GRC 89-003

WORKSHOP ON RESPONSES OF A GEOTHERMAL FIELD DURING EXPLOITATION

A RESERVOIR MANAGEMENT PLAN

June 15-16, 1989
Shattuck Hotel Conference Center
Berkeley, California

DISCLAIMER

ENVIRONMENTAL PROCESSES AND CHANGES DUE TO GEOTHERMAL EXPLOITATION - PART 2

Outline of presentation to GRC Workshop

June 15, 1986

R.G. Allis

Geothermal Research Centre, DSIR, Wairakei, New Zealand

INTRODUCTION

- Recap of key points raised by Mike Sorey

GEOTHERMAL SUBSIDENCE

- Causes
- Identifying potential subsidence areas prior to exploitation
- Effects and examples
- Counter measures

GEOTHERMALLY INDUCED SEISMICITY

- Mechanisms
- Examples
- Appropriate monitoring levels
- Mitigation measures

THERMAL ACTIVITY CHANGES

- Causes
- Examples
- Identifying potential impacts prior to exploitation

Notes for G.R.C. Workshop "Responses of a Geothermal Field during Exploitation"

June 15, 16, 1989

GEOTHERMAL SUBSIDENCE

R.G. Allis

Geophysics Division, D.S.I.R., Wairakei, Private Bag, Taupo.

INTRODUCTION

There are numerous documented cases of extraction of fluids from the ground causing surface subsidence. The cases include groundwater, oil and gas, as well as geothermal fluid withdrawal. A recent comprehensive review of all types of man-induced land subsidence was published by the Geological Survey of America (Holzer, ed. 1984). At the early stages of a geothermal power development project it is standard practice in most countries for an environmental impact report to be required. The possibility of geothermal subsidence has to be addressed, and usually it falls on the geophysicists and/or geologists to make some predictions. The advice given is vital for planning the power plant location and the borefield pipe and drain layout. It is not so much the vertical settlement that occurs with subsidence but the accompanying horizontal ground strains that can do the most damage to any man-made structure.

Nature of Subsidence

The common terminology is that subsurface compaction (i.e. loss of volume) causes deformation at the surface or subsidence. The characteristic relationship between a compacting zone and a subsidence 'bowl' is shown in Fig. 1. Note the convex curvature of the surface around the edges of the bowl which results in tensional effects, and the concave curvature in the central part of the bowl which causes compression. Subsidence over geothermal reservoirs typically has horizontal dimensions of kilometres, and vertical dimensions of usually centimetres or at most metres. Precise levelling techniques, using a network of permanent benchmarks are therefore necessary to delineate the surface deformation.

Care is needed when considering subsidence anomalies to identify whether the surface deformation could have a non geothermal origin. For

example most geothermal fields are in tectonically active zones, and there could be regional, tectonic movement within the field. Across both Broadlands and Wairakei fields in New Zealand there is the order of 5 mm/y of subsidence related to rifting in the Taupo Volcanic Zone. At The Geysers, California, reservoir compaction effects must be separated from the regional shear (Denlinger et al., 1981) associated with the San Andreas fault zone. Land slips and soil creep may disturb benchmarks, and the vibration or intermittent loading of heavy vehicles on roads can also cause local settlement. At Cerro Prieto field, Mexico, a 25 cm settlement is inferred to have occurred southeast of the Power Plant during a magnitude 6.1 earthquake in 1980 (Grannell et al., 1984). The borefield and the power station at Krafla field Iceland, tilt in accordance with inflation and deflation of the nearby volcanically active rift zone.

A combination of factor s may therefore contribute to ground movement within the borefield. If possible these should be removed to resolve the geothermal withdrawal component. Subsidence anomalies which extend far beyond inferred field boundaries, and which bear no relationship to either the shallow or deep extent of hot water should be interpreted cautiously - the anomalies may not be due to geothermal exploitation.

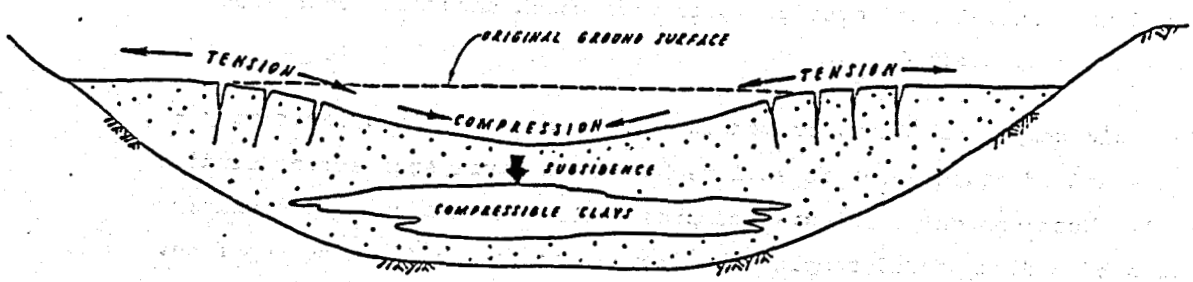

Fig. 1: Characteristic surface deformation in response to subsurface compaction (from Viets et al., 1979).

Cause of Subsidence

The theoretical basis for consolidation in porous rock is Terzaghi's concept of effective stress which states that the total stress (σ_T) is

supported by the intergranular (effective stress (σ_e) plus the pore fluid pressure (P).

i.e. $$\sigma_e = \sigma_T - P \quad (1)$$

In many hydrologic situations (especially confined aquifers) the total stress change remains relatively constant when P changes, so σ_e varies inversely with P.

Empirical studies on rock compression have shown approximately linear relation between the effective compressive stress and the resulting volume change. If $\Delta V/V$ is the fractional volume change, $\Delta\sigma_e$ the effective stress change, then

$$\Delta\sigma_e = -K\Delta V/V = -(c_b)^{-1}\Delta V/V \quad (2)$$

c_b is the bulk compressibility of the rock, which is the inverse of the bulk modulus (K). It varies by over four orders of magnitude, and is strongly dependent on porosity (Table 1). The theoretical minimum bulk compressibility is 1×10^{-6} bar^{-1}, which is the value for the mineral grains themselves (e.g. quartz, calcite). In both sedimentary and volcano-sedimentary sequences the porosity usually decreases with depth, which means the bulk compressiblity also decreases with depth. Very often in geothermal fields any formations with high porosity and high compressibility will be near surface. These formations would not have been subjected to a burial load over geologic time which naturally decreases porosity and compressibility.

The bulk compressibility, or modulus can be measured in a laboratory - it is a standard measurement in soil mechanics or civil engineering studies (Fig. 2). Most commonly, uniaxial compressibility is measured by confining the sides of a disk shaped sample, and increasing the load on the top face. The thickness of the sample is measured against the applied load, with

TABLE 1: Range of compressibility and porosity of some rock types and minerals. Multiply compressibilities by 10^{-5} to convert them to Pa^{-1}.

	Compressibility (bar^{-1})	Porosity
Clay/Pumice	10^{-1}-10^{-3}	30-80
Sand/	10^{-2}-10^{-4}	20-50
Gravel	10^{-3}-10^{-5}	10-30
Jointed rock	10^{-3}-10^{-5}	3-10
Sound rock	10^{-4}-10^{-6}	<5
Quartz	1.6×10^{-6}	-
Water	4.4×10^{-5}	-

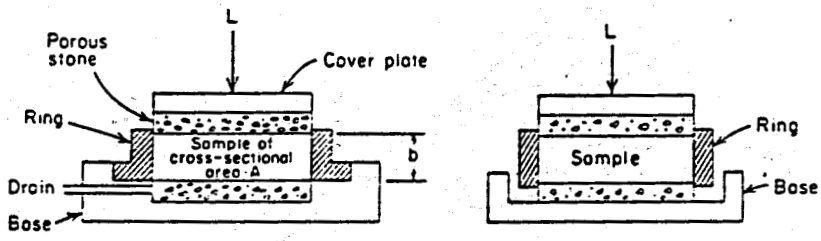

Fig. 2: Two types of consolidometer in use for compression tests of porous rocks and soils. b is the original thickness of the sample; L is the load.

fluid pressure being monitored independently. Since the area of the sample remains constant, and the rock particles/minerals are relatively incompressible, changes in thickness are equivalent to changes in pore volume. If V_p is the particle volume of the sample, V_f is the pore volume, then the ratio V_f/V_p will be proportional to the thickness of the sample (n.b. porosity = $V_f/(V_f + V_p)$. Examples of compressible behaviour of rock samples are shown in Fig. 3. Often the compressiblity increases after an initial effective stress increment. This represents a transition from a preconsolidation phase into a virgin compressibility phase. If the load is decreased, the rock behaviour is elastic if the original thickness is mostly recovered, or cataclastic if there is little recovery. Allis and Barker (1982) showed that pumice and pumice breccia samples from Wairakei field underwent cataclastic compression. This means that if field

pressures ever recovered, there would be little rebound of the ground surface. In fact the three year production test at Broadlands field (similar rock types) caused significant subsidence but no rebound occurred once fluid pressures recovered.

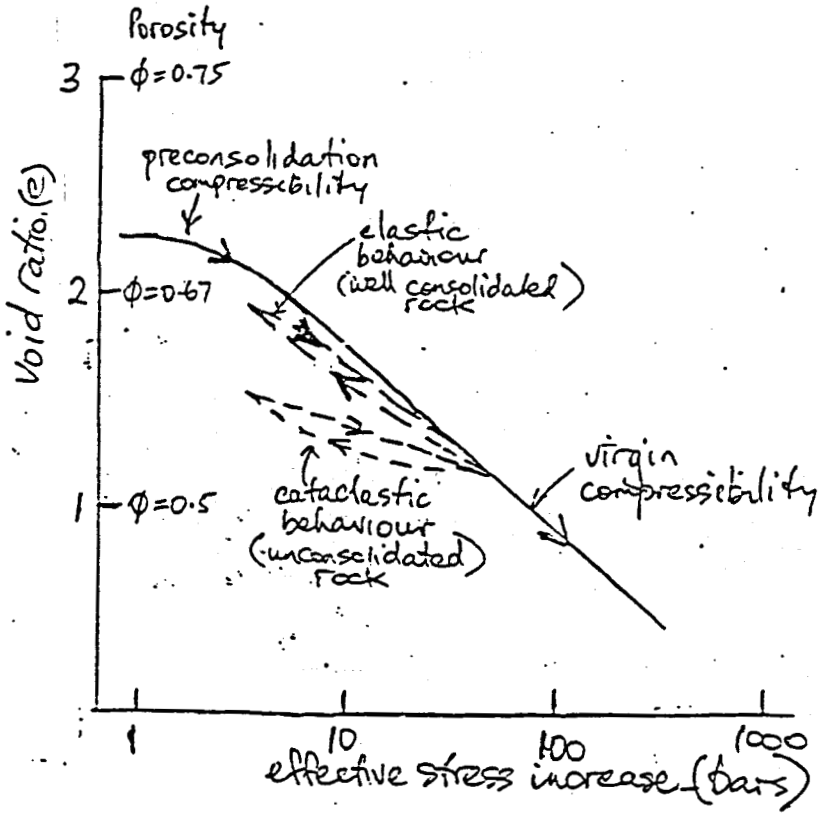

Fig. 3: Typical consolidation behaviour of rocks. The compressibility is calculated from the slope of the curve.

The uniaxial compressibility (c_m) can be calculated from the expression

$$c_m = \Delta e/(1 + e_o)/\Delta\sigma_e \qquad (3)$$

(n.b. $e = \phi/(1 - \phi)$; $\phi = e/(1 + e)$

(e_o = initial value of void ratio)

If β is the ratio of grain compressibility to bulk compressibility, then (Geertsma, 1973)

$$c_m = \frac{1}{3}\frac{(1+\nu)}{(1-\nu)}(1-\beta)\,c_b \qquad (4)$$

where ν = Poisson's ratio.

Since ν is usually in the range 0.15-0.35 and β is usually very small, $c_m \approx 0.5\ c_b$. Often the variability or uncertainty of c_b is so large that c_m and c_b can be interchangable for order-of-magnitude compaction calculations: In such cases the 1-dimensional expression for compressiblity is used:

$$c_m = \Delta h / H \Delta \sigma_e \qquad (5)$$

where H = initial thickness of formation with compressibility c_m, Δh is the amount of compaction for an effective stress increase $\Delta\sigma_e$.

QUESTION 1a: The production zone of a reservoir is fractured andesite with a compressibliity of 10^{-5} bar $^{-1}$. After 10 years of production a pressure drop of 20 bars has occurred. Assuming the production zone to be 1 km thick, calculate the compaction (i.e. subsidence - assume stress relief from mass withdrawal is insignificant).
(Answer = 20 cm)

QUESTION 1b: During the 10 years of production the average temperature has declined by 10°C. Assuming 1-d thermal contraction with a coefficient of 1×10^{-5} °C^{-1} for the andesite, calculate the thermally induced subsidence.
(Answer = 10 cm)

QUESTION 1c (optional): What was the average rate of heat extraction from the 10 km^2 area of reservoir (in MW). Assume specific heat of rock is 1×10^3 kJ/kg°C, density is 2400 kg/m^3.
(Answer 800 MW)

As mentioned earlier, when estimating the effective stress change in the reservoir it is often assumed that the total stress remains constant.

This can be shown to be approximately so at Wairakei field, where the draw-off of water has caused a 25 bar decrease. Gravity change studies have shown the average liquid saturation in the newly formed steam zone is around 0.7. That is, 30% of the pore volume has been drained. Since the porosity is around 30%, approximately 10% (0.3 x 0.3) of the rock volume has been drained of water. Therefore the stress relief caused by the mass loss is forming the steam zone is one tenth the stress increase caused by the pressure decline. The relationship between pressure change and effective stress change is shown in Fig. 4.

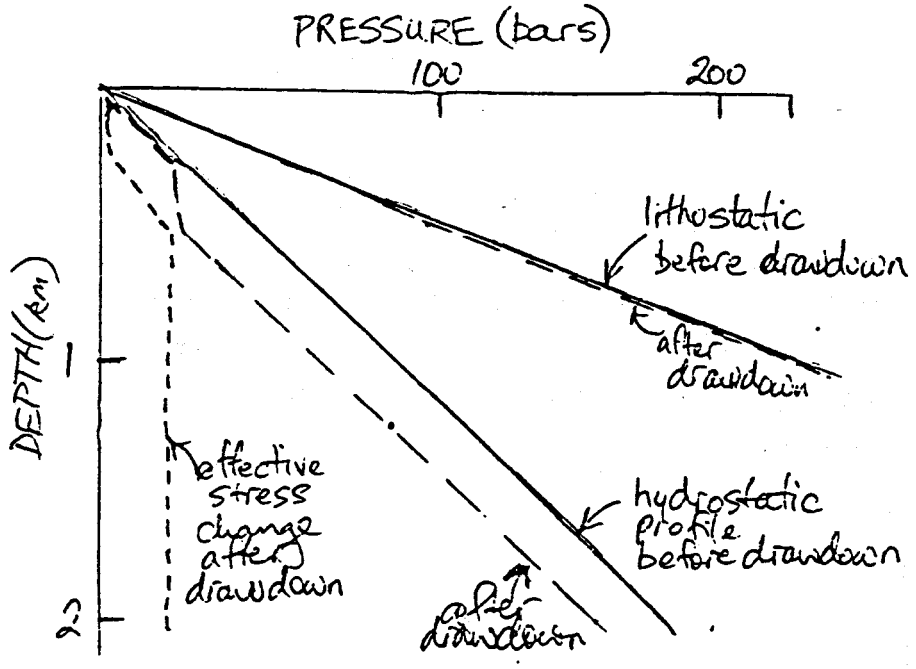

Fig. 4: Changes in pressure and stress profiles at Wairakei field as a result of 25 bars of drawdown during exploitation.

Identifying Potential Subsidence Areas

The preceding discussion has highlighted the two key parameters controlling subsidence: very compressible formations, which if present tend to be restricted to shallow depth (especially the uppermost few hundred metres), and the effective stress change, which tends to increase with depth to be a maximum in the main zone of production (usually >500 m

depth). Thus in a geothermal field, the greatest risk of a subsidence problem occurs when the deep reservoir liquid is drained from shallow parts of the field. That is, the pressure drop due to deeper production, is able to propagate to shallow depth. In general this means it is the outflow zones of liquid dominated reservoirs which present the greatest subsidence risk (Allis, 1982), as these zones represent permeable paths from the reservoir towards the surface. In addition, the alteration of the country rock in the outflow zones (especially to clays) will have enhanced the compressibility of the rock. Broadlands and Wairakei fields in New Zealand demonstrate this relationship well - the main subsidence areas are very close to the relatively small area of the field where groundwater responds to drawdown at depth.

Vapour-dominated fields , and parts of liquid-dominated fields which are capped by steam-heated thermal activity generally represent lower-risk subsidence areas. The presence of a steam zone tends to insulate deeper drawdown from propagating to shallow depth. In fact, depending on the vertical permeability in the upper few hundred metres, fluid (steam) pressures may actually increase with time during deeper drawdown of a two-phase liquid zone. Fumarole vent pressures and temperatures at Craters of the Moon thermal area in Wairakei field increased during the mid-1960's when the rate of drawdown of the deep liquid reservoir was at maximum. A summary of the subsidence characteristics of four geothermal fields is given in Table 2. More detailed discussions of geothermal subsidence case studies can be found in the references.

Effects of Subsidence

Along with vertical settlement of the ground surface in a subsidence bowl, there are associated horizontal movements towards the centre of the bowl, horizontal tension and compression zones because the horizontal movements are non-uniform, and tilt of the ground surface. In a geothermal borefield these effects can be more serious than the vertical settlement. A summary of the surface deformation around a subsidence bowl is shown in Fig. 5. Note that the horizontal movement is proportional to the first

derivative (horizontal) of the subsurface profile; and that the horizontal strain is proportional to the second derivative. The tilt, of course is the gradient of the ground surface which is the first derivative of the subsidence profile. It can be shown from simple beam theory that the proportionality constant relating the second derivative of the subsidence profile (i.e. surface curvature) and the horizontal strain is equal to the depth to the zero strain plane. Experience at Wairakei field suggests the depth to the compacting horizon lies between one two times that depth (D = 100 m at Wairakei, Allis and Barker, 1982).

TABLE 2: Comparison of four geothermal subsidence areas

	Wairakei	Broadlands	Kawerau	The Geysers
Area affected	>25 km^2	10 km^2	15 km^2	100 km^2
Area of intense subsidence	1 km^2	1 km^2	1 km^2	5 km^2
Maximum subsidence	>10 m (1985)	0.3 m (1977)	0.25 m (1982)	0.2 m (1977)
Maximum subsidence rate	0.4 m/y	0.1 m/y (1969-71)	0.02 m/y	0.05 m/y
Horizontal movement	max. 125 mm/y (1968-1979)	10 mm/y (1969-1975)	?	15 mm/y (1972-1977)
Reservoir rock type	volcanic - sedimentary	volcanic - sedimentary	volcanic - sedimentary, greywacke	greywacke
Typical production depth	500-1000 m	500-1200 m	500-1000 m	500-3000 m
Producing fluid	240°C water	260°C water	240°C water	240°C steam
Typical production rate	1500 kg/s	600 kg/s (1969-71)	200 kg/s	1200 kg/s (1977)
Pressure drawdown	max. 3 b/y (liquid) (1960-65) 0.5 b/y (steam) (1970-1980)	max. 5 b/y (1970-1971)	0.2 b/y?	maximum steam pressure drop exceeds 20 bars

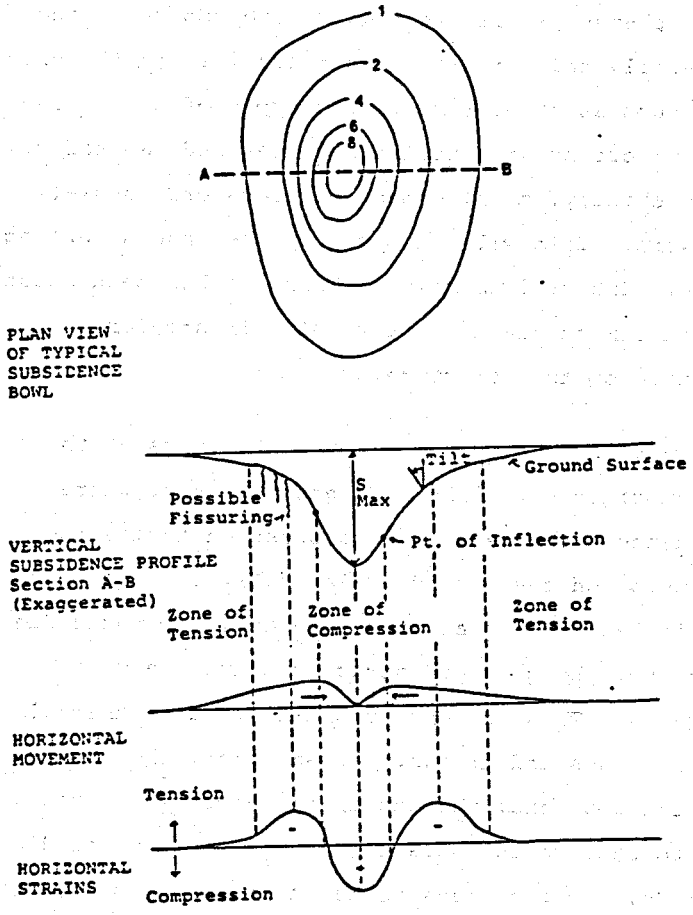

Fig. 5: Relationship between vertical and horizontal movement in a typical subsidence bowl (from Viets et al., 1979).

A very brief review of the surface effects of subsidence are given here - for a complete review, refer to Viets et al., (1979).

Vertical settlement - Because of the relatively large diameter of the subsidence in geothermal fields (~ km) the vertical movement often has a relatively small effect on surface structures. The main concern is where the water table is initially close to or at the surface. Vertical settlement causes the water level to rise relative to the ground surface, and flooding can occur. This has happened in the Wairakei Stream at Wairakei field, but fortunately the rising water level has not caused any damage.

Tilt and Differential Settlement - Tilt is towards the centre of the subsidence bowl. It is generally only important in relatively small, high amplitude subsidence bowls, such as at Wairakei. Two types of damage can result - rigid body tilt is important with tall structures and can effect the levelling of sensitive machinery, misalignment of elevators, and also micro wave beams on tall towers. Tilt will also change the grades on long drains, canals, or pipelines. The maximum tilt at Wairakei has been about one degree. Differential settlement due to tilt results in angular distortion and possible rupture of the structure.

Horizontal Movement and Strain - The maximum movement occurs at the point of inflection on the subsidence profile. Movement is everywhere towards the centre of subsidence. The result is compression inside the point of inflection, and tension on the outside. Generally the horizontal strain in rigid structures is less than that in the underlying ground due to some detachment and slipping. Long, rigid structures are the most sensitive to horizontal strains. This is very important in a geothermal borefield where there are pipelines and drains. At Wairakei, the concrete drains have cracked in the tension zone, whereas in the compression zone, a sliding joint is necessary to relieve the strain (average movement of 10 cm/y). Every five years or so, sections have to be cut out, or added, to the pipelines at Wairakei where they traverse the tension and compression zones of the subsidence bowl. Roads, curbing, and concrete floors in large buildings may also crack if under tension. The ground surface itself may crack in the high tension areas. If transmission lines pass over the subsidence bowl (as at Wairakei) then adjustments may have to be made every few years to keep the line tension even on either side of the pylons.

Subsurface Deformation - The horizontal and vertical movements occurring at the surface also occur between the compacting zone and surface, giving rise to vertical and horizontal shear stresses. If the casing in a well is poorly connected to the country rock, protrusion of the wellhead above the ground may occur (assuming the well extends below the compacting zone). However in most geothermal situations the casing at shallow depths is cemented in, so the shear stresses cause buckling, bending, or as is common at Wairakei, compressed joints (Bixley and

Hattersley, 1983). At Wairakei, the compressed joints occur over the interval of the compaction zone, and the bending that has been confirmed in one well is half way between the surface and the compaction zone. Many of the wells at Wairakei have sufferred casing damage, but none of the damage has been sufficient to cause wells to be shut-in.

Counter Measures

There is not a lot that can be done to alleviate subsidence problems once they develop in a geothermal field. Once the cause has been established (usually pressure drawdown) and the depth and thickness of the compaction zone is known, the only course of action is to minimise the drawdown in that formation. This could be done by shutting in producing wells in the vicinity, if they are known to be drawing fluid from the compaction zone. Alternatively, injecting waste water into the compacting zone may be feasible. If the compacting zone is in the steam zone this injection of water may initially condense steam and drop pressures even further. However, depending on the permeability it may be possible to keep the compacting zone liquid filled, and therefore maintain fluid pressure.

By far the best practice is to identify high-risk subsidence areas before major field development occurs and plan development around these areas if possible. Areas of intense thermal activity should be avoided because of the effects of hydrothermal alteration; in particular outflow areas where reservoir water rises to shallow depths are especially prone to subsidence, as mentioned earlier. Highly porous or clay-rich zones at less than 500 m depth which initially contain reservoir liquid may have relatively high compressibilities, and these zones may experience a large fluid pressure decline once production starts. Such formations should be identified from early wells, and their isopachs should be mapped as drilling proceeds. An early shallow well to monitor pressure and temperature in a potential compaction zone may be advisable.

Further Information

Reviews of subsidence case studies and the theoretical interpretation of subsidence data can be found in Holzer ((ed.) 1984, especially papers by Helm, and Narashimham and Goyal). Refer also to Helm (1982), and Miller et al., 1980). Wairakei Field has become a classic example of geothermal-induced subsidence, because of the extreme amplitude of subsidence (>10 m in 1985) and because the associated surface effects are so apparent. The review of Allis and Barker (1982) is therefore given as an appendix to this paper. Note that discussion in this paper on the cause of the subsidence at Wairakei differs from earlier ideas reviewed in Narasimham and Goyal (1984).

REFERENCES

Allis, R.G. 1982: Comparison of subsidence at Wairakei, Broadlands and Kawerau fields, New Zealand. In proc. 8th Stanford Geothermal Reservoir Engineering Workshop, Stanford Univ. p 183-188.

Allis, R.G. and Barker, P. 1982: Update on subsidence at Wairakei. Proc. 4th N.Z. Geothermal Workshop: 365-370.

Bixley, P.F. and Hattersley, D.S. 1983: Long term casing performance of Wairakei production wells. 1983 proc. Univ. of Auckland, N.Z. Geothermal Workshop, p 257-263.

Denlinger, R.P., Isherwood, W.F. and Kovach, R.L. 1981: A geodetic analysis of reservoir depletion at The Geysers steam field in Nth California, Jl of Geophys. Res., 86, p 6091-6096.

Geertsma, J. 1973: Land subsidence above compacting Oil and Gas reservoirs. Jl of Petroleum Technology, 25, 734-744.

Grannell, R.B., Zhou, H-W. and Wyman, R. 1984: Modeling of repetitive gravity observations at Cerro Prieto geothermal field. G.R.C. Trans., 8, 203-206.

Holzer, T.L. 1984 (ed.): Man-Induced land subsidence. Reviews in Engineering Geology, Volume VI, Geological Soc. Amer.

Helm, D.C. 1982: Conceptual aspects of subsidence due to fluid withdrawal in Narasimham, T.N. (ed.) Recent trends in hydrogeology: Geol. Soc. Amer. Spec. Pap. 189, 103-142.

Helm, D.C. 1984: Field-based computational techniques for predicting subsidence due to fluid withdrawal in Holzer, T.L. (ed.) Man-Induced land subsidence, Reviews in Engineering Geology, Vlume VI, Geol. Soc. Am., 1-22.

Miller, I., Dershowitz, W., Jones, K., Meyer, L., Roman, K. and Schauer, M. 1980: Simulation of geothermal subsidence: LBL Rep. No. 10794, 160 p.

Narasimham, T.N. and Goyal, K.P. 1984: Subsidence due to geothermal fluid withdrawal in Holzer, T.L. (ed.) Man-Induced land subsidence, Reviews in Engineering Geology, Volume VI, 35-66.

Viets, V.F., Vaughan, C.K. and Harding, R.C. 1979: Environmental and Economic Effects of Subsidence. GSRMP-1, LBL 8615, University of California, Berkeley.

Notes for G.R.C. Workshop "Responses of a Geothermal Field during Exploitation"

June 15, 16, 1989.

INDUCED SEISMICITY DUE TO GEOTHERMAL EXPLOITATION

R.G. Allis

Geophysics Division, D.S.I.R., Wairakei, New Zealand

The revelation that injection of water into the ground could trigger seismicity occurred during the pumping of waste waters into a 3.8 km deep well in the Rocky Mountain Arsenal (near Denver) during the 1960s. In analysing the data, Healy et al., (1968) attributed the anomalous seismic activity to pore pressure increases occurring at depth. Subsequently there have been many similar reports of induced seismicity, and the use of high pump pressure tests to induce hydrofracturing and to determine the magnitude of stress in the crust have become commonplace.

High pore pressure is not the only way of triggering earthquakes. Both the loading of the earth's surface with large water reservoirs (dammed lakes) and the unloading that occurs in large mines or quarries may also induce seismicity. In fact, any activity that changes the stress regime in the earth is likely to induce earthquakes. A recent review of this subject is given by Simpson (1986). Before discussing the incidence of induced seismicity in geothermal projects, a brief review of possible mechanisms is given first. Theoretical details can be found in any text book on rock mechanics (e.g. Jaeger and Cook, 1976).

Mechanisms of Induced Seismicity

Laboratory experiments on sliding or failure in rocks have established a linear relationship between the shear stress (τ) acting on a plane of weakness, and the normal stress (σ_n). This is commonly referred to as the Mohr-Coulomb failure criteria, and is expressed as:

$$\tau = \tau_o + \mu\sigma_n \qquad (1)$$

where μ = coefficient of friction (sometimes expressed as Tan ϕ - see below). and τ_o = the cohesive strength.

If the rock is filled with fluid of pressure P, the total stress on the rock is borne by the effective stress (due to grain to grain contact) and

by the fluid pressure. The effective stress is therefore the total stress minus the fluid pressure, P (in fact all principal stresses are reduced by P) . The equation above therefore becomes:

$$\tau = \tau_o + \mu(\sigma_n - P) \qquad (2)$$

Thus as fluid pressure increases, the shear stress necessary to cause failure decreases. If the rock is already close to failure, a small increase in fluid pressure may trigger a rupture. This is the essence of induced seismicity caused by pore pressure changes.

The general relationship between stress changes and rock failure can be shown diagramatically (from Simpson, 1986). σ_1, σ_2, σ_3 are the maximum, intermediate, and minimum principal (orthogonal) stresses acting on a rock. The shear stress and the normal stress acting on a plane can be related to the principal stresses by the following equations, if α is the angle between the plane and σ_3:

$$\tau = \tfrac{1}{2}(\sigma_1 - \sigma_3) \sin 2\alpha \qquad (3)$$

$$\sigma_n = \tfrac{1}{2}(\sigma_1 + \sigma_3) + \tfrac{1}{2}(\sigma_1 - \sigma_3) \cos 2\alpha \qquad (4)$$

These equations mean that τ and σ_n lie on the arc of a circle (the 'Mohr' circle) as shown in Fig. 1. Where this circle touches, or overlaps the failure line given by equation 1, the rock will fail for the appropriate value of angle α. Since the effect of a fluid pressure P is to reduce all principal stresses by P, τ remains unchanged (radius constant) but σ_n is reduced by P. Thus the Mohr circle moves closer to the failure line by the value P. Note that the σ_n in the failure line is the <u>total</u> normal stress on the rock in this case (not $\sigma_n - P$).

The various ways of causing the Mohr circle to shift towards the failure line are illustrated in Fig. 2 (after Simpson, 1986). In addition local stress perturbations may result from thermal contraction (boiling or cold water invasion in a geothermal reservoir) or from compaction induced by pressure decline. The latter is reviewed by Yerkes and Castle (1976) and has occurred during the extraction of hydrocarbons from reservoirs with highly compressible rocks.

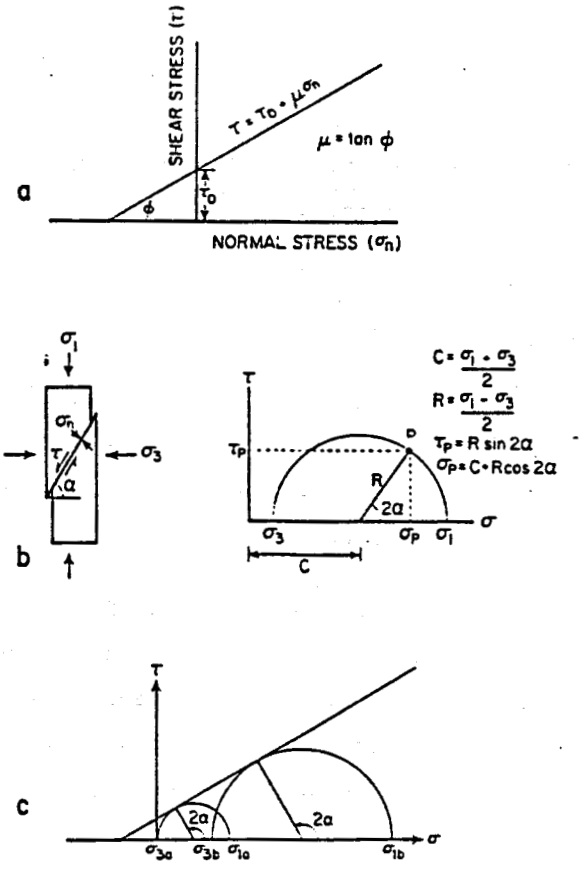

Figure 1 (*a*) Coulomb's law for failure in dry rock, showing the relationship between the shear stress (τ) required for failure and the normal stress σ_n across the plane. Here τ_0 is the cohesion and μ is the coefficient of friction. (*b*) The Mohr circle diagram, which provides a graphical method by which the principal (compressive) stresses (σ_i) can be resolved into shear (τ) and normal (σ_n) components on a plane at angle α to the σ_3 direction. (*c*) The Mohr-Coulomb failure criterion. Given maximum (σ_1) and minimum (σ_3) principal stresses, failure will occur on a plane containing the intermediate stress (σ_2) and at an angle α to σ_3 if the circle containing points σ_1 and σ_3 intersects the failure curve defined in (*a*). (from Simpson, 1986)

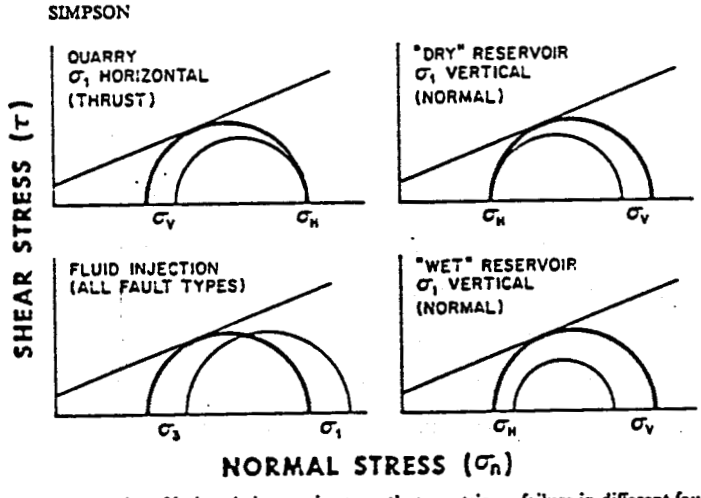

Figure 2 Examples of induced changes in stress that can trigger failure in different faulting environments. The thin circle is the original stress state and the heavy circle the state after the stress change. For simplicity, the small change in σ_H due to a lateral expansion caused by an increase in σ_V is ignored. (from Simpson, 1986)

CASE STUDIES

New Zealand

The only reported occurrence of induced seismicity in New Zealand occurred during a cold water injection experiment in 1984 (Sherburn, 1984; Allis, et al., 1985). Previous microearthquake surveys during the 1970's had shown no anomalous seismicity near borefield or geothermal areas (Evison, et al., 1976; Hunt and Latter, 1982). Over a six week period of seismic monitoring 120 local earthquakes were recorded; 90 of these occurred during the nine days of injection testing (Figs 3 and 4). The static water level in the well was 240 m below ground surface. During the pumping, wellhead pressures rose to a maximum of 35 bars g., causing a maximum overpressure of almost 60 bars. The well was initially relatively

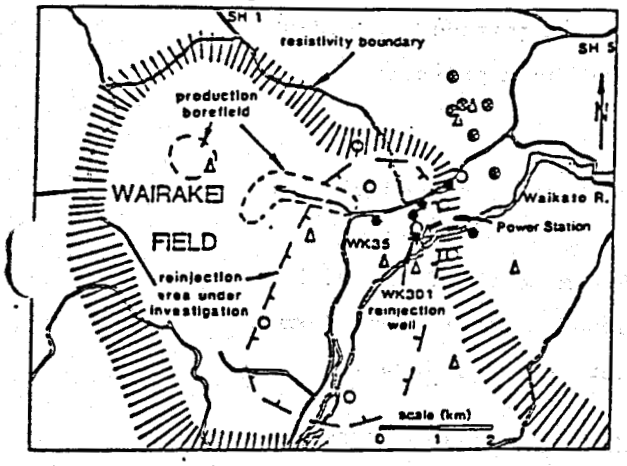

Figure 3 Location of WK301, and the reinjection area under investigation. The resistivity boundary of the field is from Risk and others (1984). Triangles denote microearthquake stations; closed circles are epicentres of earthquakes located during the first injection test; open circles are epicentres located during the second injection test; crossed circles are epicentres of a 17-minute swarm of earthquakes during the second injection test (refer to text).

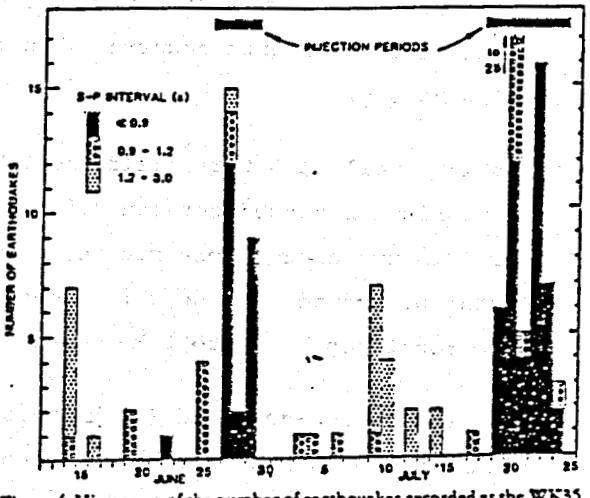

Figure 4 Histogram of the number of earthquakes recorded at the WK35 site during the monitor period. An S-P interval of 0.9 s represents approximately 3 km.

impermeable, but the injectivity increased in sudden jumps during the pumping, which were presumed to be hydrofracturing events. The jumps did not correspond to recorded seismic events. Although the largest events had a magnitude of only +1.5, they were sharply felt, because of their shallow depth. The epicentres of the induced events had a roughly elliptical

distribution about the injection well, with the more distant events occurring outside the resistivity boundary of the field. The b-value of 0.8, and the composite focal mechanism solution indicating dextral strike slip movement on a NE trending plane, were both similar to those reported in the earlier microearthquake surveys. Therefore the induced events were interpreted to be relieving the regional stress in the vicinity of the well.

Italy

Reinjection of fluids into several of Italy's geothermal fields have caused induced seismicity. Two reinjection tests into well RA1 in Torre Alfina field (approximately 100 km southeast of Larderello) in 1977 caused a clear increase in local seismicity (Batini et al., 1980). Focal depths were relatively shallow (<3 km) and concentrated around the reinjection well (generally less than 2 km distance). The maximum magnitudes exceeded 3.0. Most of the induced events occurred when the wellhead pressure exceeded about 5 bars g.

Pump tests in a well in Latera Field (near Torre Alfina) caused similar results. The magnitudes ranged between 1.5 and 2.0, with the located events clustered in two areas: one cluster about 500 m south of the well with focal depths of around 1 km depth; and the second cluster about 1 km northeast, with focal depths up to 2 km depth (Batini, et al., 1980).

Injection tests at Cesano field (40 km north of Rome), during 1978 triggered seismicity which appeared to occur above a certain pressure threshold. Later in one test, relatively little induced activity occurred despite rising fluid pressure (Batini, et al., 1980). A second injection test with slowly increasing wellhead pressure caused induced events after about 24 hours of injection, when the wellhead pressure exceed 80 bars g. The maximum magnitudes was 2.0.

The Larderello-Travale field has a high level of seismic activity, but the magnitude of the events rarely exceeds 3.0 (Batini, et al., 1985). The

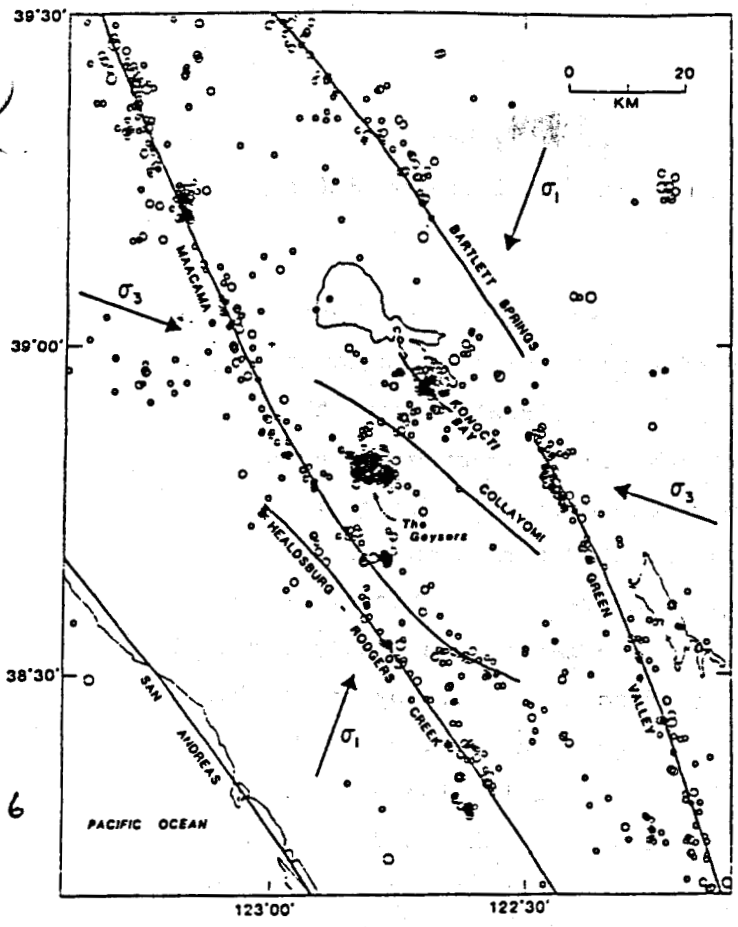

Fig. 6

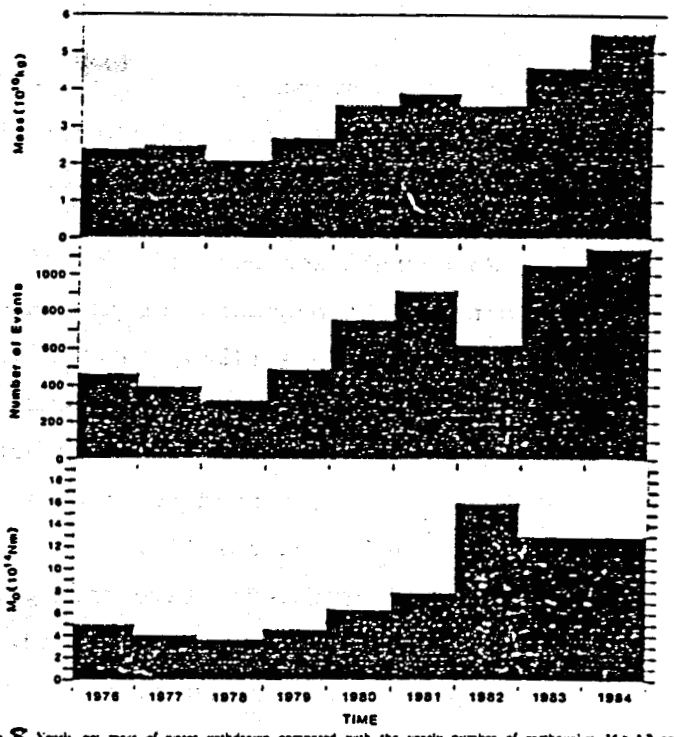

Fig. 8 Yearly net mass of water withdrawn compared with the yearly number of earthquakes $M \geq 1.2$ and quality = A–C [*Lee and Lahr*, 1975] and the associated moment sum (Table 2) for entire The Geysers geothermal reservoir. The presence of a few $M3+$ earthquakes greatly influences the moment sum calculation and explains the better correlation between yearly mass withdrawn and number of earthquakes.

(from Oppenheimer, 1986)

A
Fig 7a

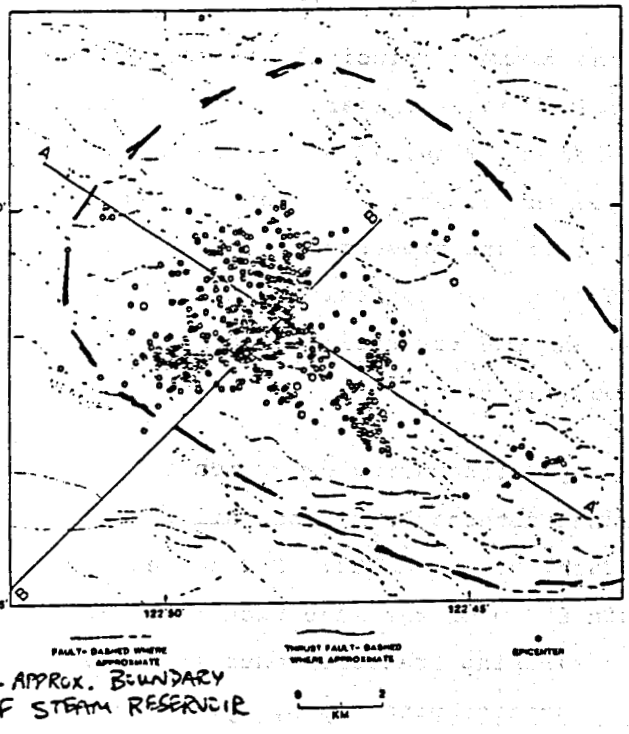

— — APPROX. BOUNDARY OF STEAM RESERVOIR

B)
Fig 7b

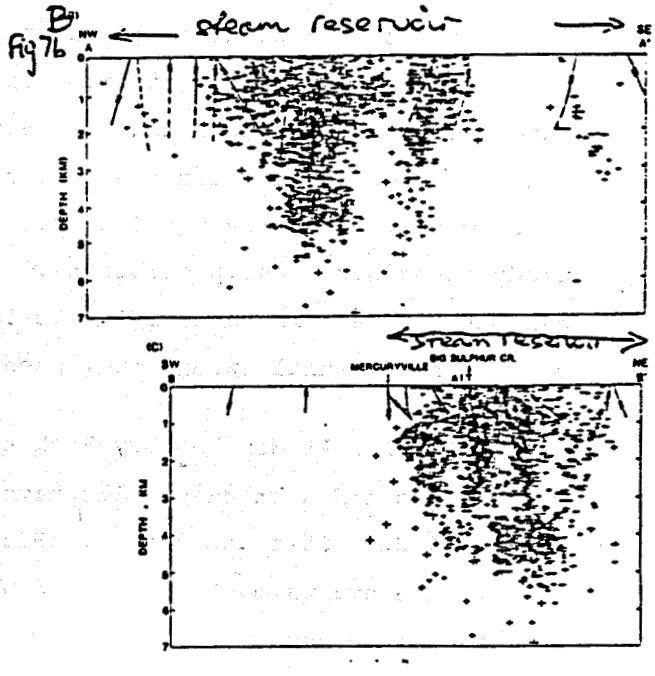

Figs 6-8: Characteristics of induced seismicity at The Geysers, California. (From Eberhart-Philips, 1984, and Oppenheimer, 1986.)

power plants starting up (Figs 7 and 8). The activity seems to be continuous rather than in swarms, with a maximum magnitude of 3 (one event per year, Ludwin and Bufe, 1980).

No correlation between injection wells and seismicity has been reported. The mechanism of the induced seismicity remains in doubt. Denlinger and Bufe (1981), and Denlinger et al., (1982) suggest that cooling and contraction on fracture surfaces are triggering the events. Allis (1981, 1982) suggests that aseismic deformation due to regional stress may be converted to stick-slip (seismic) deformation due to either an increase in the coefficient of friction on fracture surfaces, or to a large increase in effective rock pressure. The latter could only occur if the reservoir was liquid dominated, and therefore may only be applicable at >3 km depth. The former mechanism could be due to dehydration and hardening of clay and fault gauge, and by the precipitation of silica on fracture surfaces. Oppenheimer (1986) has reviewed all the data, and considers the evidence equivocal. He also points out that the earthquakes are induced at depths of up to 3 km beneath the bottom of wells, but generally only at distances of a few hundred metres laterally. This is attributed to the vertical gradient in the maximum principal stress being greater than that of the minimum principal stress (similar to the injection experiments at Cornwall, England, Batchelor and Pine, 1984). A change in the focal mechanism solutions is also apparent at about 1 km depth. At shallow depth some reverse (thrust) solutions are present in addition to predominant strike slip solutions. Below 1 km depth, fault plane solutions exhibit strike-slip to normal solutions, and the reservoir appears to be undergoing uniaxial extension (Oppenheimer, 1986).

At the Los Alamos Hot Dry Rock site, hydrofracturing experiments between two and 4 km deep wells have caused detectable microseismicity (Brown, 1982; Dash and Murphy, 1983; Cash, et al., 1983; Franke, et al., 1984). The events mostly occurred within 600 m of the injection interval. Injection into each well generated north-striking fracture zones (Fig. 9) Fracture opening pressures were found to increase with depth, typically being 200 bars less than the lithostatic pressure gradient (i.e. fracture pressures of 600-800 bars at 3.5 km depth).

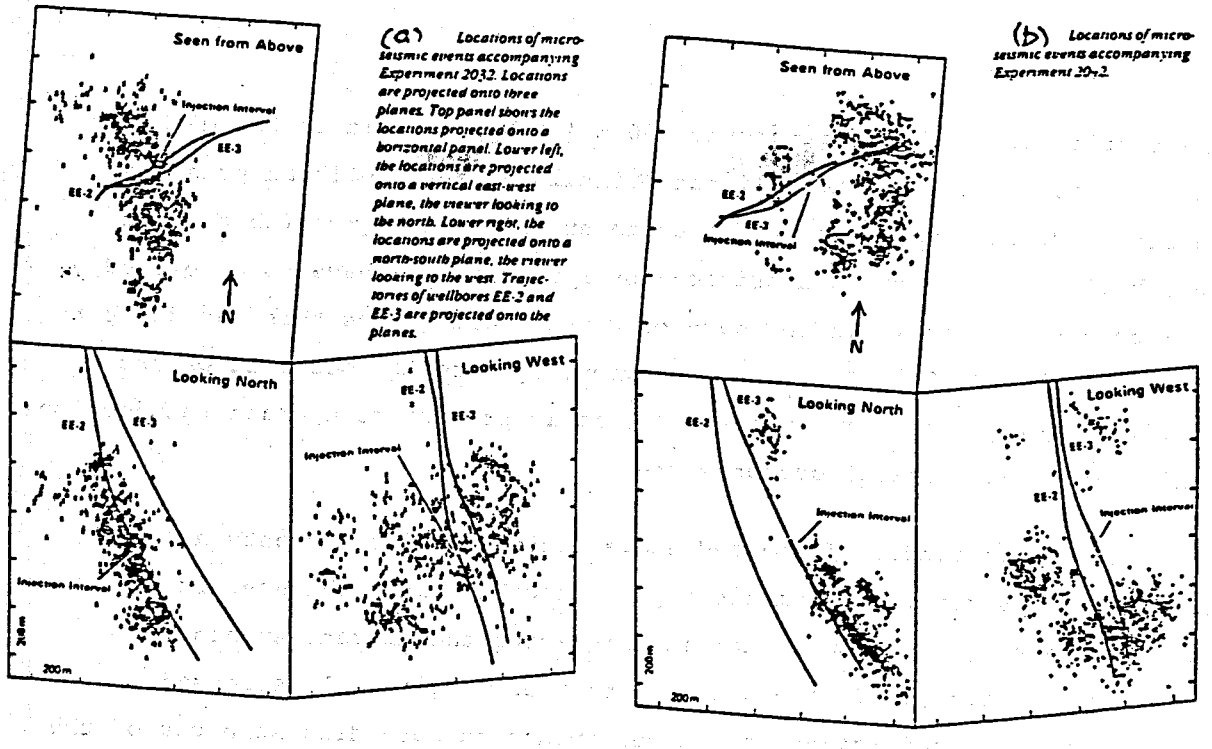

Fig. 9: Induced seismciity associated with injection into EE-2 (a), and then injection into EE-3 (b) at the Hot Dry Rock Experiment, Los Alamos. Note the clustering of events on north-trending planes in both injection experiments, suggesting a poor connection between the two wells. The injection depth are around 3.5 km depth. (Franke et al., 1984).

CONCLUSIONS

As a general rule, reinjection of geothermal fluid into the ground is liable to cause induced seismicity. The principal mechanism is the increase in pore pressure that occurs at injection depths, which reduces the effective normal stress (i.e. frictional resistance) acting on fault planes. In most areas the state of stress in the ground is close to failure, so the perturbing stress necessary to cause failure may be small (e.g. bars).

If the permeability in the injection well is high, large flows of water may be injected without a concomitant increase in downhole pressure. Conversely, the higher the pump pressure at the surface, the greater the chance of triggering seismicity. Zero wellhead pressure on the injection well is no guarantee for avoiding earthquakes either - at Southern Negros

the static water levels are around 800 m (at Wairakei it is 250 m) below the surface so filling the well but maintaining zero wellhead pressure causes an 80 bar over pressure at depth at Southern Negros (25 bars at Wairakei). In some cases a critical overpressure may have to be exceeded to induce seismicity. In the case of Denver earthquakes this was 120 bars (Healy et al., 1968). A similar behaviour appeared to occur at Cesano field, Italy. Where this is the case, it is prudent to operate reinjection wells below the critical overpressure.

Many of the studies discussed above indicate induced events at distances of several km from the injection well. In such cases it may not be the excess pore pressure that is triggering the distant events. Possibly the release of stress on one part of a critically stressed fracture will be sufficient to trigger events on more distant parts of the fracture. The vertical propagation of seismicity at both The Geysers and the Cornwall injection sites are examples of this phenomenon.

In steam-dominated reservoirs the situation is more complicated, because the injected water may disperse downwards through the reservoir without increasing pore pressure (in fact initial condensation of steam may decrease pore pressure). However if the permeability is low around the injection depth, liquid pressure may increase locally. Alternatively if the injected water drains to a deeper, liquid-dominated zone, the pore pressure may increase there and trigger seismicity. This may be the cause of the induced seismicity at Larderello. At The Geysers, the induced seismicity is not obviously caused by the reinjection of condensate.

In general it appears that production of geothermal fluids (as opposed to reinjection) does not cause induced seismicity. The reason for this is that the pore pressure declines with fluid extraction, and therefore the reservoir rock should actually increase in strength with production. The Geysers reservoir is an obvious exception - possibly its location on a transform plate boundary, and a higher level of stress (and strain) make it more sensitive to physical changes in the reservoir. Since the induced seismicity at Southern Negros may also be related to production (as well as injection), this cause of induced seismicity cannot be excluded.

In almost all cases of geothermal induced seismicity the maximum magnitude of the events does not exceed 3 (4 at The Geysers) and there have been no reports of damage. It is unclear in all the reports of induced seismicity whether the excess pore pressure mechanism is such that only low magnitude events will be triggered. In the Denver earthquake sequence a large magnitude event (5.6) did occur about a year after injection ceased. Whether the larger events would occur regardless of injection is unknown. However the risk (albiet small) of a potentially damaging event is always present, particularly when large scale injection is occurring. In such cases the installation of a seismic monitoring network is unfortunately an essential cost linked to the geothermal project. The network will enable the location and characteristics of any induced seismicity to be established, and from the magnitude frequency relationship, it will enable the estimation of recurrence times of large magnitude events.

As pointed out by Bufe and Shearer (1980), induced seismicity is not all bad news. The seismicity may delineate the direction or extent of injected fluid flowing into the reservoir. In the case of The Geysers it delineates the extent of production. The seismicity may also delineate the key fractures in a reservoir. Such fractures would be targets for additional reinjection wells, should they be needed.

REFERENCES

Allis, R.G. 1981: Comparison of mechanisms proposed for induced seismicity at The Geysers geothermal field. In Proc. New Zealand Geothermal Workshop 1981, Auckland Univ. 57-61.

Allis, R.G. 1982: Mechanism of induced seismicity at The Geysers geothermal reservoir, California. Geophysical Research Letters, 9, 629-632.

Allis, R.G., Currie, S.A., Leaver, J.D. and Sherburn, S. 1985: Results of injection testing at Wairakei Geothermal Field, New Zealand. Transactions Vol. 9, 1985, International Symposium on Geothermal Energy.

Batini, F., Bufe, C., Cameli, G.M., Console, R. and Fiordelisi, A. 1980: Seismic Monitoring in Italian Geothermal Areas I and II. Proceedings Second DOE-ENEL Workshop for Cooperative Research in Geothermal Energy, 20-85.

Batini, F., Console, R. and Luongo, G. 1985: Seismological Study of Larderello-Travale Geothermal Area.

Bromley, C.J. and Rigor, D.M. Jr 1983: Microseismic Studies in Tongonan and Southern Negros. Proceedings 5th N.Z. Geothermal Workshop, 91-96.

Bromley, C.J., Pearson, C.F. and Rigor, D.M. 1985: Induced seismicity at Southern Negros Geothermal Field, Philippines. Abstract. N.Z. Geophysical Society 1985 Symposium, Wellington.

Brown, D.W. 1982: Recent results, Los Alamos Hot Dry Rock Project. Proc. Stanford Geothermal Reservoir Engineering Workshop, Stanford University - 1982.

Bufe, C.G. and Shearer, P.M. 1980: Geothermal Induced Seismicity-Bane or Blessing. Proceedings D.O.E.-E.N.E.L. Workshop for Cooperative Research in Geothermal Energy - 1980.

Bufe, C.G.S., Marks, S.M., Lester, F.W., Ludwin, R.S. and Stickney, M.C. 1981: Seismicity of The Geysers - Clear Lake region. U.S. Geol. Survey Prof. Pap. 1141, 129-137.

Cash, D., Homuth, E.F., Pearson, C. and Sasaki, S. 1983: Fault plane solutions for microearthquakes induced at the Fenton Hill Hot Dry Rock Geothermal Site: Implications for state of stress near a Quaternary Volcanic Centre. Geophys. Res. Lett., 10, 1149-1144.

Dash, Z., and Murphy, H. 1983: Variation of fracturing pressures with depth near the Valles Caldera. Proc. Ninth Stanford Geothermal Reservoir Engineering Workshop, Stanford University.

Denlinger, R.P., Isherwood, W.F. and Kovach, R.L. 1981: A geodetic analysis of reservoir depletion at The Geysers steam field in Nth California. Jl. Geophys. Res., 86, 6091-6096.

Denlinger, R.P. and Bufe, C.G. 1982: Reservoir conditions relating to induced seismicity at The Geysers steam reservoir, northern California. Bull. Seismol. Soc. Am., 72, 1317-1327.

Eberhart-Phillips, D. and Oppenheimer, D.H. 1984: Induced seismicity in The Geysers geothermal area, California. Journal of Geophysical Research 89: 1191-1207.

Evison, F.F., Robinson, R. and Arabasz, W.J. 1976: Microearthquakes, geothermal activity, and structure, Central North Island, New Zealand. New Zealand Journal of Geology and Geophysics, 19: 625-637.

Franke, P.R., Brown, D.W., Smith, M.C. and Mathews, K.L. 1984: Hot Dry Rock Geothermal Energy Development Program. Annual Report Fiscal Year 1984, LA-10661-HDR.

Healy, J.H., Rubey, W.W., Griggs, D.T. and Raleigh, C.B. 1968: The Denver Earthquakes, Science 161, 1301-1310.

Hunt, T.M. and Latter, J.H. 1982: A Survey of Seismic Activity near Wairakei Geothermal Field, New Zealand. J. of Volcanology and Geothermal Research, 14, 319-334.

Jaeger, J.C. and Cook, N.G.W. 1976: Fundamentals of Rock Mechanics: Chapman and Hall, 585 p.

Ludwin, R.S. and Bufe, C.G. 1980: Continued seismic monitoring of The Geysers, California geothermal area. U.S. Geol. Surv. Open File Rep., 80-1060, 50 pp.

Majer, E.L. and McEvilly, T.V., 1979: Seismological investigations at The Geysers geothermal field. Geophysics, 44, 246-269.

Marks, S.M., Ludwin, R.S., Louie, K.B. and Bufe, C.G. 1978: Seismic monitoring at The Geysers geothermal field, California. U.S. Geol. Surv. Open File Rep., 78-798, 44 pp.

Oppenheimer, D.H. 1986: Extensional tectonics at The Geysers geothermal area, California. Jl. Geophys. Res. 91, 11463-11476.

Pine, R.J. and Batchelor, A.S. 1984: Downward migration of shearing in joined rock during hydraulic injection. Geothermal Energy Project, Camborne School of Mines: 48 p.

Sherburn, S. 1984: Seismic monitoring during a cold water injection experiment, Wairakei Geothermal Field. Preliminary results. Proc. 6th N.Z. Geothermal Workshop, Univ. of Auckland.

Simpson, D.W. 1986: Triggered earthquakes. Ann. Rev. Earth Planet. Sci., 14, 21-42.

Yerkes, R.F. and Castle, R.O. 1976: Seismicity and faulting attributable to fluid extraction. Eng. Geol., 10, 151-167.

Urbino, M.E.G., Zaide, M.C., Malate, R.G.M., Bueza E.L., 1986. Structural flow paths of reinjected fluids based on tracer tests - Palinpinon-1, Philippines. Proc. 8th N.Z. Geothermal Workshop. Univ. of Auckland, 53-55

CASE HISTORIES

WAIRAKEI AND KAWERAU EXPLOITATION HISTORIES COMPARED

Outline of presentation to GRC Workshop

June 16, 1989

R.G. Allis

Geothermal Research Centre, DSIR, Wairakei, New Zealand

PRODUCTION HISTORIES

DEEP RESERVOIR CHANGES

GROUNDWATER IMPACTS

MANAGEMENT STRATEGIES

Location Map

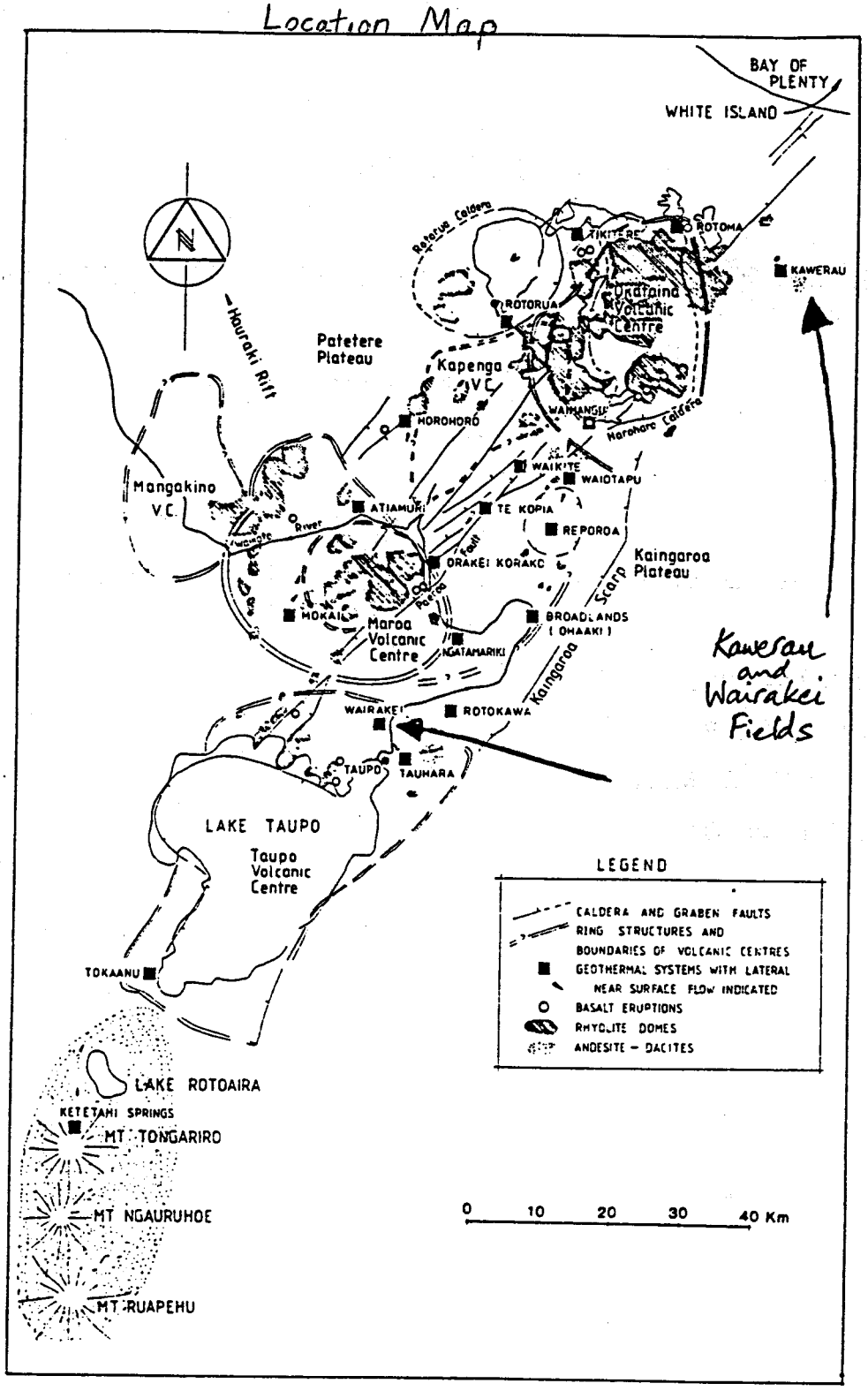

Figure 1.5a: Distribution of volcanic centres of the Taupo Volcanic Zone (adapted from Healy 1964, Healy et al. 1964, Cole 1979, Nairn 1981 and Wilson et al. 1984), principal structures and location of major geothermal fields.

Figure from Henley and Hedenquist (1986): Introduction to The Geochemistry of Active and Fossil Geothermal Systems Monograph Series on Mineral Deposits No 26, 1-22 Gebruder Borntraeger.

WAIRAKEI FIELD TRENDS

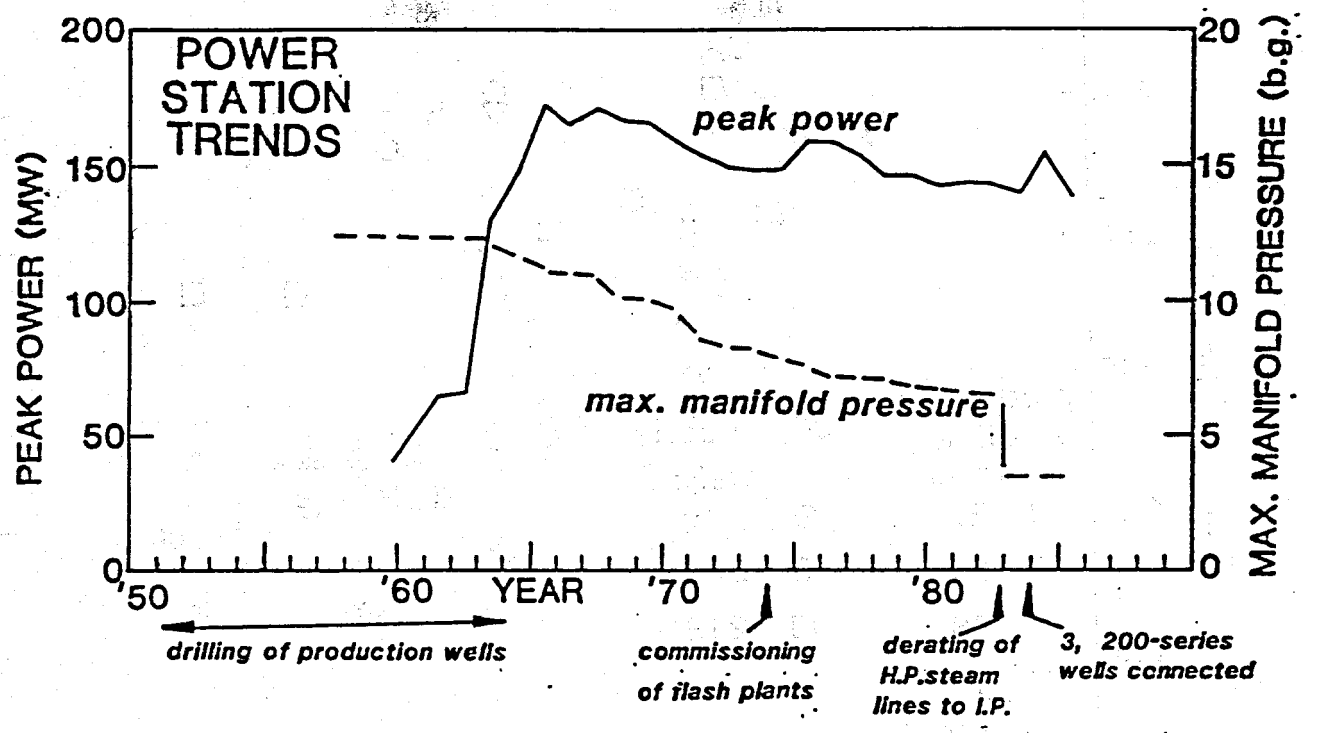

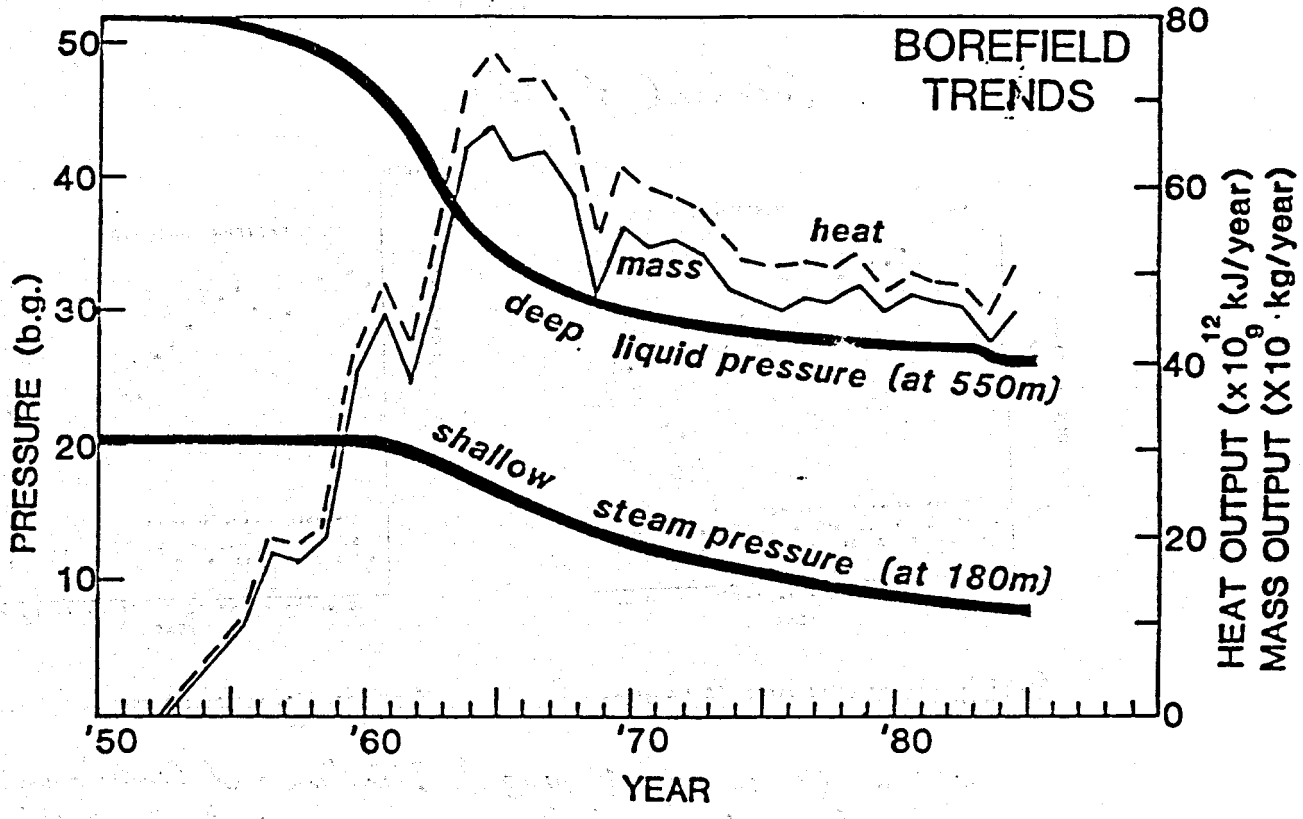

Thermal trends (Allis, unpub.)

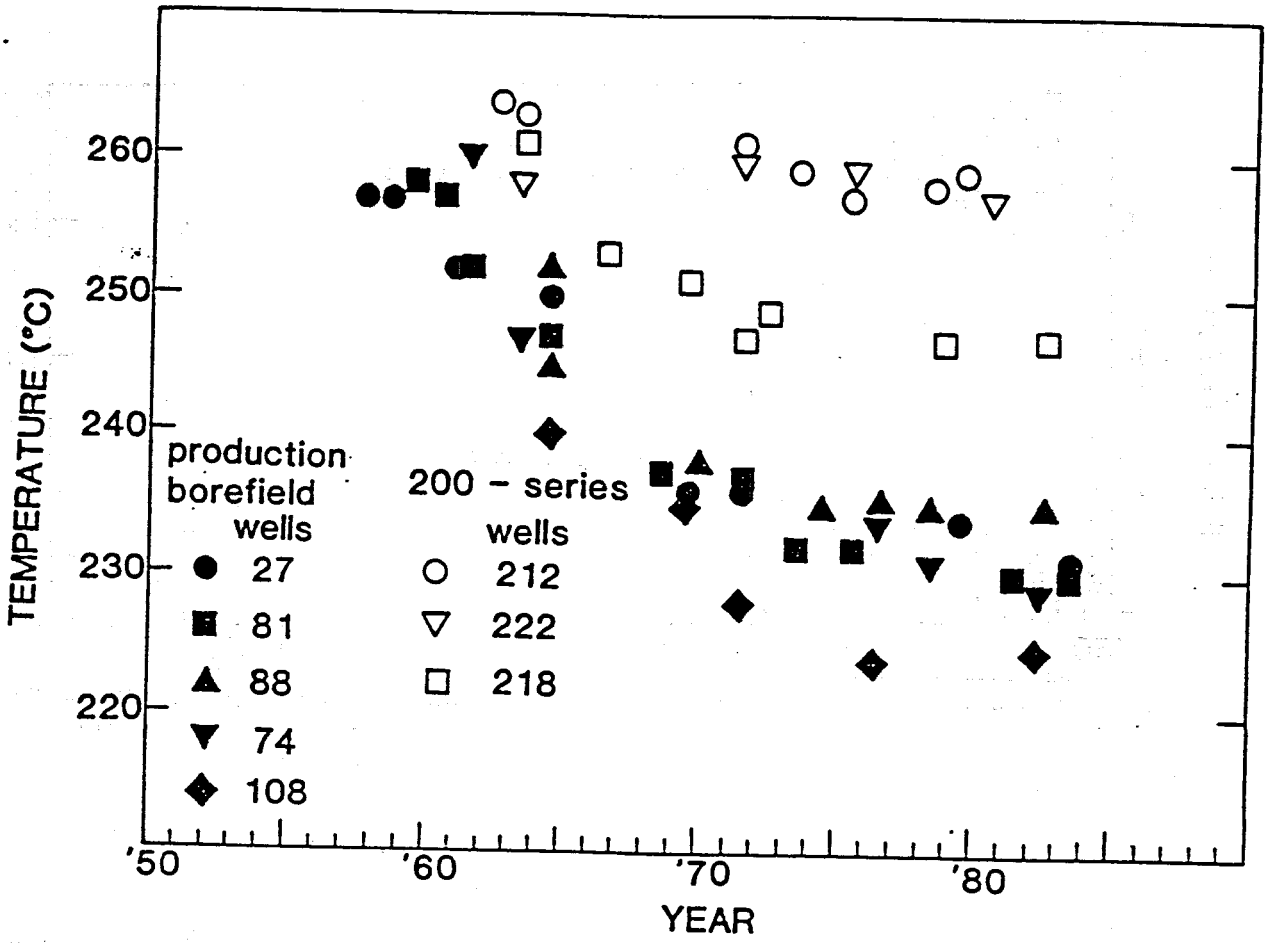

Chemical trends

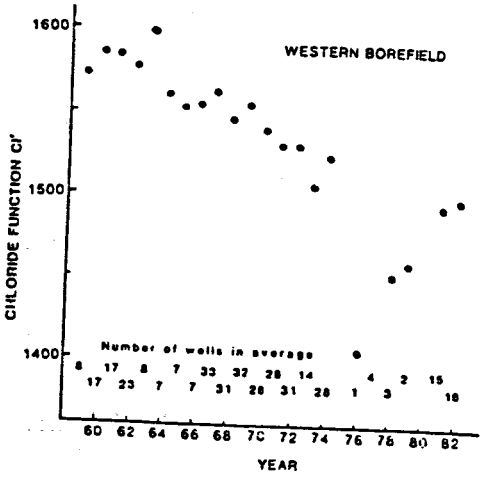

Figure 7. Flow weighted average Cl' Western Borefield.

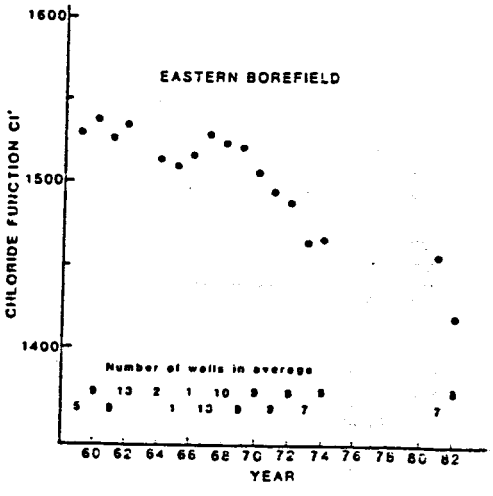

Figure 8: Flow weighted average Cl' Eastern Borefield.

Figs 7, 8, from Brown et al., 1988 "Dilution and Boiling in the Wairakei field due to exploitation, 1959-1982." in Geothermal Workshop Proc. 1988, p. 257-262.

WAIRAKEI FIELD

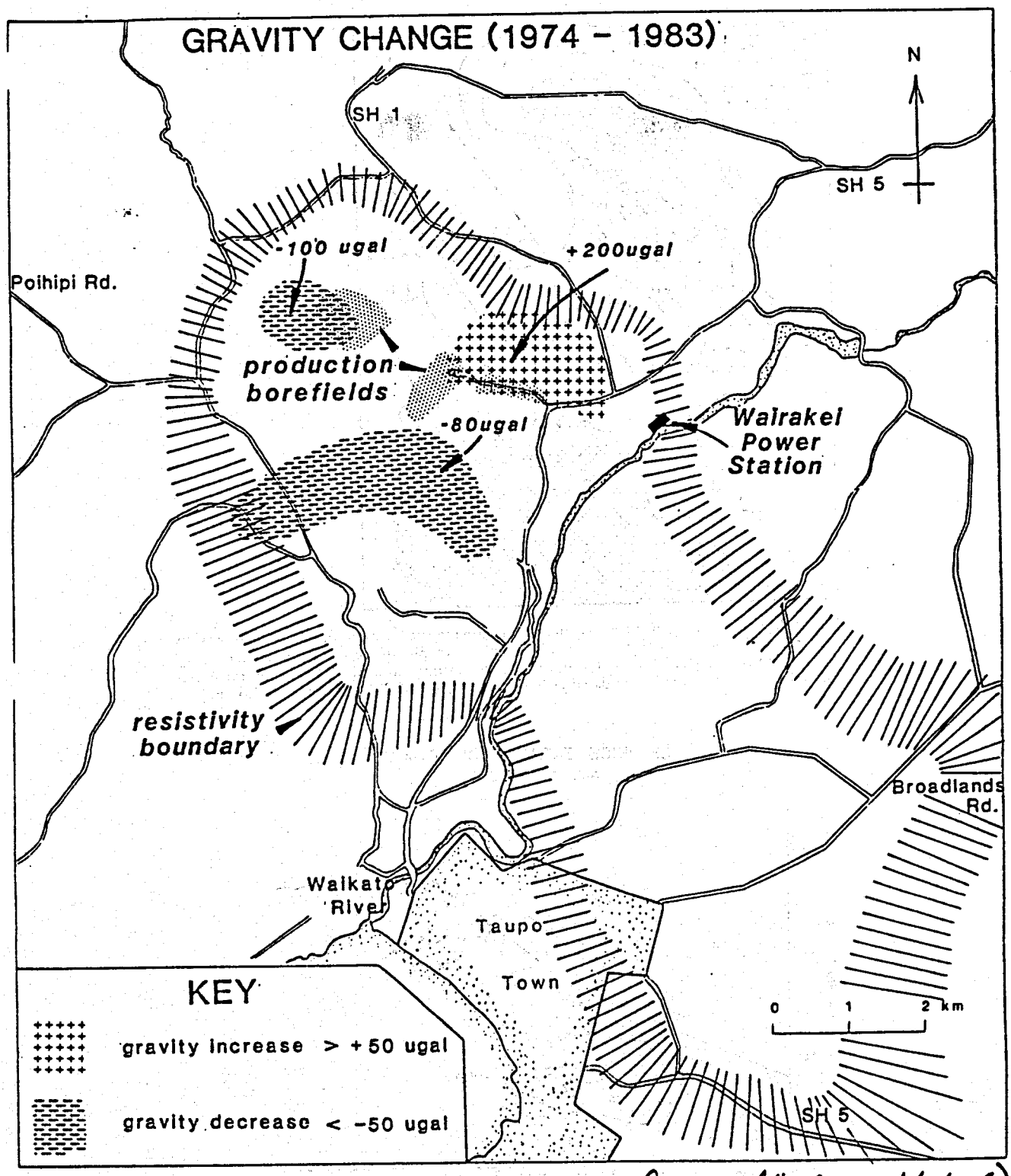

from Allis (unpublished)

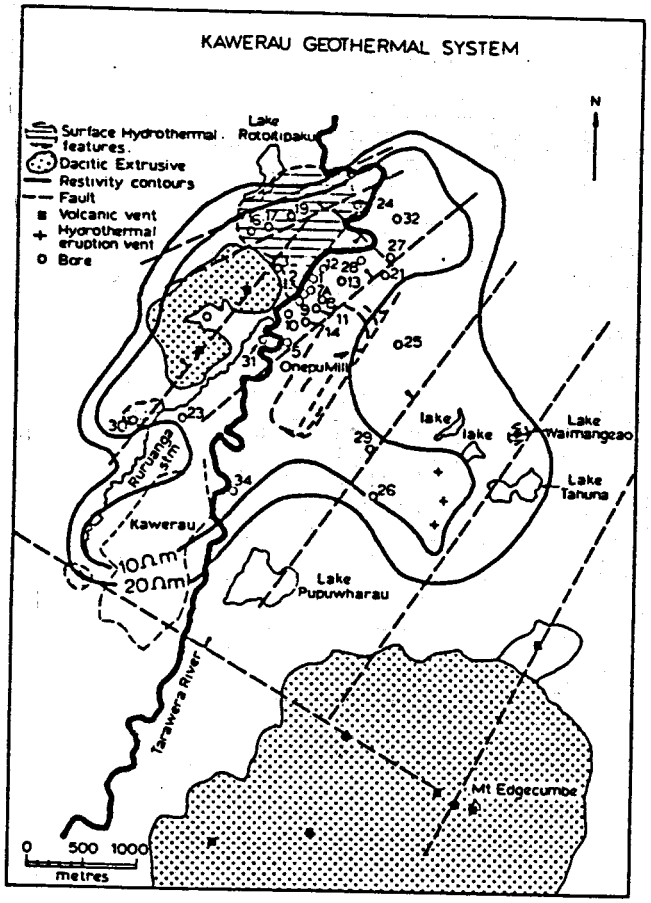

Figure 8.1: Sketch map of the Kawerau system showing the locations of 28 production wells and areas of surface hydrothermal activity. The physiography of the area is dominated by the 822 m high Mt Edgecumbe, located south of the resistivity anomaly. The dacitic extrusives located within the anomaly are dated at less than 200,000 yrs B.P. (Nairn, pers. comm.).

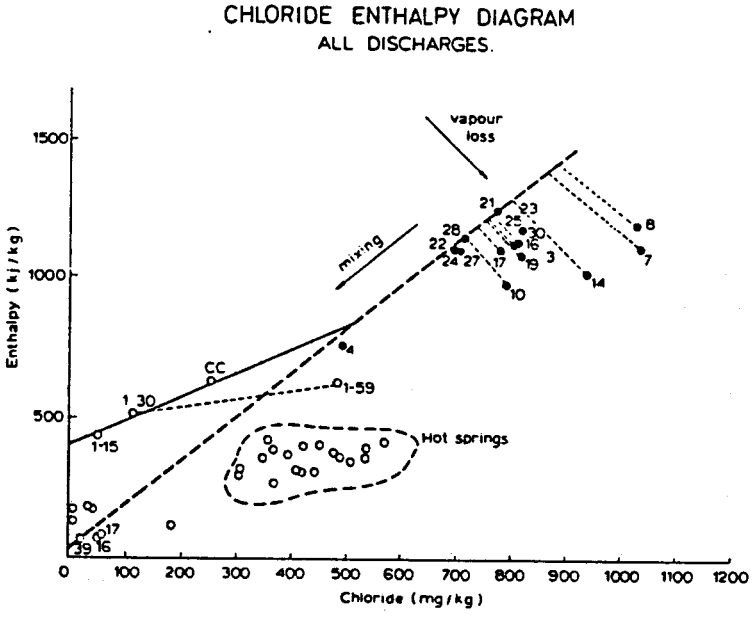

Figure 8.2: Enthalpy-chloride diagram for fluids in the Kawerau system. Enclosed circles represent deep, initial discharge fluids; samples with m or s labels are spring discharges; samples 16 and 17 are Tarawera River waters and all others are shallow well discharges. The least mixed deep fluid (from well KA8), extrapolates back to its pre-boiling composition on the deep system mixing line at about 310 °C and 870 mg/kg Cl.

Figures from Christenson, B.W. "Kawerau Geothermal Field" in Guide to Active Epithermal systems and Precious Metal Deposits of N.Z. Monograph Series on Mineral Deposits No 26. 93-106 Gebruder-Borntraeger.

the static water levels are around 800 m (at Wairakei it is 250 m) below the surface so filling the well but maintaining zero wellhead pressure causes an 80 bar over pressure at depth at Southern Negros (25 bars at Wairakei). In some cases a critical overpressure may have to be exceeded to induce seismicity. In the case of Denver earthquakes this was 120 bars (Healy et al., 1968). A similar behaviour appeared to occur at Cesano field, Italy. Where this is the case, it is prudent to operate reinjection wells below the critical overpressure.

Many of the studies discussed above indicate induced events at distances of several km from the injection well. In such cases it may not be the excess pore pressure that is triggering the distant events. Possibly the release of stress on one part of a critically stressed fracture will be sufficient to trigger events on more distant parts of the fracture. The vertical propagation of seismicity at both The Geysers and the Cornwall injection sites are examples of this phenomenon.

In steam-dominated reservoirs the situation is more complicated, because the injected water may disperse downwards through the reservoir without increasing pore pressure (in fact initial condensation of steam may decrease pore pressure). However if the permeability is low around the injection depth, liquid pressure may increase locally. Alternatively if the injected water drains to a deeper, liquid-dominated zone, the pore pressure may increase there and trigger seismicity. This may be the cause of the induced seismicity at Larderello. At The Geysers, the induced seismicity is not obviously caused by the reinjection of condensate.

In general it appears that production of geothermal fluids (as opposed to reinjection) does not cause induced seismicity. The reason for this is that the pore pressure declines with fluid extraction, and therefore the reservoir rock should actually increase in strength with production. The Geysers reservoir is an obvious exception - possibly its location on a transform plate boundary, and a higher level of stress (and strain) make it more sensitive to physical changes in the reservoir. Since the induced seismicity at Southern Negros may also be related to production (as well as injection), this cause of induced seismicity cannot be excluded.

GRC Workshop on
Responses of a Geothermal Field During Exploitation

Outline of

Physical Processes and Changes

Gudmundur S. Bodvarsson

1.0 Introduction

2.0 Physical Processes

- 2.1 Mass flow (single and two-phase)
- 2.2 Conductive heat transfer
- 2.3 Convective heat transfer
- 2.4 Boiling/condensation
- 2.5 Stress changes (subsidence)

3.0 Rock Properties

- 3.1 Matrix porosity
- 3.2 Fracture porosity
- 3.3 Rock density
- 3.4 Heat capacity
- 3.5 Matrix permeability
- 3.6 Fracture permeability
- 3.7 Relative permeability
- 3.8 Thermal conductivity

4.0 Fluid Properties (steam and water)

- 4.1 Density
- 4.2 Viscosity
- 4.3 Compressibility
- 4.4 Expansivity
- 4.5 Enthalpy
- 4.6 Two-phase mixtures

5.0 Energy Content

- 5.1 Fluid
- 5.2 Rock
- 5.3 Well outputs
- 5.4 Plant requirements

6.0 Well data

- 6.1 Lithologic data
- 6.2 Lost circulation zones
- 6.3 Completion test data
- 6.4 Static temperature and pressure profiles
- 6.5 Flow test data (flowrates and enthalpies)
- 6.6 Pressure transient test data

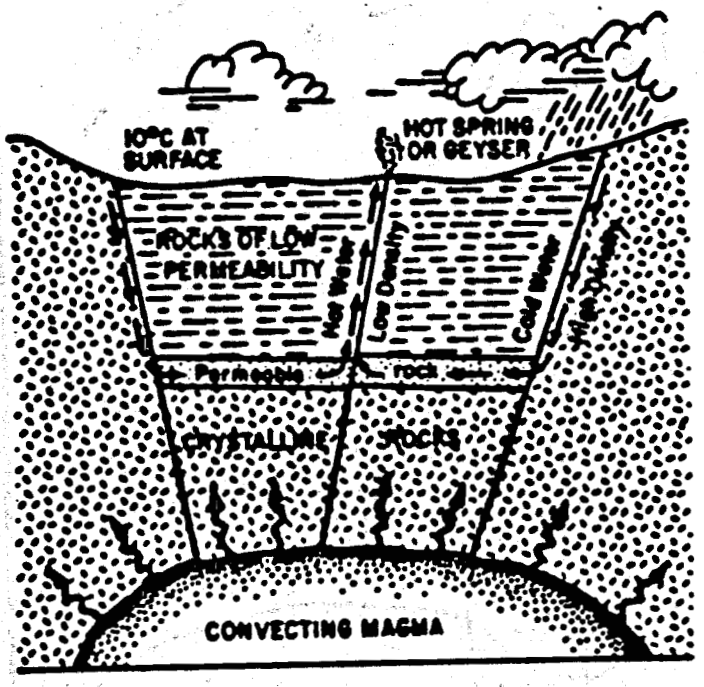

Figure 2. Conceptual reservoir model (after White, 1973).

[XBL 8111-4842]

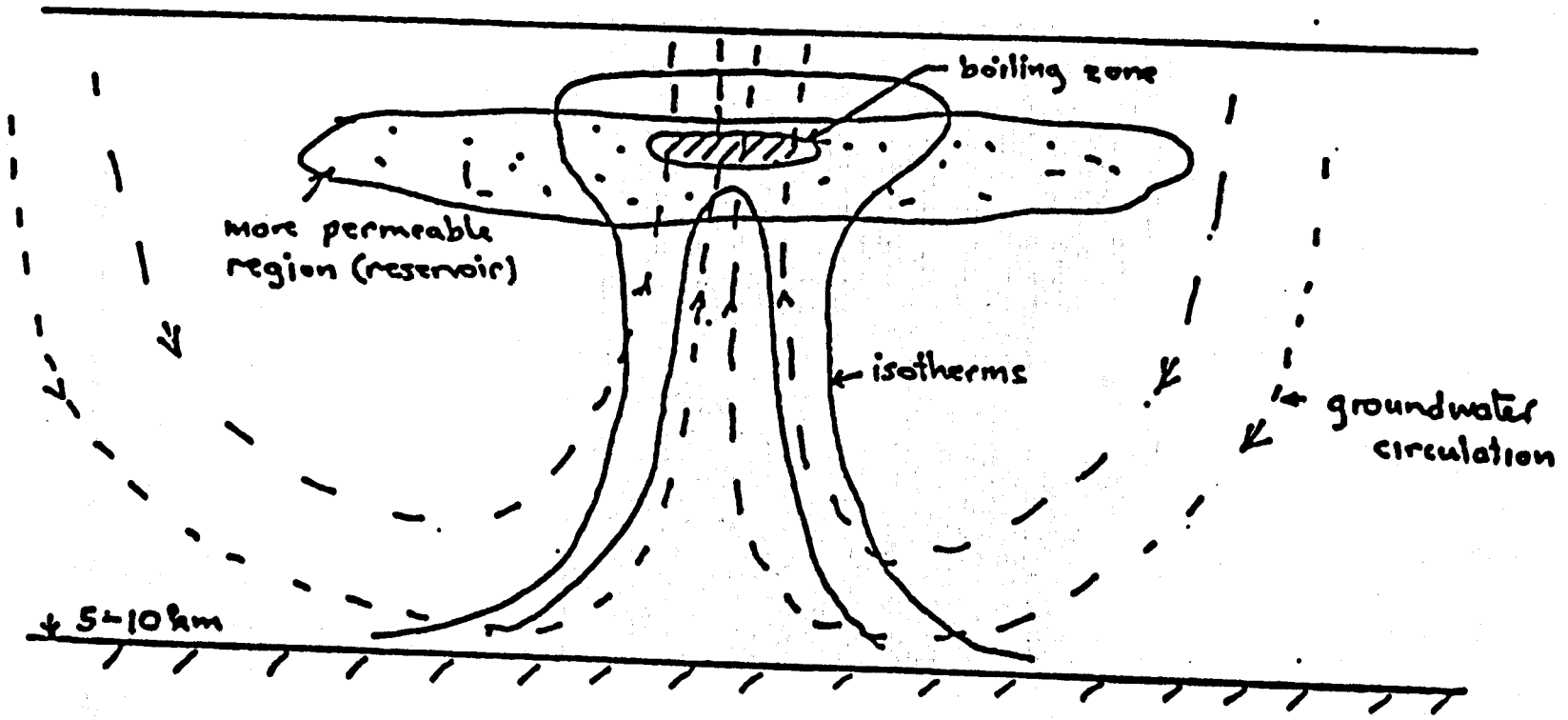

Figure 1.1.1. A hydrothermal system (Wairakei-type).

GEOTHERMAL SYSTEMS

ROCK TYPE	VOLCANIC
PERMEABILITY	FRACTURE DOMINATED
RESERVOIRS	VERY THICK (~KM)
RECOVER	HEAT (NOT FLUID)
TEMPERATURES	150° - 400°C
FLUIDS	WATER WITH DISSOLVED SOLIDS AND GASES
BASIC PROBLEM	MINE HEAT FROM ROCK

Main Processes
Occurring in the Reservoir

- Mass Flow (Liquid, Steam, Dissolved Solids, Non-Condensible Gases)
- Heat Flow (Conduction/Convection)
- Phase Changes (Boiling/Condensation)
- Stress Changes
- Mixing of Fluids
- Fluid/Fluid and Rock/Fluid Interactions

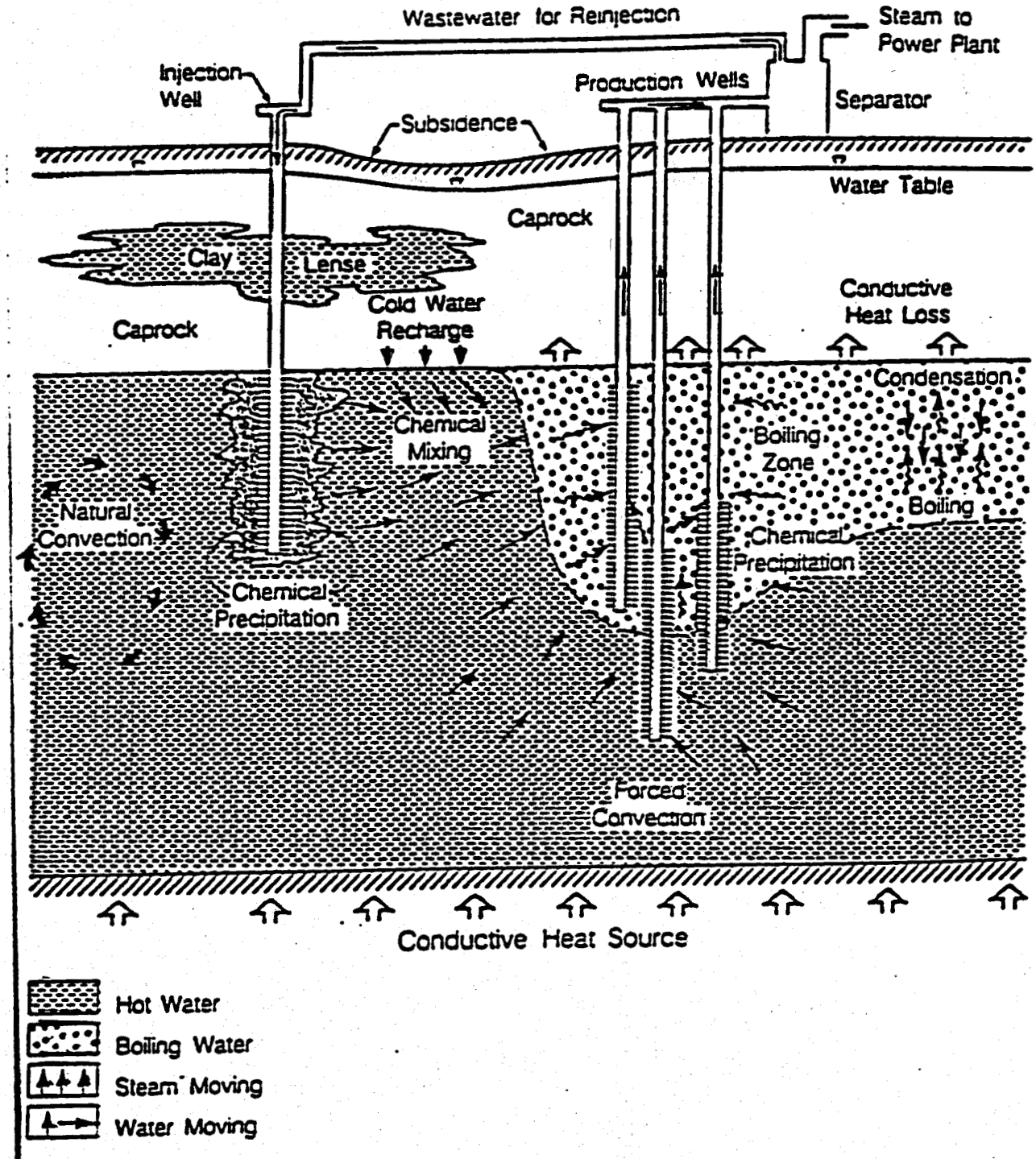

Figure 4. A schematic of different physical processes occuring in geothermal systems.

MASS FLOW

- DRIVING FORCE IS PRESSURE

$$q_m = \frac{k k_{r\ell}}{\mu_\ell} \rho_\ell A[\nabla P - \rho_\ell g] + \frac{k k_{rv}}{\mu_v} \rho_v A[\nabla P - \rho_v g]$$

- $k_{r\ell}$, k_{rv} ARE RELATIVE PERMEABILITY PARAMETERS.

HEAT FLOW

- CONDUCTIVE (DIFFUSIVE HEAT FLUX)

$$q_h = \lambda A \nabla T$$

λ : THERMAL CONDUCTIVITY

- CONVECTION (HEAT TRANSPORTED BY FLUID)

$$q_h = q_m h_f = q_{fe} h_e + q_v h_v$$

h_f : ENTHALPY (Flowing)

PHASE CHANGES

- BOILING AND CONDENSATION VERY IMPORTANT BECAUSE OF LARGE DIFFERENCE IN ENTHALPIES OF LIQUID AND VAPOR

- $h_\ell \sim 1\text{–}1.4$ MJ/kg, $h_v \sim 2.8$ MJ/kg $\Big\}$ $L \sim 1.6$ MJ/kg

- ENERGY EXCHANGE WITH ROCK

HEAT PIPES

- Counterflow of liquid and steam

$$q_l = -q_v$$

- Primary heat transfer mechanism in two-phase systems
- For a given heat flux, Q_n, have two solutions

a. $\frac{dP}{dZ} \approx -\rho_l g;\ k_{rl} \approx 1,\ k_{rv} \approx 0$

liquid-dominated

b. $\frac{dP}{dZ} \approx -\rho_l g;\ k_{rl} \approx 1,\ k_{rv} \approx 0$

vapor-dominated

ROCK-FLUID INTERACTIONS (EXAMPLES)

- DISSOLUTION/PRECIPITATION OF MINERALS
- MIXING OF FLUIDS OF DIFFERENT CHEMICAL COMPOSITION
- CLAY SWELLING

SUBSIDENCE

- EXPLOITATION CAUSES PRESSURE DECLINE AND CHANGES IN EFFECTIVE STRESS

$$\sigma_e = \sigma_t - P$$

- INFLATION AND DEFLATION OF MAGMA TRAPS

POROSITY

Matrix Porosity:

- controls reserves!
- 10-30% in sedimentary rocks (e.g., Cerro Prieto)
- 5-15% volcanic rocks (Los Azufres, Nesjavellir)
- 1-2% granitic rocks (Palinpinon)

Fracture Porosity:

- 0.1-3% (Weber and Bakker, 1981)

PERMEABILITY

Matrix Permeability:

- controls flow rate declines (and enthalpies)
- ~ mdarcies for sedimentary rocks
- ~ μdarcies for volcanic rocks
- < μdarcies granitic rocks

Fracture Permeability:

- controls initial flow rates
- 1-5 Dm for two-phase liquid dominated systems
- 10-50 Dm for "hot" single-phase system
- >30 Dm for "warm" liquid system

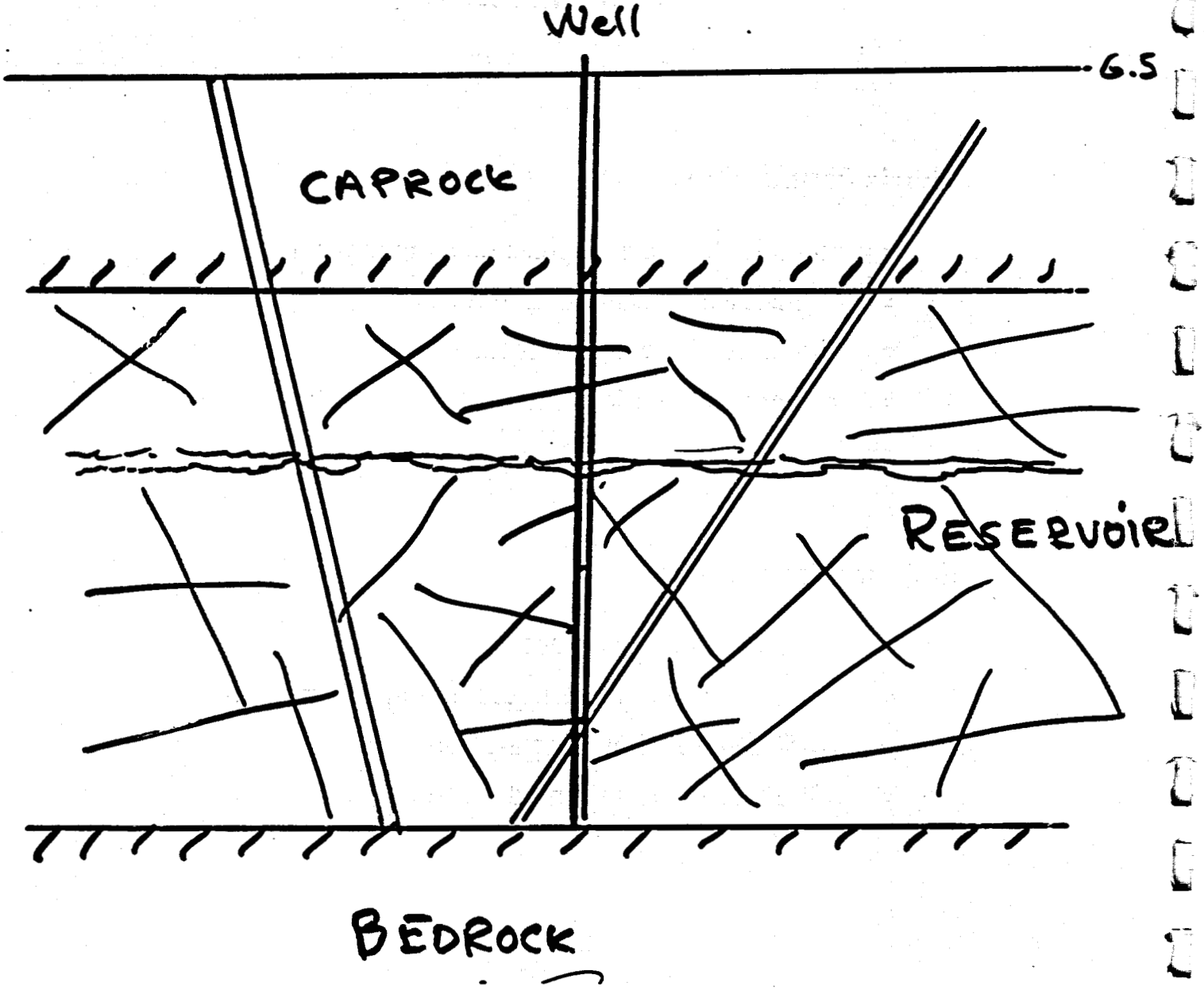
Well
6.5
CAPROCK
RESERVOIR
BEDROCK

RELATIVE PERMEABILITY

- currently unknown for geothermal reservoirs
- probably vary from field to field
- generally assume $k_{rl} + k_{rv} = 1$ for all saturations

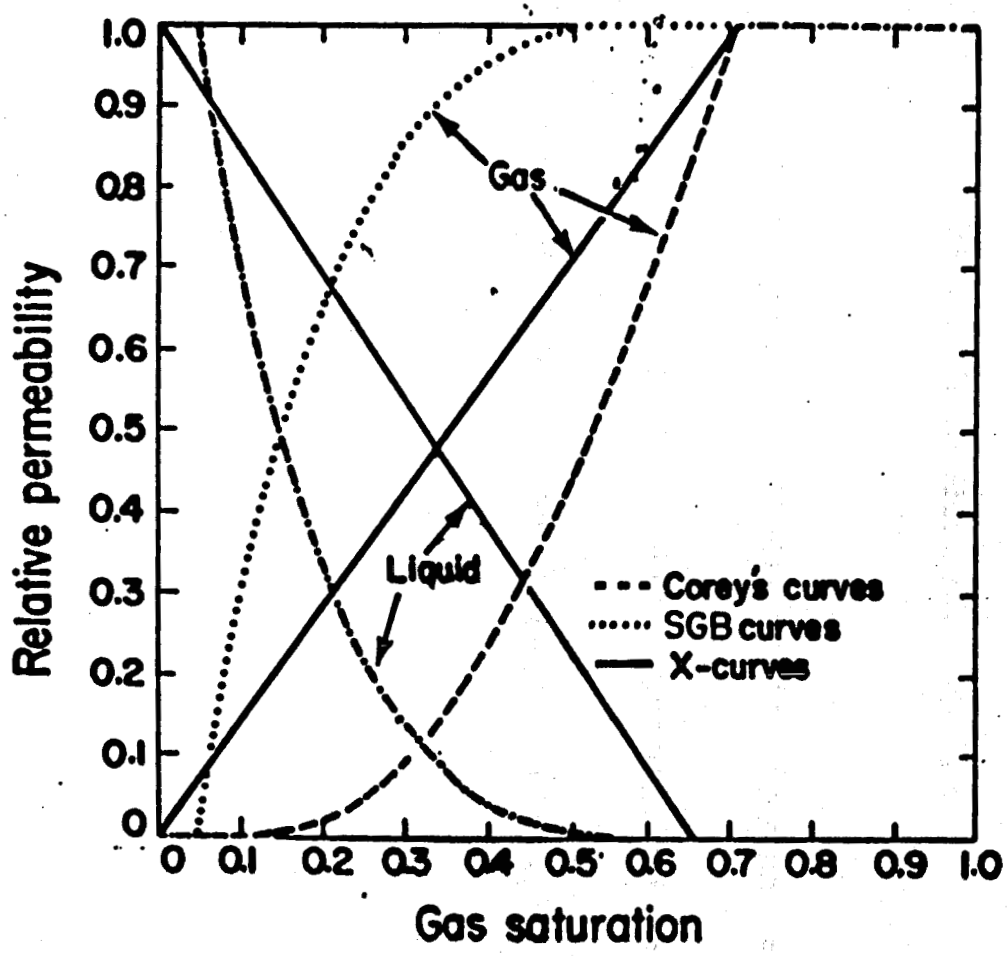
Relative permeability
1.0
0.9
0.8
0.7
0.6
0.5
0.4
0.3
0.2
0.1
0
0 0.1 0.2 0.3 0.4 0.5 0.6 0.7 0.8 0.9 1.0
Gas saturation
Gas
Liquid
Corey's curves
SGB curves
X-curves

XBL837-1901

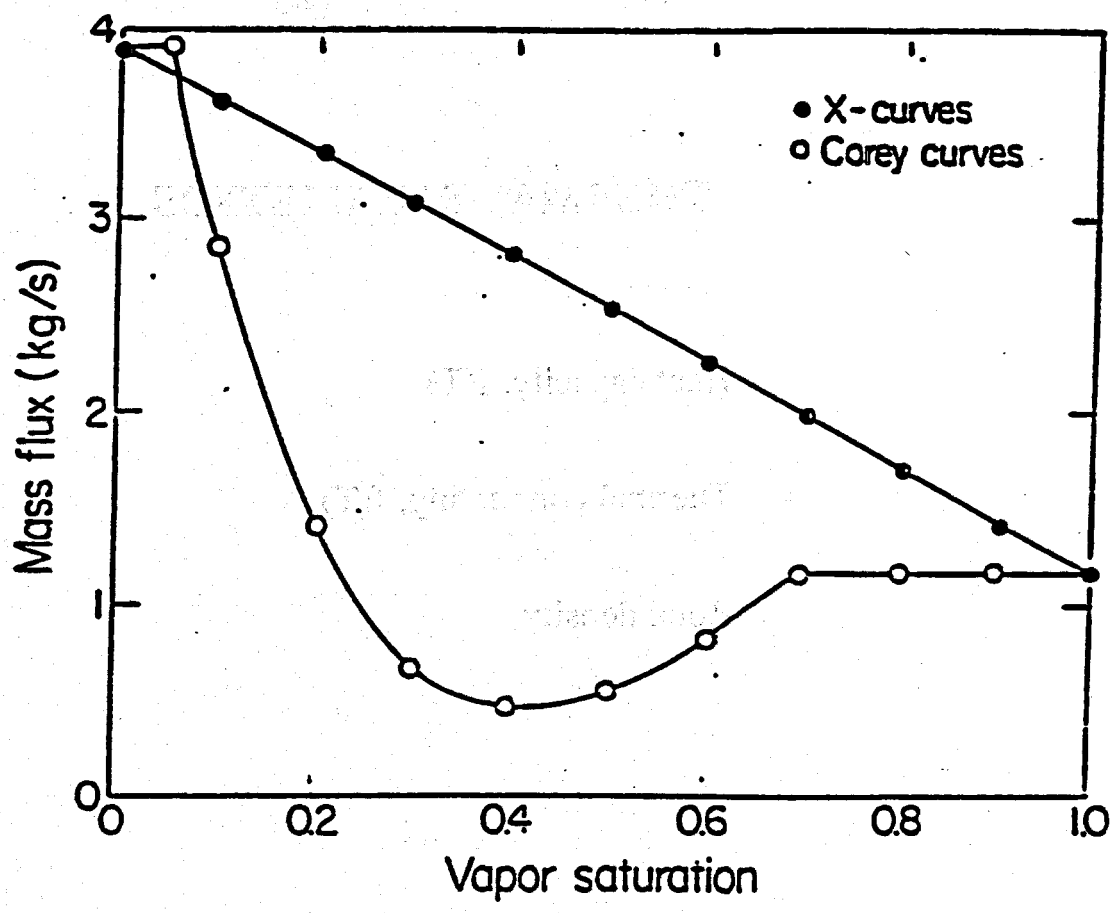

XBL 832-1211A

Figure 3. Mass flux in dependence of vapor saturation for Corey and linear relative permeability curves.

THERMAL PARAMETERS

- Heat capacity, f(T)
- Thermal conducting, f(T)
- Rock density

EXAMPLE

Nesjavellir, Iceland

- Porosity: 8-15%, $\phi_{tot} = \phi_{eff}$
- Gas permeability: 1-100 μD
  Liquid permeability: 1-10 μD
- Pore size: 80% 0.01-0.05 μm
- Fluid recovery: Centrifugal test showed 25% recovery for ΔP of 50 bars (750 psi) at T = 25°C. Correcting for temperature effects of surface tension yields ~75% recovery.

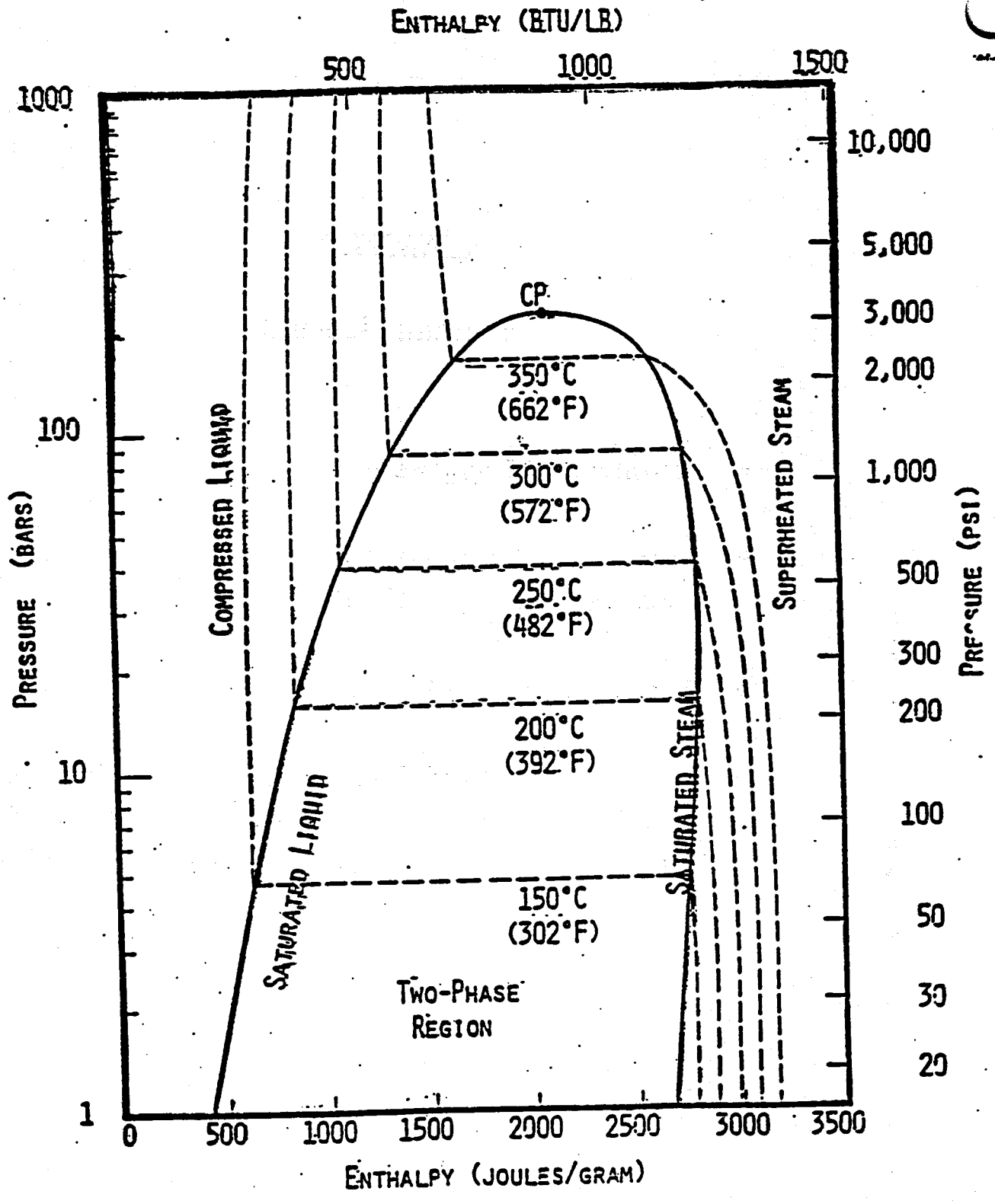
ENTHALPY (BTU/LB)
500
1000
1500
1000
100
10
1
PRESSURE (BARS)
10,000
5,000
3,000
2,000
1,000
500
300
200
100
50
30
20
PRESSURE (PSI)
CP
350°C
(662°F)
300°C
(572°F)
250°C
(482°F)
200°C
(392°F)
150°C
(302°F)
COMPRESSED LIQUID
SATURATED LIQUID
SATURATED STEAM
SUPERHEATED STEAM
TWO-PHASE
REGION
0
500
1000
1500
2000
2500
3000
3500
ENTHALPY (JOULES/GRAM)

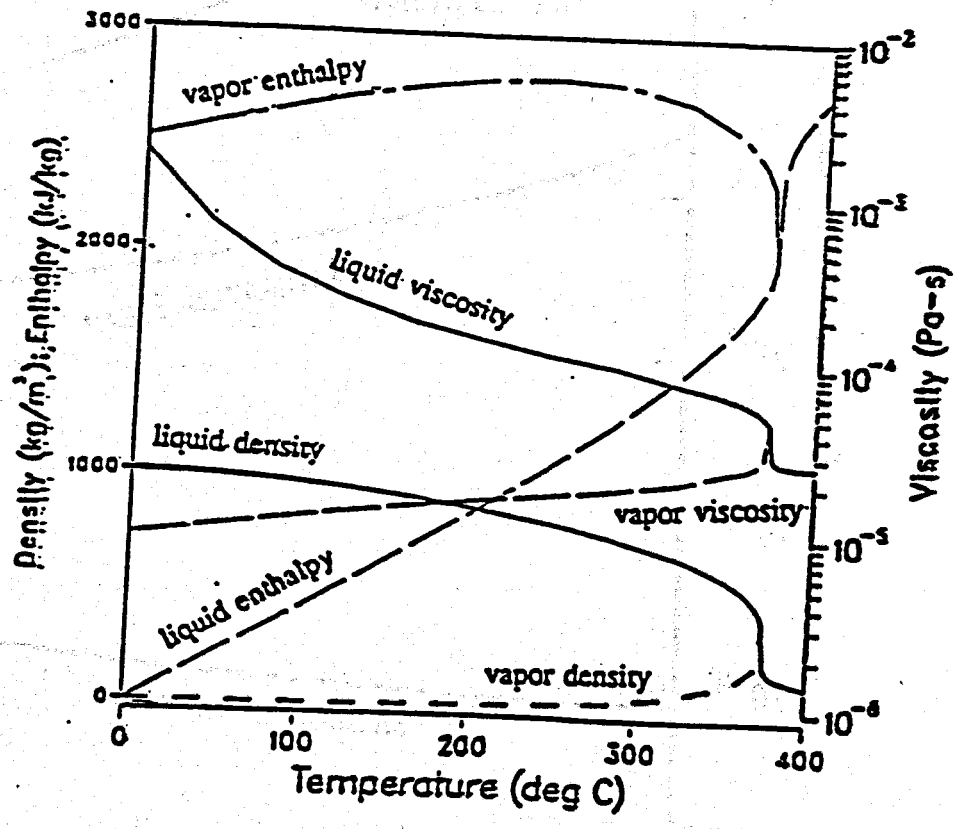

Figure 2. Density, viscosity and enthalpy of water and vapor as a function of temperature.

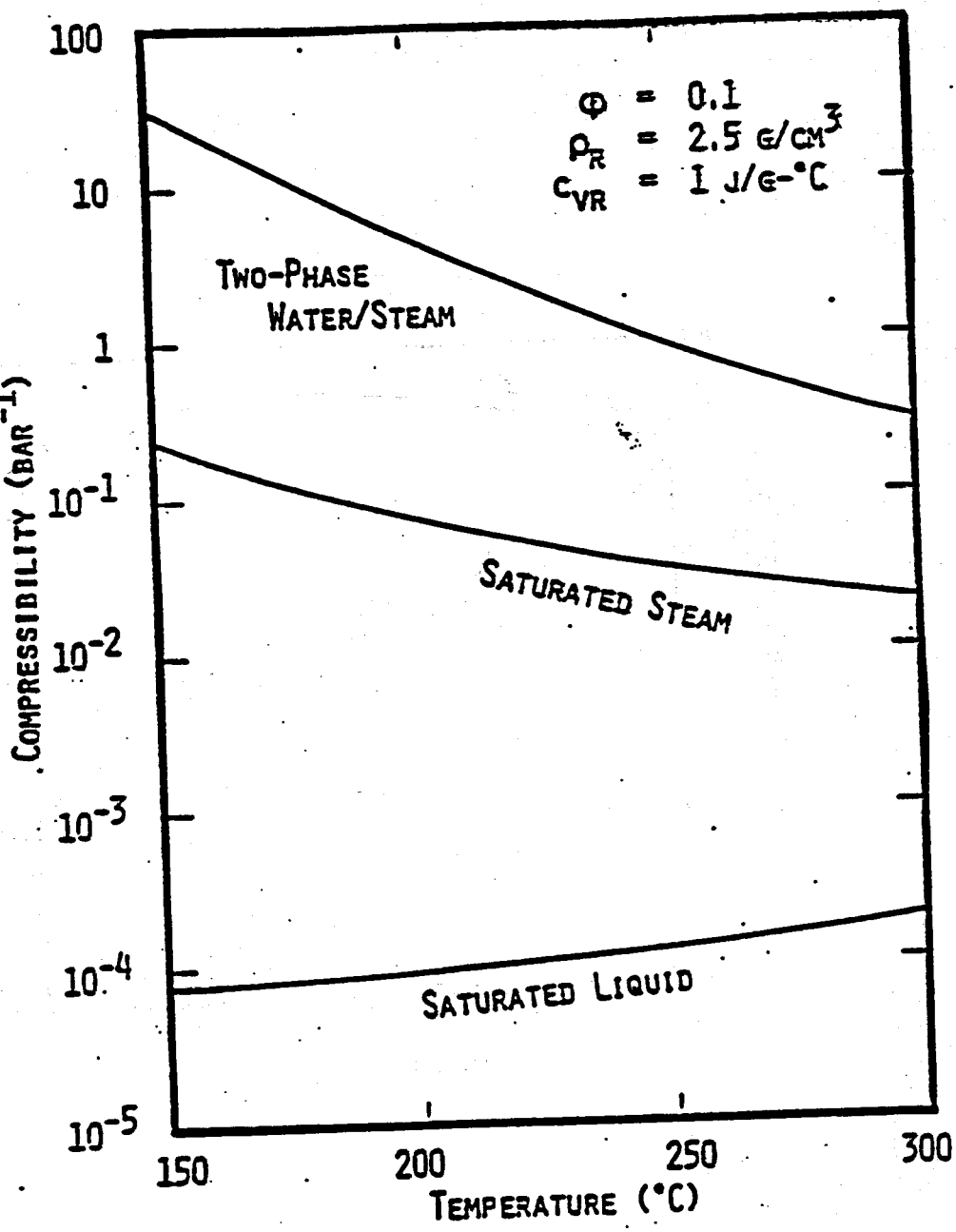
100
10
1
10^{-1}
10^{-2}
10^{-3}
10^{-4}
10^{-5}
COMPRESSIBILITY (BAR^{-1})
Φ = 0.1
ρ_R = 2.5 G/CM^3
c_{VR} = 1 J/G-°C
TWO-PHASE WATER/STEAM
SATURATED STEAM
SATURATED LIQUID
150
200
250
300
TEMPERATURE (°C)

FLUID PROPERTIES

Water Viscosity: $\mu_l = [2.414 \times 10^{-5}]\, 10^{\left[\frac{247.8}{T+133.15}\right]}$

Water Enthalpy: $h_l \approx T(°C) * C_p$

where $C_p \approx 4185$ J/kg · °C

Compressibility: $\beta = -\left[\frac{1}{\rho}\frac{d\rho}{dP}\right]_T$

Expansivity: $\varepsilon = -\left[\frac{1}{\rho}\frac{d\rho}{dT}\right]_P$

Clausius - Clapeyron Equation

$$\frac{dP_s}{dT} = \frac{\rho_w \rho_v}{\rho_w - \rho_v} \frac{L}{(T+273.15)}$$

Vapor Compressibility: $\beta_v \approx \frac{1}{P}$

Two-phase Compressibility

$$\beta_{2\phi} = \frac{\rho c}{\phi}\left[1.92 \times 10^{-5}\, p^{-1.66}\right]$$

P in bars, $\beta_{2\phi}$ in bar^{-1}, $[\rho c]$ in $J/m^3 \cdot °C$

2-PHASE MIXTURES

Saturation: $S_l + S_v = 1$

Density:
$$\begin{cases} \rho_m = \rho_l S_l + \rho_v S_v & \underline{\text{in–place}} \\ \rho_1 = \dfrac{\rho_l q_l + \rho_v q_v}{q_l + q_v} & \underline{\text{flowing}} \end{cases}$$

Enthalpy:
$$\begin{cases} h_m = \dfrac{\rho_l S_l h_l + \rho_v S_v h_v}{\rho_m} & \underline{\text{in–place}} \\ h_f = \dfrac{q_l h_l + q_v h_v}{q_l + q_v} & \underline{\text{flowing}} \end{cases}$$

ENERGY CONTENT

$T = 300°C \quad \phi = 10\%$

Liquid-dominated

Fluid: 10%
Rock: 90%

Vapor only

Fluid: 1%
Rock: 99%

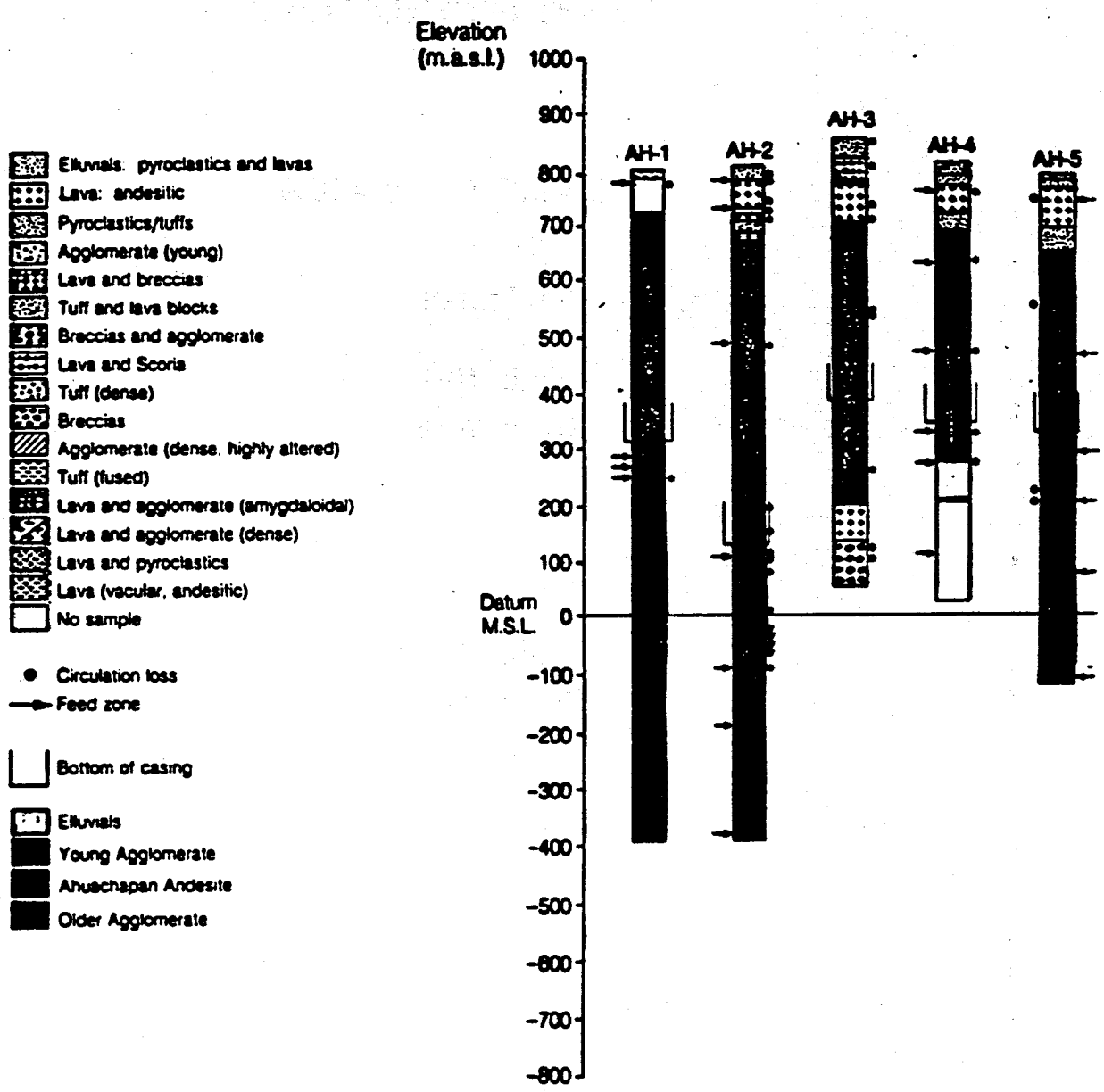

Figure 4.10a Ahuachapan well lithology

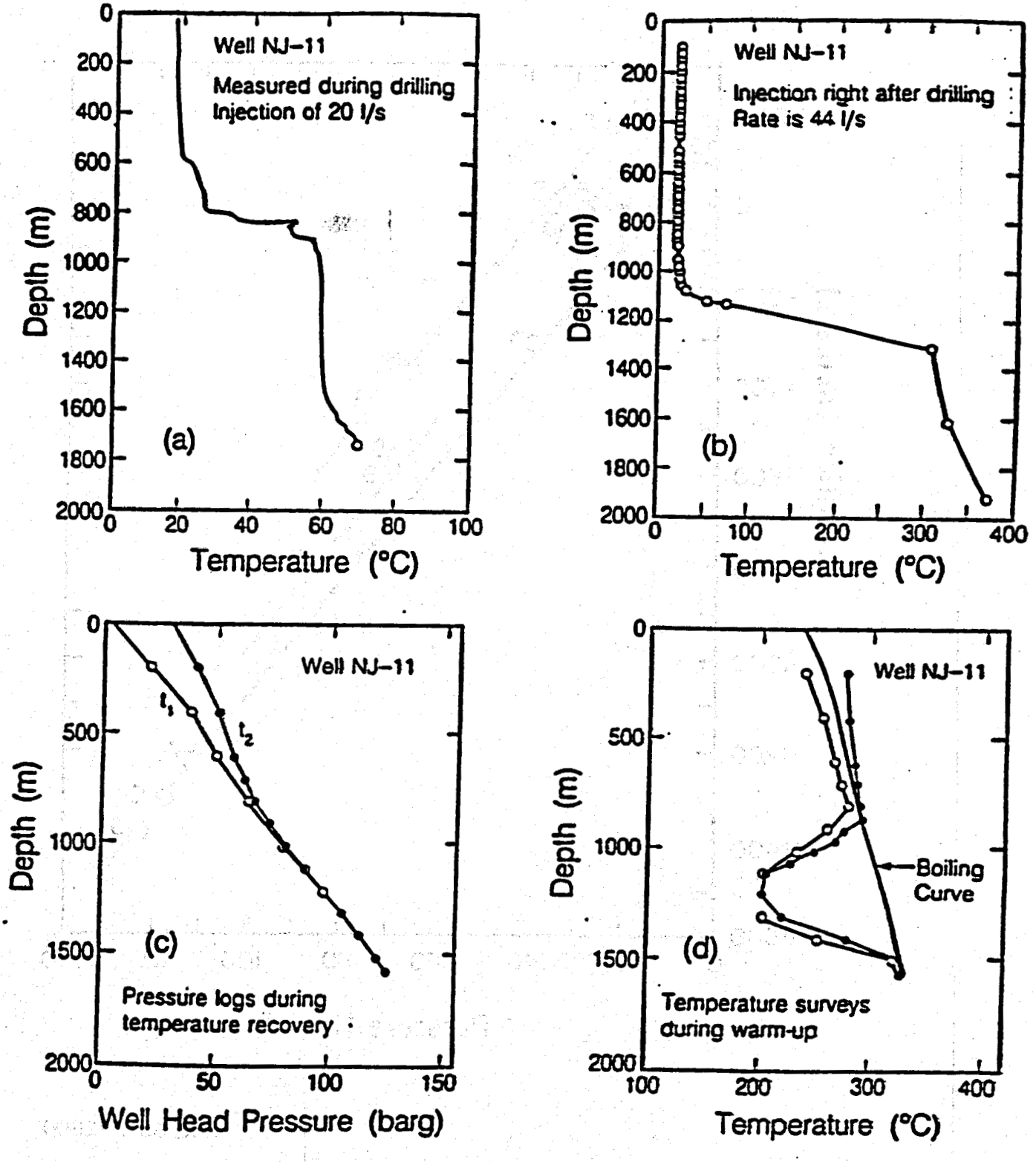

Figure 6. Temperature and pressure surveys during injection and warm-up for well NJ-11 at Nesjavellir, Iceland (B. Steingrimsson, written communications, 1988).

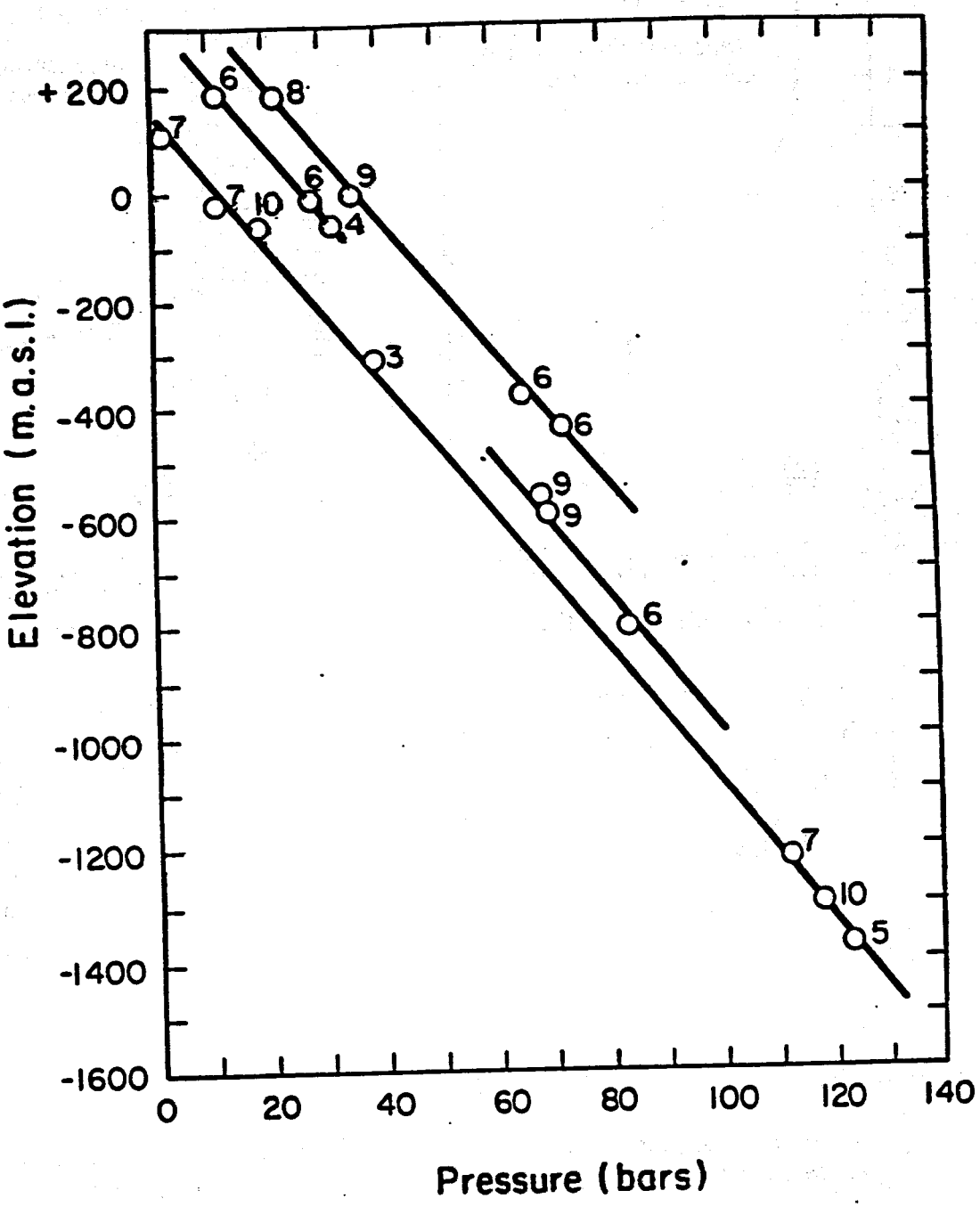

XBL 8511-12604

Figure 6. Pressures at feed zones in some of the wells (after Stefansson, 1985).

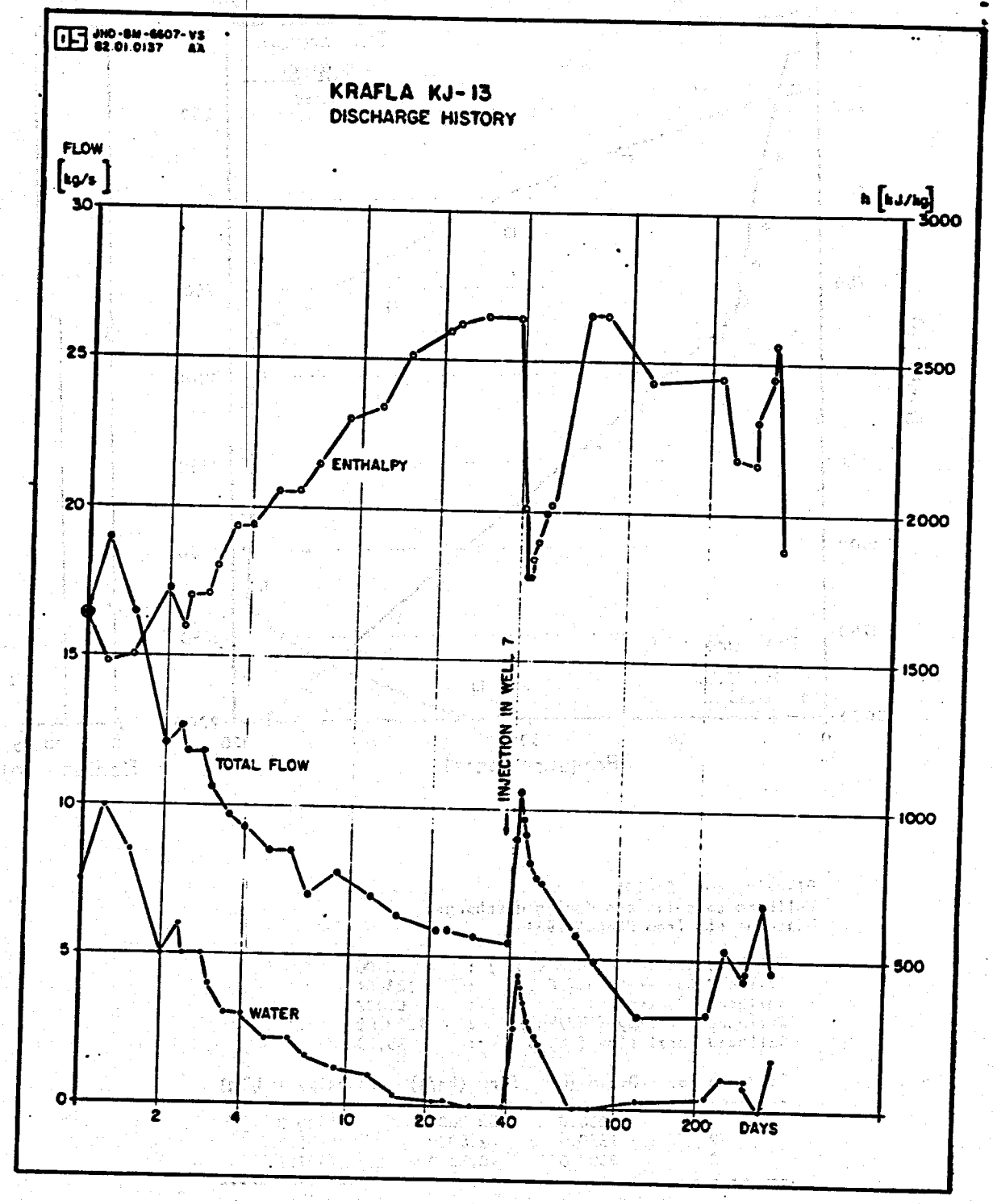
JHD-SM-6607-VS
82.01.0137 AA
KRAFLA KJ-13
DISCHARGE HISTORY
FLOW
[kg/s]
h [kJ/kg]
30
25
20
15
10
5
0
3000
2500
2000
1500
1000
500
ENTHALPY
TOTAL FLOW
WATER
INJECTION IN WELL 7
2
4
10
20
40
100
200
DAYS

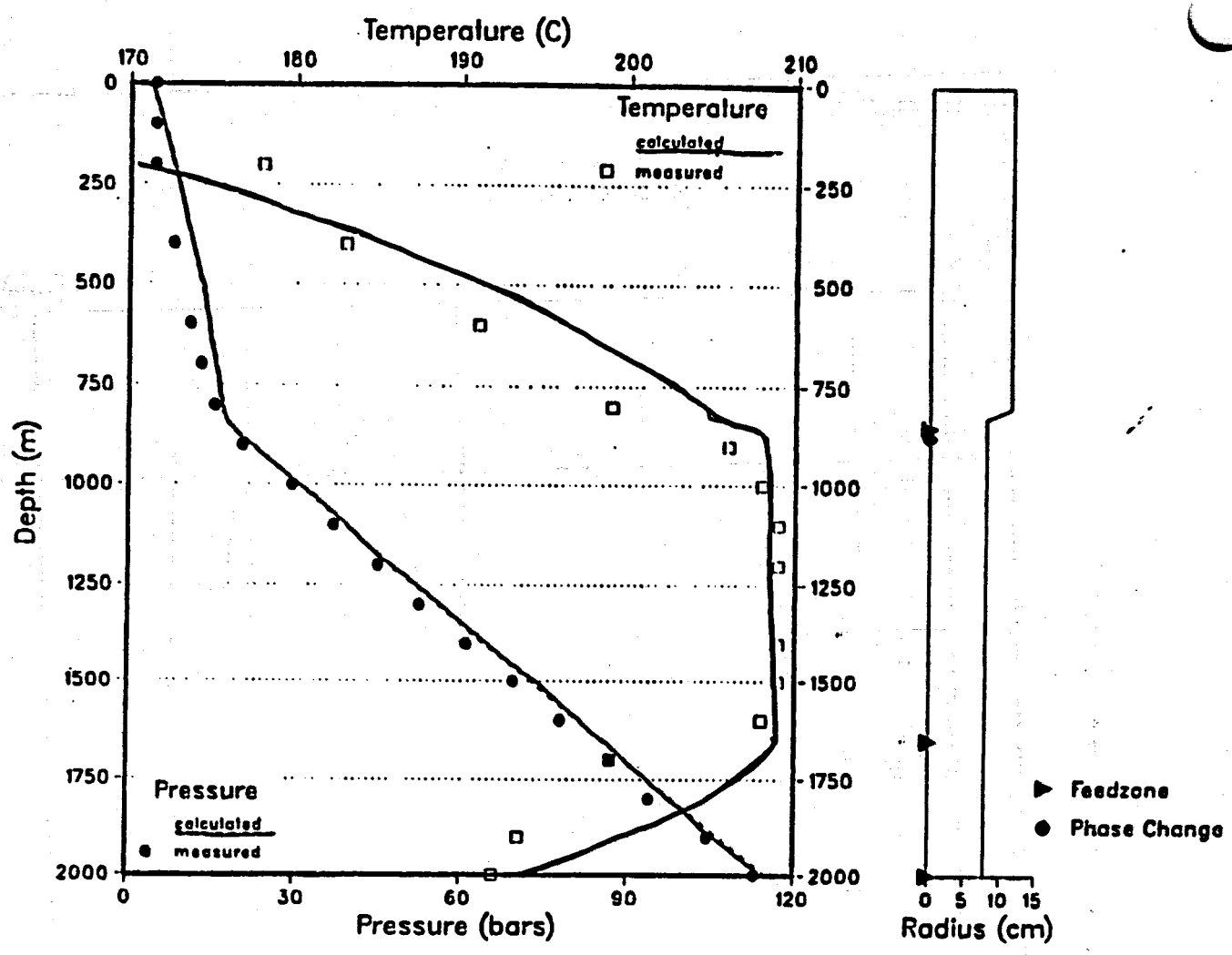

Olkaria, well OW-201
Wellbore calculations during discharge
Measurements from 22-oct-1984

Wellhead pressure (bar abs.)	:	3.00
Wellhead temperature (C)	:	133.54
Wellhead dryness	:	0.332
Wellhead enthalpy (kJ/kg)	:	1280.00
Wellhead total flow (kg/s)	:	35.50

Feedzone no:	Depth (m)	Flow (kg/s)	Enthalpy (kJ/kg)
1	850.0	33.0000	1330.0
2	1650.0	2.8000	901.6
3	2000.0	-0.3000	827.7

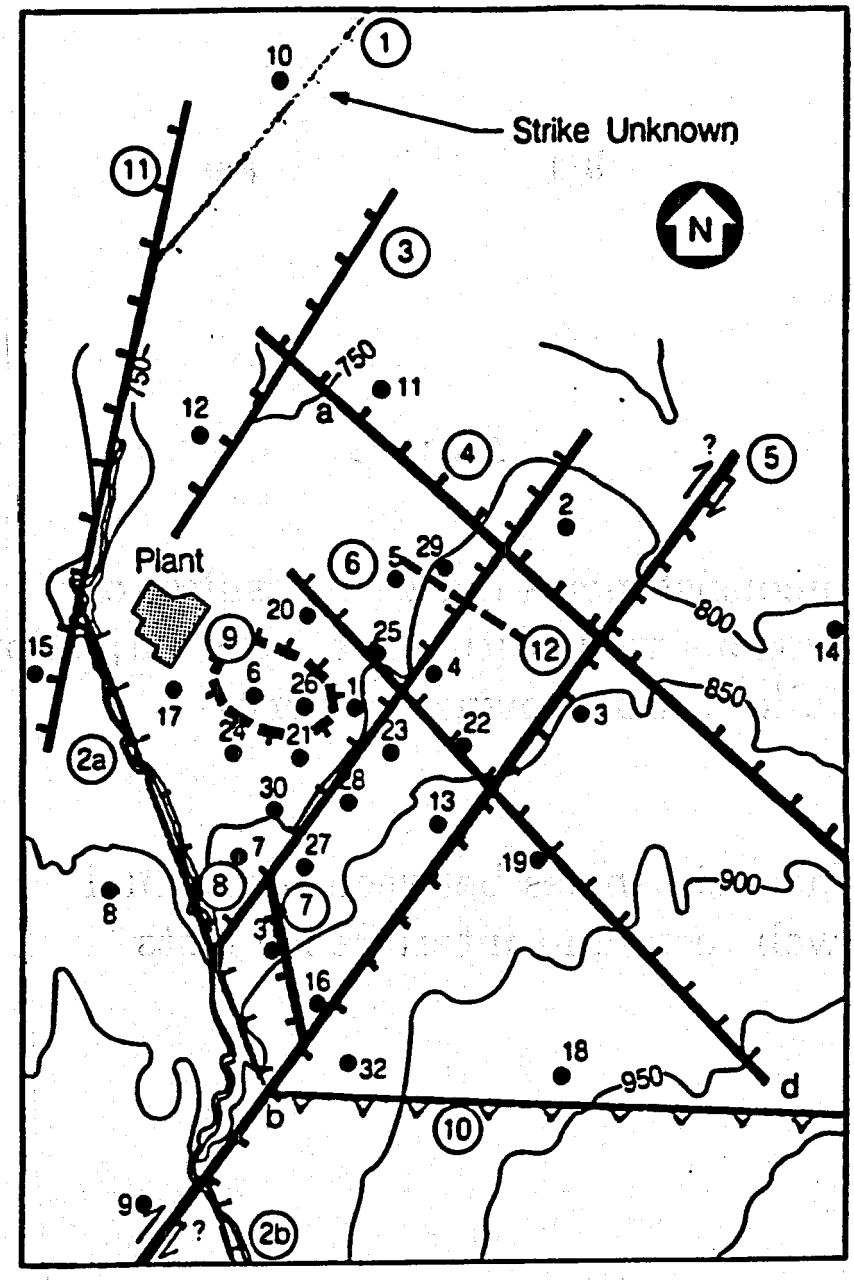

Normal Faults	Vertical Displacement	
	< 100 m	Hatches on Downthrown Side
	100-200 m	
	> 200 m	
	High Angle Reverse Fault	Sawteeth on Upthrown Block
	Right Lateral Strike-slip	

5 ● Well 5

(5) Fault No. 5

Figure 4.13 Map showing the location of the faults

Issues

- Inconsistencies between results for various well testing methods (injection, falloff, drawdown, recovery)

- Inconsistencies between individual well tests and interference tests

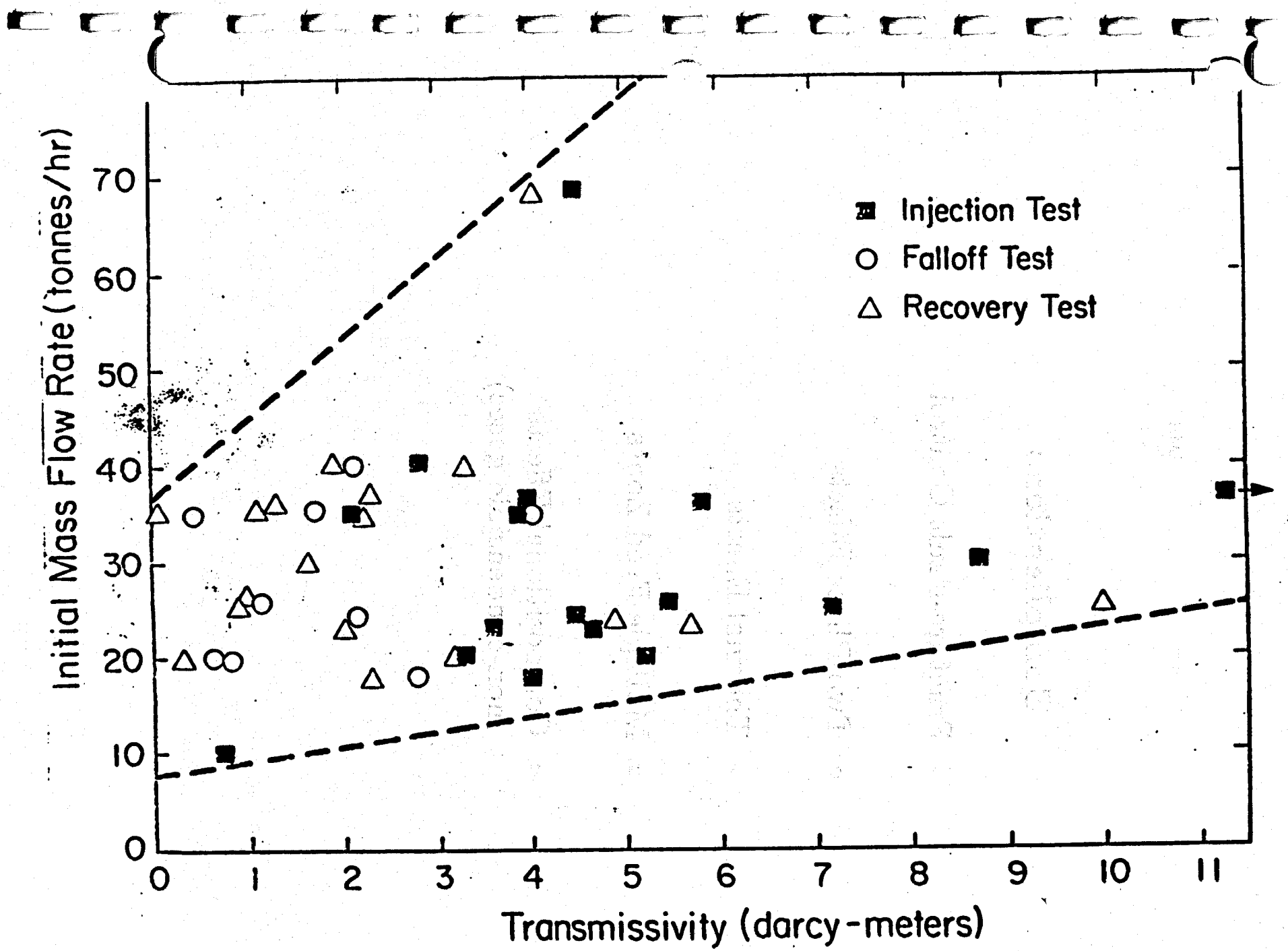

XBL 855-10506

Complications

- Fracture-Fault Control
- Two-Phase Effects
- Thermal Effects
- Multiple-Feed Zones
- Compositional Effects
  (non-condensible gases)

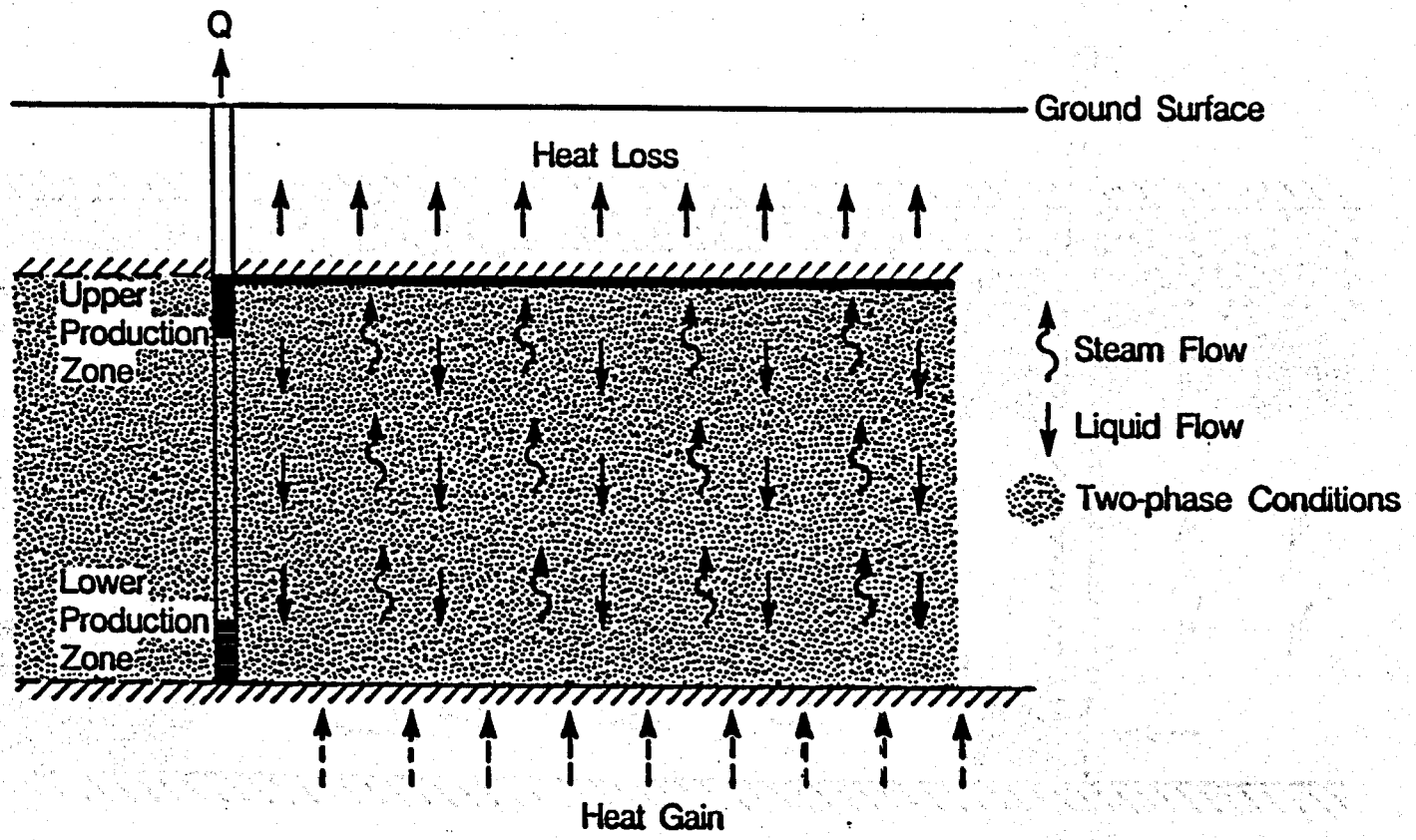

XBL 866-10846

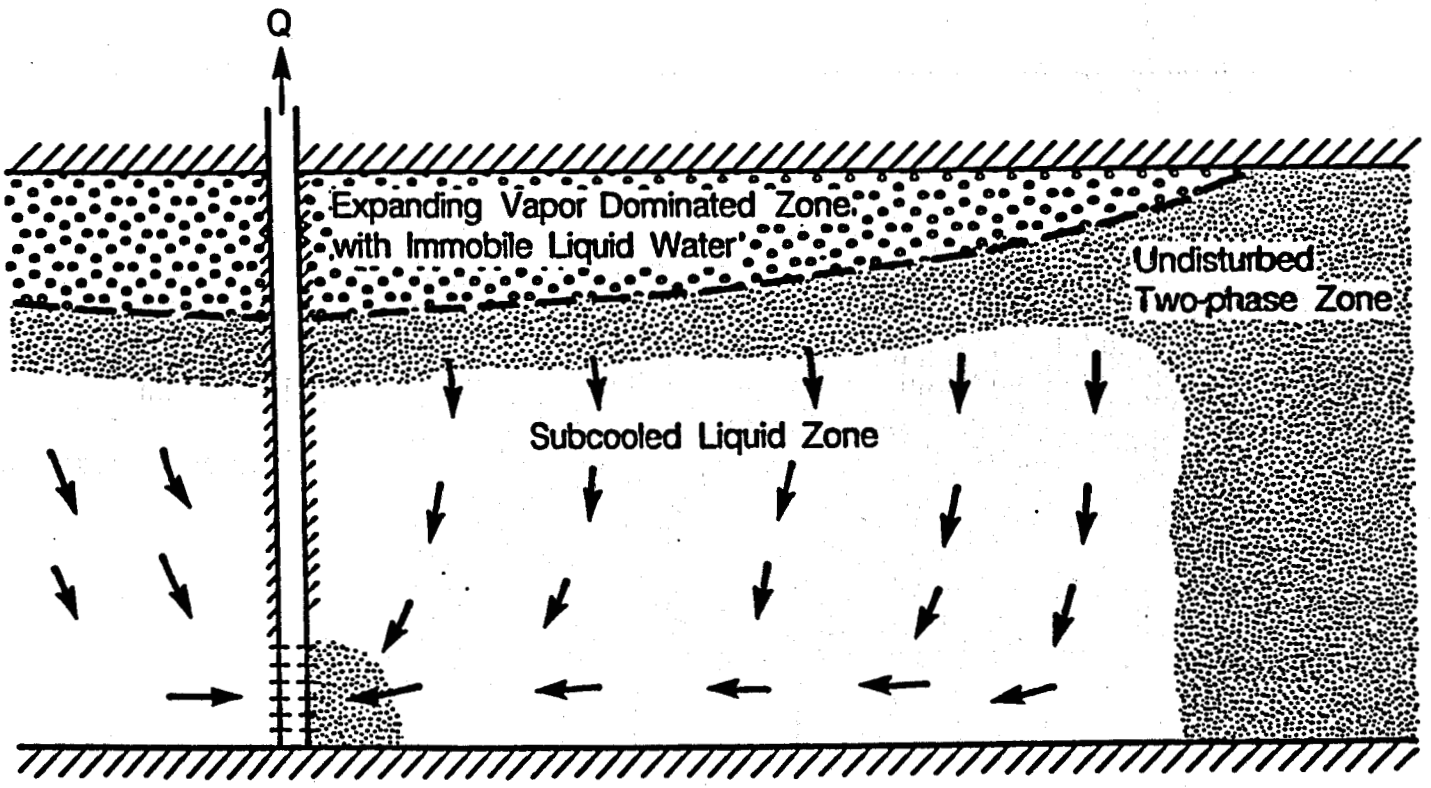

XBL 866-10863

THE EFFECTIVE STEAM PERMEABILITY

$$kk_{rv} = \frac{\mu_v}{\rho_v} \frac{\rho_a c_a (\Delta T \Delta z)_{tot}}{\rho_l g t h_v}$$

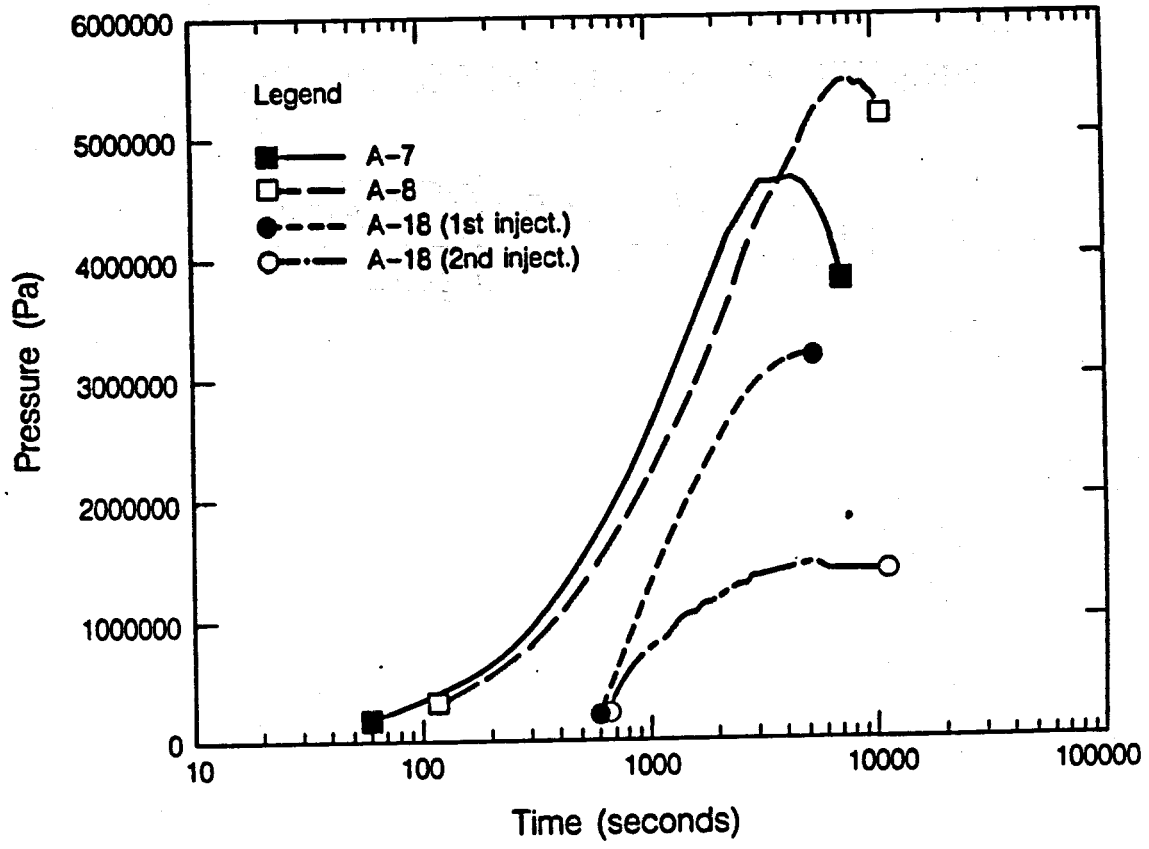

XBL 8612-12856

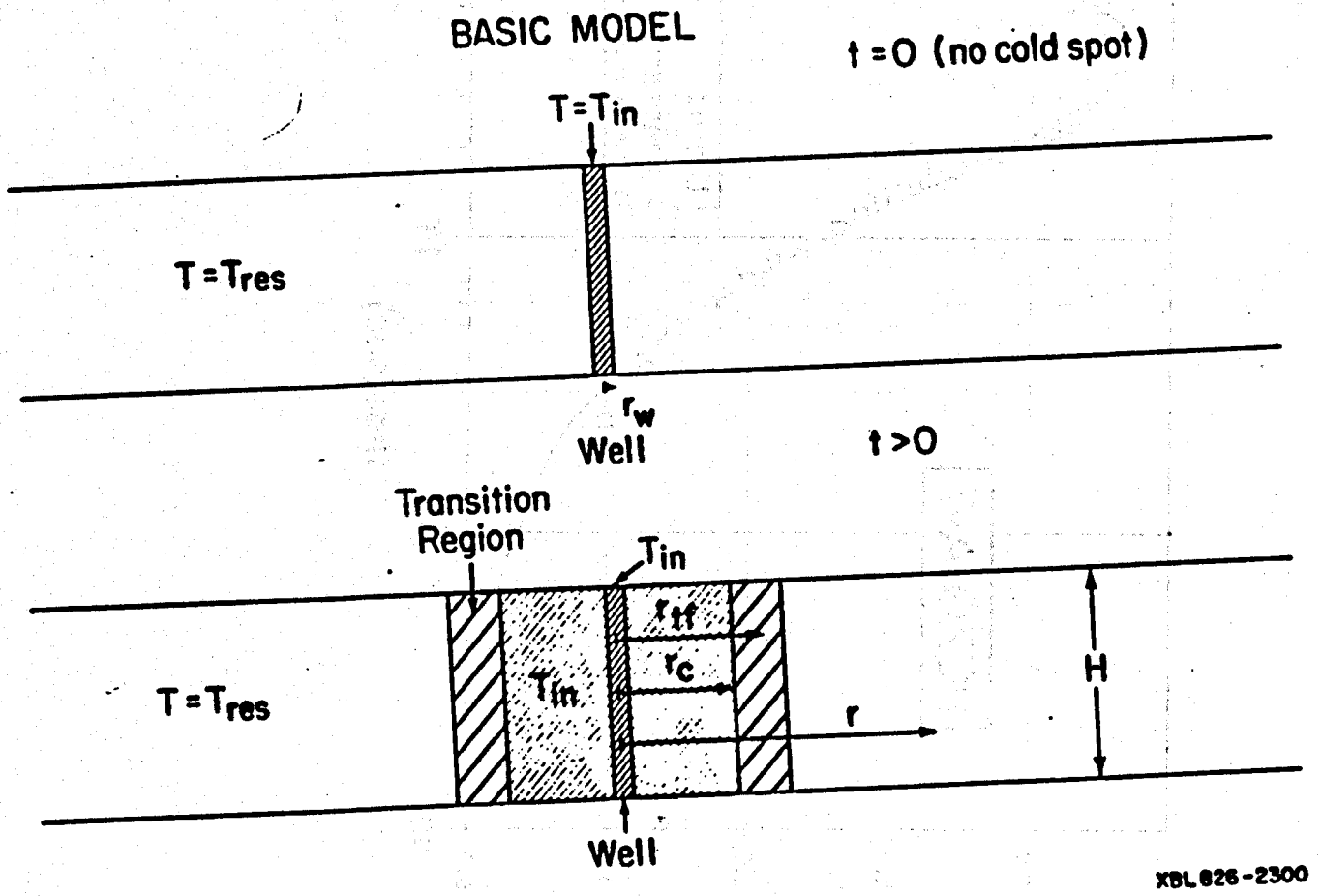
BASIC MODEL
t = 0 (no cold spot)
T=Tin
T=Tres
rw
Well
t>0
Transition Region
Tin
rtf
rc
Tin
T=Tres
r
H
Well
XBL 826-2300

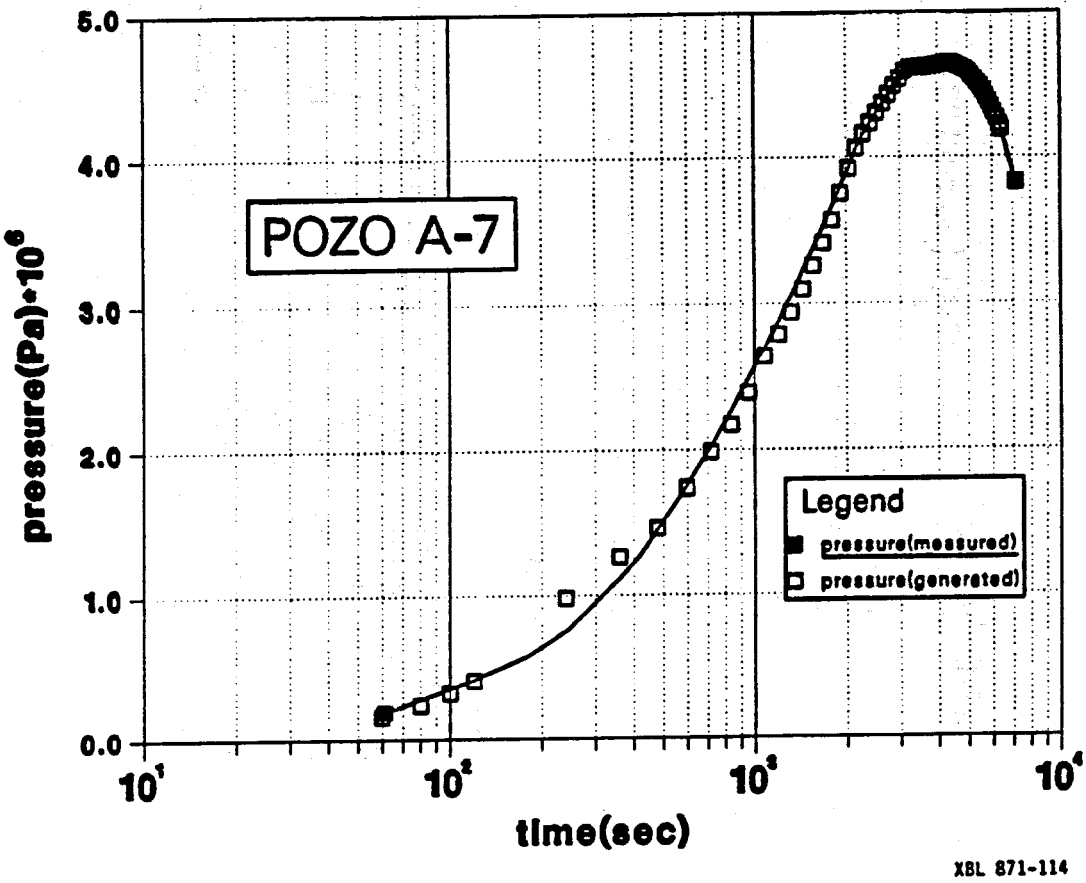
POZO A-7
pressure(Pa)*10^6
5.0
4.0
3.0
2.0
1.0
0.0
10^1
10^2
10^3
10^4
time(sec)
Legend
pressure(measured)
pressure(generated)
XBL 871-114

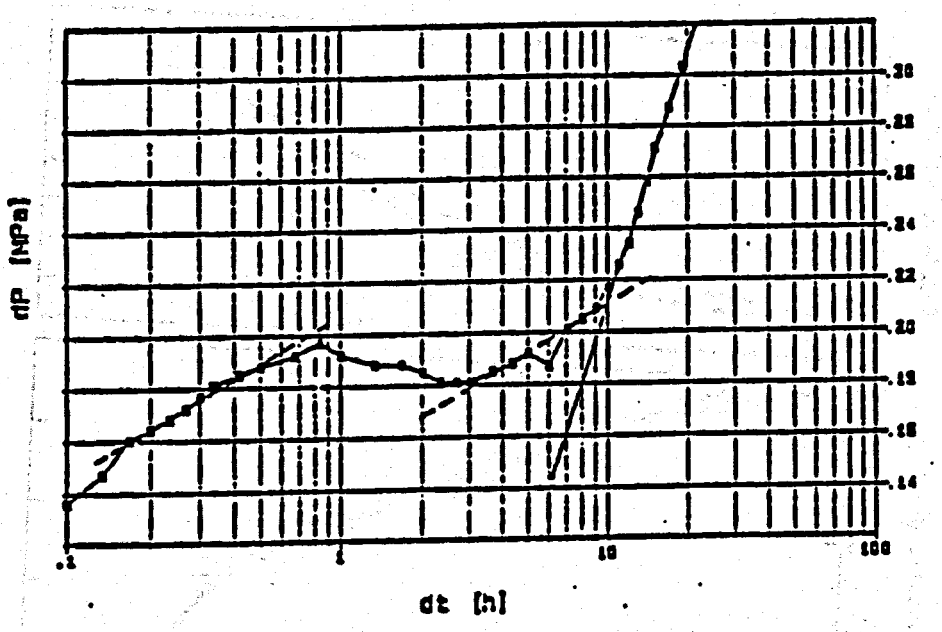

Figure 5 - Specialized plot.

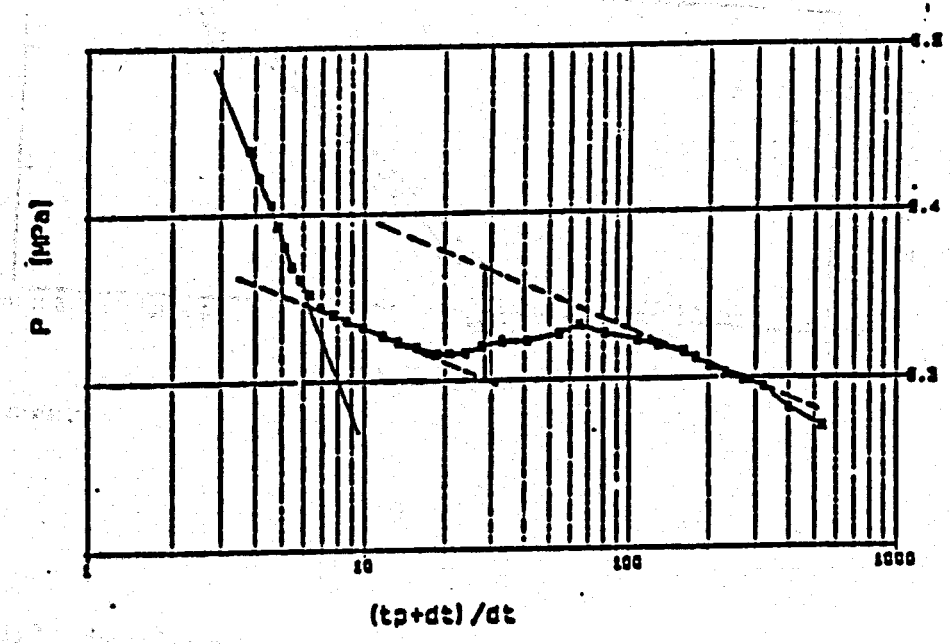

Figure 6 - Horner plot.

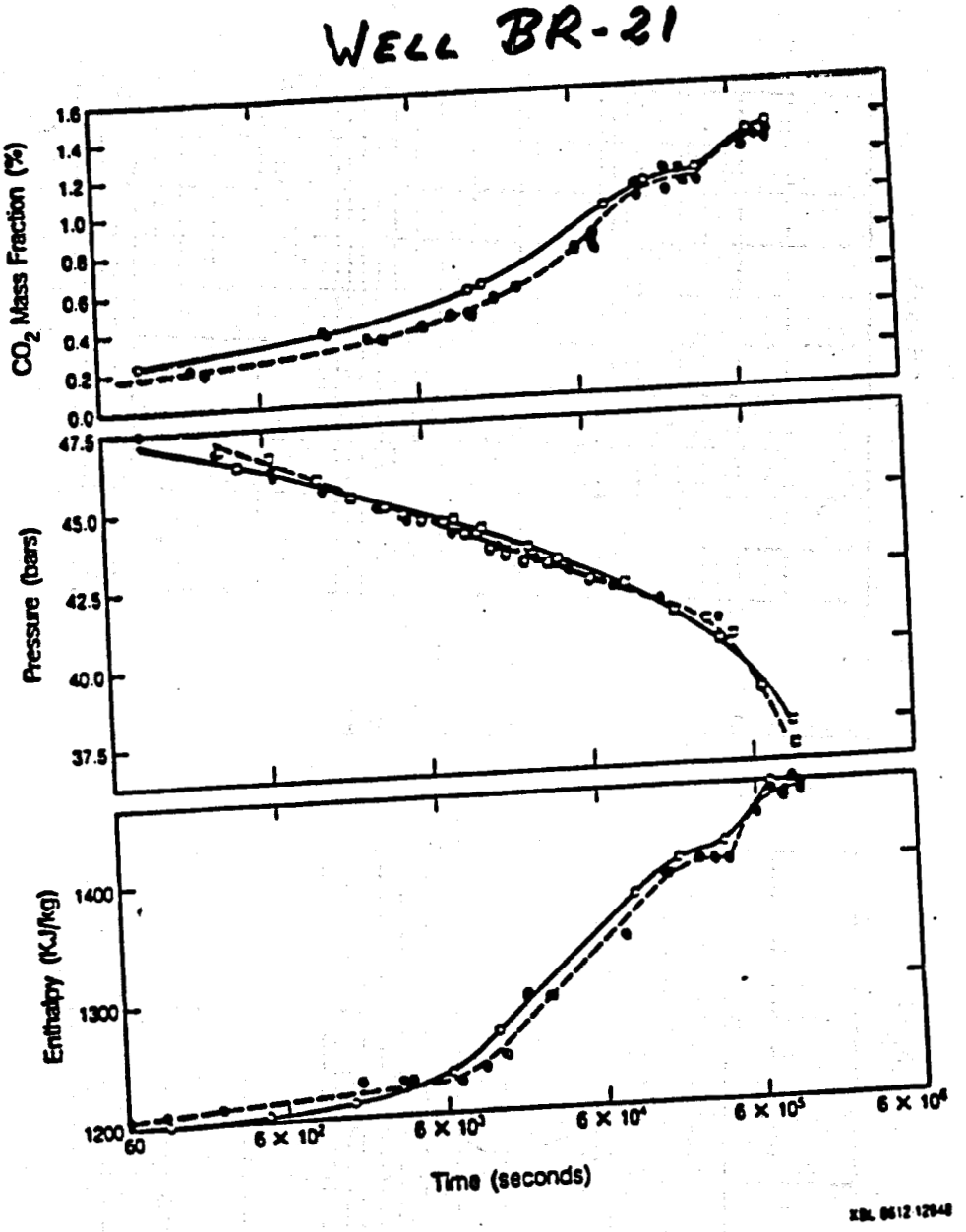

Figure (5-5). Comparison of best fit model to measured results of changes in downhole pressure, flowing mass fraction of CO_2, and flowing enthalpy with time.

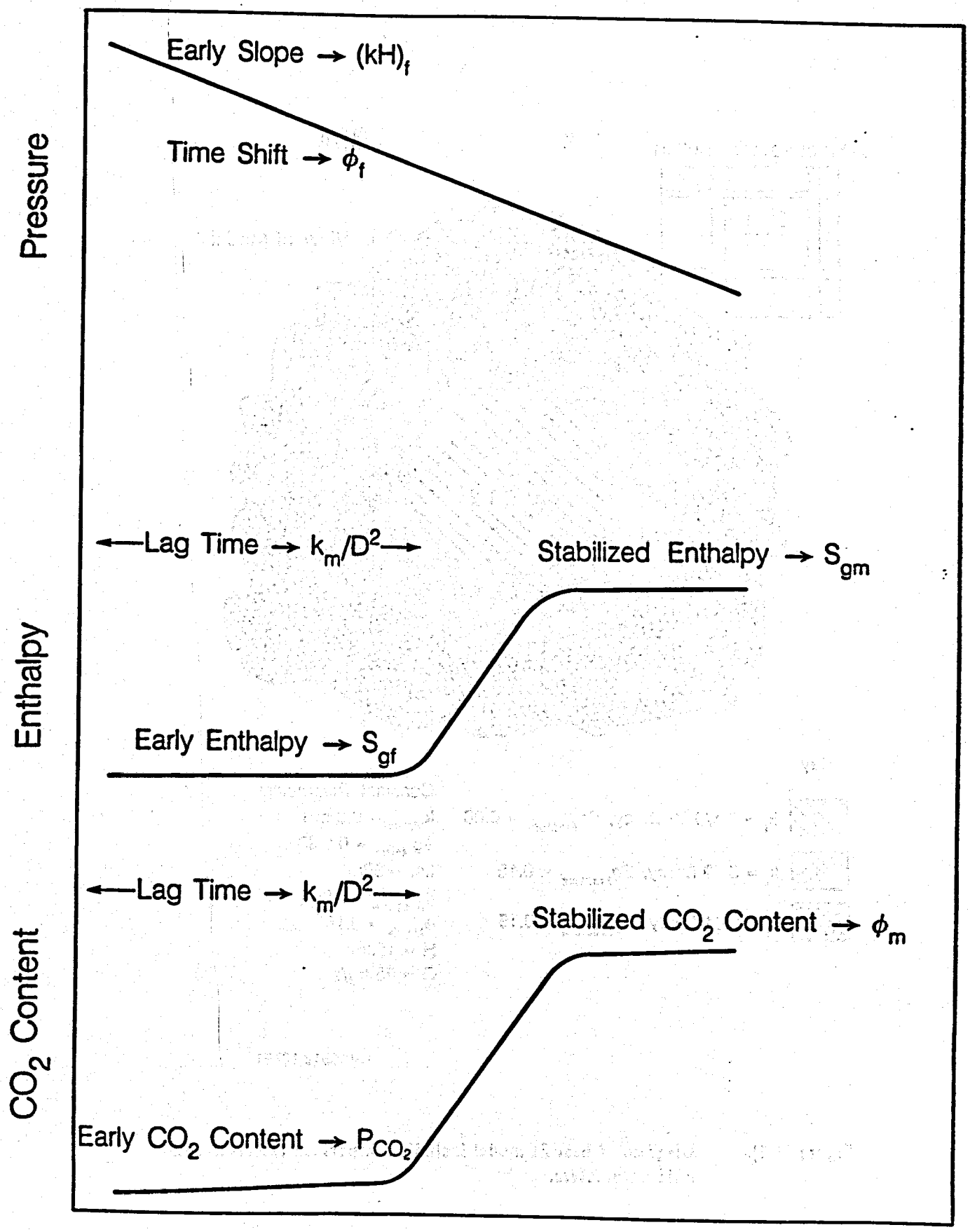

XBL 881-10010

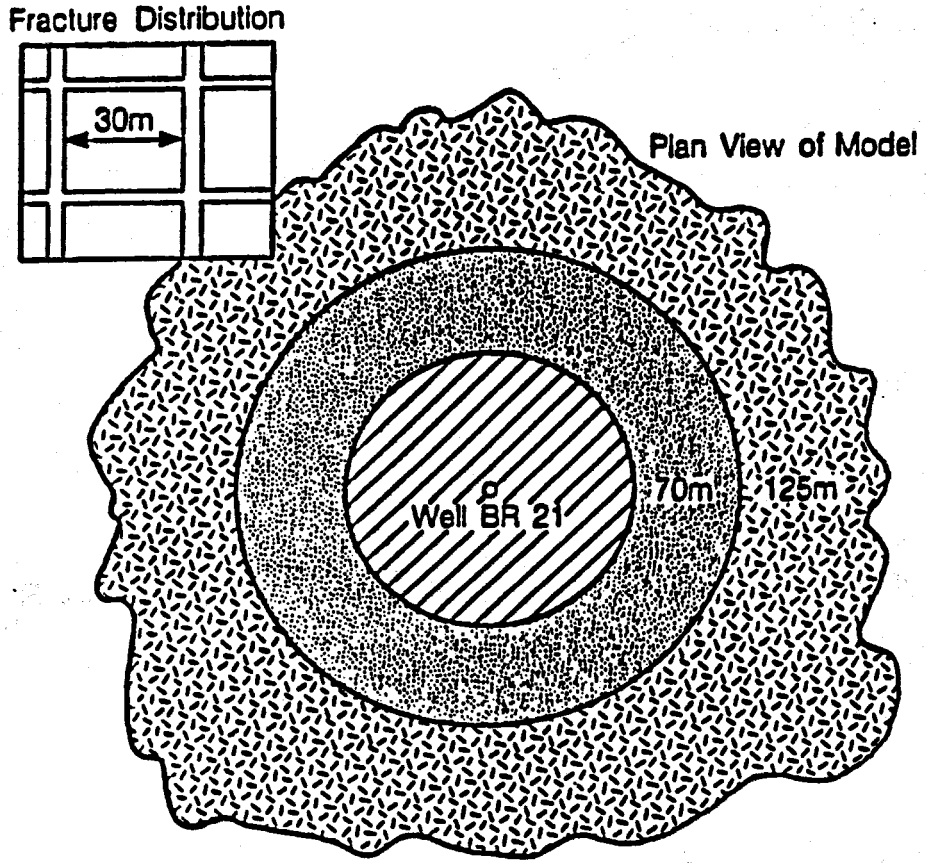

Key

k_f = 0.1/0.09 Darcy, $Sg_{Fracture}$ = 0.06

k_f = 0.09 Darcy, $Sg_{Fracture}$ = 0.15

k_f = 0.01 Darcy, $Sg_{Fracture}$ = 0.15

Constant Parameters

k_{Matrix} = 0.3 md
Sg_{Matrix} = 0.0.33
f.s. = 30m
$\phi_{Fracture}$ = 0.005
ϕ_{Matrix} = 0.18
H = 100m
Q = 25 kg/s

XBL 8612-12791

Figure (5-6). Diagram of best fit model including important reservoir and fluid parameters.

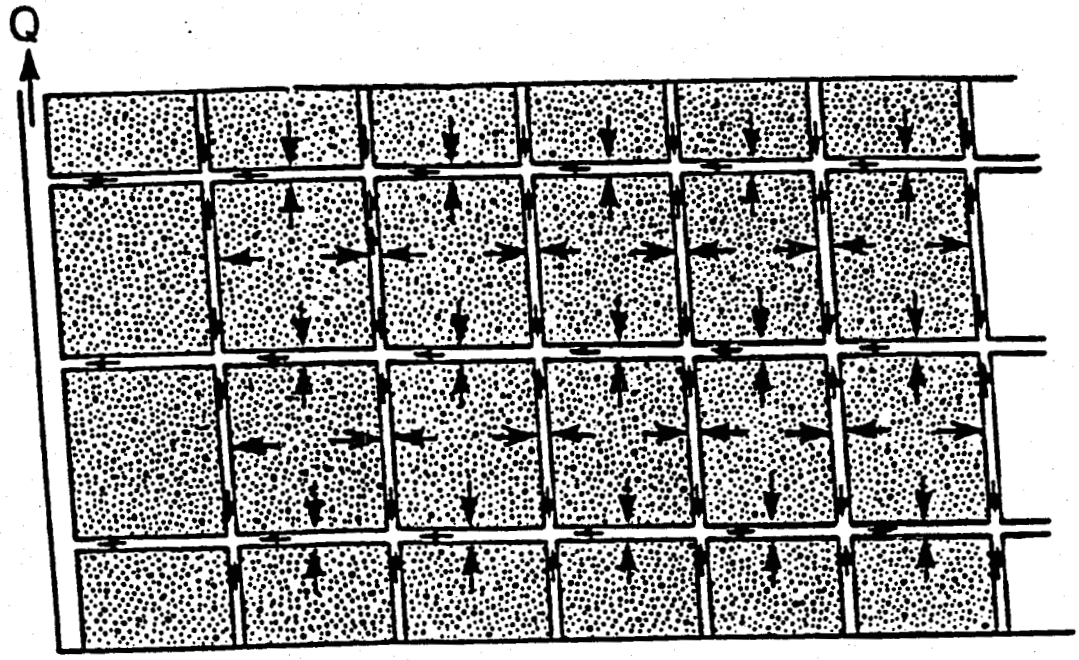

XBL 861-10551

Figure 10. Schematic view of fracture-matrix flow in a geothermal reservoir with no CO_2.

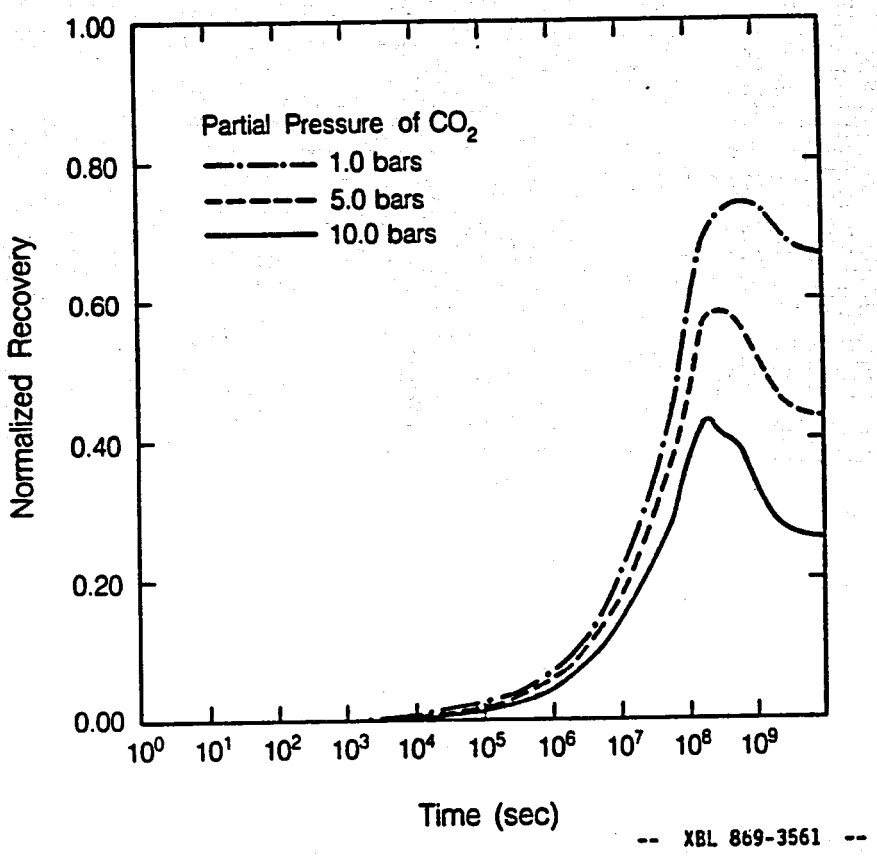

Figure (4-2). Effect of initial partial pressure of CO_2 on recovery transients normalized by the by the initial mass in the matrix.

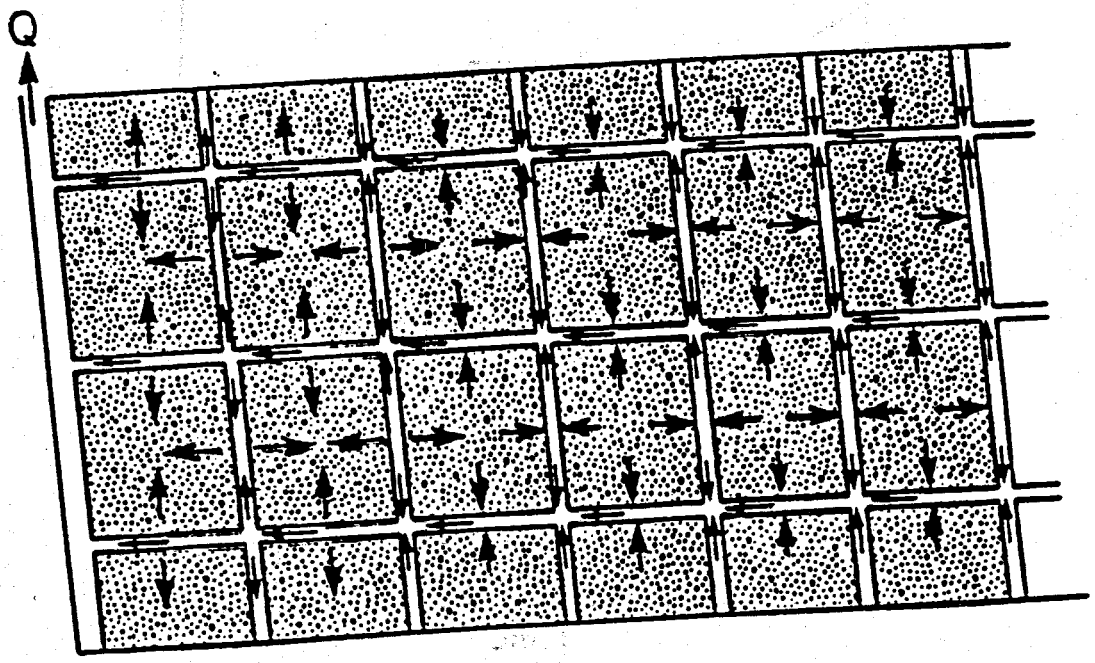

XBL 861-10552

Figure 11. Schematic view of fracture-matrix flow in a gas-rich reservoir.

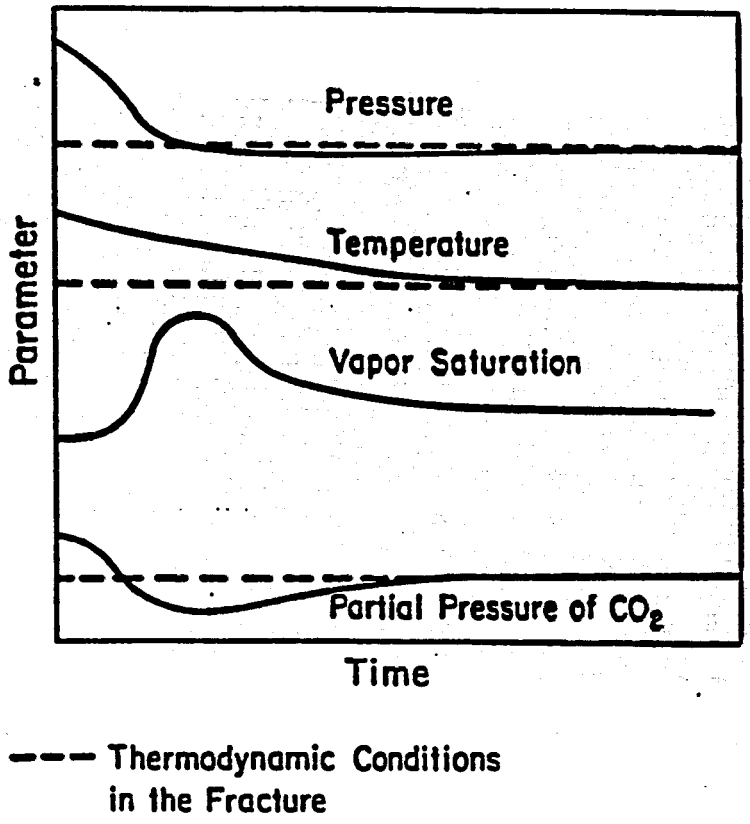

Fig. 8—Schematic results of changes in pressure, gas saturation, temperature, and CO_2 partial pressure with time in the matrix.

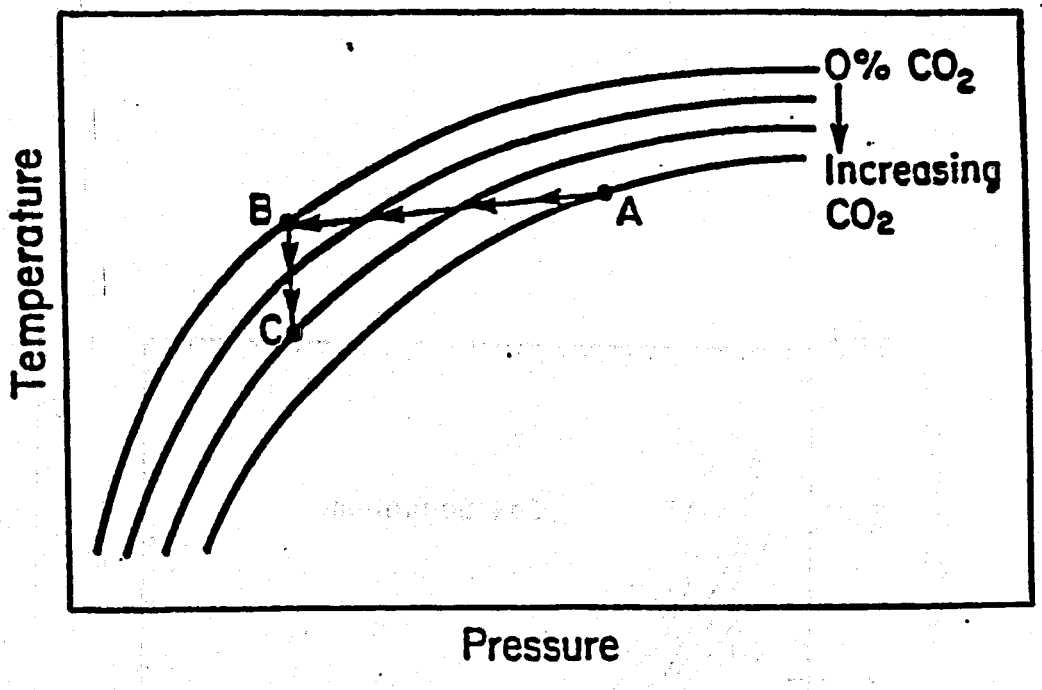

Fig. 9—Schematic diagram of pressure-temperature relationship for H_2O-CO_2 systems.

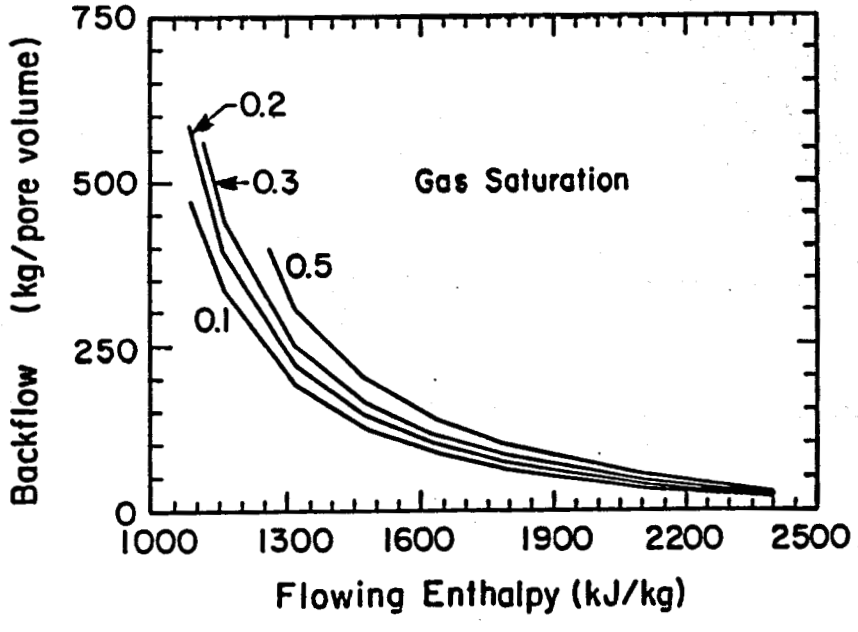

Figure (4-6). Effect of flowing enthalpy on the amount of backflow per unit pore volume for various final matrix gas saturations.

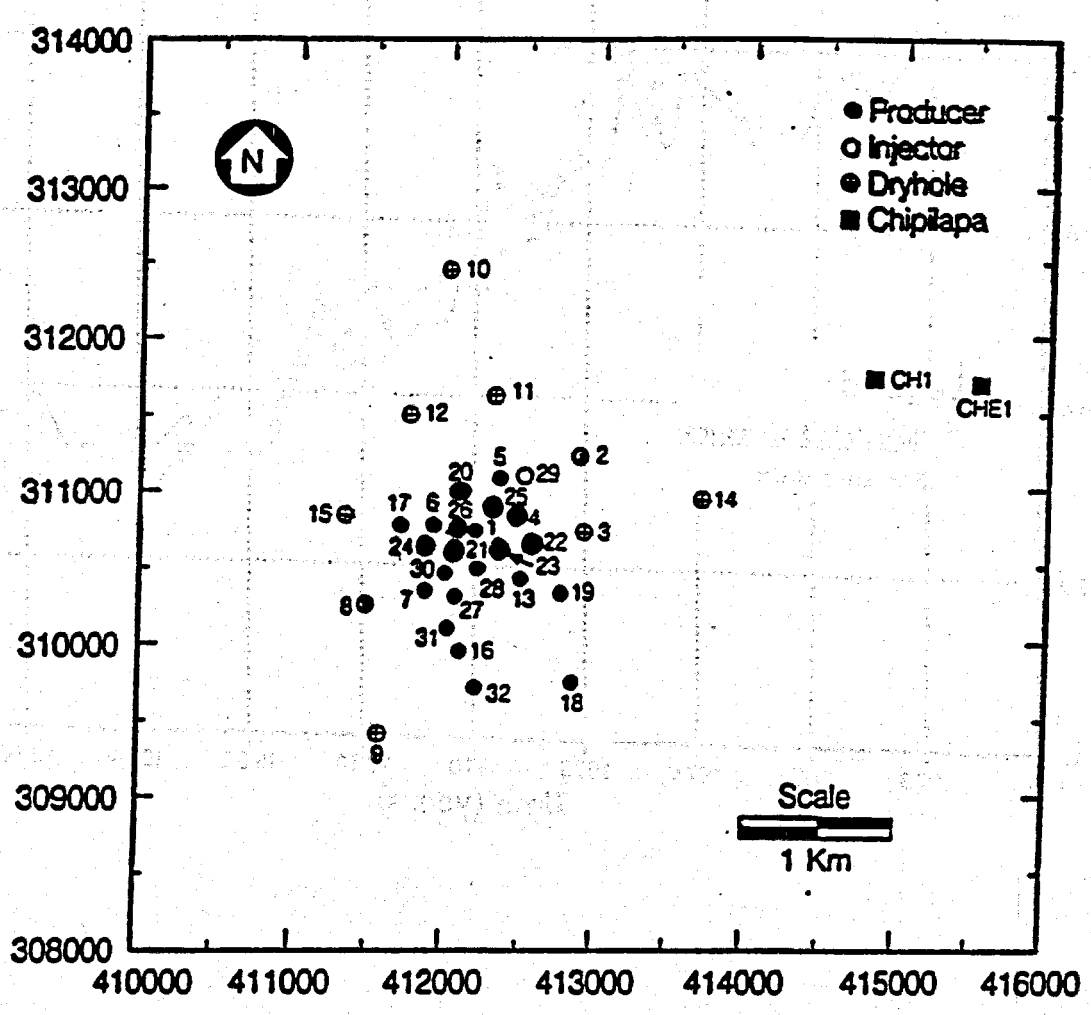
314000
313000
312000
311000
310000
309000
308000
410000
411000
412000
413000
414000
415000
416000
N
Producer
Injector
Dryhole
Chipilapa
CH1
CHE1
Scale
1 Km

XBL 891-7429

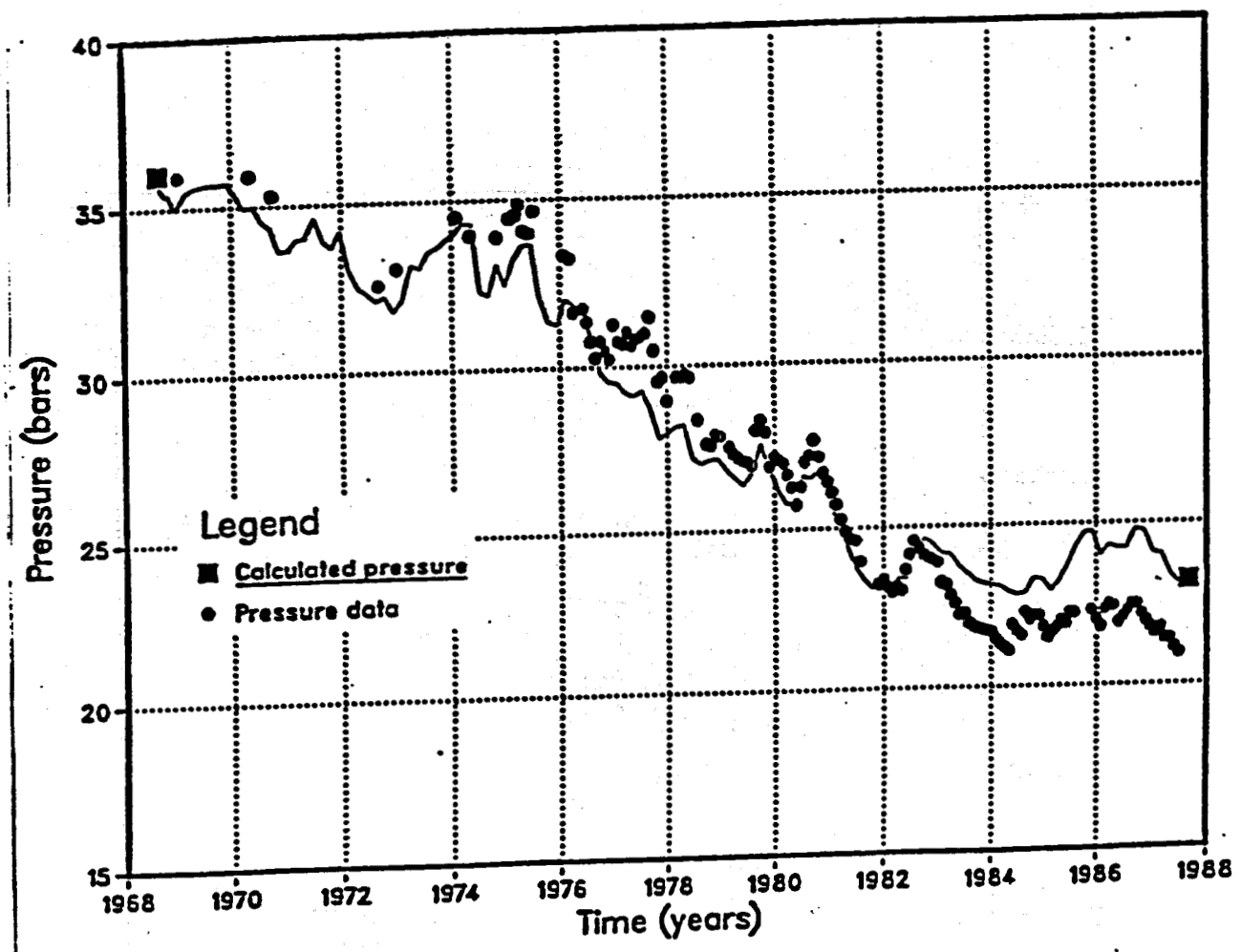
Pressure (bars)
40
35
30
25
20
15
Legend
Calculated pressure
Pressure data
1968
1970
1972
1974
1976
1978
1980
1982
1984
1986
1988
Time (years)

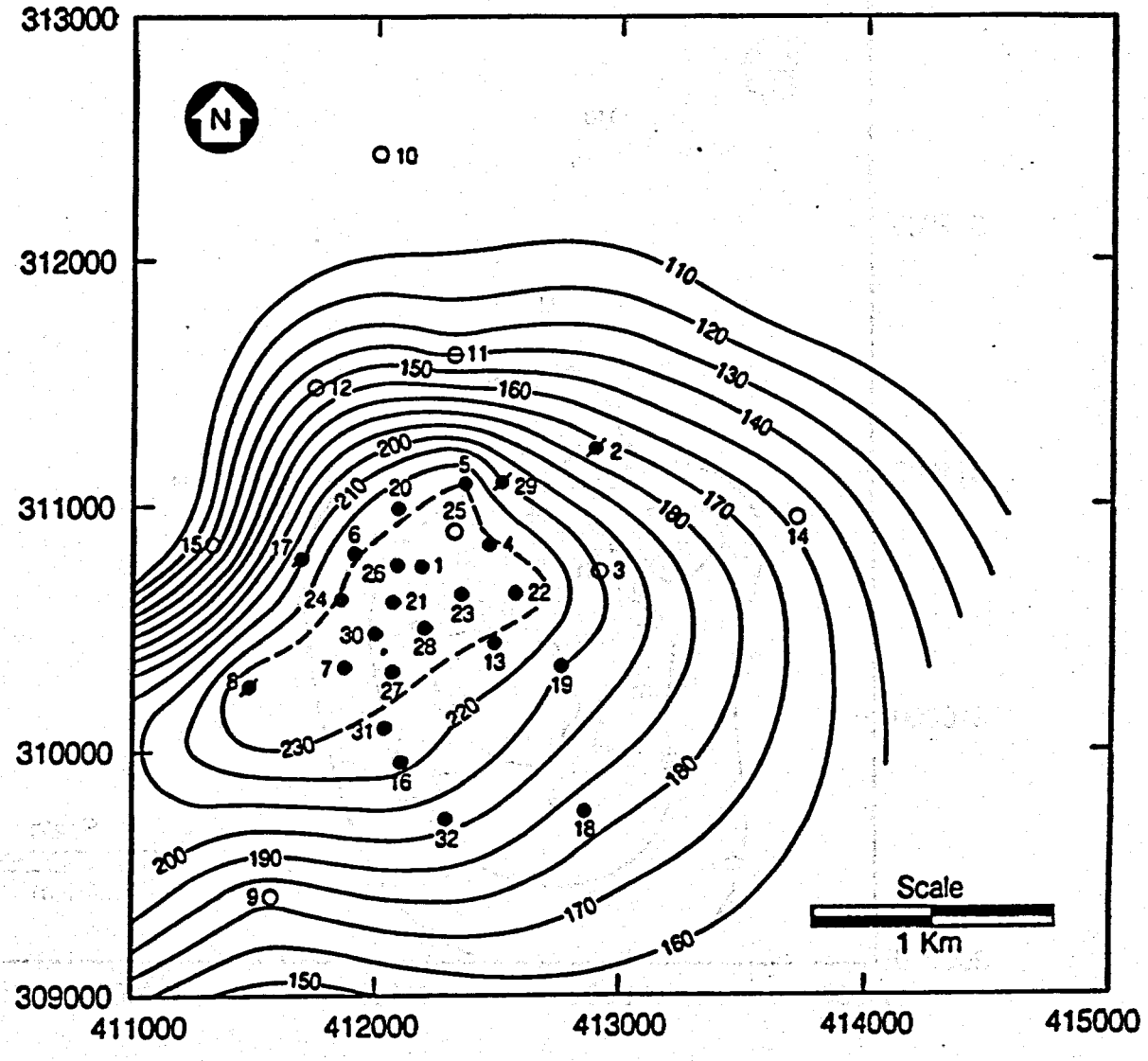

Figure 7.5. Initial temperature distribution (in °C) at 300 masl.

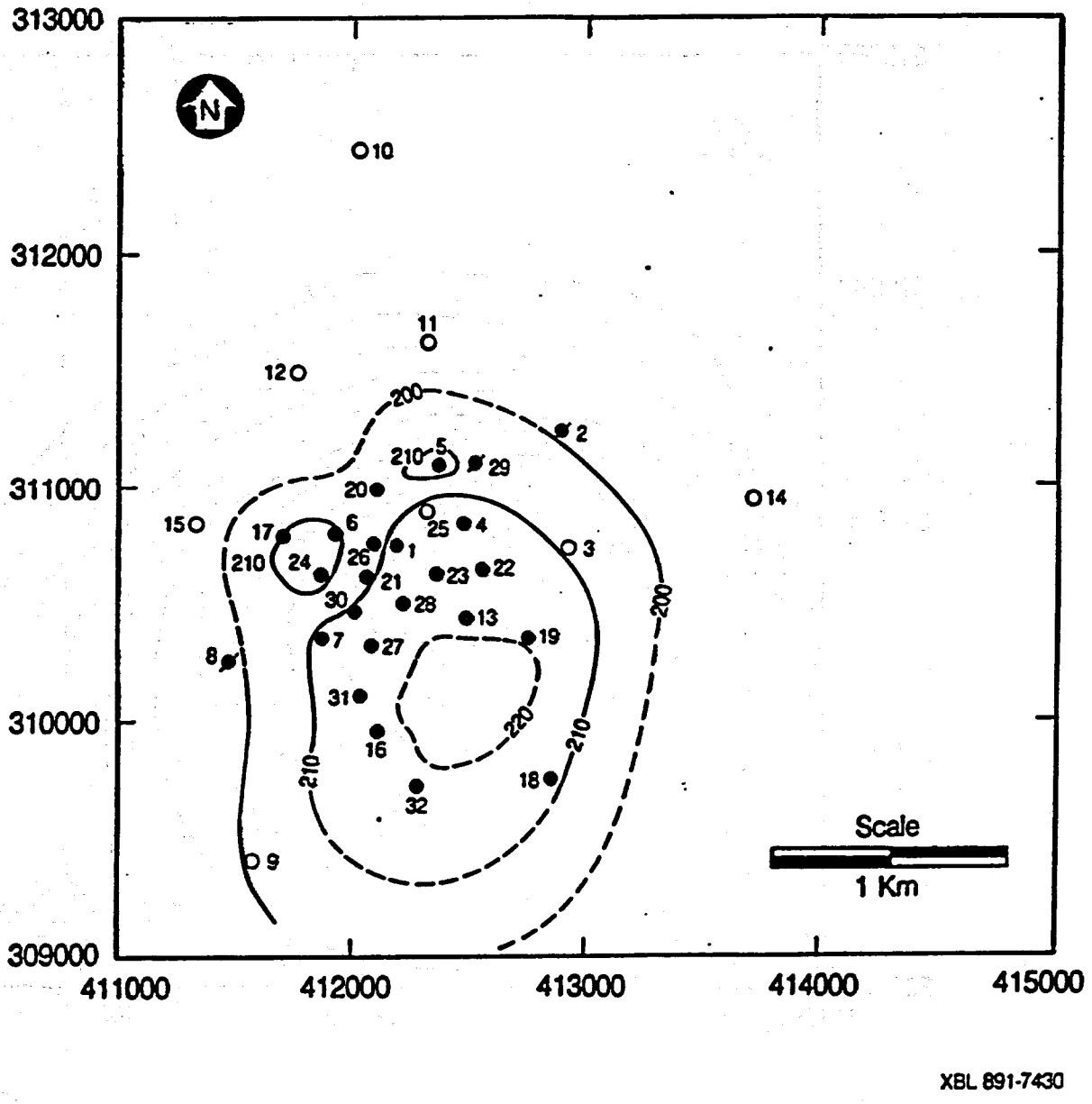

Figure 9.12. 1986 temperature contours (in °C) at 300 masl.

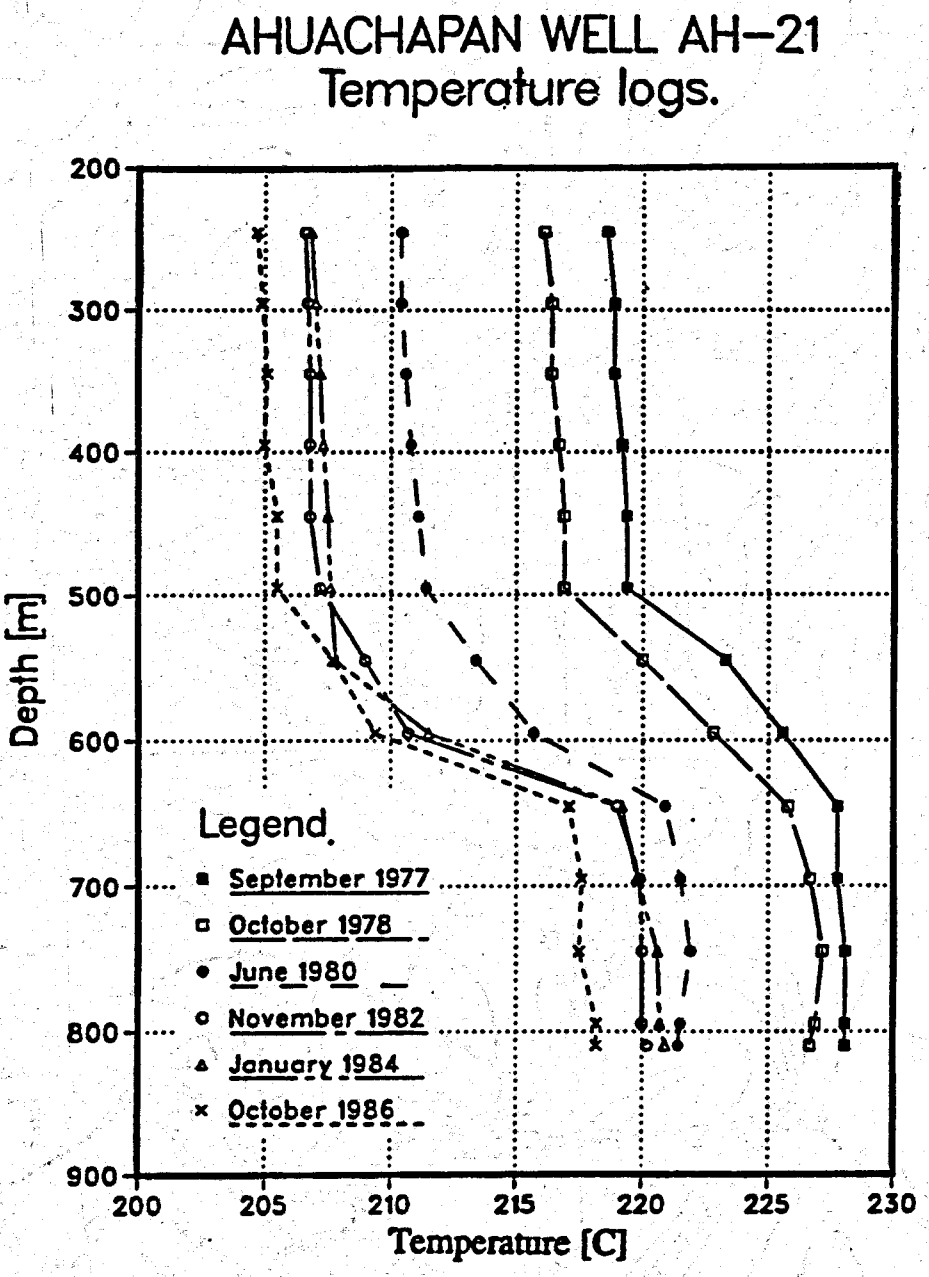

Figure 9.15. Selected temperature logs for well AH-21.

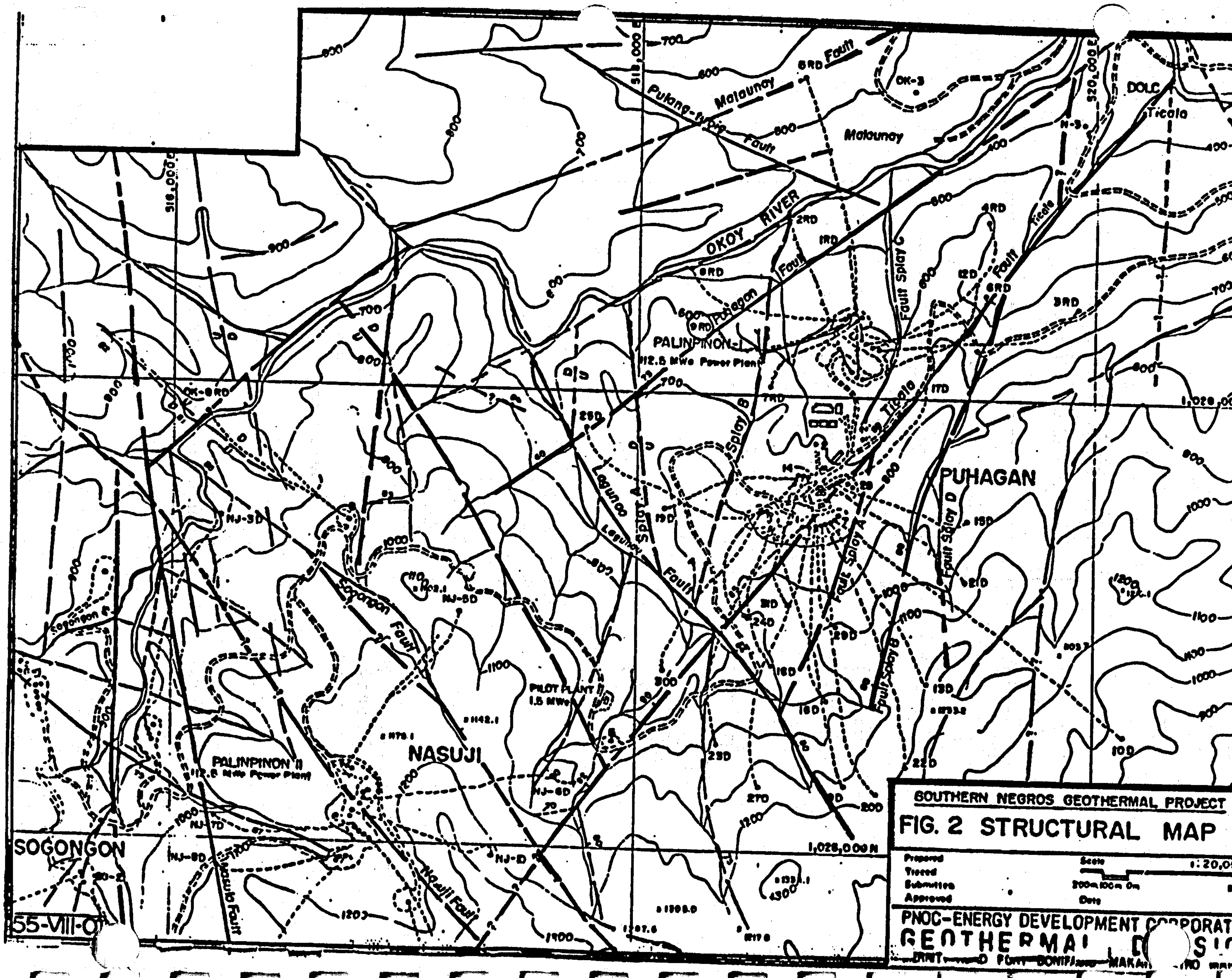

SOUTHERN NEGROS GEOTHERMAL PROJECT

FIG. 2 STRUCTURAL MAP

PNOC-ENERGY DEVELOPMENT CORPORATION
GEOTHERMAL DIVISION

FIG. 4

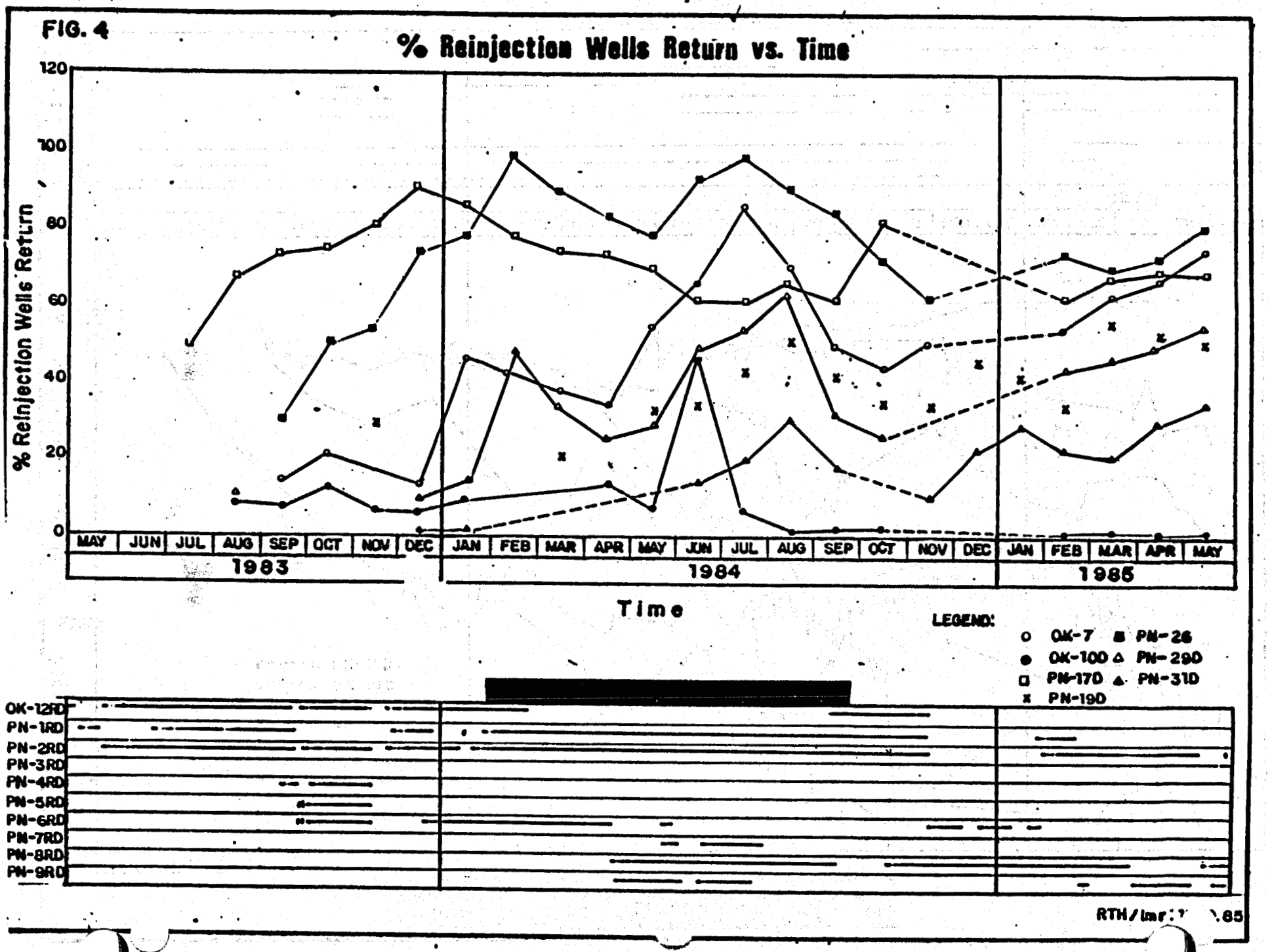
% Reinjection Wells Return vs. Time
% Reinjection Wells Return
120
100
80
60
40
20
0
MAY JUN JUL AUG SEP OCT NOV DEC JAN FEB MAR APR MAY JUN JUL AUG SEP OCT NOV DEC JAN FEB MAR APR MAY
1983
1984
1985
Time
LEGEND:
OK-7
OK-10D
PN-17D
PN-19D
PN-26
PN-29D
PN-31D
OK-12RD
PN-1RD
PN-2RD
PN-3RD
PN-4RD
PN-5RD
PN-6RD
PN-7RD
PN-8RD
PN-9RD

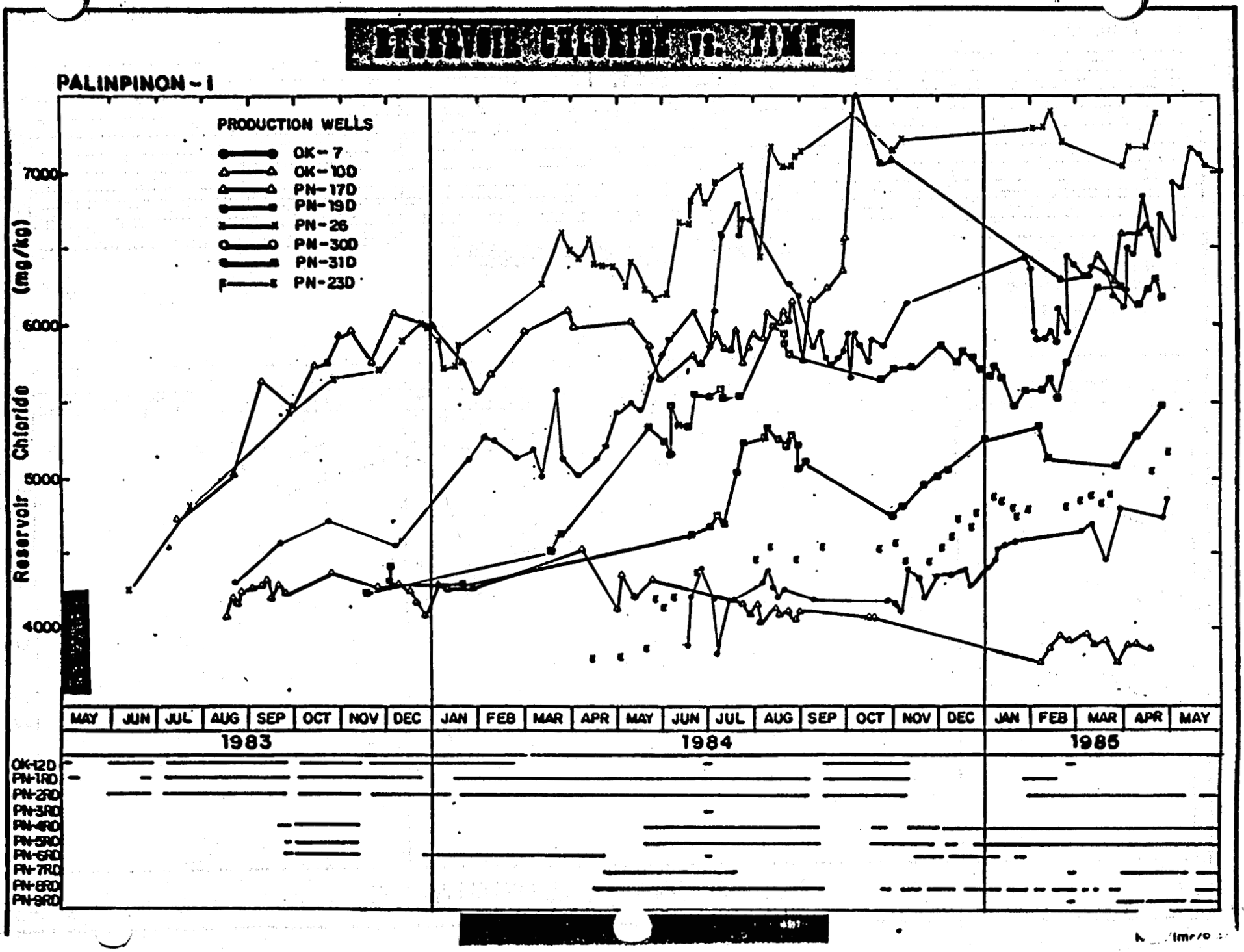
PALINPINON - I
PRODUCTION WELLS
OK-7
OK-10D
PN-17D
PN-19D
PN-26
PN-30D
PN-31D
PN-23D
Reservoir Chloride (mg/kg)
7000
6000
5000
4000
MAY JUN JUL AUG SEP OCT NOV DEC JAN FEB MAR APR MAY JUN JUL AUG SEP OCT NOV DEC JAN FEB MAR APR MAY
1983
1984
1985
OK-12D
PN-1RD
PN-2RD
PN-3RD
PN-4RD
PN-5RD
PN-6RD
PN-7RD
PN-8RD
PN-9RD

Geophysical Monitoring of Subsurface Processes in Producing Geothermal Reservoirs

Norman E. Goldstein

Lawrence Berkeley Laboratory

presented at

RESPONSES OF A GEOTHERMAL FIELD
DURING EXPLOITATION

- A Reservoir Management Plan -

Geothermal Resources Council

15-16 June 1989
Berkeley Conference Center
Berkeley, California

Geophysical Monitoring

Why?

1. To comply with state and local regulatory requirements. To monitor prossible effects of production on the environment (Imperial Valley).

   (a) Land Deformation: Leveling

   (b) Induced Seismicity: EQ Monitoring

And

2. To obtain indirect information on reservoir (fluid) behavior; e.g.,

   (a) Natural Recharge (Sources, Amounts)

   (b) Boiling and 2ϕ Conditions

   (c) Injectate Movement

Geophysical Responses to Geothermal Production

1. Electrokinetic or Streaming Potentials (SP Effect)

   Fluid withdrawal and reinjection plus natural recharge can produce a complex natural voltage pattern over the surface of hundreds of mV due to secondary electric fields induced by fluid flows.

2. Net Mass Changes (Precision Gravity)

   Withdrawal of reservoir fluids without compensating lateral recharge leads to a "drying out" of the reservoir and a drop in groundwater level. The result can be is a steady decrease in gravity that can amount to > 100 μGal.

3. Resistivity Increase Due to Natural Recharge (dc Resistivity)

   Withdrawal of reservoir fluids with lateral and/or vertical recharge of non-thermal waters can lead to a drop in groundwater levels and a general increase in resistivity above reservoir and at reservoir depths. The result can be apparent resistivity increases of ≈20% after a few years of production.

4. Increase Seismicity and Changes in Elastic Wave Parameters (Seismic Monitoring)

   Pressure drop and boiling sharply decreases bulk modulus, may increase shear modulus. The result is a 10-20% decrease in V_p/V_s and a larger decrease in the Poisson's ratio.

   Pressure drop and thermal contraction may increase seismicity.

Sources of Natural Potentials over Geothermal Fields

Man-made	Approx Size of Anomaly
• Redox-oxidizing drill casing	100's mV
• Leakage from irrigation canals	20 mV
• Grounded electric pump motors	20 mV
Natural	
• Liquid junction diffusion Mixing of waters of different salinities	< 15 mV
• Thermoelectric Secondary electric potentials driven by heat flow from a thermal source	< 10 mV
• Telluric noise	± 5 mV/km, highly variable depends on wire length
Natural and Man-Made	
• Electrokinetic (Streaming Potentials) Secondary electric potentials driven by fluid flows. Includes groundwater flow.	10 to 200 mV

$$\text{Current Flow } J = -L_{11}\,\nabla\Phi - L_{12}\,\nabla P$$

$$\text{Fluid Flow } Q = -L_{21}\,\nabla\Phi - L_{22}\nabla P$$

$$L_{12} = L_{21}$$

Streaming Potentials

If there are no external sources of current the total current J is divergenceless ($\nabla \cdot J = 0$) and

$$-\left[\frac{\nabla\Phi}{\nabla P}\right] = \frac{L_{21}}{\sigma} = C_{21}$$

Φ = Streaming potential (V)

C_{21} is the voltage coupling coefficient ($\approx$–15 to -25 mV/bar)

$$C_{21} = \frac{\varepsilon\zeta}{\eta\sigma}$$ straight capillary tube

or

$$C_{21} = \frac{\zeta\varepsilon\phi}{\eta(\phi\sigma_f + S_o\sigma_s)}$$ tortuous capillary flow in porous rock

(Ishido and Mizutani, 1981)

ε = dielectric constant of fluid

ζ = zeta potential

η = fluid viscosity

σ_f = fluid conductivity (sieman/m)

σ_s = surface conduction (S = sieman)

S_o = specific internal pore surface (m^{-1})

ϕ = porosity

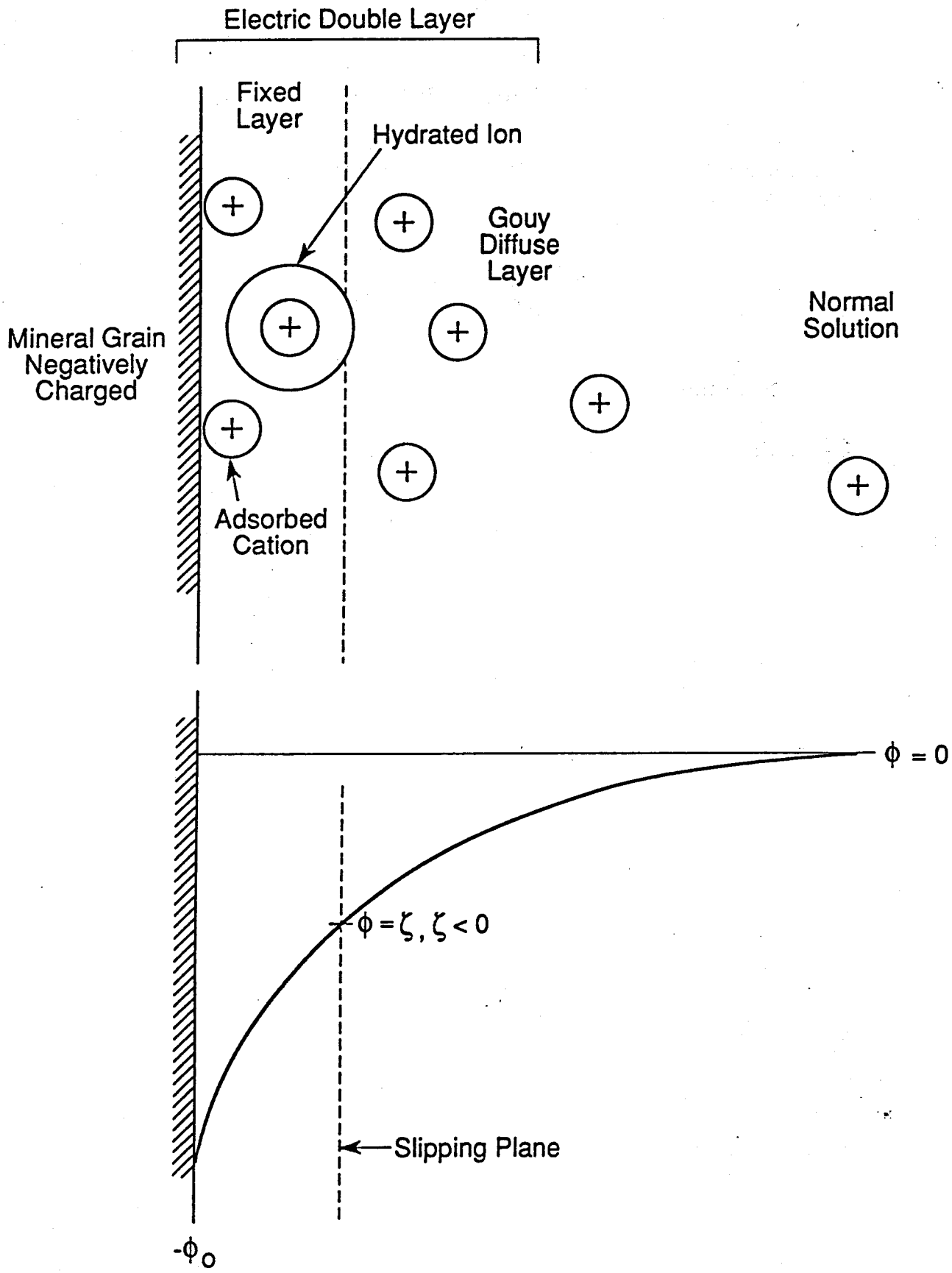
Electric Double Layer
Fixed Layer
Hydrated Ion
Gouy Diffuse Layer
Normal Solution
Mineral Grain Negatively Charged
Adsorbed Cation
ϕ = 0
ϕ = ζ, ζ < 0
Slipping Plane
-ϕo

XBL 895-7613

Sources of Conduction Current

1. Primary sources - pressure gradients cause tangential flow in pores and fractures.

2. Secondary Sources - where primary fluid flow is perpendicular to boundary where coupling coefficient and/or permeability change.

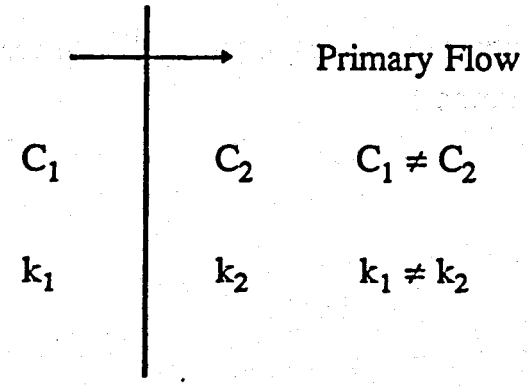

Streaming Potentials

1. Responsible for most of the SP effects observed over geothermal fields and volcanic systems in their natural states.

2. Changes in the SP anomaly over a producing geothermal field will most likely be related to

   - Changes in the size and distribution of pressure sources (ΔP terms)

   - Physical property changes associated with reservoir rocks and fluids (C_{21} terms)

Factors Affecting Streaming Potential

Pressure Gradients

Pressure gradients associated with fluid withdrawal, injection and recharge in single-phase (liquid only) systems.

Pressure gradients associated at boundaries between 2ϕ and liquid zones.

Pore Fluid Chemistry and ζ Potential

- ζ increases negatively with increasing pH.
- Increasing salinity reduces both ζ directly and C_{21} through the σ^{-1} term.

Rock Mineralogy

ζ potential depends on the surface potential of mineral grains.

Quartz and certain clays will produce large ζ potentials. Calcite coating may inhibit.

Temperature

At low T ($\leq$ 100°C) Al^{3+}, Fe^{3+} hydrolyze close to mineral surfaces, $\zeta \rightarrow 0$

$|\zeta|$ increases with T due to desorption of H^+ which increases surface potential ϕ_o, and ζ.

Boiling and Two-Phase Flow (Marsden and Wheatall, 1986)

At high liquid saturations $S > 0.5$ the presence of steam may not disturb the ionic distribution of double layer, nor change ε and σ of fluid phase.

At low liquid saturations, $S < 0.5$, ζ and $\Delta\Phi/\Delta P$ decrease.

Not clear on how ζ or $\Delta\Phi/\Delta P$ behave at $S < 0.1$. Data sparse and test run with N_2 as gas phase.

1978 SP DATA

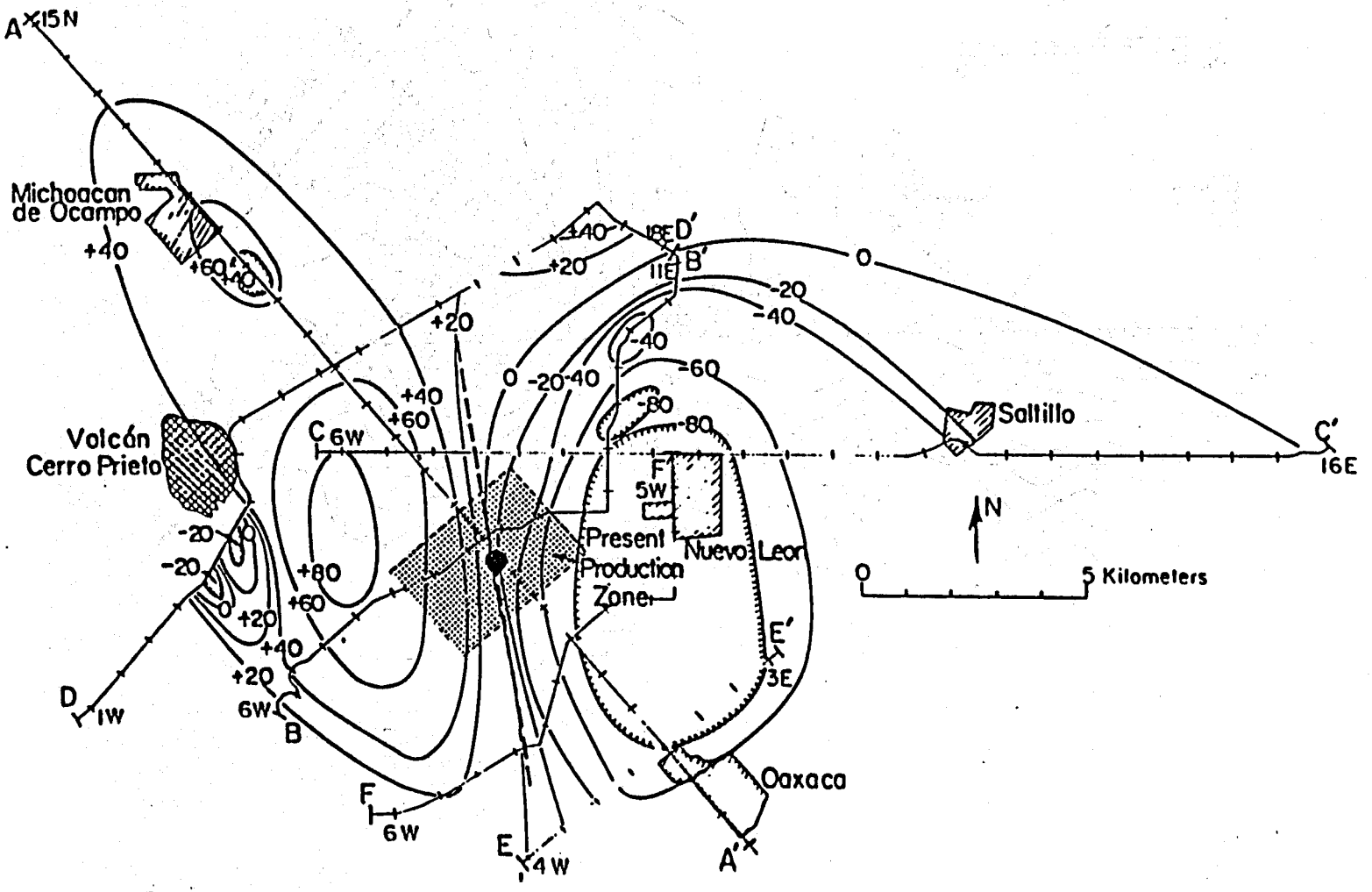

XBL787-5328A

1988 SP

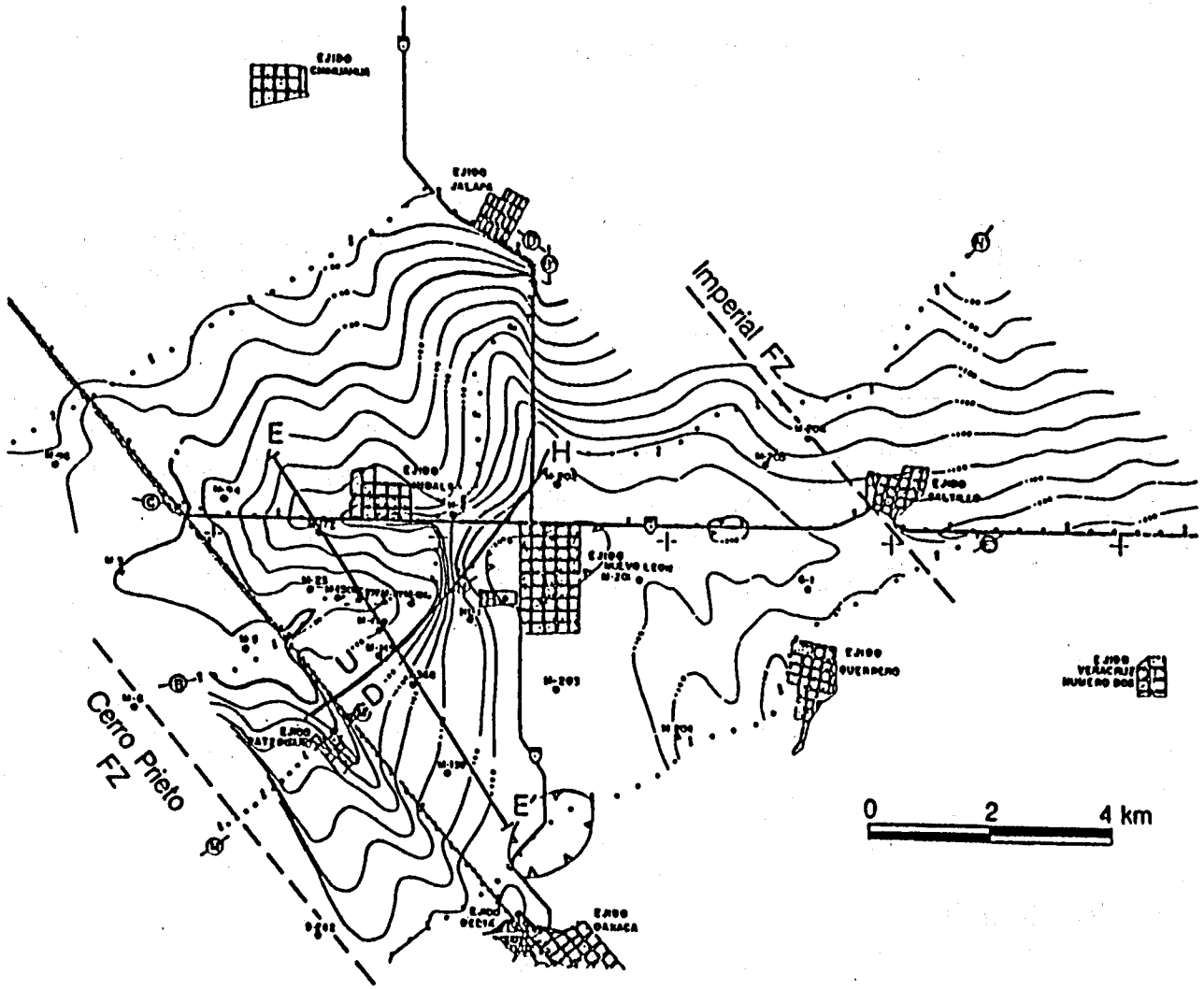

XBL 891-218A

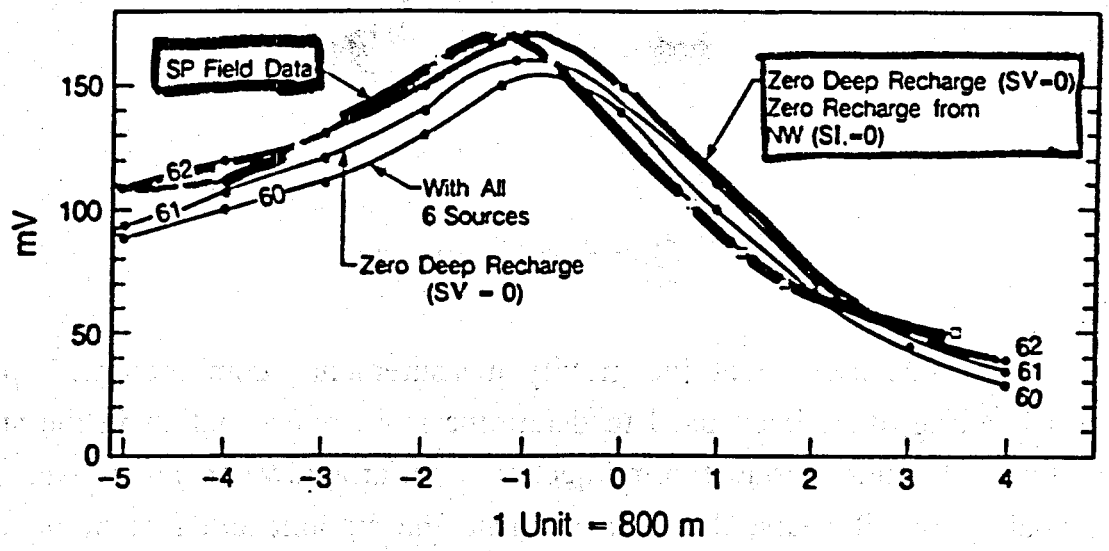

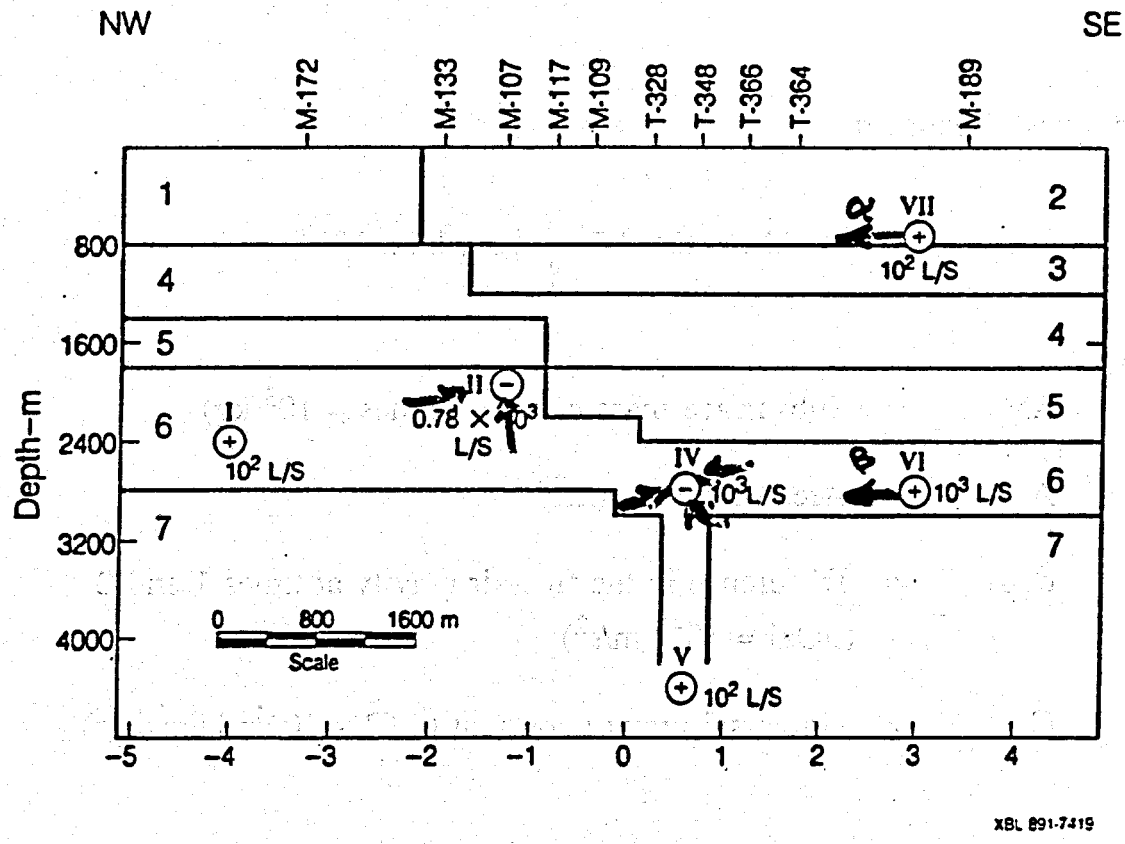

XBL 891-7419

HOT FLUID WITHDRAWAL

α → COLD WATER RECHARGE TO SHALLOW α RESERVOIR

β → COLD WATER RECHARGE TO β RESERVOIR

Gravity Changes

High-precision, repetitive gravity measurements, combined with precise leveling, have been used to determine mass redistribution in the subsurface. If fluid production/reinjection and groundwater level data are available for all years, then can estimate the amount and rate of natural recharge.

Gauss' Theorem

$$\Delta M = (2\pi G)^{-1} \int_A \delta g_{FA} dA \times 10^{-5}$$

ΔM = Subsurface mass change (tonnes = 10^3 kg)

A = Area of survey (m^2)

δg_{FA} = Difference in the free-air gravity at times 1 and 2 (μGal = 10^{-8} m/s^2)

G = Universal gravity constant (6.67×10^{-11} Nm^2/kg^2)

Free-Air Gravity

g_{FA} = observed gravity (from gravity meter)

± tidal correction (formula)

+ free-air gradient correction (approx. 308.6 μGal/m or $3.086 \times 10^{-6}/s^2$)

± meter drift error.

Instrument Precision (Lacoste & Romberg D meter) ± 1 μGal

Sources and Magnitudes of Error in High Precision Gravity Measurements
(Peter et al., 1989; Dragert et al., 1981)

"Read" error	± 2μGal
Solid Earth Tide (≈2%)	± 4μGal
Free Air (± .02 m)	± 6μGal
Atmospheric attraction and loading $\left[-0.42 \frac{\mu Gal}{mbar}\right]$	< ± 5 μGal
Meter Drift	± 20 μGal, but usually less
Ocean Loading	< 1 μGal interior sites ± 2 μGal coastal sites
Uncertainty in the seasonal groundwater level ≈±10 h (μGal) where -h/+h is the fall/rise in water level (m)	± 10 μGal
Total Possible Error	±12 to ± 22 μGal
Significant Δg_{FA}	± 24 to ± 44 μGal

Measured Fields Magnitudes of δg at Producing Geothermal Fields

Field	Reference	δg_{max} (μGal)
The Geysers	Denlinger et al., 1981	-120 ± 1974-1977
Wairakei	Allis and Hunt, 1986	-490 ± 50 1961-1967
Bulalo	Atkinson and Pedersen, 1988	-150 ± 20 (dates unknown)

Measured Magnitudes of δg Due to Natural Effects

Tectonic Deformation - Change in Elevation with Mass Redistribution	± 30 to ± 200 μGal
Seasonal Variations due to rainfall	± 10 μGal
Magmatic + fumarolic at active volcanoes	up to -800 μGal

Numerical Example (Atkinson and Pederson, 1988)

Idealized reservoir with and without natural recharge

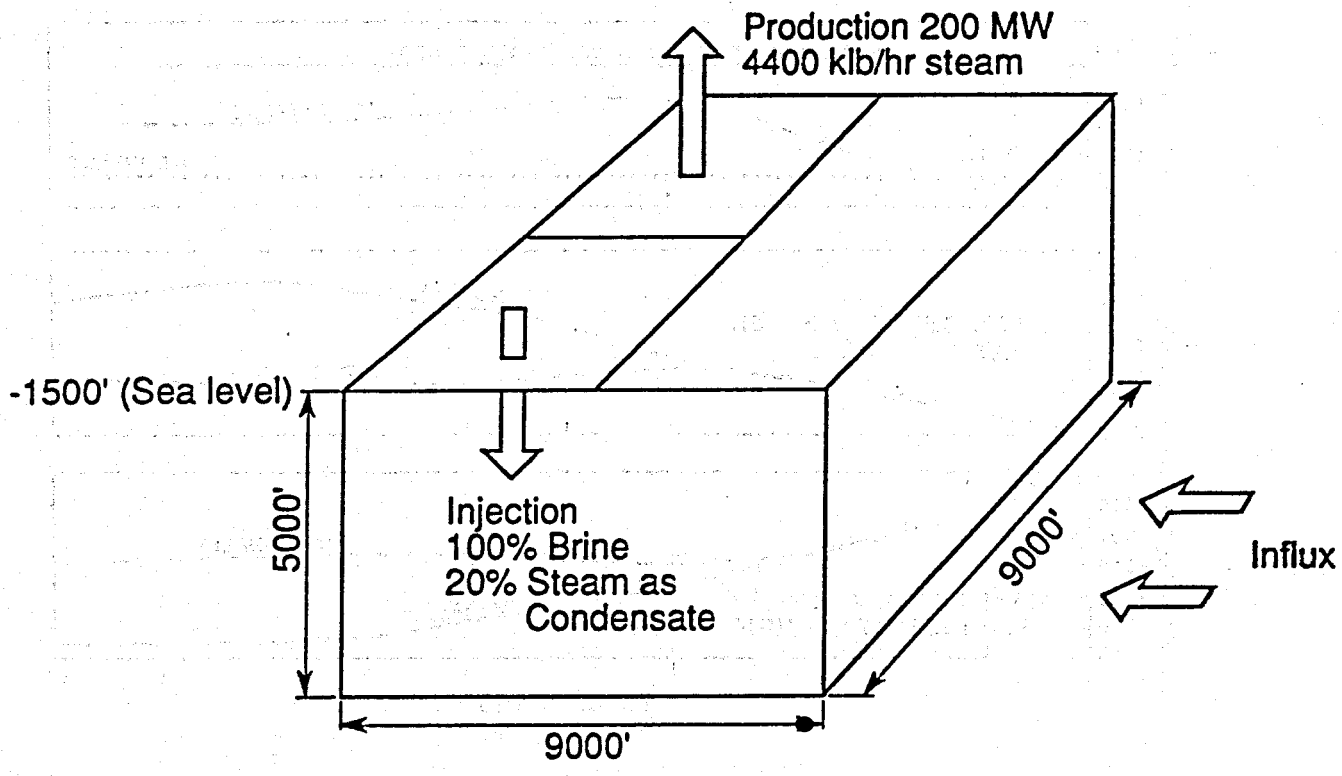

$\phi = 12\%$

$k = 100$ mD

- Initially all liquid at the boiling temperature for that depth,
- Recharge only laterally, as shown,
- Constant rates of production/injection.

XBL 895-7614

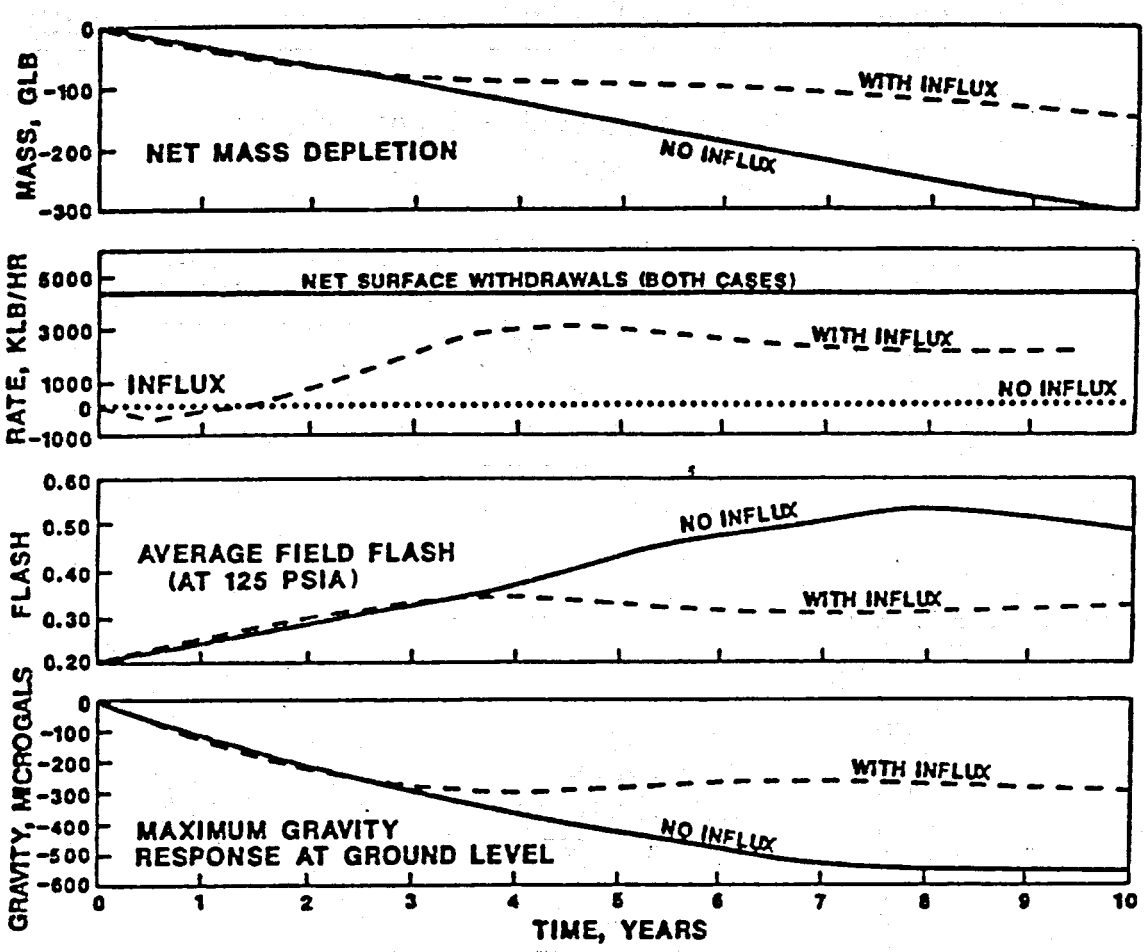

Time History of Idealized Reservoir Behavior and Change in Maximum g over the Production Area.

Effects of lateral recharge show up after 3 yrs.

Effects of injection only (no influx) show up after 5 or 6 yrs.

Some Causes of Gravity Change

Surface Deformation

- Subsidence, compaction of reservoir rocks
- Uplift, increased pore pressure due to injection.
- Subsidence/uplift due to major nearby earthquake or volcanic activity.
- Long-period motion of Earth's rotation pole changes centrifugal force.

Reservoir Conditions

- Short-Term Effects
  - Formation of a stream zone and drawdown of the top of the liquid-dominated zone.
  - Decrease in liquid saturation as steam zone dries out.
- Longer-Term Effects
  - Drop in groundwater level due to influx from shallower aquifer.
  - Increase in water density due to cooling by non-thermal water recharge.
  - Precipitation of calcite at reservoir boundaries due to heating of invading waters (minor effect)
  - Precipitation of silica due to boiling (minor effect).

Precision Gravity Caveats

1. Area of survey must extend well beyond known or inferred reservoir boundary

2. Establish 2X number of stations than needed; many will be lost to development activities.

3. Always try to carry out one precise gravity/leveling survey prior to exploitation.

4. Monitor groundwater levels during exploitation and over a large area.

5. May take 2 months to resurvey a field.

6. Gravity changes are often most pronounced during early years of field exploitation.

7. Easier to calculate ΔM than to relate it to reservoir processes.

8. Standard free-air gradient may not be correct. Can actually vary from 2.9 to > 4 μGal/cm.

9. Gravity/leveling must be tied to same stable base stations.

10. Leveling measures an "orthometric elevation change" which is distorted by local undulations in the geoid due to variations in mass distribution. Must convert to "geometric" elevation (true) change. At Cerro Prieto, the difference was 2 to 3 cm at a number of stations (Wyman, 1983).

11. Meter drift errors are assigned (usually) as if meter drift is linear with time. In fact, meter drift may be highly non-linear during first hour and so meter needs time to equilibrate after mechanical shock due to travel. Take multiple data sets and solve for station readings as a least-squares problem.

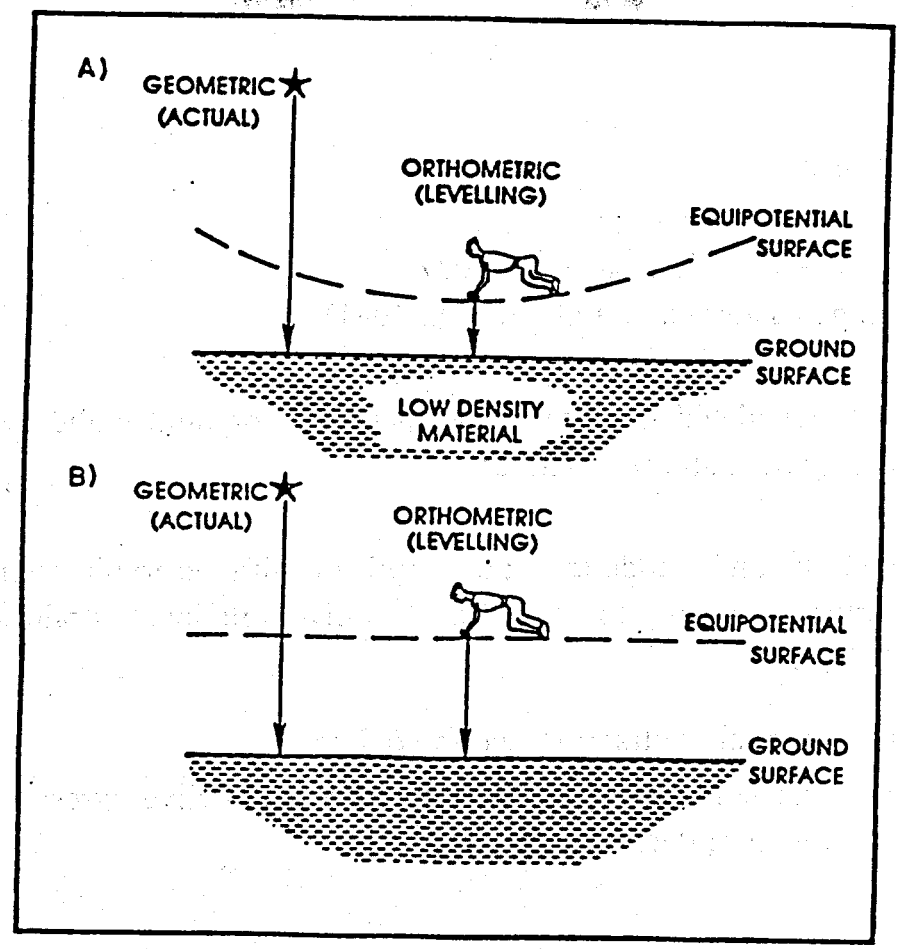

$$\Delta h_g = \frac{\Delta h_o \, \alpha/a + \Delta g}{\alpha/a - \beta}$$

Geometric Elevation Change (Whitcomb,1976)

Δh_o = Orthometric elevation change from leveling

α = 981 cm/s^2 $(\partial V/\partial Z)$

β = 3.086×10^{-6} $/s^2$ (free air gradient)

Δg = Gravity Change

a = Radius of disk-shaped region where density change is occurring

Field Example

The Geysers, California, 1974-1977
(Denlinger, Isherwood and Kovach, 1981)

1. ΔM calculated is close to the total mass of fluid withdrawn; thus negligible natural recharge.

2. Gravity and geodetic data, combined with reservoir engineering results, indicate that average negative dilational strain of 4 x 10^{-5}/y.

   - thermal contraction due to cooling
   - mechanical response to increased effective stress as pore pressure decline

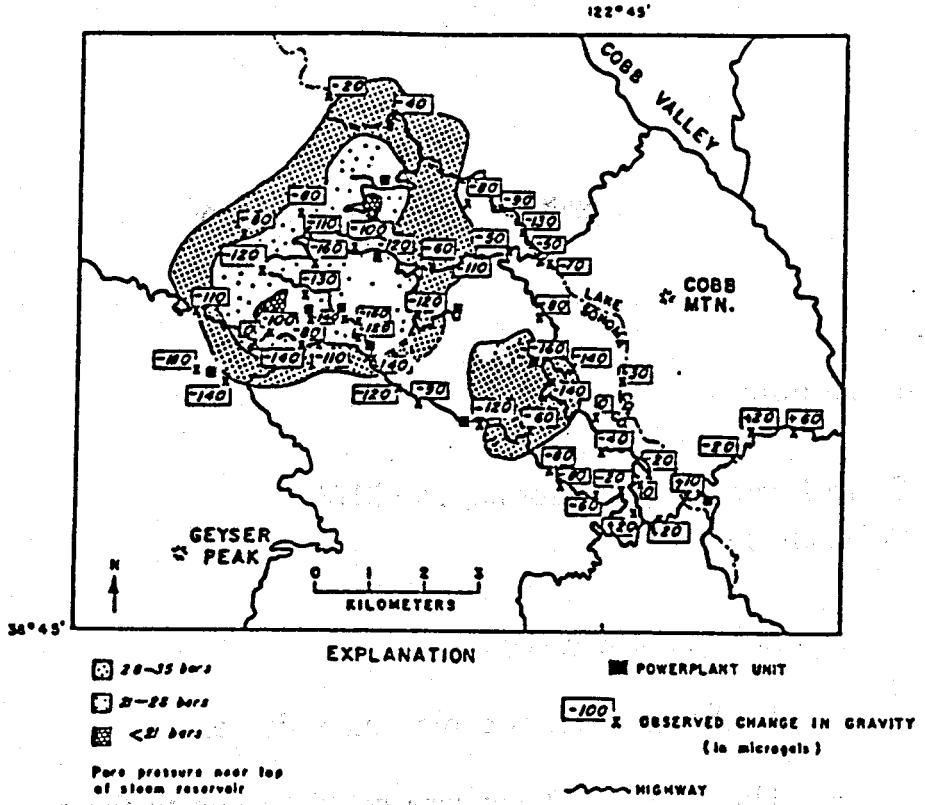

Fig. 2. Changes in surface gravity from 1974 to 1977 [*Isherwood*, 1977] compared to the pore pressure drainage near the top of the steam reservoir during early 1977 [*Lippman et al.* 1977]. In 1974 the pore pressure drainage area was approximately the same shape and about 80% of the area in 1977. The large negative values at the SW drainage boundary are suspected, since they are not corrected for elevation change.

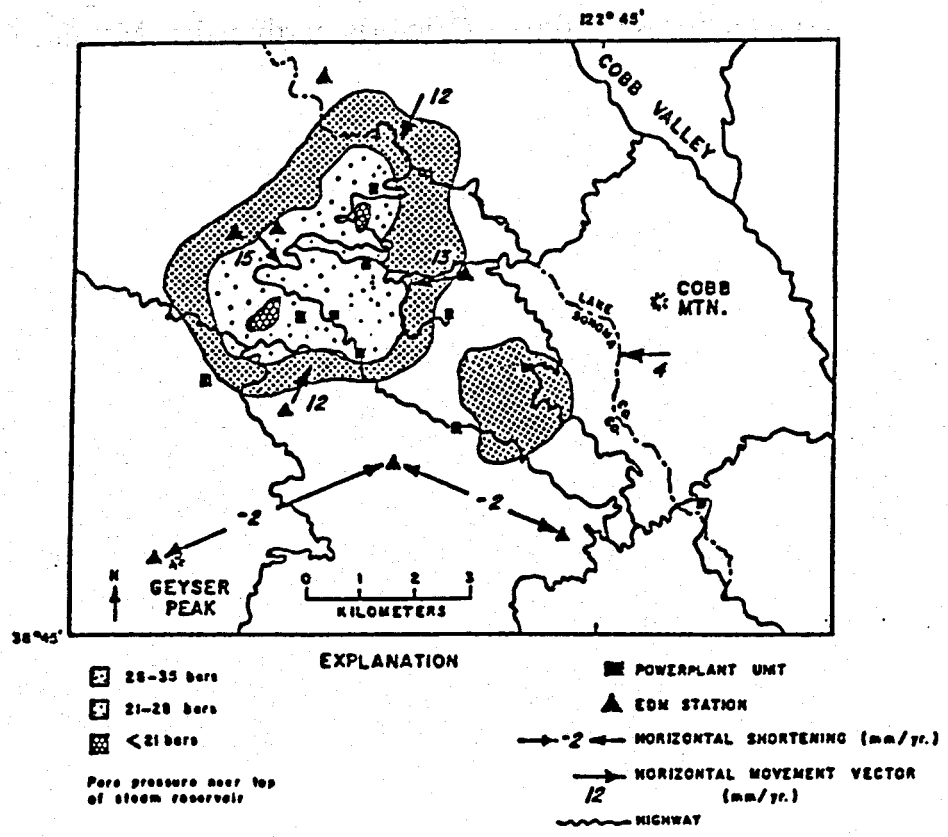

Fig. 6. Horizontal movement vectors from precision geodolite surveys [*Lofgren*, 1978] relative to the pore pressure drainage near the top of the steam reservoir during early 1977 [*Lippman et al.*, 1977].

Field Example

Cerro Prieto, Baja California, 150 MW
(Wyman, 1983)

1. Δg increased (1980-1983)

   - Recharge water is cooler, more dense.
   - Up to 10 μGal increase could be due to thermal contraction and subsidence.
   - part of the gravity increase may be due to earthquake induced compaction/subsidence (Victoria earthquake, M≈ 6+, 6/80).

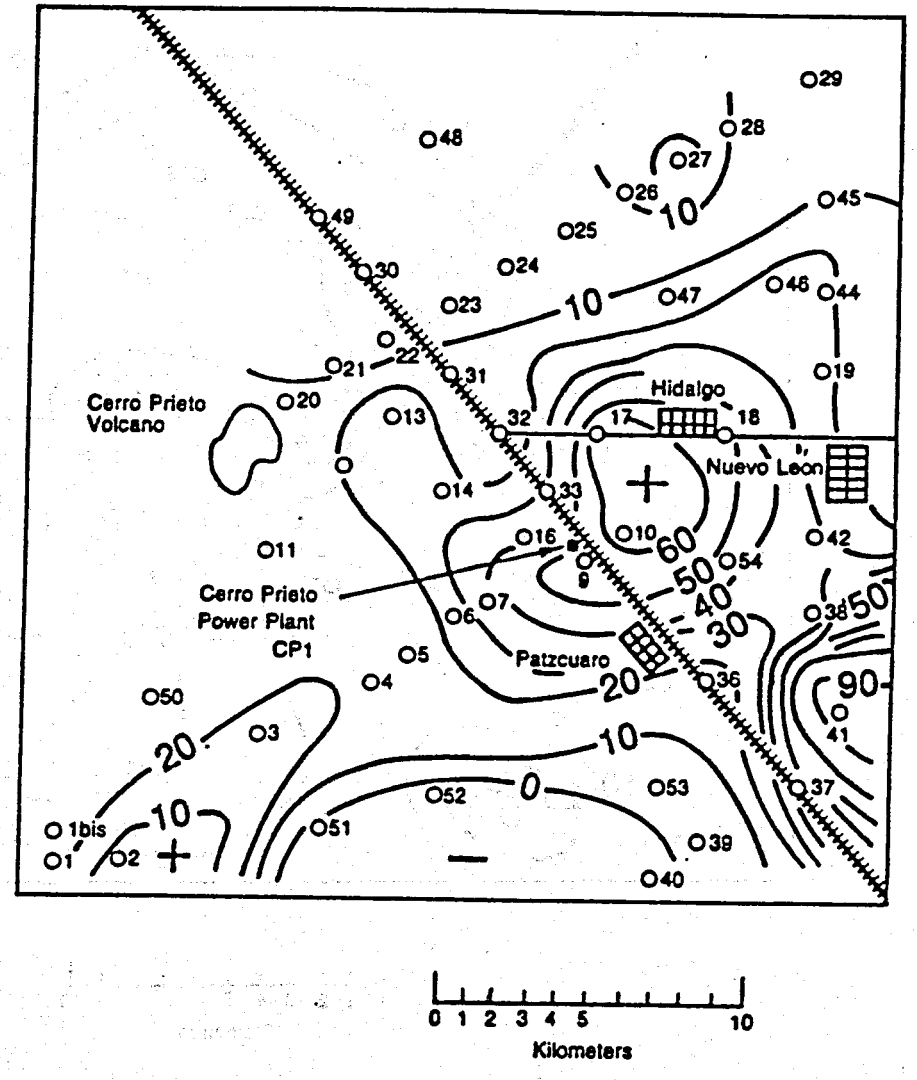

XBL 844-10312

Gravity Change 1980-1981
(Wyman, 1983)

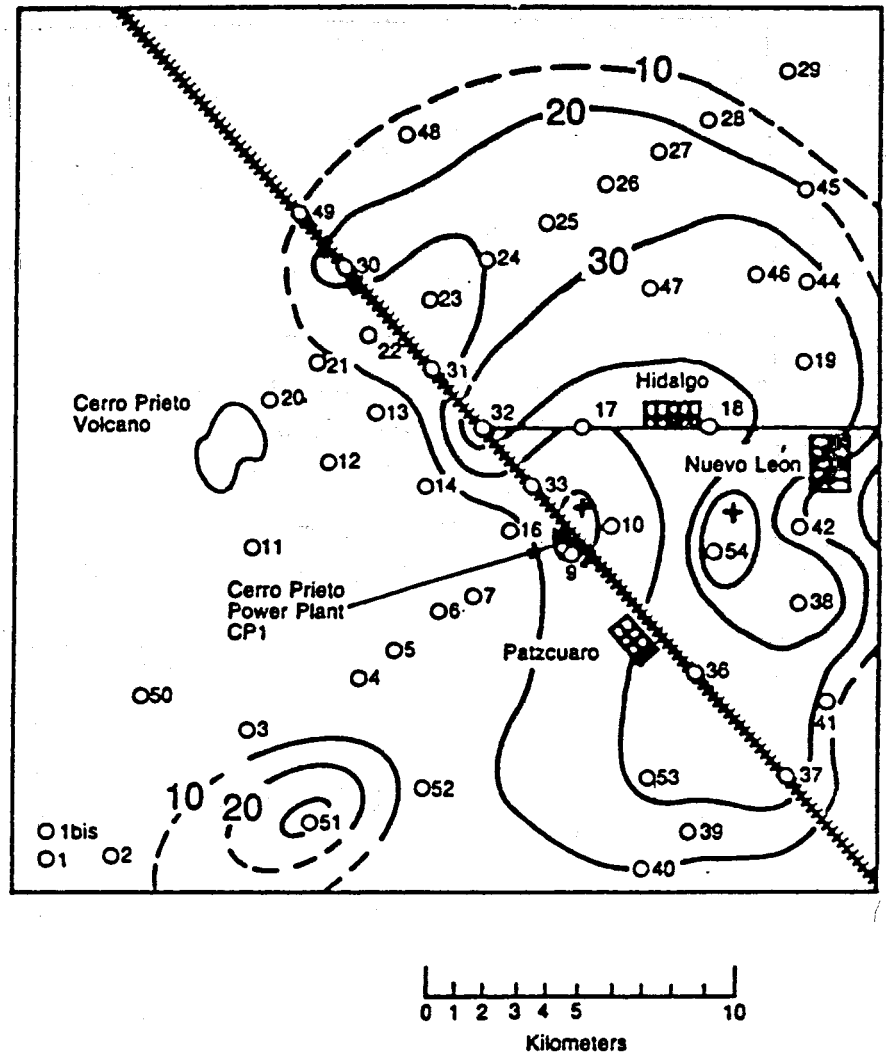

XBL 844-10317

Gravity Change 1981-1983
(Wyman, 1983)

References

Allis, R. G., and Hunt, T. V., 1986, Analysis of exploitation-increased gravity changes at Wairakei Geothermal Field: *Geophysics*, 51, 1647-1660.

Atkinson, P. G., and Pederson, J. R., 1988, Using precision gravity data in geothermal reservoir engineering modeling studies: Proc. 13th Workshop on Geoth. Reserv. Eng., Stanford Univ., Stanford, Califor., SGP-TR-113, 35-40.

Denlinger, R. P., Isherwood, W. F., and Kovach, R. L., 1981, Geodetic analysis of reservoir depletion at The Geysers steam field in northern California: *J. Geophys. Res.*, 86, 6091-6096.

Dragert, H., Lambert, A., and Liard, J., 1981, Repeated precise gravity measurements on Vancouver Island, British Columbia: *J. Geophys. Res.*, 86, 6097-6106.

Peter, G., Moose, R. E., Wessels, C. W., Faller, J. E., and Niebauer, T. M., 1989, High-precision absolute gravity observations in the United States: *J. Geophys. Res.*, 94, 5659-5674.

Whitcomb, J. H., 1976, New vertical geodesy: *J. Geophy. Res.*, 81, 4937-4944.

Wyman, R. M., 1983, Potential modeling and leveling data over Cerro Prieto geothermal field: M.S. thesis, Department of Geology, Calif. State Univ., Long Beach, Long Beach, Calif., 79 p.

DC Resistivity

Repetitive dc resistivity surveys, made at regular time intervals, can be used to monitor changes in groundwater levels and shallow recharge by less saline, non-thermal water into reservoir region.

Archie's Law

$$\rho = a\, \rho_f\, \phi^{-m}\, S^{-2},$$

where

ρ	=	bulk rock resistivity
ρ_f	=	pore fluid resistivity
ϕ	=	porosity
S	=	liquid saturation ($S \geq 0.5$)
a	=	number near unity for most rocks
m	=	number near 2 for most rocks

DC Resistivity (cont.)

DC resistivity measurements provide an apparent resistivity ρ_a value. The fractional change in ρ_a between two years is

$$\frac{\Delta\rho_a}{\rho_a} = \frac{\rho_a \text{ (year i)} - \rho_a \text{ (base year)}}{\rho_a \text{ (base year)}} ,$$

or in terms of fluid and rock parameters

$$\frac{\Delta\rho_a}{\rho_a} \approx \frac{\Delta\rho_f}{\rho_f} - \frac{2\Delta\phi}{\phi} - \frac{2\Delta S}{S} .$$

This says that the fractional change in resistivity within any discrete volume element can be expressed as the sum of effects due to

(1) change in the pore liquid resistivity
   - salinity and temperature

(2) change in connected porosity
   - compaction, chemical precipitation

(3) boiling in the reservoir
   - pore pressure changes

DC Resistivity (cont.)

In general, $\frac{\Delta\rho}{\rho}$ in the reservoir region increases with time.

$\frac{\Delta\rho_f}{\rho_f}$ increases in a positive fashion due to influx of cooler, less saline groundwater

$\frac{-2\Delta\phi}{\phi}$ increases in a positive fashion as <u>porosity decreases</u> due to pore pressure decrease, calcite, silica precipitation

$\frac{-2\Delta S}{S}$ increases in a positive fashion as <u>saturation decreases</u> due to local boiling near wells.

Of these three terms, the first is often the largest, even though the other terms contain a factor of 2.

Size of $\frac{\Delta\rho_a}{\rho}$ Expected

- 0.05 to 0.20 increase over the shallow α reservoir at Cerro Prieto between 1979 (base year) at 1983 (Wilt et al., 1984; Goldstein et al., 1985)

Size of Measurement Error Expected in $\frac{\Delta\rho_a}{\rho}$

- $\leq \pm 0.05$

Problems

- Near-surface noise effects - lead to interpretation errors
- Low resolution of $\frac{\Delta\rho}{\rho}$ at reservoir depths
- Electrode stations destroyed or inaccessible due to intensive development activities
- Need to run survey over a large area; well beyond field boundaries

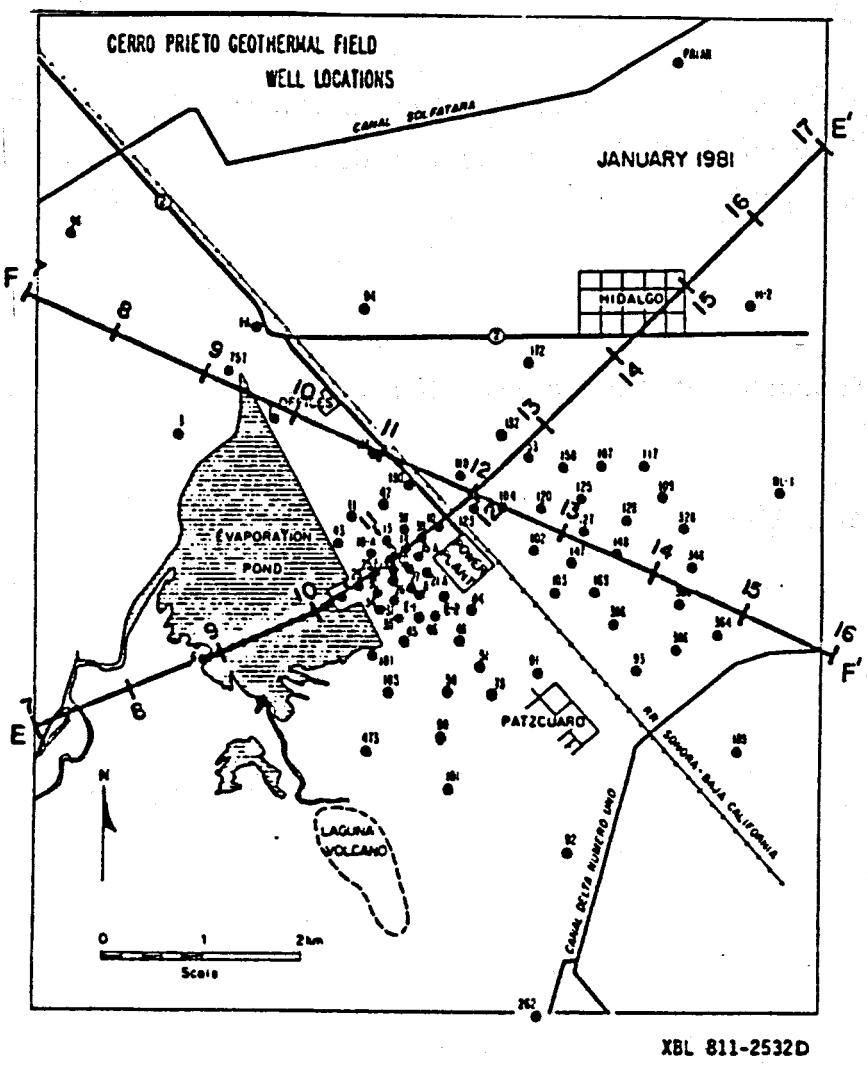

XBL 811-2532D

Fig. 1. Central part of the dipole-dipole resistivity line E-E' over the Cerro Prieto geothermal field. Wells are shown as dark circles, and those producing brine during the 1979-1983 period are mainly between electrode points 10 and 12.

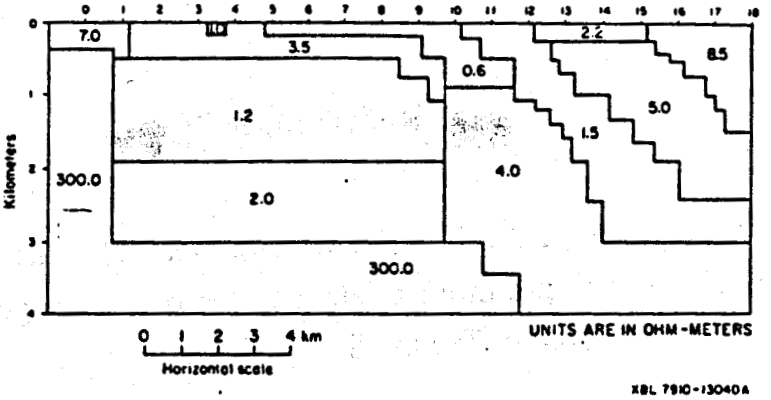

Fig. 2. Two-dimensional resistivity models for line E-E'.

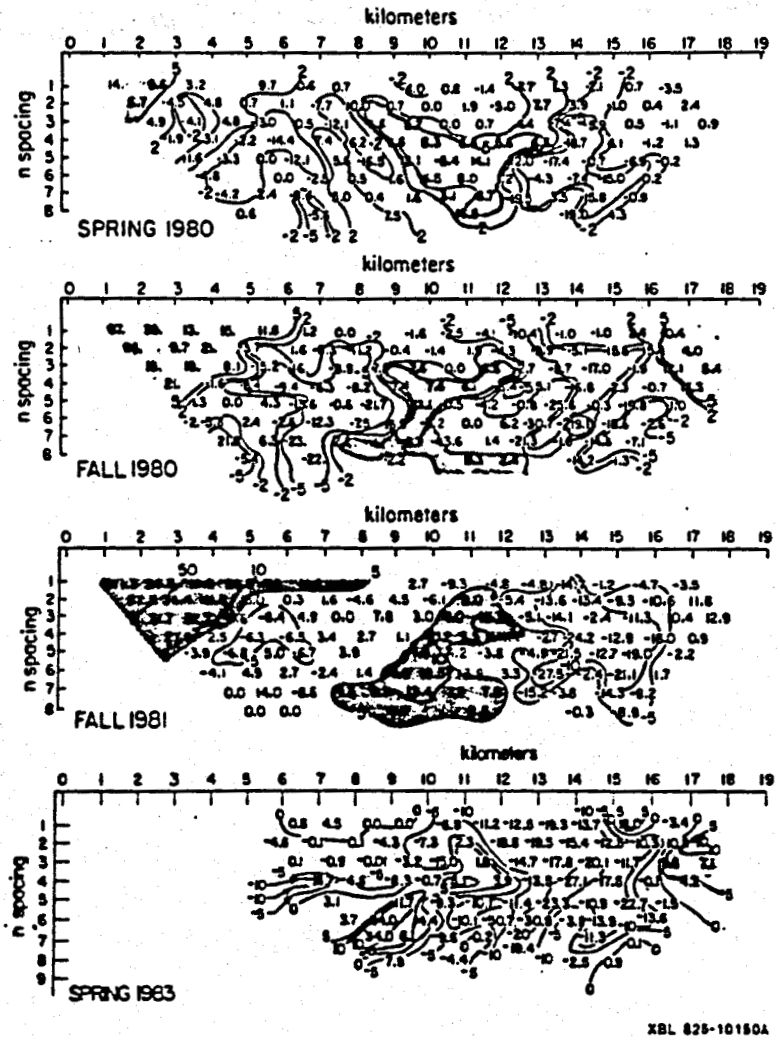

Fig. 3. Apparent resistivity pseudosections plotted as the percent change in apparent resistivity relative to the 1979 data set. Areas of dark stipple show increases >5%; areas of light stipple show decreases >5%.

References

Wilt, M. J., Goldstein, N. E., and Sasaki, Y., 1984, Long-term dipole-dipole resistivity monitoring at the Cerro Prieto geothermal field: *Geoth. Resour. Counc. Trans.*, 8, 235-240.

Goldstein, N. E. Sasaki, Y., and Wilt, M. J., 1985, Two-dimensional inversion of resistivity monitoring data from the Cerro Prieto geothermal field, Mexico: *Geoth. Resour. Counc. Trans.*, 9, pt. II, 17-24.

MEQ Monitoring

Continuous monitoring of local microearthquake (MEQ) activity indicates a close correlation between the temporal/spatial distribution and magnitudes and fluid production; e.g., The Geysers.

Causes of MEQ

- Volumetric contraction due to fluid extraction and boiling (cooling)

- Boiling and silica deposition increases coefficient of friction; aseismic deformation changes to stick-slip

The first cause is supported by subsidence and horizontal deformation measurements.

MEQ activity propagates downward with time in vicinity of production wells.

High Resolution MEQ Monitoring System

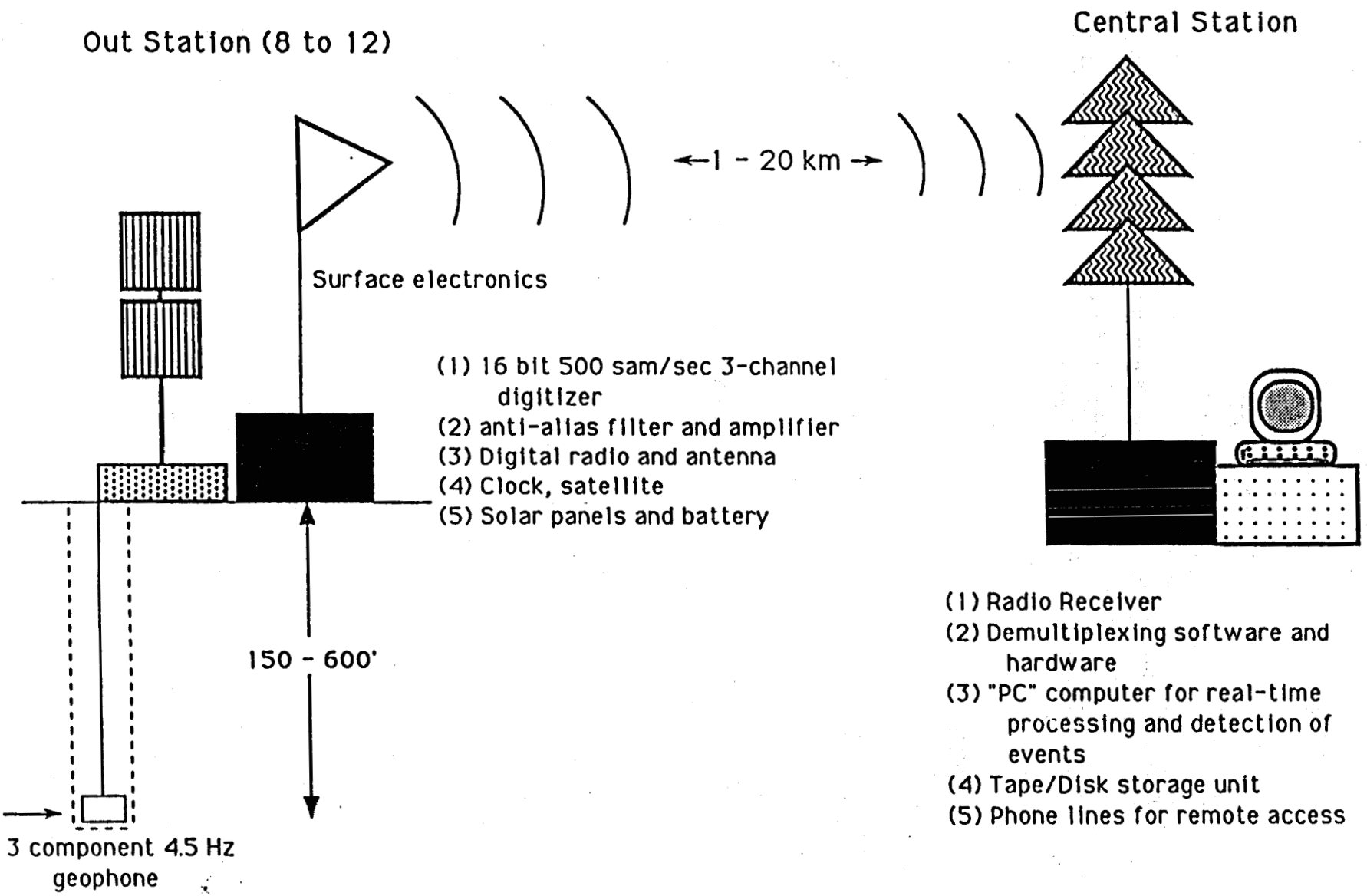

Information from Seismic Array Studies

Changes in Local Seismicity

Time history of MEQ activity indicates where pressure drops are large enough to cause large-scale boiling.

Changes in Elastic Wave Parameters

Temporal changes in P- and S-wave velocity ratio (V_p/V_s) structure with depth may help define reservoir boundaries.

$$V_p = \left[\frac{K + 4/3\mu}{\rho}\right]^{1/2}$$

$$V_s = \left[\frac{\mu}{\rho}\right]^{1/2}$$

K = bulk modulus

μ = shear modulus

$$\sigma = \frac{\left[\frac{V_p}{V_s}\right]^2 - 2}{2\left[\left[\frac{V_p}{V_s}\right]^2 - 1\right]}$$

σ = Poisson's ratio

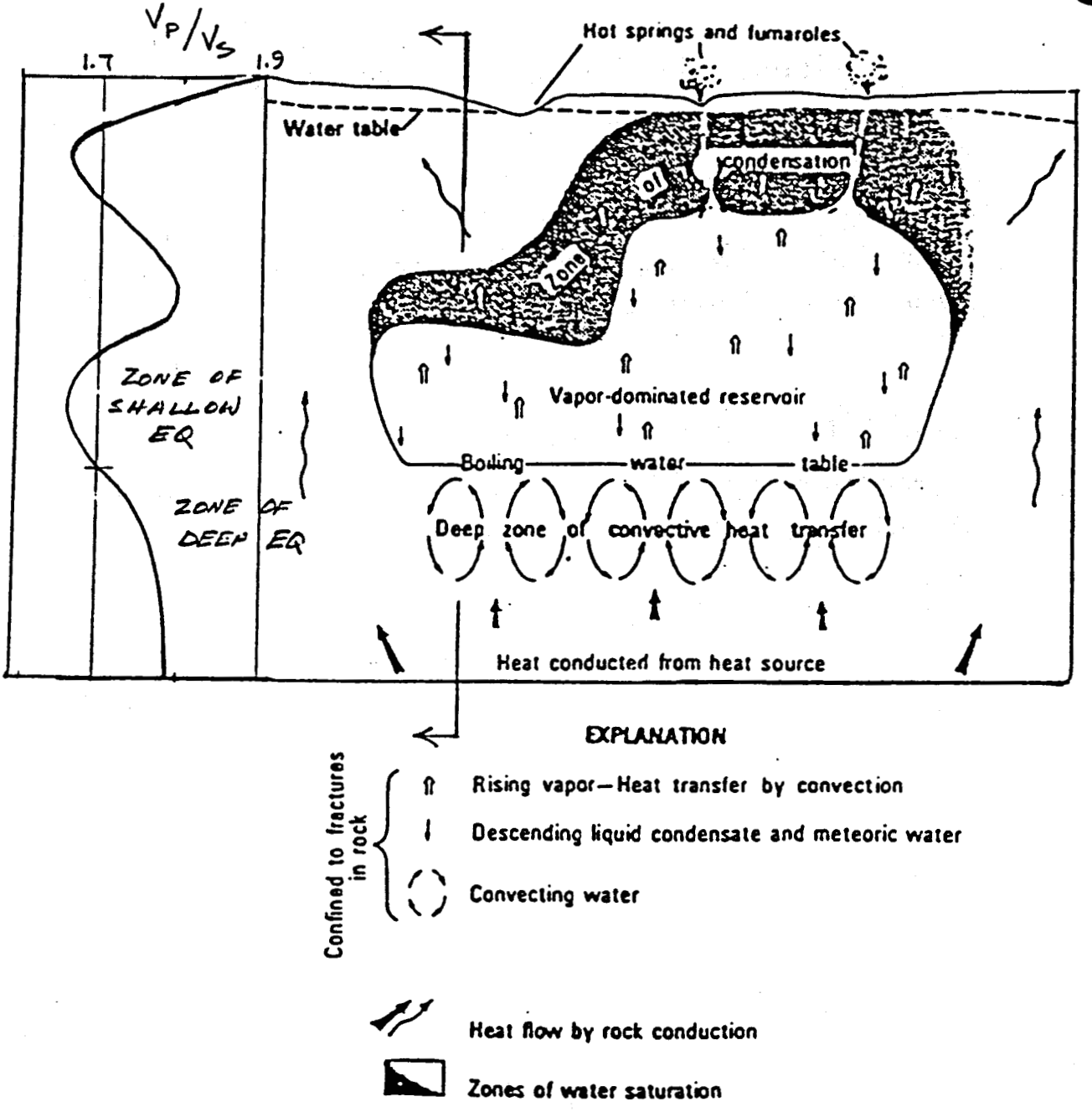

Model of a vapor-dominated system (after White et al., 1971) and the observed V_p/V_s and depths of earthquake foci at The Geysers (after O'Connell, 1986).

References

Majer, E. L., and McEvilly, T. V., 1979, Seismological investigations at The Geysers Geothermal Field: *Geophysics*, 44, 246-269.

O'Connell, D. R., 1986, Seismic velocity structure and microearthquake source properties at The Geysers, California geothermal area: Ph.D. thesis, Dept. Geology and Geophysics, Univ. California Berkeley, Lawrence Berkeley Laboratory Report, LBL-22280, 204 p.

Oppenheimer, D. H. 1985, Induced seismicity mechanism at The Geysers, California: *Geotherm. Resour. Counc. Trans.*, 9, Pt. 2, 41-44.

Toksöz, M. N., Cheng, C. H., and Timur, A., 1976, Velocities of seismic waves in porous rocks: *Geophysics*, 41, 621-645.

White, D. E., Muffler, L. J. P., and Truesdell, A. H., 1971, Vapor-Dominated hydrothermal systems compared with hot water systems: *Econ. Geol.*, 66, 57-97.

Geothermal Resources Council

Workshop on

Responses of a Geothermal Field During Exploitation

A Reservoir Management Plan

Geochemical Monitoring - Surface and Subsurface

by
Cathy Janik
U.S. Geological Survey

15 - 16 June 1989

The Shattuck Hotel

Berkeley Conference Center

Berkeley, California

Introduction

Geochemistry has wide application in each stage of geothermal reservoir assessment.

A. Exploration

Temperature, fluid chemistry, isotope composition and surface discharge rates are used to identify origin of recharge and to estimate subsurface temperatures, subsurface fluid composition, and direction of fluid flow.

B. Evaluation

Chemistry and temperature of well fluids from exploratory drill holes are used to characterize conditions in the deep system.

1. Fluid-rock interaction
2. Reservoir fluid homogeneity
3. Natural reservoir processes

C. Exploitation

Monitoring fluid chemistry and isotope compositions of well discharges to detect induced reservoir processes

1. Changes in rock-water heat transfer
2. Cold water inflow
3. Aquifer boiling
4. Mineral deposition
5. Fluid migration

Utilization of chemistry in field and power plant operations

Geochemical Monitoring

- To forecast individual well and field-wide behavior in order to establish a good field management and development program
- To detect temporal and spatial changes in chemical characteristics of thermal and non thermal fluids in the system
- To indicate favorable zones for new drilling

A. Define baseline conditions

1. Chemical characteristics of non thermal ground waters.
   a. Literature search to identify natural changes with time, location, or depth of aquifer.
   b. Determine chemical signatures for each water type recharging the system.
2. Chemical characteristics of thermal ground waters
   a. Sample springs and wells
   b. Determine reservoir fluid composition
   c. Mixing with non thermal water?
   d. Fluid-rock correlations

B. Define projected development

1. Heat extraction - chemical effects
2. Waste disposal - environmental effects
3. Injection - interaction between fluids

C. Define data requirements
   1. Sensitivity and limits of detection depend upon
      a. Chemical contrasts between different waters in the system
      b. Natural variations in chemical characteristics
      c. Environmental sensitivity and EPA constraints
      d. Well distribution density and size of the development
      e. Available analytical techniques
   2. Determine sampling frequency and distribution, significant chemical and physical parameters, and sampling and analysis methods to be utilized

Note: The primary goal of geothermal fluid sampling is to obtain representative samples that will reflect the character and chemical composition of the fluid phase(s) (water, steam, gas) present in the reservoir. To ensure a common data base to compare, classify and interpret the analytical results, a geochemical investigation should include both chemical and isotopic measurements. A minimum set of parameters for all water samples should include collection temperature, pH, Na, K, Mg, Ca, SiO_2, Cl, SO_4, HCO_3, CO_3, δD, and $\delta^{18}O$. A basic gas analysis should include CO_2, H_2S, He, H_2, Ar, O_2, N_2, and CH_4; $\delta^{13}C$ in CO_2 is optional, but highly desirable. The molar gas/steam ratio and the isotopic composition (δD and $\delta^{18}O$) of steam should be measured for samples from wells and superheated steam vents. In addition, it is essential to have physical data linked with the chemical data from two-phase well samples for calculations of aquifer compositions. These physical parameters are separation temperature (or pressure) and total discharge enthalpy (or steam and water flow rates).

D. Sample collection and analysis
   1. Natural steam vents and hot springs
   2. Design of steam-water separation and transmission equipment for wells
      a. Sampling points
      b. Portable cyclone separators
   3. Chemical stabilization and storage
      a. Evaporation
      b. Loss of volatiles
      c. Oxidation reactions
      d. Mineral precipitation
   4. Quantity requirements
   5. Note taking
   6. Field determination (on site)
   7. Laboratory measurements
   8. Sampling frequency
      a. Well test, every 1 to 2 hours at first; then daily until stable production is attained
      b. Subsequent frequency depends upon rate of observed changes, monthly to annually

E. Data storage and retrieval systems (data processing)
   1. Store data sets of analyses and sampling information
   2. Retrieve data for tabulations and graphs
   3. Process results to produce downhole concentrations, ratios of chemical constituents, chemical geothermometer temperatures, and equilibrium calculations.

F. "Tools" for interpretation and correlation of geochemical data
   1. Variations with time
      a. Chemical geothermometer temperature
      b. isotope compositions
      c. gas compositions and gas content of total discharge
      d. Chemical compositions
   2. Correlations between variables
      a. Enthalpy - Cl diagrams
      b. Cl vs SiO_2 geothermometer temperatures
      c. Gas geothermometer diagrams
   3. Variations within a field using contour diagrams

G. More on monitoring natural activity:
   Physical and chemical changes can indicate lateral spread of effects from production
   1. Decreased surface activity
   2. High-Cl springs replaced by fumaroles or steam-heated groundwater
   3. Hydrothermal blowouts

Geochemical Monitoring

Selected References

Cole, D.R., 1982. Chemical and sulfur isotope variations in a thermal spring system sampled through time. Trans. Geother. Resourc. Counc., 6:81-84.

D'Amore, F. and Panichi, C., 1980. Evaluation of deep temperatures of hydrothermal systems by a new gas geothermometer. Geochim. Cosmochim. Acta, 44:549-556.

Ellis, A.J., and Mahon, W.A.J., 1977. Chemistry and Geothermal Systems. New York, Academic Press, 392pp.

Farrar, C.D., Sorey, M.L., Rojstaczer, S.A., Janik, C.J., Mariner, R.H., Winnett, T.L., and Clark, M.D., 1985. Hydrologic and geochemical monitoring in Long Valley caldera, Mono County, California, 1982-1984. U. S. Geological Survey Water Resourc. Investig. Rept. 85-4183, 137pp.

Farrar, C.D., Sorey, M.L., Rojstaczer, S.A., Janik, C.J., Winnett, T.L., and Clark, M.D., 1987. Hydrologic and geochemical monitoring in Long Valley caldera, Mono County, California, 1985. U. S. Geological Survey Water Resourc. Investig. Rept. 87-4090, 71pp.

Fournier, R.O., 1979. A revised equation for the Na/K geothermometer. Trans. Geother. Resourc. Counc., 3:221-224.

Fournier, R.O., 1981. Application of water geochemistry to geothermal exploration and reservoir engineering, Ch. 4 in L. Rybach and L.J.P. Muffler (eds.), Geothermal Systems: Principals and Case Histories. New York, John Wiley, pp. 109-143.

Fournier, R.O. and Potter, R.W., 1982. An equation correlating the solubility of quartz in water from 25° to 900°C at pressures up to 10,000 bars. Geochim. Cosmochim. Acta, 46:1969-1974.

Fournier, R.O. and Truesdell, A.H., 1973. An empirical Na-K-Ca geothermometer for natural waters. Geochim. Cosmochim. Acta, 37:1255-1275.

Giggenbach, W.F., 1986. Graphical techniques for the evaluation of water/rock equilibration conditions by use of Na, K, Mg and Ca contents of discharge waters. Proc. 8th New Zealand Geothermal Workshop, pp. 37-43.

Giggenbach, W.F. and Goguel, R.L., 1988. Collection and analysis of geothermal and volcanic water and gas samples (3d ed.). New Zealand DSIR Rept. No. C.D. 2387, 53 pp.

Giggenbach, W.F., Gonfiantini, R., Jangi, B.L. and Truesdell, A.H., 1983. Isotopic and chemical composition of Parbati Valley geothermal discharges, N.W. Himalayas, India. Geothermics, 12:199-222.

Henley, R.W., Truesdell, A.H. and Barton, P.B., 1984. Fluid-mineral equilibria in hydrothermal systems. Rev. Econ. Geol., 1:267 pp.

Hochstein, M.P. (ed.), 1982. Introduction to Geothermal Prospecting. New Zealand, Univ of Auckland, Geothermal Institute, 155pp.
[Chapter I. Geochemistry and geochemical exploration of geothermal systems: T.A. Turney, I.1-I.12, p.1-25; P. Blattner and J.R. Hulston, I.13-I.15, p.26-33; R.W. Henley and W.A.J. Mahon, I.16-I.17, p.34-45.]

Kindle, C.H., and Woodruff, E.M., 1981. Techniques for geothermal liquid sampling and analysis. Richland, Wash., Pacific Northwest Laboratory, PNL-3801/UC-66d. 56pp.

Keenan, J.H., Keyes, F.G., Hill, P.G. and Moore, J.G., 1969. Steam tables, thermodynamic properties of water including vapor, liquid and solid phases. New York, Wiley, 162 pp.

Klyen, L.E., 1982. Sampling techniques for geothermal fluids. New Zealand, Dept. of Scientific and Industrial Research Rept. C.D. 2322, 88pp.

Mahon, W.A.J., 1966. A method for determining the enthalpy of a steam-water mixture discharged from a geothermal drill hole. New Zealand J. Sci., 9:791-800.

McKenzie, W.F. and Truesdell, A.H., 1977. Geothermal reservoir temperatures estimated from the oxygen isotope compositions of dissolved sulfate and water from hot springs and shallow drill holes. Geothermics, 5:51-61.

Nehring, N. L., and D'Amore, F., 1984. Gas chemistry and thermometry of the Cerro Prieto, Mexico, geothermal field. Geothermics, 13:75-89.

Nehring, N.L. and Truesdell, A.H., 1978. Collection of chemical, isotope and gas samples from geothermal wells, in Proc., 2nd Workshop on Sampling Geothermal Efficients, Las Vegas, Nevada, February 1977. Environmental Protection Agency Rept. EPA-600/7-78-121, pp. 130-140.

Owen, L.B., and Michels, D.E., 1984. Geochemical Engineering Reference Manual. Dept. of Energy Rept. DOE/SF/11520-T1, 530pp.

Pimentel, K.D., Ireland, R.R., and Tompkins, G.A., 1978. Chemical fingerprints to assess the effects of geothermal development on water quality in Imperial Valley. Trans. Geother. Resourc. Counc., 2:527-530.

Sheppard, D.S. and Giggenbach, W.F., 1985. Methods for the analysis of geothermal and volcanic waters and gases. New Zealand DSIR Rept. No. C.D. 2364, 78 pp.

Sheppard, D.S. and Truesdell, A.H., 1985. A GC-system for the analysis of residual geothermal gases. Chromatographia, 20:681-682.

Sorey, M.L., 1986. Hot spring monitoring at Lassen Volcanic National Park, Calif. 1983-1985. Proc. 11th Workshop on Geother. Reservoir Eng., Stanford Univ., Stanford, Calif., pp. 141-147.

Sorey, M.L., 1988. A hyrologic monitoring program to detect potential impacts of geothermal development in Long Valley caldera, California. Proc. 13th Workshop on Geother. Reservoir Eng., Stanford Univ., Stanford, Calif., pp. 121-124.

Truesdell, A.H., 1976. Summary of section III, Geochemical techniques in exploration, in Proc. 2nd U.N. Symp. on the Development and Use of Geothermal Resources, San Francisco, Calif., 1975, v. 1, pp. liii-lxxix.

Truesdell, A.H. and Fournier, R.O., 1977. Procedure for estimating the temperature of a hot-water component in a mixed water by using a plot of dissolved silica versus enthalpy. J. Res. US Geol. Surv., 5:49-52.

Truesdell, A.H., Nathenson, M. and Rye, R.O., 1977. The effects of subsurface boiling and dilution on the isotopic compositions of Yellowstone thermal waters. J. Geophys. Res., 82:3694-3703.

Trujillo, P., Counce, D., Grigsby, C., Goff, F. and Shevenell, L., 1987. Chemical analysis and sampling techniques for geothermal fluids and gases at the Fenton Hill Laboratory. Los Alamos National Laboratory Rept. LA-11006-MS, 84 pp.

U.S. Standard Atmosphere, 1962. U.S. Com. on Extension of the Standard Atmosphere, NASA, USAF and USWB report.

Weiss, R., 1978. Ground water monitoring methodology for geothermal development. Trans. Geother. Resourc. Counc., 2:709-712.

References for Gas Equilibria

D'Amore, F. and Celati, C., 1983, Methodology for calculating steam quality in geothermal reservoirs: Geothermics, v. 12, no. 2-3, p. 129-140.

D'Amore, F., Celati, R., Calore, C., 1982, Fluid geochemistry applications in reservoir engineering (vapor-dominated systems): Proceedings, 8th Workshop on Geothermal Reservoir Engineering, Stanford, December 14-16, 1982, p. 295-308.

D'Amore, F., Fancelli, R., Saracco, L., and Truesdell, A.H., 1987, Gas geothermometry based on CO content--Application in Italian geothermal fields: Proceedings, 1987 Stanford Geothermal Reservoir Engineering Workshop Vol. 12, p. 247-252.

D'Amore, F. and Truesdell, A.H., 1980, Gas thermometry for drillhole fluids from vapor-dominated and hot-water geothermal fields: Proceedings, 6th Workshop on Geothermal Reservoir Engineering, Stanford, December 1980, p. 351-360.

D'Amore, F. and Truesdell, A.H., 1985, Calculation of geothermal reservoir temperatures and steam fraction from gas compositions: 1985 International Symposium on Geothermal Energy, Geothermal Resources Council Transactions, v. 9, pt. 1, p. 305-310.

Ellis, A.J., 1957, Chemical equilibrium in magmatic gases: American Journal of Science, v. 255, p. 416-431.

Giggenbach, W.F., 1980, Geothermal gas equilibria: Geochimica et Cosmochimica Acta, v. 44, p. 2021-2032.

Hulston, J.R. and McCabe, W.J., 1962, Mass spectrometer measurements in the thermal areas of New Zealand. Part 1. Carbon dioxide and residual gas analyses: Geochimica et Cosmochimica Acta, v. 26, p. 383-397.

King, M.B., 1969, Phase equilibria in mixtures, v. 9 of International series of monographs in chemical engineering: Oxford, Pergamon Press, 584 p.

Nieva, D., Fausto, J.J., Gonzalez, J., and Garibaldi, F., 1982, Vapor flow into the feeding zone of Cerro Prieto I wells: Proceedings, 4th Symposium on the Cerro Prieto Geothermal Field, Baja California, Mexico, p. 455-467.

Truesdell, A.H., 1980, Aquifer boiling may be normal in exploited high-temperature geothermal systems: Proceedings, 5th Workshop on Geothermal Reservoir Engineering, Stanford, December 1979, p. 299-303.

Truesdell, A.H., D'Amore, F., and Nieva, D., 1984, The effects of localized aquifer boiling on fluid production at Cerro Prieto: Geothermal Resources Council Transactions, v. 8, p. 223-229.

Truesdell, A.H., and Janik, C.J., 1986, Reservoir processes and fluid origins in the Baca geothermal system, Valles Caldera, New Mexico: Journ. Geophys Res., v. 91, p. 1817-1833.

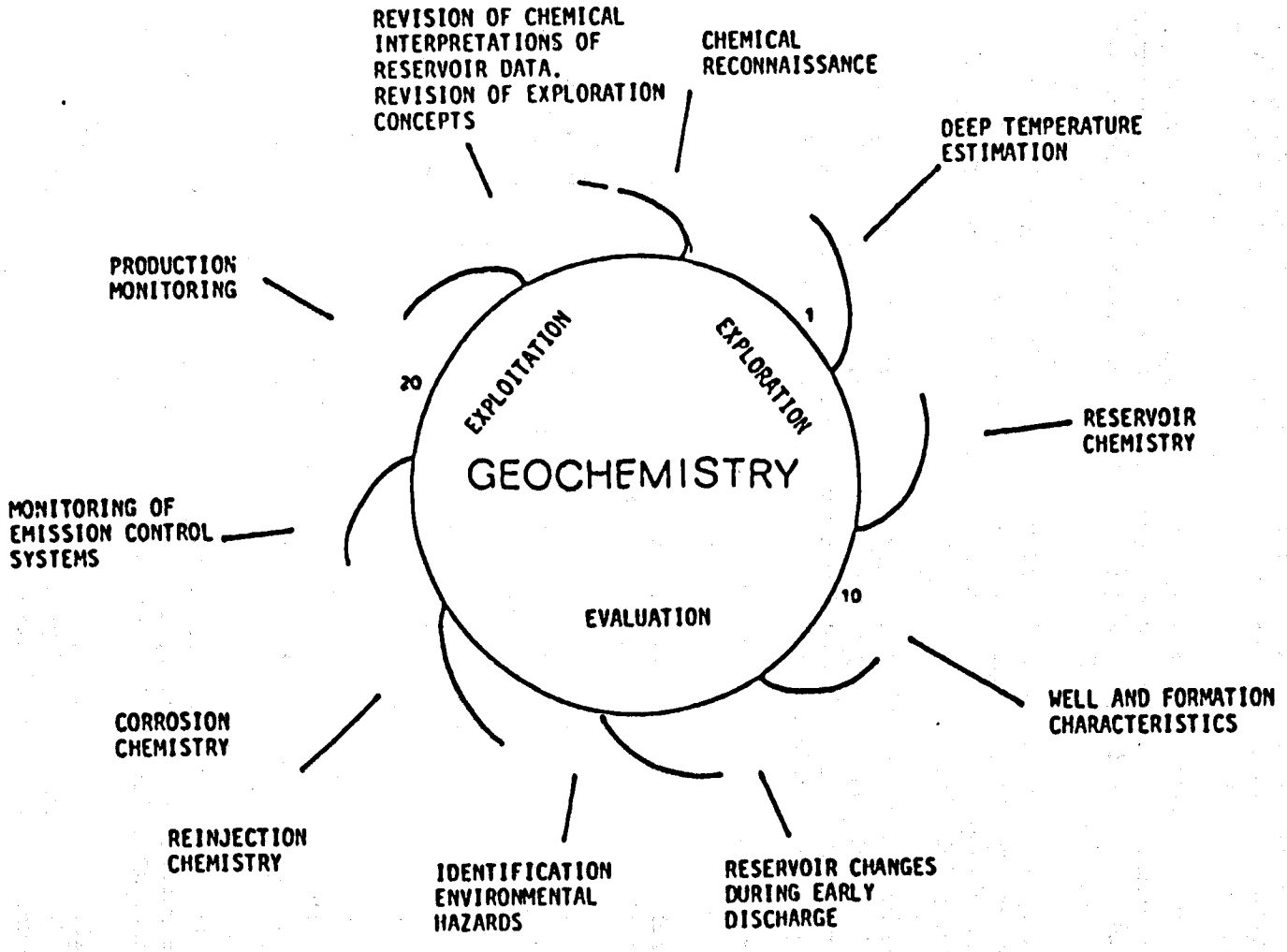

The geochemical "whirlwind": illustrating the continuity of chemical studies and interpretation from the exploration to exploitation stages and the feedback into the exploration of systems in other areas. (The numbers 1, 10, 20 indicate the approximate number of deep wells available at different stages).

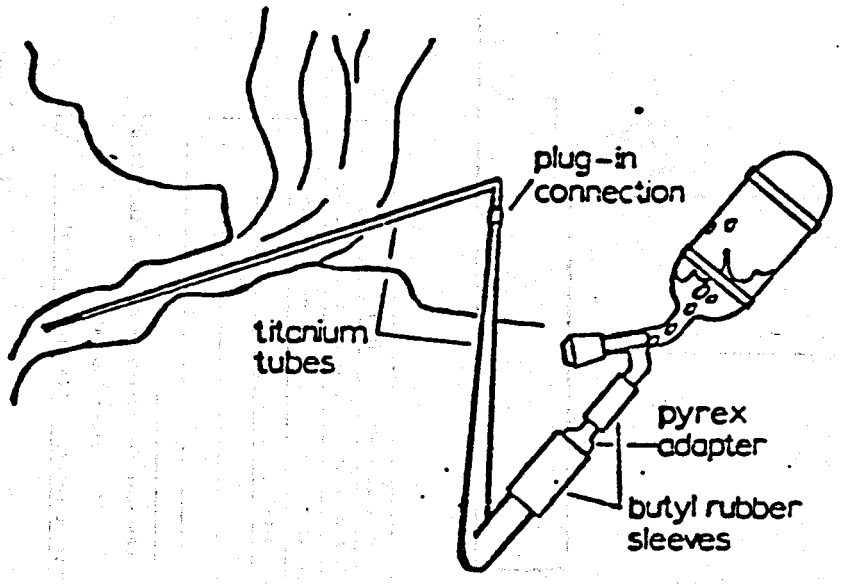

Sampling of steam vents

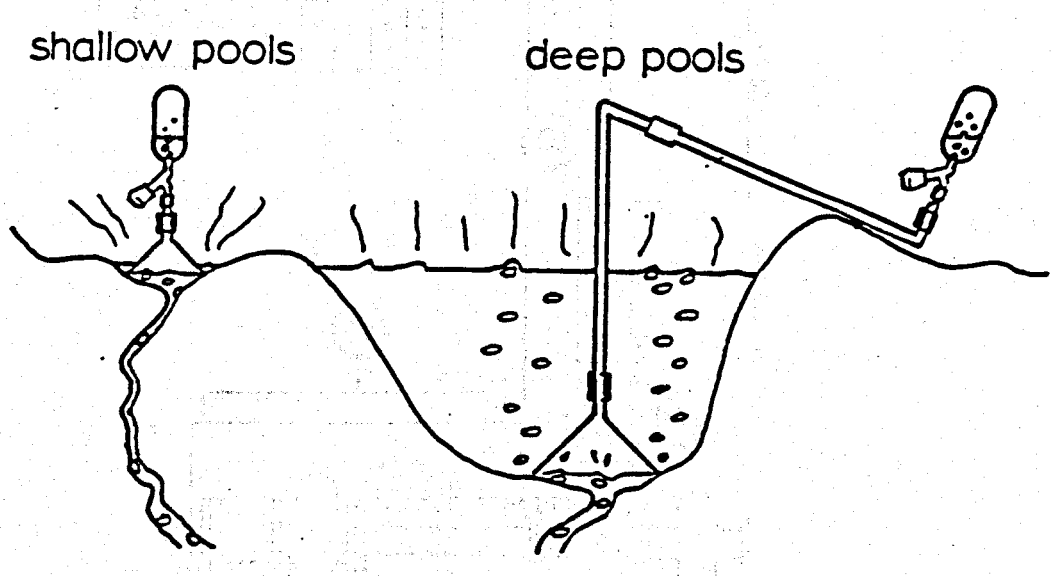

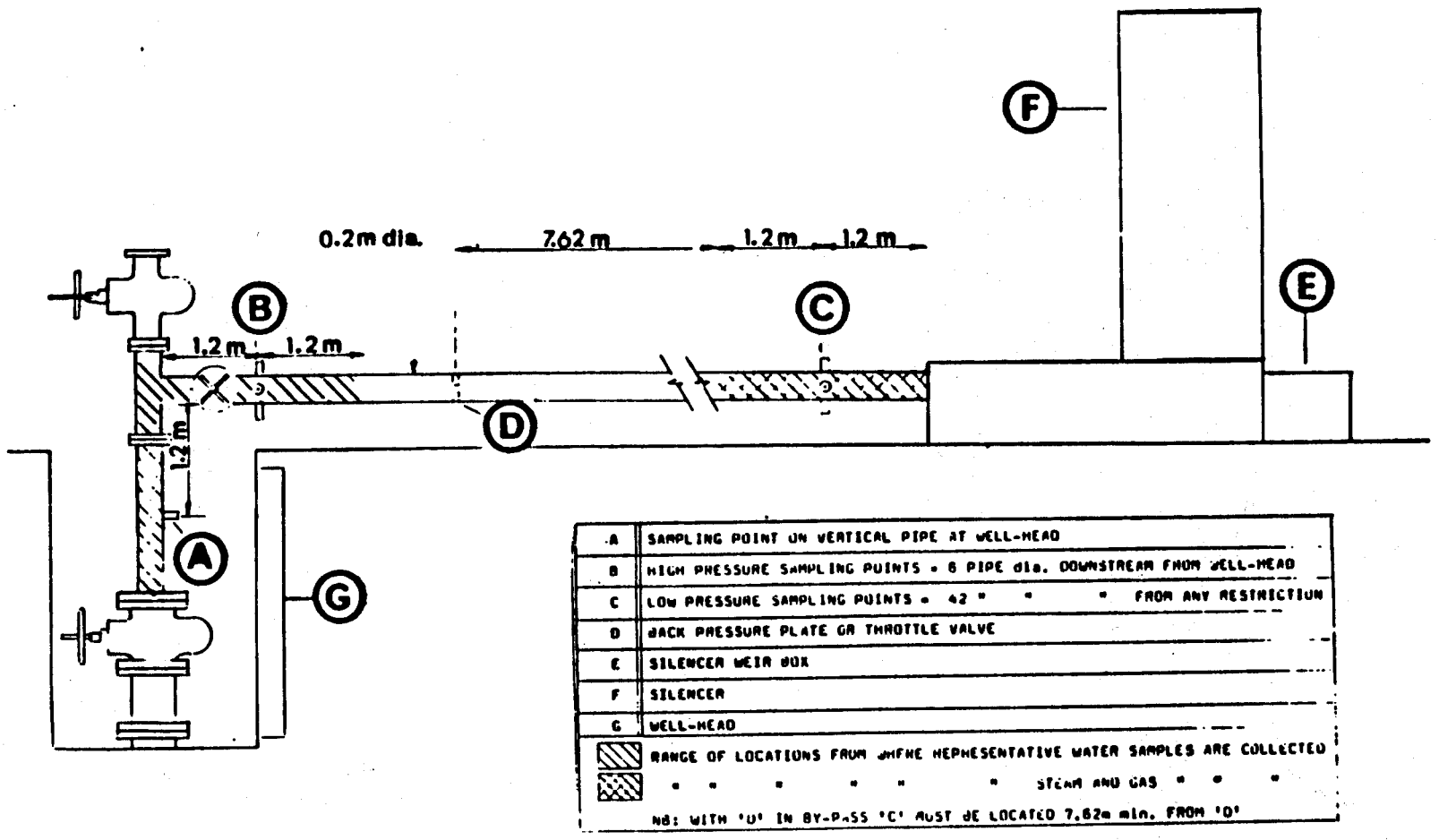

A	SAMPLING POINT ON VERTICAL PIPE AT WELL-HEAD
B	HIGH PRESSURE SAMPLING POINTS = 6 PIPE dia. DOWNSTREAM FROM WELL-HEAD
C	LOW PRESSURE SAMPLING POINTS = 42 " " " FROM ANY RESTRICTION
D	BACK PRESSURE PLATE OR THROTTLE VALVE
E	SILENCER WEIR BOX
F	SILENCER
G	WELL-HEAD
	RANGE OF LOCATIONS FROM WHERE REPRESENTATIVE WATER SAMPLES ARE COLLECTED
	" " " " " " STEAM AND GAS " " "

NB: WITH 'D' IN BY-PASS 'C' MUST BE LOCATED 7.62m min. FROM 'D'

L.E. Klyen

Figure 1. A simple by-pass installation

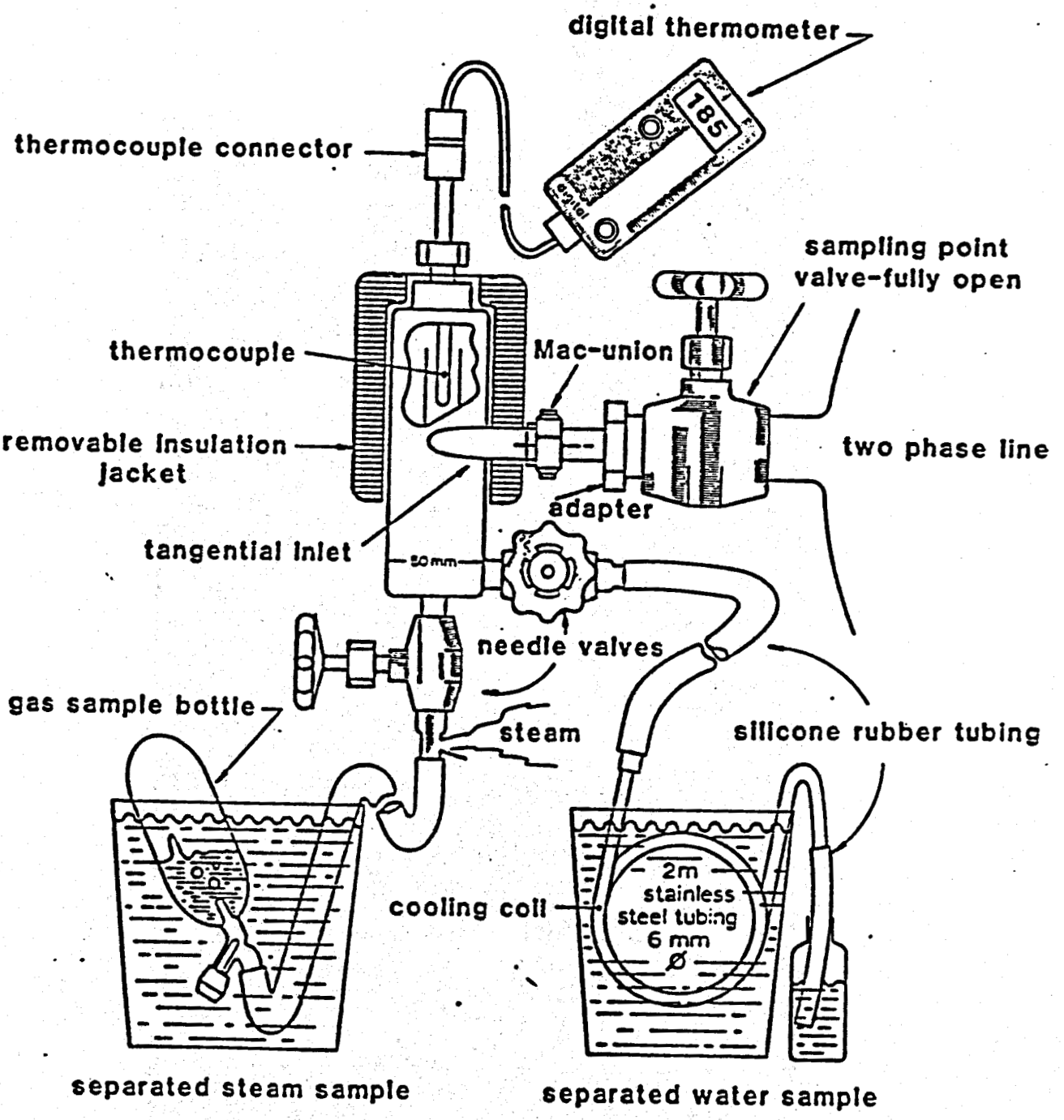
digital thermometer
thermocouple connector
sampling point valve-fully open
thermocouple
Mac-union
removable insulation jacket
two phase line
adapter
tangential inlet
50mm
needle valves
gas sample bottle
steam
silicone rubber tubing
2m stainless steel tubing 6 mm ø
cooling coil
separated steam sample
separated water sample

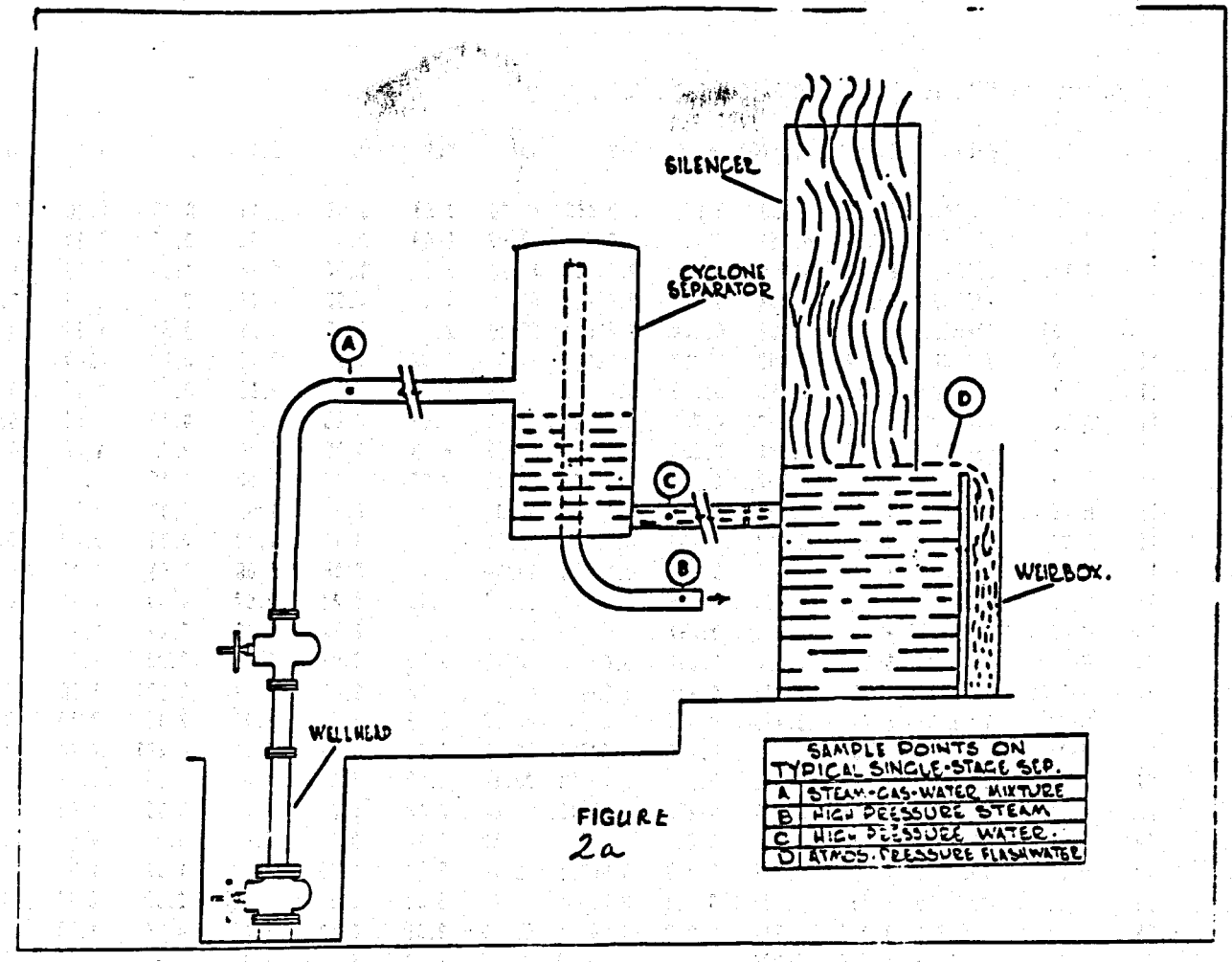

FIGURE 2a

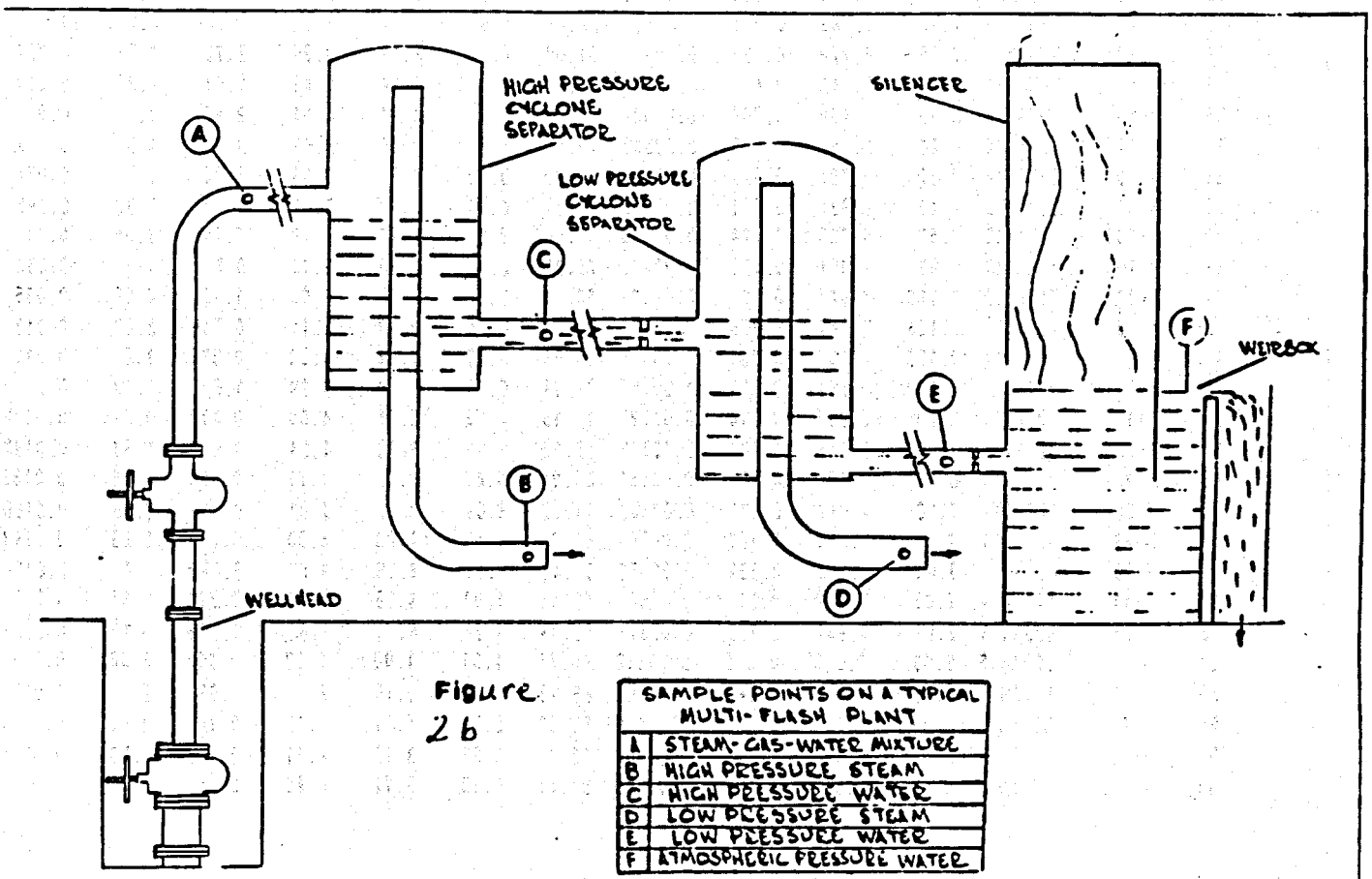

Figure 2b

SAMPLE POINTS ON A TYPICAL MULTI-FLASH PLANT	
A	STEAM-GAS-WATER MIXTURE
B	HIGH PRESSURE STEAM
C	HIGH PRESSURE WATER
D	LOW PRESSURE STEAM
E	LOW PRESSURE WATER
F	ATMOSPHERIC PRESSURE WATER

GEOTHERMAL GAS ANALYSES FROM CERRO PRIETO [illegible]

Rec#	Well	Date	Psep(f)	Psep(w)	Ysep	G/S	CO2	H2S	H2	CH4	N2	NH3	Ar	He
5	M-5	77APR29	5.836	6.259	0.287	0.00446	78.86	7.63	4.66	5.18	0.60	2.28	0.014	-
6	M-8	77APR27	6.398	6.751	0.284	0.00924	92.02	2.59	2.33	1.51	0.15	1.47	0.0037	-
7	M-11	77APR19	6.328	6.259	0.279	0.00564	71.30	5.69	1.77	4.26	11.0	3.98	1.091	-
8	M-14	77APR20	6.328	6.188	0.244	0.00781	81.75	4.99	4.52	4.86	0.51	2.97	0.013	-
9	M-19A	77APR27	6.679	6.962	0.289	0.00588	82.19	7.91	2.86	3.98	0.51	2.31	0.014	-
10	M-20	77APR20	6.012	5.802	0.227	0.00912	91.65	2.32	1.98	1.77	0.23	2.07	0.0059	-
11	M-21A	77APR22	6.91	6.997	0.342	0.01010	87.93	3.17	3.97	2.95	0.27	1.77	0.0038	-
12	M-25	77APR27	6.328	6.399	0.284	0.00693	82.73	7.07	2.25	3.39	0.46	3.00	0.0097	-
13	M-26	77APR20	6.996	7.384	0.243	0.00485	80.89	8.33	4.09	4.26	0.63	1.80	0.016	-
14	M-27	77APR21	6.855	6.892	0.262	0.00919	86.13	3.82	4.42	3.50	0.45	1.75	0.013	-
15	M-29	77APR21	6.588	6.069	0.217	0.00525	82.88	4.94	2.98	4.99	0.82	2.73	0.014	-
16	M-30	77APR21	6.890	6.927	0.269	0.00463	82.52	5.80	4.14	4.12	0.71	2.40	0.019	-
17	M-31	77APR22	6.539	6.540	0.257	0.00656	80.87	5.76	5.46	5.08	0.65	2.24	0.016	-
18	M-35	77APR26	-	7.736	0.285	0.00708	91.10	2.63	2.21	2.07	0.30	1.71	0.0091	-
19	M-42	77APR29	-	7.736	0.257	0.00548	81.50	6.14	2.24	4.43	0.49	4.58	0.0083	-
20	M-5	79JAN30	6.679	6.610	0.294	0.00585	80.19	3.34	3.07	3.89	7.22	2.10	0.135	0.0011
21	M-8&46	79JAN30	7.312	7.173	0.306	0.00604	83.13	4.02	6.48	3.92	0.834	1.90	0.0021	0.0
22	M-11	79FEB01	6.96	6.470	0.301	0.00491	86.53	2.39	2.35	4.12	2.12	2.30	0.043	0.001
23	M-14	79JAN31	6.53	7.032	0.212	0.00791	85.72	3.65	3.55	4.74	0.667	1.70	0.019	0.0
24	M-19A	79MAY15	7.31	7.032	0.290	0.00501	82.34	3.29	4.08	4.65	3.20	2.12	0.065	0.0
25	M-21A	79MAY15	6.50	6.681	0.272	0.00646	82.84	2.46	4.20	3.73	3.90	2.42	0.80	0.0
26	M-26	79JAN31	7.488	-	0.251	0.00522	85.50	4.40	0.0	0.0	0.0	0.0	0.0	0.0
27	M-27	79JAN30	6.996	6.329	0.307	0.00796	82.49	5.17	4.85	4.28	1.92	1.51	0.037	0.0
28	M-29	79MAY15	6.71	6.681	0.191	0.00553	84.07	3.49	2.57	4.52	2.99	2.17	0.062	0.0
29	M-31	79FEB01	7.207	7.314	0.250	0.00604	85.16	3.38	4.42	4.42	0.78	1.73	0.021	0.003
30	M-35	79FEB01	6.996	7.806	0.328	0.00373	84.11	5.14	3.58	3.14	0.87	3.12	0.020	0.0006
31	M-42	79MAY16	7.20	7.314	0.237	0.00576	83.50	3.44	1.75	4.56	4.41	1.99	0.088	0.0
32	M-45	79FEB01	6.81	6.751	0.473	0.00620	82.31	4.00	8.07	3.61	0.65	1.69	0.020	0.0
33	M-48	79MAY15	7.90	9.283	0.324	0.00420	82.03	4.80	7.97	1.02	1.74	2.20	0.0	0.0066
34	M-50	79MAY14	7.55	8.228	0.327	0.00780	81.09	4.60	5.18	4.29	2.76	1.25	0.057	0.0
35	M-51	79MAY14	8.08	9.142	0.405	0.00555	73.80	11.40	6.14	2.45	4.97	2.26	0.098	0.0
36	M-53	79MAY16	6.89	6.962	0.398	0.00644	84.48	2.94	4.71	4.54	2.99	1.46	0.0	0.0
37	M-84	79MAY14	7.20	8.087	0.503	0.00543	78.65	5.62	7.79	3.03	3.67	1.37	0.063	0.0
38	M-90	79MAY14	7.62	7.384	0.328	0.00533	82.39	3.92	4.92	3.69	3.30	1.75	0.054	0.0059
39	M-91	79MAY15	8.40	8.931	0.371	0.00390	81.67	4.13	3.90	3.83	4.08	2.32	0.085	0.0
40	M-103	79MAY15	6.53	6.329	0.424	0.00340	81.00	2.98	5.41	3.28	5.40	1.68	0.11	0.0027
41	M-105	79MAY17	7.97	9.001	0.401	0.00470	78.35	6.60	5.60	3.74	3.83	1.84	0.058	0.0018
42	M-114	79FEB02	7.769	7.947	0.223	0.00394	83.94	5.50	1.27	5.55	1.13	2.27	0.035	0.0022
43	M-130	79JAN31	7.488	7.947	0.305	0.00461	83.21	6.44	3.10	4.14	0.745	2.23	0.017	0.0022
44	M-5	82JAN14	7.170	6.962	0.301	0.00579	85.64	4.87	3.14	4.23	0.536	1.6	0.0127	0.00046
45	M-11	82JAN14	7.10	6.751	0.314	0.00452	84.87	5.79	2.09	3.79	1.6	1.83	0.0283	0.00063
46	M-14	82JAN11	6.60	6.962	0.214	0.0172	85.15	3.63	6.54	4.00	0.472	0.624	0.0112	0.00016
47	M-19A	82JAN12	7.10	7.173	0.283	0.00565	85.35	5.38	3.20	4.04	0.566	1.57	0.0137	0.00047
48	M-25	82JAN11	6.60	7.103	0.333	0.00554	85.04	5.69	3.16	4.11	0.550	1.55	0.0139	0.00012
49	M-26	82JAN14	7.10	7.947	0.271	0.00602	84.42	6.69	2.66	4.01	0.618	1.55	0.0160	0.00022
50	M-29	82JAN11	8.36	8.650	0.188	0.00709	86.73	4.53	2.88	3.80	0.571	1.59	0.0143	0.00044
51	M-30	82JAN11	7.03	7.173	0.269	0.00472	84.49	5.57	3.85	3.68	0.662	1.94	0.0184	0.00049
52	M-31	82JAN12	7.03	7.032	0.286	0.00605	82.43	5.81	4.58	5.10	0.726	1.51	0.0186	0.00031
53	M-35	82JAN14	6.81	6.962	0.280	0.00373	82.33	5.26	4.11	5.68	0.953	1.70	0.0238	0.0
54	M-42	82JAN15	6.89	6.610	0.226	0.00612	86.33	4.51	1.80	4.29	0.602	2.36	0.0148	0.00061
55	M-43	82JAN15	6.60	-	0.244	0.00490	85.48	5.88	2.15	3.85	0.673	2.00	0.0159	0.000
56	M-48	82JAN12	7.38	7.103	0.370	.0.00294	83.00	5.56	5.47	3.12	0.783	2.49	0.0214	0.0
57	M-50	82JAN13	8.01	7.454	0.303	0.00524	83.86	5.57	3.80	4.31	0.741	1.73	0.0205	0.00026
58	M-51	82JAN13	8.43	7.595	0.351	0.00605	84.41	5.43	3.72	4.40	0.642	1.47	0.0162	0.00026

CP DOUBLE SEP CHEM DATA

Rec#	Well	Date	Code	Psep1	Psep2	Pcol	Fstm1	Fstm2	Fwat	Enth	pH	Na	K	Ca	Mg	Cl	SiO2	HCO3	SO4
563	T-350	88/05/11	BF901	11.95	-	0	58.5	-	123.7	346.0	5.85	12728	2809	667	-	23635	1144	19	9.1
564	T-364	78/09/14	BF700	-	-	0	-	-	-	-	7.3	9315	2111	407	-	16872	1108	4	-
565	T-364	86/02/04	BF255	13.01	5.06	0	64.4	13.3	149.6	328.1	-	9517	2419	428	-	17520	-	-	-
566	T-364	86/03/31	BF312	13.01	5.41	0	61.8	12.6	162.5	315.7	6.81	9622	2384	421	0.16	17089	904	32	0.14
567	T-364	86/04/17	BF329	13.01	5.41	0	61.8	12.6	162.5	315.6	7.51	9482	2452	416	-	17669	1382	30	-
568	T-364	86/05/05	BPT2	13.01	5.52	5.52	58.2	12.1	148.1	318.9	7.33	8210	1832	371	0.105	15730	781	15	3
569	T-364	86/08/07	BF437	13.57	6.33	0	62.9	11.3	166.6	317.7	7.09	9635	2431	425	-	18463	1333	26	-
570	T-364	86/09/29	BF492	14.77	5.41	0	40.7	7.0	68.2	366.9	7.08	8765	2258	431	-	16886	1276	44	-
571	T-364	87/02/25	BF623	13.92	5.91	0	56.3	9.9	119.0	339.0	8.33	9266	2428	433	-	17167	1174	85	-
572	T-364	87/03/17	BF646	13.50	5.77	0	57.0	10.9	144.8	320.0	7.29	8469	2365	426	-	16118	1103	32	-
573	T-364	87/04/09	BPT2	13.50	5.77	5.77	57.2	10.9	144.8	320.0	6.24	8480	1693	350	0.23	16000	830	5.4	0
574	T-364	87/06/01	BF685	13.15	5.62	0	50.0	12.0	146.0	308.9	6.96	9147	2366	432	-	17168	1089	35	-
575	T-364	87/09/14	BF700	13.15	5.62	0	50.0	12.0	146.0	309.0	7.30	9315	2111	407	-	16872	1108	4	2.9
576	T-364	88/02/24	BPT2	12.8	4.30	4.30	38.7	12.7	140.5	291.3	5.30	8330	1980	353	0.16	15570	752	10.1	1
577	T-364	88/03/11	BF703	13.08	4.43	0	49.6	14.3	155.7	219.6	6.80	9578	2093	421	-	17394	847	32	4.0
578	T-366	84/09/24	BF112	6.02	-	0	107	-	107.5	-	5.9	10738	2866	293	-	19702	1183	19	-
579	T-366	86/02/24	BF335	13.22	4.78	0	77.7	17.1	181.7	326.8	-	11016	3058	446	-	20334	-	-	-
580	T-366	86/03/31	BF372	12.94	5.41	0	66.6	20.5	266.9	280.1	6.19	10589	2919	461	0.29	19335	1456	27	0.32
581	T-366	86/04/17	BF389	12.94	5.41	0	66.6	20.5	266.9	280.1	-	11008	3000	406	-	20401	1332	24	-
582	T-366	86/05/06	BPT2	13.57	5.69	5.69	69.9	20.5	221.9	300.1	6.11	9260	2271	393	0.226	18050	918	7	5
583	T-366	86/05/09	BF404	13.57	5.69	0	69.9	20.5	221.9	300.1	6.5	10998	2982	450	-	20890	1481	30	-
584	T-366	86/08/08	BF496	13.36	5.70	0	70.9	16.4	202.9	310.6	6.71	11454	3149	467	-	21761	1425	20	-
585	T-366	86/09/29	BF549	13.01	5.34	0	67.4	13.8	157.4	328.5	6.19	10303	2969	461	-	19738	1367	28	-
586	T-366	87/03/09	BF698	13.01	4.92	0	47.5	12.8	100.0	335.0	7.3	10399	2910	470	-	19710	1275	21	-
87	T-366	87/06/04	BF766	13.01	4.78	0	57.4	16.3	175.5	304.5	7.57	10250	2906	464	-	19261	875	21	-
588	T-366	87/07/10	BF729	12.58	4.57	0	51.6	14.9	159.9	302.0	7.36	10570	2926	461	-	20273	1320	21	-
589	T-366	88/02/25	BKT	12.3	-	0	74.5	-	145.6	354.3	6.92	10300	2760	434	0.34	19450	793	12.8	1
590	T-366	88/03/11	BF781	12.09	-	0	74.0	-	105.6	388.4	-	10312	2380	447	-	19132	1325	-	1.9
591	T-388	84/09/29	BF101	5.61	-	0	66	-	113.2	-	6.7	9385	2465	349	-	17407	930	33.0	-
592	T-388	86/02/13	BF304	11.81	4.36	0	31.2	7.6	85.3	311.2	-	9105	2508	363	-	17142	-	-	-
593	T-388	86/03/31	BF353	11.95	4.22	0	16.7	8.7	98.3	253.8	7.37	9193	2475	364	0.17	16470	1293	55	0.24
594	T-388	86/05/05	BPT2	12.09	4.29	4.29	16.6	6.6	72.8	272.7	7.96	8140	1980	322	0.102	15120	793	26	1
595	T-388	86/05/07	BF388	12.09	4.29	0	16.6	6.6	72.8	272.7	8.0	9104	2477	378	-	17060	1340	45	-
596	T-388	86/08/07	BF461	12.31	4.78	0	26.0	8.2	99.3	285.5	7.53	9259	2407	395	-	16819	1287	49	-
597	T-388	86/09/29	BF516	13.08	5.06	0	26.9	5.4	67.9	320.3	7.14	9024	2521	361	-	17043	1216	54	-
598	T-388	88/05/11	BF631	13.71	4.57	0	39.1	4.2	52.8	382.5	6.49	9911	2188	393	-	18190	1217	21	6.1
599	T-388	84/12/04	BF258	-	-	0	-	-	-	-	-	10595	2910	394	-	23231	1529	17.0	-
600	T-388	84/12/05	BF266	-	-	0	-	-	-	-	-	10597	2993	393	-	19513	1529	-	-
601	T-388	85/11/24	BF720	12.3	-	0	73.6	-	163	-	-	1810	2934	424	-	20232	-	-	-
602	T-388	86/02/11	BF765	11.25	4.71	0	72.9	10.8	133.8	348.8	-	10812	2769	440	-	20211	1350	-	-
603	T-388	86/04/23	BF818	11.95	5.77	0	68.1	9.1	123.1	353	6.18	10302	2767	437	0.76	19171	1333	28	0.34
604	T-388	86/05/06	BPT2	11.60	4.64	4.64	74.1	12.8	149.6	339.3	6.37	9830	2389	409	0.187	17990	1027	11	3
605	T-388	86/05/08	BF835	11.60	4.64	0	74.1	12.8	149.6	339.3	6.67	10793	2882	435	-	20533	1453	29	-
606	T-388	86/08/19	BF939	14.21	5.56	0	62.2	11.4	128.1	343.9	6.72	10828	2649	441	-	19937	1439	19	-
607	T-388	86/10/10	BF970	14.06	5.34	0	48.7	9.3	94.0	350.1	6.33	10154	2780	444	-	19643	1281	34	-
608	T-388	87/02/27	BF1098	13.71	4.71	0	58.6	12.6	112.2	349.0	6.06	10634	2887	449	-	19649	1270	20	-
609	T-388	87/03/19	BF1111	10.69	4.22	0	64.8	10.4	124.1	341.0	6.01	10828	2853	443	-	20141	1212	22	-
610	T-388	87/04/09	BPT2	11.60	4.71	4.71	59.1	13.6	162.1	312.0	6.16	9410	2142	373	0.33	18440	886	5.0	0
611	T-388	87/06/01	BF1168	11.25	4.36	0	57.0	10.0	104.3	350.0	6.13	10526	2880	445	-	19674	1216	22	-
612	T-388	87/09/01	BF1189	12.16	4.22	0	50.7	10.6	106.0	336.0	5.56	10633	2553	457	-	19440	1326	43	1.8
613	T-388	88/02/23	BPT2	12.3	3.24	3.24	27.3	6.4	61.0	330.8	4.90	9510	2420	393	0.28	18210	889	6.6	2

CP DOUBLE SEP CHEM DATA

Rec#	Well	Date	Code	Cat	An	Bal	Na/Cl	Ca/Cl	TE	TQA	TNK-F	TKNg	T13	CT13	Ysepe
563	T-350	88/05/11	BF901	662.6	667.2	-0.341	0.539	0.0282	318	300	296	-	292	14430	0.456
564	T-364	78/09/14	BF700	482.4	476	0.668	0.552	0.0241	-	296	299	-	292	10280	-
565	T-364	86/02/04	BF255	500.2	494.2	0.608	0.543	0.0244	305	-	313	-	302	10260	0.423
566	T-364	86/03/31	BF312	503.3	482.5	2.1	0.563	0.0246	296	277	309	416	300	10080	0.4
567	T-364	86/04/17	BF329	498.9	498.9	0.00721	0.537	0.0235	296	320	315	-	304	10270	0.4
568	T-364	86/05/05	BPT2	424.8	444.1	-2.22	0.522	0.0236	298	276	297	411	289	11200	0.314
569	T-364	86/08/07	BF437	505.4	521.2	-1.54	0.522	0.023	298	315	312	-	302	10820	0.404
570	T-364	86/09/29	BF492	463.1	477	-1.48	0.519	0.0255	332	310	314	-	300	9946	0.495
571	T-364	87/02/25	BF623	489.8	485.6	0.428	0.54	0.0252	313	302	316	-	304	9981	0.443
572	T-364	87/03/17	BF646	453.3	455.2	-0.202	0.525	0.0264	299	296	324	-	307	9240	0.408
573	T-364	87/04/09	BPT2	431.7	451.5	-2.25	0.53	0.0219	299	282	284	370	281	11730	0.314
574	T-364	87/06/01	BF685	482.8	484.8	-0.205	0.533	0.0252	291	295	315	-	302	10050	0.387
575	T-364	87/09/14	BF700	482.4	476	0.662	0.552	0.0241	291	296	299	-	292	10280	0.388
576	T-364	88/02/24	BPT2	433.2	439.5	-0.716	0.535	0.0227	277	271	304	399	295	10620	0.272
577	T-364	88/03/11	BF703	494	491.2	0.285	0.551	0.0242	215	271	295	-	289	10720	0.222
578	T-366	84/09/24	BF112	558.3	556	0.201	0.545	0.0149	-	302	319	-	315	10850	-
579	T-366	86/02/24	BF335	583.4	573.5	0.851	0.542	0.0219	304	-	324	-	313	11310	0.421
580	T-366	86/03/31	BF372	561.9	545.8	1.45	0.548	0.0238	268	321	323	407	311	10870	0.334
581	T-366	86/04/17	BF389	579.4	575.8	0.307	0.54	0.0199	268	315	321	-	313	11360	0.334
582	T-366	86/05/06	BPT2	483.4	509.5	-2.63	0.513	0.0218	284	292	308	396	299	12370	0.275
583	T-366	86/05/09	BF404	580.5	589.7	-0.784	0.526	0.0215	284	321	321	-	311	11740	0.371
584	T-366	86/08/08	BF496	605.8	614.1	-0.684	0.526	0.0215	292	321	322	-	313	12120	0.391
585	T-366	86/09/29	BF549	550	557.2	-0.653	0.522	0.0234	306	319	328	-	314	10930	0.424
586	T-366	87/03/09	BF698	553.5	556.3	-0.25	0.528	0.0238	310	310	325	-	312	11050	0.436
587	T-366	87/06/04	BF766	546.8	543.6	0.289	0.532	0.0241	287	274	326	-	312	10750	0.379
588	T-366	87/07/10	BF729	560.9	572.2	-0.994	0.521	0.0227	285	314	323	-	311	11380	0.375
589	T-366	88/02/25	BKT	543.5	549	-0.503	0.53	0.0223	324	266	319	395	309	11060	0.472
590	T-366	88/03/11	BF781	535	539.7	-0.433	0.539	0.0234	344	314	301	-	295	11520	0.535
591	T-386	84/09/29	BF101	492	491.5	0.0474	0.539	0.02	-	280	317	-	307	9954	-
592	T-386	86/02/13	BF304	481.9	483.5	-0.164	0.531	0.0212	293	-	323	-	310	9681	0.392
593	T-386	86/03/31	BF353	484.1	465.5	1.96	0.558	0.0221	245	311	320	417	308	9378	0.285
594	T-386	86/05/05	BPT2	423.4	427	-0.426	0.538	0.0213	261	276	307	420	298	10210	0.235
595	T-386	86/05/07	BF388	481.7	481.9	-0.0269	0.534	0.0222	261	316	321	-	308	9710	0.32
596	T-386	86/08/07	BF461	487.3	475.2	1.26	0.551	0.0235	272	311	315	-	304	9752	0.344
597	T-386	86/09/29	BF516	477.9	481.6	-0.386	0.529	0.0212	299	305	324	-	311	9577	0.409
598	T-386	88/05/11	BF631	509.7	513.5	-0.377	0.545	0.0216	341	305	296	-	292	11090	0.524
599	T-388	84/12/04	BF258	557.8	655.5	-8.06	0.456	0.017	-	321	322	-	313	12930	-
600	T-388	84/12/05	BF266	556.9	550.4	0.591	0.543	0.0201	-	321	326	-	316	10730	-
601	T-388	85/11/24	BF720	178.7	570.7	-52.3	0.0895	0.021	-	-	683	-	443	-	-
602	T-388	86/02/11	BF765	566.8	570.1	-0.288	0.535	0.0218	320	317	313	-	306	11630	0.461
603	T-388	86/04/23	BF818	544.2	541.2	0.275	0.537	0.0228	323	315	319	362	309	10890	0.469
604	T-388	86/05/06	BPT2	511.8	507.8	0.391	0.546	0.0227	313	301	307	409	299	12120	0.364
605	T-388	86/05/08	BF835	568.5	579.6	-0.973	0.526	0.0212	313	321	319	-	310	11620	0.444
606	T-388	86/08/19	BF939	564	562.7	0.122	0.543	0.0221	316	321	308	-	302	11680	0.452
607	T-388	86/10/10	BF970	538.2	554.6	-1.5	0.517	0.0226	321	310	322	-	310	11110	0.464
608	T-388	87/02/27	BF1098	562.2	554.6	0.688	0.541	0.0229	320	309	321	-	310	11090	0.462
609	T-388	87/03/19	BF1111	569.5	568.5	0.0911	0.538	0.022	314	304	317	-	308	11470	0.447
610	T-388	87/04/09	BPT2	485.5	520.3	-3.46	0.51	0.0202	293	287	299	375	294	12710	0.309
611	T-388	87/06/01	BF1168	557.2	555.3	0.168	0.535	0.0226	321	305	322	-	311	11080	0.464
612	T-388	87/09/01	BF1189	554.1	549.1	0.451	0.547	0.0235	311	315	306	-	299	11520	0.438
613	T-388	88/02/23	BPT2	498.5	513.9	-1.52	0.522	0.0216	307	285	313	392	303	11800	0.361

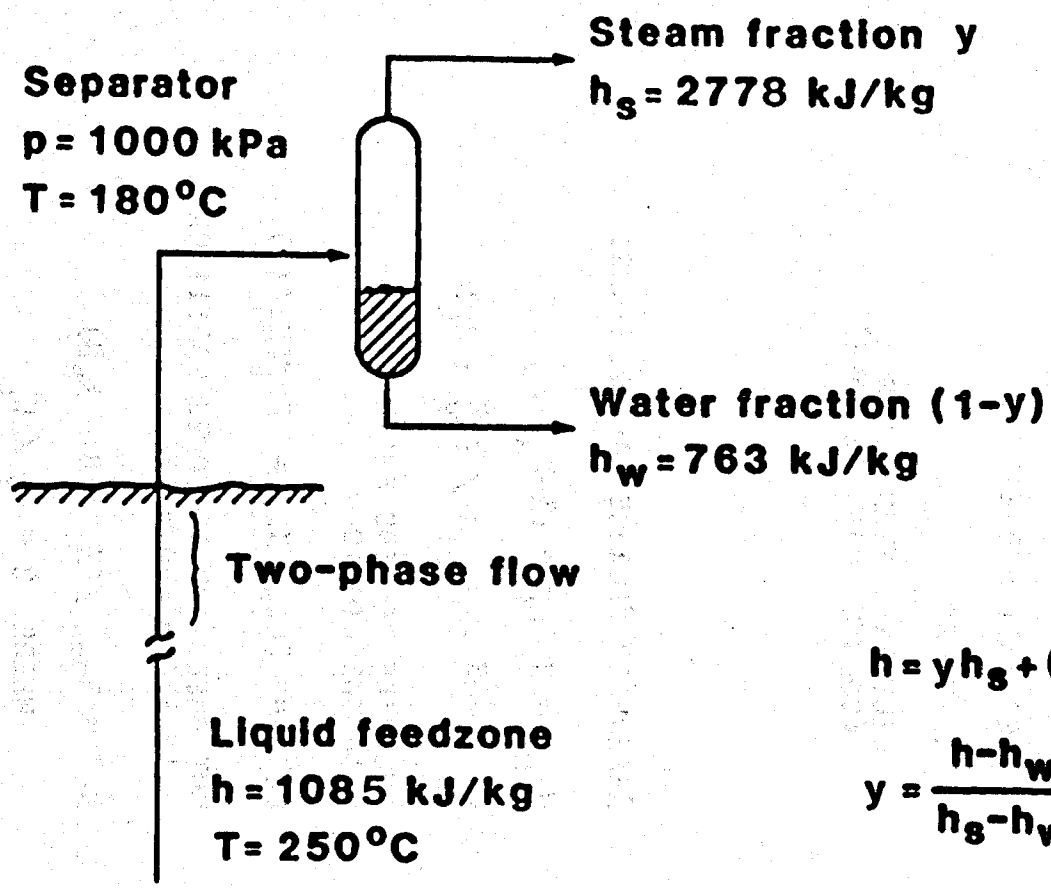

$$h = y h_s + (1-y) h_w$$

$$y = \frac{h - h_w}{h_s - h_w} = 0.16$$

Separation of steam and water, energy and mass balance.

MASS AND ENERGY BALANCES:

$$H_{TOT} = x\, H_L + (1-x)\, H_V$$

$$C_{TOT} = x\, C_L + (1-x)\, C_V$$

$$\delta_{TOT} = x\, \delta_L + (1-x)\, \delta_V$$

WHERE X = LIQUID FRACTION

DATA NEEDED:

ANALYSES OF SEPARATED WATER AND STEAM

SEPARATION PRESSURE

ENTHALPY

GEOTHERMOMETER TEMPS (SOLUTE, GAS, ISOTOPE)

RESERVOIR BALANCE CALCULATIONS:

$$H_{TOT} = X_R\, H_L^R + (1-X_R)\, H_V^R$$

$$X_R = (H_V^R - H_{TOT}) \,/\, (H_V^R - H_L^R)$$

CHLORIDE REMAINS ENTIRELY IN THE LIQUID

$$CL_L^R = CL_{TOT}/X_R = CL_L^S(X_S/X_R)$$

BUT GASES AND ISOTOPES PARTITION IN STEAM AND WATER

$$N_{2L}^R = N_{2TOT}/(X_R + B - X_R B)$$

WHERE $B = C_V / C_L$

$$\delta D_L^R = \delta D_{TOT} + (1-X_R)\, 10^3 \text{ LN } \alpha_{L-V}$$

Equations expressing the temperature dependence of selected geothermometers. C is the concentration of dissolved silica. All concentrations are in mg/kg. (Modified from Fournier, 1981).

Geothermometer	Equation	Restrictions
Quartz-no steam loss	$t\,°C = \frac{1309}{5.19 - \log C} - 273.15$	t = 0-250°C
Quartz-maximum steam loss	$t\,°C = \frac{1522}{5.75 - \log C} - 273.15$	t = 0-250°C
K-Mg	$t\,°C = \frac{4410}{\log\,(Mg/K^2) - 13.95} - 273.15$	t > 100°C
Na/K (Fournier)	$t\,°C = \frac{1217}{\log\,(Na/K) + 1.483} - 273.15$	t > 150°C
Na-K-Ca	$t\,°C = \frac{1647}{\log\,(Na/K) + \beta[\log(\sqrt{Ca}/Na) + 2.06] + 2.47} - 273.15$	t < 100°C, β = 4/3 t > 100°C, β = 1/3

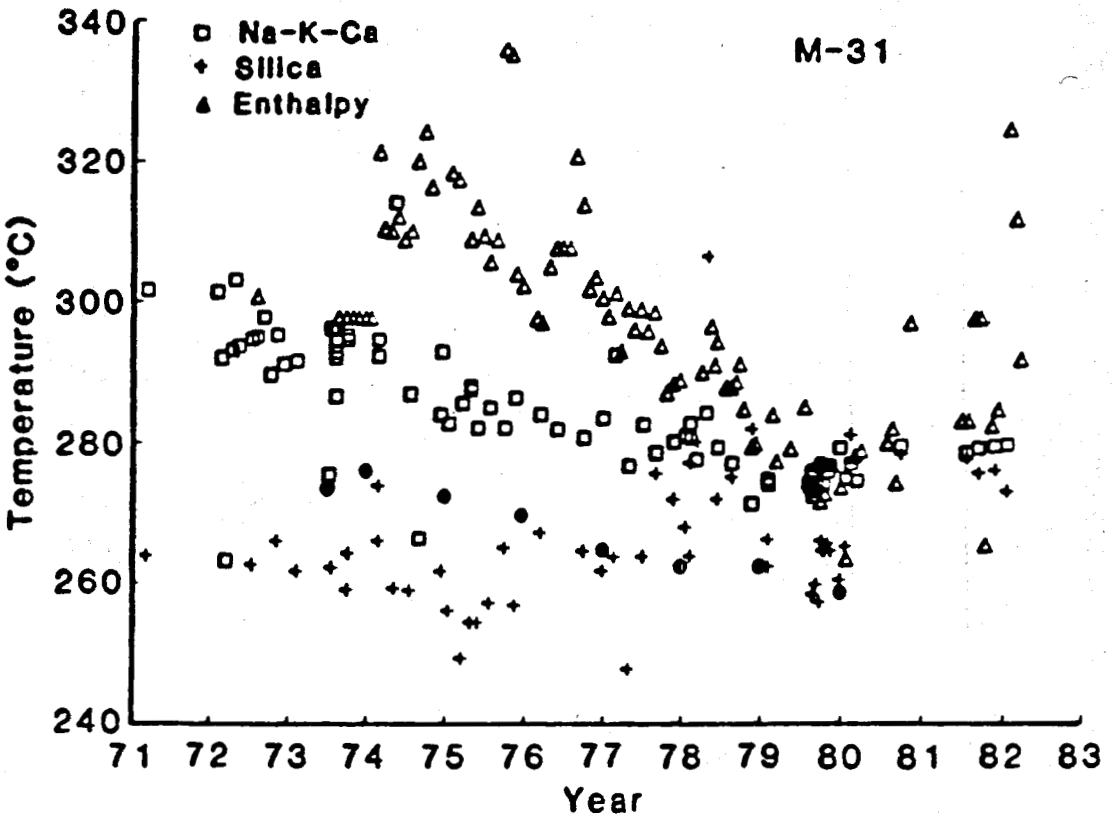

Time plot of temperatures indicated from Na-K-Ca and silica geothermometers and measured enthalpy for fluid produced from well M-31 at Cerro Prieto, Mexico. Dots show calculated well bottom temperatures based on a wellbore flow model

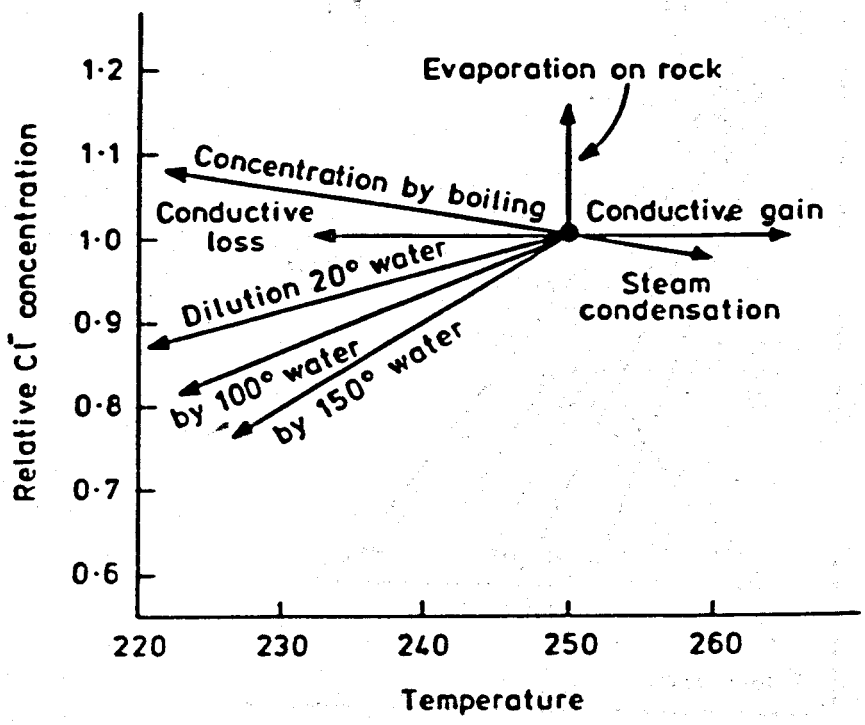

Trend lines relating changes in deep-water chloride concentrations to various physical processes.

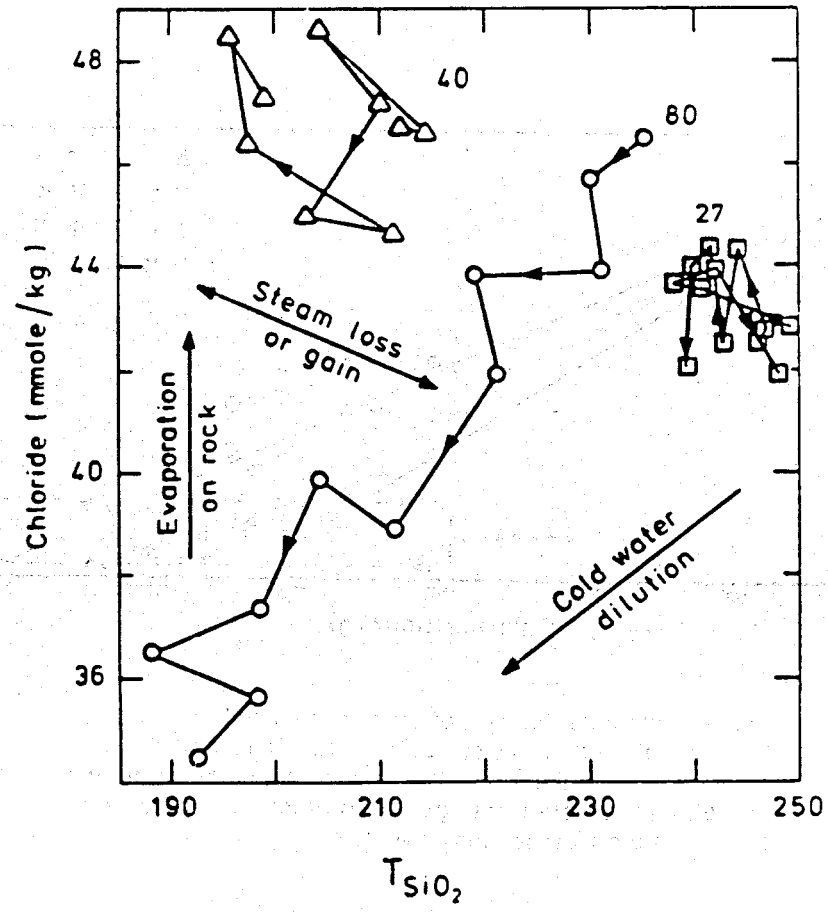

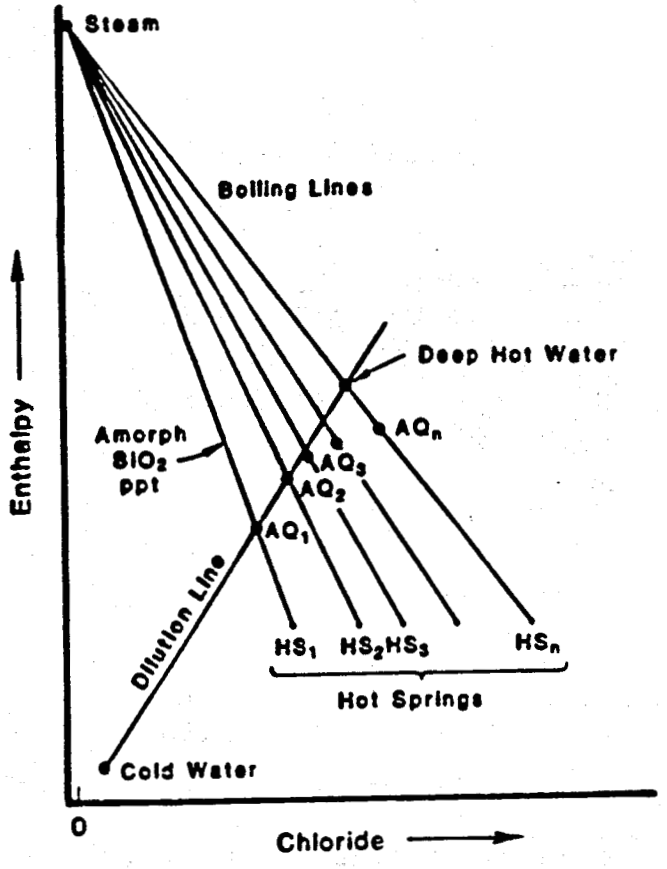

Hypothetical plot of enthalpy relative to chloride for various waters that result from the mixing of hot and cold waters Enthalpies of deep waters are estimated using the silica content of hot-spring waters (modified from Truesdell and Fournier, 1976).

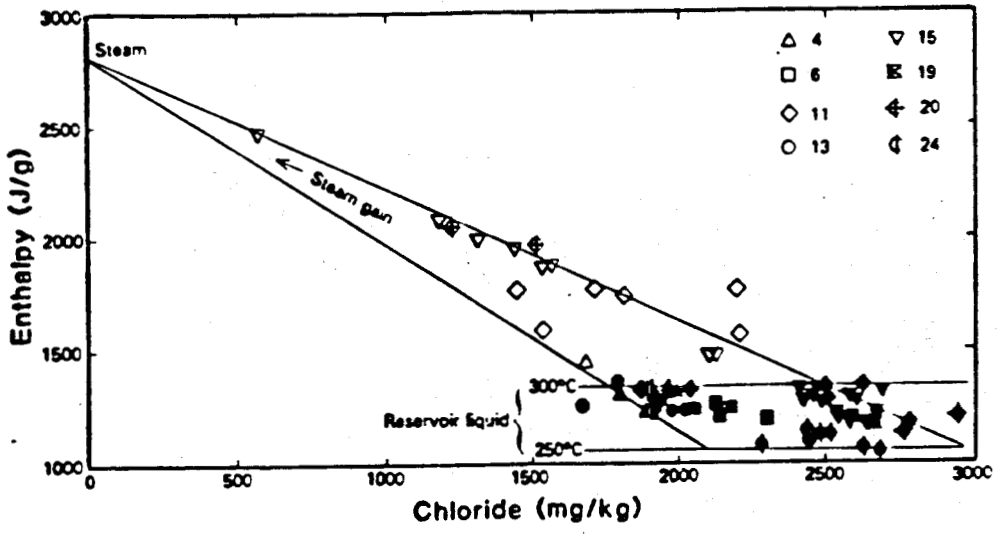

Enthalpy-chloride diagram of produced fluids from the Baca Geothermal Field Open symbols are total fluid enthalpy and chloride, closed symbols are reservoir liquid chloride and enthalpy (calculated from geothermometer temperatures) (modified from Truesdell and Janik, 1986)

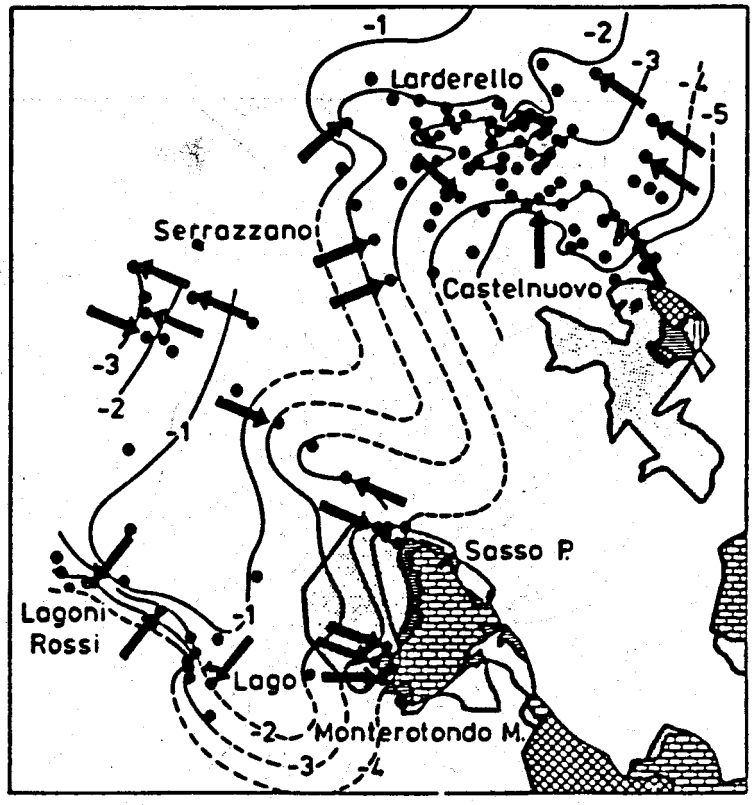

Contours about the Larderello field of changes in $\delta^{18}O$ values with time during the period 1960-1970.

Cerro Prieto

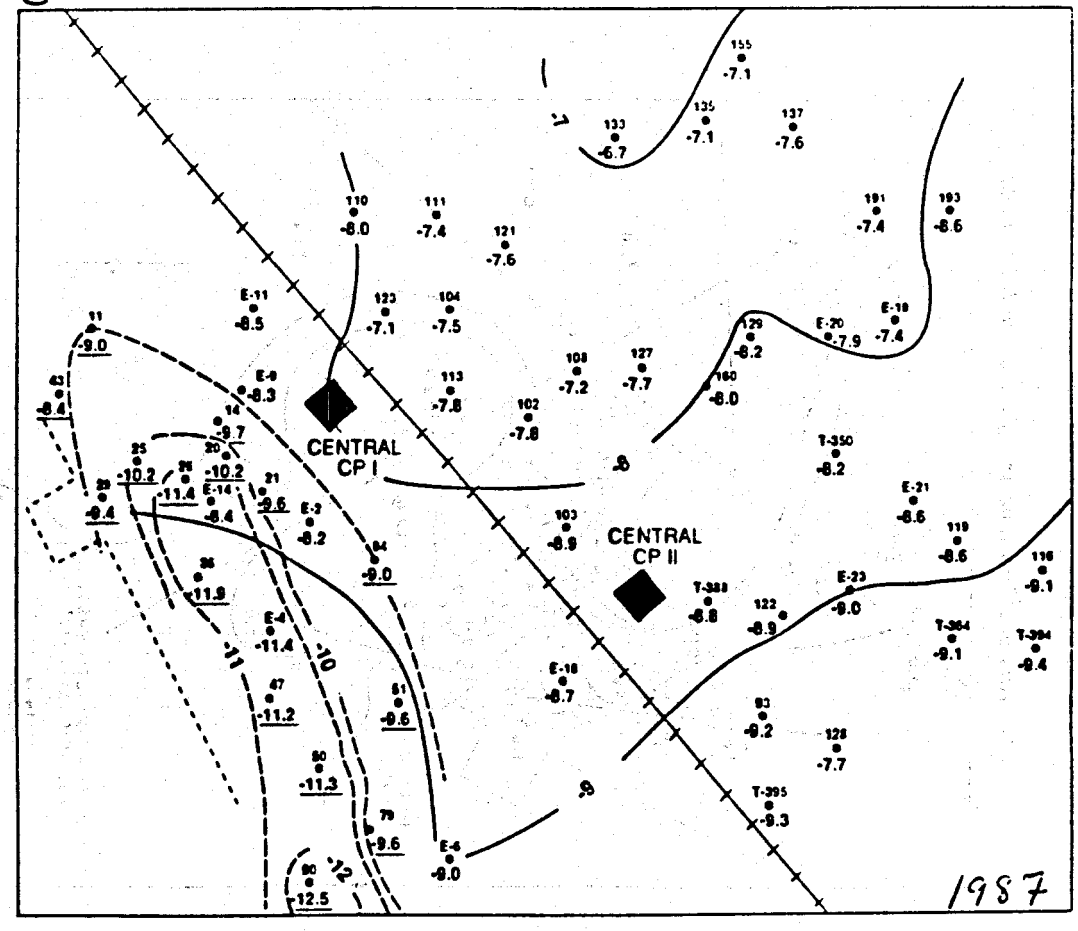

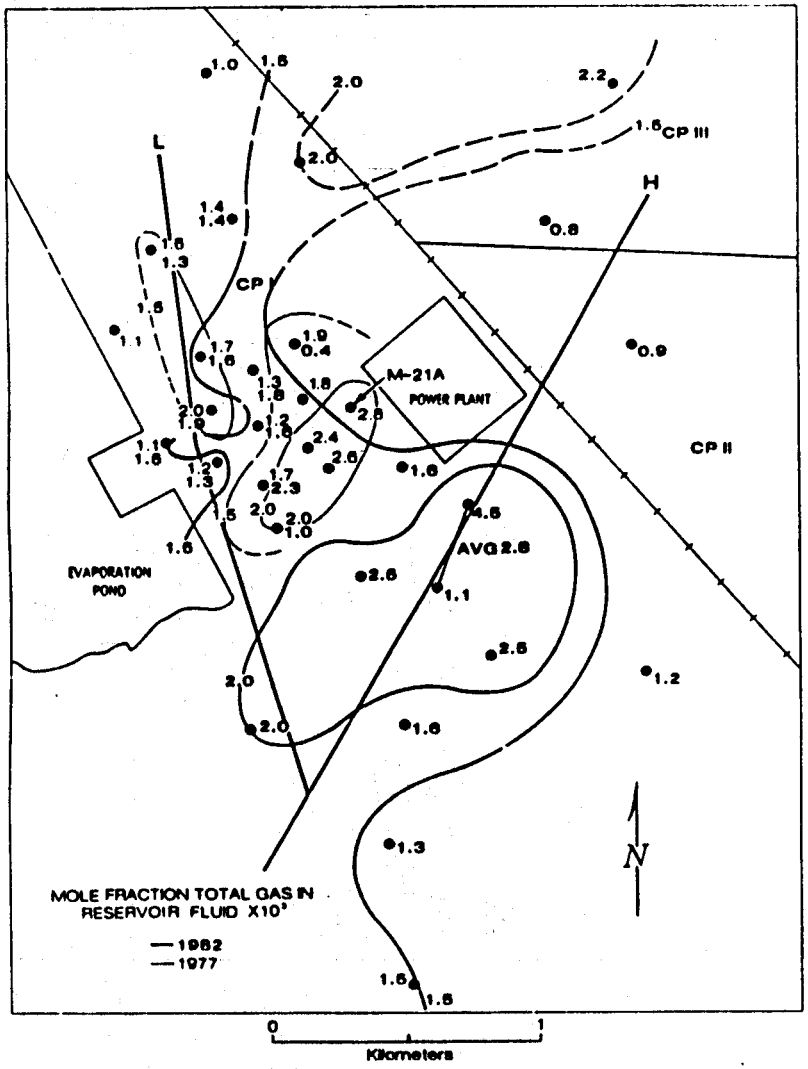

Fig. 3. Mole fraction of total gas in reservoir fluid × 10³. Data from 1977 show boiling around M-21A and along fault L. Data from 1982 show boiling along fault H, and imply that fault H provides major structural control for fluid movement (steam fraction × gas/stream = mole fraction of total gas).

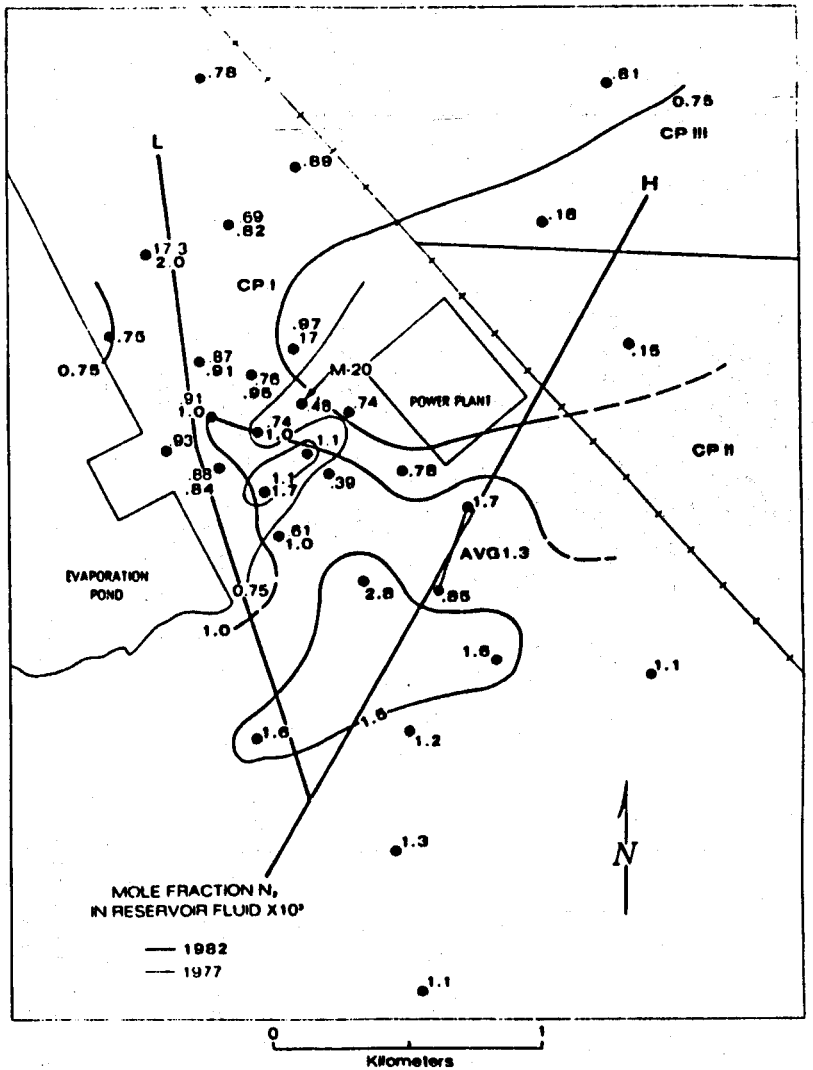

Fig. 4. Mole fraction of N_2 in reservoir fluid × 10². Data from 1977 reflect drawdown of cold water into the reservoir fluid (steam fraction × gas/steam × $\%N_2$ = mole fraction N_2).

GAS EQUILIBRIA--E.G. METHANE BREAKDOWN

$$CH_4 + 2H_2O = CO_2 + 4H_2$$

$$K_C = (P_{CO2} * P_{H2}^4) / (P_{CH4} * P_{H2O}^2)$$

FOR EACH GAS

$$(C/H_2O)_{WH} = Y_R(C/H_2O)_V^R + (1-Y_R)(C/H_2O)_L^R$$

Y_R = RESERVOIR STEAM FRACTION

$$B = C_V / C_L$$

$$P = P_{H2O}\ (C/H_2O)_V^R$$

THEREFORE

$$P = P_{H2O}\ (C/H_2O)_{WH} / (Y_R + (1-Y_R)/B)$$

PUTTING THESE EXPRESSIONS INTO LOG FORM

$$\log K_C = \log P_{CO2} + 4 \log P_{H2} - \log P_{CH4} + 2 \log P_{H2O}$$

AND

$$\log P_R = \log P_{H2O} + \log (C/H_2O)_{WH} - \log A$$

WHERE $A = (Y_R + (1-Y_R)/B)$

COMBINING

$$4 \log (H_2/H_2O) + \log (CO_2/CH_4) = \log K_C + 2 \log P_{H2O} + 4 \log A_{H2} + \log (A_{CO2}/A_{CH4})$$

K_C, B, AND P_{H2O} ARE KNOWN FN OF T, SO GIVEN T, THE EQUATION CAN BE SOLVED FOR Y.

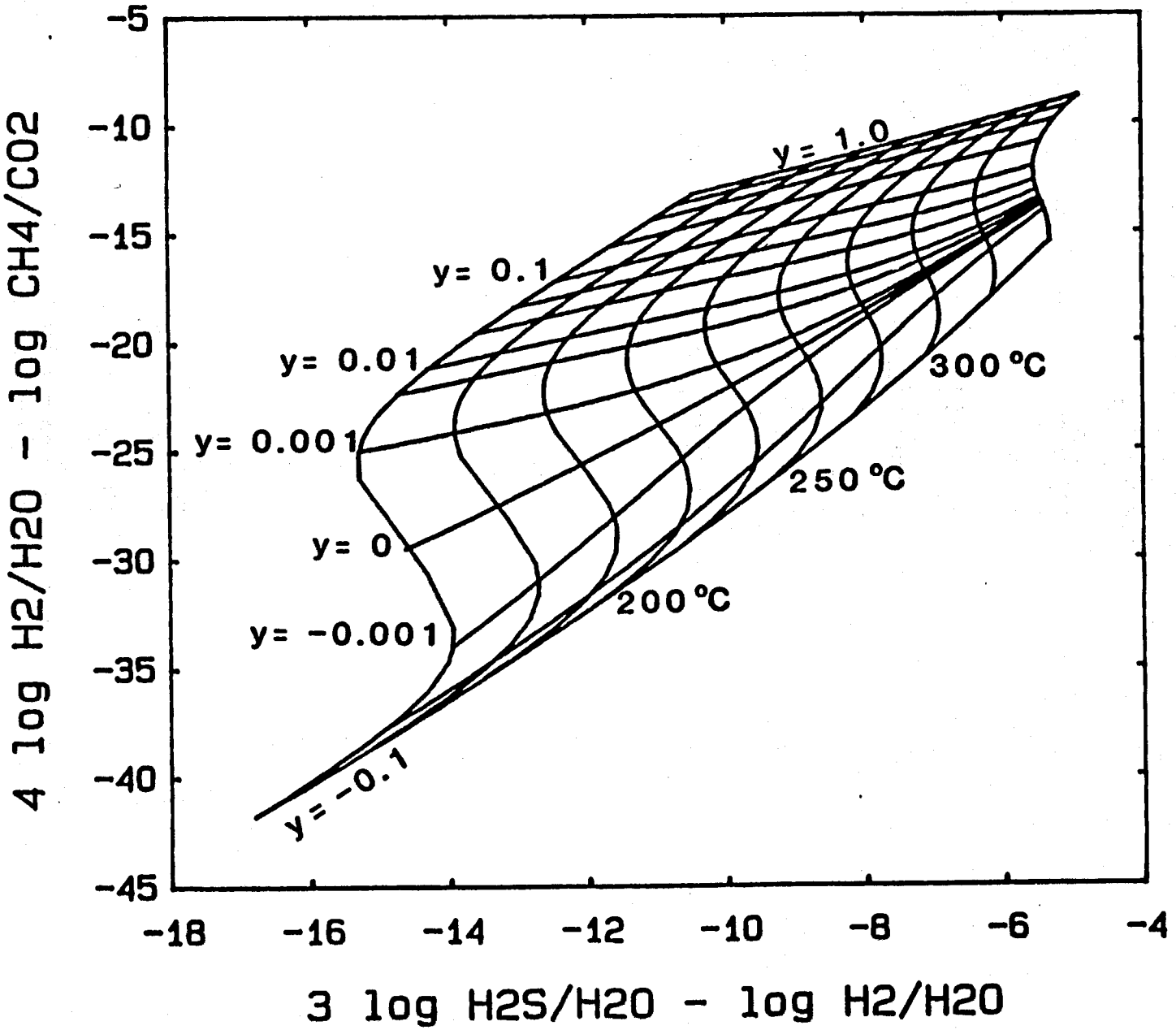
-5
-10
-15
-20
-25
-30
-35
-40
-45
-18
-16
-14
-12
-10
-8
-6
-4
4 log H2/H20 - log CH4/C02
3 log H2S/H20 - log H2/H20
y= 1.0
y= 0.1
y= 0.01
y= 0.001
y= 0
y= -0.001
y= -0.1
300 °C
250 °C
200 °C

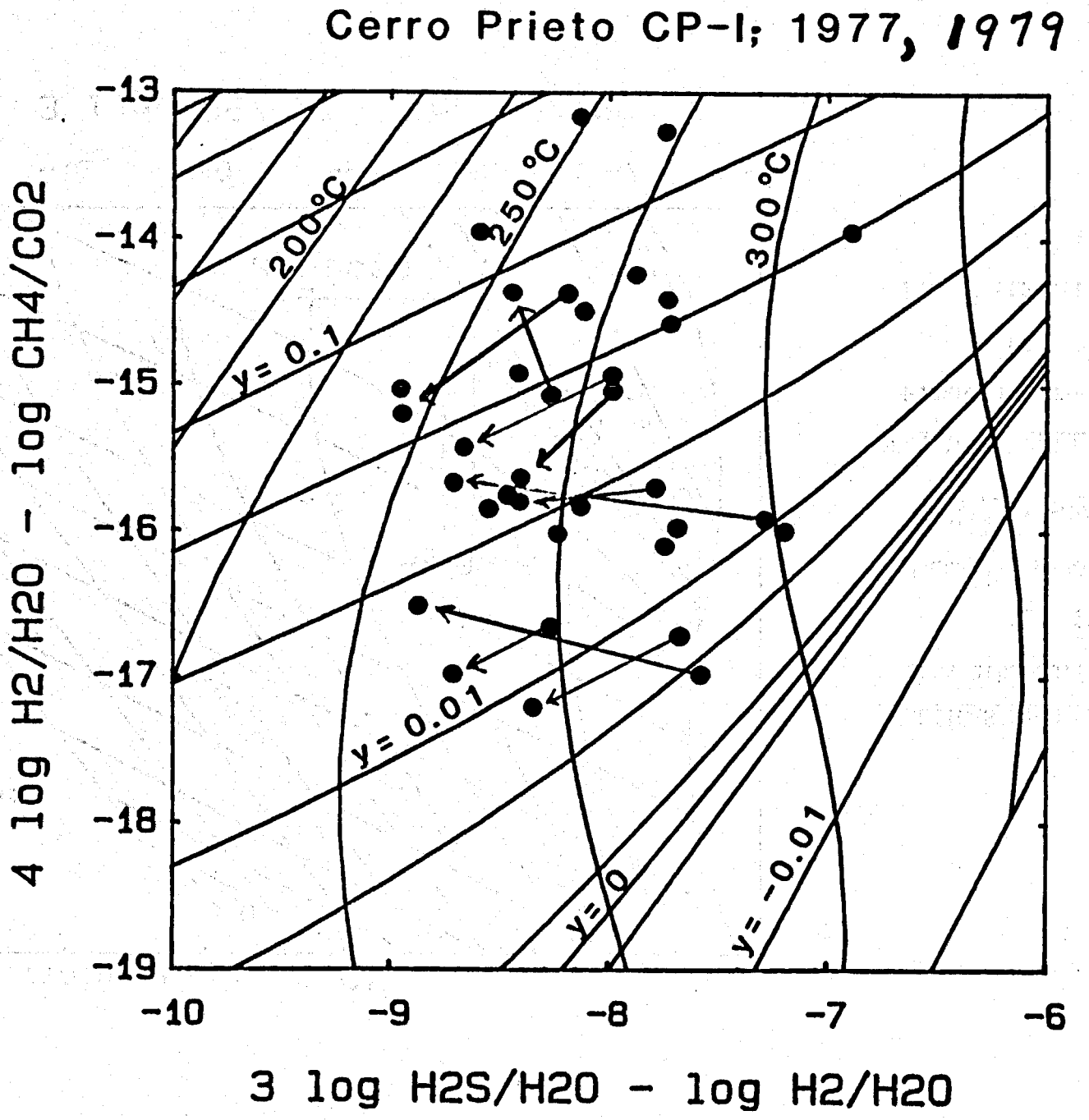
Cerro Prieto CP-I; 1977, 1979
-13
-14
-15
-16
-17
-18
-19
-10
-9
-8
-7
-6
200°C
250°C
300°C
y= 0.1
y= 0.01
y= 0
y= -0.01
4 log H2/H20 - log CH4/CO2
3 log H2S/H20 - log H2/H20

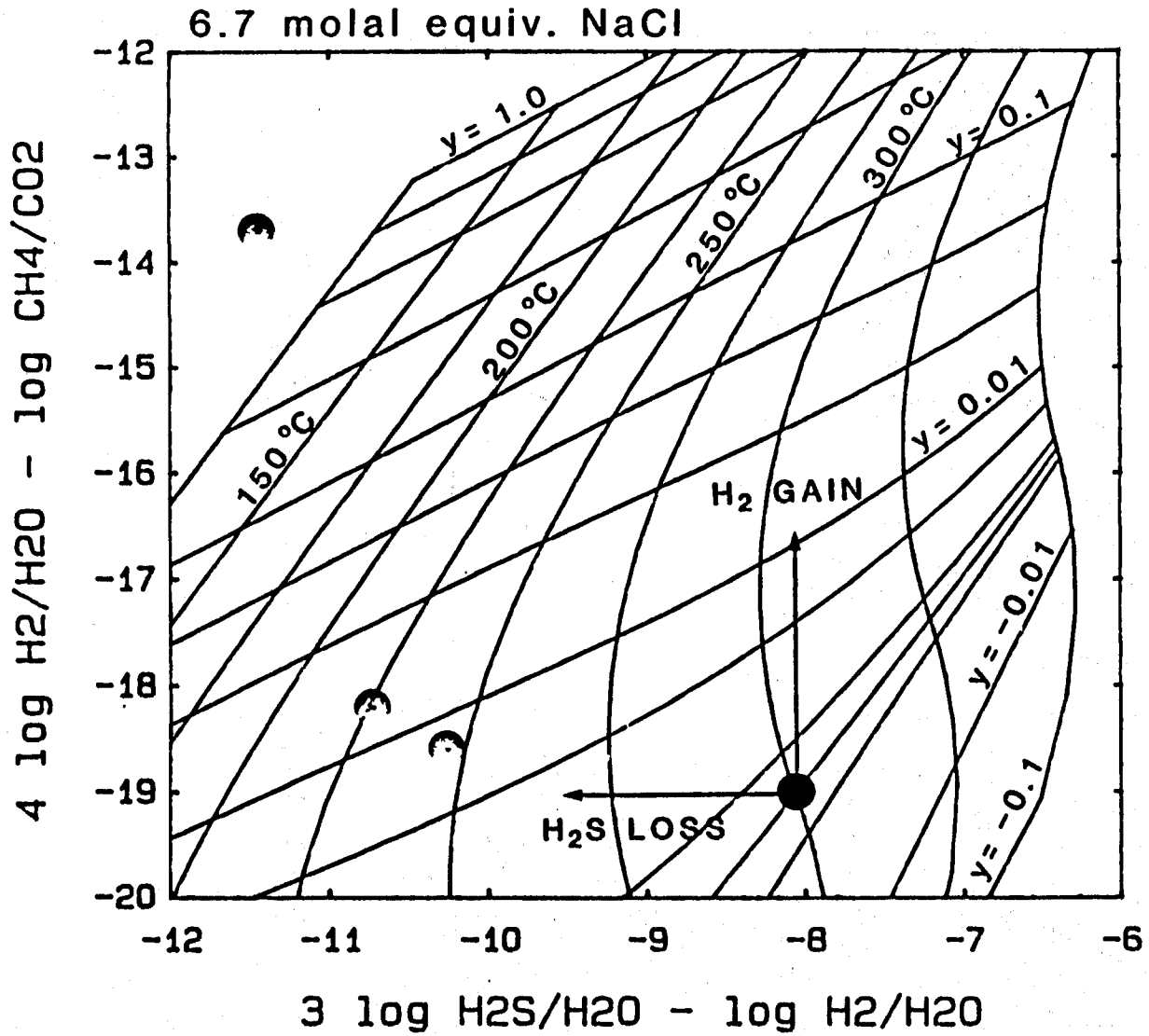

REACTIONS WITH WATER

IRON DISSOLUTION

$$Fe + 2H^+ \rightleftarrows Fe^{2+} + H_2$$

MAGNETITE DEPOSITION

$$3Fe^{2+} + 4H_2O \rightleftarrows Fe_3O_4 + H_2 + 6H^+$$

REACTIONS WITH H_2S

PYRRHOTITE DEPOSITION

$$Fe^{2+} + H_2S \rightleftarrows FeS + H_2$$

PYRITE DEPOSITION

$$Fe^{2+} + 2H_2S \rightleftarrows FeS_2 + 2H_2$$

Changes with Time in Enthalpy and Gas Concentrations for Total Discharge for Well 11, Broadlands"

	Date				
	9/17/68	10/15/68	11/27/68	1/21/69	3/21/69
Enthalpy (cal/g)	296	317	333	374	356
CO_2 (mmole/100 moles)	223	370	480	560	855
CO_2/H_2S ratio	43	44	49	50	59

" At a wellhead pressure of 13.8 bars gage.

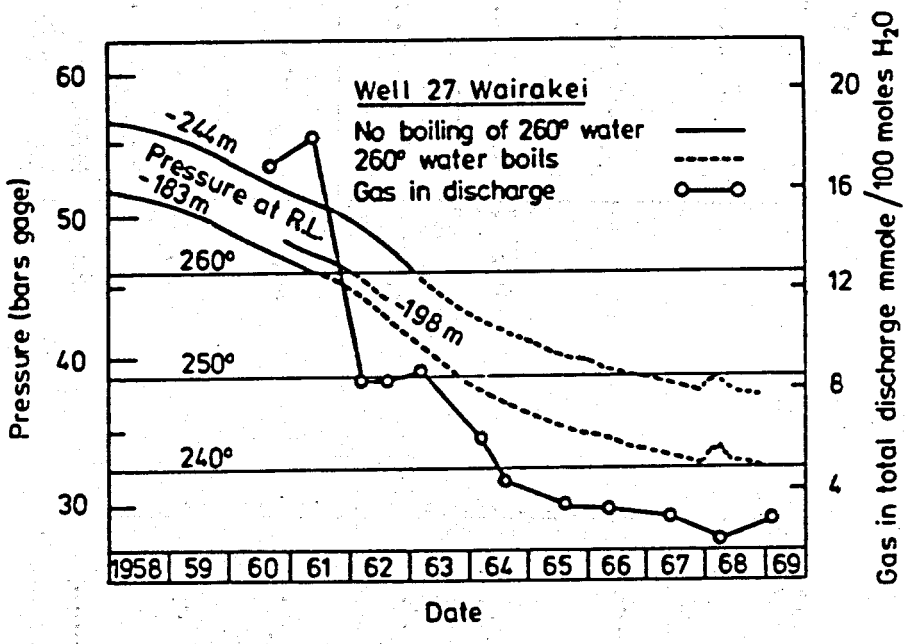

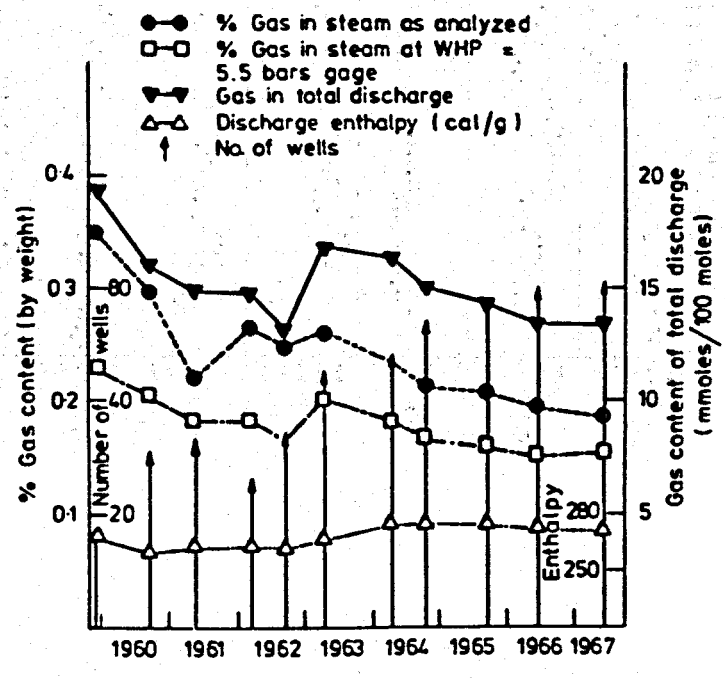

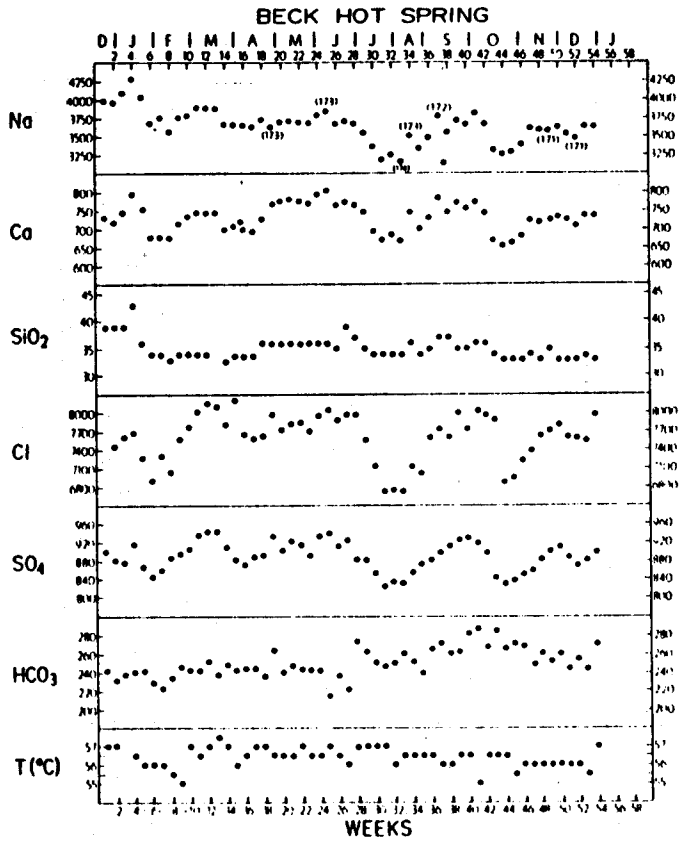
BECK HOT SPRING
Na
Ca
SiO2
Cl
SO4
HCO3
T(°C)
WEEKS

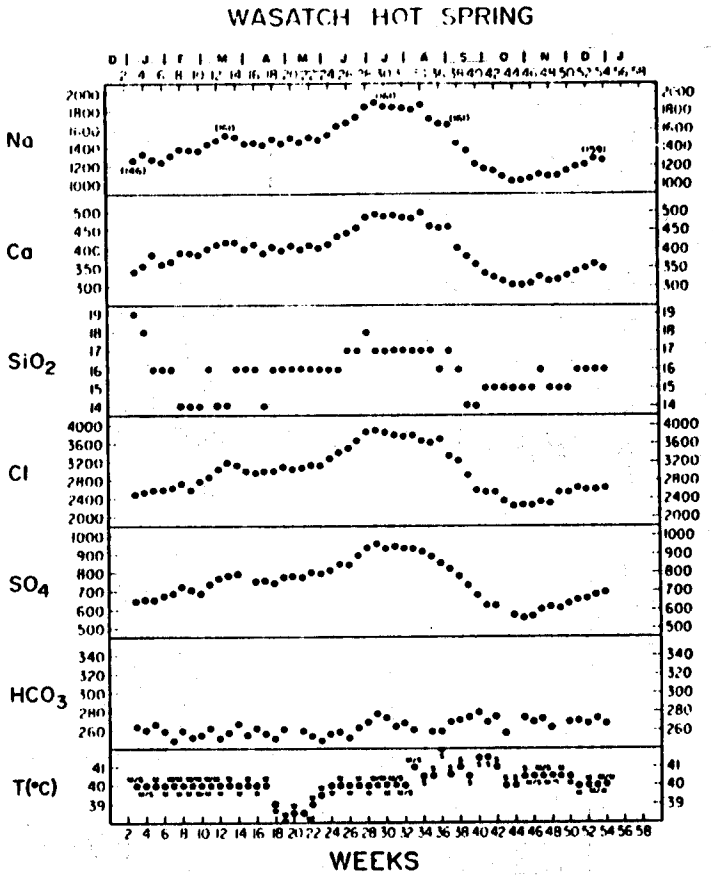
WASATCH HOT SPRING
Na
Ca
SiO2
Cl
SO4
HCO3
T(°C)
WEEKS

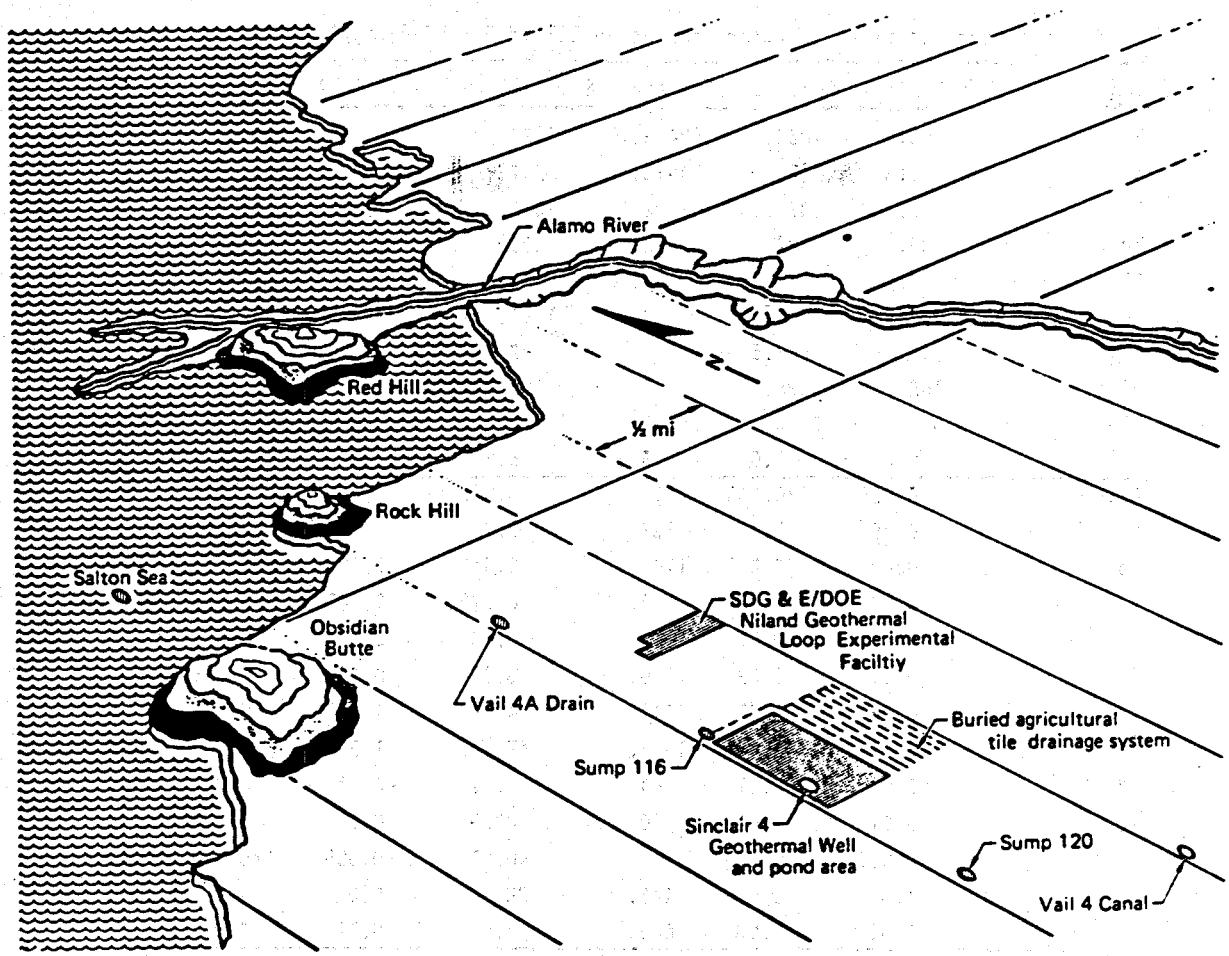

Water sample sites near the Sinclair 4 Geothermal Well in the Salton Sea KGRA used in the Vail 4A Drain case study.

Recommended maximum concentrations of trace elements in water

	Drinking	Irrigation
As	0.05	2.0
B		2.0-10.0
Ba	1.0	
Cu	1.0	5.0
F	1.4-2.4	15.
Fe	0.3	20.
Li		2.5
Mn	0.05	10.
Ni		2.
Pb	0.05	10.
Se	0.01	0.020
Zn	5.0	10.

Nat. Acad. Sci., Water Quality Criteria (1972).

Average concentrations in water samples in Salton Sea KGRA, mg/l.

Ion	Vail4 Canal	Sump 120	Sinclair 4	Sump 116	Vail4A Drain	Alamo River	Salton Sea
Na	168.	1080.	58442.	2470.	970.	607.	10600.
K	6.3	20.	14918.	247.	66.	15.	195.
Ca	93.	373.	26992.	2050.	437.	201.	850.
Mg	35.	187.	736.	385.	160.	120.	1200.
Cl	158.	989.	154590.	8540.	1870.	760.	14700.
SO_4	357.	1990.	19.	1590.	1480.	960.	8100.
CO_3	15.	<2.5		<2.5	<2.5	<2.5	63.
HCO_3	152.	338.	0.	380.	330.	205.	143.
TDS	928.	5030.	266560.	17700.	5970.	3000.	38600.
pH	8.2	7.0	5.3	6.8	7.6	7.7	8.8
As	0.005	<0.005	10.	0.005	0.005	0.007	<0.01
B	0.25	1.1	332.	9.7	2.	0.76	6.8
Ba	0.09	0.097	1100.	0.54	0.093	0.12	0.07
Cu	<0.005	0.005	3.	0.075	0.007	0.014	0.08
F	0.5	0.57	14.	0.48	0.05	0.66	1.1
Fe	0.03	0.08	1240.	0.26	0.08	0.045	0.24
Li	0.08	0.31	344.	14.3	1.24	0.23	3.2
Mn	0.01	0.30	1475.	47.	1.9	0.035	0.08
Ni	0.01	<0.01	<4.	0.31	<0.01	<0.01	<0.2
Pb	<0.01	0.01	60.	0.29	0.02	0.01	<0.1
Se	<0.005	<0.005		<0.01	<0.005	<0.005	0.02
Sr	1.3	5.0	448.	38.	6.0	3.2	13.5
Zn	0.02	0.03	600.	7.8	0.12	0.02	0.03
K/Na × 10	0.38	0.19	2.55	1.0	0.68	0.25	0.18
Cl/SO_4	0.44	0.50	8140.	5.36	1.26	0.79	1.82

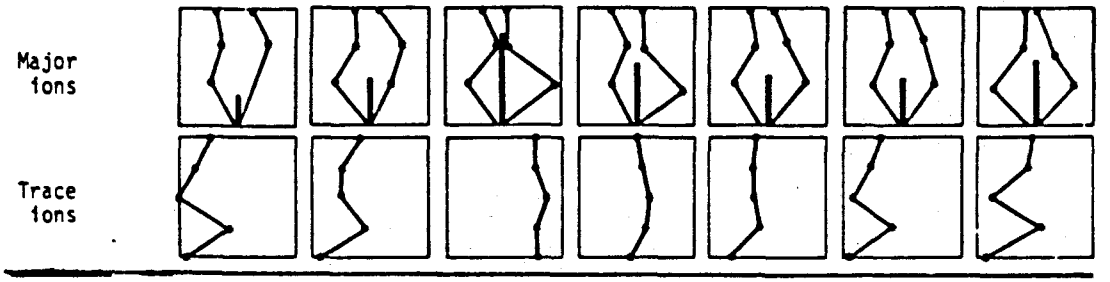

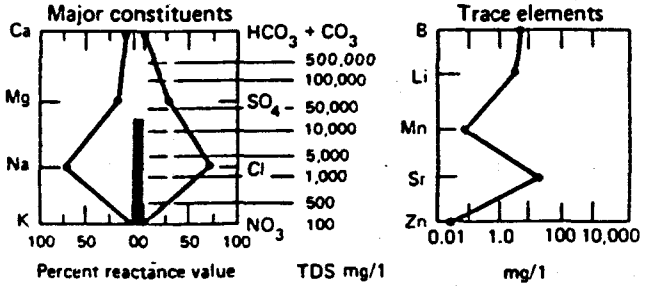

Stiff diagram of major constituents and logarithmic diagram of trace elements

TABLE 17.1: Cost estimate for analytical geochemistry laboratory (data supplied by J.B.Finlayson)

Instrumentation		
Analysis		
pH, HCO_3, CO_2, B	pH meter, bench model	$2000
	Combination pH electrodes	500
Na, K, Ca, Mg, Si, etc.	Atomic Absorption/Emission Spectrophotometer*	35000
	Hollow cathode lamps (Li, Mg, Fe, Mn, Si)	1800
	Gas cylinders and two stage regulators for acetylene, H_2, Air, N_2O, Ar	1000
Si, SO_4	UV-Visible spectroscopy*	12800
	1 set quartz cells	200
		$53300
(* prices quoted for instruments suitable for permanent laboratory)		
Miscellaneous Equipment		
Analytical balance (160-200 g max, 0.0001 g min)		$ 2500
Top loading balance		1800
Water still		700
Water bath (12 holes)		360
Vacuum pump		900
		$6260
Laboratory supplies		
General glassware		= $2000
Reagents		= 3000
		= $5000
Other equipment		
Gas chromatography (incl. vac. pump, gas regulators, recorder)		$10000
Webre separator		4000
Downhole sampling bottle		6500
		$85500

* Costs are specified in $NZ which at the time of writing (June 1982) has an equivalent value of $US 0.76.

Classification of Geothermal (Hydrothermal) Reservoirs

from *O'Sullivan, M. J. and McKibbin, R.*
Geothermal Reservoir Engineering (draft February 1989),
University of Auckland, New Zealand

- **Warm water reservoirs-** Usually includes systems with temperatures in the range 90-180°C and where boiling will not occur in the reservoir even during exploitation. Usually they are useful only for non-electrical purposes. Examples of warm water reservoirs are Tianjin (P.R. China) and Waiwera (New Zealand).

- **Hot water reservoirs-** These systems are all hot water in their pre-production state but may boil after extensive production. Temperatures are usually in the range 200-250°C (the presence of gas may cause some reservoirs in this temperature range to boil). Wairakei with maximum initial temperatures of 260-270°C and a small initial boiling region is often called a hot water system but perhaps fits better into the next category. Ahuachapán, Salton Sea and the upper reservoir at Krafla are hot water types.

- **Two-phase liquid-dominated reservoirs-** In these reservoir a two-phase region containing a mixture of steam and liquid water overlying a deeper hot liquid layer is present in the natural state (Wairakei and Cerro Prieto are examples). Temperatures vary (220-300°C) with the presence of gas causing boiling at lower temperatures (for example Ohaaki-Broadlands, Ngawha).

- **Two-phase vapor-dominated reservoirs-** Vapor-dominated systems also contain an upper two-phase layer. In this case, however, the liquid phase is sparse, widely dispersed and immobile and so wells produce only steam (Geysers and Lardarello). Again temperatures vary (say 230-330°C) depending on depth and gas content.

When drilling first occurs in a geothermal reservoir it may be classified into one of the above categories quite easily. If it is vapor-dominated then a low downhole pressure and the production of dry steam will serve to identify it. The remaining categories can be distinguished by temperature distribution with depth.

High–Temperature Geothermal (Hydrothermal) Systems

TYPICAL CHARACTERISTICS OF PRODUCING FIELDS

Rock Type:
Volcanic (sedimentary, plutonic, metamorphic)

Permeability:
Related to fractures (primary pores)

Reservoir Depth:
Generally between 500 and 2500 meters

Reservoir Thickness:
Hundreds to thousands of meters

Reservoir Transmissivity:
1 to 100 darcy-meters

Reservoir Temperature:
150 to 350°C

Reservoir Fluids:
Total dissolved solids (0.2 to 25 % weight)
Non-condensible gases (0 to 10% weight; 0 to 5 bars CO_2 partial pressure)

For additional details see Bjornsson, G. and Bodvarsson, G.S. (1989), " A survey of geothermal reservoir properties ", paper submitted to Geothermics (Lawrence Berkeley Laboratory report LBL-26892).

- Hydrothermal convective systems are dynamic in nature

- Complex geologic structures may control the convective heat transport in these systems.

- Complex processes occur in these systems under natural conditions and in response to exploitation.

- In order to understand the behavior of these systems one has to analyze field data obtained through a carefully designed exploration and monitoring program.

- For most geothermal systems the geological and thermodynamic complexities are such that numerical models are required for testing conceptual models and for predicting reservoir response to exploitation.

Conceptual Model of a Geothermal System

Definition

The conceptual model reflects our current knowledge of a given geothermal system and its dynamics. It is a descriptive or qualitative model that incorporates the essential features, and physical and chemical processes that affect the system. The model should be capable of matching the characteristics and salient behavior of the geothermal system.

Definition based on:

Bodvarsson, G.S., Pruess, K. and Lippmann, M.J., 1986. Modeling of Geothermal Systems, Jour. Petr. Tech., Vol. 38, No. 10, pp. 1007-1021.

Grant, M.A., Donaldson, I.G., and Bixley, P.F., 1982. Geothermal Reservoir Engineering, Academic Press, 369 p.

Main Processes Occurring in the Reservoir

- Mass Flow (Liquid, Steam, Dissolved Solids, Non-Condensible Gases)
- Heat Flow (Conduction/Convection)
- Phase Changes (Boiling/Condensation)
- Stress Changes
- Mixing of Fluids
- Fluid/Fluid and Rock/Fluid Interactions

Hydrothermal Systems are Described/Characterized by Conceptual Models that Range —

FROM:

SIMPLE MODELS

That correspond to systems presenting

Uncomplicated geometry/geologic structure
Porous medium porosity/permeability
Low temperature (< 200°C)
Single phase fluid
Single low salinity fluid
Low amounts of non-condensible gases

TO:

COMPLEX MODELS

That correspond to geothermal systems presenting

Complicated geometry/geologic structure
Fractured medium porosity/permeability
High temperatures (> 200°C)
Two-phase fluid(s)
High salinity fluid(s)
High amounts of non-condensible gases

To Develop the Conceptual Model of a Geothermal System

one has to consider/analyze:

a) Geological data
(lithology, hydrothermal alteration, faults)

b) Drilling/well completion data
(depth of lost circulation zones, casing data)

c) Location and characteristics of surface manifestations
(fluid composition, temperature, flow rate)

d) Geophysical data
(surface and downhole data)

e) Downhole temperature, pressure and flow rate data
(vertical and horizontal distribution)

f) Wellhead data
(pressure, enthalpy, fluid composition)

and the changes of c) to f) with time (i.e., in response to the exploitation of the system).

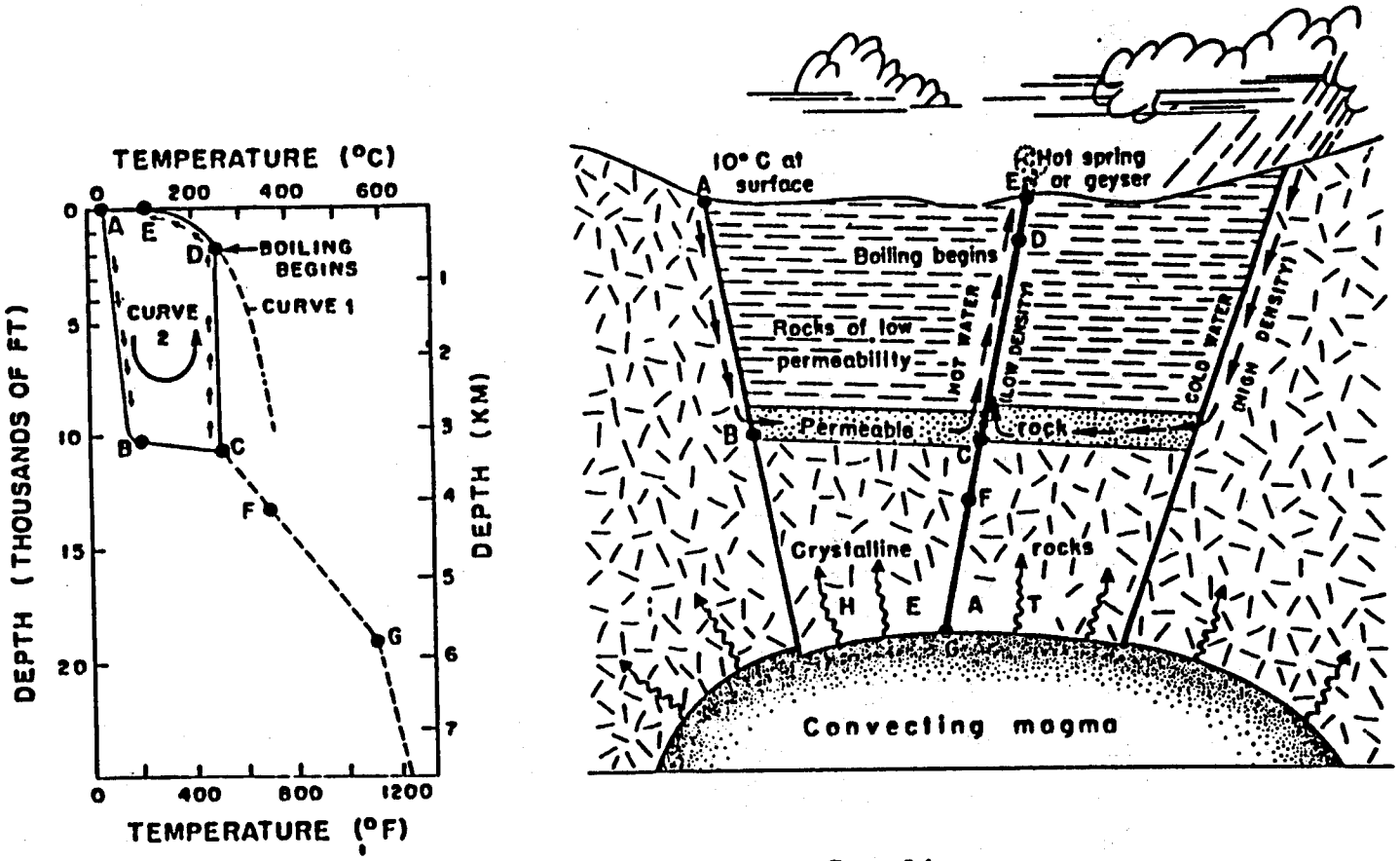

Model of a high-temperature hot-water geothermal system. Curve 1 is the reference curve for the boiling point of pure water. Curve 2 shows the temperature profile along a typical circulation route from recharge at point A to discharge at point E.

(From D.E. White, 1973).

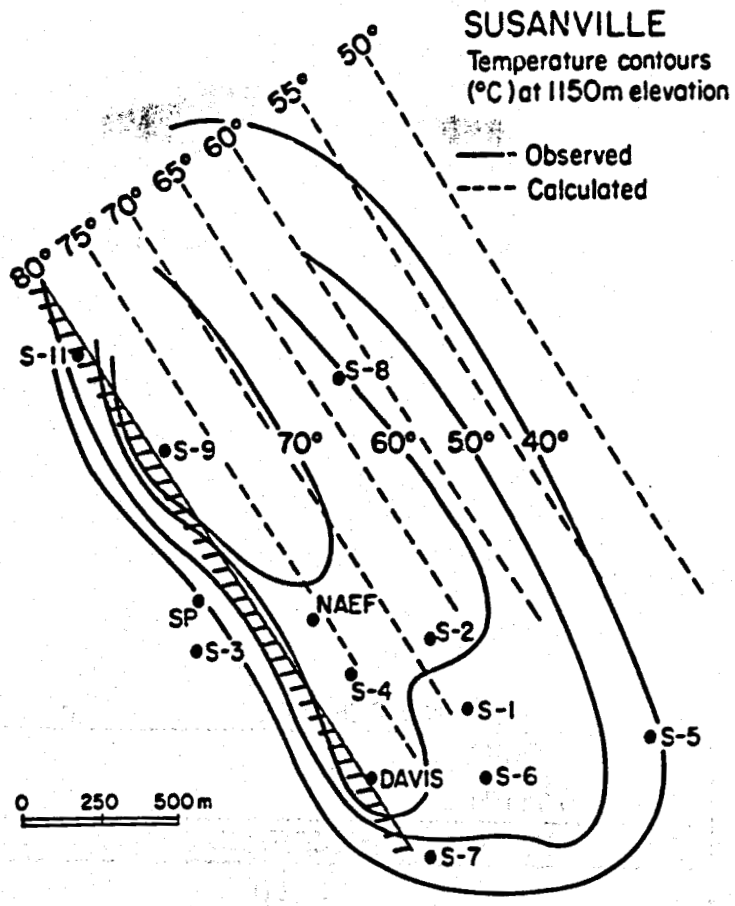

Susanville, California. Comparison between observed and calculated temperature countour data (Bodvarsson, G.S., et al., 1981).

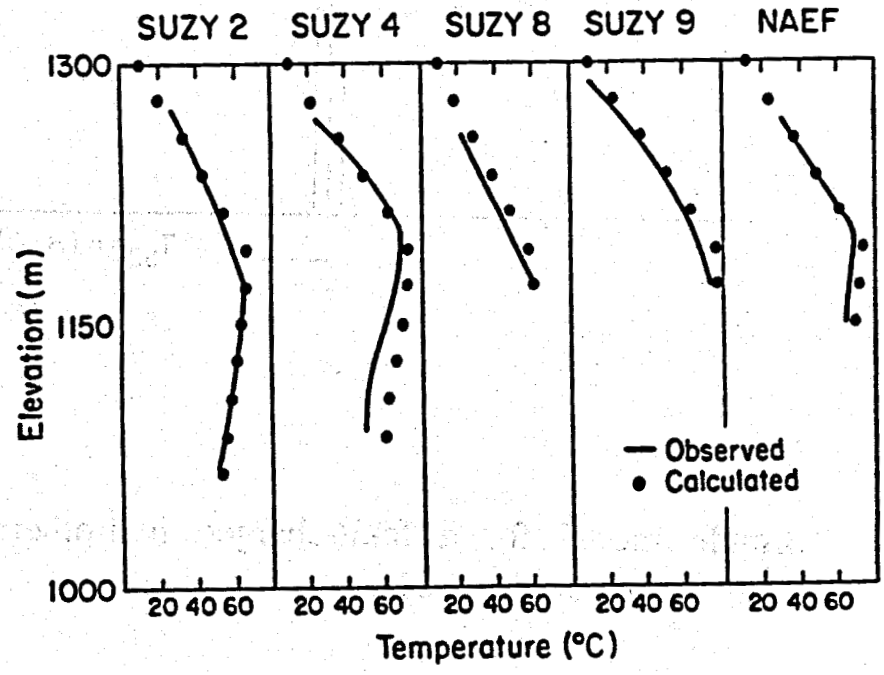

Susanville, California. Comparison between observed and calculated downhole temperature profiles (Bodvarsson, G.S., et al., 1981).

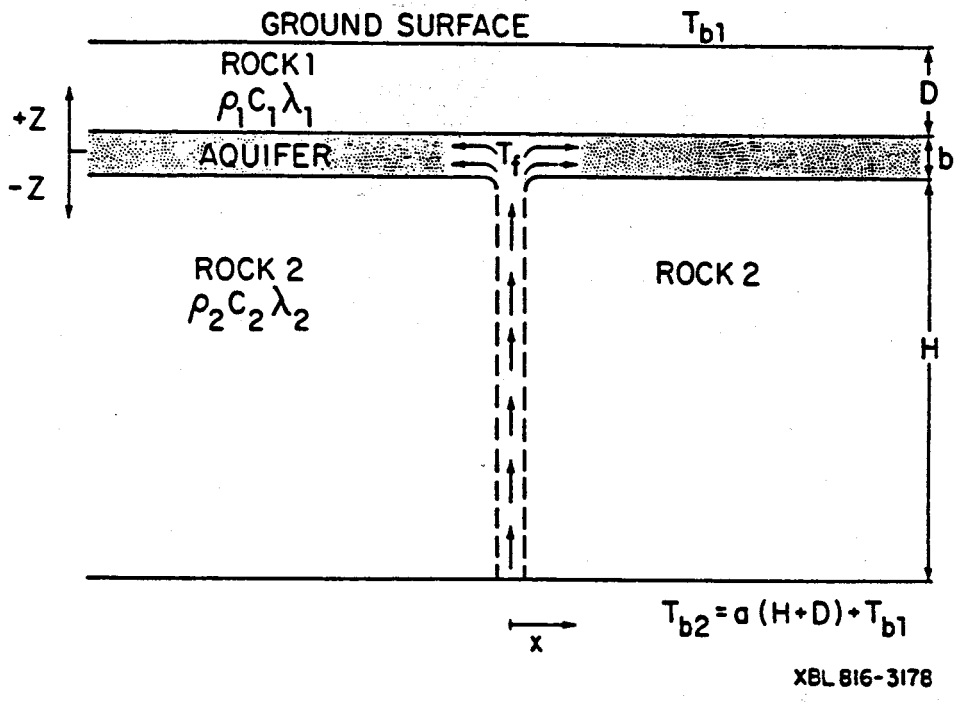

Simple model for a fault-charged hydrothermal system (G.S. Bodvarsson, et al., 1981).

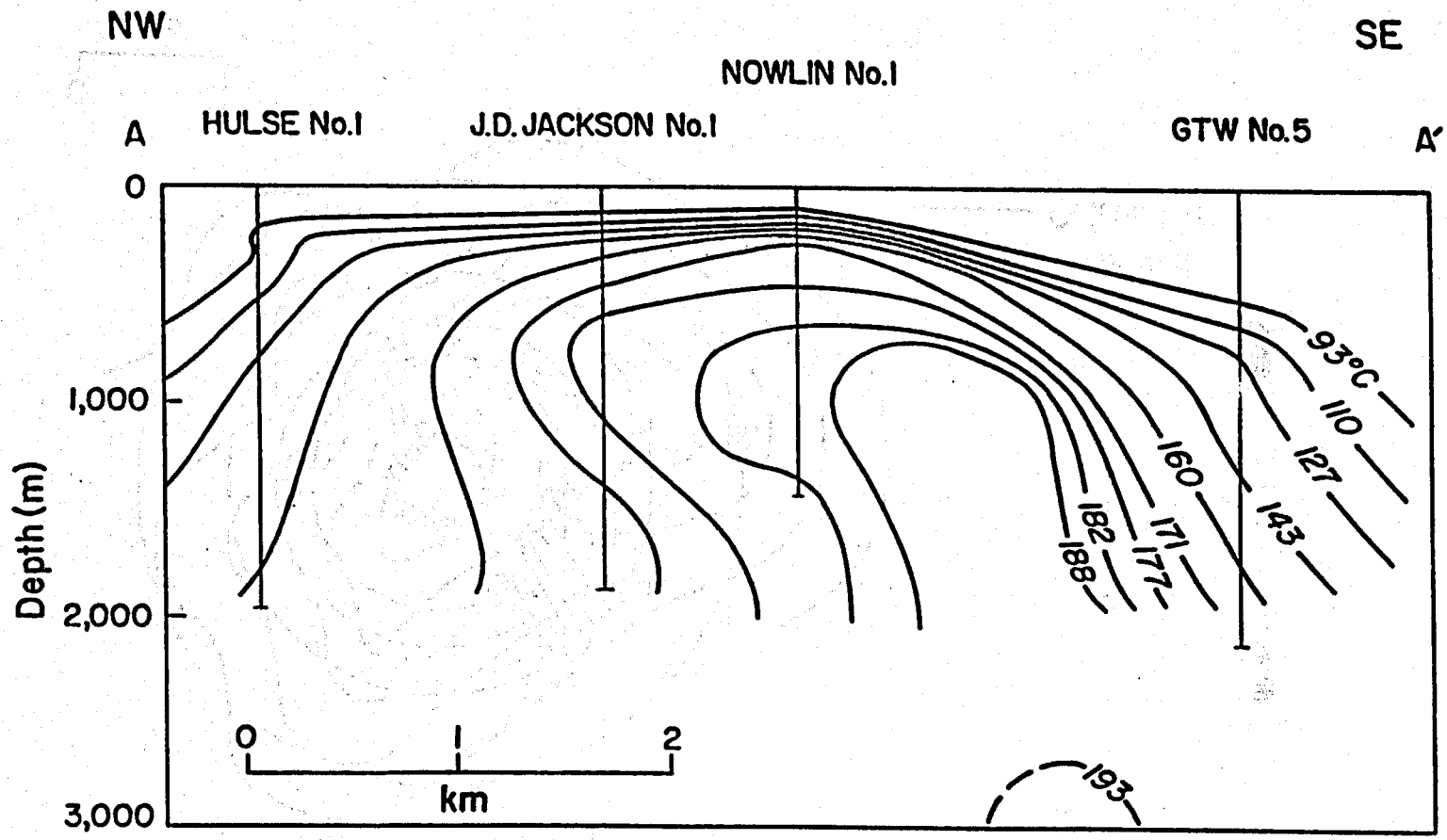

Temperature distribution in the Heber geothermal field (based on Salveson and Cooper, 1981).

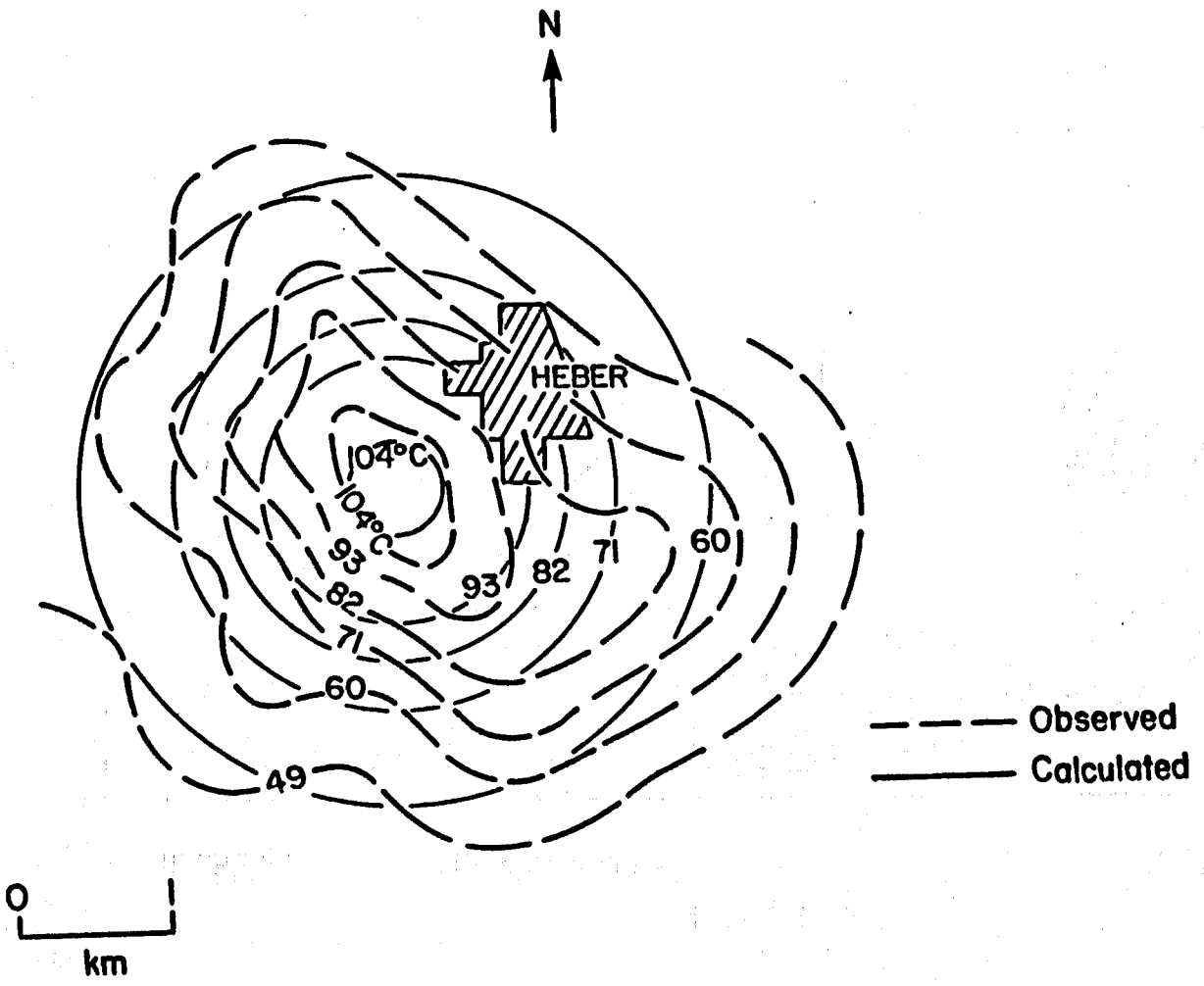

Heber. Comparison between observed temperatures at 146 m depth and computed steady state temperatures (Lippmann and Bodvarsson, 1985).

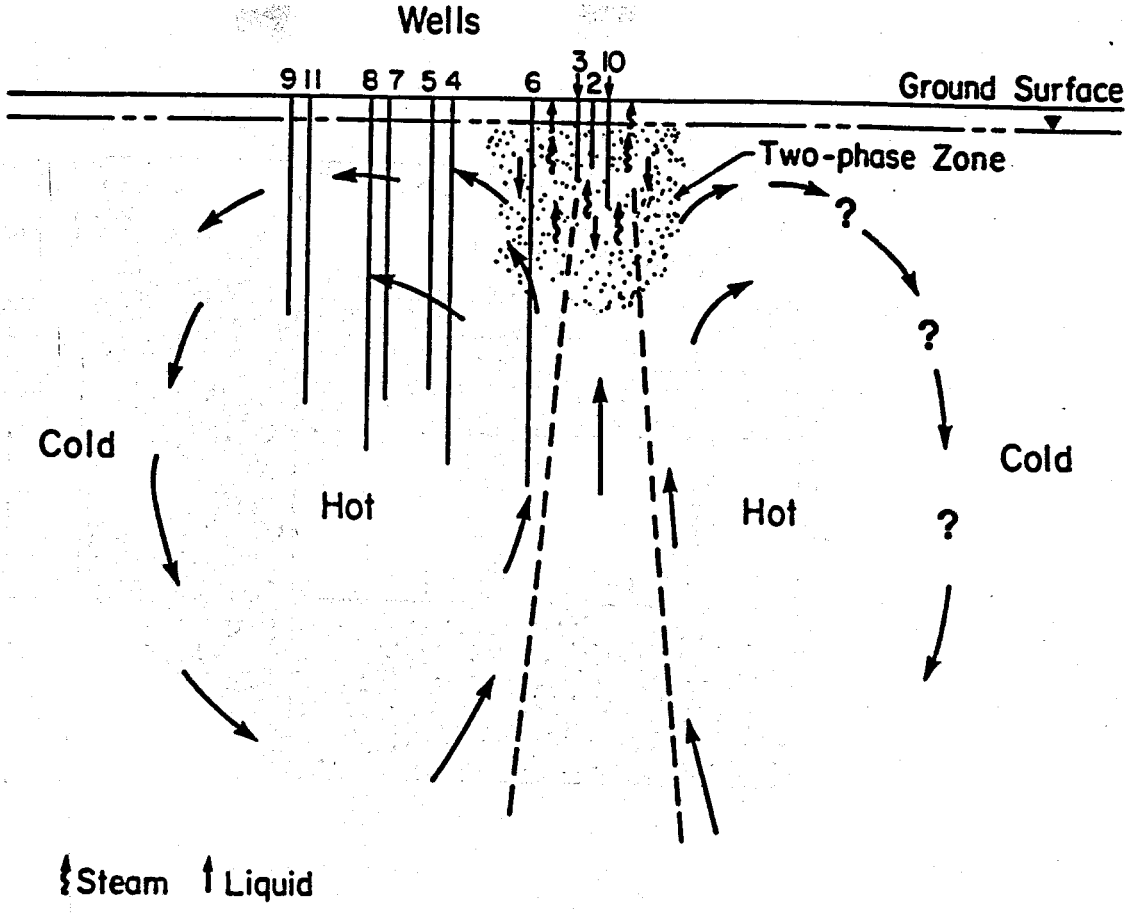

Conceptual model of Svartsengi, Iceland.

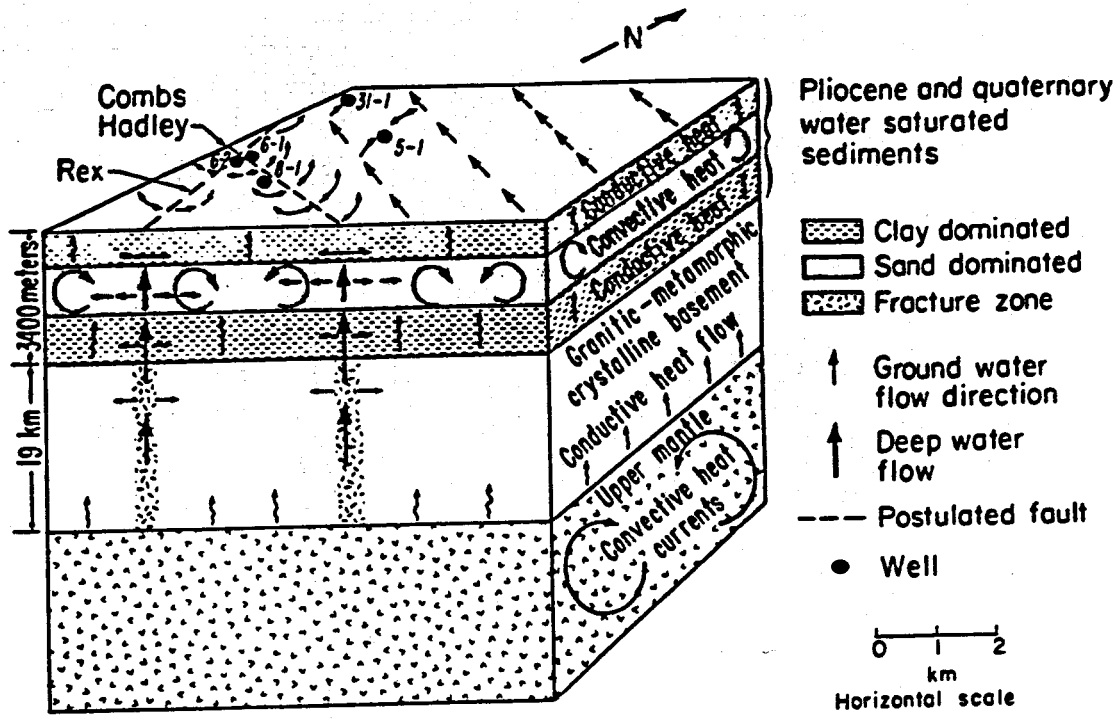

Conceptual model of the East Mesa anomaly (based on Bailey, 1977).

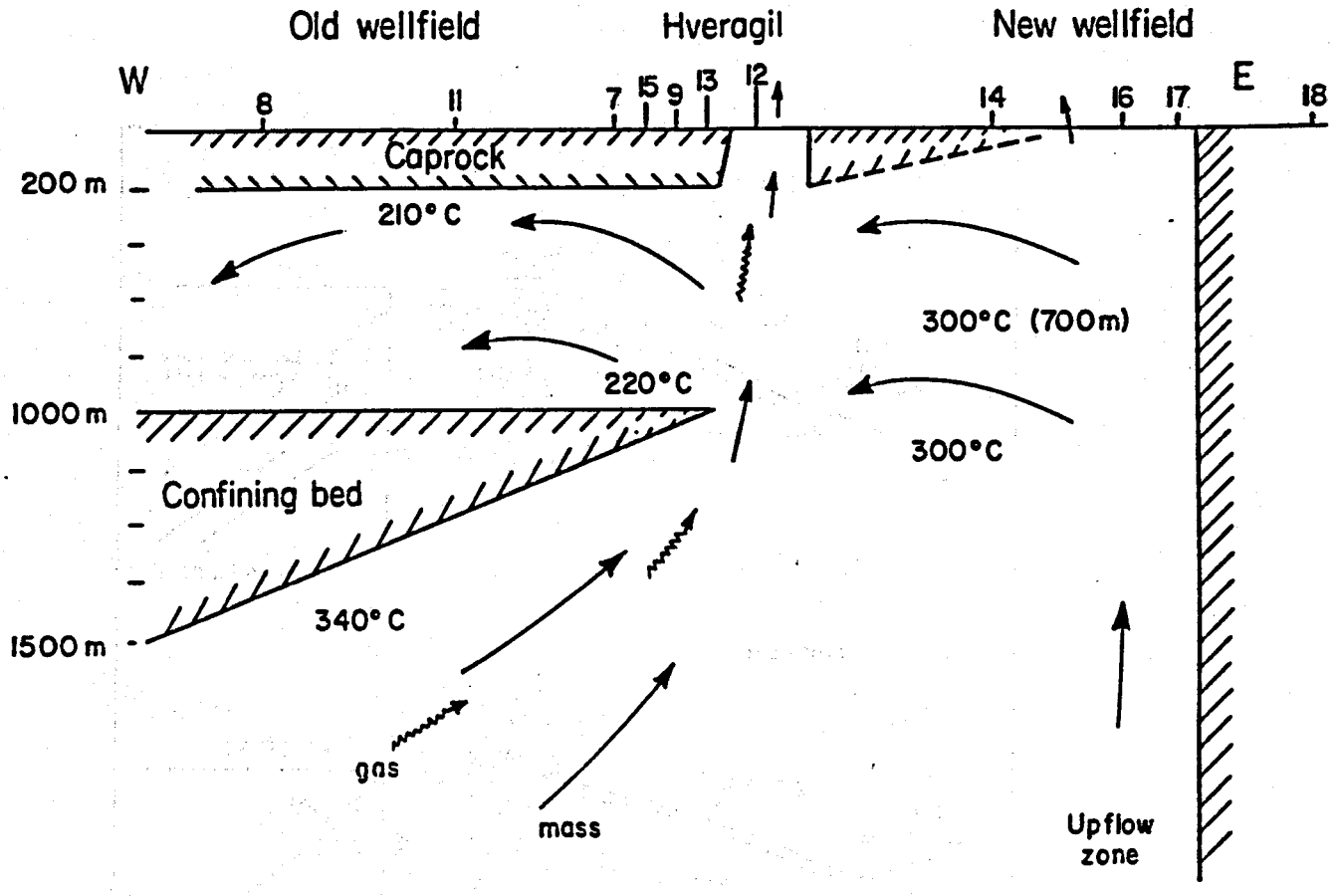

Conceptual model of the Krafla field (G.S. Bodvarsson et al., 1984).

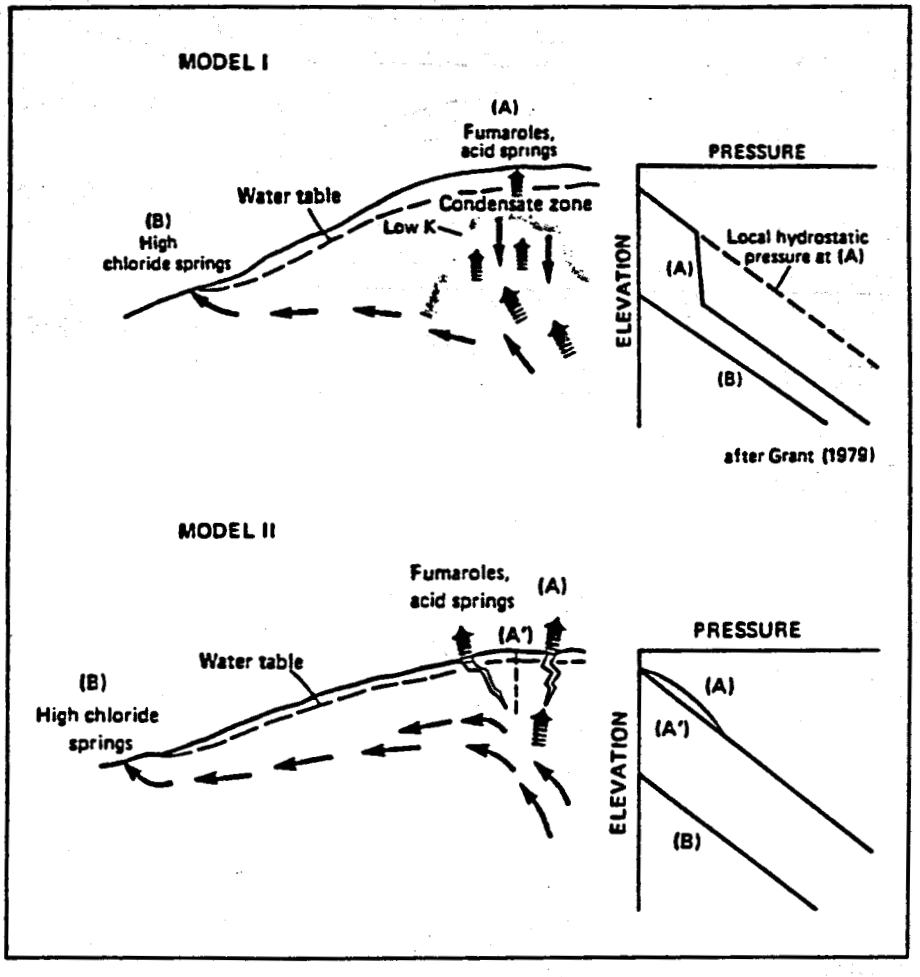

Conceptual models applicable to the Lassen Hydrothermal System. Both models involve lateral flow that links acid-sulfate features at higher elevations with high-chloride discharge at lower elevations. Solids arrows: liquid flow; Broken arrows: steam flow (from Ingebritsen, S.E. and Sorey, M.L., 1987).

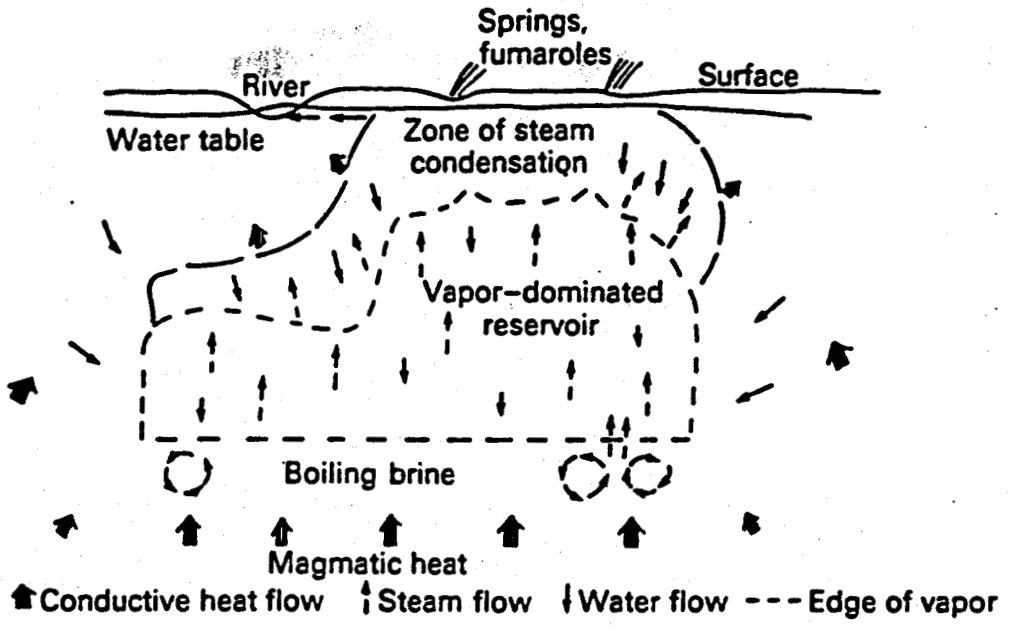

Conceptual model of the natural state fluid flow in a vapor-dominated reservoir (after White et al., 1971).

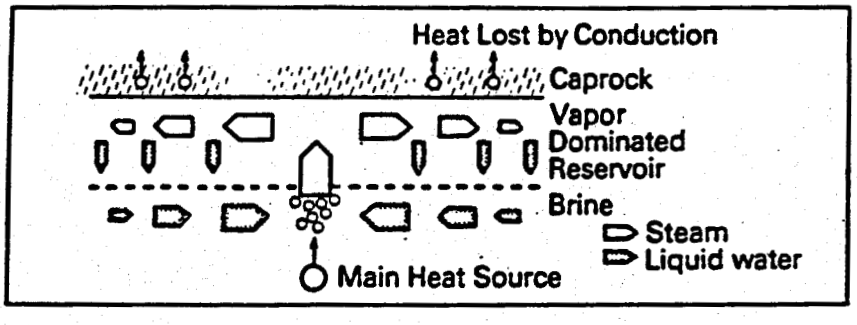

Conceptual model of the natural state of a vapor-dominated reservoir (D'Amore and Truesdell, 1979).

Development of the Conceptual Model of Cerro Prieto

(evolution of the model with time)

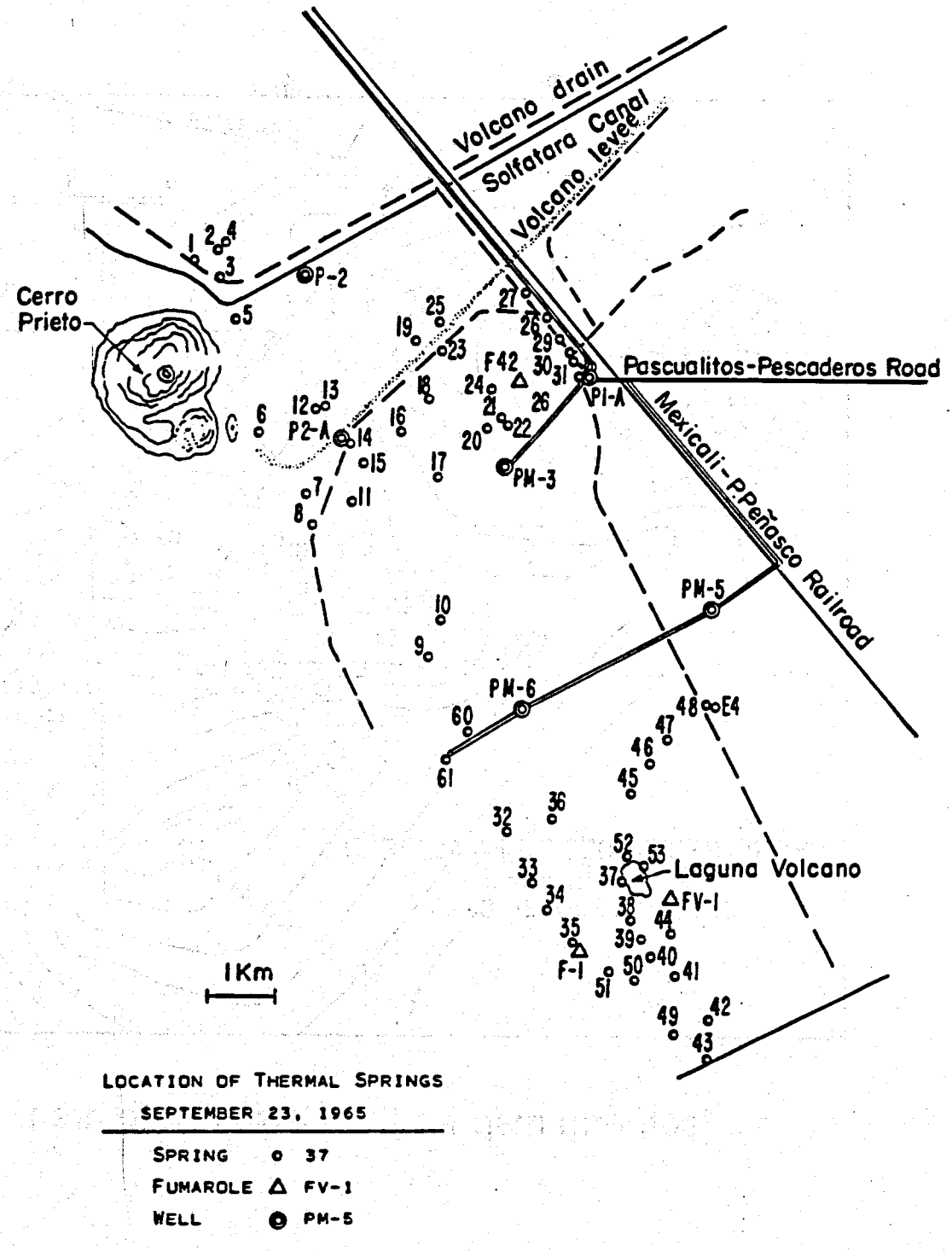

Location of surface manifestations in the Cerro Prieto area (Mañón et al., 1977).

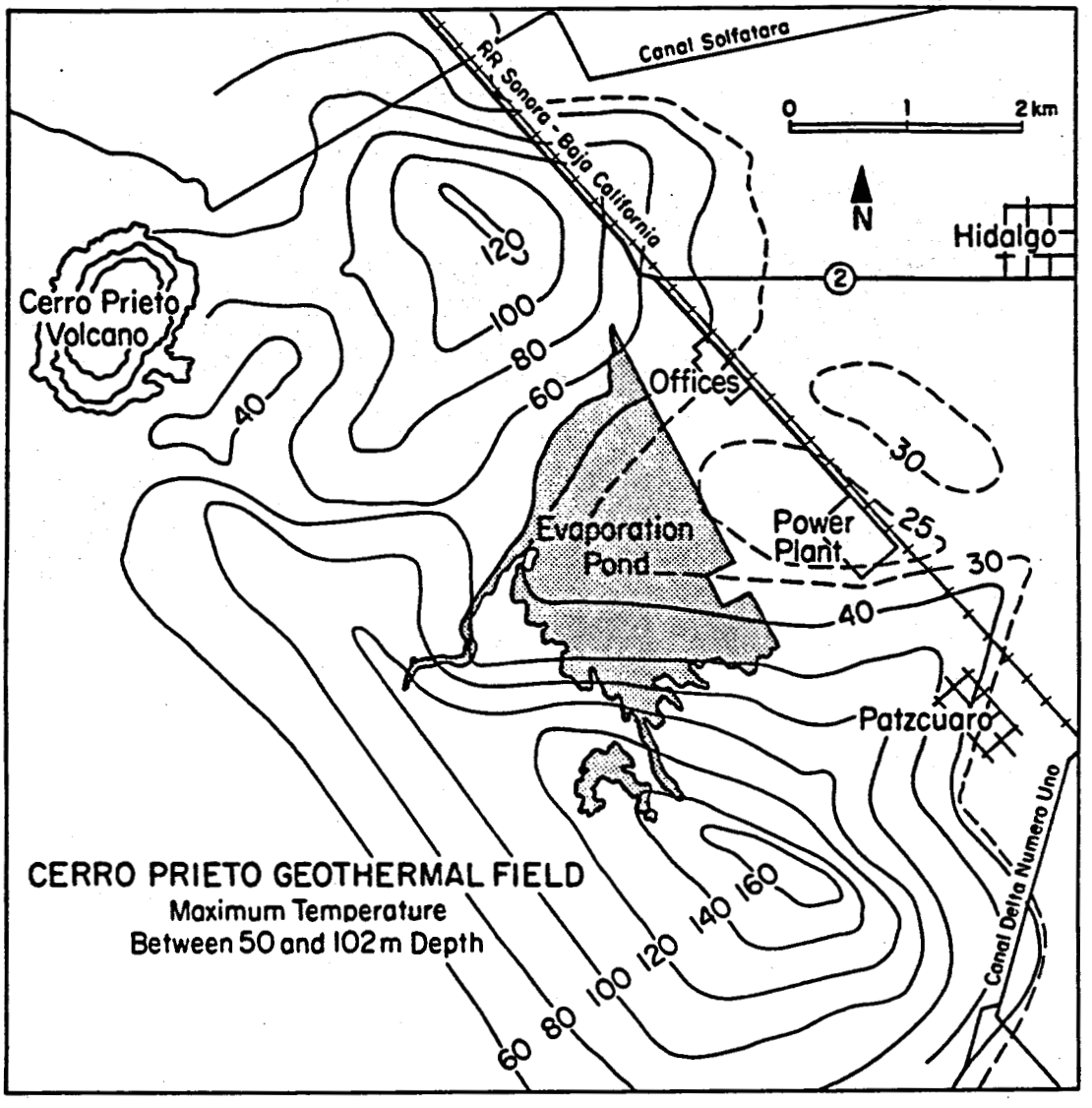

Isotherm map for the Cerro Prieto area.

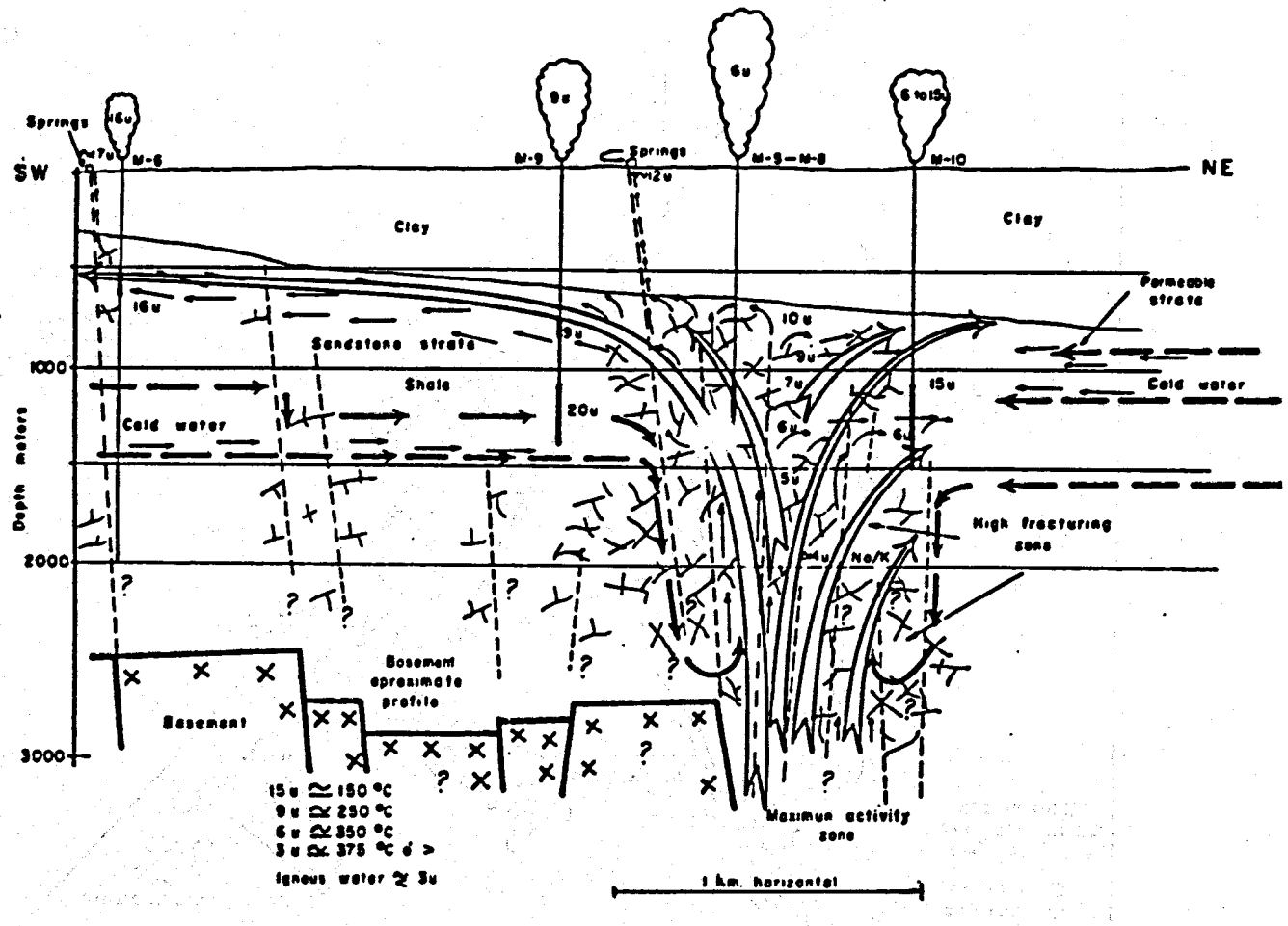

Cerro Prieto. Fluid flow model and Na/K distribution (Mercado, 1970).

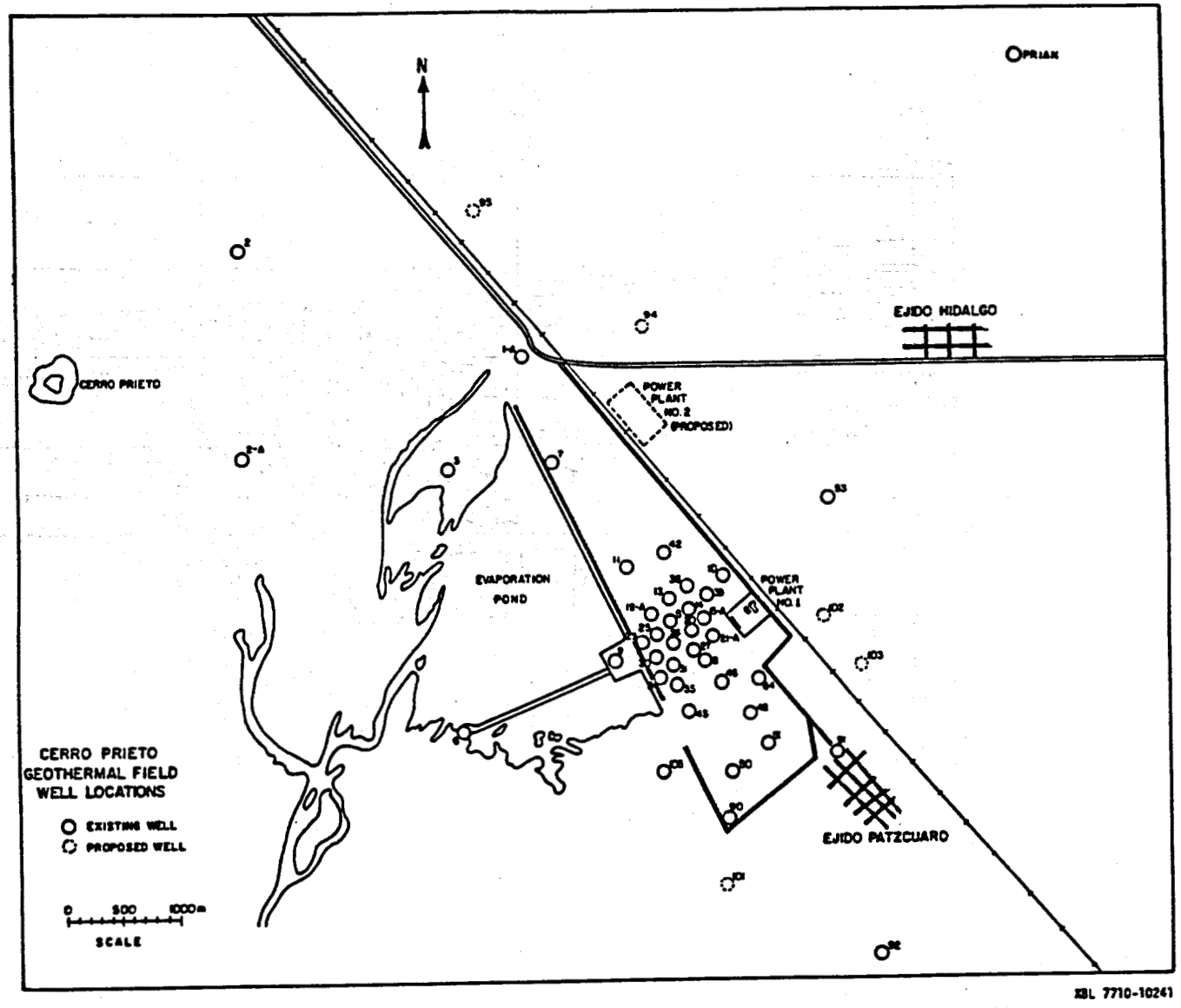

Well locations at Cerro Prieto (1977).

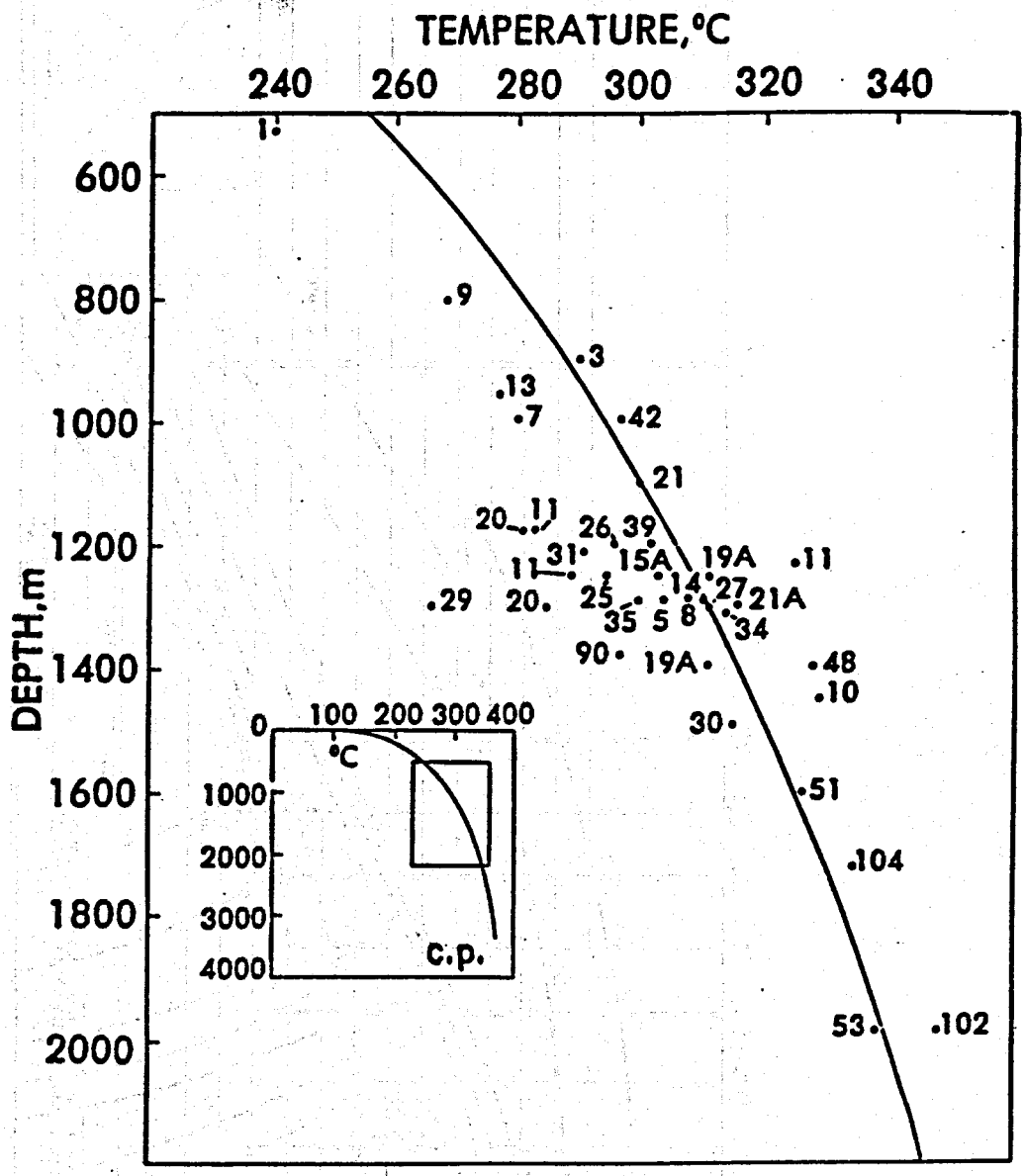

Cerro Prieto. Increase of temperature with depth; most wells fall close to the boiling-point-to-depth curve (Grant et al., 1984).

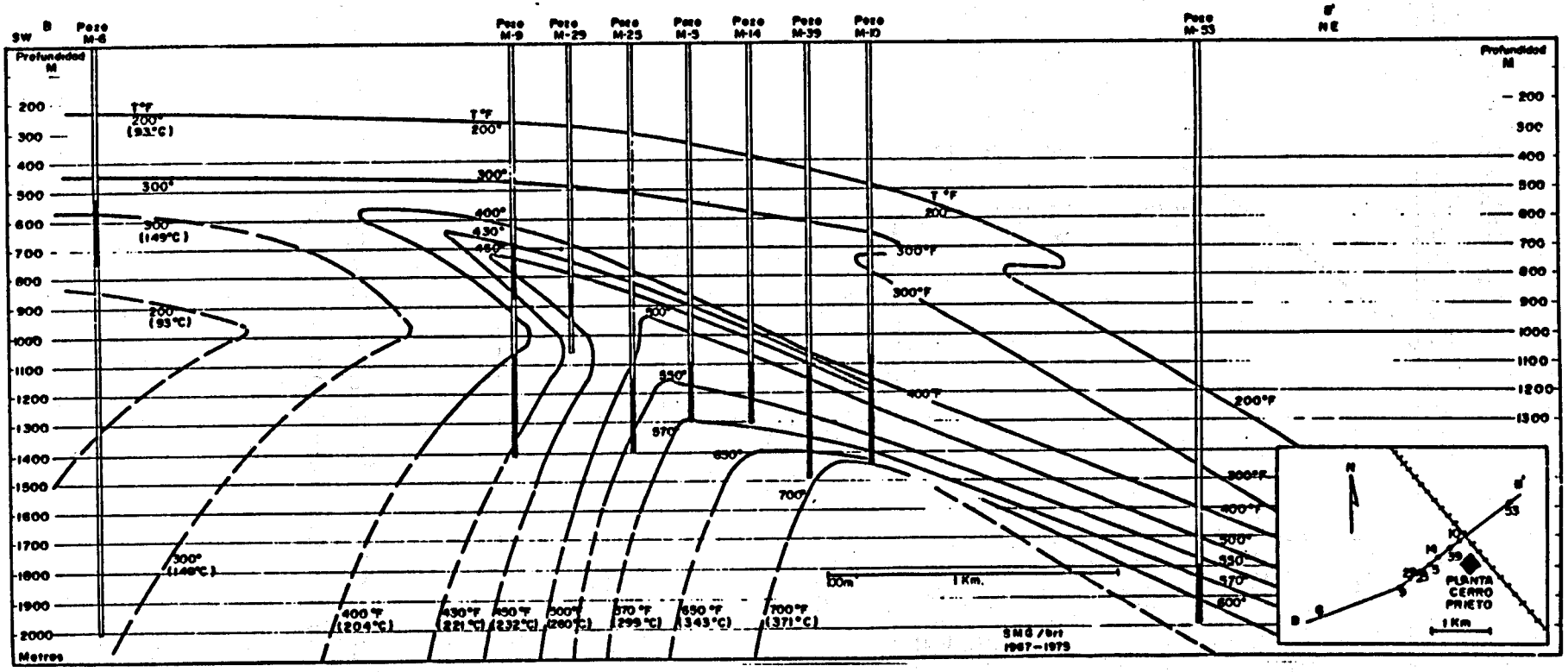

Cerro Prieto. Temperature distribution (Mercado, 1976).

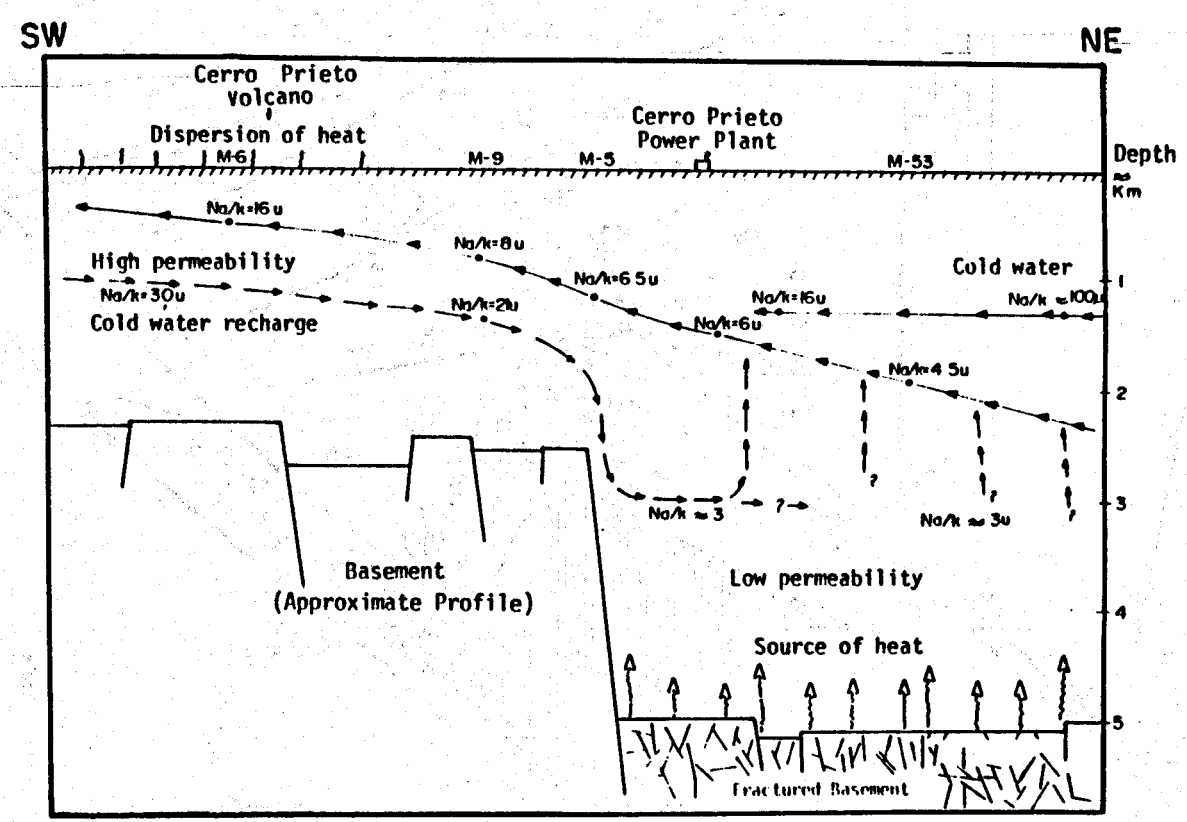

Mercado's (1976) convective model for the Cerro Prieto system.

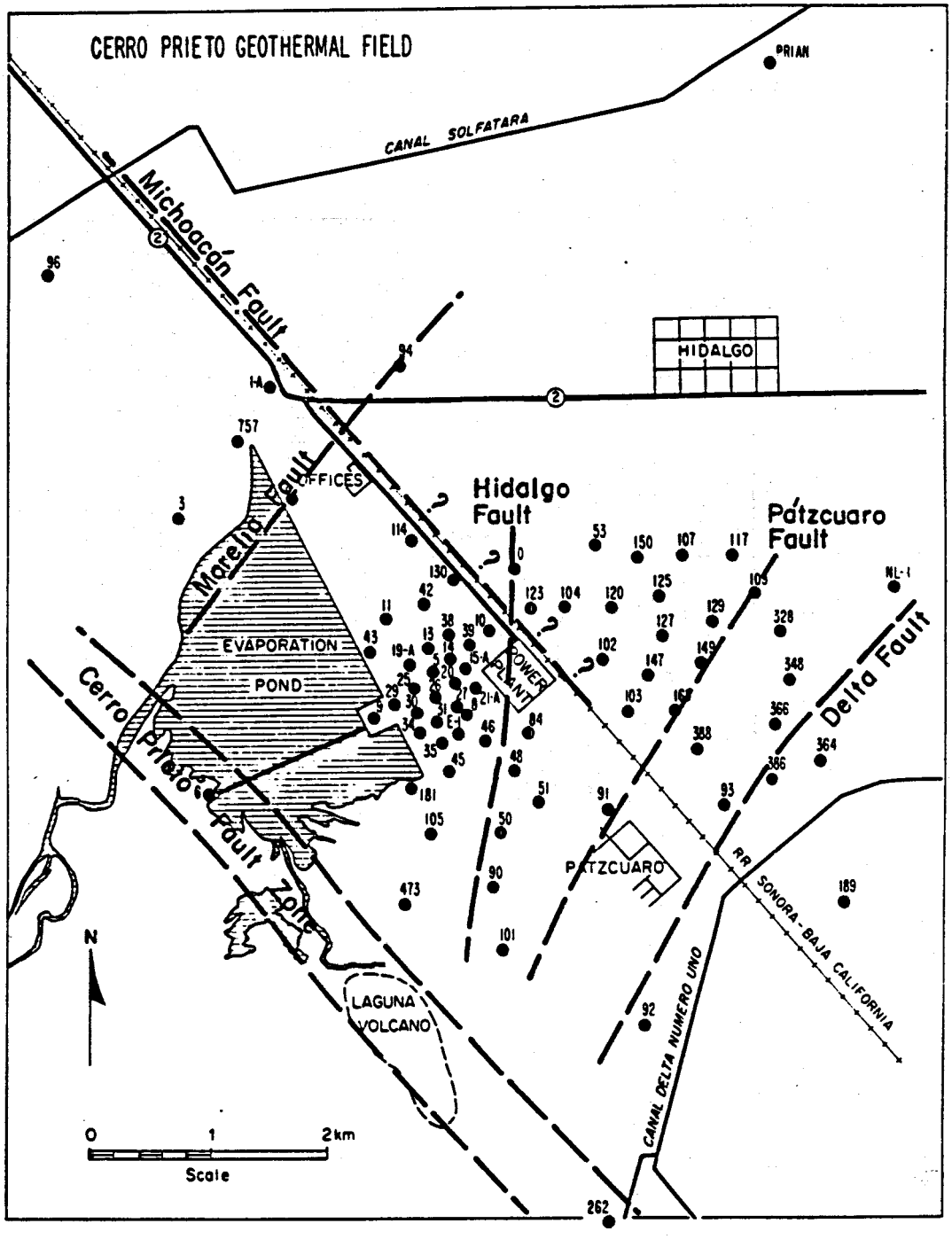

Schematic fault map for the Cerro Prieto area developed in 1980.

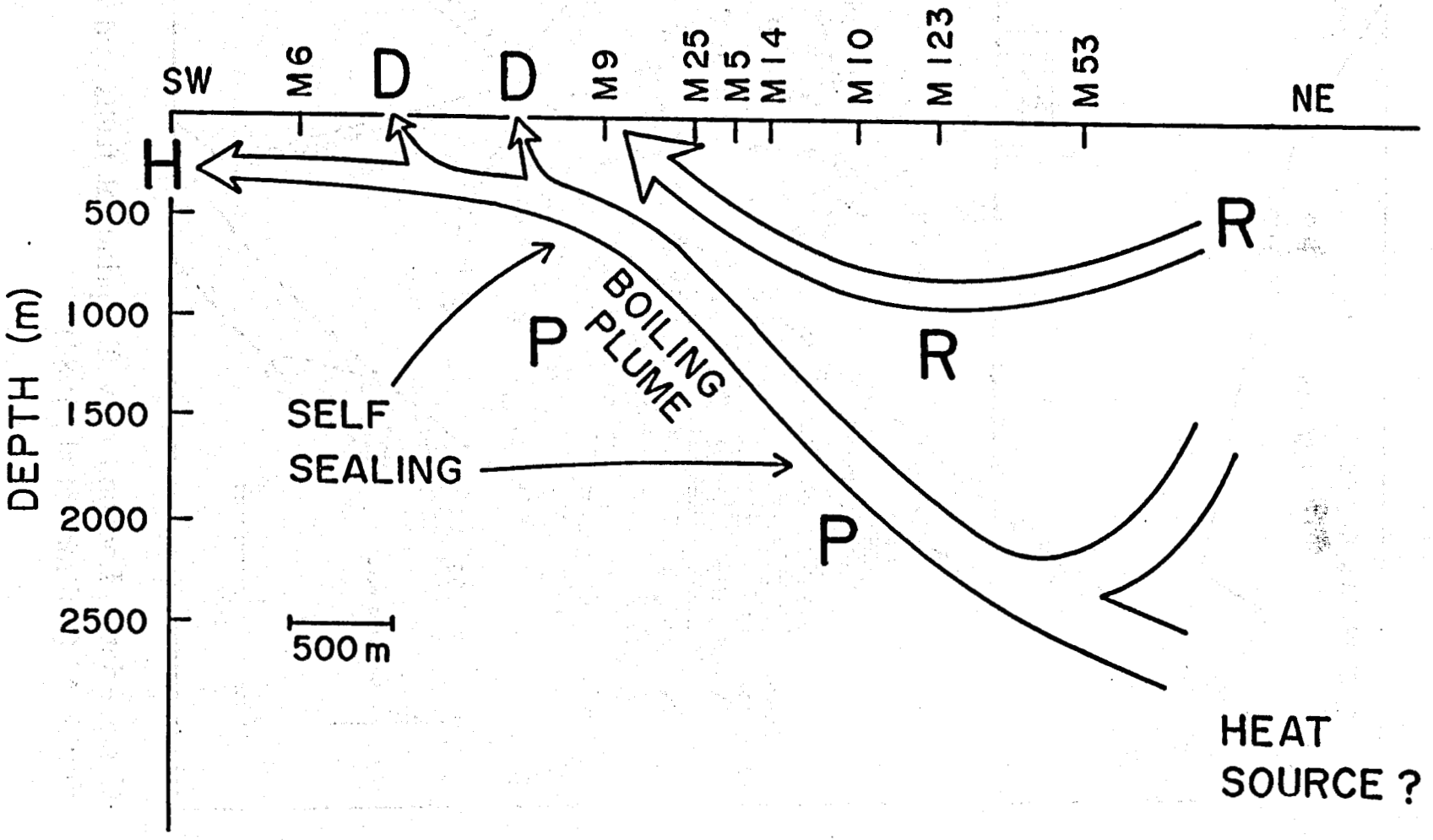

Proposed flow pattern at Cerro Prieto (Elders et al., 1984).

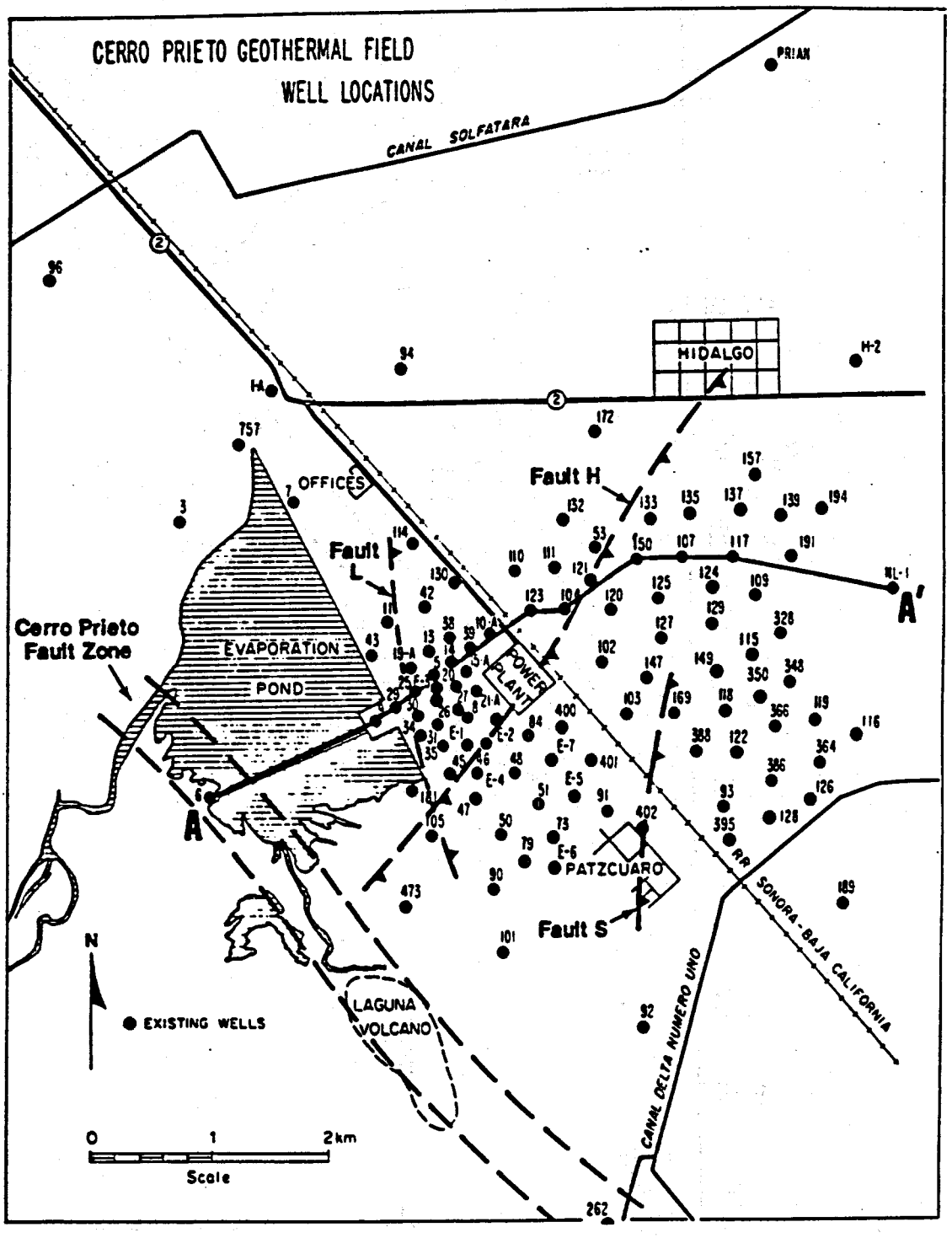

Cerro Prieto. Location of wells, principal faults and cross section A-A' (Halfman et al., 1984).

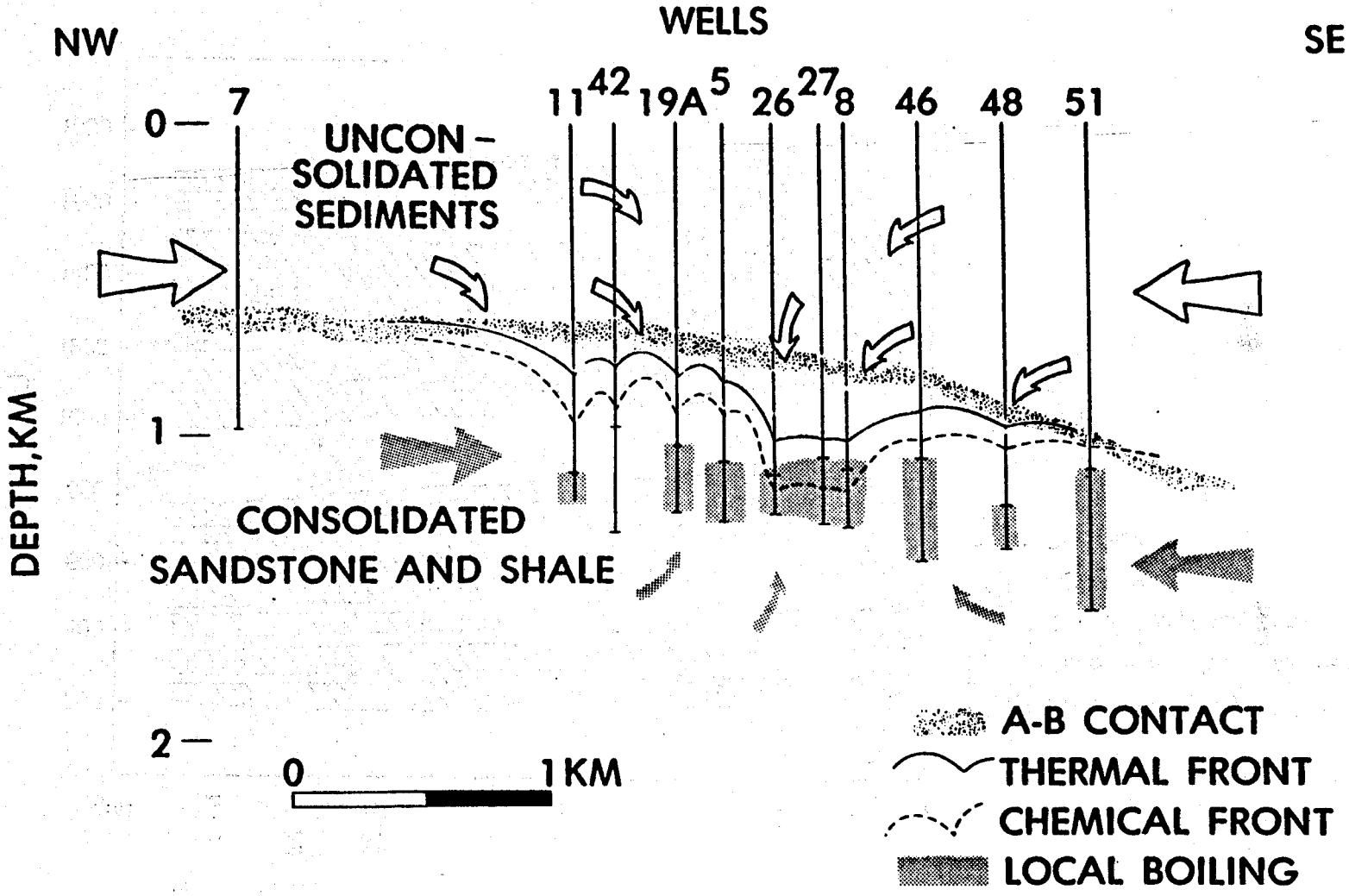

Schematic section across the western Cerro Prieto reservoir showing flows of hot and cold water toward the producing wells, the chemical fronts and zones of near-well boiling (Grant et al., 1984).

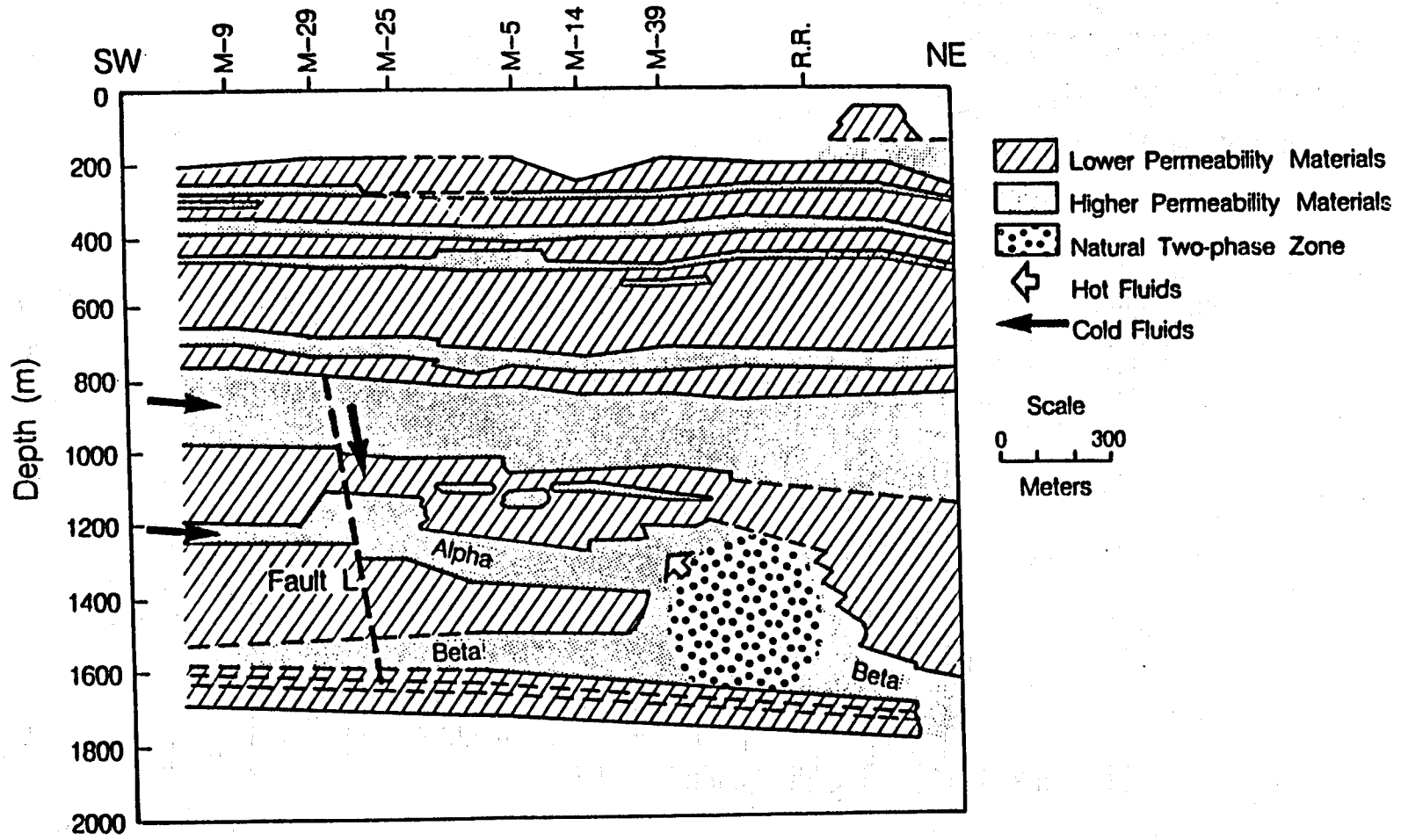

Postulated fluid recharge pattern in the Cerro Prieto alpha reservoir resulting from its exploitation (from Truesdell and Lippmann, 1986).

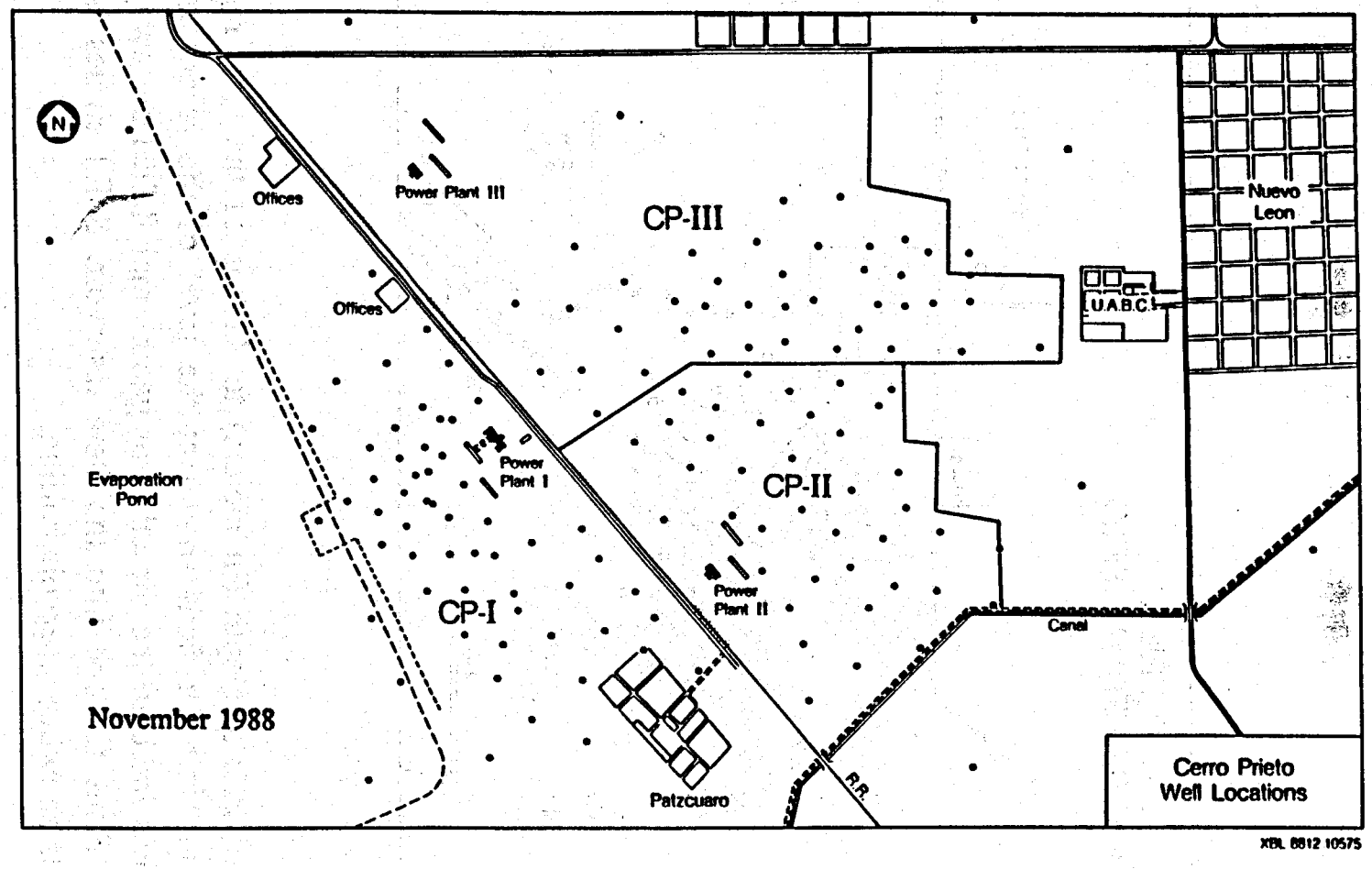

Cerro Prieto. Well locations (November 1988).

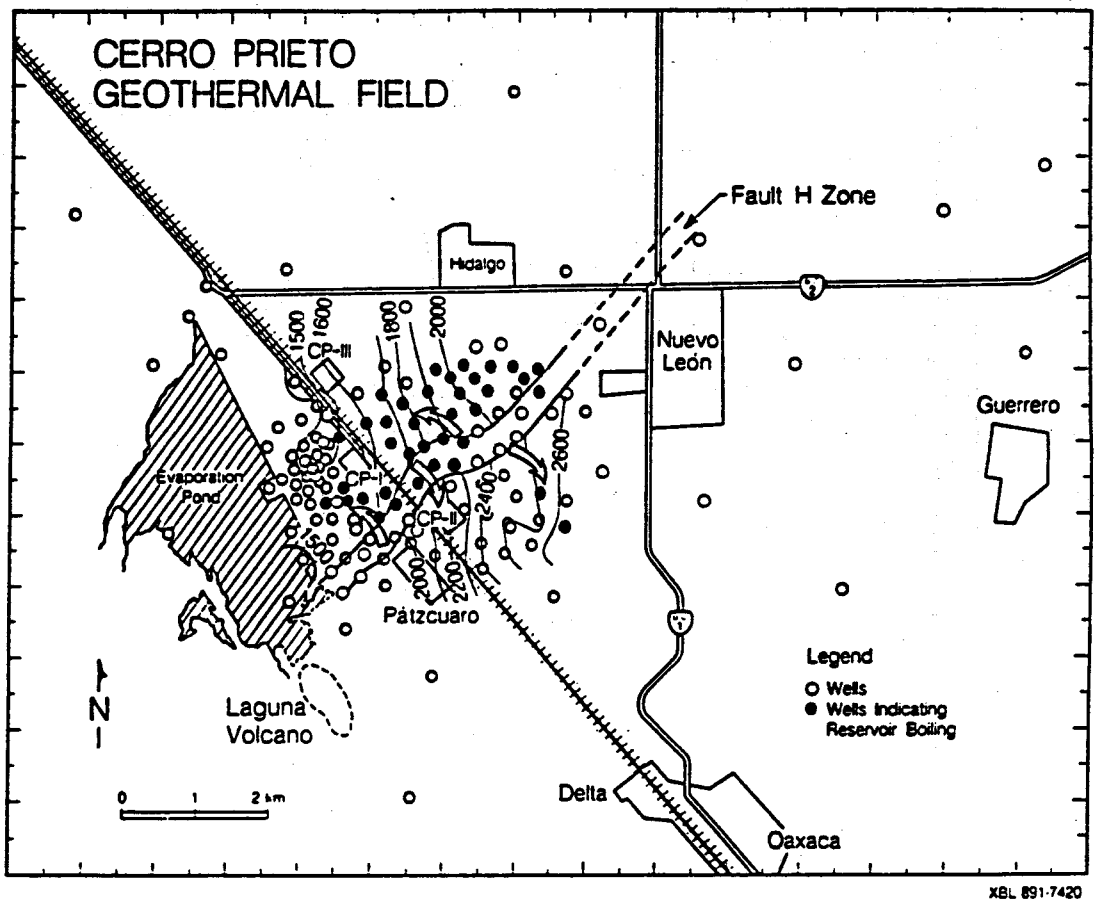

Cerro Prieto. Depth (in meters) to the top of the Beta reservoir (Sand Unit Z); fault shown at the level of the reservoir. The arrows indicate the direction of geothermal fluid flow away from the Fault H zone into the Beta reservoir. Solid circles indicate wells showing reservoir boiling.

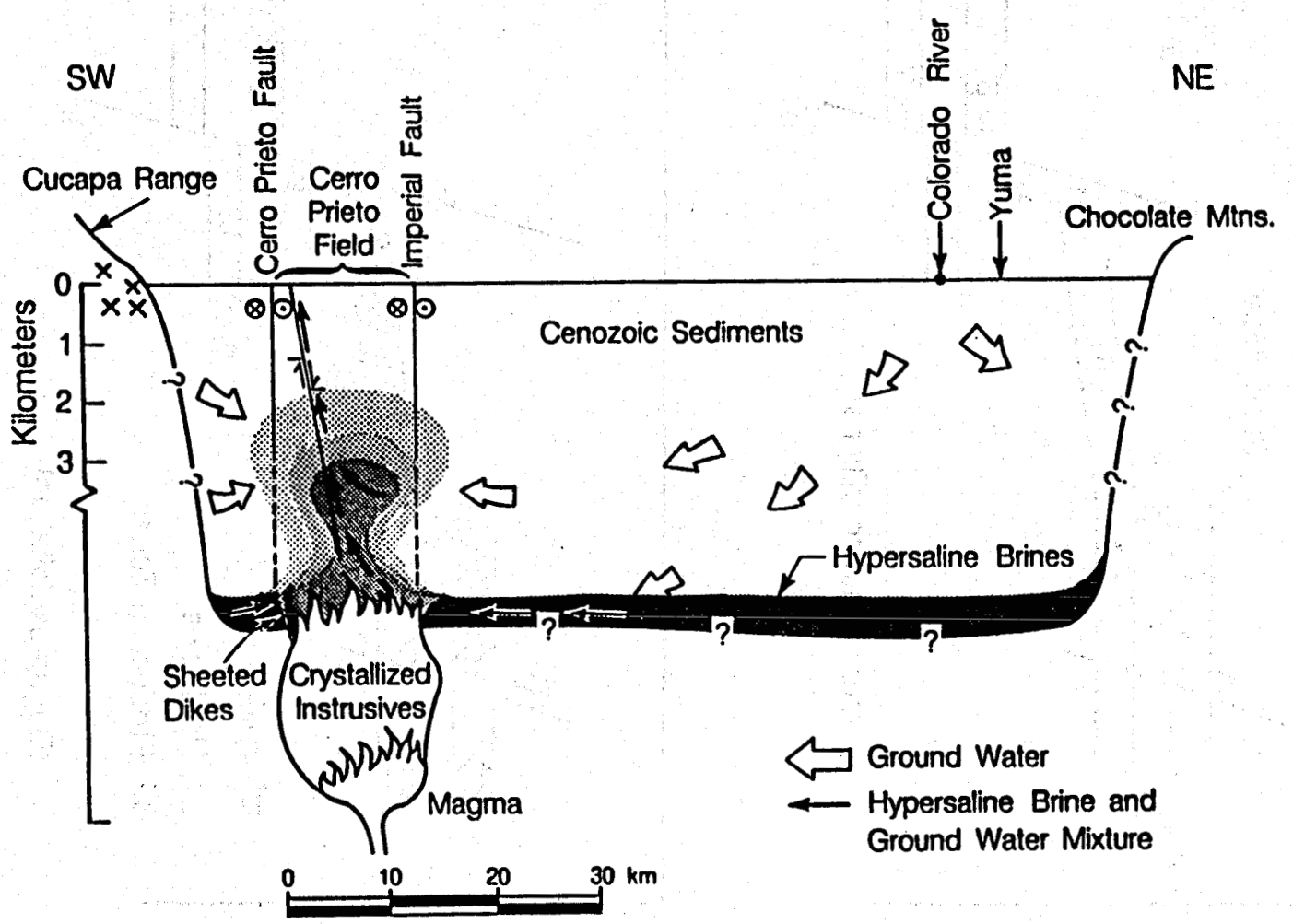

Schematic diagram of the geology and fluid flow across the Mexicali Valley (Halfman et al., 1986.)

Schematic Geothermal Fluid Flow Model for Cerro Prieto

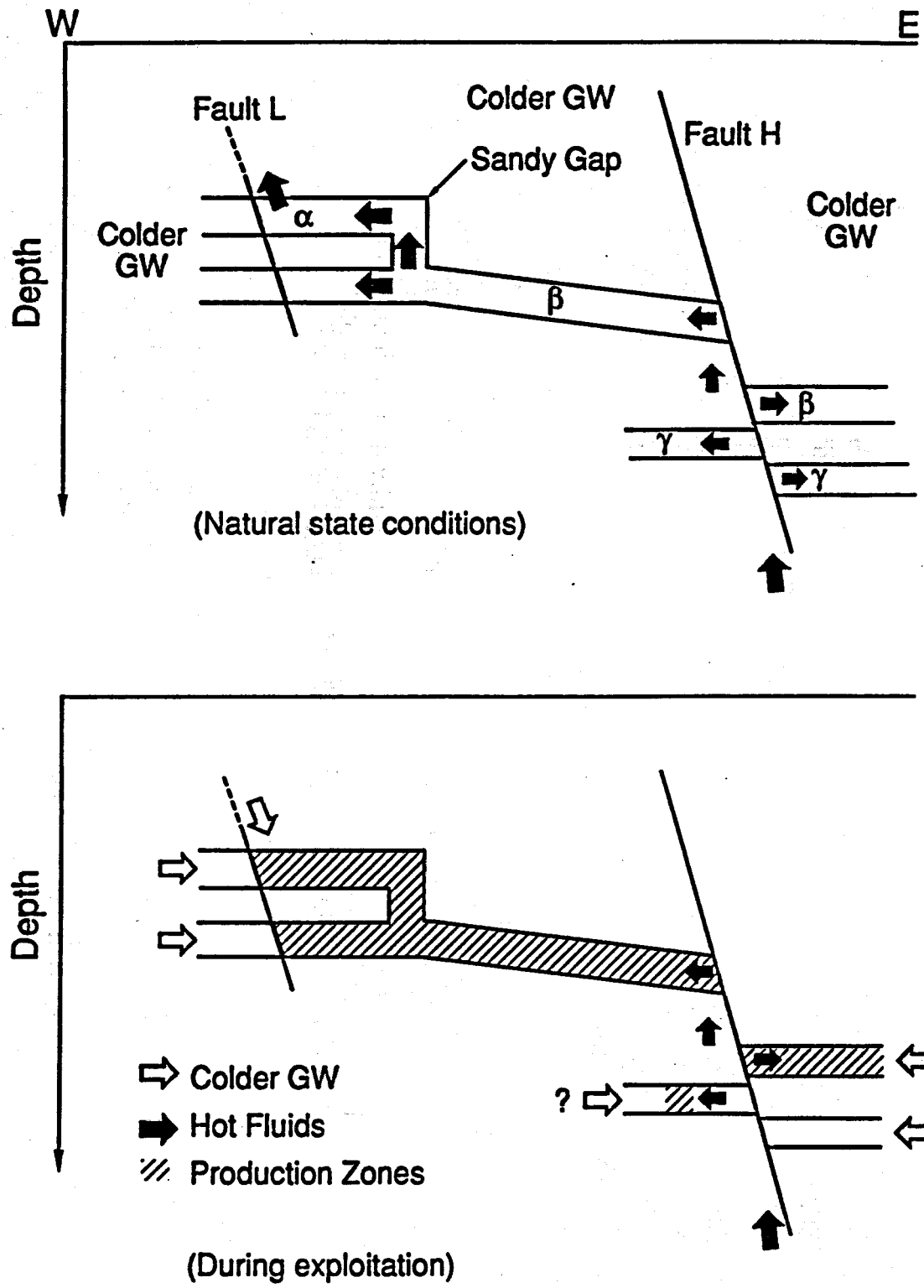

Schematic west-east cross section of the Cerro Prieto field showing geothermal fluid flow and cold groundwater (GW) recharge (a) prior to and (b) during exploitation (Lippmann et al., 1989).

"Early" References
on the Exploration and Development of Cerro Prieto

Comisión Federal de Electricidad, 1979. Proceedings Second Symposium on the Cerro Prieto geothermal field, 17-19 October, 1979, Mexicali, Mexico.

Comisión Federal de Electricidad, 1982. Proceedings Fourth Symposium on the Cerro Prieto geothermal field, 10-12 August, 1982, Guadalajara, Mexico.

Halfman, S.E., Lippmann, M.J., Zelwer, R., and Howard, J.H., 1984. Geologic interpretation of geothermal fluid movement in Cerro Prieto field, Baja California, Mexico, *Amer. Assoc. Petroleum Geologists Bull.*, Vol. 68, No. 1., pp. 18-30.

Halfman, S.E., Mañón, A. and Lippmann, M.J., 1986. Update of the hydrogeologic model of the Cerro Prieto field based on recent well log data, Geothermal Resources Council Trans., Vol. 10, pp. 369-375.

Lawrence Berkeley Laboratory, 1978. Proceedings First Symposium on the Cerro Prieto geothermal field, 20-22 September, 1978, San Diego, CA, report LBL-7098.

Lawrence Berkeley Laboratory, 1981. Proceedings Third Symposium on the Cerro Prieto geothermal field, 24-26 March 1981, San Francisco, CA, report LBL-11967.

Lippmann, M.J., 1983. Overview of Cerro Prieto studies, *Geothermics*, Vol. 12, No. 4, pp.265-289.

Lippmann, M.J., Goldstein, N.E., Halfman, S.E., and Witherspoon, P.A., 1984. Exploration and development of the Cerro Prieto geothermal field, *Journal Petroleum Engineering*, Vol. 36, No. 10, pp. 1579-1591.

Mercado, S., 1976. Movement of geothermal fluids and temperature distribution in the Cerro Prieto geothermal field, Baja California, Mexico. Proc. Second U.N. Symposium Development and Use Geothermal Resources, May 1975, San Francisco, CA., Vol. 1, pp.487-494.

RECENT PAPERS ON CERRO PRIETO (In English)

Halfman-Dooley, S.E., Lippmann, M.J., and Bodvarsson, G.S., 1989. Progress report on LBL's numerical modeling studies on Cerro Prieto, paper presented at the DOE/CFE Symposium on Geothermal Energy, San Diego, CA, April 4-5, 1989.

Goldstein, N.E., Alvarez, J., 1989. Self-potential anomaly changes at the Cerro Prieto geothermal field, paper presented at the DOE/CFE Symposium on Geothermal Energy, San Diego, CA, April 4-5, 1989.

Lippmann, M.J. and Mañón, A., 1987. The Cerro Prieto geothermal field, *Geothermal Science and Technology*, Vol. 1, No. 1, pp. 1-38.

Lippmann, M.J., Truesdell, A.H., Mañón M., A. and Halfman, S.E., 1989. The hydrogeologic-geochemical model of Cerro Prieto revisited, paper presented at the 14th Workshop on Geothermal Reservoir Engineering, Stanford, CA, January 24-26, 1989.

Mercado, S. and Bermejo, F., 1988. Ecological aspects on Cerro Prieto geothermal field, Trans. Geothermal Resources Council, Vol. 12, pp. 95-99.

Mercado, S., Bermejo, F., Hurtado, R., Terrazas, B., and Hernández, L., 1989. Scale incidence on production pipes of Cerro Prieto geothermal wells, *Geothermics*, Vol. 18, No. 1/2, pp. 225-232.

Truesdell, A.H., 1988. Geochemical models for reservoir processes at Cerro Prieto, Mexico, Proc. Intern. Symp. on Geothermal Energy, Nov.10-14, 1988, Kumamoto and Beppu, Japan, pp. 59-62.

Truesdell, A.H., Terrazas, B., Hernández, L., Janik, C., Quijano, L., and Tovar, R., 1989. The response of the Cerro Prieto reservoir to exploitation as indicated by fluid chemistry, paper presented at the DOE/CFE Symposium on Geothermal Energy, San Diego, CA, April 4-5, 1989.

Conceptual Models of Geothermal Systems

SUMMARY

— The conceptual model is a plausible and coherent "mental picture" one develops for the system.

— The model is useful in targeting and designing exploration, confirmation, production and injection wells.

— The development of a conceptual model is the first and fundamental step in the process of evaluating a given geothermal system and designing reservoir management plans.

— The model changes (evolves) as additional information becomes available during the exploration, confirmation and development stages of a project.

Thus,

— The conceptual model of a geothermal system is mainly a function of:

a) the data available (i.e., type, amount and quality of the data)

and

b) the experience of the "modeler" (i.e., the person has to have a good understanding of the processes that occur in the system and use the appropriate data interpretation methods).

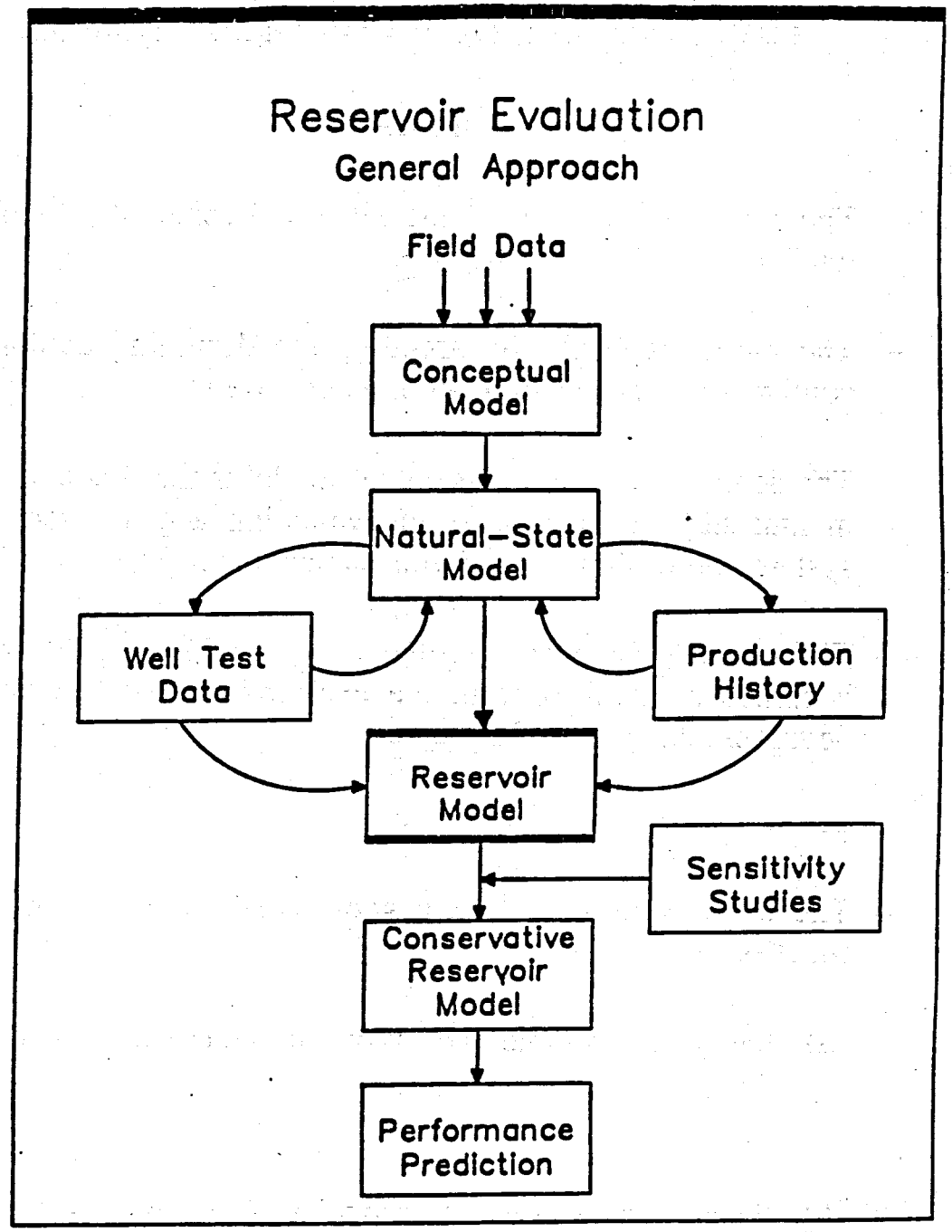

General approach to reservoir evaluation (G.S. Bodvarsson, 1986).

GeothermEx, Inc.

SUITE 201
5221 CENTRAL AVENUE
RICHMOND, CALIFORNIA 94804-5829

(415) 527-9876
CABLE ADDRESS GEOTHERMEX
TELEX 709152 STEAM UD
FAX (415) 527-8164

RESPONSES OF A GEOTHERMAL FIELD DURING EXPLOITATION - A RESERVOIR MANAGEMENT PLAN

Reservoir Engineering and Hydrologic Monitoring Techniques: Surface and Subsurface

Anthony J. Menzies

Senior Reservoir Engineer

GeothermEx, Inc.
SUITE 201
5221 CENTRAL AVENUE
RICHMOND, CALIFORNIA 94804-5829

(415) 527-9876
CABLE ADDRESS GEOTHERMEX
TELEX 709152 STEAM UD
FAX (415) 527-8164

Introduction

The main parameters of interest to a reservoir engineer that should be monitored on a routine basis during exploitation are:

- mass flow rate (steam, water, total)
- enthalpy
- pressure (wellhead, downhole)
- temperature (wellhead, downhole)

By monitoring the above parameters, it is possible to follow changes in well behavior and relate these changes to reservoir processes. The purpose of this presentation is to summarize the basic techniques used to measure these parameters and the practical problems that can be encountered in obtaining the measurements.

Geothermal Systems

There are presently 3 general categories of geothermal system that are presently being successfully exploited for both electricity generation

GeothermEx, Inc.
SUITE 201
5221 CENTRAL AVENUE
RICHMOND, CALIFORNIA 94804-5829

(415) 527-9876
CABLE ADDRESS GEOTHERMEX
TELEX 709152 STEAM UD
FAX (415) 527-8164

and heating purposes. They can be characterized as follows:

- **dry steam systems:** these are systems where the discharged fluid is either saturated or superheated steam that can be used directly to produce electricity using a steam turbine or binary plant (The Geysers, Larderello, Kamojang, Cove Fort),

- **hot water systems:** these are systems that contain hot water of greater than 180°C (356°F) and the fluid is produced by natural well flow and flashed to steam in a surface separator vessel. The separated steam is then used in a steam turbine to produce electricity (Wairakei, Tongonan, Hatchobaru, Cerro Prieto, Salton Sea, Coso, Olkaria, Dixie Valley, Heber),

- **moderate temperature systems:** these are systems in which the temperature is generally less than 180°C (356°F) and the fluid is produced for heating or to either a binary or flash plant using downhole production pumps (Ormesa plants, Geo East Mesa I, Steamboat, Amedee, Mammoth-Pacific).

GeothermEx, Inc.
SUITE 201
5221 CENTRAL AVENUE
RICHMOND, CALIFORNIA 94804-5829

(415) 527-9876
CABLE ADDRESS GEOTHERMEX
TELEX 709152 STEAM UD
FAX (415) 527-8164

The equipment used in these different systems for monitoring surface and subsurface changes in flow rate, enthalpy, pressure and temperature are similar. However, each geothermal system is different and it is necessary to recognize these differences when designing the surface plant layout and monitoring equipment.

Dry Steam Systems

A typical well in a dry steam system produces steam that is either saturated or superheated and can be used directly in a steam turbine to produce electricity. In some wells, separators may be required but this is not typical. In The Geysers, automated monitoring systems are now common and are used to monitor all wellhead measurements on a routine basis. These systems typically monitor pressure, temperature, flow rate and valve position.

Well flow rates are generally measured by using either an orifice plate (figure 1) or "annubar" (figure 2) in the individual well flow lines and in the steam lines to the power plant. Other types of flow meters are available but are not used to the same extent. Annubars are preferred over orifice plates as they cause a smaller permanent pressure loss in

GeothermEx, Inc.
SUITE 201
5221 CENTRAL AVENUE
RICHMOND, CALIFORNIA 94804-5829

(415) 527-9876
CABLE ADDRESS GEOTHERMEX
TELEX 709152 STEAM UD
FAX (415) 527-8164

the flow line. Both methods have been proven over the years but reliability is affected by the tendency of the steam to cause scaling etc.

The discharge enthalpy of a dry steam well is relatively easy to measure, particularly if the steam is superheated. Under these conditions, wellhead temperature and pressure measurements taken in the flow line are sufficient to define the thermodynamic state of the steam at the wellhead. By using these parameters that are routinely measured, it is possible to define trends in wellhead superheat with time. This is illustrated in figure 3 which shows how the production data from a well varies with time.

If the steam is not superheated, a "calorimeter" (figure 4) can be used to estimate the enthalpy of the steam. The data collected with the calorimeter test are used with a "Mollier" diagram or steam tables to obtain the steam enthalpy and steam "wetness".

The measured steam enthalpy at the surface can be very different from the subsurface fluid conditions. In the past few years it has been possible to obtain more information on downhole fluid enthalpy by running pressure-temperature-spinner (PTS) logs. These logs are now run

GeothermEx, Inc.
SUITE 201
5221 CENTRAL AVENUE
RICHMOND, CALIFORNIA 94804-5829

(415) 527-9876
CABLE ADDRESS GEOTHERMEX
TELEX 709152 STEAM UD
FAX (415) 527-8164

on a routine basis by a number of operators in The Geysers field and provide a method of monitoring changes in downhole enthalpy with time in superheated steam wells. Figure 5 shows the results from a PTS log to illustrate the enthalpy changes that occur within the wellbore. PTS logs also provide information on flow velocity within the wellbore and this data is useful for identifying where inflows are occurring to the well. By running repeat logs it is possible to see how these inflows change with time.

Pressure measurements in dry steam systems are generally taken at the wellhead in production wells, injection wells and observation wells using standard pressure gauges or using an automated monitoring system with wellhead transducers. It is possible to obtain information on reservoir pressure decline in the production area by analyzing production well pressure and flow rate data. Figure 6 presents calculated pressure declines compared with data measured during shut-in periods from the same well and shows that the calculation technique can provide valid information on pressure decline.

Wellhead pressure data from inactive wells can also provide information on reservoir pressure decline. However, these wells are not generally located within the production areas. Downhole pressure changes can also

GeothermEx, Inc.
SUITE 201
5221 CENTRAL AVENUE
RICHMOND, CALIFORNIA 94804-5829

(415) 527-9876
CABLE ADDRESS GEOTHERMEX
TELEX 709152 STEAM UD
FAX (415) 527-8164

be monitored in observation wells using downhole capillary tubing connected to a surface pressure gauge or transducer. This is discussed in more detail in the next section.

Hot Water Systems

With hot water systems, we generally have a two-phase mixture of steam and water at the surface. The steam must therefore be separated before being used in a steam turbine. Typical surface layouts for this type of field are shown in figures 7 and 8; figure 7 shows the layout in Matsukawa where individual separators are provided at each well while figure 8 shows the layout in Tongonan where central separator stations are used. At the wellhead, only wellhead pressure and possibly temperature are monitored on a routine basis.

In hot water systems, the flow rate and enthalpy are usually calculated simultaneously either by mass and energy balances over individual separators (figure 9) or by using the James method. The steam and water flow rates are generally measured using orifice plates or annubars although problems do arise, particularly with the measurement of water flow rates.

GeothermEx, Inc.
SUITE 201
5221 CENTRAL AVENUE
RICHMOND, CALIFORNIA 94804-5829
(415) 527-9876
CABLE ADDRESS GEOTHERMEX
TELEX 709152 STEAM UD
FAX (415) 527-8164

The basic layout used for the James method is shown in figure 10. The James method is generally used during initial testing of geothermal wells but may also be used during exploitation if it is possible to divert production wells to an atmospheric silencer as required. The James method may be the only technique available for monitoring changes in individual well performance when multiple wells are connected to a single separator.

Surface enthalpy can also be monitored by using chemical techniques where samples of either the water or gas are collected at different pressures. By knowing the enthalpy of the steam and water at the different pressures and the change in chemical constituent concentrations, it is possible to calculate the total fluid enthalpy. This technique is presently being used at the Coso field.

In wells where flashing is occurring in the wellbore, such as at Dixie Valley, changes in subsurface enthalpy can be monitored by running repeat temperature and pressure surveys to find where flashing is occurring in the wells and also the temperature and pressure conditions at the flash point. An example of this type of survey is shown in figure 11.

GeothermEx, Inc.
SUITE 201
5221 CENTRAL AVENUE
RICHMOND, CALIFORNIA 94804-5829

(415) 527-9876
CABLE ADDRESS GEOTHERMEX
TELEX 709152 STEAM UD
FAX (415) 527-8164

As with dry steam wells, PTS logs are also used in hot water systems to establish where inflows are occurring to the well. However, it is not possible to use these logs to accurately estimate enthalpy unless the fluid is flashing within the wellbore. Example PTS logs from a hot water geothermal well are shown in figure 12.

Pressure changes in hot water systems are generally monitored by using observation wells, with measurement of downhole pressure. At present, temperature limitations restrict the use of downhole transducers for this purpose to wells with water level temperatures of less than 80°C (176°F). In hotter wells, downhole pressures can be monitored by using capillary tubing within the well connected to a surface pressure gauge or pressure transducer. This type of equipment is now used extensively in geothermal fields to monitor for pressure interference.

Moderate Temperature Systems

By using pumped production wells, the hot geothermal water is maintained under single phase conditions and it is therefore possible to use relatively standard techniques for monitoring changes in well conditions. A typical pump installation usually includes a "bubbler" tube for measuring downhole pressure, surface monitoring of discharge

GeothermEx, Inc.
SUITE 201
5221 CENTRAL AVENUE
RICHMOND, CALIFORNIA 94804-5829

(415) 527-9876
CABLE ADDRESS GEOTHERMEX
TELEX 709152 STEAM UD
FAX (415) 527-8164

pressure, annulus pressure and flow temperature and flow rate monitoring.

The flow rates are generally measured in the individual flow lines with either orifice plates or annubars.

Changes in discharge enthalpy can be monitored by measuring wellhead temperature.

Downhole pressure measurements can be taken from the production wells by using a "bubbler" tube installed in the annulus of the well and with the end of the tube located just above the pump intake. The pressure is monitored on the surface using a pressure gauge or transducer.

Downhole pressure measurements can also be taken in observation wells using the same equipment as for the hot water systems.

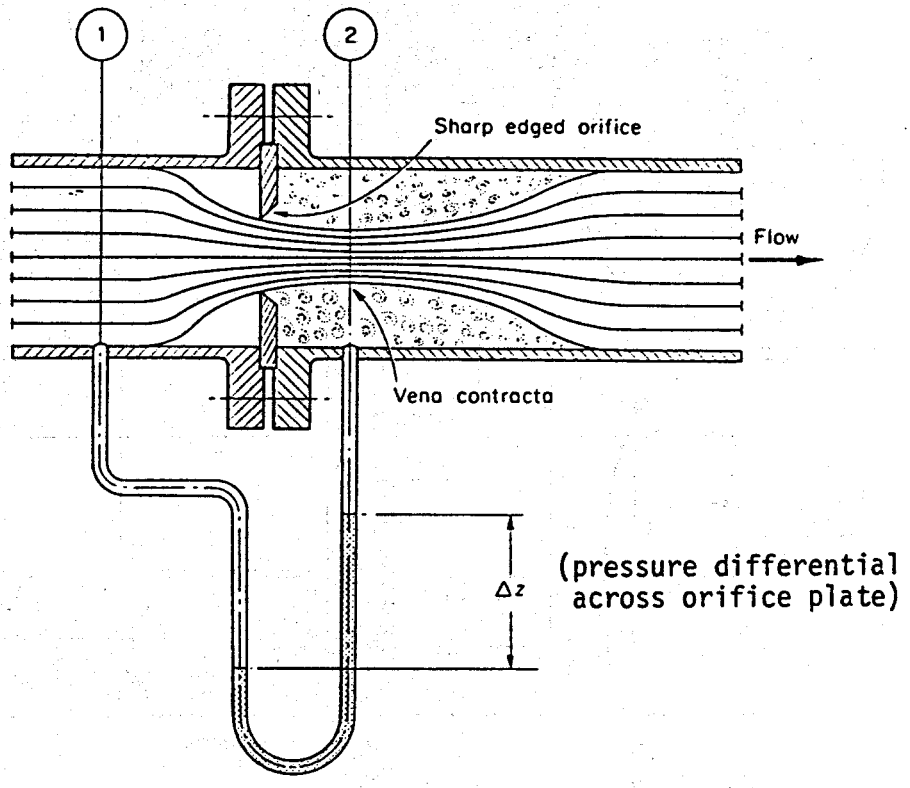

FIGURE 1: ORIFICE PLATE INSTALLATION

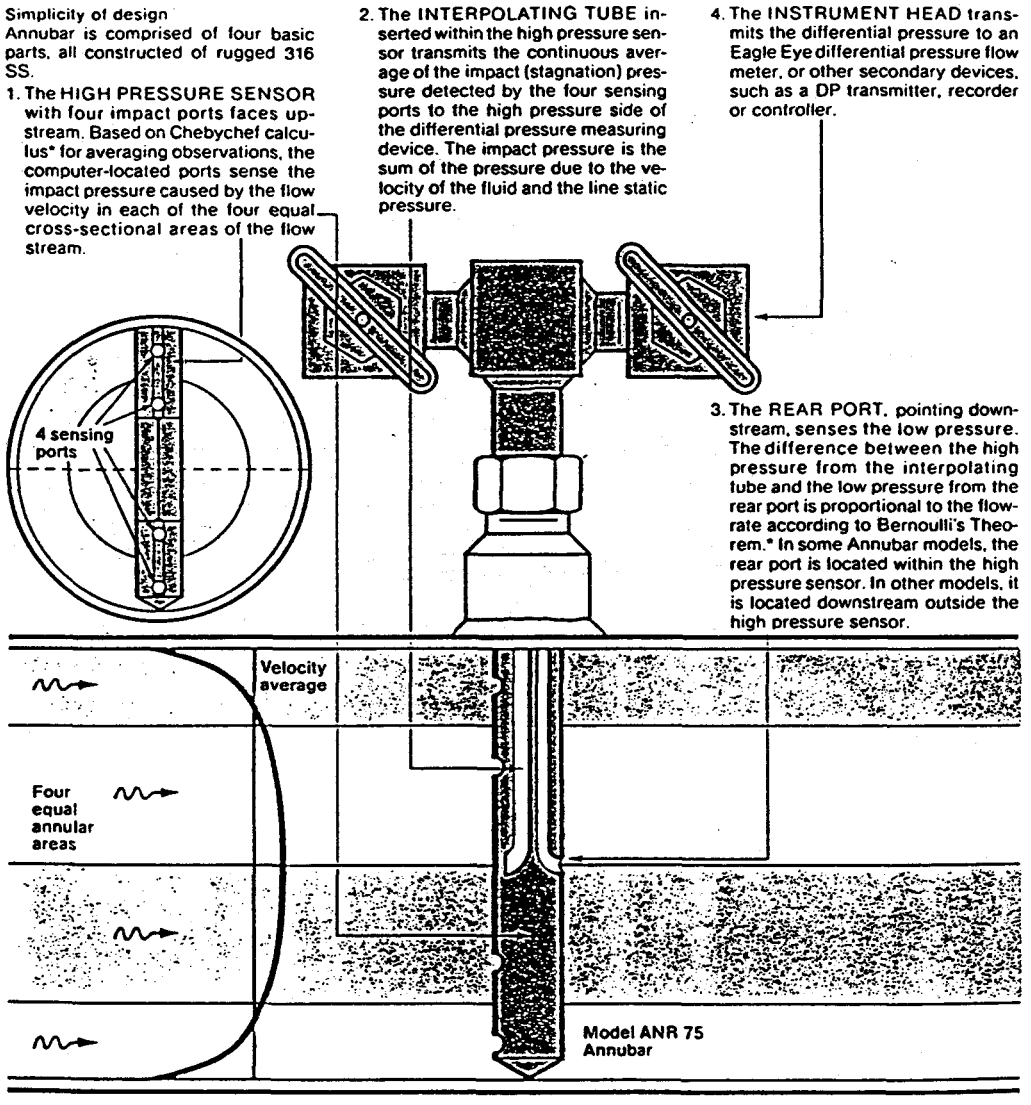

FIGURE 2: ANNUBAR INSTALLATION

FIGURE 3 : FLOWRATE, PRESSURE, TEMPERATURE and SUPERHEAT CHANGES vs TIME

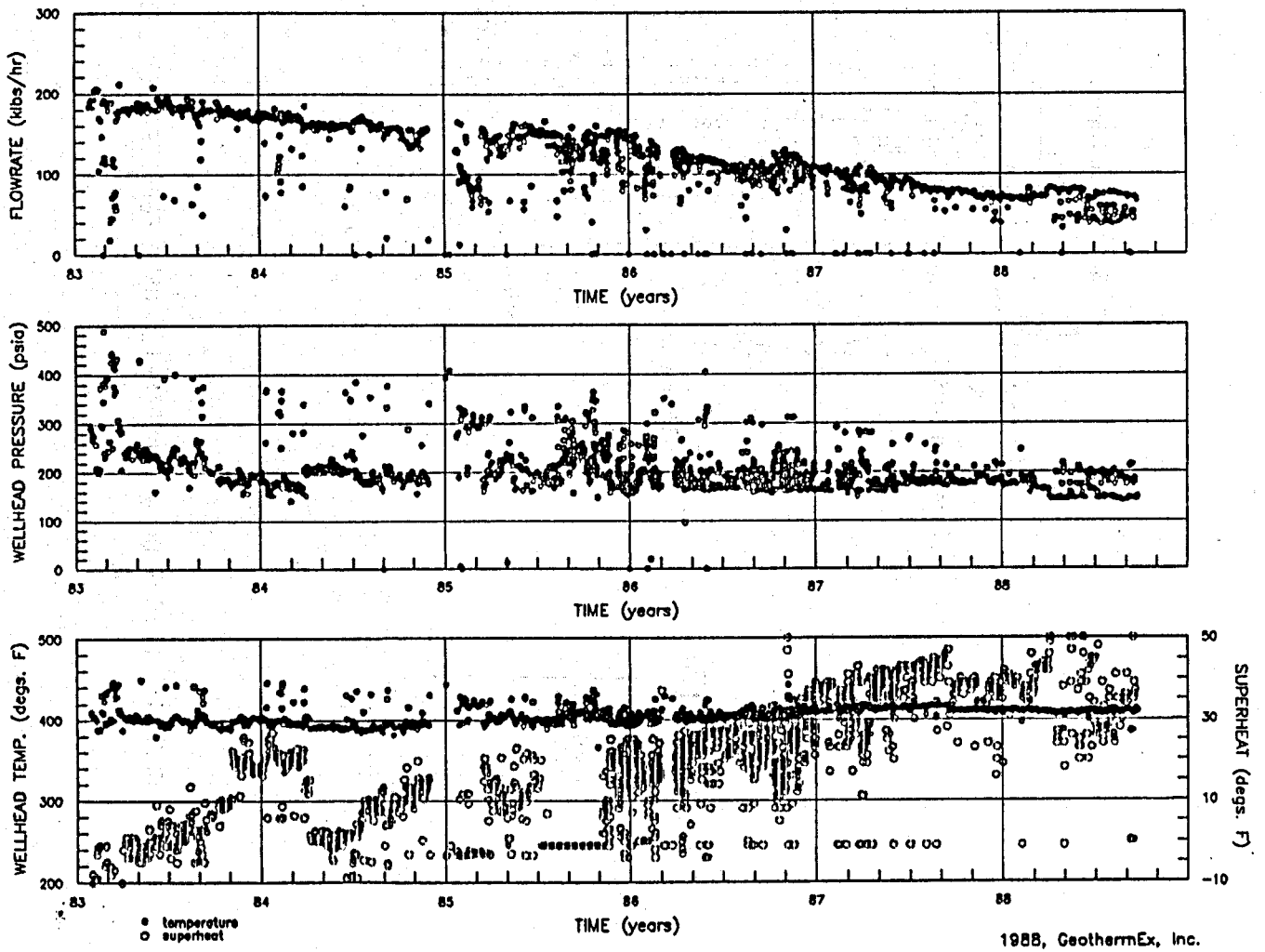

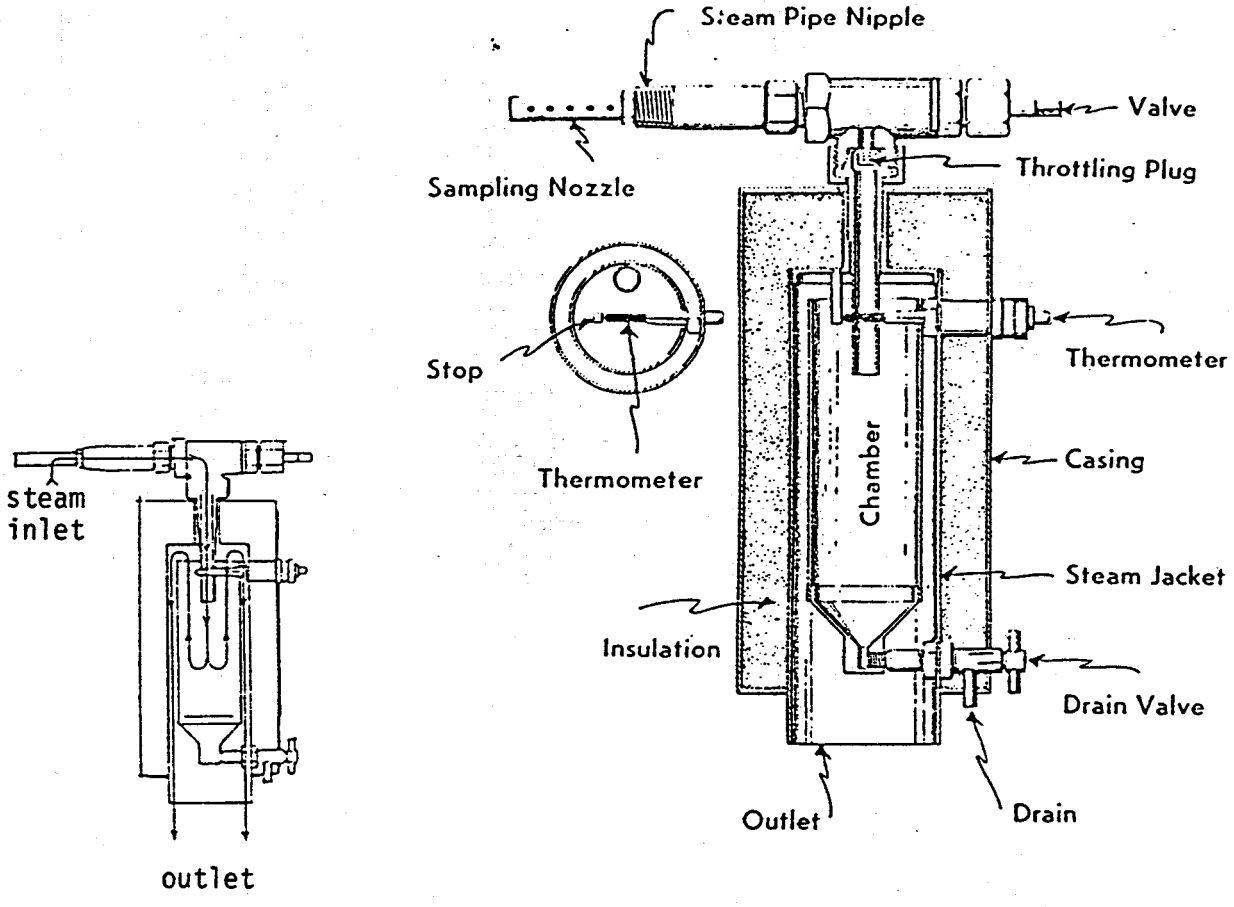

FIGURE 4: LAYOUT OF A CALORIMETER USED FOR STEAM QUALITY DETERMINATION

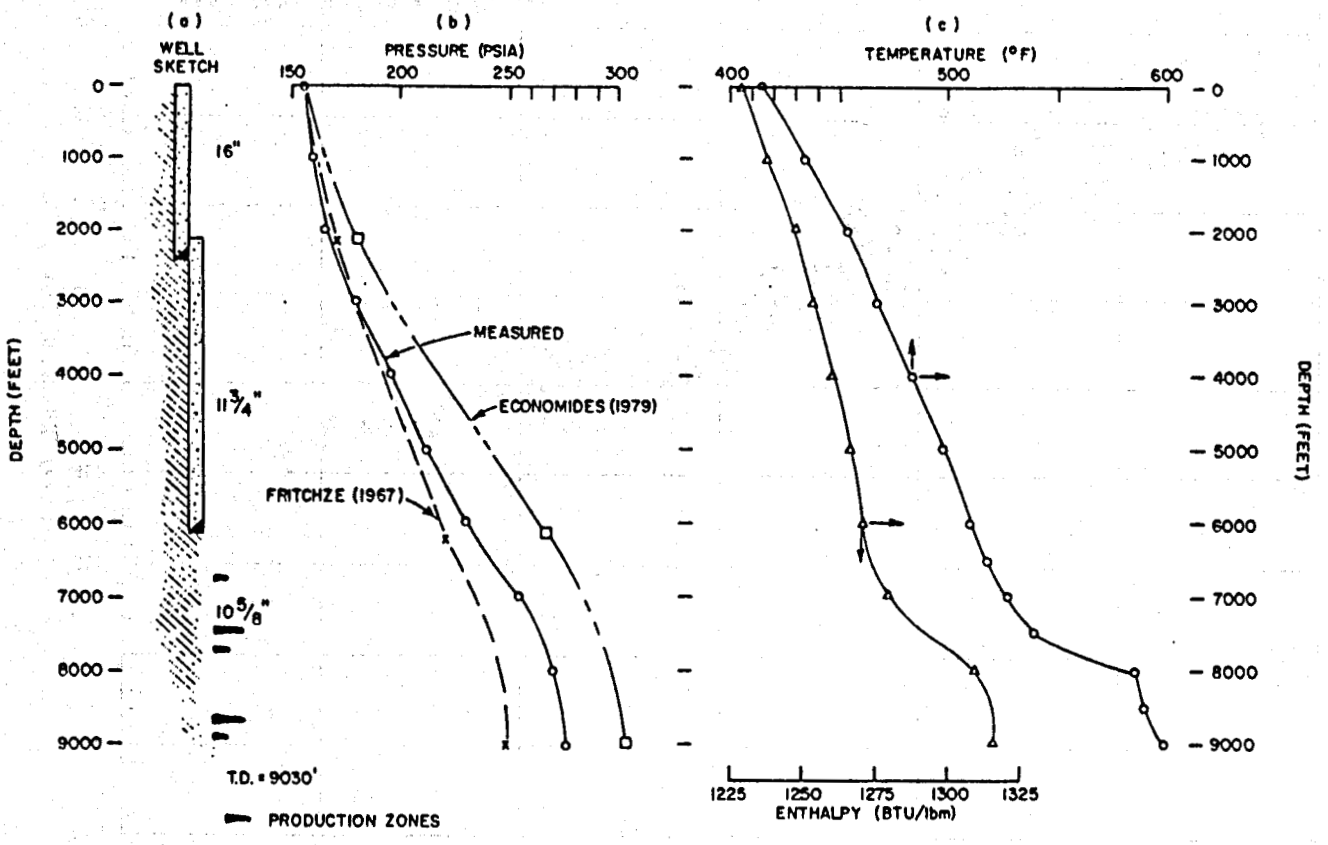

FIGURE 5: PTS LOGGING IN A DRY STEAM WELL

FIGURE 6 : CHANGES IN STATIC PRESSURE WITH TIME

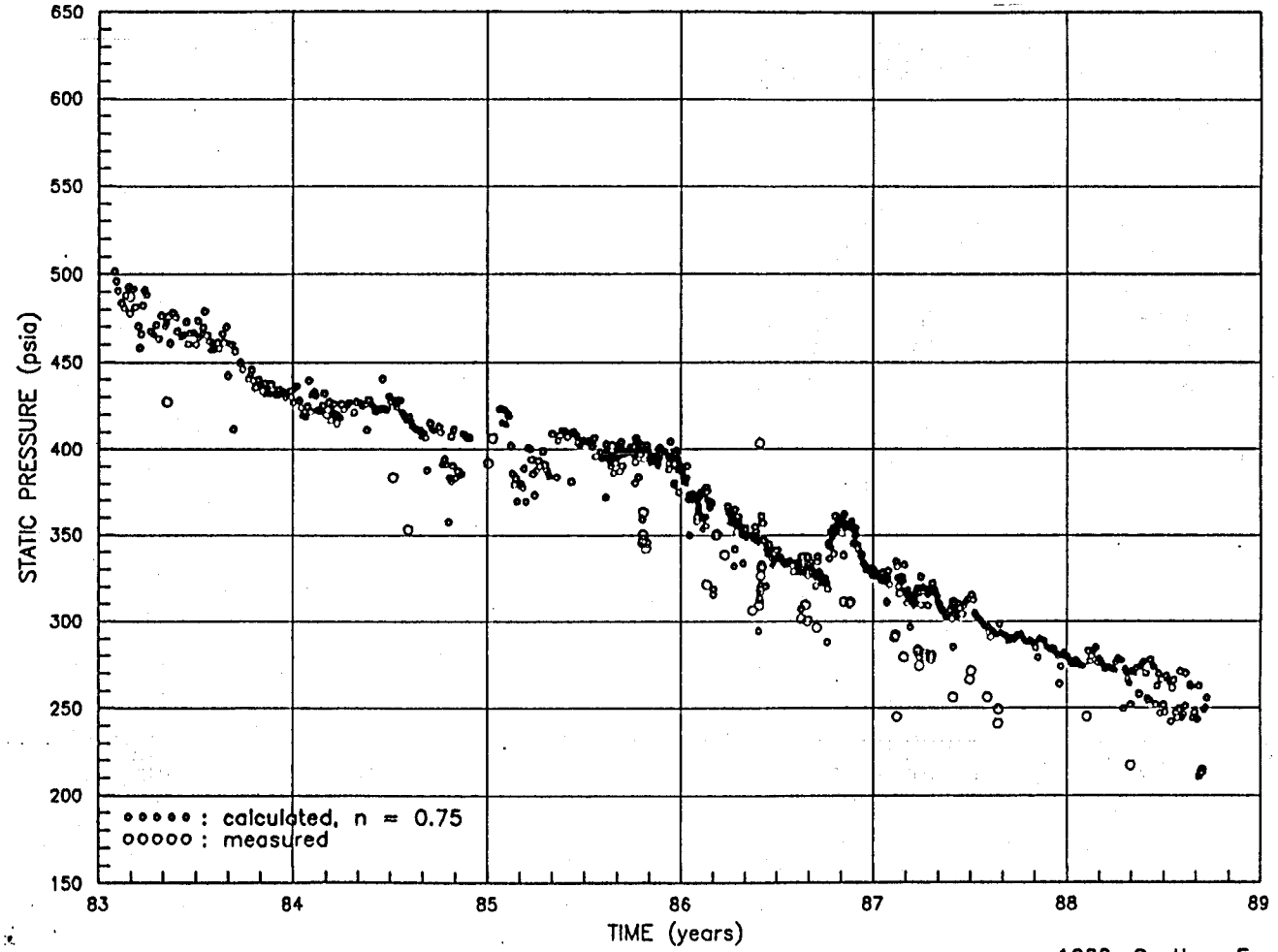

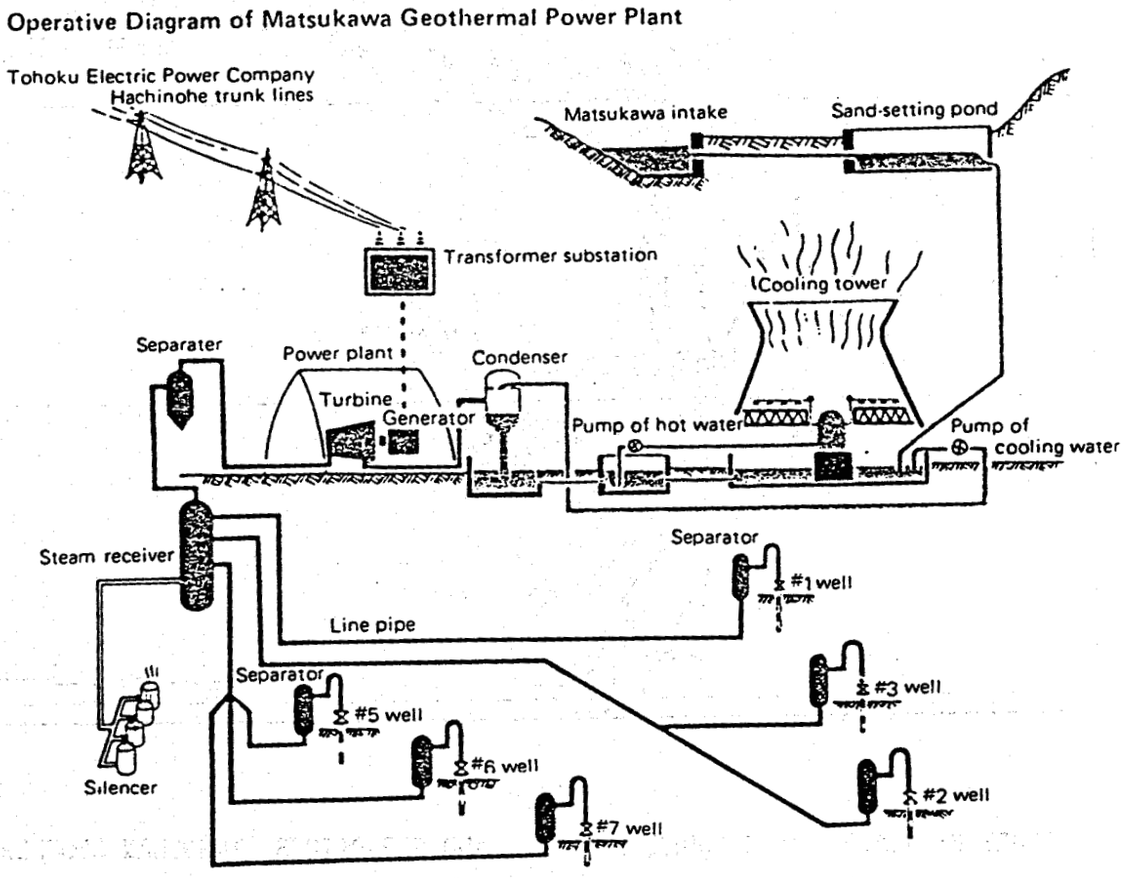

FIGURE 7: LAYOUT OF SURFACE EQUIPMENT, MATSUKAWA GEOTHERMAL FIELD

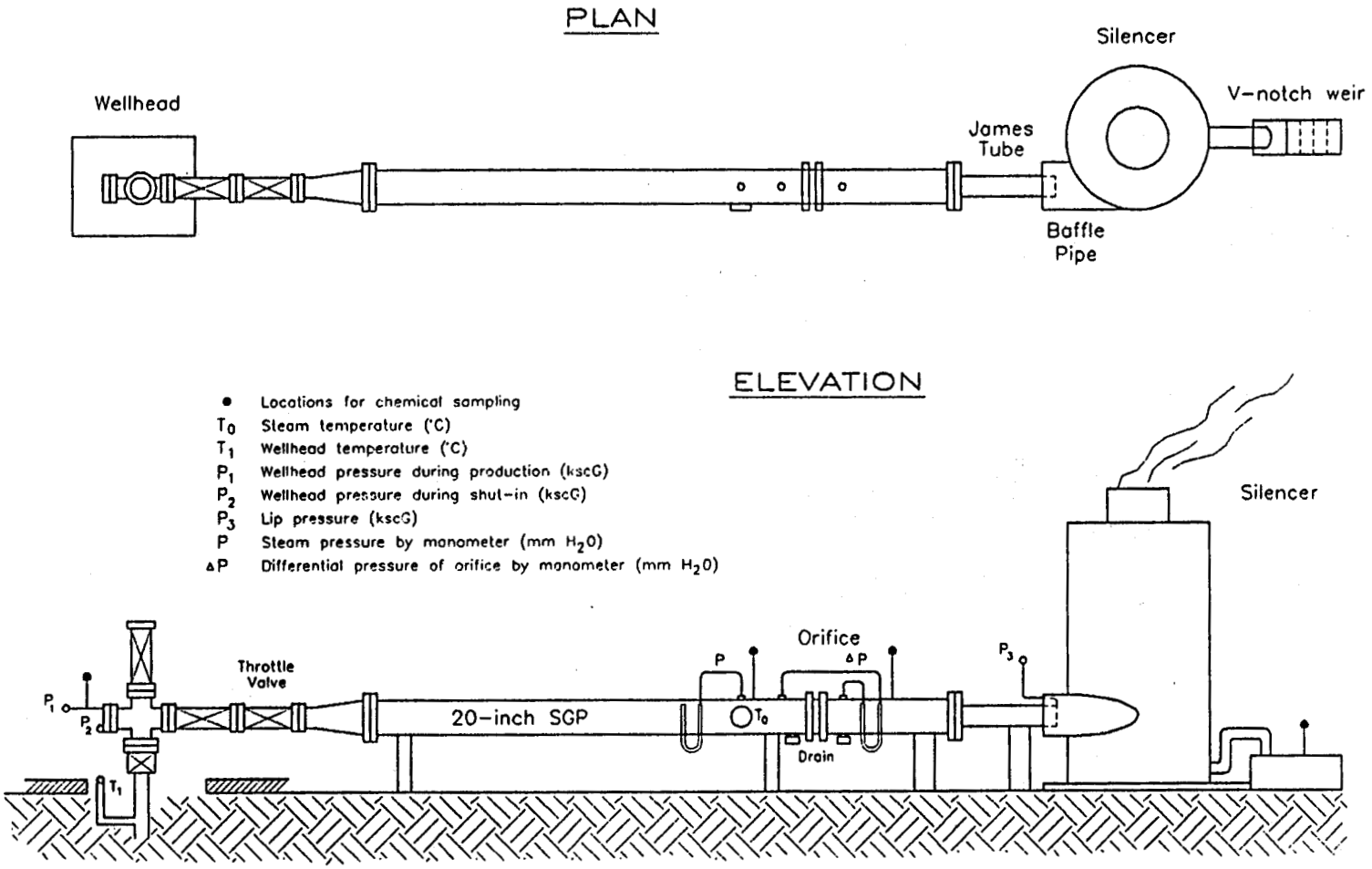

FIGURE 10: SURFACE EQUIPMENT SETUP FOR USING JAMES METHOD

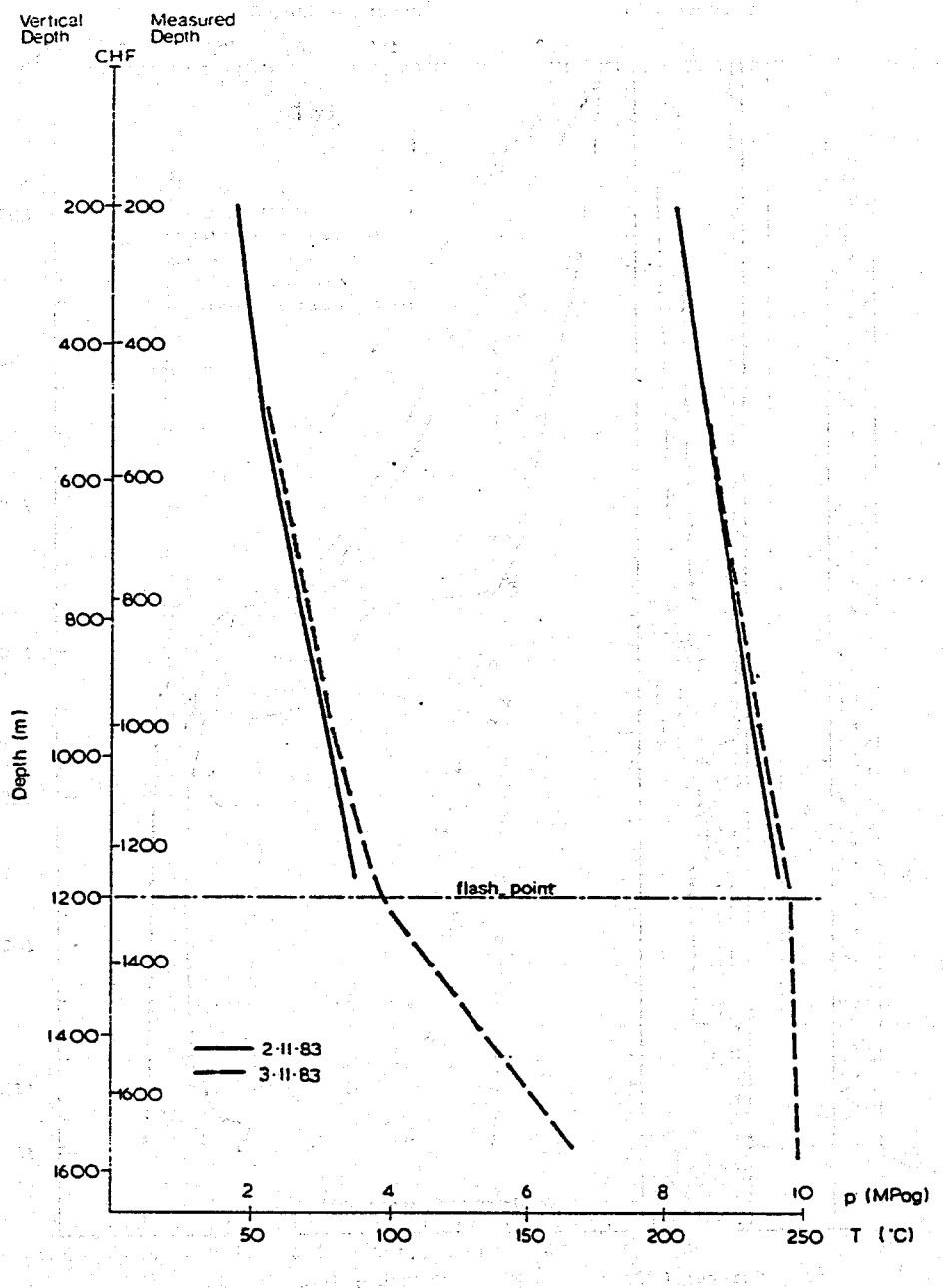

FIGURE 11: FLOWING PRESSURE/TEMPERATURE SURVEYS TO LOCATE FLASH POINT

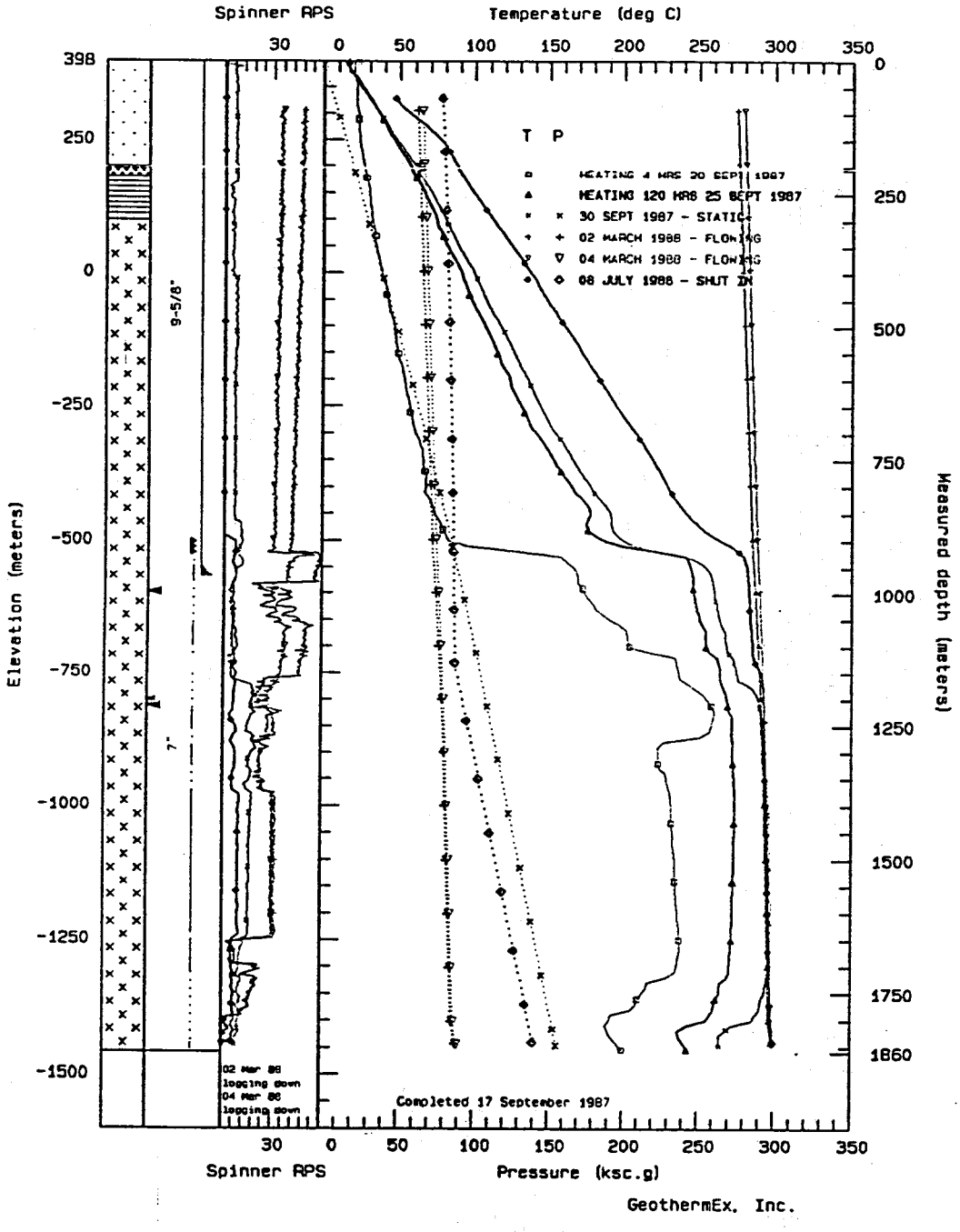

FIGURE 12: PTS LOGGING IN A HOT WATER WELL

GEOTHERMAL RESOURCES COUNCIL
WORKSHOP – JUNE 14-15, 1989

RESPONSES OF A GEOTHERMAL FIELD DURING EXPLOITATION

CHEMICAL PROCESSES AND CHANGES

HOW DOES GEOTHERMAL WATER BOIL??

by
Donald E. Michels
DON MICHELS ASSOCIATES

One may be said to "understand" a boiling system if they know the temperature, pressure, phase compositions, heat balance, densities, and dynamic relationships for a complete process. The process may be considered as beginning with a single-phase liquid, overpressured in the sense that no vapor is initially present. The process continues with the extensive development of vapor, mostly H_2O, but with prominent gases, and includes heat losses and partitioning of components between liquid and vapor. Partitioning may be continuous, as in a wellbore, or stepped, as through an orifice plate or steam separator, possibly with multiple stages.

WHAT IS BOILING?

Boiling concerns the balance between internal pressure, external pressure, volume available for expansion, and losses (or inputs) of heat, for a vapor-liquid system. Specifically, we consider a system dominated by the thermophysical properties of H_2O, but with substantial effects due to other materials.

One may consider the pressure, required to confine a watery mixture of liquid and vapor, as the collective effect of "escaping tendencies" by the molecules of H_2O and other gases. Furthermore, when no vapor phase is physically present, it is realistic and useful to consider an internal pressure of a single-phase liquid, due to those escaping tendencies of the components.

A liquid has an internal pressure due to its temperature and composition. This pressure can be measured directly only in the cases where the liquid and its vapor are both present.

Confining pressures are considered to be mechanical and/or hydraulic. They can be measured with ordinary pressure gauges. They may exceed or be equal to the internal pressures of the liquid-gas mixture, but they can never be less.

Temperature is the main factor which controls the escaping tendencies of vapor and gases. The presence of dissolved, non-volatile materials in the liquid has some effects on the escaping tendencies. Usually, they decrease the escaping tendencies for H_2O while increasing the escaping tendencies for non-H_2O gases. For the H_2O component, one may visualize the pressures given in a steam table. For non-H_2O components, Henry's Law pressures may be visualized. Both kinds of visualization need to include thoughts of effects due to dissolved salts, etc.

In some cases the gas pressures of CO_2 exceed the H_2O vapor pressures, bringing into question the meaning of boiling" initiation. Also extreme are geopressured fluids, in which methane pressures are so high, relative to H_2O vapor pressures, that the energetics of the system are no longer dominated by the H_2O component.

In ordinary geothermal developments, gases are collectively important for the Henry's Law pressures they contribute for incipient boiling. They are also important during the early stages of boiling, particularly when redistribution of gases initiates chemical reactions in the residual liquid. During boiling, gases preferentially enter

the vapor phase and their pressure effects diminish sharply once boiling begins.

Geothermal Boiling

Several kinds of boiling concepts are useful when considering geothermal situations.

- Boiling-pressure-with-depth, for "static" systems;
- Boiling, with nearly adiabatic pressure/temperature conditions, in a discharging wellbore;
- Incipient boiling conditions in a reservoir, due to pressure drop related to well discharge;
- Selected boiling pressures in power plants, where steam separations are made for engineered purposes.

In all of these, the temperature or pressure is to be related to some geologic or engineering factor. Usually, it is important to consider also the composition of the fluid mixture. For some aspects, the distribution of mass between phases is required, and sometimes it is necessary to know the partitioning of components between the phases. It generally is useful, and sometimes necessary, to know the heat losses that complicate calculations about distributions of components between phases.

Boiling-Pressure-with-Depth

Heat flow from geologic depths may warm a water-saturated zone of near-surface rock enough to cause boiling at the higher levels. Eventually, a temperature profile may develop so that the pressure at any depth, due to the weight of overlying water (a hydraulic head) is equal to the vapor pressure of the water at that point. Then, the temperature profile can be estimated from the density and vapor pressure for saturated water (or brine).

Selected profiles are shown in Figure 1. Usually, the profile is computed for salt-free, gas-free water. The effects due to small amounts of salt are negligible. However, the curve is markedly flattened if the salt content is high, as in hypersaline brines.

The presence of CO_2 causes small alterations in the shape of the curve, due to variations in solubility with temperature. This invites consideration of alternatives, such as "constant CO_2 concentration" through the profile, versus "constant CO_2 pressure". The simulataneous presence of salt and CO_2 causes both distortion and shifting of the boiling pressure profile.

Since gases are normally present, in real geothermal liquids, the parts of temperature profiles, computed for shallow places, are not likely to be found in nature. These upper levels, where boiling may be active, are dominated instead, by thermal features which involve strong changes to the composition of fluids moving upwardly from below. They are also vulnerable to effects of fluids moving laterally, in response to the shallow hydrologic features of the area.

The deeper places in a boiling-pressure-with-depth zone represent a physical system that is close to static, yet unstable, veritably ready to explode. Wellbores should not be completed in this zone unless some specific, and clever production strategies are involved. Such wells cannot be discharged without inducing boiling in the rocks beyond the wellbore. That boiling invites deposition of scale which tends to cause short lifetimes for the well's productivity. Also, the well's energy outputs are not stable when a boiling front relentlessly moves away from the bore.

Geothermal boiling is not like gases escaping from petroleum, nor can geothermal two-phase mixtures be practically imitated or modeled by mixtures, such as gaseous nitrogen and cool water.

PRESSURE-TEMPERATURE-COMPOSITION RELATIONSHIPS

In a system of pure boiling water, information about pressure is redundant with information about temperature. Specifying one defines the other, as can be seen by reference to steam tables.

The situation is not greatly complicated by small concentrations of dissolved salts. However, for total dissolved salt (TDS) concentrations above about 15,000 ppm, brine properties are enough different from pure water

that an accounting must be made if the work is to be considered as "good".

Even for waters of low salt content, the pressures of gases are highly significant at the initiation of boiling and during the early stages of steam formation. As a consequence, it often is impractical to use pressure as a thermodynamic "independent" variable.

For two or more components, (measureable) temperature and composition are simpler to use as independent variables. Then, total pressure may be readily computed as the sum of separately calculable pressures associated with certain components. Approached in this way, the total pressure has a uniquely determined value. Then, the measured (field) pressure serves as a check on the model and the measurements.

The alternative, of using composition and (measureable) total pressure as independent variables requires successive approximations (iterations) to determine the temperature. The mass distribution of H_2O between phases must be computed, whether a temperature approach or a pressure approach is involved. But the total pressure is not accurately correlatable with fluid enthalpies when gases are dynamically re-partitioning between phases. This is because the multiple gases and salts have significant pressure effects, but negligible enthalpy effects.

Consequently, the discussion below relates to mathematical modeling of boiling systems by using temperature and composition as inputs. Outputs include proportions of phases, distribution of components between phases, specific enthalpy of phases, specific volumes, pressure, etc. This fits the engineering applications for which reservoir and fluid properties are used to compute engineering properties of the fluids that are relevant to the energy extraction apparatus.

Components

The most important pressure component usually is water vapor pressure. For hypersaline brines, correlations between temperature and enthalpy, or density, or pressure, etc., are greatly different from dilute waters. Not only is it necessary to account for the salt effects, but the salt concentrations change enough during the boiling process (due to steam formation) that continuous adjustment of the correlations is required for any practical model.

Dissolved gases in geothermal liquids are not considered as part of the TDS, although their concentrations are generally significant in a relative way. That is, the ppm concentrations of gases may exceed the ppm concentrations of dissolved solids. The pressure variations of gases in boiling systems have physical and chemical aspects that make geothermal boiling distinct from all other boiling processes.

- The most important gas in terms of pressure usually is carbon dioxide (CO_2).
- In some systems nitrogen (N_2) may be more significant, particularly at incipient boiling.
- Methane (CH_4) is the most important pressure component for "geopressured" systems, as near the Gulf Coast, but it is only occasionally significant in circumstances usually considered as geothermal.
- Hydrogen sulfide (H_2S) seldom has a pressure large enough to be worth considering as a component of the total pressure. But, corrosion, toxicity, and regulatory issues require that it never be disregarded til clearly shown as negligible in all three aspects.
- Ammonia seldom, if ever, has a pressure that is significant, but its chemical effects are sometimes important.
- Hydrogen, helium, argon, and higher hydrocarbon gases are generally too scarce to have significant pressure effects. However, their presence and proportions, in relation to other gases, have geochemical implications that may be important.

Functional Relationships

Pressure of H_2O in a boiling system follows $\log(P) = A/T$, where A represents the energy contrast between liquid and vapor (heat of vaporization). "A" varies regularly with

temperature, hence a plot of log(P) versus 1/T is highly linear. Dissolved materials (salts) affect the value of log(P), but not A. Thus, for salty water with no gases, log(P) = A/T + f(N). [N = salt concentration and f(N) indicates a convenient functional relationship.

Figure 2 shows plots of log(P) versus $1/T_{abs}$ for water and two concentrations of NaCl. Plots are "least squares" straight lines through tabular data from Haas (1976). The system appears highly linear in an engineering sense and the effect of salt on log(P) is uniform over the interesting range of temperature.

It is significant that a boiling H_2O system does not follow the mathematics of PV = nRT. [Pressure, Volume, absolute Temperature, number of moles of gas in the system, R is a physical constant].

The log(P) = A/T relationship is one way to explain why hot, two-phase water systems cannot be accurately imitated by experiments with mixtures of cool water and gas(es) which do follow the mathematics of PV = nRT.

Non-H_2O gases in the geothermal vapor phase follow PV = nRT, but V is determined by the amount of H_2O vapor generated, in accordance with the energy balance between liquid and vapor. In the early stages of boiling, the "n" moles of non-H_2O gas in the system are partitioned between liquid and vapor. Often, it is necessary to account for the partitioning, until boiling has progressed so that negligible amounts of a gas are left in the residual liquid.

The pressures of the several gas species are independent, permitting the total vapor pressure of the system to be given by the simple, algebraic sum of the individual species pressures, plus the H_2O pressure

Henry's Law

Each gas species in a boiling system has a unique relationship among temperature, pressure of the species, and other components in the system. At a single temperature and overall composition, the pressure of any single gas species is directly proportional to its concentration in the liquid. This linear proportionality between vapor pressure and concentration "dissolved" in the liquid is known as Henry's Law.

At "high" pressures, the pressure/concentration relationship becomes non-linear. In ordinary exploited geothermal systems, the gas pressures are not high enough for non-linear effects to be significant. That is, non-H_2O gases may be treated as ideal without introducing errors that have engineering significance.

Gas solubilities obey Henry's law at any temperature, but the proportionality factors vary with temperature. Each gas species has a "temperature of minimum solubility". Most minima occur below 150C. Practical correlations between gas vapor pressure and the concentration in the liquid phase are given, for salt-free water, by equations of the form, [pres/conc = C + D/T], where C and D are unique constants for each gas species, and T is the absolute temperature (Himmelblau, 1960).

Unfortunately, the solubility minimum for CO_2 occurs at about 175 C, so a practical equation for its pres/conc relationship is more complicated. Data from different laboratory studies on the solubility of CO_2 in pure water and in salty waters are not in good agreement. My preference is the data by Ellis and Golding (1960), which included results for pure water and for three concentrations of sodium chloride, the highest being 2 molar. Those results have been fitted to an equation of the form:

$$psi/ppm = a + b|T_t - T_m|^c + d(e + fT_t)N$$

where N is the salt concentration, T_t is the temperature of interest, T_m is the temperature of minimum solubility, and |...| represents absolute values. Figure 3 shows the data and the fitted lines.

Gas Distribution Factor

A partial alternative to the Henry's Law approach for handling gas concentrations in a boiling system involves the factor "B" (see Giggenbach, 1980). It does not concern pressures directly, but describes the distribution of a gas species between phases.

calculation stopped before the long-term process is completed.

The third variant might be modeled to include a separate accounting for the steam derived from boiling. However, validation of the model requires some means to identify the proportion of total steam which comes from the vapor zone of the reservoir.

Boiling pressure: The collective vapor pressures of the fluid components at any position along the two-phase flowpath.

In a wellbore, this "chemical" pressure is identical to the sum of pressures usually considered in mechanical terms, as, for example, friction, weight of overlying components, accelerations, etc.

Boiling initiation pressure: The pressure at the time (position) where bubbles of vapor first begin to form. It corresponds to the boiling initiation temperature in concept and position. It can be computed from the temperature and fluid composition.

It may be identified in a pressure profile for a wellbore as a place where the pressure gradient in the deeper parts (due to a single phase liquid density) becomes less, due to development of vapor (bubbles).

Boiling Process: The evolution of events, thermophysical and dynamic characteristics, and chemical relationships between the point of boiling initiation and cessation of steam development.

Brine: The liquid phase produced from a geothermal well or residing in a geothermal reservoir, whether or not it is substantially salty. The liquid portion of a two-phase (liquid-vapor) steam-water mixture.

Fluid: Either steam or brine or a mixture of the two in any proportions.

Steam: The H_2O vapor plus a host of other substances, generally in minor amounts, generally including carbon dioxide, hydrogen sulfide, nitrogen, ammonia, methane, a variety of other hydrocarbons, and noble gases. Produced steam often contains physically entrained droplets of brine and sometimes, exotic substances, but for modeling purposes, these non-vapor components are normally disregarded.

Non-condensable gas: The naturally present non-H_2O gases in geothermal steam that do not redissolve in liquid when the steam is condensed. Mainly, these are carbon dioxide, methane, nitrogen, some higher hydrocarbons and noble gases.

Condensable gas: Any of the non-H_2O vaporous components in geothermal steam that tend to re-enter the liquid phase upon condensation of the steam. Mainly, this is ammonia. Its solubilization is aided by carbon dioxide, which, with H_2O forms an ionic compound. Hydrogen sulfide may be intentionally solubilized by additives.

REFERENCES

Ellis, A.J. and R.M. Golding, 1963, The solubility of carbon dioxide above 100°C in water and in sodium chloride solutions: Amer. Jour. Sci., v. 261, pp. 47-61.

Giggenbach, W.F., 1980, Geothermal gas equilibria: Geochim. et Cosmochim. Acta, v. 44, pp. 2021-2032.

Haas, J.L., Jr., 1976, Thermodynamic properties of the coexisting phases and thermochemical properties of the NaCl component in boiling NaCl solutions: U.S. Geol. Surv. Bul. 1421-B, Revised, 71 pp., U.S. Govt. Print Off.

Himmelblau, D.M., 1960, Solubilities of inert gases in water 0°C to near the critical point of water: Jour. Chem. and Engrg. Data, v. 5, n. 1, p.10-15.

Figure 1:

BOILING PRESSURE WITH DEPTH

Selected Conditions

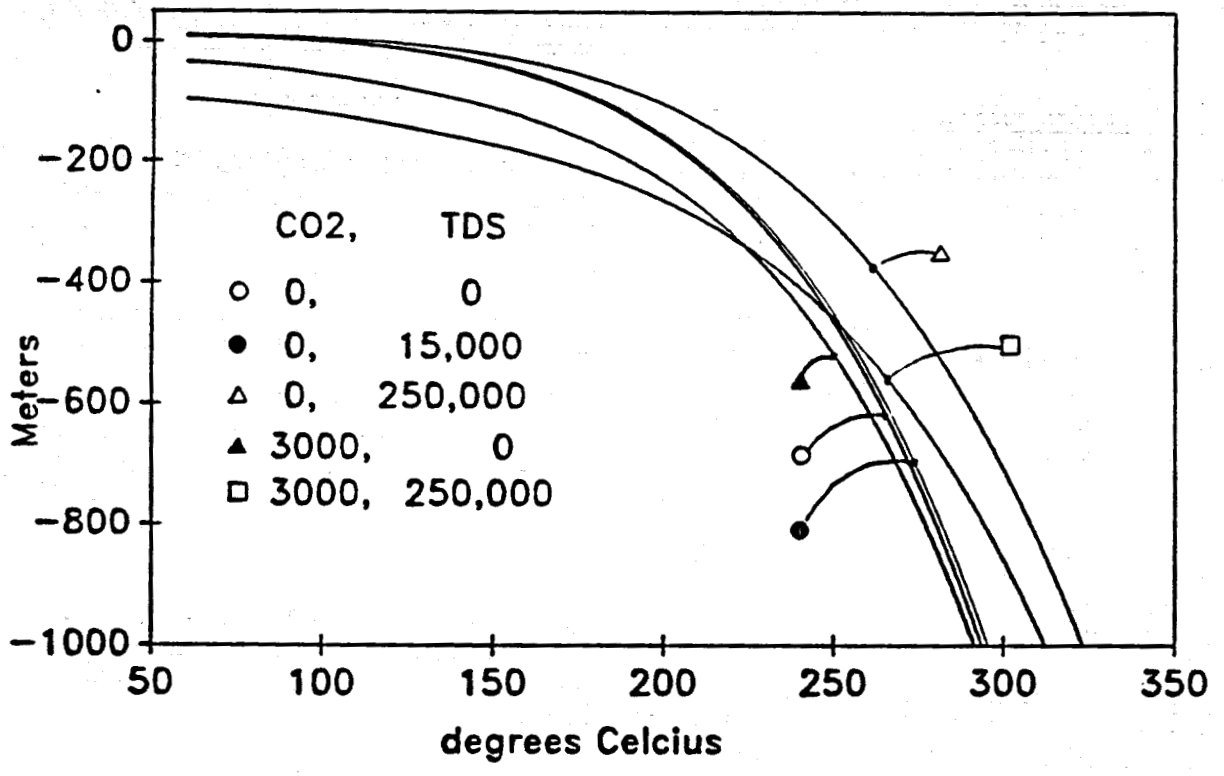

Figure 2:

BOILING TEMPERATURE–PRESSURE FOR SALTY WATERS (Haas, 1976)

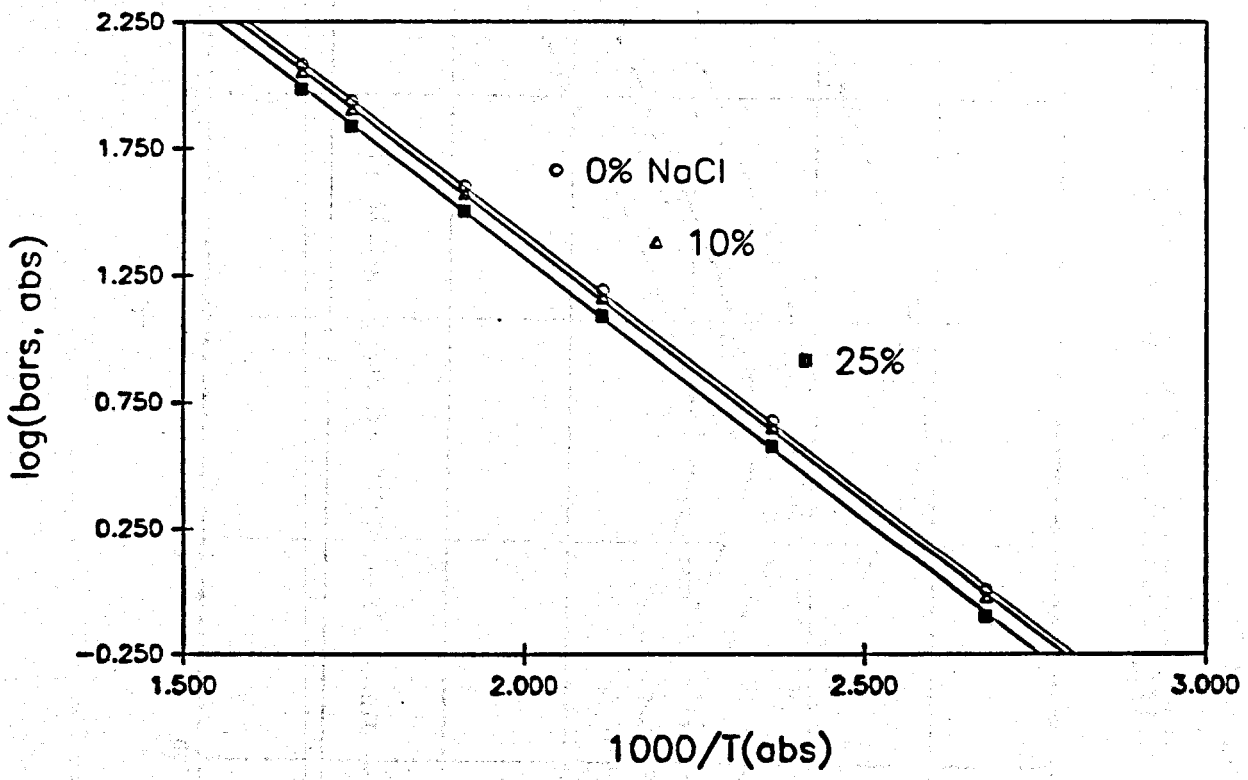

Figure 3:

CO_2 SOLUBILITY IN NaCl SOLUTIONS

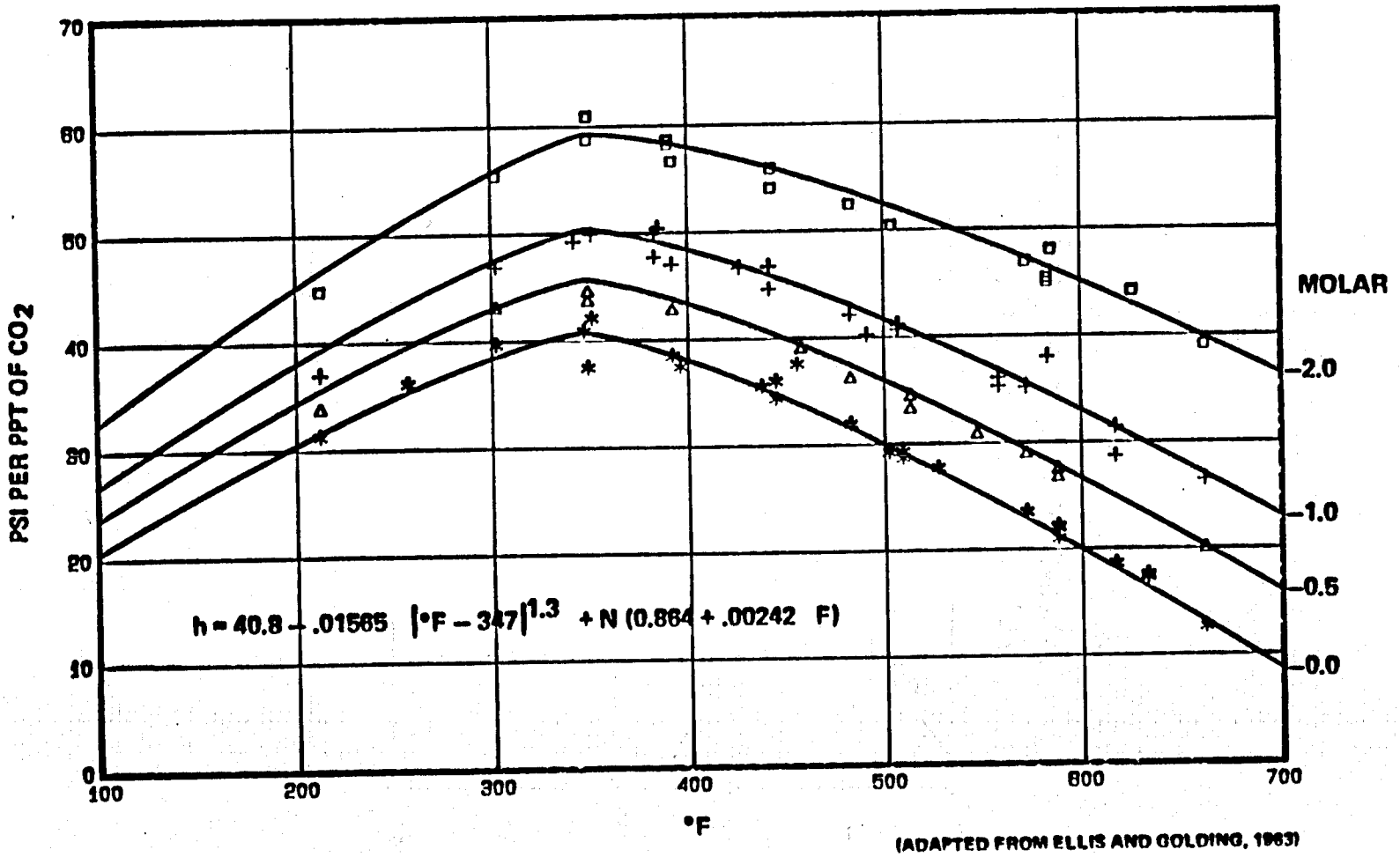

(ADAPTED FROM ELLIS AND GOLDING, 1963)

Figure 4:

VAPOR PRESSURE CURVES FOR PURE WATER AND 10 wt. % NaCl WITH DATA FROM WELL MESA 6-2

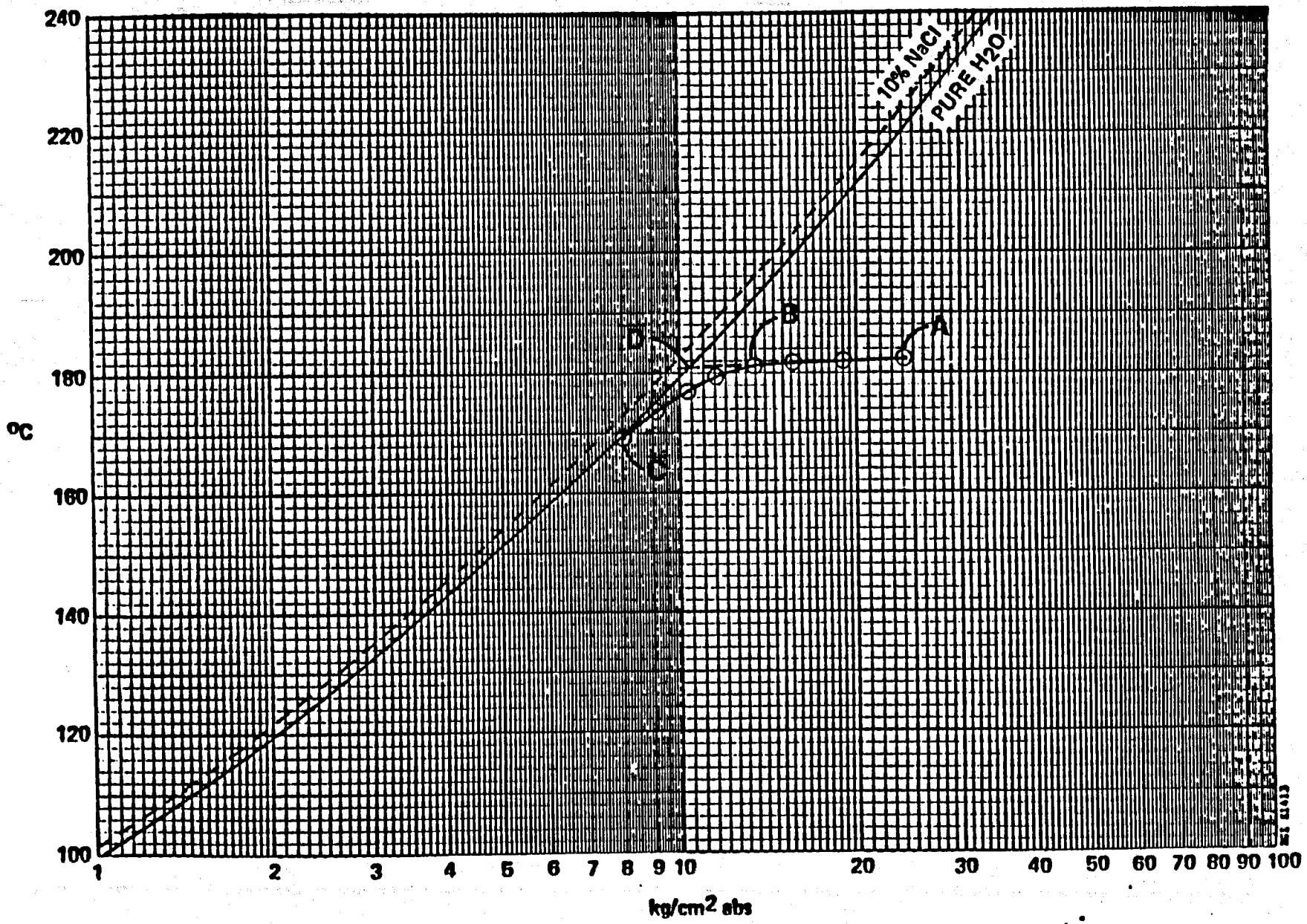

Figure 5:

FLOW SHEET FOR COMPUTATION OF STEAM YIELDS

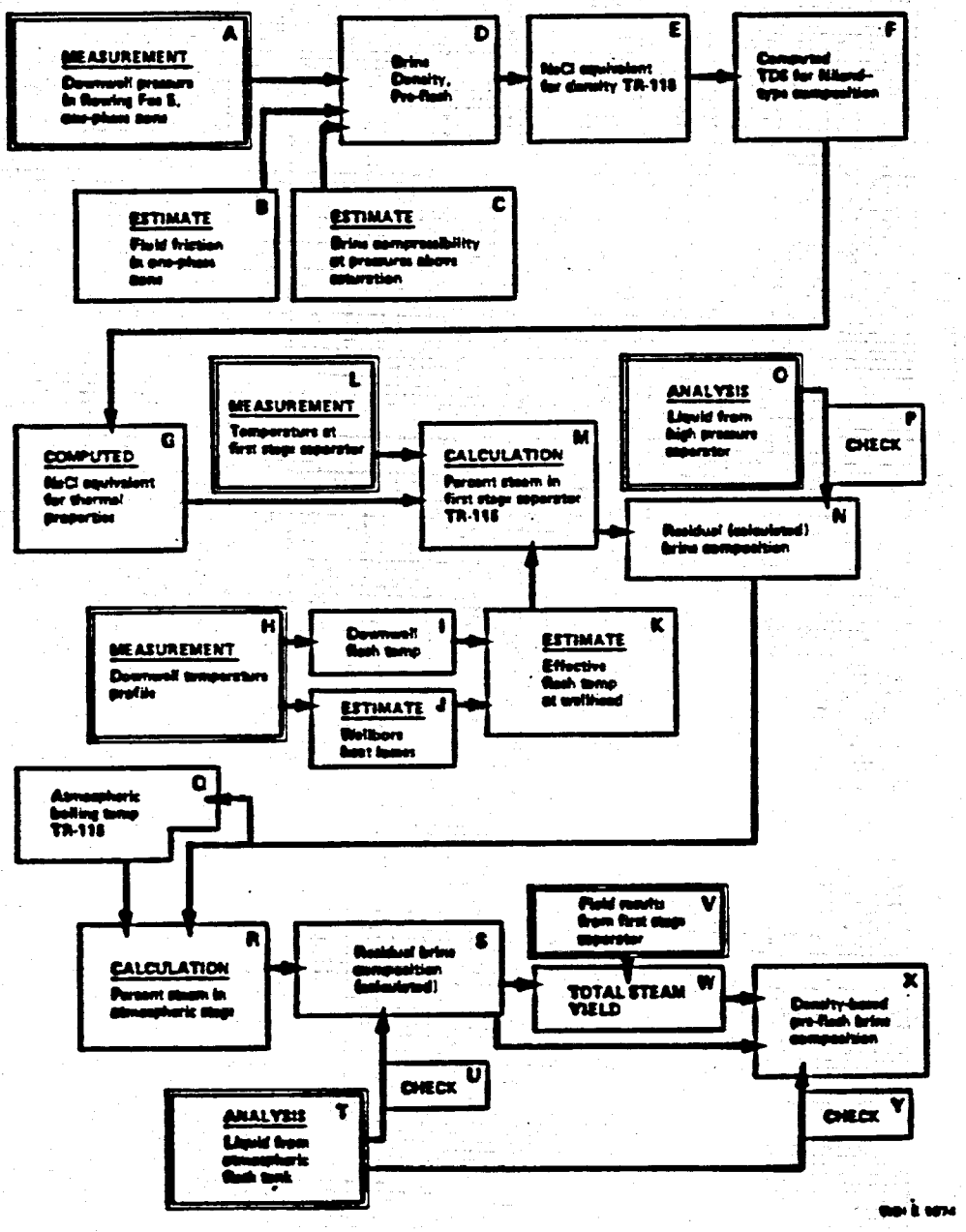

FLAGASA:
by
DON MICHELS ASSOCIATES

COMPUTATION OF COMPOSITION AND PHYSICAL PROPERTIES
FOR FLASHING GEOTHERMAL FLUIDS
Working Version

Example Calculations for:
GRC Workshop
RESPONSES OF A GEOTHERMAL FIELD DURING EXPLOITATION

Setchenow 1.02
Henry's Law CO2 41.5 BRINE-n 1
CH4 769 BRINE-d 0.902
N2 728

FLASH INITIATION AT: 350 F
PRE-FLASH TDS 5000 ppm
CO2 1000 ppm
CH4 10 ppm
N2 40 ppm

INITIAL HENRY'S LAW PRESSURES
H2O 130.7
CO2 41.6
CH4 7.9
N2 29.8
TOTAL 209.9

Table 1: Low-Salt, Low-Gas, Low-Temperature

DEG F	ENTHALPIES LIQUID	EVAP	FLASH FRACTION	--SPECIFIC VOLUMES-- STEAM	LIQUID	NET	VAPOR VOLUME FRAC	TDS ppm	Setch Coeff	PSIA/1000 CO2	CH4	N2	WEIGHT FRACTION OF INITIAL GAS REMAINING IN LIQUID CO2	CH4	N2	ppm OF GASES IN VAPOR PHASE CO2	CH4	N2	PARTIAL PRESSURES CO2	CH4	N2	H2O	TOTAL PRESSURE PSIA	KPA	DEG C
350	319.5	866.7	0.0000	3.355	0.0181	0.0181	0.000	5000	1.02	41.6	786	744	1.000	1.000	1.000				42	7.86	29.77	130.7	210	1447	176.7
349	318.4	867.5	0.0012	3.397	0.0181	0.0222	0.187	5006	1.02	41.6	789	747	0.533	0.140	0.089	276580	7001	28990	22	1.10	2.67	129.0	155	1068	176.1
348	317.4	868.4	0.0024	3.440	0.0181	0.0264	0.318	5012	1.02	41.6	792	750	0.361	0.074	0.046	207762	3785	15414	15	0.59	1.38	127.3	144	995	175.6
347	316.3	869.2	0.0037	3.483	0.0181	0.0307	0.414	5018	1.02	41.7	796	753	0.271	0.050	0.031	166435	2595	10506	11	0.40	0.93	125.6	138	953	175.0
346	315.2	870.1	0.0049	3.527	0.0180	0.0351	0.489	5024	1.02	41.6	799	756	0.216	0.037	0.023	138854	1976	7973	9	0.30	0.69	124.0	134	924	174.4
345	314.2	870.9	0.0061	3.571	0.0180	0.0396	0.548	5031	1.02	41.6	802	759	0.179	0.029	0.018	119150	1596	6428	7	0.24	0.55	122.4	131	900	173.9
340	308.9	875.1	0.0121	3.804	0.0180	0.0637	0.721	5061	1.02	41.5	818	775	0.093	0.014	0.008	69886	816	3275	4	0.11	0.26	114.5	119	819	171.1
335	303.7	879.3	0.0180	4.054	0.0179	0.0906	0.806	5092	1.02	41.3	835	790	0.060	0.008	0.005	49604	551	2206	3	0.07	0.17	107.0	110	757	168.3
330	298.4	883.4	0.0239	4.325	0.0178	0.1206	0.856	5122	1.02	41.0	852	806	0.044	0.006	0.004	38541	416	1668	2	0.05	0.12	100.0	102	703	165.6
325	293.2	887.5	0.0297	4.617	0.0178	0.1541	0.888	5153	1.02	40.8	869	822	0.033	0.004	0.003	31576	336	1344	1	0.04	0.09	93.3	95	654	162.8
320	287.9	891.6	0.0356	4.933	0.0177	0.1916	0.911	5183	1.02	40.5	886	839	0.026	0.003	0.002	26788	282	1127	1	0.03	0.07	87.0	88	608	160.0
310	277.5	899.5	0.0466	5.646	0.0176	0.2601	0.940	5245	1.02	39.9	921	872	0.018	0.002	0.001	20631	214	856	1	0.02	0.05	75.5	76	526	154.4
300	267.2	907.4	0.0576	6.485	0.0175	0.3903	0.958	5306	1.02	39.3	957	906	0.012	0.001	0.001	16842	173	693	1	0.01	0.03	65.2	66	453	148.9
290	256.9	915.2	0.0684	7.478	0.0173	0.5277	0.969	5367	1.02	38.6	994	941	0.009	0.001	0.001	14276	146	584	0	0.01	0.02	56.1	57	390	143.3
280	246.6	922.8	0.0790	8.658	0.0172	0.6994	0.977	5429	1.02	37.9	1032	977	0.007	0.001	.000	12422	127	506	0	0.01	0.02	48.1	48	334	137.8
270	236.4	930.3	0.0893	10.070	0.0171	0.9144	0.983	5490	1.02	37.2	1072	1014	0.005	.000	.000	11020	112	448	0	0.01	0.01	41.0	41	285	132.2
260	226.3	937.8	0.0994	11.767	0.0170	1.1845	0.987	5552	1.02	36.4	1112	1052	0.004	.000	.000	9924	101	402	0	.00	0.01	34.9	35	242	126.7
250	216.2	945.1	0.1092	13.822	0.0169	1.5249	0.990	5613	1.02	35.6	1154	1092	0.003	.000	.000	9042	92	366	0	.00	0.01	29.5	30	204	121.1
240	206.2	952.3	0.1189	16.326	0.0167	1.9562	0.992	5675	1.03	34.8	1197	1132	0.003	.000	.000	8318	84	336	0	.00	0.01	24.8	25	172	115.6
230	196.3	959.3	0.1284	19.400	0.0166	2.5054	0.994	5737	1.03	34.0	1241	1174	0.002	.000	.000	7713	78	311	0	.00	.00	20.8	21	144	110.0
220	186.4	966.3	0.1377	23.206	0.0165	3.2090	0.996	5798	1.03	33.1	1287	1218	0.002	.000	.000	7200	73	290	0	.00	.00	17.3	17	120	104.4

FLAGASA:
by
DON MICHELS ASSOCIATES

COMPUTATION OF COMPOSITION AND PHYSICAL PROPERTIES
FOR FLASHING GEOTHERMAL FLUIDS
Working Version

Example Calculations for:
GRC Workshop
RESPONSES OF A GEOTHERMAL FIELD DURING EXPLOITATION

Setchenow 1.07
Henry's Law CO2 43.3 BRINE-n 1
CH4 769 BRINE-d 0.911
N2 728

FLASH INITIATION AT: 350 F
PRE-FLASH TDS 15000 ppm
CO2 2000 ppm
CH4 20 ppm
N2 80 ppm

INITIAL HENRY'S LAW PRESSURES
H2O 129.7
CO2 86.6
CH4 16.4
N2 62.1
TOTAL 294.7

Table 2: Moderate-Salt, Moderate-Gas, Low-Temperature

DEG	ENTHALPIES		FLASH	--SPECIFIC VOLUMES--			VAPOR VOLUME	TDS	Setch	PSIA/1000			WEIGHT FRACTION OF INITIAL GAS REMAINING IN LIQUID			ppm OF GASES IN VAPOR PHASE			PARTIAL PRESSURES				TOTAL PRESSURE		
F	LIQUID	EVAP	FRACTION	STEAM	LIQUID	NET	FRAC	ppm	Coeff	CO2	CH4	N2	CO2	CH4	N2	CO2	CH4	N2	CO2	CH4	N2	H2O	PSIA	KPA	DEG C
350	315.1	875.0	0.0000	3.359	0.0179	0.0179	0.000	15000	1.07	43.3	820	776	1.000	1.000	1.000				87	16.39	62.07	129.7	295	2031	176.7
349	314.1	875.9	0.0012	3.401	0.0179	0.0220	0.185	15018	1.07	43.3	823	779	0.529	0.132	0.084	441419	14347	57892	46	2.18	5.26	128.0	181	1250	176.1
348	313.0	876.7	0.0024	3.444	0.0179	0.0261	0.315	15036	1.07	43.3	826	782	0.357	0.070	0.043	350806	7752	31139	31	1.16	2.72	126.3	161	1111	175.6
347	312.0	877.6	0.0036	3.487	0.0179	0.0303	0.411	15054	1.07	43.4	830	785	0.267	0.047	0.029	291161	5315	21313	23	0.78	1.82	124.7	151	1038	175.0
346	310.9	878.4	0.0048	3.531	0.0179	0.0346	0.485	15072	1.07	43.3	833	789	0.213	0.035	0.021	248902	4046	16210	19	0.59	1.36	123.0	144	989	174.4
345	309.9	879.3	0.0059	3.575	0.0179	0.0390	0.544	15090	1.07	43.3	836	792	0.176	0.028	0.017	217413	3267	13085	15	0.47	1.08	121.4	138	953	173.9
340	304.7	883.4	0.0118	3.808	0.0178	0.0625	0.718	15179	1.07	43.2	853	808	0.091	0.013	0.008	133504	1671	6685	8	0.22	0.51	113.6	122	843	171.1
335	299.5	887.6	0.0176	4.058	0.0177	0.0888	0.804	15269	1.07	43.0	871	824	0.059	0.008	0.005	96624	1127	4506	5	0.14	0.32	106.2	112	771	168.3
330	294.3	891.8	0.0233	4.329	0.0177	0.1182	0.854	15338	1.07	42.7	888	841	0.043	0.006	0.003	75890	852	3409	4	0.10	0.23	99.2	103	712	165.6
325	289.1	895.9	0.0290	4.621	0.0176	0.1510	0.887	15448	1.07	42.5	906	858	0.033	0.004	0.002	62602	687	2747	3	0.08	0.17	92.6	96	660	162.8
320	284.0	899.9	0.0346	4.938	0.0176	0.1876	0.910	15537	1.07	42.2	924	875	0.026	0.003	0.002	53360	576	2305	2	0.06	0.14	86.3	89	612	160.0
310	273.7	907.9	0.0456	5.651	0.0174	0.2742	0.939	15716	1.07	41.6	961	909	0.017	0.002	0.001	41345	438	1750	2	0.04	0.09	74.9	76	527	154.4
300	263.5	915.8	0.0563	6.490	0.0173	0.3820	0.957	15896	1.07	41.0	999	945	0.012	0.001	0.001	33879	354	1417	1	0.03	0.06	64.7	66	454	148.9
290	253.3	923.6	0.0669	7.486	0.0172	0.5164	0.969	16075	1.07	40.3	1038	983	0.009	0.001	0.001	28789	299	1194	1	0.02	0.05	55.6	56	389	143.3
280	243.2	931.2	0.0772	8.665	0.0171	0.6844	0.977	16254	1.07	39.6	1079	1021	0.007	0.001	.000	25096	259	1035	1	0.02	0.03	47.7	48	333	137.8
270	233.2	938.8	0.0873	10.077	0.0170	0.8947	0.983	16434	1.07	38.9	1120	1060	0.005	.000	.000	22295	229	916	0	0.01	0.03	40.7	41	284	132.2
260	223.2	946.2	0.0971	11.775	0.0168	1.1589	0.987	16614	1.07	38.1	1164	1101	0.004	.000	.000	20097	206	823	0	0.01	0.02	34.6	35	241	126.7
250	213.3	953.5	0.1068	13.831	0.0167	1.4920	0.990	16793	1.07	37.3	1208	1144	0.003	.000	.000	18327	187	748	0	0.01	0.02	29.2	30	204	121.1
240	203.4	960.7	0.1163	16.336	0.0166	1.9139	0.992	16973	1.07	36.4	1255	1187	0.002	.000	.000	16871	172	688	0	0.01	0.01	24.6	25	171	115.6
230	193.6	967.8	0.1255	19.412	0.0165	2.4512	0.994	17153	1.08	35.6	1303	1233	0.002	.000	.000	15653	159	637	0	.00	0.01	20.6	21	143	110.0
220	183.9	974.8	0.1346	23.218	0.0164	3.1396	0.995	17333	1.08	34.7	1353	1280	0.002	.000	.000	14618	149	594	0	.00	0.01	17.2	17	119	104.4

FLAGASA:
by
DON MICHELS ASSOCIATES

COMPUTATION OF COMPOSITION AND PHYSICAL PROPERTIES
FOR FLASHING GEOTHERMAL FLUIDS
Working Version

Example Calculations for:
GRC Workshop
RESPONSES OF A GEOTHERMAL FIELD DURING EXPLOITATION

Setchenow 1.10
Henry's Law CO2 33.0 BRINE-n 1
CH4 374 BRINE-d 0.812
N2 354

FLASH INITIATION AT: 500 F
PRE-FLASH TDS 15000 ppm
CO2 2000 ppm
CH4 20 ppm
N2 80 ppm

INITIAL HENRY'S LAW PRESSURES
H2O 675.3
CO2 66.2
CH4 8.2
N2 31.2
TOTAL 780.9

Table 3: Moderate-Salt, Moderate-Gas, High-Temperature

DEG	ENTHALPIES		FLASH	--SPECIFIC VOLUMES--			VAPOR VOLUME	TDS	Setch	PSIA/1000 ppm			WEIGHT FRACTION OF INITIAL GAS REMAINING IN LIQUID			ppm OF GASES IN VAPOR PHASE			PARTIAL PRESSURES				TOTAL PRESSURE		
F	LIQUID	EVAP	FRACTION	STEAM	LIQUID	NET	FRAC	ppm	Coeff	CO2	CH4	N2	CO2	CH4	N2	CO2	CH4	N2	CO2	CH4	N2	H2O	PSIA	KPA	DEG C
500	476.6	725.7	0.0000	0.673	0.0201	0.0201	0.000	15000	1.10	33.1	411	389	1.000	1.000	1.000				66	8.22	31.15	675.3	781	5382	260.0
499	475.5	726.9	0.0015	0.679	0.0201	0.0211	0.049	15023	1.10	33.2	413	392	0.872	0.578	0.452	143907	5521	28007	58	4.78	14.19	669.1	746	5142	259.4
498	474.4	728.1	0.0030	0.686	0.0201	0.0221	0.096	15046	1.10	33.3	416	394	0.771	0.403	0.289	130920	3918	18382	51	3.36	9.14	662.9	727	5010	258.9
497	473.3	729.3	0.0045	0.692	0.0201	0.0231	0.136	15069	1.10	33.4	418	396	0.690	0.307	0.211	120111	3038	13693	46	2.58	6.72	656.7	712	4909	258.3
496	472.2	730.5	0.0061	0.699	0.0201	0.0242	0.175	15091	1.10	33.5	420	398	0.622	0.247	0.165	110974	2483	10918	42	2.09	5.30	650.6	700	4824	257.8
495	471.0	731.7	0.0075	0.706	0.0200	0.0252	0.211	15114	1.10	33.5	423	401	0.566	0.206	0.135	103148	2100	9083	38	1.75	4.36	644.5	689	4748	257.2
490	465.5	737.6	0.0150	0.740	0.0200	0.0307	0.360	15228	1.10	34.0	435	412	0.381	0.108	0.068	76413	1191	4959	26	0.95	2.27	614.8	644	4441	254.4
485	460.0	743.5	0.0223	0.776	0.0199	0.0367	0.471	15341	1.10	34.5	447	423	0.279	0.070	0.043	60850	835	3428	20	0.64	1.50	586.1	608	4190	251.7
480	454.5	749.4	0.0296	0.815	0.0198	0.0432	0.555	15455	1.09	34.9	459	435	0.215	0.050	0.031	50664	646	2630	15	0.47	1.10	558.5	576	3967	248.9
475	449.0	755.1	0.0365	0.855	0.0197	0.0502	0.621	15568	1.09	35.3	471	446	0.171	0.038	0.023	43477	528	2139	13	0.37	0.85	531.9	546	3762	246.1
470	443.6	760.7	0.0434	0.898	0.0196	0.0578	0.675	15680	1.09	35.8	483	458	0.140	0.029	0.018	38135	447	1807	10	0.30	0.69	506.3	518	3569	243.3
460	432.6	771.7	0.0569	0.992	0.0195	0.0749	0.755	15906	1.09	36.6	509	482	0.098	0.019	0.012	30719	344	1387	8	0.21	0.48	458.1	466	3215	237.8
450	421.7	782.5	0.0701	1.097	0.0193	0.0949	0.811	16130	1.09	37.5	534	506	0.072	0.013	0.008	25818	282	1131	6	0.15	0.36	413.5	420	2894	232.2
440	410.9	793.0	0.0828	1.216	0.0192	0.1183	0.851	16355	1.09	38.3	561	531	0.054	0.010	0.006	22336	239	959	4	0.12	0.27	372.4	377	2601	226.7
430	400.1	803.2	0.0952	1.350	0.0190	0.1458	0.882	16579	1.09	39.1	588	557	0.041	0.007	0.004	19734	208	836	4	0.09	0.22	334.7	339	2334	221.1
420	389.3	813.2	0.1073	1.501	0.0189	0.1780	0.905	16803	1.08	39.8	615	583	0.032	0.005	0.003	17715	185	743	3	0.08	0.17	300.0	303	2089	215.6
410	378.6	823.0	0.1191	1.673	0.0187	0.2157	0.923	17028	1.08	40.5	644	610	0.026	0.004	0.003	16103	167	670	2	0.06	0.14	268.2	271	1866	210.0
400	367.9	832.6	0.1305	1.868	0.0186	0.2601	0.938	17252	1.08	41.2	673	637	0.020	0.003	0.002	14786	153	611	2	0.05	0.11	239.2	241	1663	204.4
390	357.2	841.9	0.1417	2.091	0.0185	0.3122	0.949	17477	1.08	41.9	703	665	0.016	0.003	0.002	13689	141	563	2	0.04	0.09	212.7	214	1478	198.9
380	346.6	851.1	0.1527	2.346	0.0183	0.3736	0.958	17703	1.08	42.5	734	694	0.013	0.002	0.001	12761	131	523	1	0.03	0.08	188.7	190	1311	193.3
370	336.1	860.1	0.1634	2.637	0.0182	0.4461	0.966	17929	1.08	43.0	765	724	0.011	0.002	0.001	11966	122	489	1	0.03	0.07	166.9	168	1158	187.8
360	325.6	868.9	0.1738	2.973	0.0181	0.5316	0.972	18155	1.08	43.5	798	755	0.009	0.001	0.001	11277	115	460	1	0.02	0.05	147.1	148	1021	182.2
350	315.1	877.5	0.1840	3.360	0.0179	0.6330	0.977	18383	1.08	43.9	831	787	0.007	0.001	0.001	10675	109	434	1	0.02	0.05	129.3	130	897	176.7
340	304.7	886.0	0.1940	3.809	0.0178	0.7534	0.981	18611	1.08	43.7	865	819	0.006	0.001	.000	10143	103	412	1	0.02	0.04	113.3	114	786	171.1
330	294.3	894.3	0.2038	4.330	0.0177	0.8967	0.984	18840	1.08	43.3	901	852	0.005	0.001	.000	9670	98	392	1	0.01	0.03	98.9	100	686	165.6
320	284.0	902.5	0.2134	4.939	0.0176	1.0678	0.987	19069	1.08	42.8	937	887	0.004	.000	.000	9247	94	375	0	0.01	0.03	86.1	87	597	160.0
310	273.7	910.5	0.2228	5.652	0.0174	1.2729	0.989	19300	1.08	42.2	975	922	0.004	.000	.000	8866	90	359	0	0.01	0.02	76.7	75	517	154.4
300	263.5	918.4	0.2320	6.492	0.0173	1.5195	0.991	19531	1.08	41.6	1013	959	0.003	.000	.000	8522	86	345	0	0.01	0.02	64.5	65	447	148.9
290	253.3	926.2	0.2410	7.486	0.0172	1.8173	0.993	19763	1.08	40.9	1053	997	0.002	.000	.000	8210	83	332	0	0.01	0.02	55.5	56	384	143.3
280	243.2	933.9	0.2499	8.667	0.0171	2.1784	0.994	19996	1.08	40.2	1095	1036	0.002	.000	.000	7925	80	320	0	0.01	0.01	47.6	48	329	137.8
270	233.2	941.4	0.2585	10.080	0.0170	2.6185	0.995	20230	1.09	39.4	1137	1077	0.002	.000	.000	7663	77	309	0	.00	0.01	40.6	41	281	132.2
260	223.2	948.8	0.2670	11.778	0.0168	3.1576	0.996	20465	1.09	38.7	1182	1118	0.001	.000	.000	7423	75	299	0	.00	0.01	34.5	35	239	126.7
250	213.3	956.1	0.2754	13.834	0.0167	3.8217	0.997	20700	1.09	37.9	1228	1162	0.001	.000	.000	7202	73	290	0	.00	0.01	29.2	29	202	121.1
240	203.4	963.4	0.2836	16.340	0.0166	4.6451	0.997	20937	1.09	37.0	1275	1207	0.001	.000	.000	6997	71	282	0	.00	0.01	24.5	25	170	115.6
230	193.6	970.5	0.2916	19.416	0.0165	5.6728	0.998	21174	1.09	36.2	1324	1253	0.001	.000	.000	6807	69	274	0	.00	.00	20.6	21	142	110.0
220	183.9	977.5	0.2994	23.223	0.0164	6.9654	0.998	21412	1.10	35.3	1376	1302	0.001	.000	.000	6630	67	267	0	.00	.00	17.1	17	119	104.4

FLAGASA:
by
DON MICHELS ASSOCIATES

COMPUTATION OF COMPOSITION AND PHYSICAL PROPERTIES
FOR FLASHING GEOTHERMAL FLUIDS
Working Version

Example Calculations for:
GRC Workshop
RESPONSES OF A GEOTHERMAL FIELD DURING EXPLOITATION

Setchenow 3.61
Henry's Law CO2 78.7 BRINE-n 1
CH4 209 BRINE-d 0.991
N2 198

FLASH INITIATION AT: 580 F
PRE-FLASH TDS 250000 ppm
CO2 3000 ppm
CH4 20 ppm
N2 40 ppm

INITIAL HENRY'S LAW PRESSURES
H2O 1118.1
CO2 236.3
CH4 15.1
N2 28.6
TOTAL 1398.1

Table 4: HYPERSALINE, Modeled as NaCl

DEG F	ENTHALPIES LIQUID	EVAP	FLASH FRACTION	--SPECIFIC VOLUMES-- STEAM	LIQUID	NET	VAPOR VOLUME FRAC	TDS ppm	Setch Coeff	PSIA/1000 CO2	CH4	N2	WEIGHT FRACTION OF INITIAL GAS REMAINING IN LIQUID CO2	CH4	N2	ppm OF GASES IN VAPOR PHASE CO2	CH4	N2	PARTIAL PRESSURES CO2	CH4	N2	H2O	TOTAL PRESSURE PSIA	KPA	DEG C
580	409.2	735.7	0.0000	0.353	0.0165	0.0165	0.000	250000	3.61	78.8	754	715	1.000	1.000	1.000				236	15.08	28.61	1118.1	1398	9637	304.4
579	408.3	737.1	0.0011	0.356	0.0165	0.0168	0.023	250278	3.59	78.9	758	719	0.890	0.393	0.281	228487	10817	25267	211	5.96	8.08	1109.0	1334	9195	303.9
578	407.5	738.5	0.0022	0.359	0.0165	0.0172	0.046	250555	3.58	79.0	762	723	0.801	0.243	0.162	212161	6787	14903	190	3.71	4.69	1100.0	1299	8952	303.3
577	406.7	739.9	0.0033	0.362	0.0165	0.0176	0.068	250832	3.56	79.1	766	726	0.727	0.175	0.113	198059	4950	10580	173	2.69	3.30	1091.1	1270	8755	302.8
576	405.9	741.3	0.0044	0.365	0.0164	0.0180	0.090	251108	3.55	79.2	770	730	0.664	0.136	0.087	185754	3899	8209	159	2.11	2.55	1082.2	1245	8584	302.2
575	405.1	742.7	0.0055	0.368	0.0164	0.0184	0.110	251384	3.54	79.3	773	734	0.611	0.111	0.070	174924	3218	6711	146	1.73	2.07	1073.4	1223	8432	301.7
570	401.0	749.2	0.0109	0.384	0.0164	0.0204	0.205	252757	3.47	79.8	793	752	0.429	0.057	0.035	135715	1727	3527	104	0.91	1.06	1030.1	1136	7830	298.9
565	396.9	755.8	0.0162	0.400	0.0164	0.0226	0.287	254119	3.41	80.3	812	770	0.324	0.037	0.023	111196	1187	2406	79	0.61	0.71	988.1	1069	7367	296.1
560	392.8	762.2	0.0214	0.418	0.0163	0.0249	0.359	255471	3.35	80.8	830	787	0.256	0.027	0.016	94396	908	1834	63	0.45	0.52	947.5	1012	6975	293.3
555	388.8	768.4	0.0265	0.436	0.0163	0.0274	0.422	256814	3.29	81.3	849	805	0.208	0.021	0.013	82159	738	1487	52	0.36	0.41	908.2	961	6626	290.6
550	384.7	774.4	0.0316	0.455	0.0162	0.0301	0.477	258149	3.24	81.8	867	822	0.173	0.017	0.010	72843	623	1253	44	0.30	0.34	870.2	915	6306	287.8
540	376.6	785.7	0.0414	0.496	0.0162	0.0361	0.570	260804	3.14	82.8	904	857	0.125	0.011	0.007	59567	477	958	32	0.21	0.25	797.9	831	5727	282.2
530	368.5	796.8	0.0510	0.542	0.0161	0.0429	0.644	263432	3.05	83.7	941	892	0.095	0.008	0.005	50576	389	780	25	0.16	0.19	730.4	756	5209	276.7
520	360.5	807.3	0.0603	0.592	0.0160	0.0508	0.703	266044	2.96	84.6	977	926	0.073	0.006	0.004	44068	329	660	20	0.13	0.15	667.4	687	4739	271.1
510	352.5	817.3	0.0694	0.648	0.0159	0.0598	0.752	268641	2.89	85.4	1015	961	0.058	0.005	0.003	39132	287	574	16	0.11	0.12	608.8	625	4308	265.6
500	344.5	826.8	0.0783	0.710	0.0159	0.0702	0.792	271229	2.82	86.2	1052	997	0.047	0.004	0.002	35256	254	510	13	0.09	0.10	554.2	567	3911	260.0
490	336.5	835.9	0.0870	0.780	0.0158	0.0822	0.825	273810	2.75	87.0	1090	1033	0.038	0.003	0.002	32129	229	459	11	0.07	0.09	503.6	515	3547	254.4
480	328.5	844.7	0.0955	0.857	0.0157	0.0961	0.852	276387	2.70	87.8	1130	1070	0.031	0.003	0.002	29551	209	418	9	0.06	0.07	456.7	466	3211	248.9
470	320.6	853.1	0.1038	0.944	0.0157	0.1120	0.875	278963	2.64	88.5	1170	1108	0.025	0.002	0.001	27387	192	385	8	0.05	0.06	413.3	421	2902	243.3
460	312.7	861.2	0.1120	1.040	0.0156	0.1304	0.894	281539	2.60	89.2	1212	1148	0.021	0.002	0.001	25544	178	357	6	0.05	0.05	373.2	380	2617	237.8
450	304.8	868.9	0.1201	1.149	0.0155	0.1516	0.910	284118	2.56	89.8	1255	1188	0.018	0.001	0.001	23955	166	333	5	0.04	0.04	336.3	342	2356	232.2
440	297.0	876.4	0.1280	1.271	0.0154	0.1762	0.924	286701	2.52	90.4	1300	1231	0.015	0.001	0.001	22570	156	312	5	0.03	0.04	302.3	307	2116	226.7
430	289.2	883.6	0.1358	1.409	0.0154	0.2047	0.935	289290	2.49	91.0	1346	1275	0.012	0.001	0.001	21351	147	294	4	0.03	0.03	271.2	275	1896	221.1
420	281.4	890.5	0.1435	1.565	0.0153	0.2377	0.945	291886	2.46	91.5	1395	1321	0.010	0.001	.000	20270	139	279	3	0.02	0.03	242.6	246	1696	215.6
410	273.6	897.2	0.1511	1.741	0.0152	0.2760	0.953	294491	2.43	92.0	1445	1369	0.009	0.001	.000	19305	132	265	3	0.02	0.02	216.5	219	1512	210.0
400	265.9	903.6	0.1585	1.941	0.0152	0.3206	0.960	297106	2.41	92.5	1498	1419	0.007	0.001	.000	18437	126	252	2	0.02	0.02	192.8	195	1345	204.4
390	258.2	909.9	0.1659	2.170	0.0151	0.3726	0.966	299731	2.39	92.9	1554	1472	0.006	.000	.000	17652	120	241	2	0.02	0.02	171.1	173	1194	198.9
380	250.5	915.9	0.1732	2.430	0.0150	0.4333	0.971	302369	2.38	93.3	1613	1527	0.005	.000	.000	16940	115	231	2	0.01	0.02	151.5	153	1056	193.3
370	242.9	921.7	0.1804	2.728	0.0150	0.5044	0.976	305019	2.36	93.5	1674	1585	0.004	.000	.000	16289	111	222	1	0.01	0.01	133.7	135	932	187.8
360	235.3	927.4	0.1875	3.071	0.0149	0.5879	0.979	307683	2.36	93.8	1739	1647	0.004	.000	.000	15693	107	213	1	0.01	0.01	117.7	119	820	182.2
350	227.7	932.8	0.1945	3.467	0.0149	0.6862	0.983	310362	2.35	93.8	1808	1712	0.003	.000	.000	15144	103	206	1	0.01	0.01	103.2	104	719	176.7
340	220.2	938.1	0.2014	3.924	0.0148	0.8022	0.985	313056	2.35	93.4	1881	1780	0.003	.000	.000	14637	99	199	1	0.01	0.01	90.3	91	629	171.1
330	212.7	943.2	0.2083	4.455	0.0147	0.9396	0.988	315766	2.35	92.7	1957	1853	0.002	.000	.000	14168	96	192	1	0.01	0.01	78.7	79	548	165.6
320	205.3	948.2	0.2151	5.075	0.0147	1.1029	0.990	318492	2.35	91.8	2039	1930	0.002	.000	.000	13733	93	186	1	0.01	0.01	68.3	69	476	160.0
310	197.8	953.0	0.2218	5.801	0.0146	1.2977	0.991	321235	2.36	90.9	2126	2012	0.002	.000	.000	13327	90	180	1	.00	.00	59.1	60	412	154.4
300	190.4	957.7	0.2284	6.654	0.0145	1.5309	0.993	323996	2.37	90.0	2218	2099	0.001	.000	.000	12948	88	175	0	.00	.00	51.0	51	355	148.9
290	183.1	962.2	0.2349	7.663	0.0145	1.8114	0.994	326775	2.38	89.0	2316	2192	0.001	.000	.000	12594	85	170	0	.00	.00	43.8	44	305	143.3
280	175.8	966.6	0.2416	8.861	0.0144	2.1504	0.995	329571	2.40	87.9	2421	2291	0.001	.000	.000	12261	83	166	0	.00	.00	37.5	38	260	137.8
270	168.5	970.8	0.2479	10.293	0.0144	2.5621	0.996	332387	2.42	86.8	2533	2397	0.001	.000	.000	11949	81	161	0	.00	.00	31.9	32	222	132.2
260	161.3	974.4	0.2542	12.014	0.0143	3.0649	0.997	335220	2.44	85.7	2653	2511	0.001	.000	.000	11655	79	157	0	.00	.00	27.0	27	188	126.7
250	154.1	977.6	0.2605	14.095	0.0142	3.6826	0.997	338073	2.47	84.5	2782	2633	0.001	.000	.000	11378	77	154	0	.00	.00	22.8	23	159	
240	147.0	980.4	0.2667	16.630	0.0142	4.4463	0.998	340944	2.50	83.3	2921	2764	.000	.000	.000	11117	75	150	0	.00	.00	19.2	19	133	

$CACO_3$ DEPOSITION
NEAR AN ORIFICE PLATE

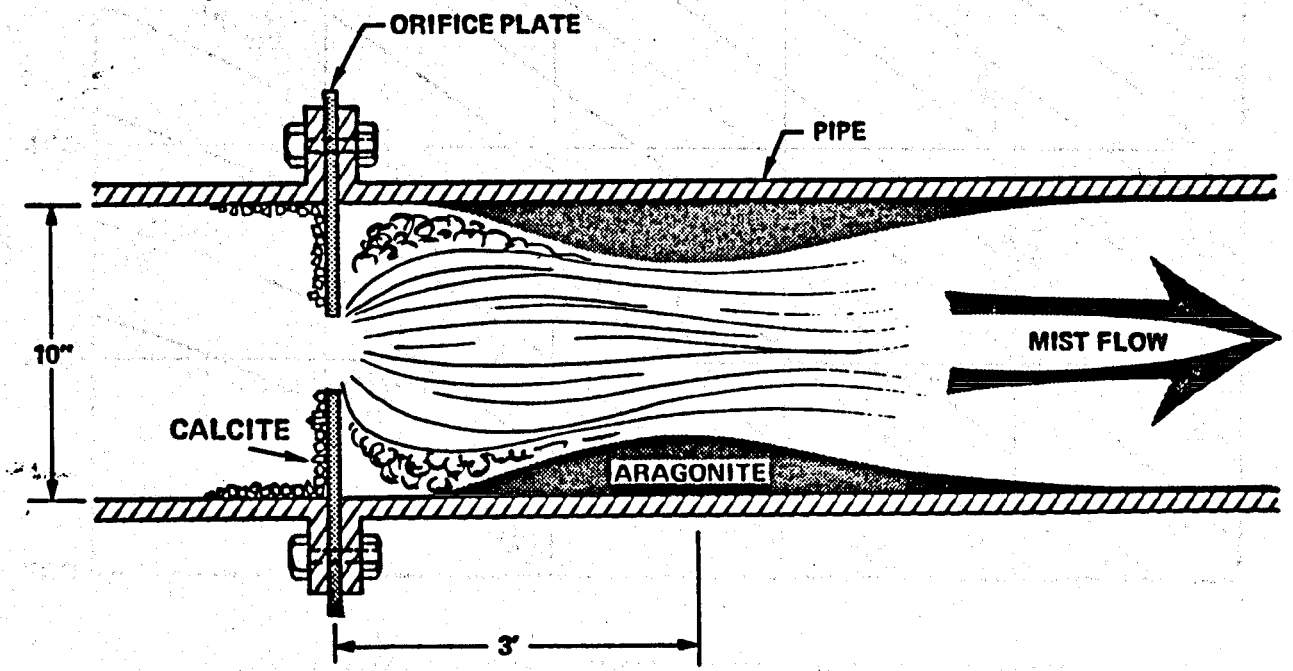

RGI E 1671.

PATHWAYS FOR THREE THERMAL PROCESSES

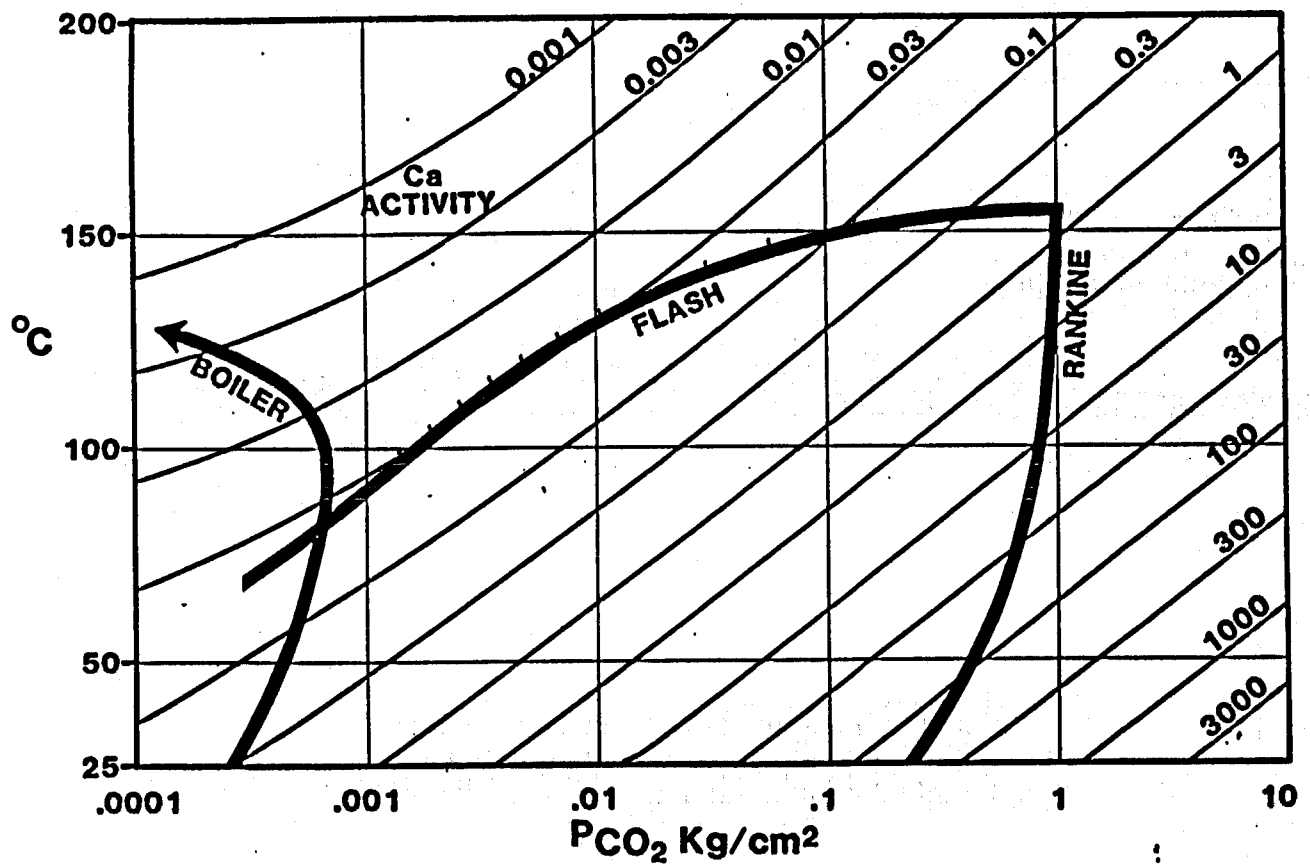

RLE E 1668

Geothermal Resources Council
WORKSHOP -- June 14-15, 1989

RESPONSES OF A GEOTHERMAL FIELD DURING EXPLOITATION

Example Calculations
by
DON MICHELS ASSOCIATES

Analyzed Composition	ppm	mmol/kg	Adjusted mmol/kg
Sodium	554	24.09	24.01
Calcium	1.15	0.03	0.03
Potassium	80.1	2.05	2.04
Magnesium	0.14	0.01	0.01
Lithium	6.59	0.95	0.95
Ammonium	0.1	0.01	0.01
Chloride	768	21.66	21.73
Bicarbonate	203	3.33	3.34
Carbonate		0.00	0.00
Sulfate	96	1.00	1.00
Boron	26	2.58	2.58
Silica	443	7.38	7.38
Sum	2178	63.08	63.08
m-equivalents (+,-)		54.15	54.15
Charge Balance		0.0031	.0000
Ionic strength		mol/kg	0.0281

FLASH INITIATION AT: 473 F
PRE-FLASH TDS 2178 ppm
CO2 4100 ppm
CH4 0.05 ppm
N2 18.5 ppm

CALCITE SCALING COMPUTATION

Activity Coefficients SO4	HCO3	CO3	CO2	Ca	CaX(aq) /Ca x100	K1Ks/K2	Ca solubility activity	ppm	mg/kg Ca to Calcite inc.	cumulat	Calcite Deposits mg/kg cumul	Cu.Ft/10-6 lb inc	cumul	Temp F	C
0.304	0.744	0.304	1.02	0.339	0.00102	-8.76	0.0000266	3.146	0	0	0.00	0.00	0.0	473	245.0
0.305	0.745	0.305	1.02	0.341	0.00106	-8.73	0.0000207	2.439	0.714	0.714	1.79	10.60	10.6	471	243.9
0.307	0.745	0.307	1.02	0.342	0.00110	-8.70	0.0000174	2.039	0.404	1.119	2.80	6.00	16.6	469	242.8
0.308	0.746	0.308	1.02	0.343	0.00114	-8.67	0.0000151	1.772	0.270	1.389	3.47	4.01	20.6	467	241.7
0.309	0.747	0.309	1.02	0.345	0.00118	-8.64	0.0000136	1.583	0.192	1.581	3.95	2.85	23.5	465	240.6
0.312	0.749	0.312	1.02	0.348	0.00129	-8.56	0.0000111	1.288	0.301	1.882	4.71	4.47	27.9	460	237.8
0.315	0.751	0.315	1.02	0.351	0.00141	-8.48	0.0000098	1.127	0.166	2.048	5.12	2.46	30.4	455	235.0
0.318	0.752	0.318	1.02	0.354	0.00153	-8.41	0.0000090	1.029	0.103	2.151	5.38	1.53	31.9	450	232.2
0.321	0.754	0.321	1.02	0.357	0.00167	-8.33	0.0000086	0.966	0.067	2.219	5.55	1.00	32.9	445	229.4
0.324	0.756	0.324	1.02	0.360	0.00182	-8.26	0.0000083	0.926	0.045	2.264	5.66	0.67	33.6	440	226.7
0.327	0.758	0.327	1.02	0.363	0.00199	-8.18	0.0000081	0.901	0.030	2.294	5.73	0.45	34.0	435	223.9
0.330	0.759	0.330	1.02	0.365	0.00217	-8.11	0.0000080	0.886	0.020	2.313	5.78	0.29	34.3	430	221.1
0.332	0.761	0.332	1.02	0.368	0.00236	-8.04	0.0000080	0.880	0.012	2.325	5.81	0.18	34.5	425	218.3
0.335	0.762	0.335	1.02	0.371	0.00257	-7.97	0.0000081	0.880	0.006	2.331	5.83	0.09	34.6	420	215.6
0.338	0.764	0.338	1.02	0.374	0.00280	-7.90	0.0000082	0.884	0.001	2.332	5.83	0.02	34.6	415	212.8
0.340	0.765	0.340	1.02	0.376	0.00305	-7.83	0.0000083	0.893	-0.002	2.330	5.82	-0.04	34.6	410	210.0
0.343	0.767	0.343	1.02	0.379	0.00333	-7.76	0.0000085	0.905	-0.005	2.324	5.81	-0.08	34.5	405	207.2
0.345	0.768	0.345	1.02	0.381	0.00362	-7.69	0.0000087	0.920	-0.008	2.317	5.79	-0.12	34.4	400	204.4
0.350	0.771	0.350	1.02	0.386	0.00431	-7.55	0.0000092	0.958	-0.022	2.295	5.74	-0.32	34.0	390	198.9
0.355	0.773	0.355	1.02	0.391	0.00512	-7.42	0.0000097	1.002	-0.027	2.267	5.67	-0.41	33.6	380	193.3
0.360	0.776	0.360	1.02	0.396	0.00610	-7.29	0.0000103	1.052	-0.032	2.236	5.59	-0.47	33.2	370	187.8
0.364	0.779	0.364	1.02	0.401	0.00728	-7.16	0.0000110	1.106	-0.034	2.201	5.50	-0.51	32.7	360	182.2
0.369	0.781	0.369	1.02	0.405	0.00872	-7.04	0.0000117	1.164	-0.037	2.165	5.41	-0.55	32.1	350	176.7
0.373	0.783	0.373	1.02	0.410	0.01047	-6.92	0.0000126	1.237	-0.048	2.117	5.29	-0.71	31.4	340	171.1
0.377	0.786	0.377	1.02	0.414	0.01261	-6.80	0.0000136	1.318	-0.054	2.063	5.16	-0.80	30.6	330	165.6
0.382	0.788	0.382	1.02	0.418	0.01525	-6.69	0.0000146	1.401	-0.053	2.010	5.02	-0.79	29.8	320	160.0
0.386	0.790	0.386	1.02	0.422	0.01854	-6.58	0.0000156	1.483	-0.052	1.958	4.90	-0.76	29.0	310	154.4
0.390	0.792	0.390	1.02	0.427	0.02264	-6.47	0.0000166	1.562	-0.048	1.910	4.78	-0.71	28.3	300	148.9
0.394	0.794	0.394	1.02	0.431	0.02782	-6.36	0.0000175	1.636	-0.043	1.867	4.67	-0.63	27.7	290	143.3
0.398	0.796	0.398	1.02	0.435	0.03437	-6.26	0.0000184	1.702	-0.036	1.831	4.58	-0.53	27.2	280	137.8
0.402	0.798	0.402	1.02	0.438	0.04272	-6.16	0.0000192	1.759	-0.028	1.804	4.51	-0.41	26.8	270	132.2
0.405	0.800	0.405	1.02	0.442	0.05345	-6.06	0.0000199	1.804	-0.018	1.786	4.46	-0.27	26.5	260	126.7
0.409	0.802	0.409	1.02	0.446	0.06728	-5.97	0.0000204	1.835	-0.007	1.778	4.45	-0.11	26.4	250	121.1
0.413	0.804	0.413	1.02	0.450	0.08523	-5.87	0.0000207	1.850	0.004	1.782	4.46	0.06	26.4	240	115.6
0.417	0.805	0.417	1.02	0.453	0.10861	-5.78	0.0000208	1.848	0.017	1.799	4.50	0.25	26.7	230	110.0
0.420	0.807	0.420	1.02	0.457	0.13921	-5.70	0.0000208	1.828	0.029	1.829	4.57	0.44	27.1	220	104.4

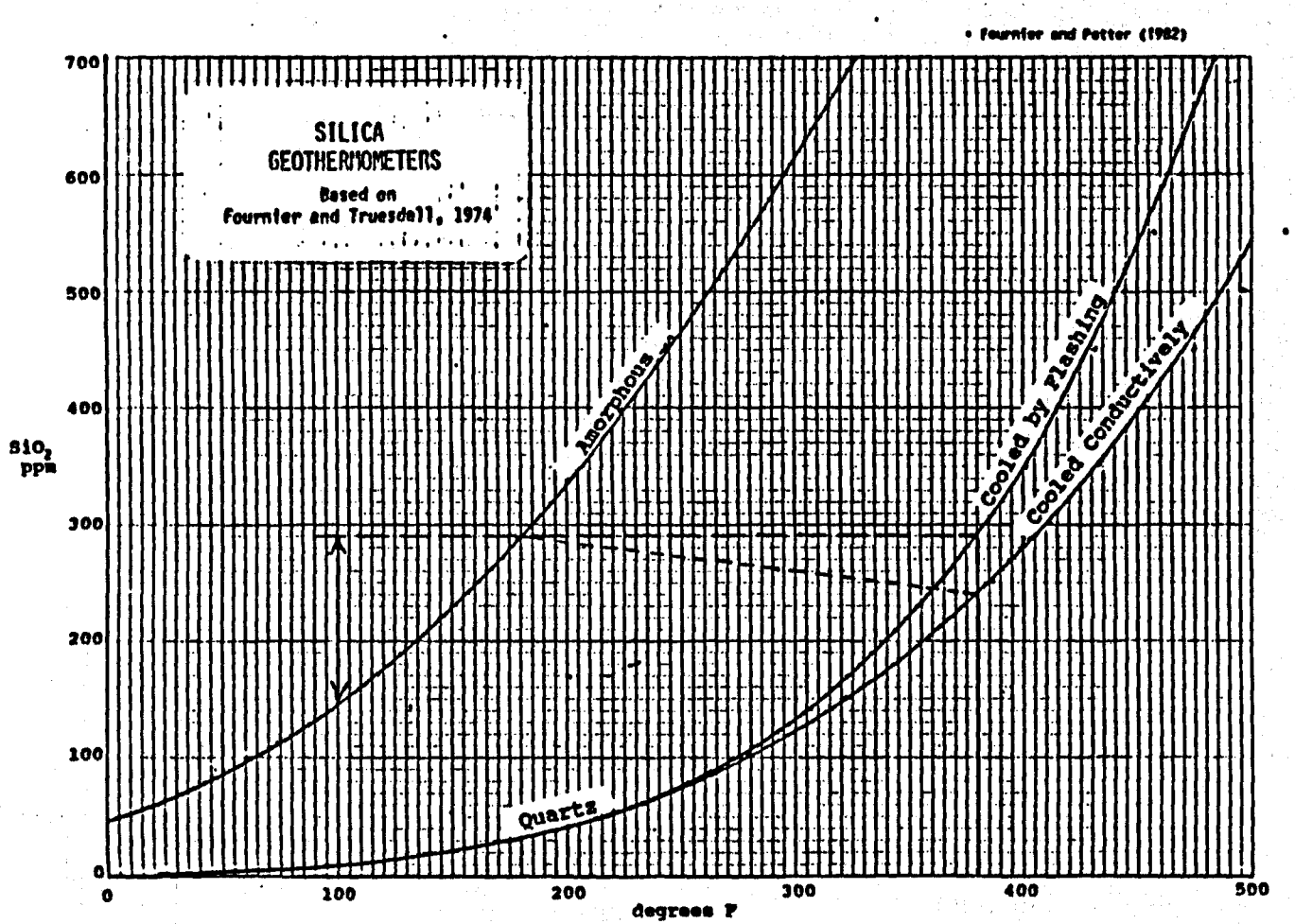
• Fournier and Potter (1982)
SILICA
GEOTHERMOMETERS
Based on
Fournier and Truesdell, 1974
Amorphous
Cooled by flashing
Cooled Conductively
Quartz
SiO2 ppm
degrees F
0
100
200
300
400
500
600
700

Weres, et al, 1980

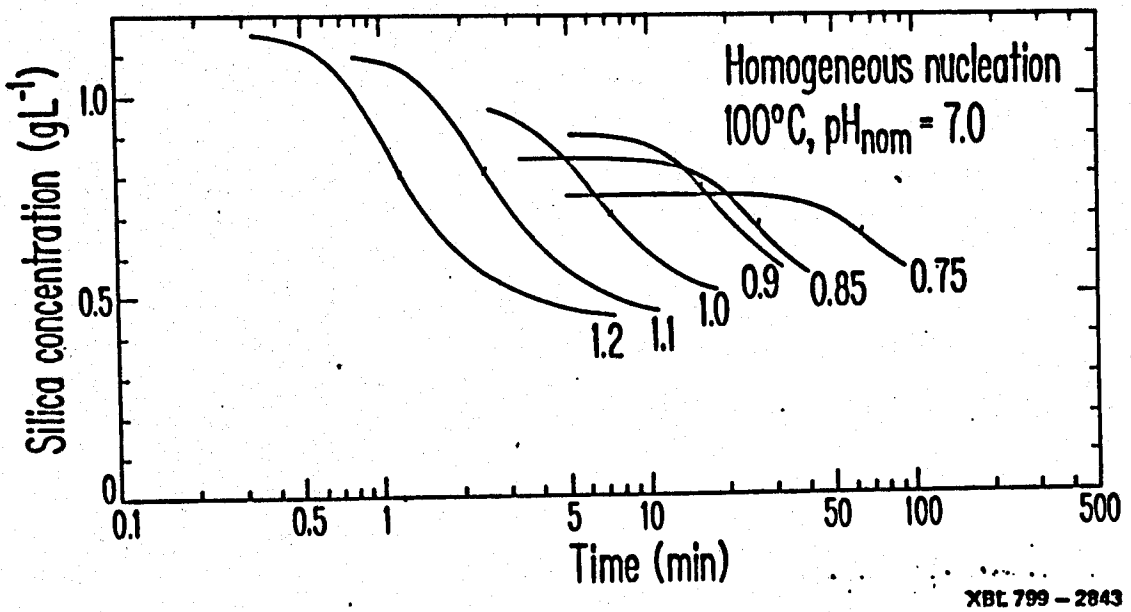

XBL 799 – 2843

CASE HISTORY OF THE BULALO FIELD IN THE PHILIPPINES

OUTLINE

INTRODUCTION

1. Location

   south-central Luzon, 70 km south of Manila

2. Prospect Basis

   chloride hot springs along Laguna de Bay

   local steaming ground and acid sulfate springs

3. Geologic Setting

   SE flank of andesitic stratovolcano (Mt. Makiling)

   associated with 0.5Ma dacite dome (Mt. Bulalo)

   reservoir rocks propylitic tuffs and andesite lavas

4. Conceptual Model

   2 (or 3) upflows neutral chloride brine

   rise into two-phase zone with local steam cap

   spread laterally in tuffaceous aquifers

   outflow west and north

   reservoir margin sealed along south and east

   no reservoir floor found in production area

5. Development History

   Bulalo #1 discovery well, drilled late 1974

exploratory drilling continued through 1976

followed by development drilling into 1983

Units 1 & 2 (110 MWe) startup late 1979

Units 3 & 4 mid 1980, Units 5 & 6 mid 1984

6. Present Project

55 production wells

8 hot brine injection wells

3 cold brine injection wells

6 satellite stations for steam separation

test separators at each station for enthalpy/sampling

RESERVOIR CHANGES

1. Pressure

initially liquid dominated, saturated above 3,500'ss

now two-phase above 2500'ss

maximum 400 psi drop at 2500'ss - mid 1987

rate of pressure decline slowed after 1984

2. Enthalpy

average steam fraction increased from 25% to 55%

Most wells intermediate enthalpy - few single phase

significant enthalpy swings in many wells

3. Flowrate

common increased steam rate with increased enthalpy

current fieldwide steam decline 4%/yr

no makeup drilling 1983-1988

augmented steam supply with acid stimulations

4. Injectivity

injection deep at field margins

moved progressively outward to prevent breakthru damage

well injectivity usually improves with time

problems with corrosion in cold water system

FLUID GEOCHEMISTRY CHANGES

1. Initial Conditions

highest TDS and NCG in southeast upflow

enthalpy-chloride relationships

boiling & dilution / multiple sources

2. Typical Well Behavior

cyclic enthalpy without boiling effects

supersaturated silica with respect to quartz

3. Dilution

influx from edges - return of outflow

dilution slugs in shallow wells - tritium

GEOPHYSICAL CHANGES

1. Subsidence

field area levelled to 2nd order biannually

maximum 20 cm subsidence 1979 - 1987

2. Gravity

field area surveyed with L&R D-meter annually

maximum 300 microgals (0.3 mgal) 1980 - 1988

pattern like subsidence except open to north

reservoir simulator match is good

excess mass in center of field (BM66)

mass deficiency at Mt. Bulalo (BM39) & Tigsa River

significant rainfall effect in observations

3. Microearthquake Activity

5-10 local events per week, occasional swarms

4. Thermal Areas

monitoring has detected no changes

Proc. 10th New Zealand Geothermal Workshop 1988

DEVELOPMENT AND PERFORMANCE OF THE BULALO GEOTHERMAL FIELD

Pio J. Benavidez[1] Mark D. Mosby[2] John K. Leong[2] Ver C. Navarro[1]

(1) National Power Corporation

(2) Phil. Geothermal, Inc. (UNOCAL)

ABSTRACT

The Bulalo Geothermal Field has generated electricity from geothermal steam since 1979. The wells produce two phase fluid from a 260-316 deg C benign, low gas, liquid dominated reservoir which is made up of fractured and intensely altered interlayered volcanics. Separated steam from six satellite stations, flows to NPC's six 55 MW power plants while the residual brine is reinjected back into the reservoir on the periphery of the production area. Through 1988, the reservoir's performance has been excellent. The maximum field-wide steam supply decline rate observed thus far is approximately four percent per year. The power plants, through mid-year 1988, have generated a cumulative total of 15,375 GWh of electricity. The plants are now generating 14 percent of NPC's Luzon grid energy and are currently the top performing plants in the Philippines.

INTRODUCTION

The Bulalo Geothermal Field (hereafter called Bulalo) is located approximately 70 km south of Manila and has been commercially operating since April 1979. Bulalo is one of two geothermal projects developed by the National Power Corporation (NPC) of the Philippine Government and Philippine Geothermal, Inc. (PGI), a wholly owned subsidiary of Union Oil Company of California. After the 1973 signing of a service contract that includes the Bulalo area, exploration work began. The first production test, Bul-1 was drilled in late 1974 and completed as a discovery to 5722' (1744 m) T.D. In a 1975 flow test, the well produced a total mass rate of 467 kph (thousand lbs per hour) (211.8 T/h). Since then, 72 wells have been drilled and completed. These wells provide the steam and reinjection capacity required to operate NPC's six 55 MW Mitsubishi direct contact condensing turbine generators.

This paper briefly summarizes Bulalo's development, reservoir and generation performance through mid-year 1988. Extensive technical work has been carried out by both NPC and PGI on Bulalo. The results of selected studies will be presented in this paper.

GEOLOGICAL SETTING

Bulalo is located on the southeast flank of Mt. Makiling, an 800 m high extinct and partially eroded andesitic stratovolcano (Figure 1). The field is directly associated with the Mt. Bulalo dacite dome after which it is named. This parasitic dome was formed 500,000 years ago on the southeast flank of Mt. Makiling. Bulalo's main production area as delineated by development and exploratory drilling is approximately 7 to 8 square kilometers.

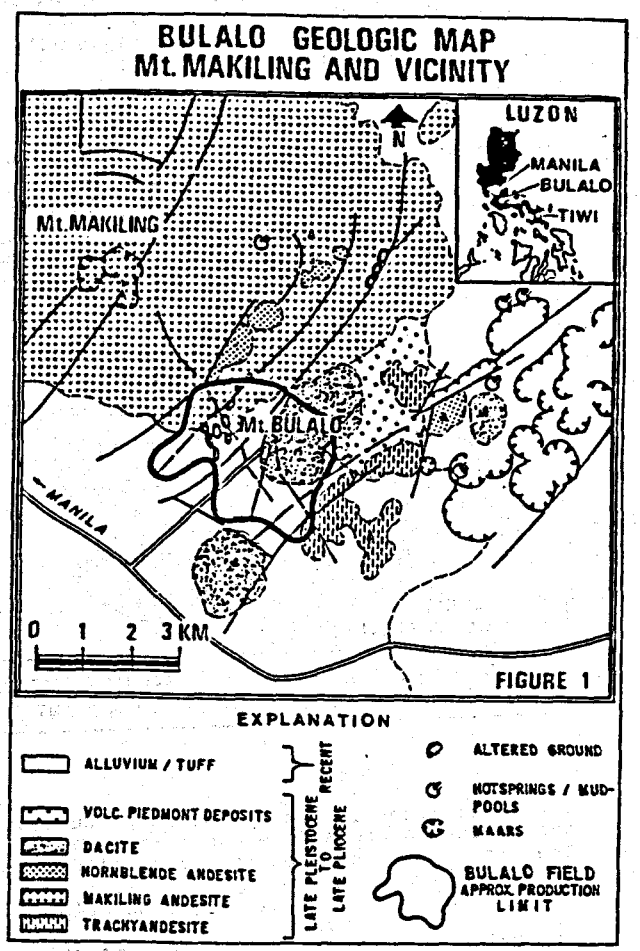

Several southwest-northeast trending regional and Makiling ring faults cross the field. These are normal faults downthrown towards Mt. Makiling. These faults have been intersected by northwest-southeast trending normal faults downthrown toward the south. Surface areas of acid sulfate steaming ground are located along the traces and at intersections of these fault systems. These thermal features reflect the venting of steam and gases from a two phase zone that overlies Bulalo's deep reservoir brine. The first well, Bul-1, was drilled within a low resistivity anomaly that is associated with these thermal features.

DEVELOPMENT

Bulalo's geothermal development continued over a span of 14 years. In late 1974 exploratory drilling started and continued through 1976. After the initial drilling results were evaluated, development drilling commenced and continued until 1983.

The first two 55 MW power plants Units 1 & 2 (Plant A) were completed in late 1979, followed by Units 3 & 4 (Plant B) in 1980. After extensive testing and analysis of production withdrawal associated with Units 1-4 operations, PGI notified NPC that Bulalo's reservoir could support another two 55 MW power plants. As a result, Units 5 & 6 (Plant C) were constructed and generation started in late 1984.

With each development phase the steam gathering and waste brine injection facilities were modified to accomodate increased reservoir mass withdrawal and power plant steam line piping flexibility. These modifications included facility changes to improve well testing capability, steam quality, waste brine injection capability and production-generation efficiency.

Figure 2: BULALO FIELD

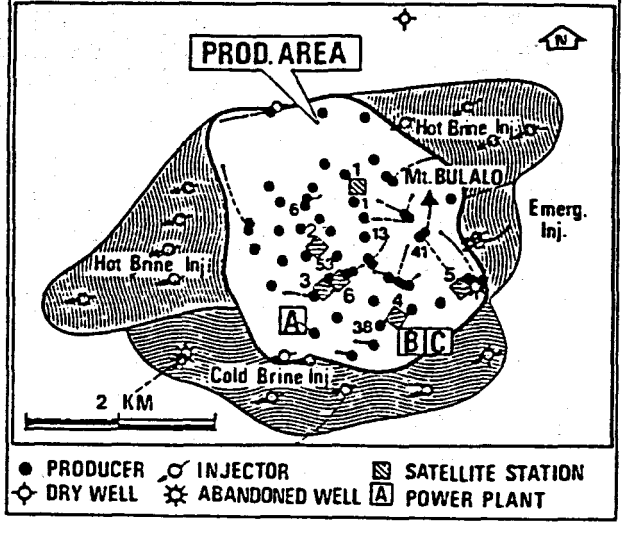

The generalized layout of Bulalo production and injection areas is shown in Figure 2. The field is subdivided into the following:

Prod. Area - Includes all production wells
Hot Brine Inj. - Separated brine injection area 175 deg C, single flash
Cold Brine Inj.- NPC blowdown, brine flashed to atmosphere
Emergency Inj. - Emergency injection wells

The producing area includes 55 production wells. The average steam and total mass flowrates of these wells are approximately 125 kph (56.7 T/h) and 220 kph (99.8 T/h) respectively. The hot brine injection area includes eight wells that can take up to 6000 kph (2721.6 T/h) while the cold brine area includes three active injection wells for the NPC coldwell blowdown and PGI's sump water. These cold brine injection wells handle approximately 1000 kph (453.6 T/h) of brine.

Three additional wells located within the production area are available for reinjection during injection wellbore or pipeline system problems. These wells are either non commercial or marginal producing wells. They provide the field with injection system redundancy and flexibility.

Figure 3 : STEAM PIPING SCHEMATIC

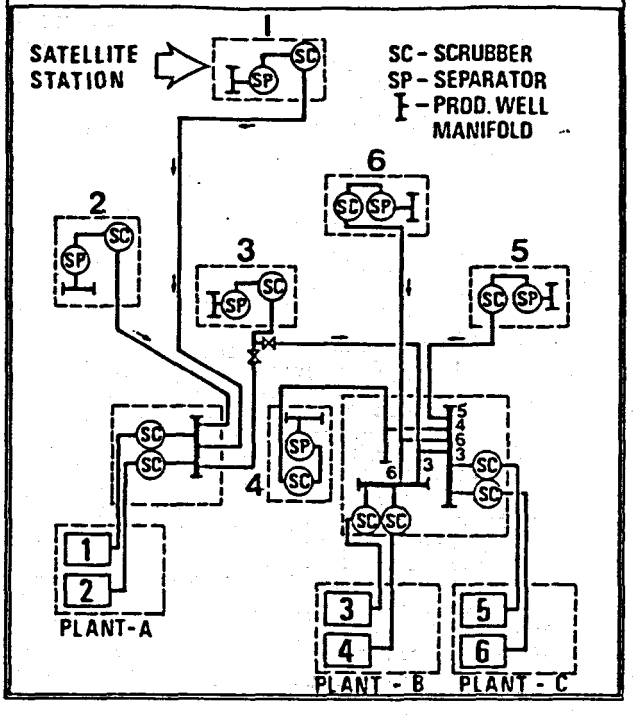

Steam Gathering System

Bulalo's steam gathering system is a satellite station type. There are six satellite stations at strategic locations within the field's production area. Each station consists of a primary separator, scrubber and a pumping station (Figure 3). Six to eight wells per satellite station, at an average flowing WHP of 180 psig (12.7 kg/sq.cm) produce fluids into the production well manifold which feeds into the main separator (Figure 3).

The production area has different characteristics of enthalpy, brine and steam fraction, non-condensible gas (NCG) and brine concentration depending on the well location. The southeast quarter (near satellite station no. 5) is characterized by higher Cl-SiO_2 and NCG concentrations. This is attributed to close proximity to the reservoir upflow zone. Table 1 shows these characteristics for six typical wells from the satellite stations.

SAT. STATION	1	2	3	4	5	6
PLANT	A	A	B	C	C	B
WELL NO.	1	6	53	38	41	13
Month/Yr.	04/87	04/87	08/87	03/87	07/87	03-87
WHP (PSI)	251	215	200	188	241	200
SEP (PSI)	183	150	145	152	162	160
STEAM (%)	64.6	28.8	47.1	81.7	51.4	88.3
ENTH. (BTU/LB)	900	586	741	1040	783	1097
TMP (DEG)	387.7	558.7	327.2	221.8	434.2	273.5
NA	1606	1554	1238	2085	2010	1581
K	305	267	326	509	508	281
CA	26	34	16	28	28	26
MG	0.12	0.09	0.06	0.09	0.24	0.02
CL	2808	2648	2112	3739	3498	2657
HCO_3	19	32	19	26	26	13
SO_4	14	13	13	16	13	18
B	69	41	41	118	105	88
SiO_2	486	551	593	643	650	546
STM NCG Wt %	0.18	0.23	0.34	1.37	1.54	0.29
CO_2 mole %		92.04	92.06	95.81	94.02	81.84
H_2 mole %		1.88	0.95	0.57	0.24	2.57
CH_4 mole %		0.10	1.08	0.09	0.06	0.12
N_2 mole %		1.90	0.98	0.60	0.51	5.47
NH_3 ppm		0.7	0.90	0.6	1.10	0.5
H_2S ppm		170.0	160.0	200.0	270.0	350.0

Table 1. Bulalo Field 1987 geochemical and enthalpy data for selected satellite station sector wells. The analysis is corrected for steam flash. For the well location, see Figure 2

The throughput of each satellite station is approximately 1100 kph (498.9 T/h) of steam which meets the requirements of one 55 MW unit. The field-wide design specific steam consumption rates for the NPC power plants vary between 18,050 and 19,050 LB/MW (8.19-8.64 T/h) depending on whether the steam ejectors or gas compressors are operating. Steam flows from the satellite at 135 psig (9.5 kg/sq.cm) and through 36 inch steam lines into secondary scrubbers at approximately 105 psig (7.4 kg/sq.cm) prior to entering the turbine. These scrubbers remove both condensate and any residual brine carry-over from the satellite station. The steam enters the turbine at an inlet pressure of 80 psig (5.6 kg/sq.cm) and with chloride and silica concentrations less than 1 ppm. At maximum loading steam gathering system pressure drop from the wells to the turbine inlet is approximately 100 psig (7.0 kg/sq.cm).

After attaining operating experience with Bulalo's steam gathering system some modifications were introduced. These focused on improving the steam gathering system capability for testing wells and reducing the amount of atmospheric stacked steam. These modifications have improved Bulalo's overall resource management plan.

From 1974 through 1985, welltesting was frequently completed with skid mounted test separators. This work was cumbersome and required steam to be vented to the atmosphere during the test. In 1985 permanent test separators were installed in all the satellite stations. With this arrangement, the wells are tested at pressures higher than the system pressure while producing to the power plants. Well testing is important to characterize the reservoir conditions and to update steam supply forecasts. Two to three tests per well for three day periods are completed every year.

Atmospheric steam venting due to power plant upset conditions and excess hydropower curtailments was a problem until 1987. Wellsite two phase throttling valves have been installed which have helped reduce atmospheric stacked steam. The current system is designed to throttle wells to save steam, equivalent to an 80 MW curtailment. Planned improvements will expand and automate the two phase throttling system. By mid-year 1989, the system will provide curtailment of steam production equivalent to 140 MW.

Brine Injection Systems

Two brine injection systems have been installed in Bulalo: 1) Hot brine and 2) Cold brine. These two systems are mandatory because Bulalo is a landlocked geothermal system.

The hot brine system provides for reinjecting separated reservoir brine. From the satellite stations 175 deg C brine is pumped by 400-440 HP motor and steam driven pumps to injection wells through an interconnected network of 18 inch pipelines. The normal operating pressure for the system is 300 psig (21.1 kg/sq.cm), with a tripping discharge pressure of 365 psig (25.6 kg/sq.cm). The combined injection capacity of the eight injection wells at normal pressures is about 6000 kph (2721.6 T/h). Problems with this system have been minimal and include scaling in strainers, pumps and pipelines.

A second injection system operates in order to reinject excess NPC blowdown and PGI sump water. This system has many problems that are related to corrosion associated with the cooling tower blowdown. The blowdown is characterized by either low pH and/or high concentrations of disssolved oxygen. Pump casings, pipelines and wellbore failures have occurred due to the corrosive blowdown. Two wellbore failures which required well abandonment have occurred due to corroded casing. Future plans are to reinject excess blowdown directly from the NPC hotwell pump condenser discharge line for Units 1-4. This will greatly reduce the level of dissolved oxygen, and has already been completed for Units 5 & 6.

RESERVOIR

Physical Description

Extensive production testing, reservoir and geoscientific studies have been completed to evaluate and develop a conceptual model of Bulalo's reservoir. The results indicate that the reservoir is driven by a strong thermal upflow that rises beneath the south western edge of Mt. Bulalo from depths greater than 3,000 meters subsea to as shallow as sea level (Figure 4).

CROSS-SECTION
BULALO 75-BULALO 19

Figure 4

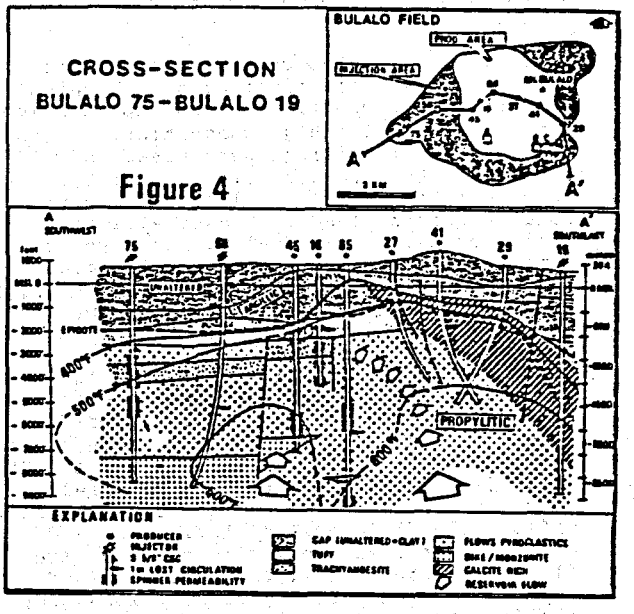

The upflow migrates through intensely altered fractured andesitic flows, tuffs and volcaniclastics along multiple near vertical permeable fault zones. The rising geothermal fluids encounter lower pressures, boil and form a two phase zone above the reservoir brine.

The more porous and permeable formations adjacent to the upflow planes such as tuffs and volcaniclastics become charged with the ascending geothermal fluids. These formations are primary reservoir aquifers which are characterized by intense propylitic alteration, lost circulation during drilling and production influx zones during well flowing. The geothermal fluids flow laterally through these aquifers to the west and north. Flow to the east and south appears to be limited based on observed low well productivity and which may be related to abundant secondary mineralization (calcite). The thick calcite rich zone is related to the boiling of reservoir fluids as they ascend. This zone appears to be a lateral permeability boundary in the southeast part of the field.

The reservoir volume is very large, it expands in size and increases in temperature with depth. Approximately 70 percent of the reservoir volume exists below 1500 meters subsea. The cores and drillcuttings analyzed below this depth are all intensely altered with the reservoir propylytic mineralogical assemblage. Below this depth there are no significant mineralogical or temperature gradient reversals and approximately 60 percent of the estimated reservoir volume is at temperatures exceeding 288 deg C. The cores from this part of the reservoir have mean porosities of 11.4 percent.

Geochemistry

Table 1 gives the geochemical composition of separate brine (corrected for flash) and NCG for characteristic wells of Satellite Stations 1 to 6 . The data shows that Bulalo's reservoir fluids are a neutral chloride brine with low salinities and low gas content. In order to characterize and compare fluid geochemistry with reservoir processes, the following classification of the fluids based on chloride enthalpy and chloride-boron relationships is utilized. This geochemical discussion is based on a pre-exploitation model.

Wells located in the central upflow zone such as Bul-41, are distinguished by high concentrations of chloride and NCG and high temperatures. The high concentrations result from reservoir boiling where steam and NCG is released. The NCG accumulates near the reservoir top and the well produces high concentrations of NCG. These wells are called transient flow wells. Some wells completed above this zone typically produce from steam caps and contain moderate to high NCG, high boron, low chloride and lower temperatures.

The lowest NCG wells are located in the western part of the field. These wells are distinguished by their moderate chloride concentrations, low geochemical temperatures, low NCG and high chloride/boron ratios. The boron fluids are thought to be modified brine which originated in the upflow zone. During upflow, the fluid boiled, losing NCG and boron to the steam, becoming cooler. The fluids are stored in lithologic aquifers which act as the primary outflow zones for fluids from the upflow regions.

The edge wells are further classified into two categories. Those along the western margin of the field have low NCG contents which indicate mixing of dilute ground waters with the brine stored in the reservoir acquifers. Those along the northern and southern margins of the field have moderately high gas concentrations which may indicate mixing of dilute ground waters with the upflowing thermal brine.

Exploitation Effects

Initially the Bulalo reservoir was a liquid dominated system with a two phase zone present at depths above 600 meters subsea. Exploitation reduced the pressure which has caused the steam-brine interface to drop from 600 m to 1070-1220 m subsea. Both vapor and reservoir brine pressure decline rates were high up to 1984. After late 1984, the vapor pressure has stabilized and the brine pressure decline rate has slowed down.

The stabilized vapor pressure supports the presence of near vertical fractures which act as conduits for recharging vapor zones from deeper boiling fluids. The slowing down of the brine pressure decline rate appears to be related to deep reservoir influx of either natural recharge or injection fluids. Thermal breakthrough of the injection fluids has been minimal.

Figure 5 : BULALO 79-88 PRODUCTION

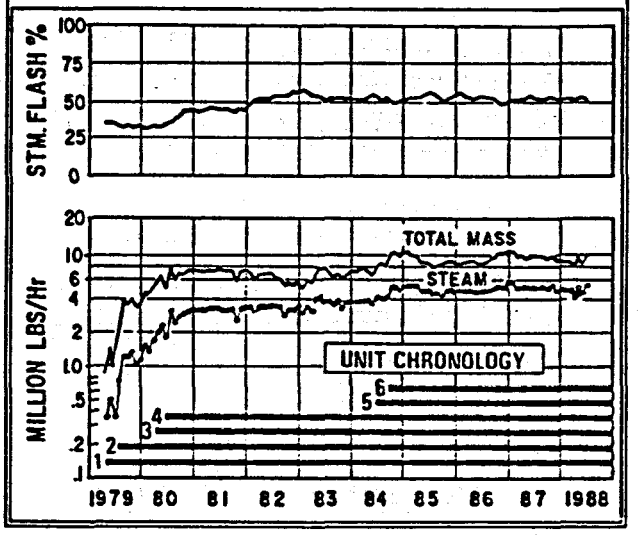

Figure 5 shows Unit chronologies steam quality, and monthly flow rates for steam and mass during the development period up to August 1988. Presently the yearly average withdrawal from the reservoir is approximately 5000 kph (2268.0 T/h) of steam and 4000 kph (1814.4 T/h) of brine. All the brine has been reinjected back into the reservoir. The average steam quality has risen from below 25 percent to approximately 55 percent. Some of the wells are still drying up and these exhibit little or no total mass decline rate An example is Bul-3A as shown in Figure 6.

Figure 6 : WELL BUL 3A PRODUCTION

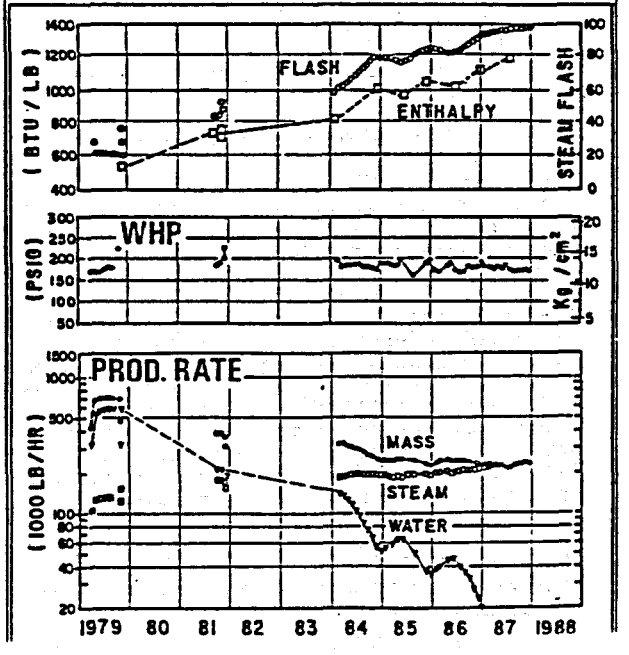

Currently the largest well in the field is Bul-1, the 1974 discovery well. This well is now producing 250 kph (113.4 T/h) of steam as compared to it's 1975 steam flowrate of 150 kph (68.0 T/h). This improvement is partly due to a 30 percent increase in enthalpy.

Since 1983, make-up steam supply optimization has been ongoing. The last production well, Bul-66 was drilled 5-1/2 years ago. Additional steam supply has been obtained by converting idle injectors into producers, reducing pipeline pressure losses, and acidizing wells. Figure 7 shows the results of acidizing six producers with hydrochloric and hydrofluoric acids. Through 1988 all these efforts combined with the reservoir's high porosity and excellent vertical communication have resulted in a low total field steam decline rate of approximately four percent per year.

Figure 7 : BULALO STIMULATION

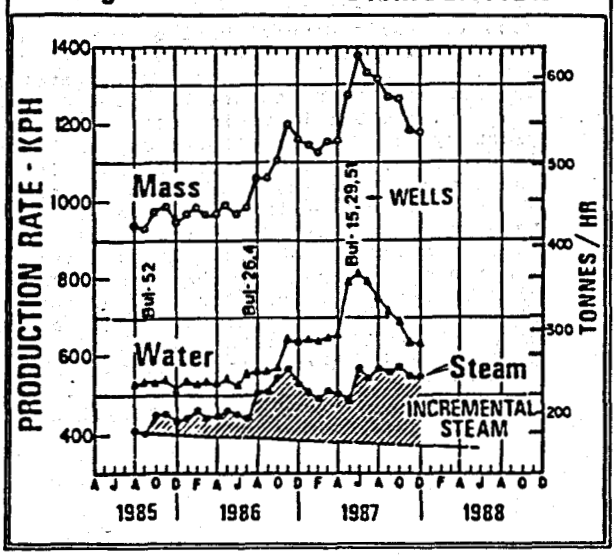

GENERATION PERFORMANCE

Generation

For the past nine years, Mak-Ban has been one the best performing power plant cycles in the Philippines. Figure 8 shows yearly generation bar graphs from 1979 to 1988.

Figure 8 : 1979-1988
GENERATION PERFORMANCE

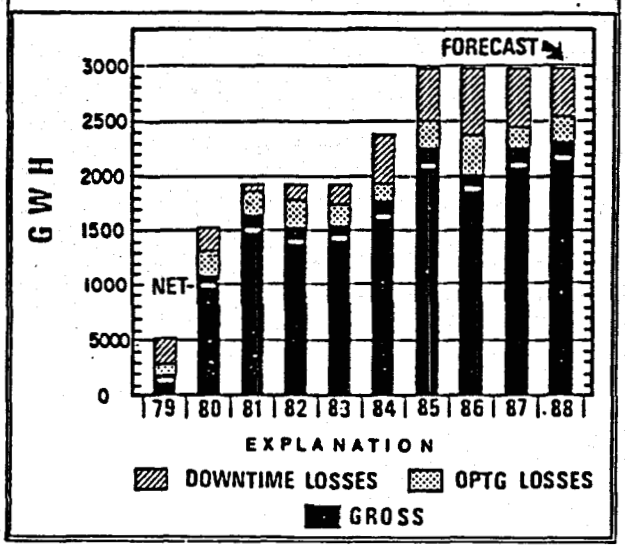

The field's generation output has increased every year with the exception of 1982, 83 and 86. This increasing trend will hold true in 1988, assuming there are no major forced outage incidents during the remaining part of the year. Table 2 shows the generation performance indicators for the last three years up to August 1988. The theoretical output load from the power plants minus annual scheduled maintenance and overhaul downtime is 290.2 MW. The past three year

PERFORMANCE INDICATORS	1985	1986	1987	1988 AUG.	AVERAGE
FACTORS (%, MW)					
Avail.	86.7	81.8	84.4	85.7	84.7
Capacity	77.7	69.8	77.7	77.1	75.6
Pd. Ld. Ave.	256.6	230.4	254.1	254.1	249.4
EQUIV. LOAD (MW)					
Optg. Losses	29.6	39.8	22.1	28.4	30.0
Excess DT	4.0	20.1	11.6	7.4	10.8
TOTAL (MW)	33.6	59.9	33.7	35.8	40.8
THEORETICAL (%)	11.6	20.6	11.6	12.3	14.1

Table 2. Mak-Ban 1985 thru 1988 August generation performance indicators. By meeting the downtime schedule of 6336 hours per year, (Per Unit: 1-35 day/overhaul and 3-3 day quarterly maintenance shutdowns) the maximum availability and capacity factors are both 87.9% or 290.2 MW ("0" operating or excess downtime losses). The total under equivalent load is the potential gain per year in load if both operating and excess downtime losses are eliminated. Pd - Period.

average of 249.4 MW is 86 percent of this theoretical amount. The 14 percent deficiency is attributed to both extended overhaul/maintenance periods and operating generation losses. NPC is addressing this deficiency and is implementing programs to reduce the losses. One successful program has been turbine steam scrubbing. Unit 6 has had steep load declines due to turbine scale build-up, on the first stage nozzles since initial startup (Figure 9). A successful steam scrubbing experiment has been ongoing since February 1988, reducing turbine scale-induced generation losses by approximately 15,000 MWh. This has reduced the unit's average load decline from 1.3 MW/month to 0.3 MW/month (Figure 9). NPC and PGI are currently designing a permanent steam scrubbing system for Units 3, 4, 5 & 6. Once operational, the steam scrubbing program is expected to increase the annual generation levels by 120 to 140 GWh.

Figure 9 : LOAD DECLINE

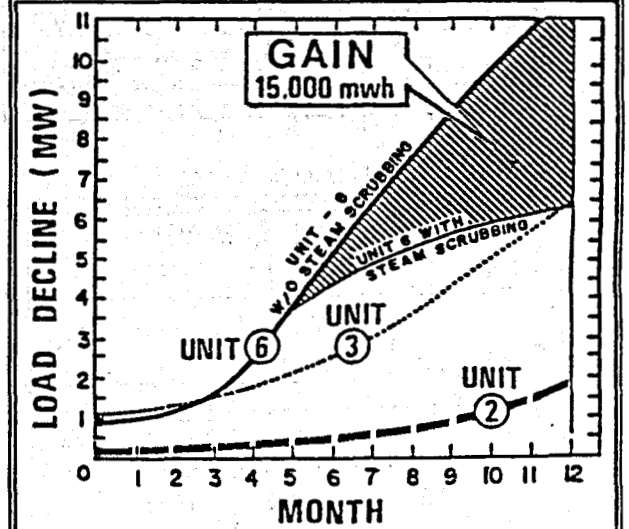

In order to maximize unit availability, NPC plans are underway to eliminate excess downtime losses. These improvements are needed in order to optimize the performance of Bulalo's reservoir capacity. At this time, Bulalo's available reservoir steam is 10 to 20 percent higher than the operating capacity of the power plants.

Specific Steam Consumption

Bulalo's overall production generation efficiency is indicated by the specific steam consumption ratio. This ratio represents the following:

CONSUMER STEAM (lb)		STACKED STEAM (lb)	
NPC - Turbine NPC - Steam Ejector NPC - Gland Seal Ejector PGI - Turbine Pumps PGI - Scrubber Drains	+	LDO NPC Upset NPC Maintenance PGI Upset Cont. Venting	= lb/MW

Metered Gross Generation (MW)

This ratio together with monthly generation numbers are shown in Figure 10. The ratio is plotted against the field design rate of 18,050 lb/MW (8.19 T/MW) (using gas compressors - G.C.). This design rate includes all steam consumers listed above. There are some high ratios in 1985 and 1986 that are attributed to LDO (excess hydro power), Peoples Power and Luzon grid contingency plans. In all cases, excess stacked steam occurred as a result of load curtailments. The years 1987 and 1988 have been the best years for production generation efficiency. In 1988, the field average specific steam consumption ratio through August is 19,850 lb/MW (9.00 T/MW). With the planned expansion and automation of the two phase throttling system, it is expected that this number will become lower in the future.

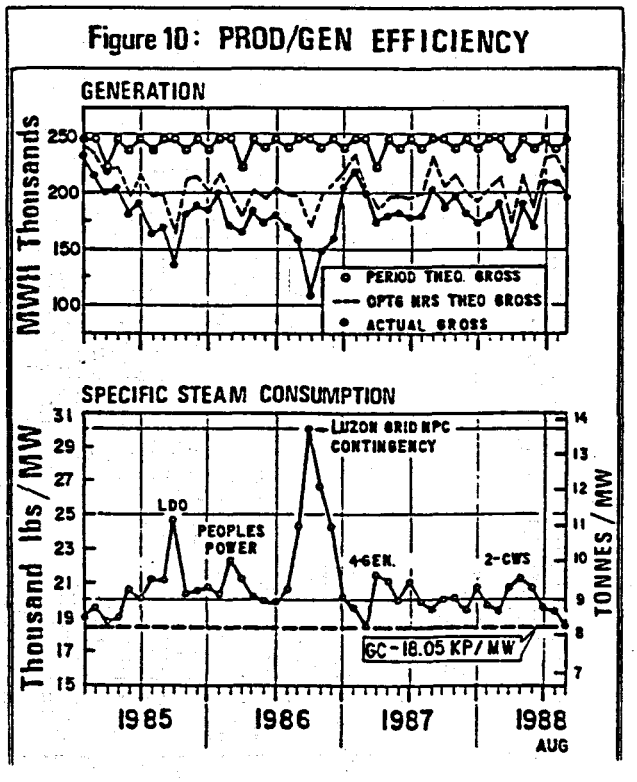

Figure 10: PROD/GEN EFFICIENCY

CONCLUSIONS

The Bulalo geothermal power plant cycle is reliable due to the presence of a very large and efficient reservoir, dependable steam gathering and waste brine injection systems and well-designed power plants. For the last eight years, Bulalo has been the top performing power plant cycle in the Philippines. NPC and PGI are introducing additional design improvements that will improve Bulalo's performance. NPC and PGI are currently studying the feasibility of adding more capacity to the field in the form of several small units.

ACKNOWLEDGEMENTS

The authors gratefully acknowledge NPC's President E. M. Aboitiz, Operations Sr. Vice President A. C. Plata, UNOCAL's Vice President of Foreign Operations Chester F. Budd and PGI's General Manager Tony Chasteen for granting permission to publish this paper. We are also particularly grateful to the NPC and PGI personnel that operate and maintain the Bulalo field geothermal power plant cycle. Their efforts are instrumental in maintaining the high performance levels of the cycle. The reservoir and steam gathering system sections of this paper are based on technical unpublished contributions of PGI engineers and scientists. In particular, mention must be made of the high quality work of Mike Barnes, Calvin Strobel, Wilson Clemente, Paul Atkinson, Dave Rohrs and Doug Cope. Their work together with the work of many other geothermal professionals has contributed significantly to the successful operations of the Bulalo geothermal field.

USING PRECISION GRAVITY DATA IN GEOTHERMAL RESERVOIR ENGINEERING MODELING STUDIES

Paul G. Atkinson and Jens R. Pedersen

Unocal Geothermal Division
3576 Unocal Place
Santa Rosa, CA 95401

ABSTRACT

Precision gravity measurements taken at various times over a geothermal field can be used to derive information about influx into the reservoir. Output from a reservoir simulation program can be used to compute surface gravity fields and time histories. Comparison of such computed results with field-measured gravity data can add confidence to simulation models, and provide insight into reservoir processes. Such a comparison is made for the Bulalo field in the Philippines.

INTRODUCTION

Reservoir engineering calculations of mass and energy balances on producing geothermal reservoirs require information about in- and out-flows from the reservoir. Such information is usually available for surface flows: production and injection rates can be measured; and natural discharge rates can be estimated. Values for subsurface in- or out-flows are much more elusive. One method commonly used to estimate aquifer influx is via a history matching process whereby reservoir performance is computed for various strengths of influx, and then matched against observed performance (Gudmundsson, and Olsen, 1985). The best match is then considered to represent an estimate of influx into the reservoir. This methodology is directly analogous to the use of influx models in material balance calculations in the oil and gas industry (Craft and Hawkins, 1959).

A more direct and independent method of estimating influx is through repeat precision gravity surveys over a producing field. When such surveys are carried out with appropriate accuracy, they allow an estimate of mass loss between surveys to be made. This estimate can then be compared with net surface withdrawals (production minus injection) to compute influx. Such calculations have been made for the Wairakei field (Hunt, 1970; Hunt, 1977; Allis and Hunt, 1986).

This paper first reviews the basic principles of repeat gravity surveys as they pertain to estimating influx into producing geothermal reservoirs. It then describes the coupling of precision gravity data with reservoir simulation models. Three examples of such a coupling are then presented: two for idealized reservoirs; and one for the Bulalo field in the Philippines.

GRAVITY: THEORY AND MEASUREMENT

Gravity relates, through fundamental elements of physics, the force exerted on a body on the surface of a planet to the mass distribution surrounding the body. The gravitational pull on the surface of the earth is not uniform, and in fact, subtle variations in gravity are commonly used to identify the presence of ore bodies or geological structures. This use of gravity measurement as a geophysical prospecting tool is described in standard references such as Dobrin (1960). The magnitude of gravity on the surface of the earth is approximately 980 gals. Exploration geophysics is usually looking at variations on the order of milligals. Precision gravity measurements discussed in this paper deal with variations on the order of 0.01 milligals, or 10 microgals; hence the term "precision".

As mass is removed from a geothermal reservoir, the gravity field above the reservoir will decrease. By measuring the surface gravity field at two points in time over a producing reservoir, the change in gravity over the reservoir during the time interval can be determined. This delta-gravity field can be used in various ways. These are:

1. To qualitatively identify 100% influx, as for example was done for Wairakei, when the delta-gravity values approached zero. (Hunt, 1977);

2. To integrate under the delta-gravity contours to obtain the net mass loss implied by the contours (Hunt, 1977); and

3. To model the areal detail of the observed delta-gravity contours with calculations derived from a reservoir simulator.

Instruments are commercially available to measure gravity with a precision of $\pm$ 1 microgal (e.g., LaCoste & Romberg, Model D gravimeters). When making comparisons of repeat measurements at a given site, known

temporal effects need to be corrected for. Three major effects requiring correction are subsidence (3 microgals/cm), earth tides (up to 230 microgals) and meter drift (assumed linear with time after removal of earth tides). Our field wide surveys in the Philippines are run using a tight network configuration (Lambert and Beaumont, 1977). Approximately 125 benchmarks are measured using 300 independent estimates of gravity differences between benchmark pairs. The survey takes about two months to complete. After corrections for known subsidence, earth tides and meter drift, the network is least-squares adjusted (Eckhardt, 1986). The resulting average error at a benchmark is ± 7 microgals. By comparison, typical reservoir effects can be expected to be about 100 microgals per 4 million megawatt-hrs of production. Other non-reservoir effects due mainly to seasonal effects of rainfall are ± 10 microgals.

Correcting for subsidence effects through high order levelling surveys is probably the single most expensive element of carrying out meaningful precision gravity surveys over a producing geothermal field. In general, both the gravity and levelling surveys need to extend far beyond the limits of the producing field.

NUMERICAL MODELLING OF GRAVITY FIELDS

We have developed a program which uses information from a three-dimensional reservoir simulator to compute surface gravity fields corresponding to any state of the simulator. The gravity calculation procedure uses the method of Nagy (1966) to compute the gravity effect at any surface point resulting from a subsurface stacked set of rectangular prisms comprising the cartesian discretization of a reservoir problem. Thus, we can compute the surface delta-gravity field between two times resulting from the change in mass distribution in the reservoir. The following presents such calculations for two idealized reservoirs and then presents both field results and calculations for the Bulalo field in the Philippines.

IDEALIZED RESERVOIR WITH NO INFLUX

Figure 1 presents gravity profiles at two different times over hypothetical Reservoir A in order to illustrate various points. The computed delta-gravity field has a well-defined maximum directly above the reservoir, and extends far past the edges of the reservoir. In principle such a field is measurable with an instrument whose precision is ± 1 microgal. As net mass loss from the reservoir increases, the volume under the delta-gravity surface can be seen to increase. Gauss' theorem states that this volume is directly proportional to the net mass loss from the reservoir (Hammer, 1945; LaFehr, 1965). Thus, integrating under the 10-year surface would result in twice the volume under the five-year curve.

IDEALIZED RESERVOIR WITH INFLUX

A series of calculations were next made for a rectangular hypothetical porous medium Reservoir B, in order to illustrate the impact of influx on surface gravity. The reservoir has dimensions 9000 ft x 9000 ft x 5000 ft deep, and top at a plane at 1500 ft subsea. It is initially filled with liquid at boiling-point-with-depth conditions, has 12% porosity, and 100 md permeability. Steam for 200 MW is produced from the upper part of one quadrant. 100% of the associated brine

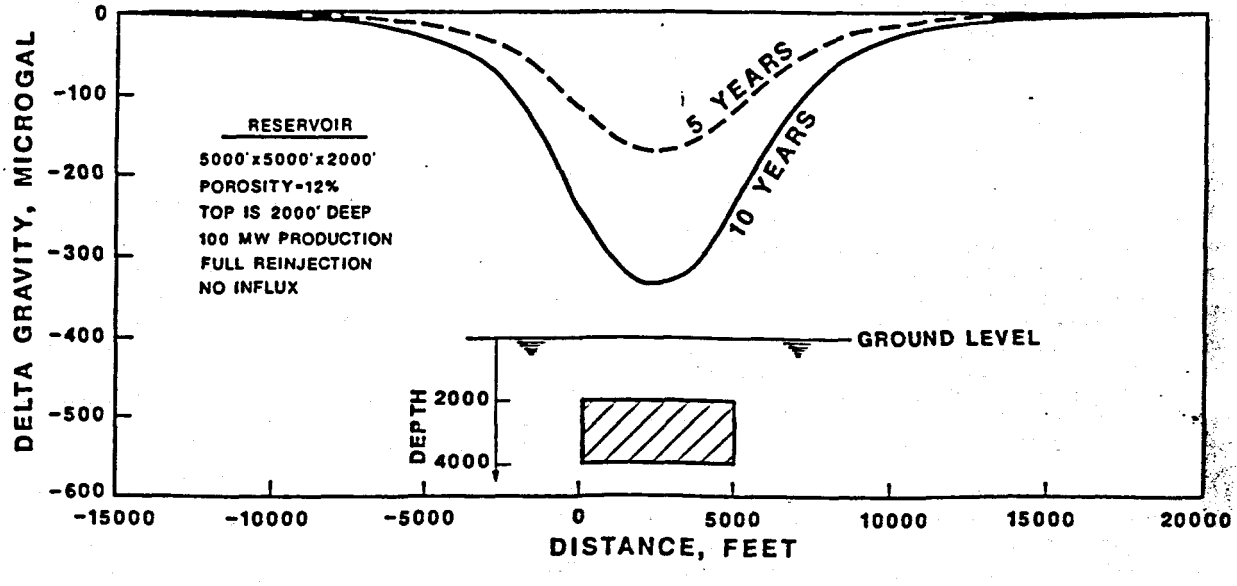

Figure 1. Delta gravity profiles over center of idealized Reservoir A

and 20% of the steam are injected as liquid into an adjacent quadrant. Case 1 was run with no influx, and Case 2 with deep hot influx along the bottom edge of the two remaining quadrants. Figure 2 illustrates this system. Both cases develop an extensive two-phase zone around the producing wells.

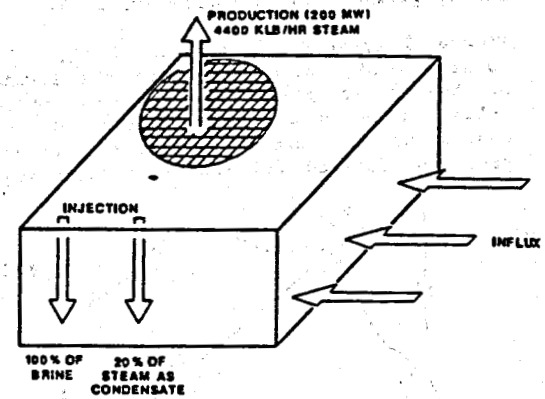

Figure 2. Schematic of idealized Reservoir B

Figure 3 illustrates the time history of gravity and various computed reservoir parameters during the ten-year period. Net mass depletion falls linearly with time for no influx. Influx has little effect on system performance until after three years of production, at which time its effects become important. The computed gravity response over the reservoir can be seen to mimic the net mass depletion curve. The details of the gravity response shown are certainly detectable with a well planned gravity survey program.

Figure 3 depicts the impact of influx on gravity as well as more traditional reservoir engineering measures for the specific configuration of Reservoir B. The effects of reservoir physics on surface gravity are subtle, and other configurations may act differently.

PRECISION GRAVITY AT BULALO

The Bulalo Geothermal Field is located in the Philippines approximately 30 miles south of Manila. The field is operated by Philippine

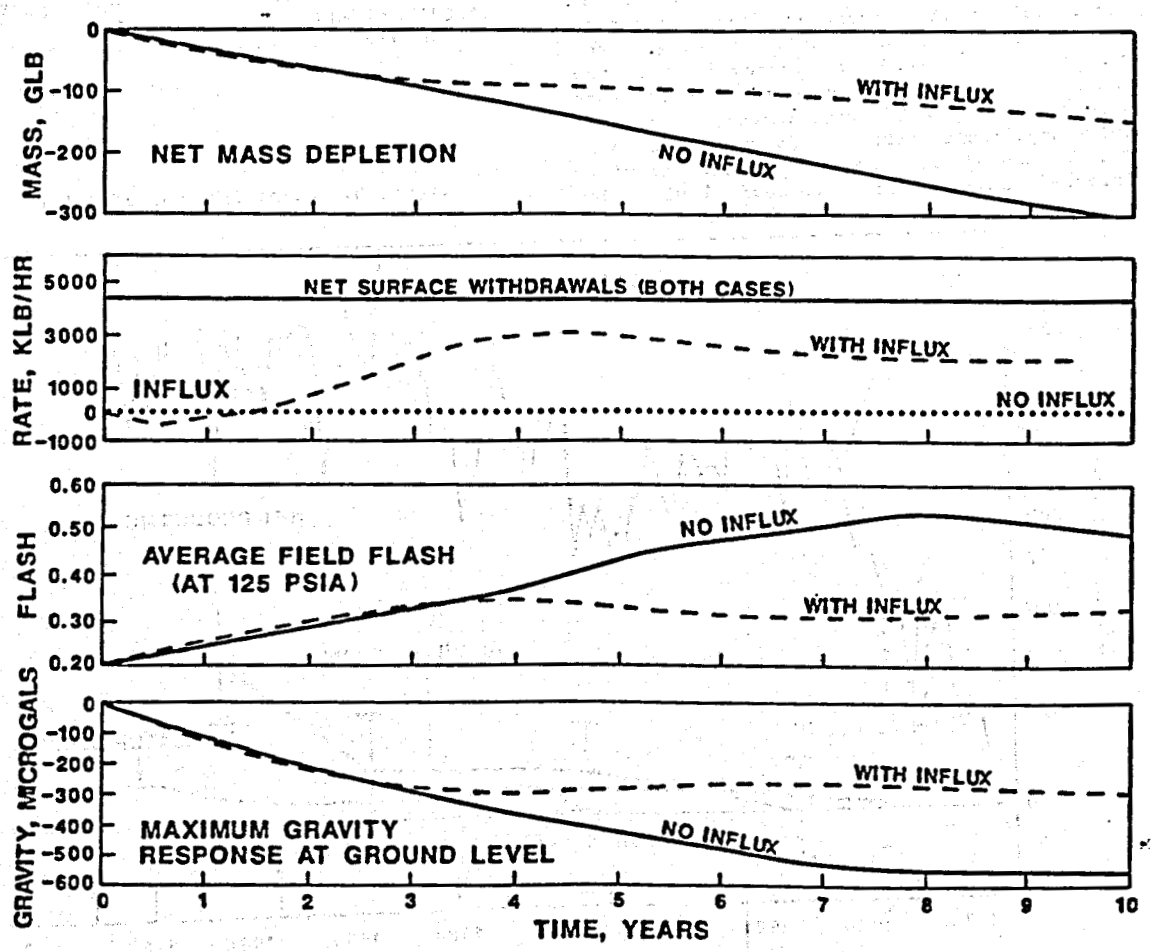

Figure 3. Computed history of Reservoir B performance

Geothermal, Inc. (PGI, a subsidiary of Unocal) under a contract with the National Power Corporation of the Philippines. The field has been producing commercially since 1979, and currently has 330 MW of installed capacity. Figure 4 presents the history of net surface production at Bulalo since 1979.

Five fieldwide precision gravity surveys have been carried out at Bulalo since 1980, as indicated on Figure 4. After 1980, each new precision gravity survey can be used to infer overall mass loss from the system over the intervening time period. When this is compared with net surface production (production minus injection), influx can be computed. Figure 4 presents the resulting influx rates averaged over each time period. Up through 1985 gravity-inferred influx is a small fraction of net production. During 1986 and 1987 gravity-inferred influx has increased significantly.

Figure 4 also presents the influx rate computed by a three-dimensional reservoir simulation model of the Bulalo Field. The model describes the Bulalo reservoir with a 1100 block double-porosity configuration. It as been calibrated against histories of individual well pressures and producing enthalpies through 1985. While the calibration can still be improved upon, the important elements of reservoir performance were reasonably well approximated by allowing only negligible influx into the reservoir. This behavior is consistent with gravity-inferred influx rates through 1985. The recent increase in gravity-inferred influx is anomalous, and is not associated with any obvious changes in reservoir performance. Our current hypothesis is that it is associated with subtle near surface or data processing effects, rather than a real increase in influx rate. The next gravity survey will be run in April-May, 1988.

Figure 5 presents a simplified map of the Bulalo field. Also shown are the locations of the power plants and various outlying wells. BM66 is a benchmark located in the center of the production area. Figure 6 presents observed and simulator delta-gravity

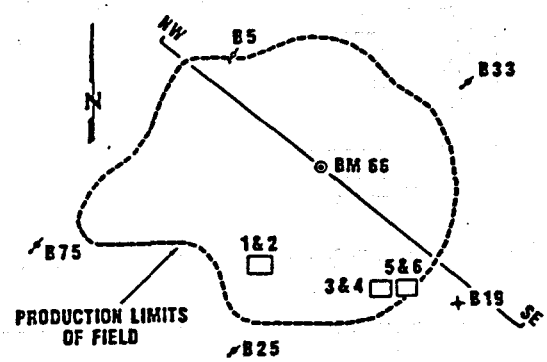

Figure 5. Simplified map of Bulalo

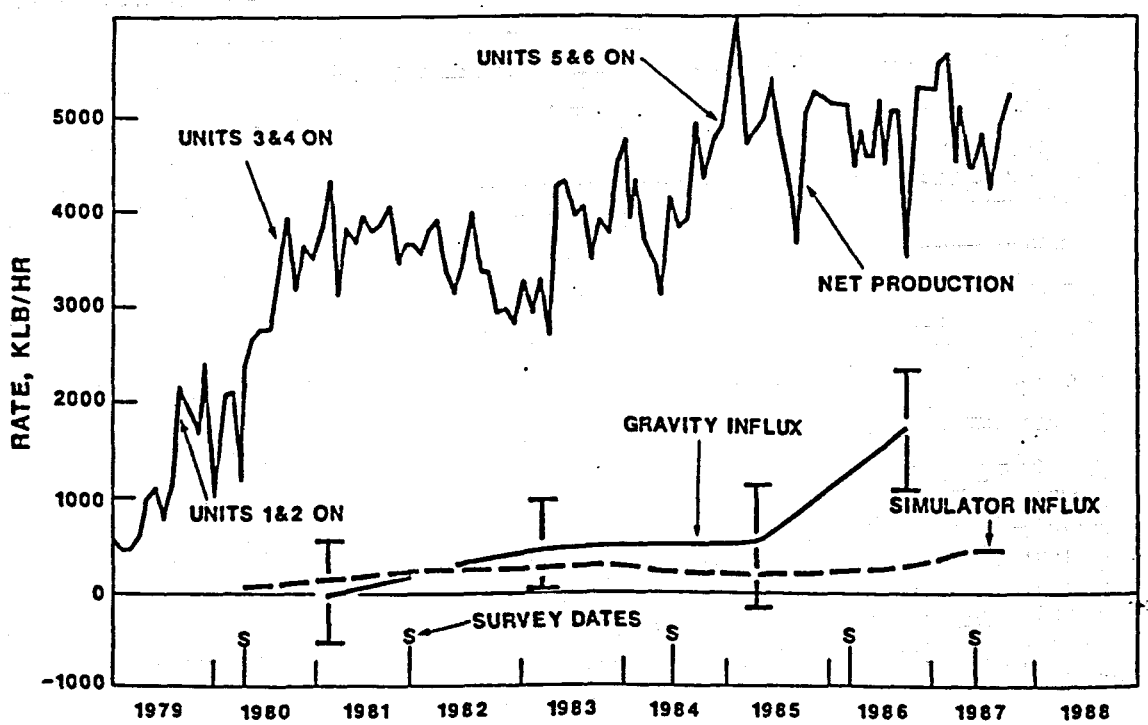

Figure 4. Bulalo Field net production and influx rates

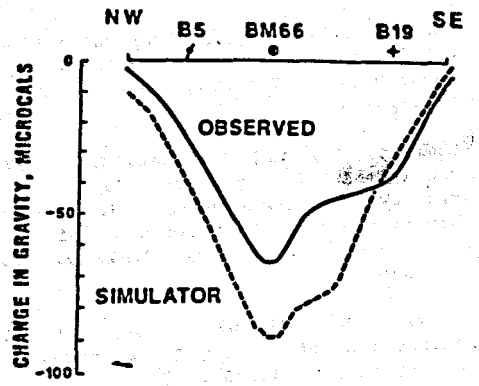

Figure 6. Observed and computed delta-gravity profiles across Bulalo for 1984 to 1986

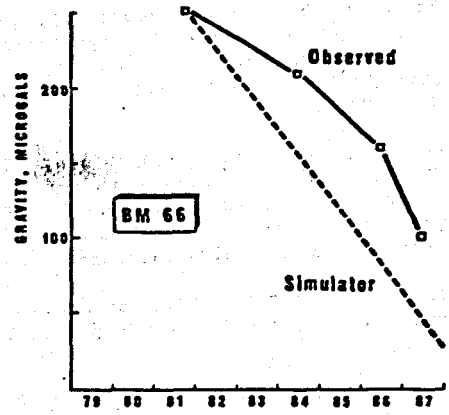

Figure 7. Observed and computed histories of gravity at Bulalo benchmark BM66

profiles on a NW-SE section through BM66, corresponding to the 1984-1986 time frame. The maximum observed gravity change is almost 70 microgals, whereas that derived from the reservoir simulation model is 90 microgals. The smaller area under the observed curve suggests that the reservoir is experiencing substantially more influx than the simulation model. However, another possibility is that depletion in the reservoir is occurring deeper than in the numerical model. This latter possibility is consistent with two observations:

1. The shapes of the two profiles in Figure 6 are similar, suggested that the fundamental reservoir physics of depletion contained in the model is a good representation of that in the reservoir; and

2. The impact of near-surface effects on precision gravity data is to add variations of ± 10 microgals to the delta-gravity field away from the productive area. This causes the tails of the observed delta-gravity distribution to be noisy. It results in uncertainty in mass loss calculations because stable benchmarks cannot be accurately defined. The error bars on the gravity-inferred influx rates in Figure 4 result partly from this effect. Thus, it may be that the observed data should be shifted down.

Figure 7 presents observed and computed delta-gravity histories for benchmark BM66. This benchmark was first installed in 1981 in the center of the field. A total observed change of 150 microgals over almost six years can be seen. The observed data initially show a flatter trend, implying either less depletion, or deeper depletion in the field than in the model.

We are currently reviewing both field and model data in order to provide a basis for improving the match between observed and simulation gravity results. Past experience with such reviews have taught us that while the gravity data can provide important insights into reservoir behavior, it can also display misleading features that have nothing to do with reservoir behavior. Sometimes these features appear to have been associated with weather patterns. We suspect that the gravity-inferred increase in influx in 1986-87 shown on Figure 4 may actually be an effect unrelated to the reservoir.

CONCLUSION

Precision gravity monitoring can be used to infer influx into geothermal reservoirs. Such data must be gathered in the field with great care, as data interpretation requirements push the limits of commercially available technology. Even when the data gathering is sufficiently accurate, non reservoir effects such as near-surface aquifer recharging due to rainfall can complicate data interpretation.

Gravity-inferred influx rates for the Bulalo field have been compared with those used in a simulation model. Conversely, simulation-computed gravity fields have been compared with observed results. These comparisons have provided us with confidence in the basic structure of the simulation model.

REFERENCES

Allis, R.G., and Hunt, T.M. (1986), "Analysis of exploitation-induced gravity changes at Wairakei geothermal field, Geophysics, v. 51, no. 8, 1647-1660.

Craft, B.C., and Hawkins, M.F. (1959), Applied Petroleum Reservoir Engineering, Prentice-Hall, Chapters 4 and 5.

Dobrin, M.B. (1960), Introduction to Geophysical Prospecting, Second Edition, McGraw-Hill.

Eckhardt, D. (1986), "Isomorphic geodetic and electrical networks: An application to the analysis of airborne gravity gradiometer survey data", Geophysics, v. 51, no. 11, 2145-2159.

Gudmundsson, J.S., and Olsen, G. (1985), "Water influx modeling of Svartsengi geothermal field, Iceland," SPE 13615, presented at the SPE 1985 California Regional Meeting, Bakersfield, California, March 27-29.

Hammer, S. (1945), "Estimating ore masses in gravity prospecting", Geophysics, v. 10, 50-62.

Hunt, T.M. (1970) "Gravity changes at Wairakei geothermal field, New Zealand", Geological Society of America Bulletin, v. 81, 529-536.

Hunt, T.M. (1977), "Recharge of water in Wairakei geothermal field determined from repeat gravity measurements", N.Z. Jour. Geol. & Geophys., v. 20, no. 2, 303-317.

LaFehr, T.R. (1965), "The estimation of the total amount of anomalous mass by Gauss's theorem", J. Geophys. Res., v. 70, no. 8, 1911-1919.

Lambert, A., and Beaumont, C. (1977), "Nano variations in gravity due to seasonal groundwater movements: Implications for gravitational detection of tectonic movements", J. Geophys. Res., v. 82, no. 2, 297-306.

Nagy, D. (1966), "The gravitational attraction of a right rectangular prism", Geophysics, v. 31, 362-371.

ACKNOWLEDGEMENTS

All reservoir simulation calculations described in this paper were made with a program developed under joint sponsorship with Technical Software & Engineering, Inc. T.D. Anderson of Unocal's Science and Technology Division wrote the software for computing surface gravity fields.

CASE HISTORY OF A GEOTHERMAL FIELD IN ITALY: LATERA FIELD IN NORTHERN LATIUM

by

S. K. SANYAL

GeothermEx, Inc.

Geothermal Resources Council
Workshop on
Responses of a Geothermal Field During Exploitation

16 June 1989

ACKNOWLEDGEMENT

THE SPEAKER GRATEFULLY ACKNOWLEDGES THE EXCEPTIONALLY HIGH CALIBER OF DATA GATHERING AND EVALUATION CONDUCTED BY ENEL/AGIP JOINT VENTURE AT LATERA, WHICH FORMED THE BASIS ON WHICH THE GEOTHERMEX STUDY WAS CONDUCTED (UNDER A CONTRACT FROM AGIP).

SPECIAL ASPECTS OF THE LATERA RESERVOIR

- COMPLEX GEOLOGY AND GEOCHEMISTRY
- HIGHLY ANISOTROPIC AND HETEROGENEOUS
- STRONG SCALING POTENTIAL
- HIGH CO_2 CONTENT
- INCIPIENT GAS CAP IN INITIAL STATE
- NON-CONDENSIBLE GAS TO BE INJECTED WITH WASTE WATER

TOPICS DISCUSSED

- HYDROGEOLOGIC MODELING
- ANALYTICAL MODELING OF PRESSURE BEHAVIOR
- TWO-DIMENSIONAL NUMERICAL SIMULATION
- THREE-DIMENSIONAL NUMERICAL SIMULATION
- RESERVOIR MANAGEMENT

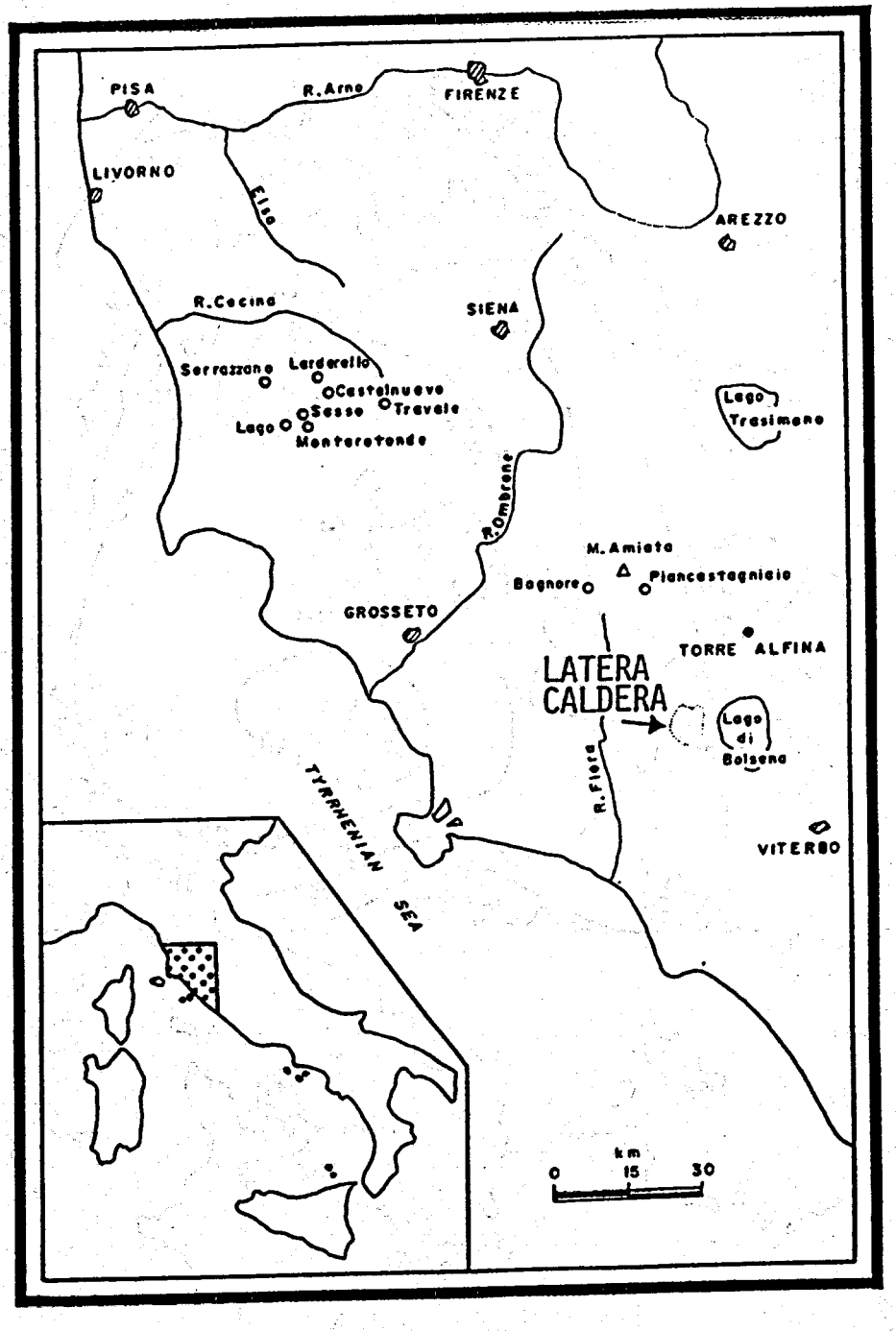

Figure 1.1: Location of Latera geothermal area

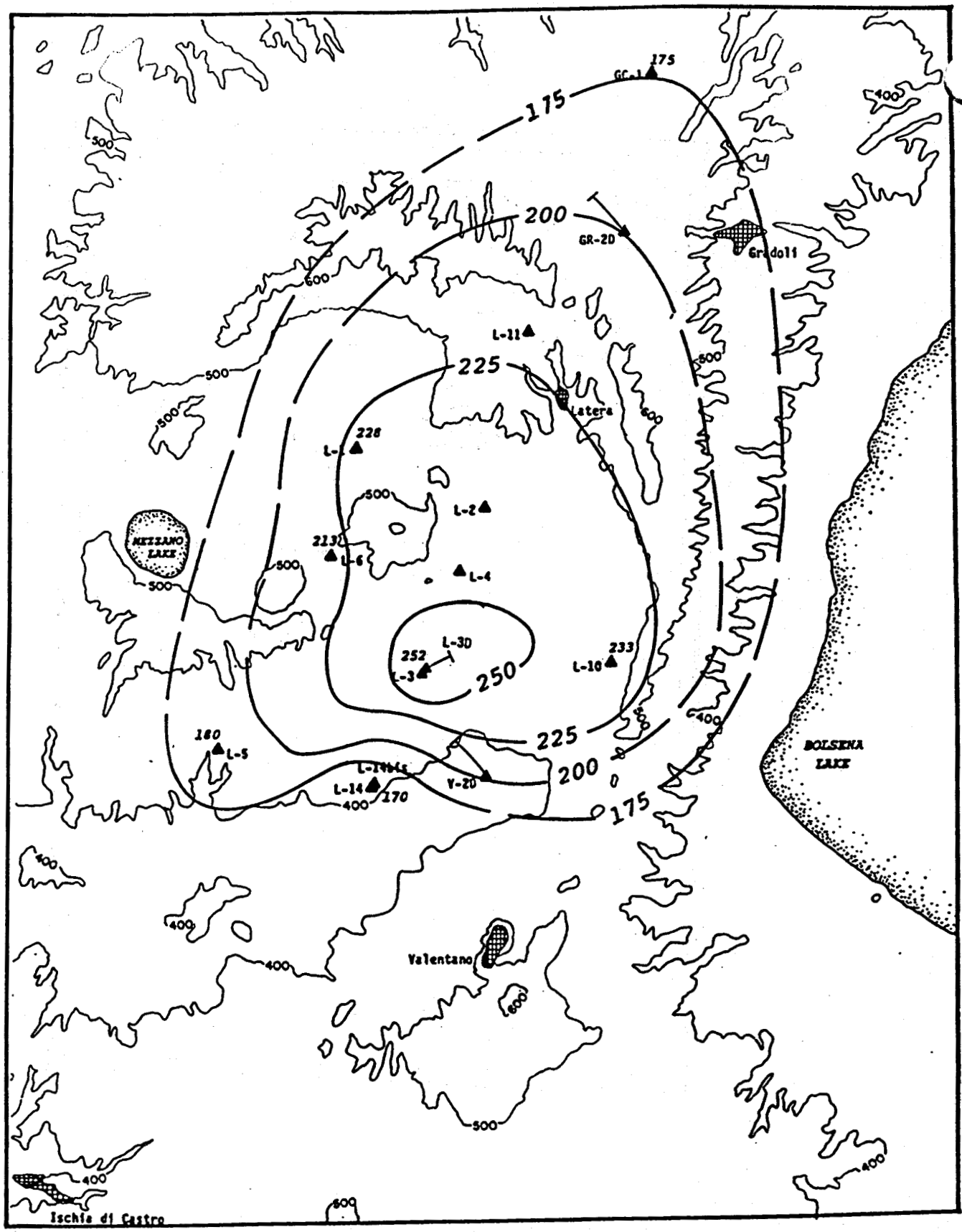

Figure 4.4 Temperature contours, -1500 meters (m.s.l.)

LEGEND

——100 Isotherm, °C; dashed where uncertain

N

0 1 2 km

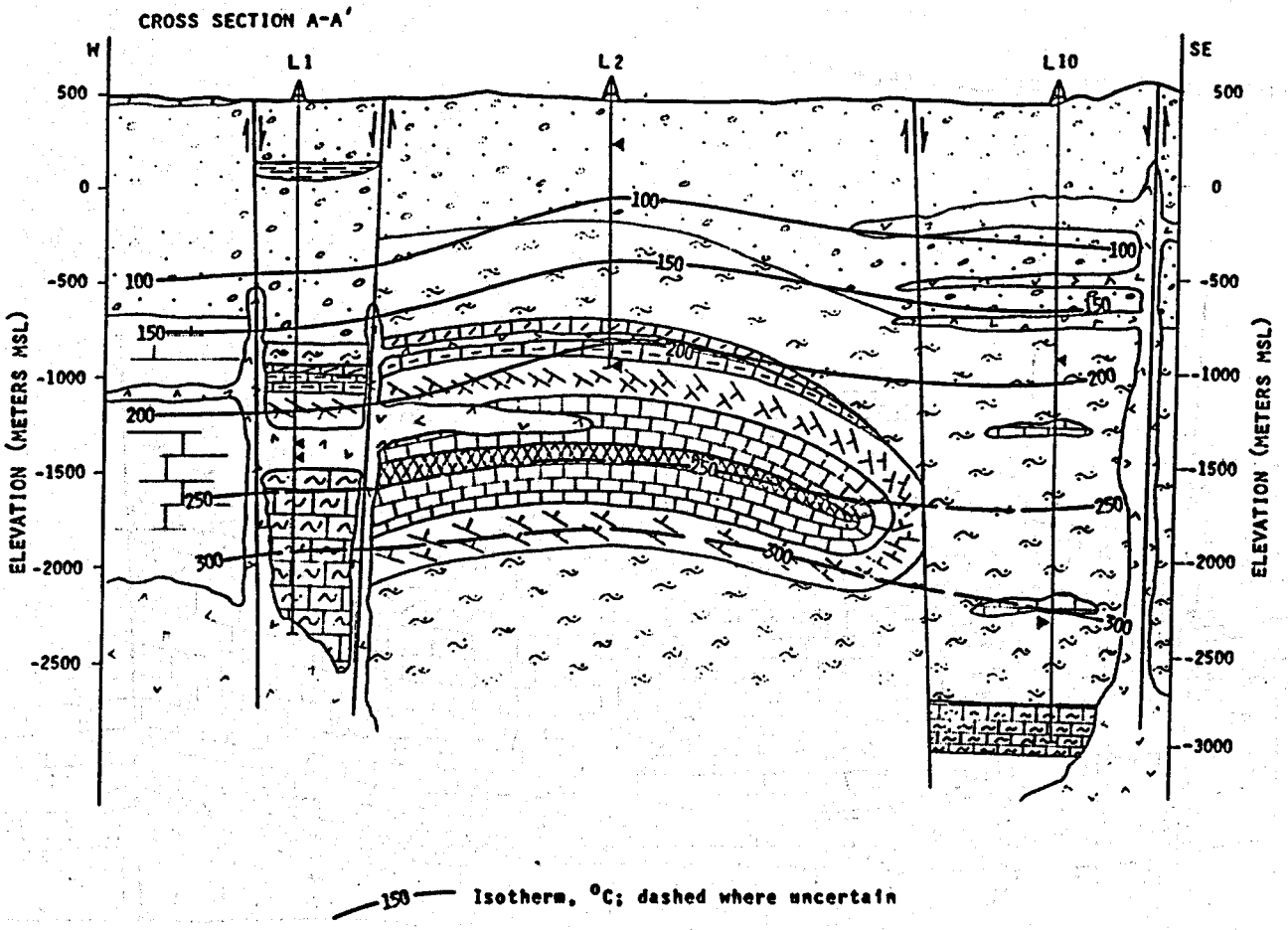

Figure 4.5 Cross-section A-A' with temperature contours

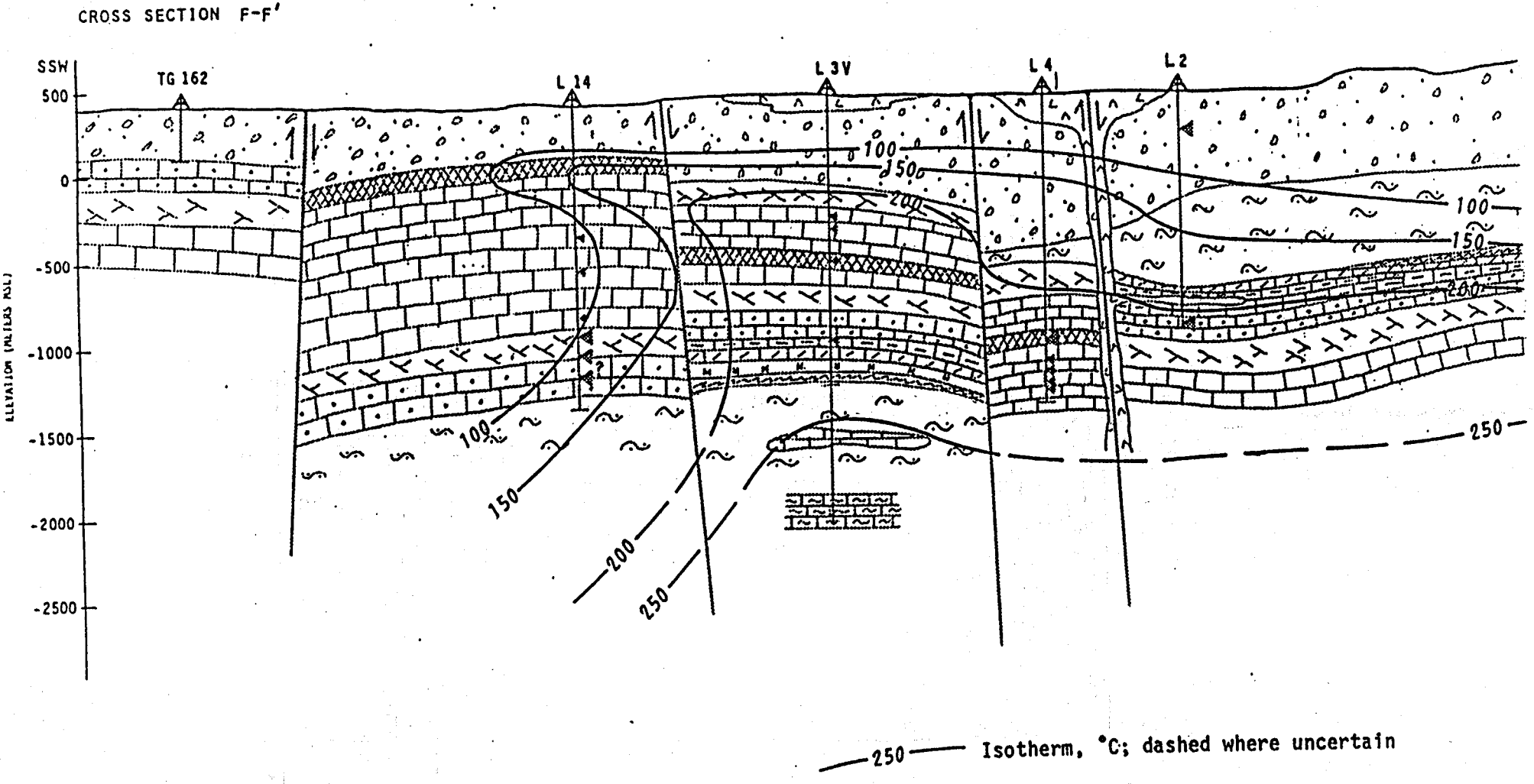

Figure 4.10 Cross-section F-F' with temperature contours.

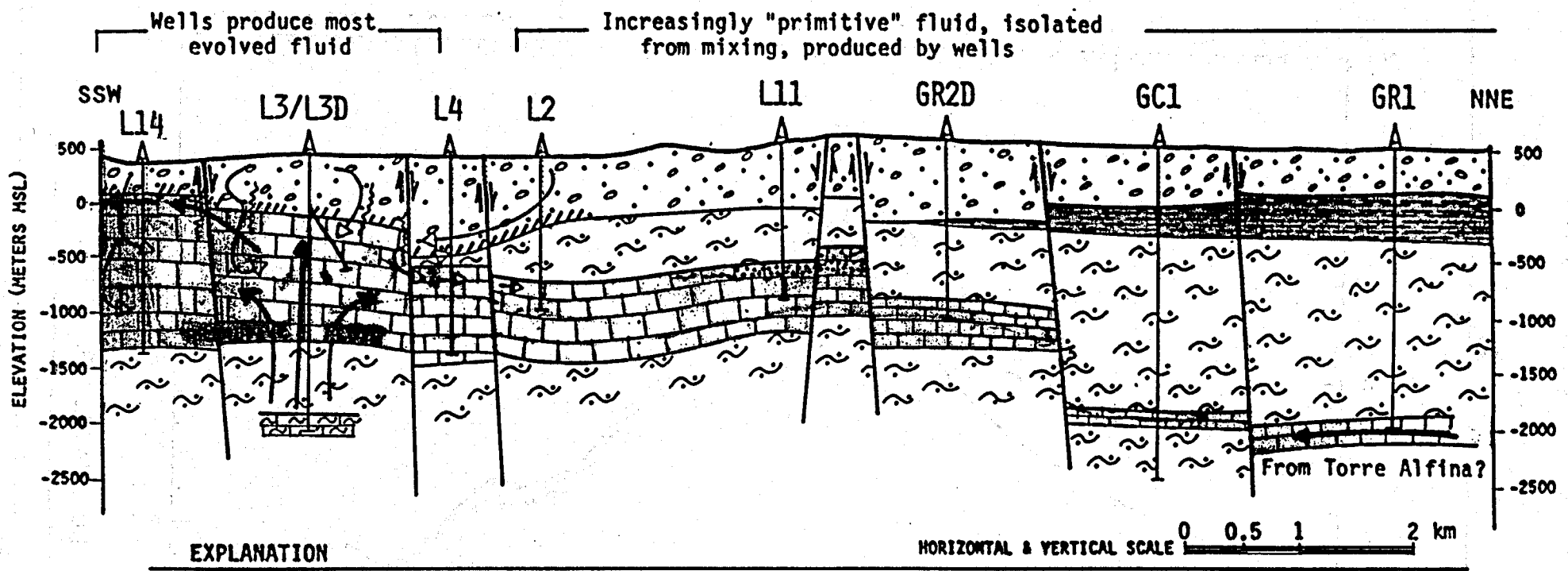

Figure 4.11 Schematic representation of fluid movement and mixing in the Latera geothermal field

FIGURE 5.13: MEASURED and CALCULATED WATER LEVELS, WELL L1

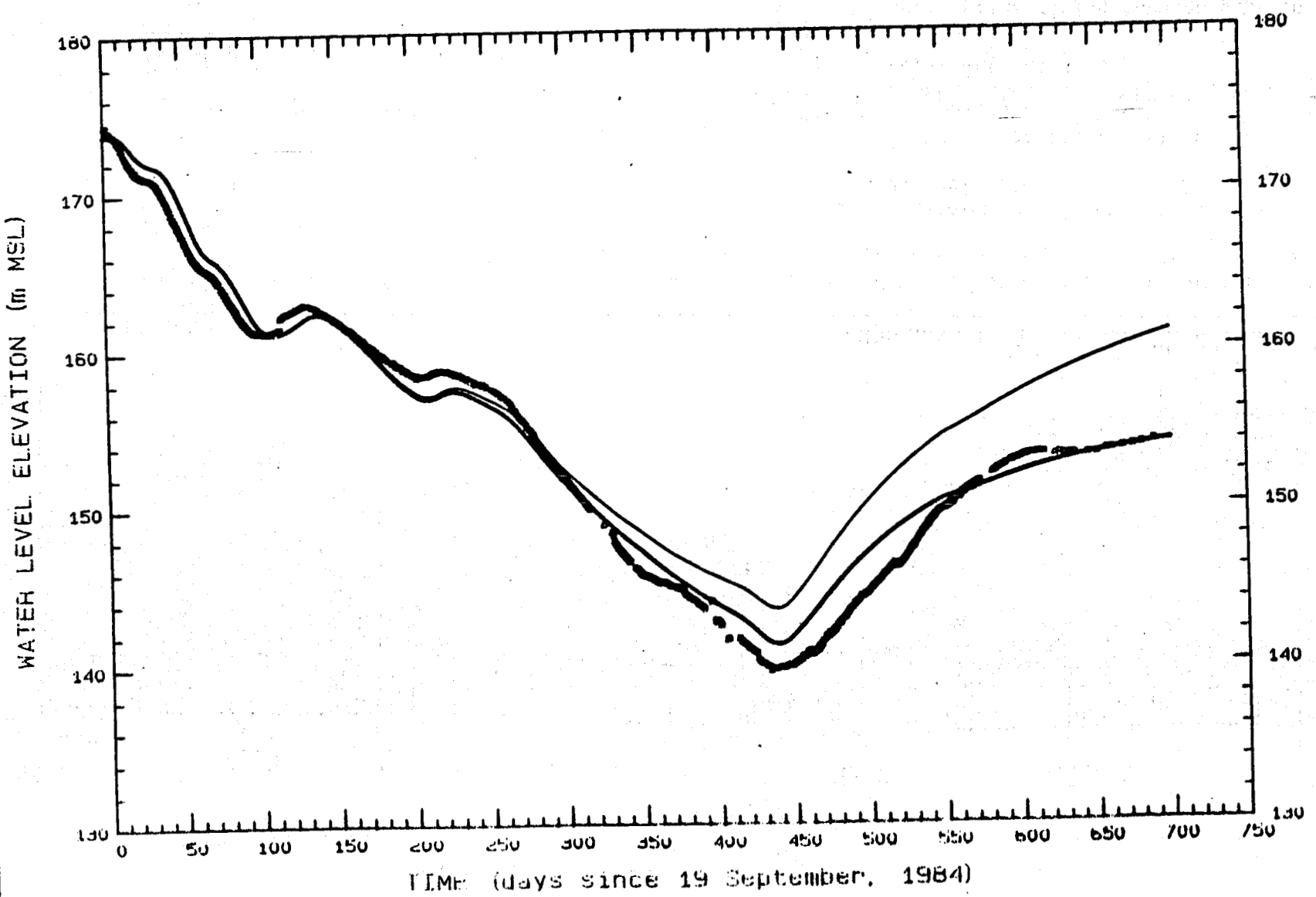

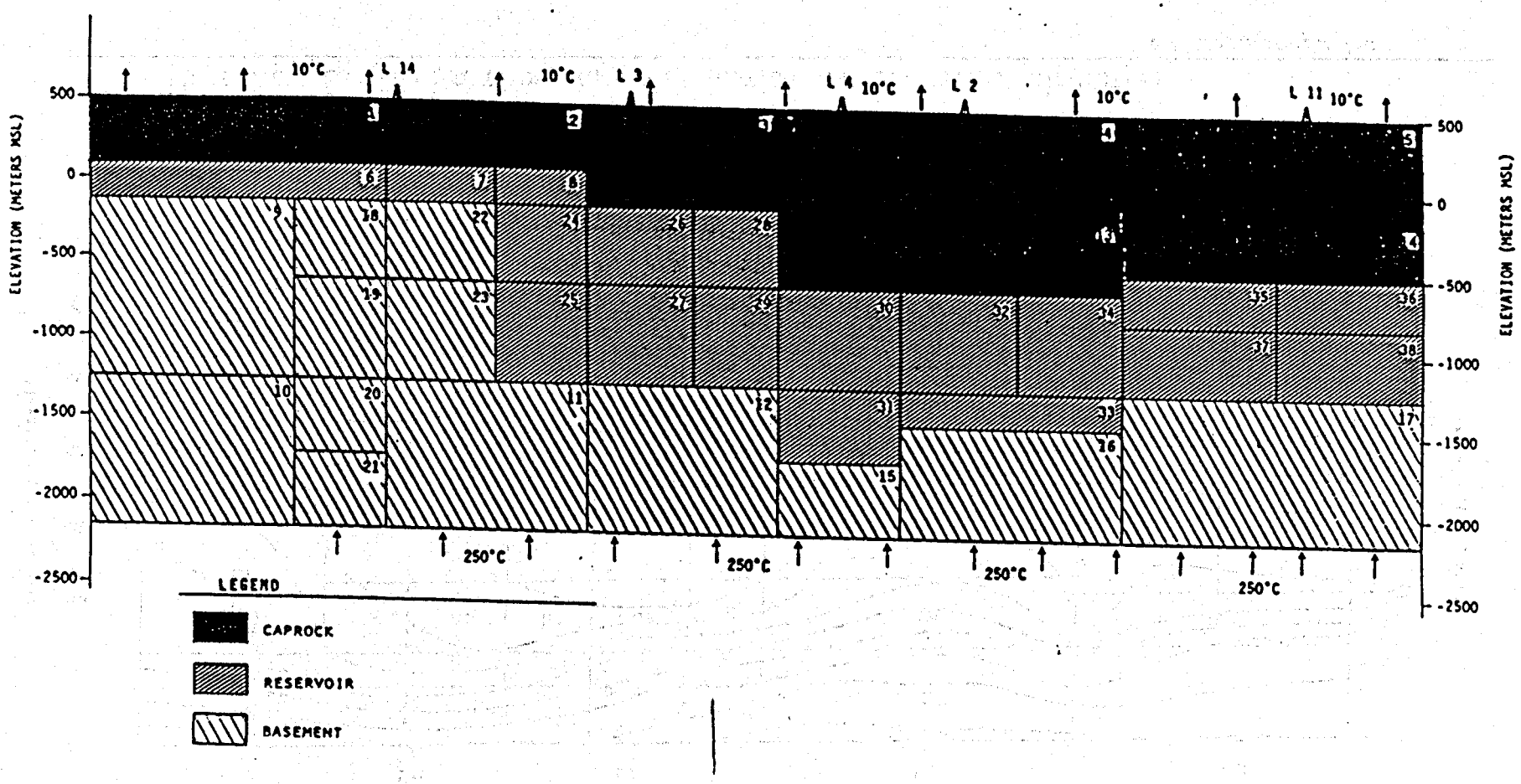

Figure 6.1 Grid layout of the vertical, two-dimensional model used for simulation of the initial state of the Latera field.

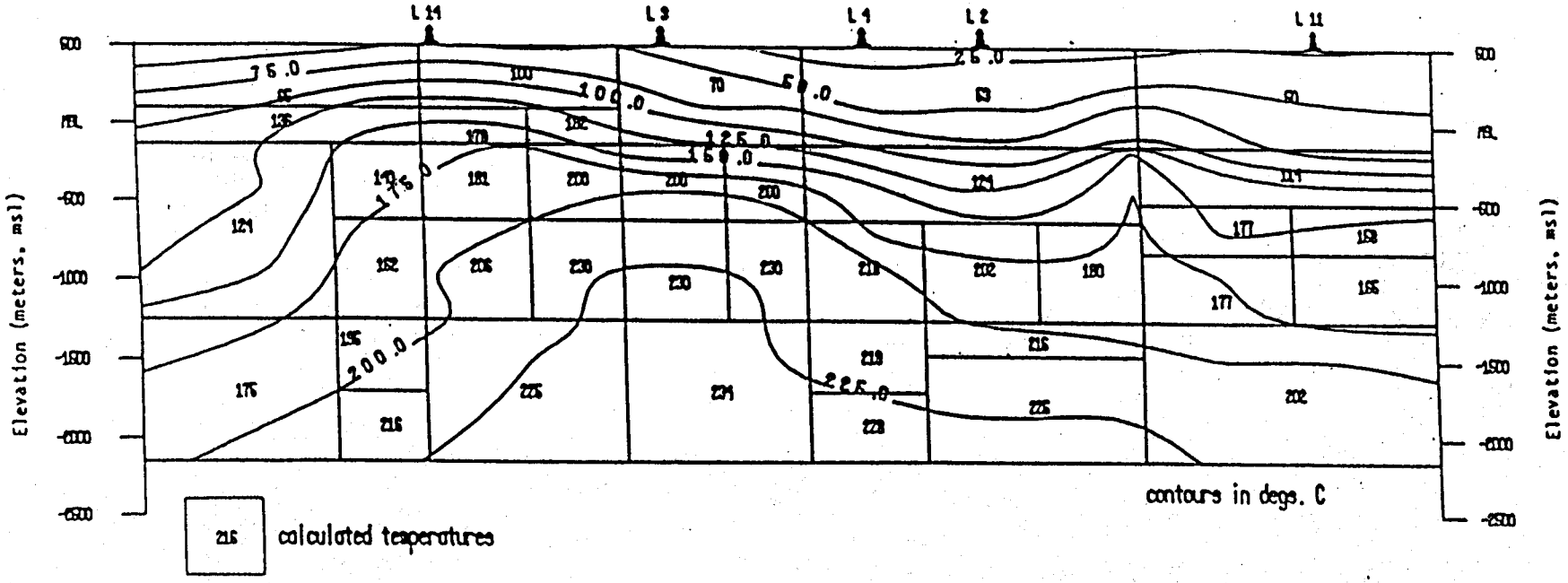

Figure 6.2: Equilibrium temperature distribution, two-dimensional simulation

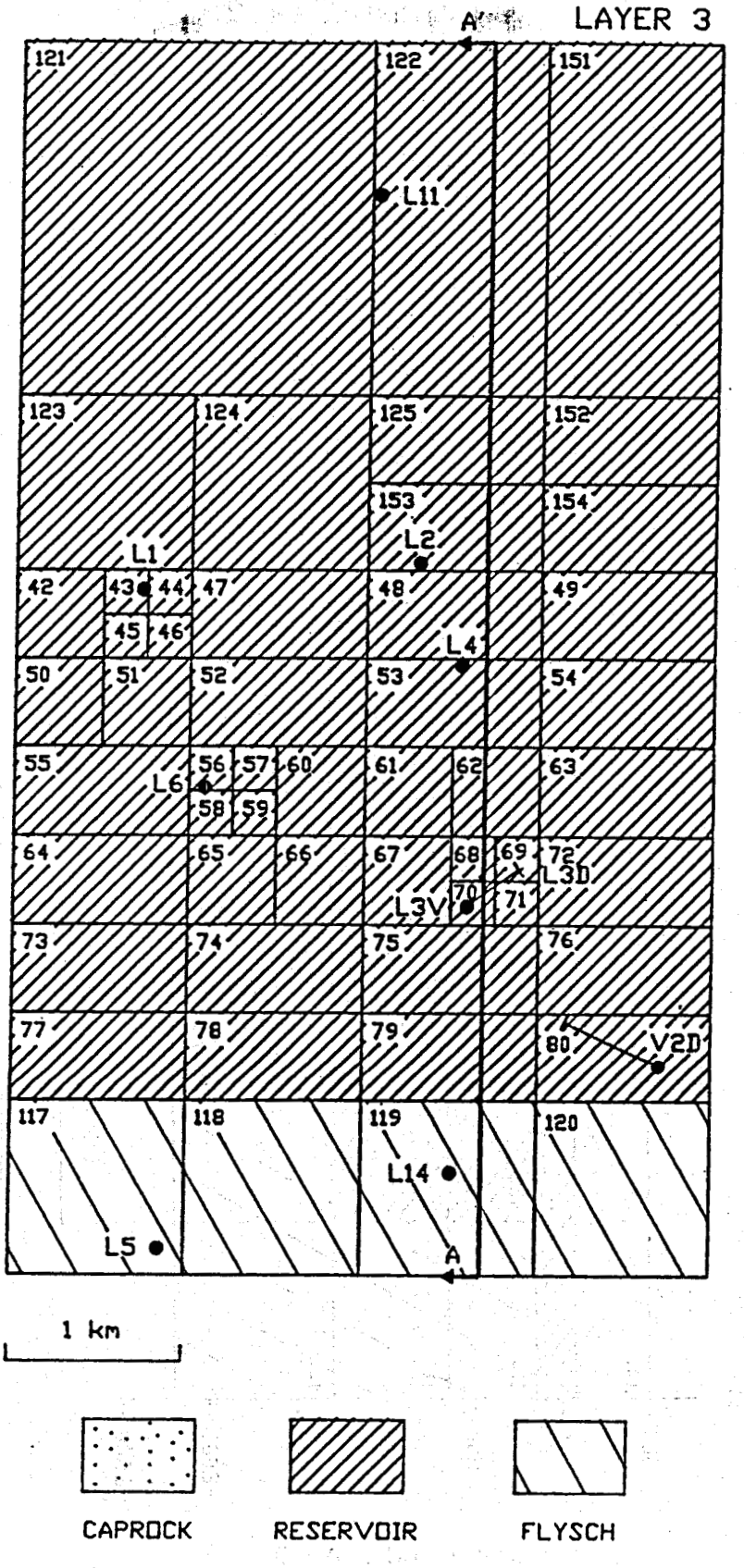

Figure 6.6: Horizontal grid layout for three-dimensional simulation (Layer 3).

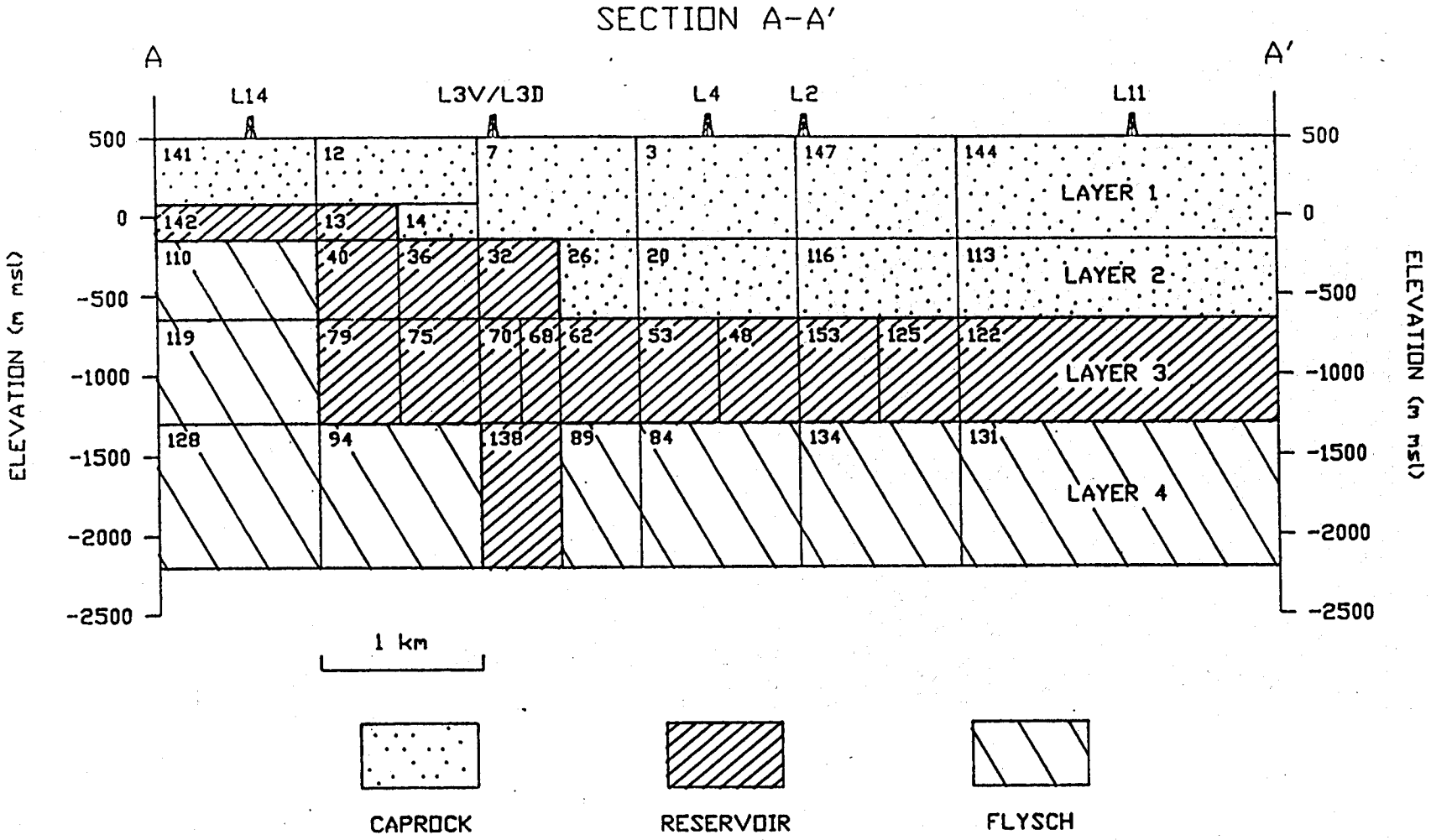

Figure 6.8: Grid layout, three dimensional simulation (Section A-A').

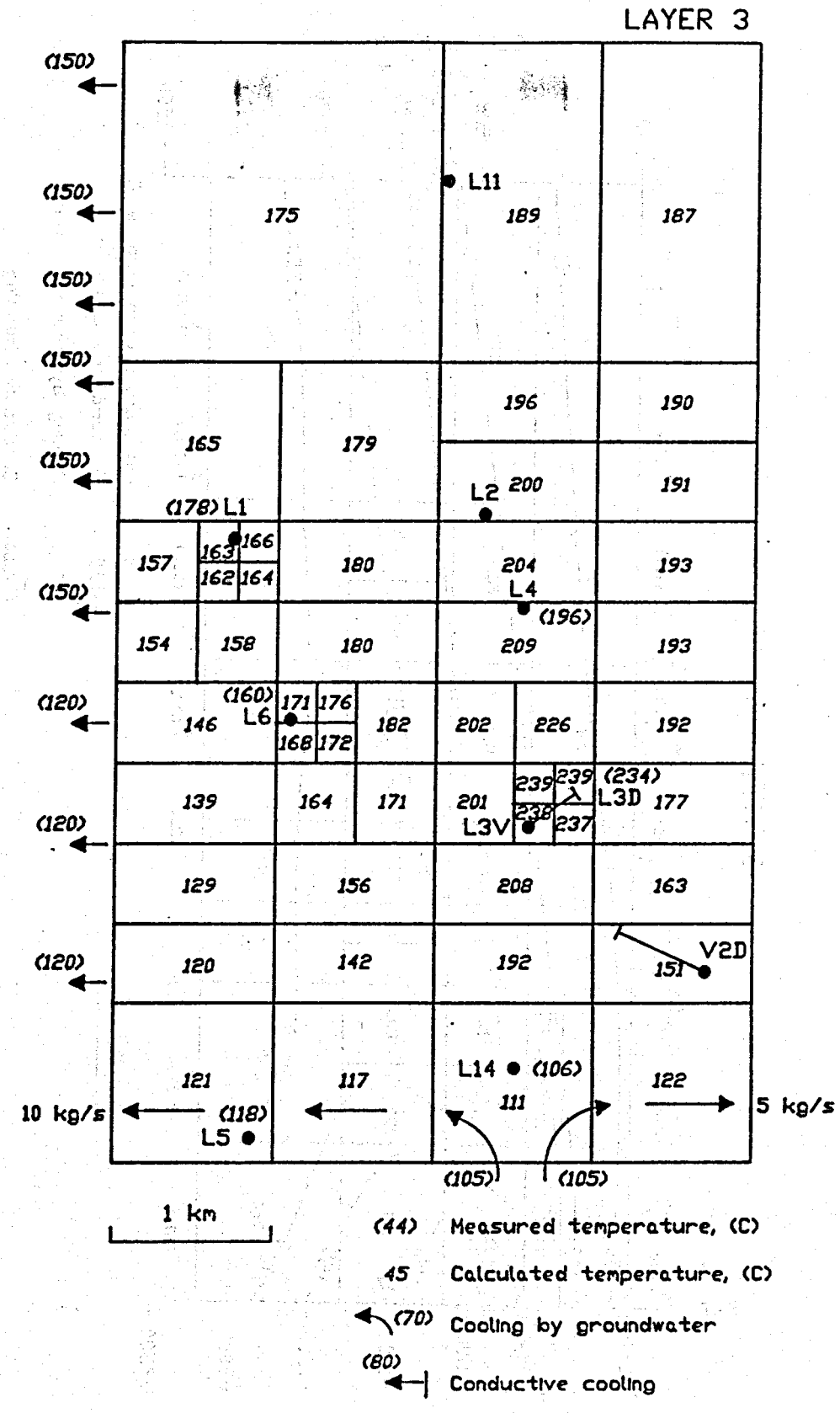

Figure 6.11: Equilibrium temperature distribution (Layer 3, -965 m msl).

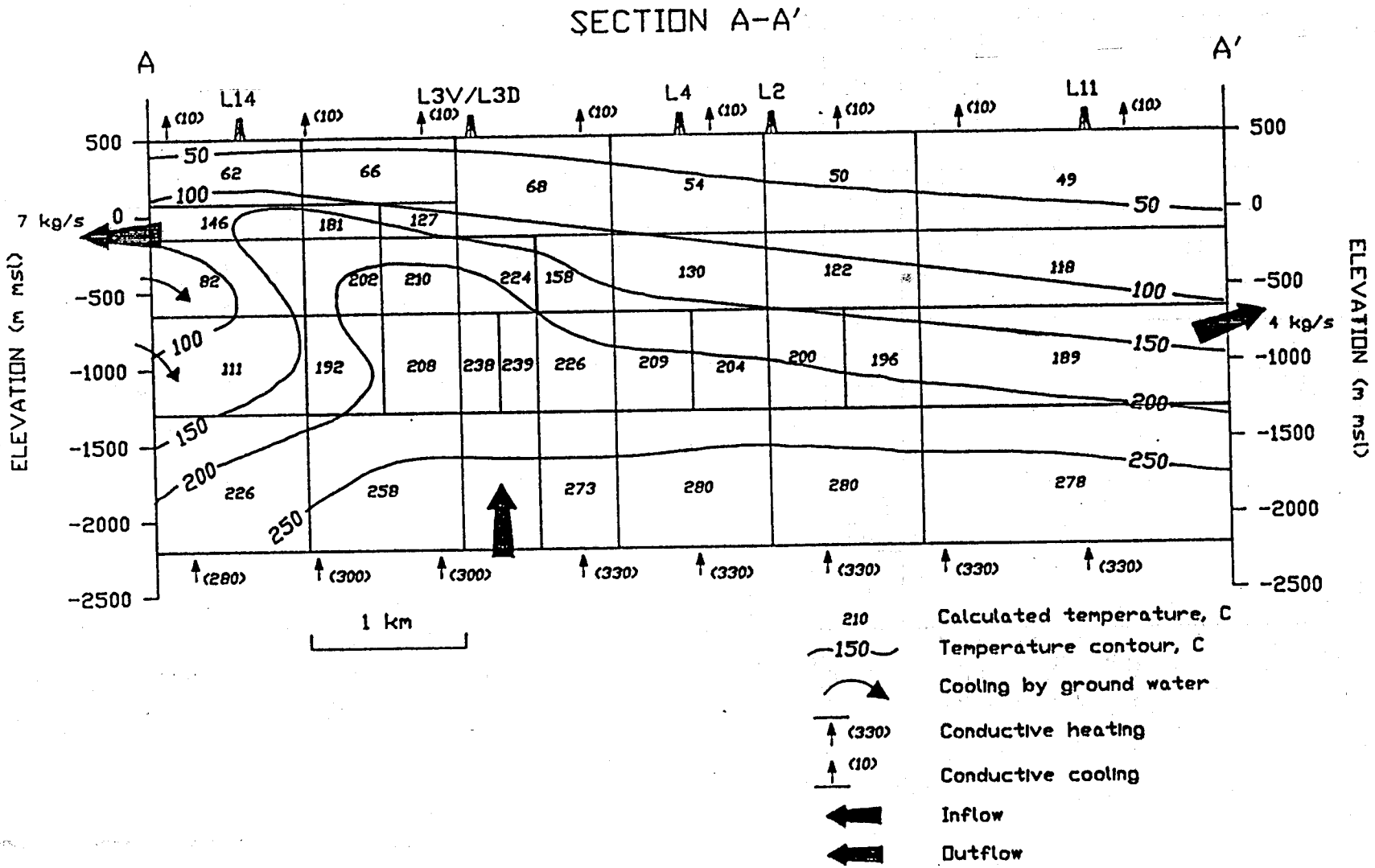

Figure 6.13: Equilibrium temperature distribution (Section A-A').

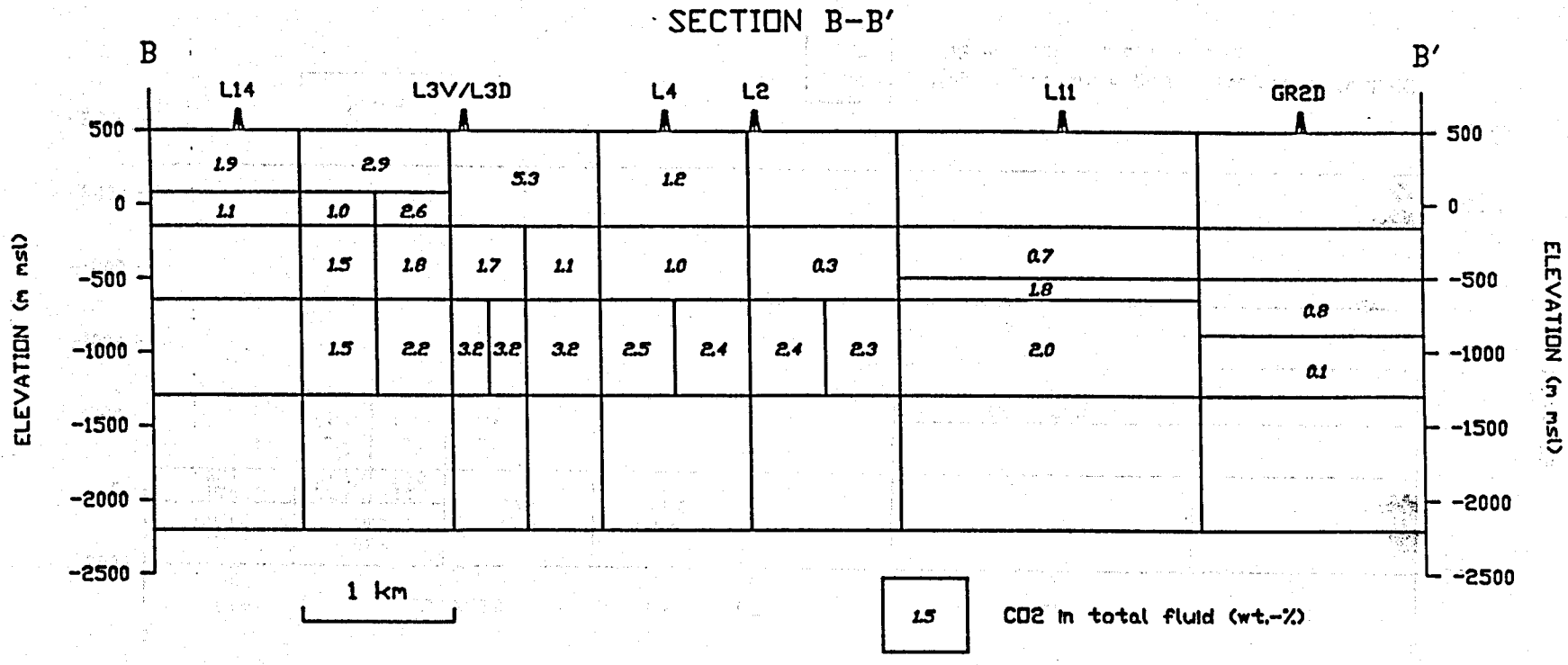

Figure 6.23: Equilibrium distribution of CO2 in total fluid (modified 3-D simulation).

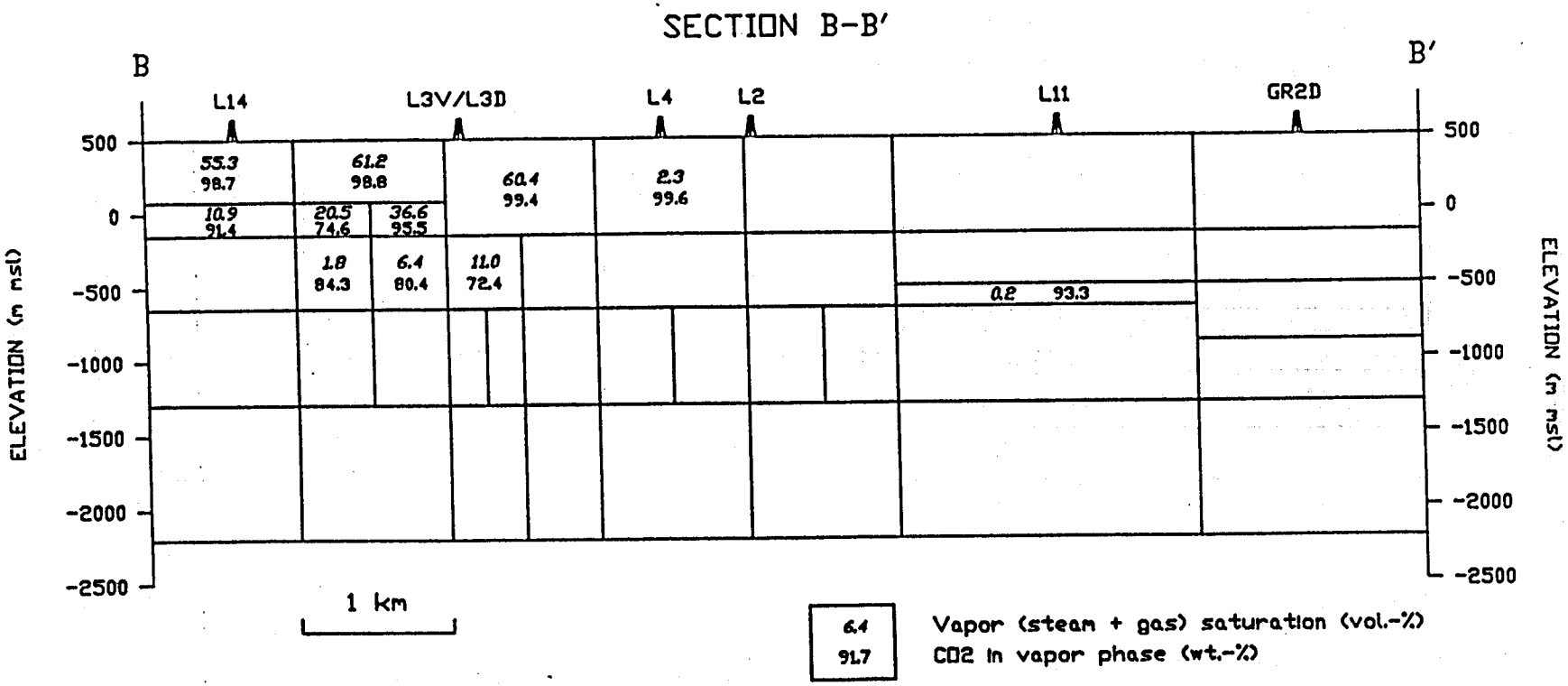

Figure 6.24: Equilibrium distribution of vapor saturation and CO2 in vapor phase (modified 3-D simulation).

1987, GEOTHERMEX, INC.
LATER624.DVG

FIGURE 6.25: MEASURED and CALCULATED WATER LEVELS FROM SIMULATION, WELL

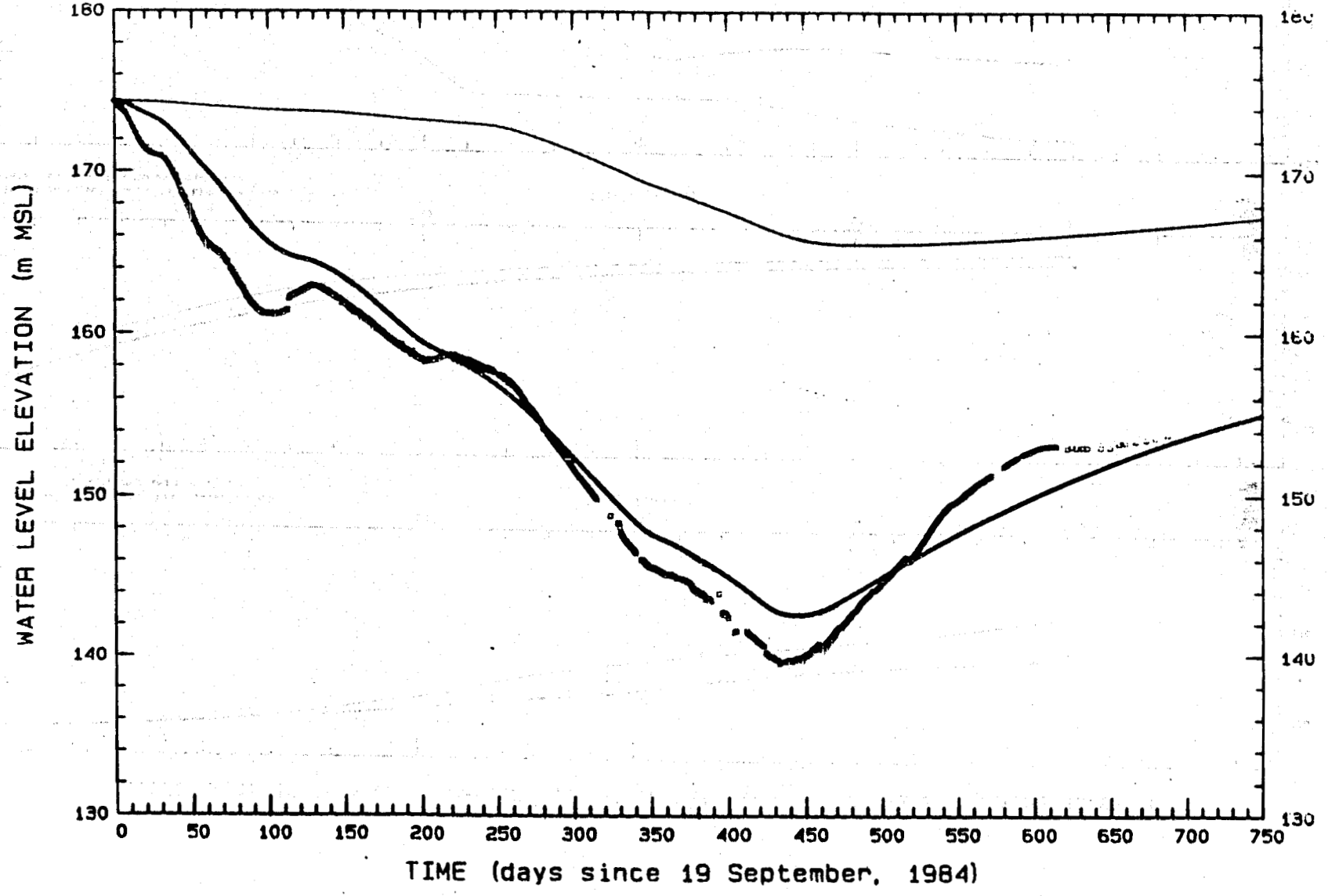

GeothermEx, Inc.
04-15-1987 A:L1MLE.PLT

FIGURE 6.33: TEMPERATURE, PRESSURE and STEAM SATURATION at BLOCK 69 vs TIME (CASE G)

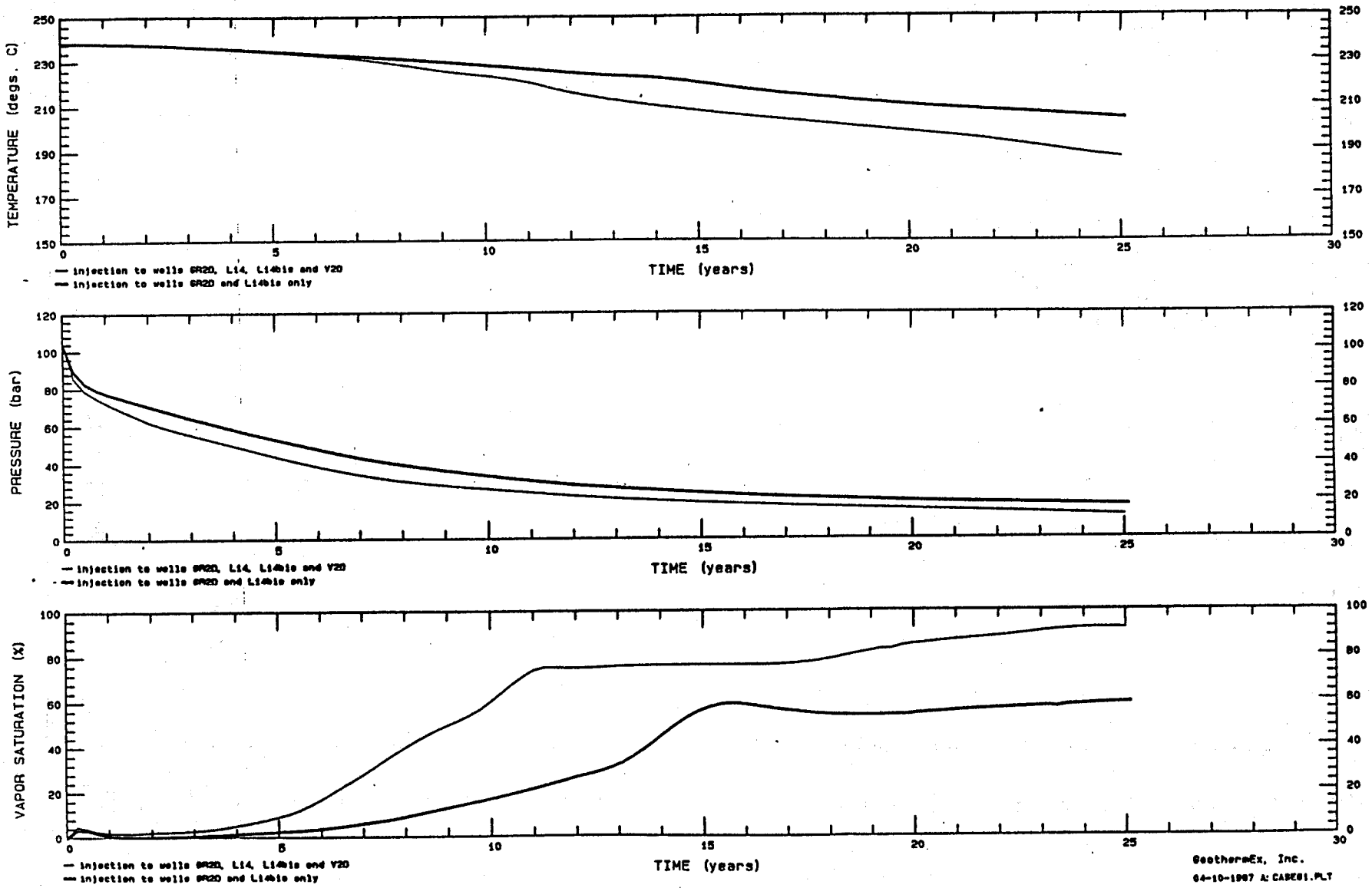

CHANGE IN FLOW RATE WITH DRAWDOWN FOR TYPICAL COMPLETION

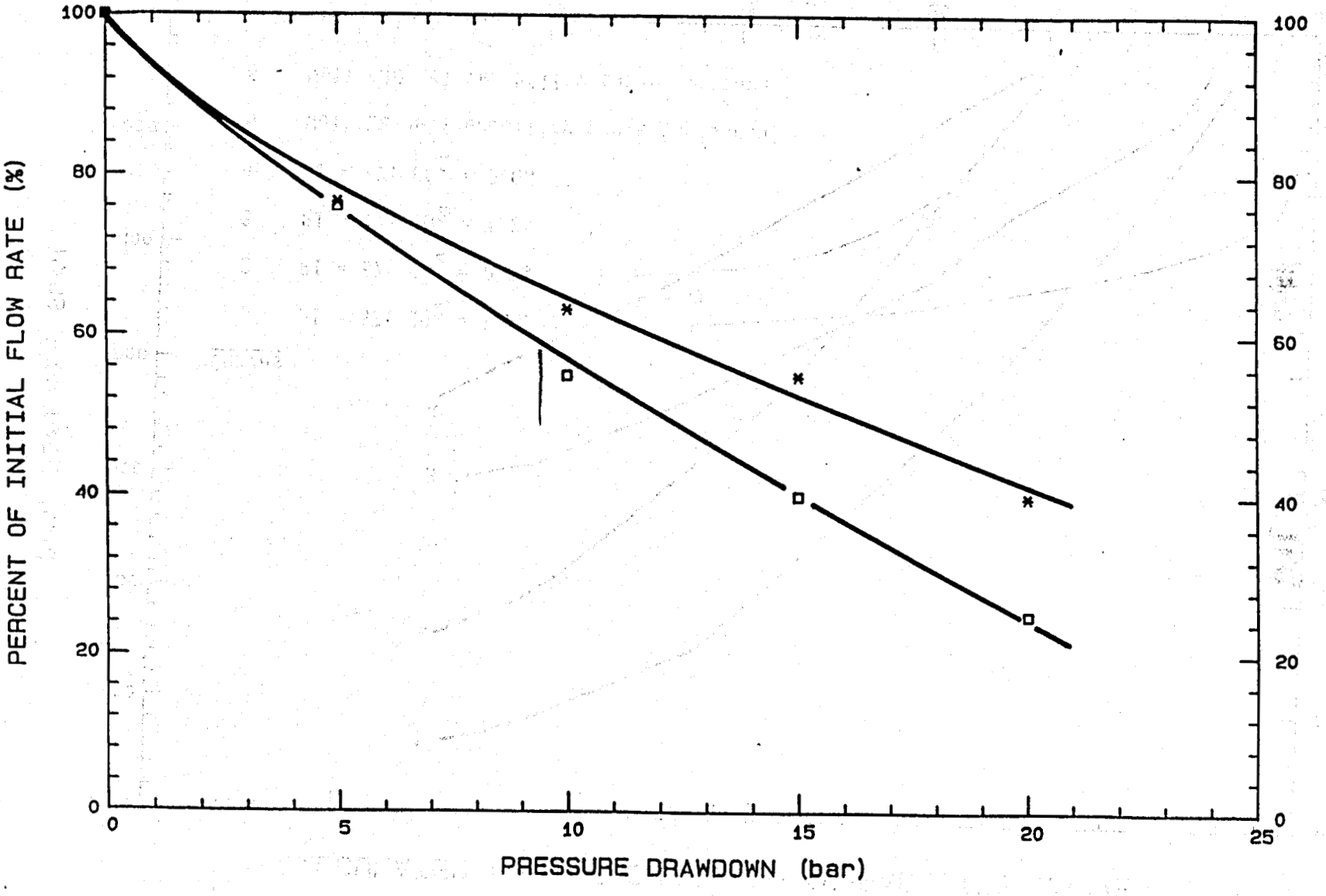

□ for wellhead pressure = 14 bar
* for wellhead pressure = 10 bar

GeothermEx, Inc.
05-04-1987 A:WELLSIM.PLT

CALCULATED and MEASURED DELIVERABILITY CURVES

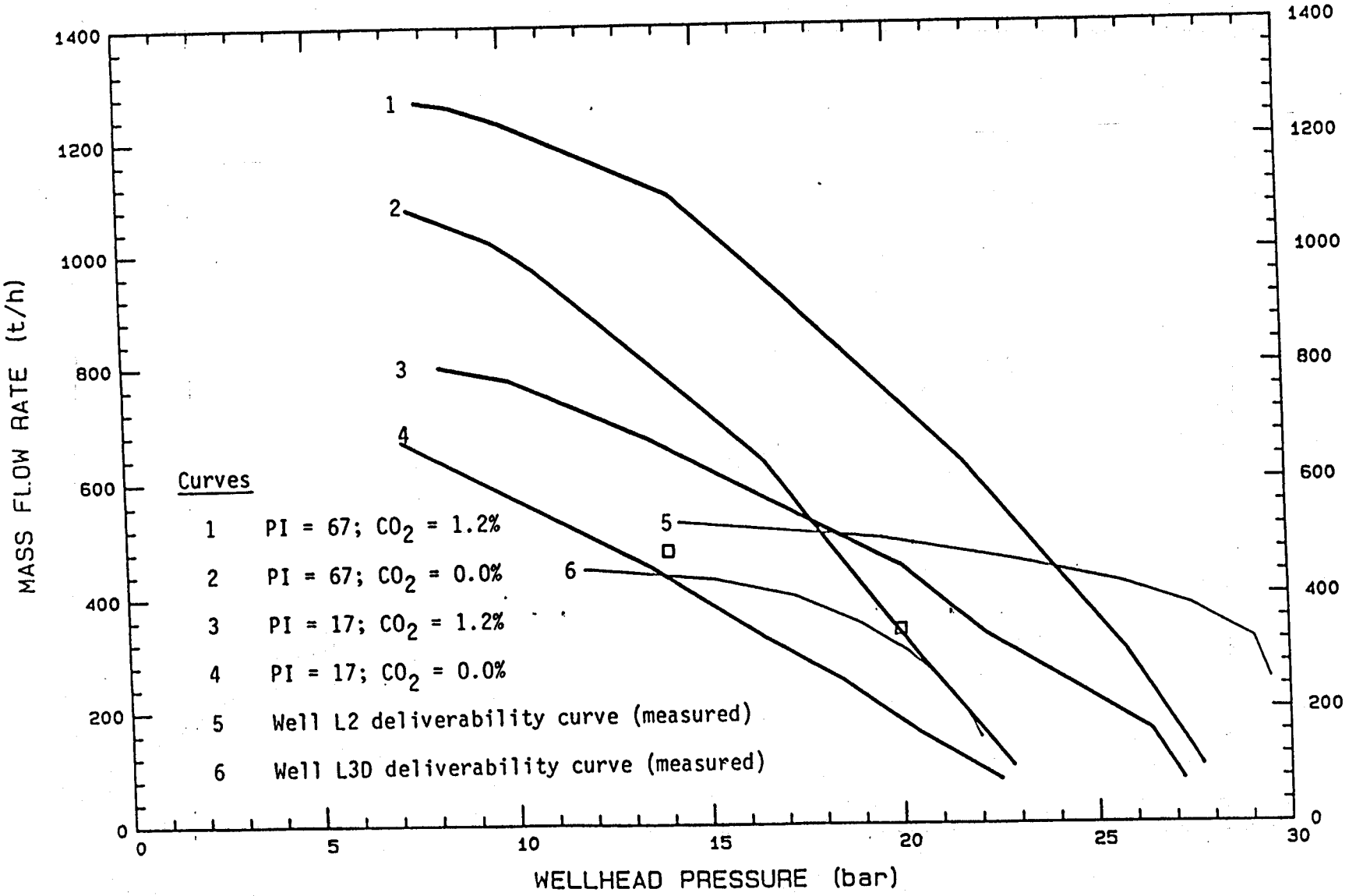

□ Well L3D; 1986 measured data

GeothermEx, Inc.

05-08-1987 A:L3DDEL2.PLT

CHANGE IN FLOW RATE WITH DRAWDOWN FOR TYPICAL COMPLETION

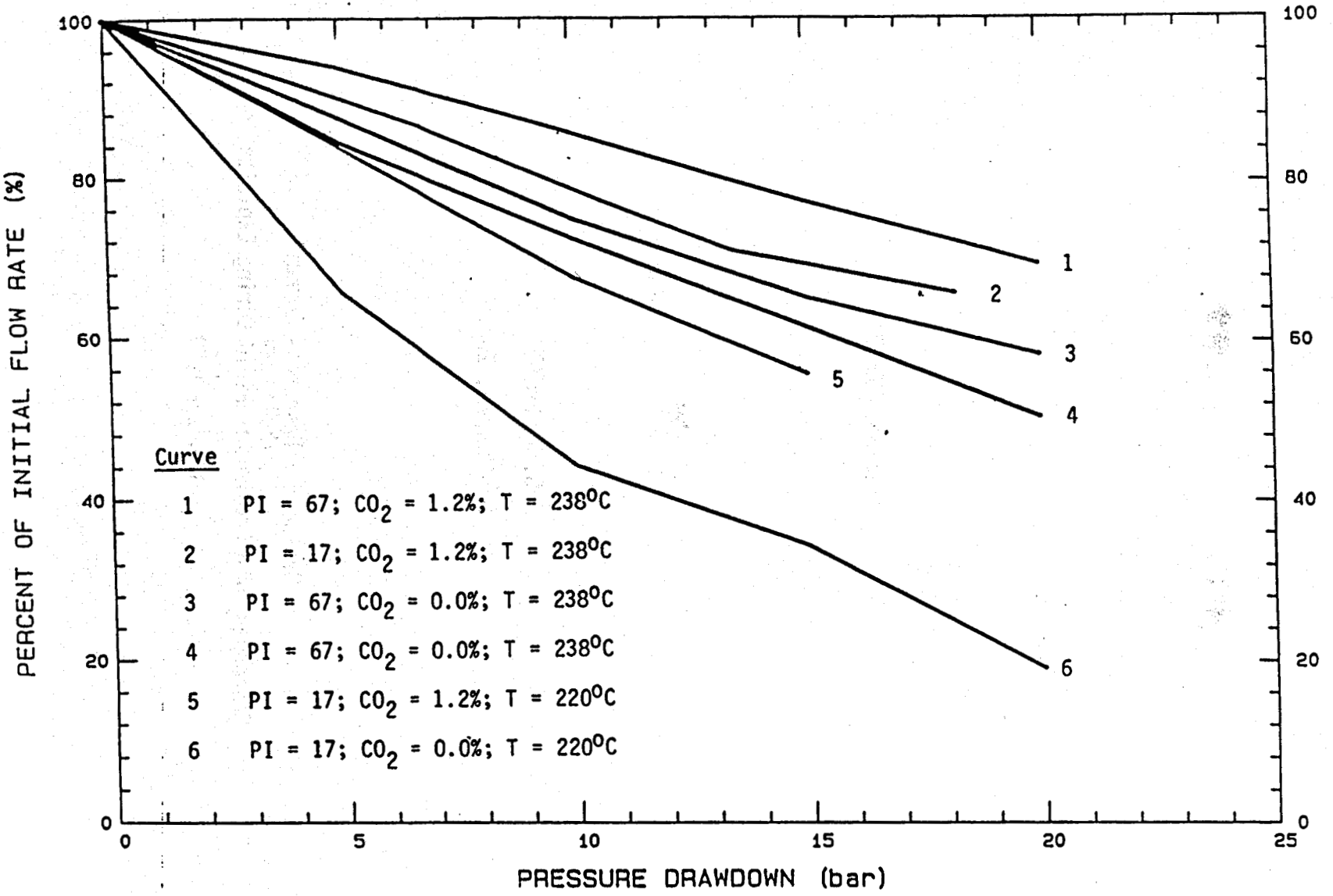

GeothermEx, Inc.
05-08-1987 A:DECLINE.PLT

CONCLUDING REMARKS

by

S. K. SANYAL

GeothermEx, Inc.

Geothermal Resources Council
Workshop on
Responses of a Geothermal Field During Exploitation

16 June 1989

GOALS OF RESERVOIR MANAGEMENT

- MAINTAINING A SAFE AND ENVIRONMENTALLY BENIGN OPERATION

- MAXIMIZING PROFIT

SAFETY AND ENVIRONMENTAL CONCERNS

- BLOWOUT AND OTHER MECHANICAL HAZARDS
- GAS EMISSIONS
- NOISE
- GROUNDWATER POLLUTION
- INTERFERING WITH HOT SPRINGS AND FUMAROLES
- SUBSIDENCE

PROFITABILITY CONCERNS

- DEBT SERVICE
- PLANT CAPACITY FACTOR
- COST OF MONEY
- FUEL COMPONENT OF ELECTRICITY PRICE
- OPERATION AND MAINENANCE COST
  - WORKOVER
  - MAKE-UP WELL DRILLING
  - OTHER OPERATIONS (INJECTION, CORROSION/SCALE ABATEMENT, GAS EMISSIONS CONTROL, MAINTENANCE OF SURFACE FACILITIES)
  - ADMINISTRATION/MANAGEMENT

SENSITIVITY TO RATE VARIABLES

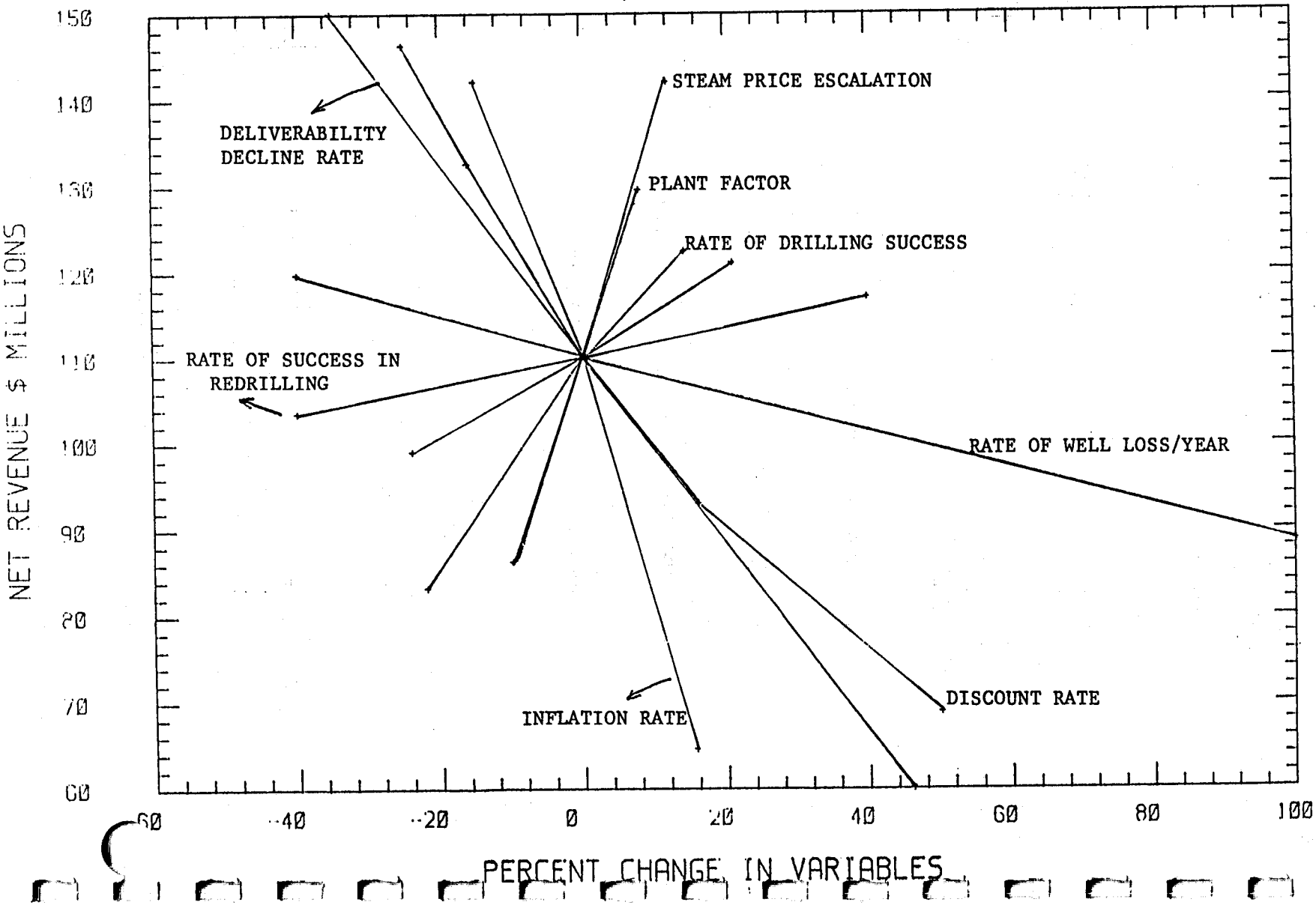

SENSITIVITY TO COST VARIABLES

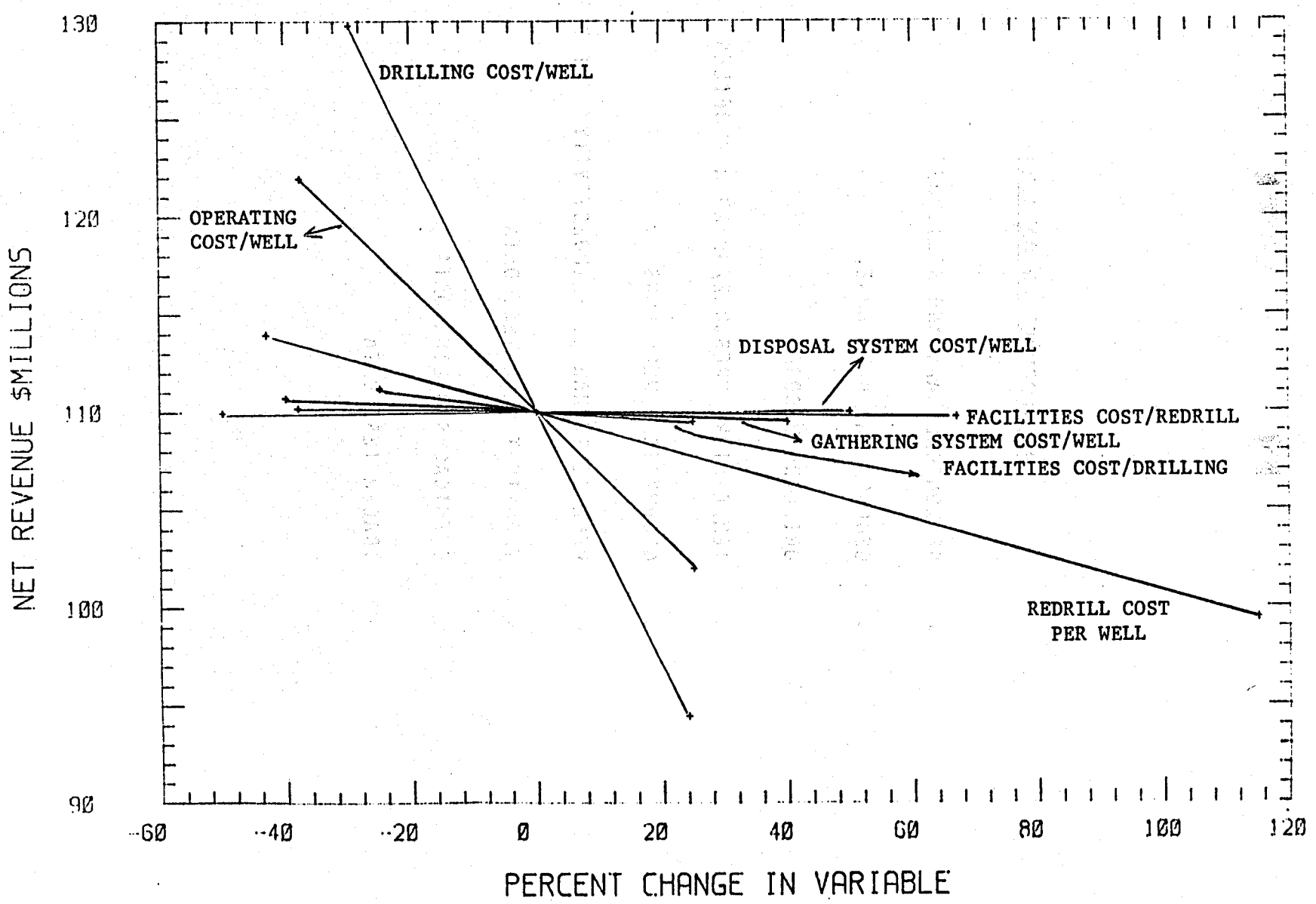

PRE-PRODUCTION DATA BASE

- GEOLOGICAL MAPS AND SECTIONS
- GEOCHEMICAL DATA BASE
- DRILLING RECORDS
- TEMPERATURE/PRESSURE/SPINNER PROFILES
- GEOPHYSICAL WELL LOGS
- WELL DELIVERABILITY/INJECTIVITY/TEST DATA
- TRANSIENT WELL TEST DATA
- CHEMICAL SAMPLING DATA
- TRACER TEST DATA

DATA BASE GENERATED DURING PRODUCTION

- MONITORING DATA FROM OLD WELLS:
  - MASS RATE VERSUS TIME
  - ENTHALPY VERSUS TIME
  - WELLHEAD PRESSURE VERSUS TIME
  - WELLHEAD TEMPERATURE VERSUS TIME
  - DOWNHOLE PRESSURE VERSUS TIME
  - TRACER CONCENTRATION VERSUS TIME
  - CHANGES IN FLUID CHEMISTRY WITH TIME

FORECAST OF RESERVOIR AND WELL BEHAVIOR

- FUTURE CHANGES IN FLUID PRESSURE, ENTHALPY AND CHEMISTRY
- FUTURE CHANGES IN PLANT/SURFACE EQUIPMENT DESIGN
- FUTURE MAKE-UP WELL REQUIREMENT
- FUTURE WORK OVER REQUIREMENT
- FUTURE CHANGES IN WELL SITING AND DRILLING
- FUTURE CHANGES IN SUSTAINABLE PLANT CAPACITY
- ECONOMICS OF FUTURE PRODUCTION
- EXPANSION IN INSTALLED POWER CAPACITY

DATA ANALYSIS APPROACH

QUANTITATIVE MODELING OF RESERVOIR AND WELL BEHAVIOR

- LUMPED PARAMETER MODELING
- ANALYTICAL MODELING OF PRESSURE BEHAVIOR
- NUMERICAL MODELING OF PRESSURE/TEMPERATURE/ENTHALPY/SATURATION/CHEMICAL BEHAVIOR
- WELLBORE SIMULATION
- TRACER FLOW MODELING

DATA ANALYSIS APPROACH

EMPIRICAL ANALYSIS OF PRODUCTION TRENDS

- NORMALIZED PRODUCTION RATE
- ENTHALPY TREND
- DELIVERABILITY TREND
- FLUID CHEMISTRY TREND
- TRACER RESPONSE TREND
- SATURATION TREND

DATA ANALYSIS APPROACH

UPDATING OF CONCEPTUAL, HYDROGEOLOGICAL MODEL

- INTEGRATION OF ALL NEW WELL DATA
- VERIFICATION AND/OR MODIFICATION OF THE ORIGINAL MODEL
- UPDATED EVALUATION OF RESERVES

DATA BASE GENERATED DURING PRODUCTION

- WORKOVER AND WELL MAINTENANCE RECORDS:
  - CASING CALIPER LOGS
  - TEMPERATURE/PRESSURE/SPINNER PROFILES WITH TIME
  - TRANSIENT PRESSURE TESTS
  - SCALE REMOVAL RECORDS
  - CORROSION MONITORING RECORDS
  - WORKOVER RECORDS

DATA BASE GENERATED DURING PRODUCTION

- NEW WELL DATA:
  - DRILLING RECORDS
  - TEMPERATURE/PRESSURE/SPINNER PROFILES
  - GEOPHYSICAL WELL LOGS
  - WELL DELIVERABILITY/INJECTIVITY TEST DATA
  - TRANSIENT WELL TEST DATA
  - CHEMICAL SAMPLING DATA

WELL/RESERVOIR BEHAVIOR FORECASTING:
METHODS IN INCREASING ORDER OF COMPLEXITY

- DECLINE CURVE ANALYSIS
- MATERIAL BALANCE
- ANALYTICAL SIMULATION OF PRESSURE BEHAVIOR
- NUMERICAL SIMULATION OF SINGLE-PHASE RESERVOIR
- NUMERICAL SIMULATION OF SINGLE-PHASE RESERVOIR WITH DISSOLVED SOLIDS
- NUMERICAL SIMULATION OF TWO-PHASE RESERVOIR
- NUMERICAL SIMULATION OF TWO-PHASE RESERVOIR WITH DISSOLVED GAS

PROBLEMS IN NUMERICAL RESERVOIR MODELING

- BUDGET
- CONCEPTUAL MODEL
- WHAT NUMERICAL MODEL - 0-D? 1-D? 2-D? 3-D? SINGLE PHASE? 2-PHASE? WITH GAS? WITHOUT GAS? HOW MANY BLOCKS?
- RELATIVE PERMEABILITY CHARACTERISTICS
- BOUNDARY CONDITIONS
- MODEL CALIBRATION
- IS INITIAL-STATE MODELING NECESSARY?
- LEVEL OF CONFIDENCE

ENVIRONMENTAL PROCESSES AND CHANGES

GRC WORKSHOP June 15-16, 1989

Mike Sorey

U.S. Geological Survey

I. INTRODUCTION TO ENVIRONMENTAL ASPECTS

A. Surficial thermal features

1. Hot springs: neutral ph-high chloride or acid-sulfate
2. Fumaroles: boiling point or superheated
3. Heat flow: conductive or advective (water or steam)

B. Subsidence: pressure or temperature induced

C. Seismicity: natural or induced

II. IMPACTS ON SURFICIAL THERMAL FEATURES

A. Types of impacts

B. Subsurface processes

1. Pressure changes
   a. Effects of injection and boundaries
   b. Rate of spread of pressure changes
2. Boiling and excess steam generation
3. Temperature changes: from injection and/or recharge

III. FIELD EXAMPLES

A. Impacted areas: Steamboat Springs, NV; Long Valley, CA;
Beowawe, NV; Klammath Falls, OR; Geysers, CA
Wairakei and Rotorua, NZ, Other fields

B. New Zealand fields

1. Wairakei

2. Rotorua

C. Steamboat Springs

1. Development status

2. Geyser activityu

3. Thermal-water inflow to Steamboat Creek

D. Long Valley caldera

1. Development status

2. Hot Springs

3. Subsidence

IV. MITIGATION AND MONITORING

A. Injection: pressure support versus thermal breakthrough

B. Monitoring programs and legislation

1. Public and private lands

2. National Parks

GEOTHERMAL EXPLOITATION EXPERIENCE

CASE HISTORIES FOR THREE GEOTHERMAL FIELDS IN ICELAND

BENEDIKT STEINGRÍMSSON

ORKUSTOFNUN, GEOTHERMAL DIVISION

GRENSÁSVEGUR 9, 108 REYKJAVÍK, ICELAND

PREPARED FOR GRC WORKSHOP ON:

RESPONSES OF A GEOTHERMAL FIELD DURING EXPLOITATION

BERKELEY, CALIFORNIA

June 15-16, 1989

INTRODUCTION

Hydrothermal activity is widespread in Iceland. The numerous warm spring, geysers, mudpools and fumaroles surprised the first Norwegian settlers in 876 A.D., and many localities have since been named after thermal manifestations, such as the capital Reykjavík (Smoky bay) which draws it name from thermal springs now within the city limits. Although the geothermal manifestations filled the ancient Icelanders with wonders and some fear, we have very few historical accounts where this energy resource was put to use. Certainly this use was on a small scale and limited to bathing, washing and cooking and was so for centuries.

The first commercial exploitation of geothermal fields in Iceland dates at least back to the 12.th century. However it was not the thermal energy but the sulphur deposits of the fields that were exploited. Sulphur mining continued until this century. Most of the sulphur was exported to Denmark and used there in gunpowder production.

More or less simultaniously with the decay of the sulphur mining industry a large scale exploitation of the geothermal fields was initiated. Geothermal water was used for district heating and greenhouse farming. The first district heating system, in Reykjavík, was put on line in 1930, supplying hot water to 70 buildings, including a school house and a swimming pool. The water, 15 l/s, 93 ° C, was taken from hot springs and shallow wells in what now is known as the Laugarnes field. The Reykjavik heating system was expanded considerably in the 1940's and later in the 1960's, when downhole pumps were installed in wells, in order to increase the fluid production. Concurrant with the expansion of the district heating system in Reykjavík rapid developments followed in other parts of the country, especially after the impetus given by the increase in oil prices during the 1970's. The main emphasis was on space heating, but other uses emerged gradually. In 1967 the diatomite plant at lake Mývatn began operation using steam from the Námafjall field for drying. A 3 MW non-condensing electric turbine was put on line in Námafjall in 1969 and the Krafla electric power plant (30 MW) began operation in 1977. At the Svartsengi field a high temperature brine has been used since 1976 to heat up cold ground water for space heating, but also to generate 8 MW of electricity. Currently a thermal power plant is under construction at the Nesjavellir field to harness the high temperature there for space heating and cogeneration of electricity.

Today geothermal energy plays an important role in the energy economy of Iceland. About 40 geothermal district heating systems are in operation meeting about 85% of the energy demand for space heating in the country. The total annual geothermal energy consumption, however, constitutes about 40% of the total energy sold to users.

GEOTHERMAL FIELDS IN ICELAND.

The geothermal areas are divided into two categories on the basis of the

subsurface temperature in the systems. By definition, fields with temperatures exceeding 200 ° C at 1 km depth are classified as high-temperature fields, but low-temperature fields if the temperature at this depth is lower than 150 ° C.

The high-temperature fields are all confined to the active volcanic zones that bisect Iceland from southwest to northeast. To date, 28 potential high-temperature fields have been identified. Major reservoir rock types are hyaloclastides, basaltic lava flows and igneous intrusives, but the common surface manifestations are thermally altered ground, mudpools, fumaroles and steaming ground.

The major low-temperature fields are found on the flanks of the volcanic zones in Quaternary formations, but smaller fields are found almost all over the country. Over 600 thermal springs have been recognized in about 250 localities. Flowrate from springs generally varies in the range of few liters upto tens of liters per second. The maximum flowrate from a single vent is 180 l/s of 100 degree hot water.

EXPLOITATION EFFECTS.

The exploitation of several geothermal fields in Iceland has now lasted for some decades. Initially, the exploitation was limited to natural discharge at surface from hot springs or free flow from shallow wells. Where demand has exceeded the natural discharge or free flow from wells has diminished, downhole pumps have been installed in order to increase the water production. It is not uncommon today that production from a field exceeds the original natural discharge by a factor of 10-30. The geothermal systems have responded to this large scale exploitation in several ways: Surface activity has diminished or even disappeared, areas have subsided, reservoir pressures have declined and fluctuated in harmony with production rates, production temperature and fluid chemistry has changed due to increasing recharges to the system and in the high-temperature fields two phase regions have developed and expanded.

Table 1 summarizes the utilization and its effects on some of the major fields. Most of them had natural discharge, as thermal springs, before exploitation started. A summary for some of the explored high-temperature fields is given in Table 2. The Krafla field is used for electricity generation. The presently available steam suffices 35 MW_e production of which 30 MWsude are connected. The Svartsengi field is used for district heating (120 MW_t) and generation of 8 MW_e of electricity. Cogeneration of thermal and electric power is also planned for the Nesjavellir field where 100 MW_t thermal power and 5 MW_e electric power will be on-line in 1990 with possible expansion later to 300 MW_t and upto 70 MW_e.

Following is a summary of the development and utilization of three geothermal fields. Examples of observed responses due to their exploitation will be given during the presentation.

THE LAUGARNES FIELD.

The Reykjavík Municipal District Heating Service utilizes geothermal water from three separate fields, two of

which are located within the city limits, the Laugarnes and the Elliðaár field. Drilling for hot water began in the Laugarnes field in 1928 and exploitation was initiated in 1930. Available flowrate was 15 l/s of 93 ° C hot water. In 1940's two more wells were drilled adding 6 l/s of free flowing water. During 1957-63, 14 medium deep wells were drill increasing the artesian flow to 50-60 l/s. Deep (>1000 m) drilling began in 1958, and the first downhole pump was installed a year later. Artesian flow ceased in 1965, and since then downhole pumps have been operated in 12 deep wells. Today a total of 26 deep wells have been drilled in the field, the deepest one reaching down to 3085 m depth. The production from the field increased steadily during the 1960's but has since 1968 averaged at 5-6 Gl per year. Maximum production during the coldest part of the year is about 300 l/s.

Exploration data has revealed three separate major aquifers in the Laugarnes field, designated A, B and C. Aquifer A extends from 250- 650 m depth and contains water at 110-120 ° C, aquifer B from 730-1250 m depth with 135 ° C water and finally aquifer C below 2150 m depth with water temperatures of 145-160 ° C. The aquifers were all artesian prior to the exploitation of the field but their initial pressure potential was never recorded. The fluid from Laugarnes was low in total dissolved solids, about 350 ppm, of which 35 ppm was chloride.

Production from the Laugarnes field has caused a considerable pressure drawdown within the production wellfield and vicinity. The total area affected by exploitation is 6-7 sq.km, more than twice the size of of the production field. As the initial pressure potential of the field is unknown, so is the total drawdown. Since 1963, however, has the well head pressure and later the water level in observation wells been monitored carefully. The total drawdown to this date is of the order of 120 m.

The exploitation of the field has not had any effect on production temperatures, but some gradual changes have been measured in the fluid chemistry. The concentration of chloride has dobbled in production fluid and few wells produce now water with 100-200 ppm chloride concentration. The concentration of silica and fluoride has on the other hand showed a small decline during the exploitation years. The chemical changes are believed to be caused by an infiltration of a highly saline water into the uppermost part of the reservoir, aquifer A. Some of this fluid enters the reservoir through wells due to shallow casings. The mixing of the reservoir fluid with more saline ground water within the wellbores has caused calcite deposition in downhole pumps in wells where chloride concentrations have reached 100 ppm. Steps have been taken to stop the leakage of saline water in the reservoir. Idle wells which show downflow of saline water have been plugged with cement and new production wells will be cased deeper than present production wells.

THE ELLIDAÁR FIELD.

The Ellidaár field was discovered in 1967, when the first deep well was drilled in the area. To this date 16 deep wells (900-2300 m) have been drilled in the area. Production from the field started in january 1968 and since 1970

the annual fluid production has been in the range of 4 to 5 Gl. The peak pumping rate from six producing wells has been about 180 l/s.

Three aquifers have been revealed in the Ellidaár reservoir, aquifers A,B and C. Aquifer A is found above 300-500 m depth, with water temperature of 40-90 ° C. Aquifer B extends down to 1100 m depth and overlies aquifer C, which extends to the bottom of the deepest well. The temperature within the B aquifer is as high as 110 ° C, but 70-115 ° C in the C aquifer. Aquifers A to C were artesian prior to exploitation of the field, leading to a well head pressure of 1,7 and less than 7 bar, respectively.

The pressure history of the field shows a rapid drawdown or recovery each time pumping from the field is changed. At a constant pumping rate for 1-2 mounths, pressure stabilization occurs, indicating a massive recharge of fluid to the reservoir. Monitoring of production temperatures and fluid chemistry shows, that the recharge is of groundwater origin. Cooling, of up to 20 ° C, has been observed since 1968 and the concentration of silica and fluoride has decreased at the same time as the concentration of oxygen in the water has increased drastically.

THE SVARTSENGI HIGH-TEMPERATURE FIELD.

The Svartsengi field is located within the active volcanic zone on the Reykjanes peninsula. Unlike most other high-temperature fields in Iceland only minor geothermal manifestations were seen on the surface. The existence of the field was proved in 1971, when the first well was drilled to a depth of 240 m. Today eleven wells have been drilled in an area of 1.5 km2 to a depth of 240-1998 m. Seven wells are used as producers and one well for reinjection purposes.

The Svartsengi system is liquid dominated and contains fluid with a salinity of 2/3 that of seawater. Reservoir temperature is 240 ° C. The top of the reservoir is found at about 500 m depth, except in the eastern part of the wellfield where a two phase zone extends to the surface. The rest of the system is overlain by a warm groundwater aquifer, which initially had about 6 bar higher pressure potential than the geothermal reservoir.

Production data, including fluid extraction and reinjections rates, pressure drawdown, fluid chemistry and downhole temperatures, have been monitored closely since the start of production on 18 October 1976. The rate of fluid production increased steadily for the first five years, but has since leveled out at about 300 kg/s. From the start of production, all spent fluid have been disposed at the surface. A minor reinjection test was carried out in 1982 when cold groundwater was injected for 24 days, but in the reinjection program, that has been executed since 1984, the injection fluid has been 80 °C freshwater. The average reinjections rates have been about 50 kg/s.

The production data from Svartsengi shows several effects caused by the fluid production from, and reinjection into, the system. Rapid drawdown of more then 100 m in monitoring wells has been observed in the wellfield and a drawdown of 5 bar has been measured during 1983-1989 in Eldvörp, a high temperature area at about 5 km distance

from Svartsengi. The nearsurface two phase zone in the eastern part of the well field has expanded and the discharge of the only producing well from this zone has consisted exclusively of dry steam since 1984. The gas content of the discharged fluids have steadily decreased, and degassing of the reservoir appears to be taking place. This is supported by a steady rise in H_2S/ CO_2 ratio and a decline in the magnesium concentration of the fluid. Some long-period oscillations have been observed in measured downhole temperatures and these agree with variations seen in silica geothermometer temperatures. These variations have not been explained but, it is speculated that tectonic events in the volcanic zone may have led to fracture movements causing a burst of cold water into the system.

The reinjection well (well 12) in Svartsengi is located within the production wellfield. The injection of warm freshwater during the last few years has influenced the production characteristics of at least one well (well 6), located about 300 m away from the injector. A significant temperature drop (12 ° C) has been measured in that well and a decline by a least a quarter has been observed in the concentration of most dissolved minerals in fluids from well 6 since 1984.

ACKNOWLEDGEMENTS.

I thank the District Heating Services of Reykjavík and Sudurnes for permission to use data from their fields in this presentation. Special thanks are extended to Einar Gunnlaugsson at Reykjavíks Municipal District Heating Service, Snorri Páll Kjaran at Vatnaskil Consulting Engineers and my colleagues at Orkustofnun for their contributions.

TABLE 1. Low-temperature geothermal fields. A summary from 1985.

Geothermal field	Utilization Start up year	Utilization Duration years	Accum. volume Gl	Ave. flow l/s	Pressure* and Temperature Initial bar	Initial °C	Present bar	Present °C	Decay bar	Decay °C	Remarks
Blonduos	1978	7	7	23	29	71	17	71	12	0	
Dalvik	1969	-	-	45	-	-	-	-	-	-	
Deildartunga	1981	3	8	160	-	-	-	-	-	-	Free flow
Egilsstadir	1979	4	3	22	4	66	3	51	1	15	
Ellidaar	1968	16	58	127	7	102	-4	92	11	10	
Hrisey	1973		-	6	1	68	1	59	0	9	
Husavik	1970		-	50	-	-	-	-	-	-	Free flow
Hvammstangi	1973		-	21	-	-	-	-	-	-	
Laugaland	1977	6	16	51	19	95	-16	95	35	0	
Laugal.Holtum	1982	2	2	21	12	101	-2	101	14	0	
Laugarnes	1930	55	111	158	8	125	-6	-	14	-	
Olafsfjordur	1944		-	31	-	-	-	-	-	-	
Reykholar	1974		-	2	-	-	-	-	-	-	Free flow
Reykir	1944	39	590	982	8	86	-3	85	11	1	
Saudarkrokur	1953	31	60	87	6	70	2	69	4	1	Free flow
Selfoss	1948	36	-	90	2	90	-4	81	6	9	
Seltjarnarnes	1972	14	15	46	1	107	-4	107	5	0	
Siglufjordur	1975	9	7	25	16	67	-2	67	18	0	
Sudureyri	1977	7	-	12	3	63	0	63	3	0	
Thorlakshofn	1979			21	3	135	3	135	0	0	Free flow

* Reference to mean sea level

TABLE 2. High-temperature geothermal fields.

Geothermal field	Reservoir	Start drill. year	No.of wells	Max.temp °C	Total avail. flow rate kg/s	Remarks
Eldvorp		1983	1	260	165.0	Exploration
Krafla	Upper-Leirbotnar	1974	14	210-220	178.2	
	Deeper-	1974		298-344		Decay 5 bars
	Sudurhlidar	1980	6	280-340	51.3	
	Hvitholar	1982	3	250-260	63.0	
Namafjall		1967	12	255-340	42.0	2 wells operating
Nesjavellir		1965	18	220-400	400	Under exploration
Svartsengi		1972	12	229-240	1060.0	Decay 9 bars
Reykjanes		1969	9		246.6	2 wells operating

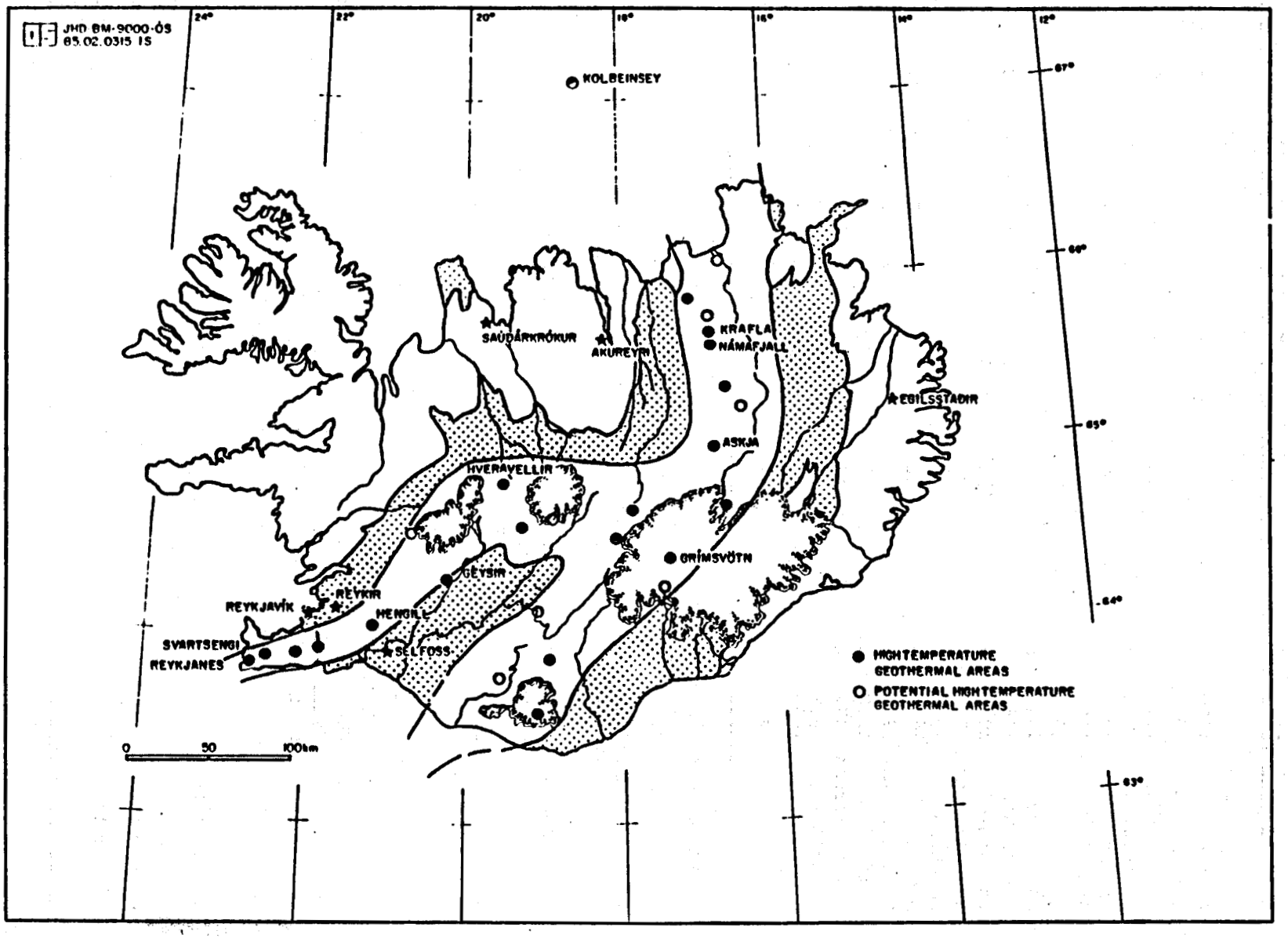
JHD BM-9000-ÓS
85.02.0315 IS
24°
22°
20°
18°
16°
14°
12°
67°
66°
65°
64°
63°
KOLBEINSEY
SAUÐÁRKRÓKUR
AKUREYRI
KRAFLA
NÁMAFJALL
EGILSSTAÐIR
ASKJA
HVERAVELLIR
GRÍMSVÖTN
GEYSIR
REYKIR
REYKJAVÍK
HENGILL
SVARTSENGI
REYKJANES
SELFOSS
0
50
100km
HIGHTEMPERATURE GEOTHERMAL AREAS
POTENTIAL HIGHTEMPERATURE GEOTHERMAL AREAS

OS-JHD
89-06-09 BS

TYPICAL PRESSURE CONDITIONS PRIOR TO EXPLOITATION

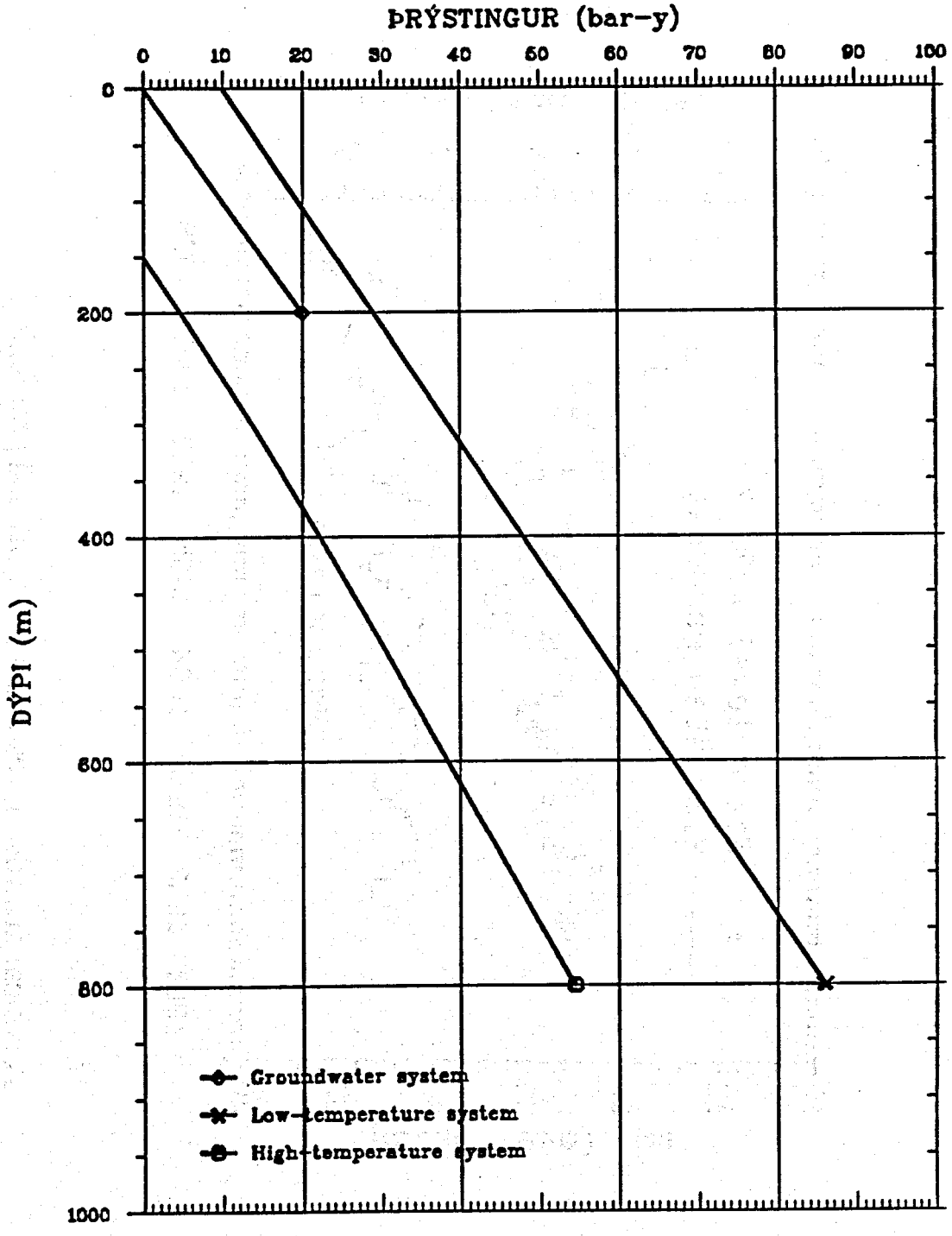

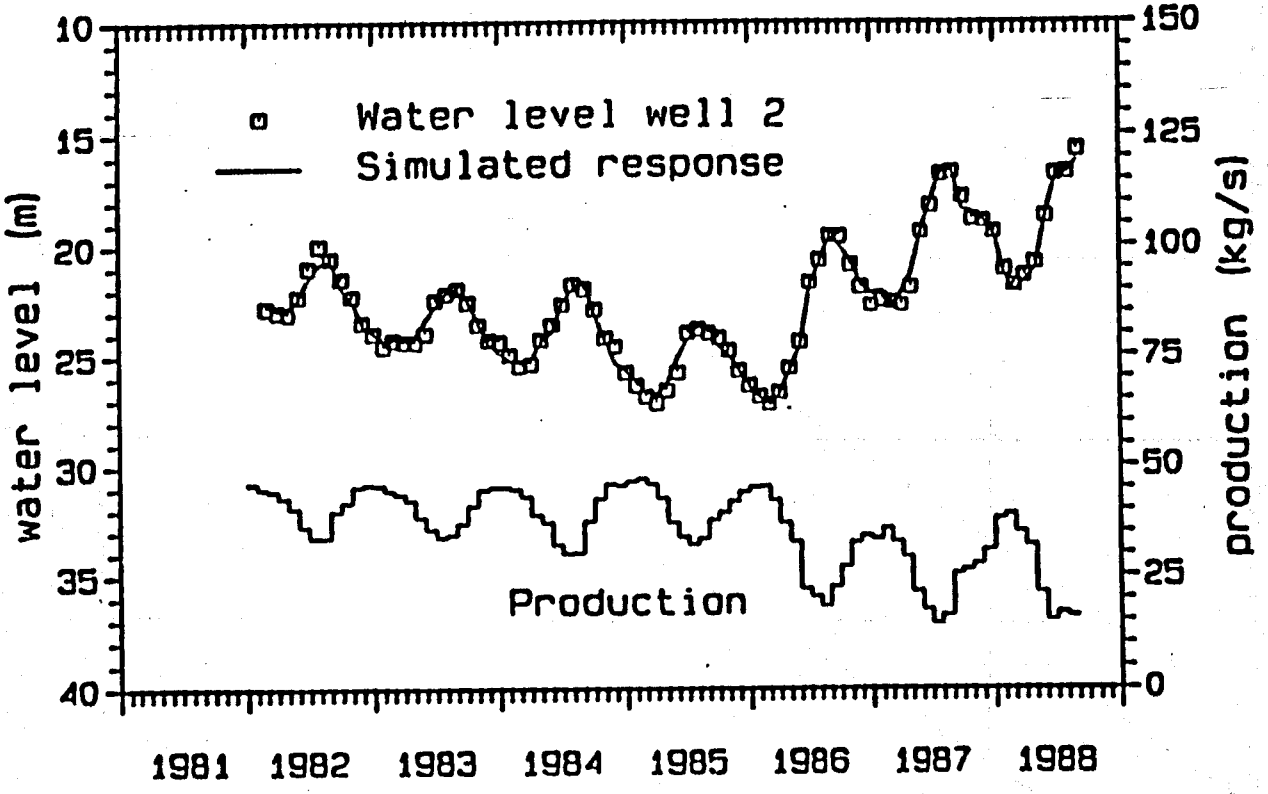

A typical drawdown response to a seasonal production from a low temperature field in Iceland.

OS-JHD
89-06-04 BS

HLEMMISKEID WELL H-2
Several temperature logs

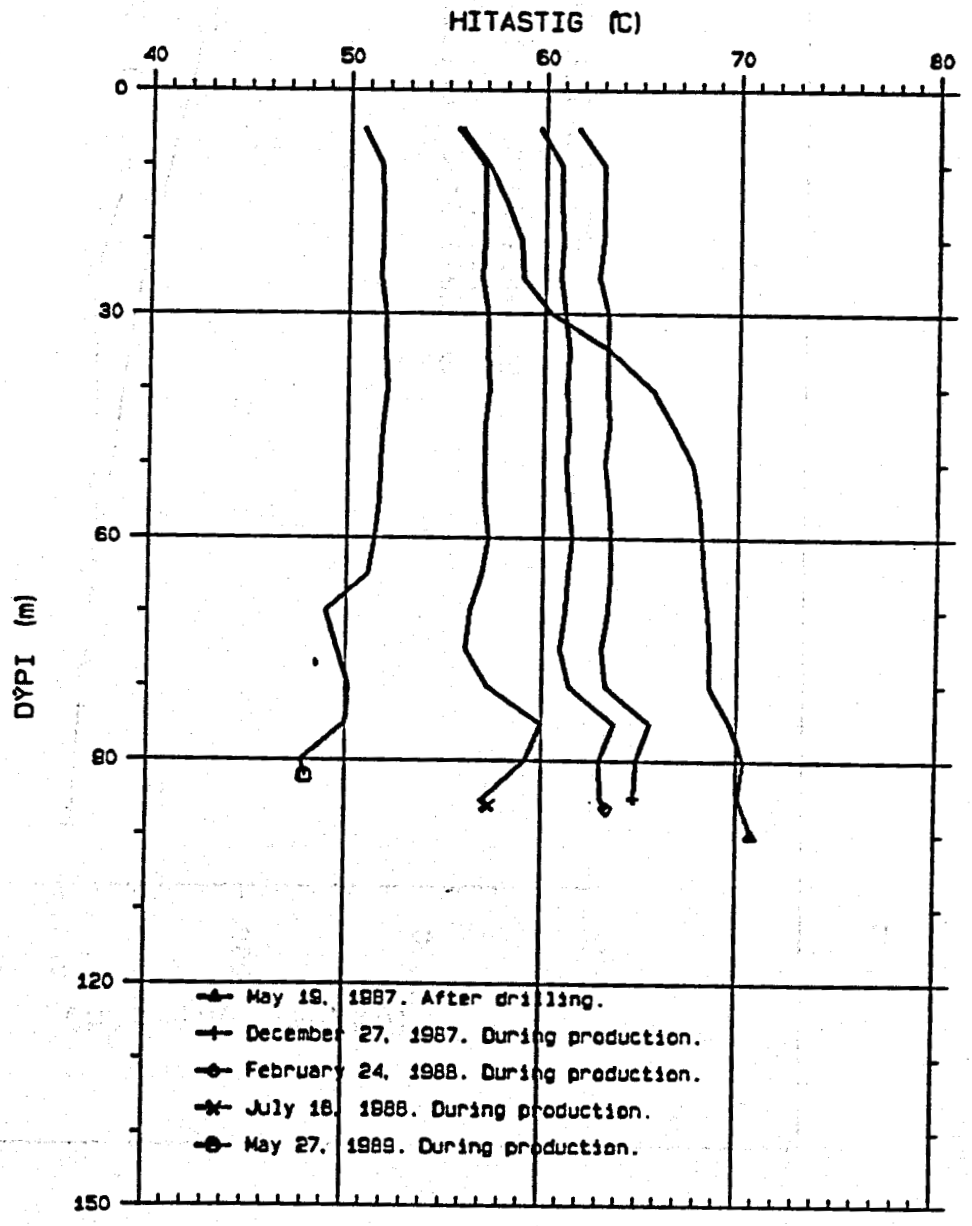

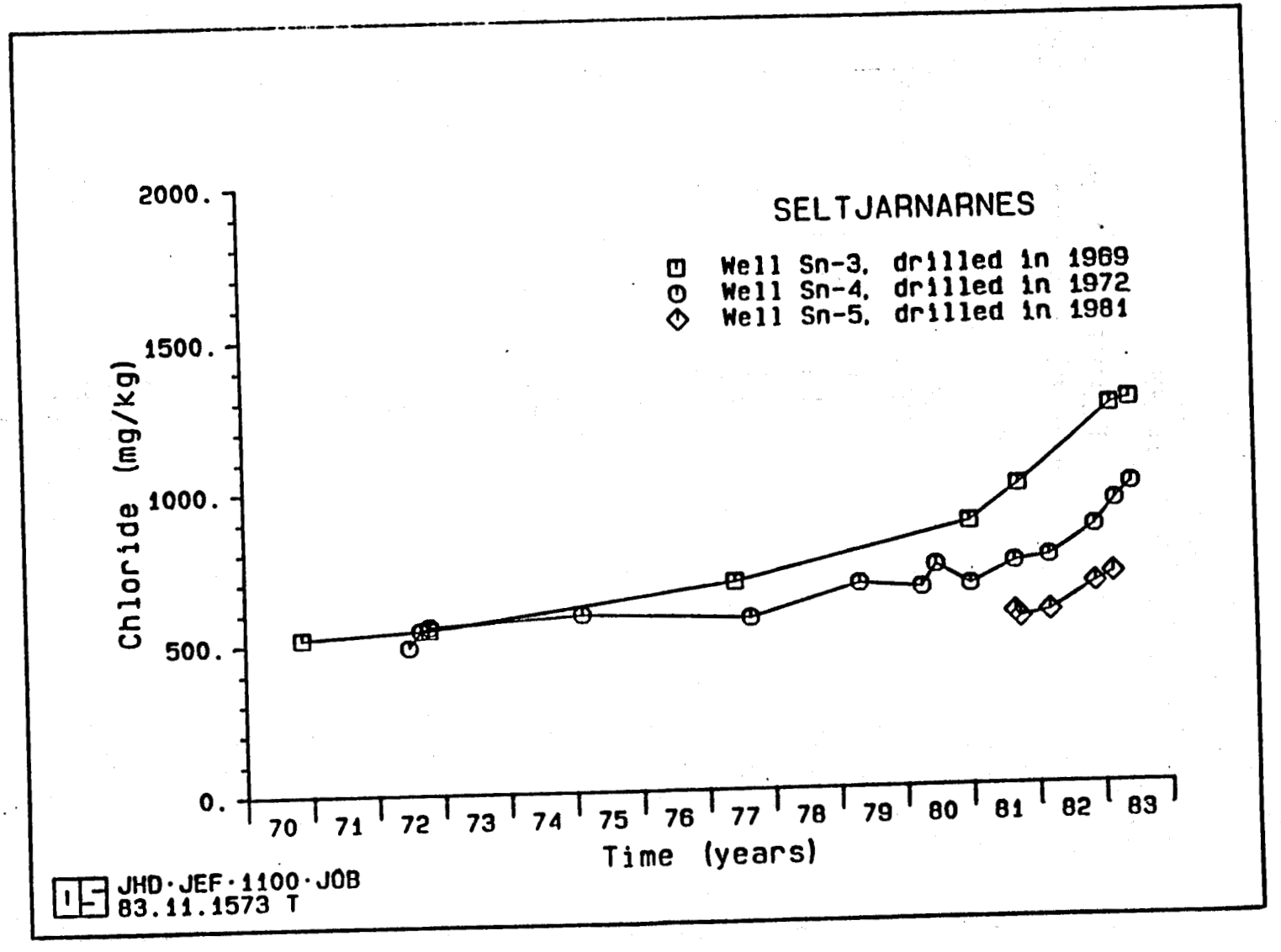
SELTJARNARNES
Well Sn-3, drilled in 1969
Well Sn-4, drilled in 1972
Well Sn-5, drilled in 1981
Chloride (mg/kg)
2000.
1500.
1000.
500.
0.
70
71
72
73
74
75
76
77
78
79
80
81
82
83
Time (years)
JHD·JEF·1100·JOB
83.11.1573 T

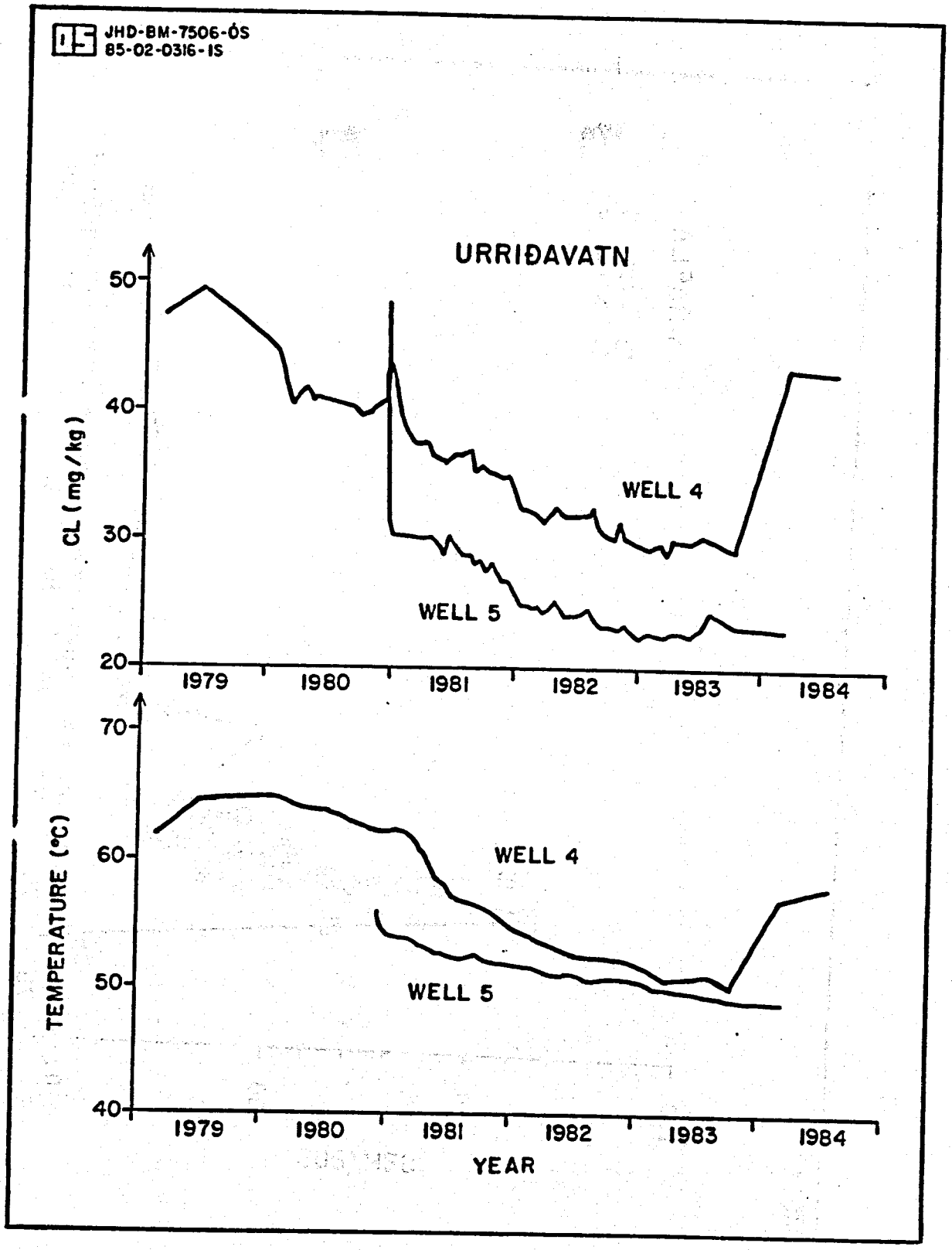
JHD-BM-7506-ÓS
85-02-0316-IS
URRIÐAVATN
CL (mg/kg)
50
40
30
20
WELL 4
WELL 5
1979
1980
1981
1982
1983
1984
TEMPERATURE (°C)
70
60
50
40
WELL 4
WELL 5
1979
1980
1981
1982
1983
1984
YEAR

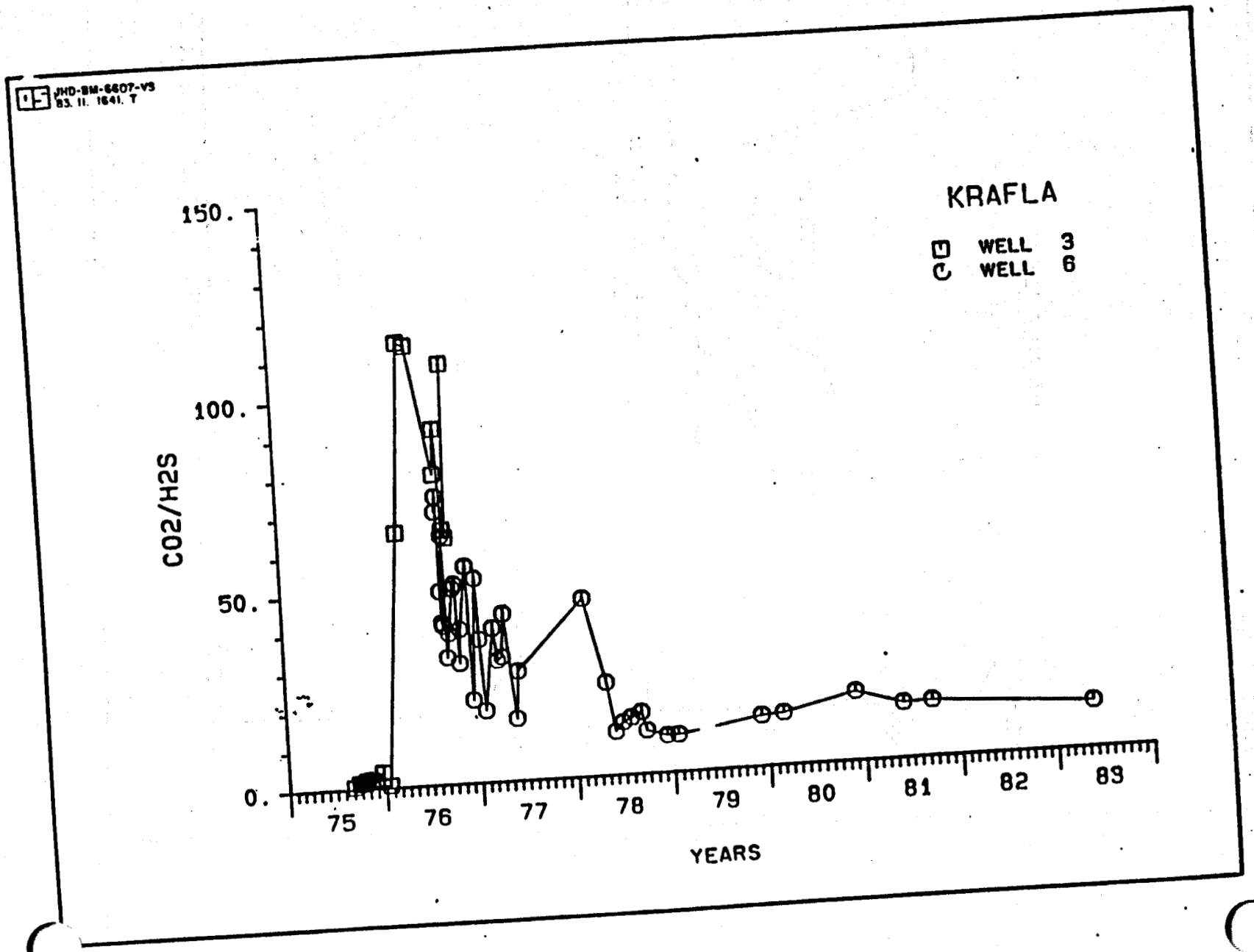
JHD-BM-6607-V3
83. 11. 1641. T
KRAFLA
WELL 3
WELL 6
150.
100.
50.
0.
CO2/H2S
75
76
77
78
79
80
81
82
83
YEARS

KRAFLA POWER PLANT

Land elevation 1975-1989

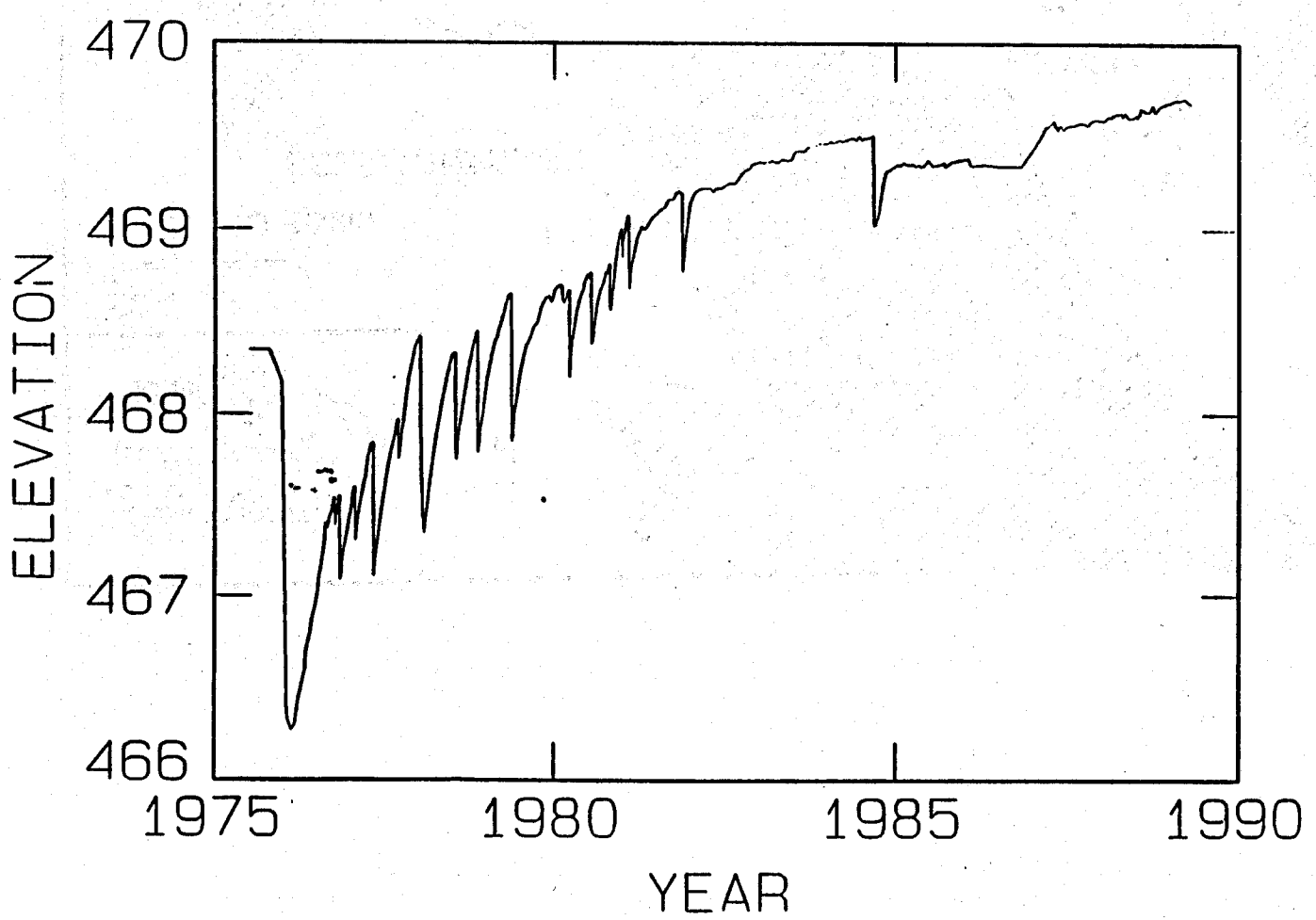

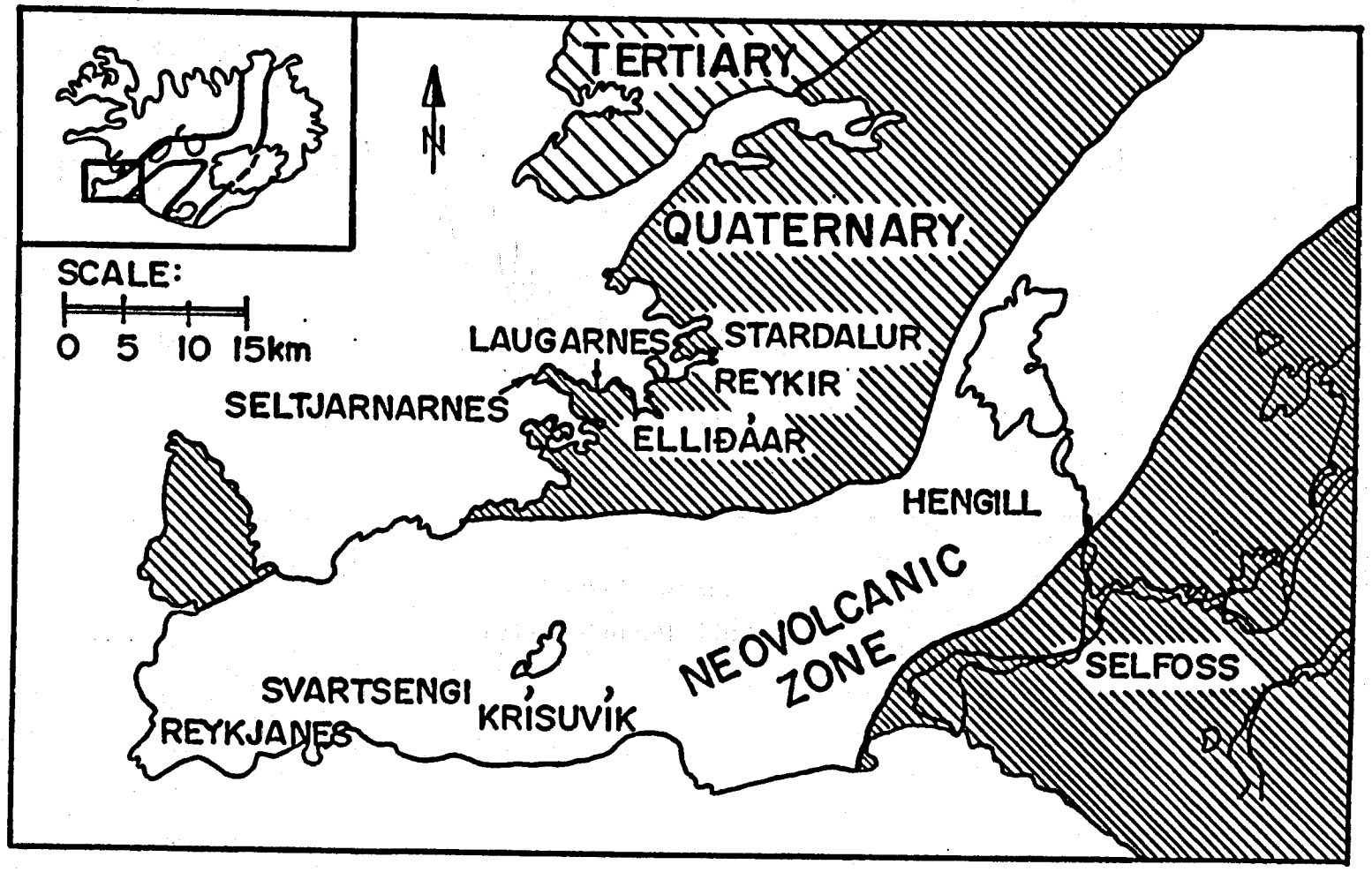
TERTIARY
QUATERNARY
N
SCALE:
0 5 10 15km
LAUGARNES
STARDALUR
REYKIR
SELTJARNARNES
ELLIÐÁAR
HENGILL
NEOVOLCANIC ZONE
SELFOSS
SVARTSENGI
KRÍSUVÍK
REYKJANES

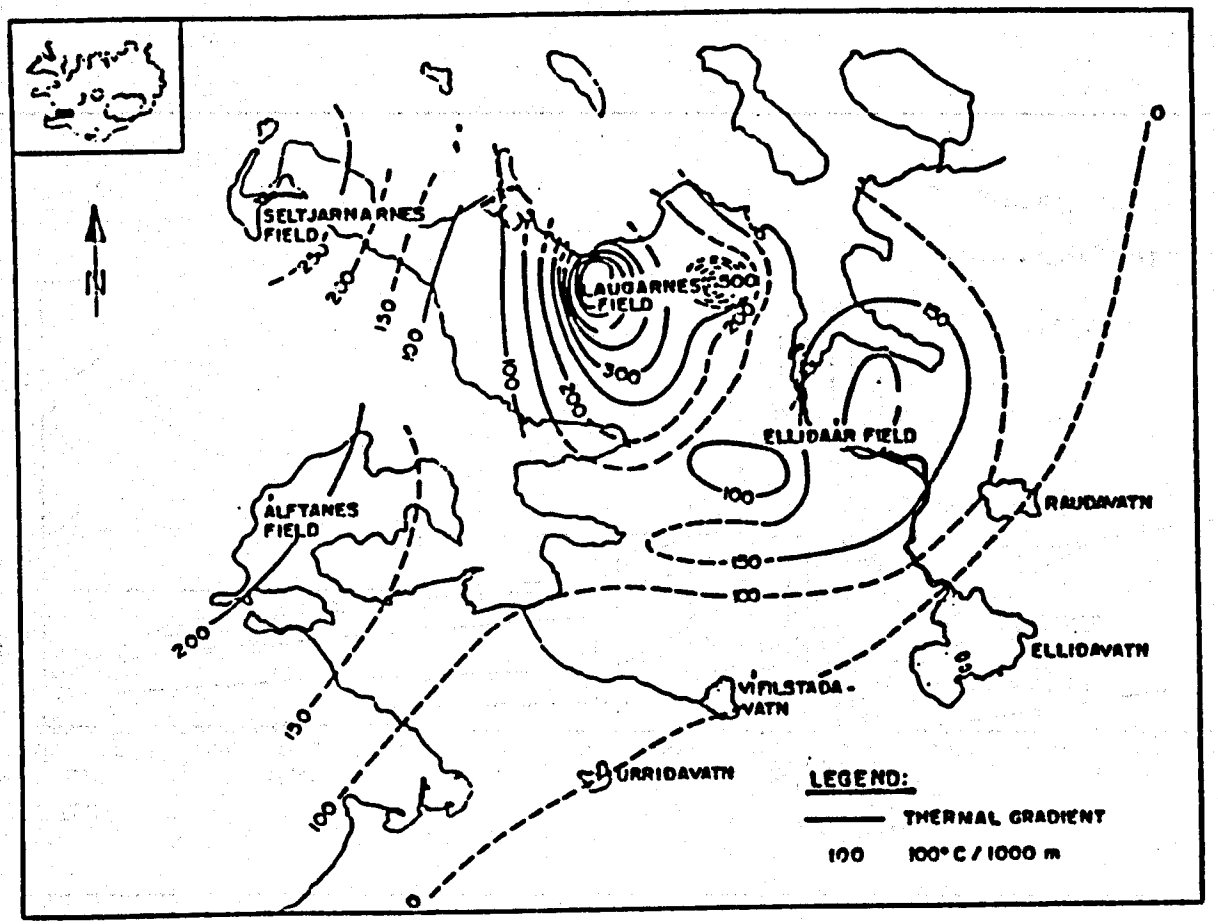

Thermal gradient map of Reykjavík and vicinity.

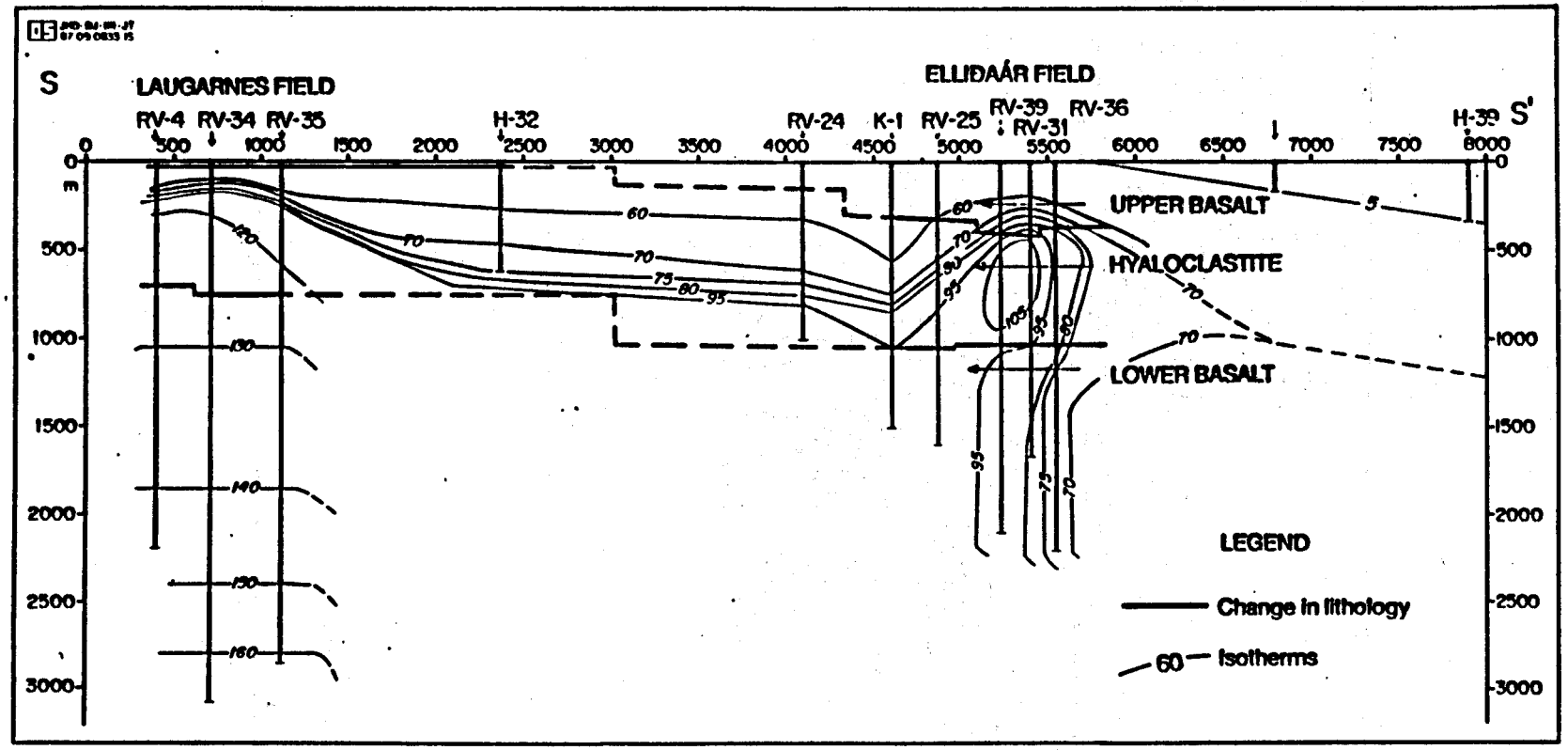
S
LAUGARNES FIELD
ELLIÐAÁR FIELD
RV-4
RV-34
RV-35
H-32
RV-24
K-1
RV-25
RV-39
RV-31
RV-36
H-39
S'
0
500
1000
1500
2000
2500
3000
3500
4000
4500
5000
5500
6000
6500
7000
7500
8000
m
UPPER BASALT
HYALOCLASTITE
LOWER BASALT
LEGEND
Change in lithology
60 Isotherms

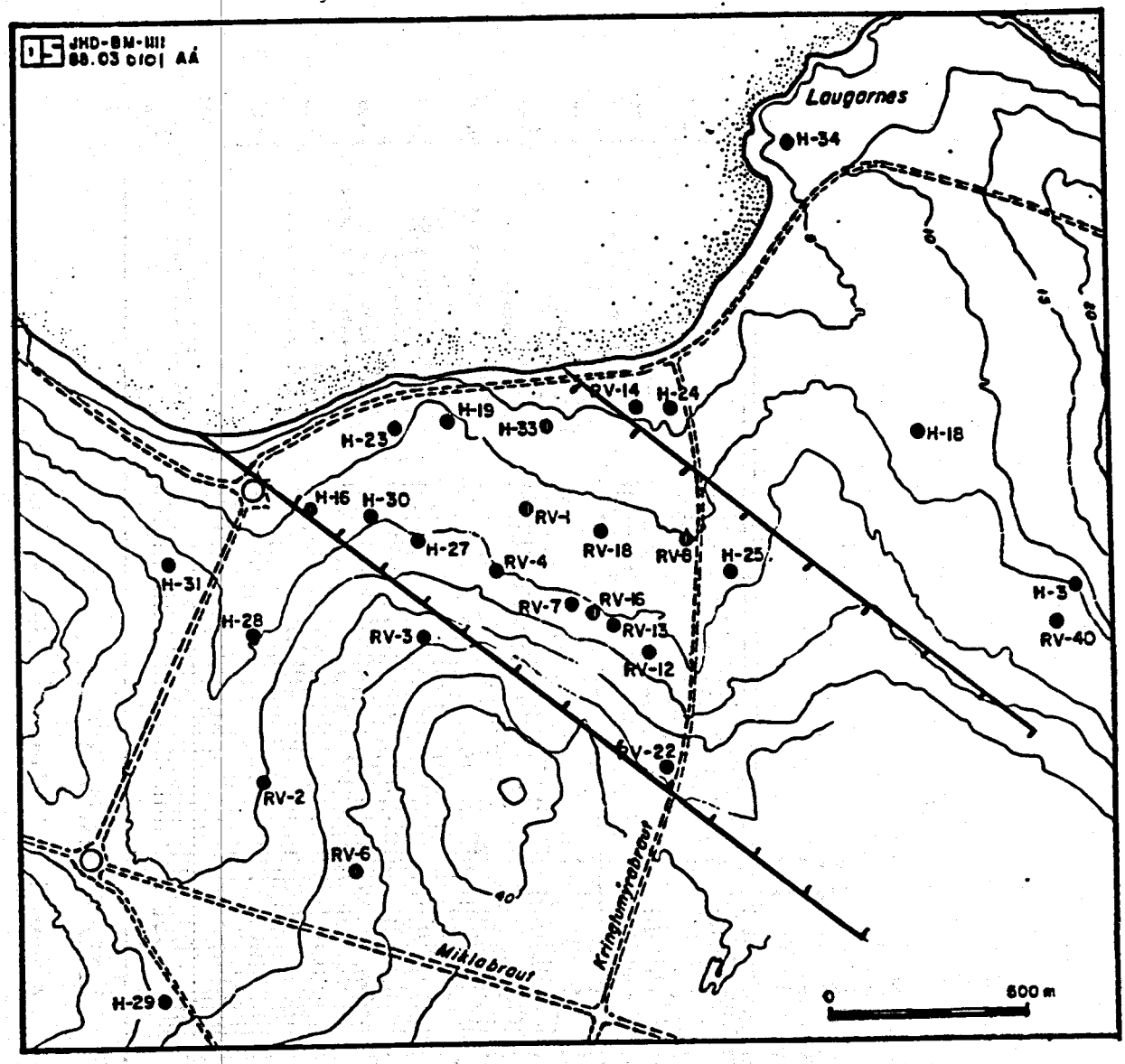

LAUGARNES FIELD.

Location of wells and faults inferred from well data.

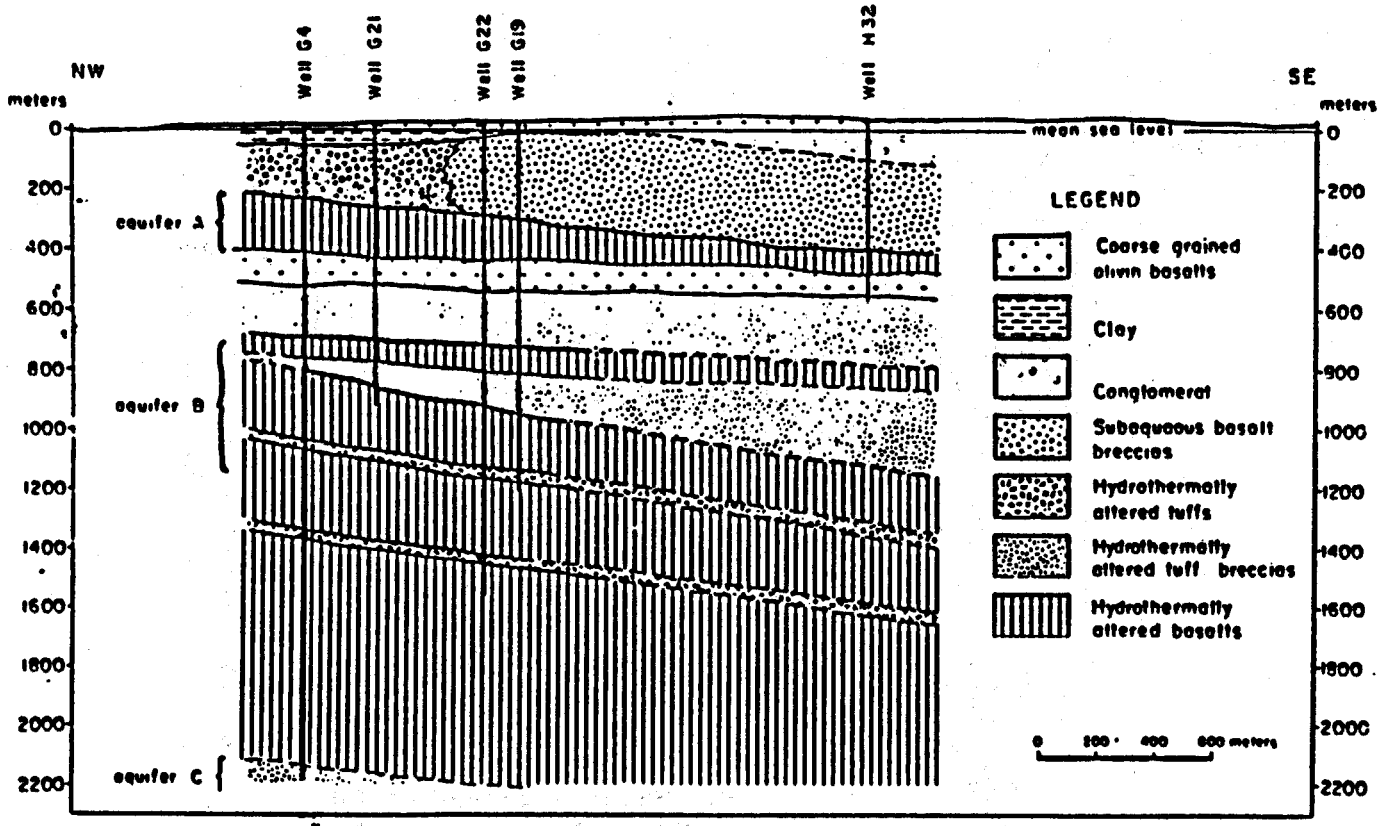

LAUGARNES FIELD.

A generalized NW to SE geologic cross-section.

LAUGARNES FIELD.

Annual mass extraction 1963-1988.

The extraction 1928-1963 is estimated 10 Gl.

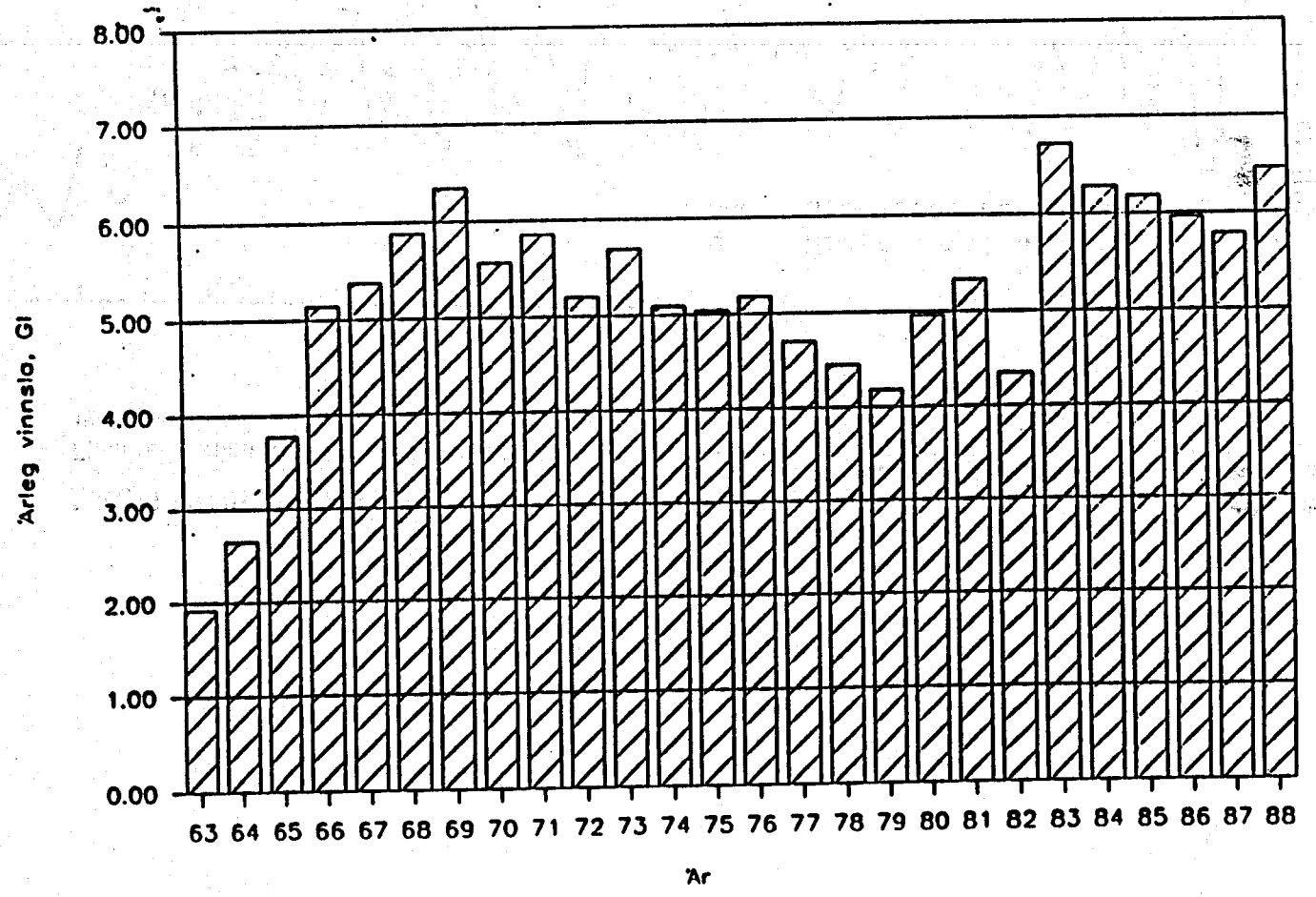

LAUGARNES FIELD.

Fluid production from the field and observed and calculated water level fluctuations; 1962-1982.

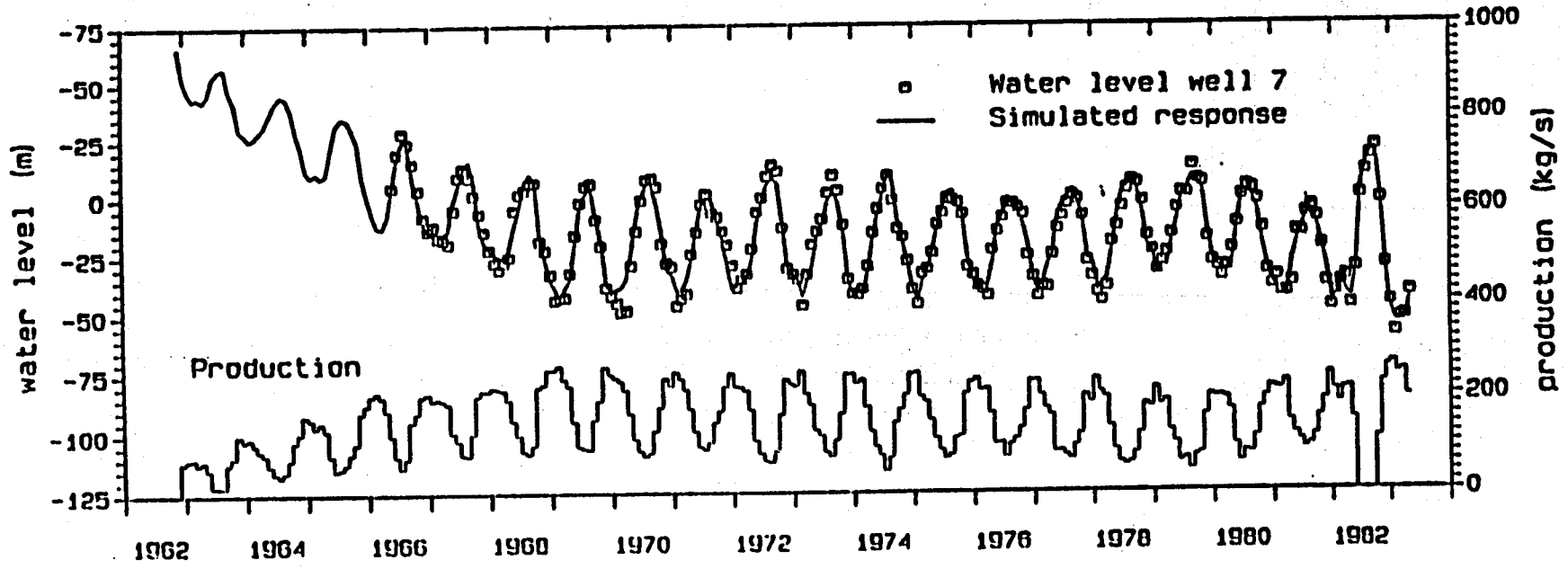

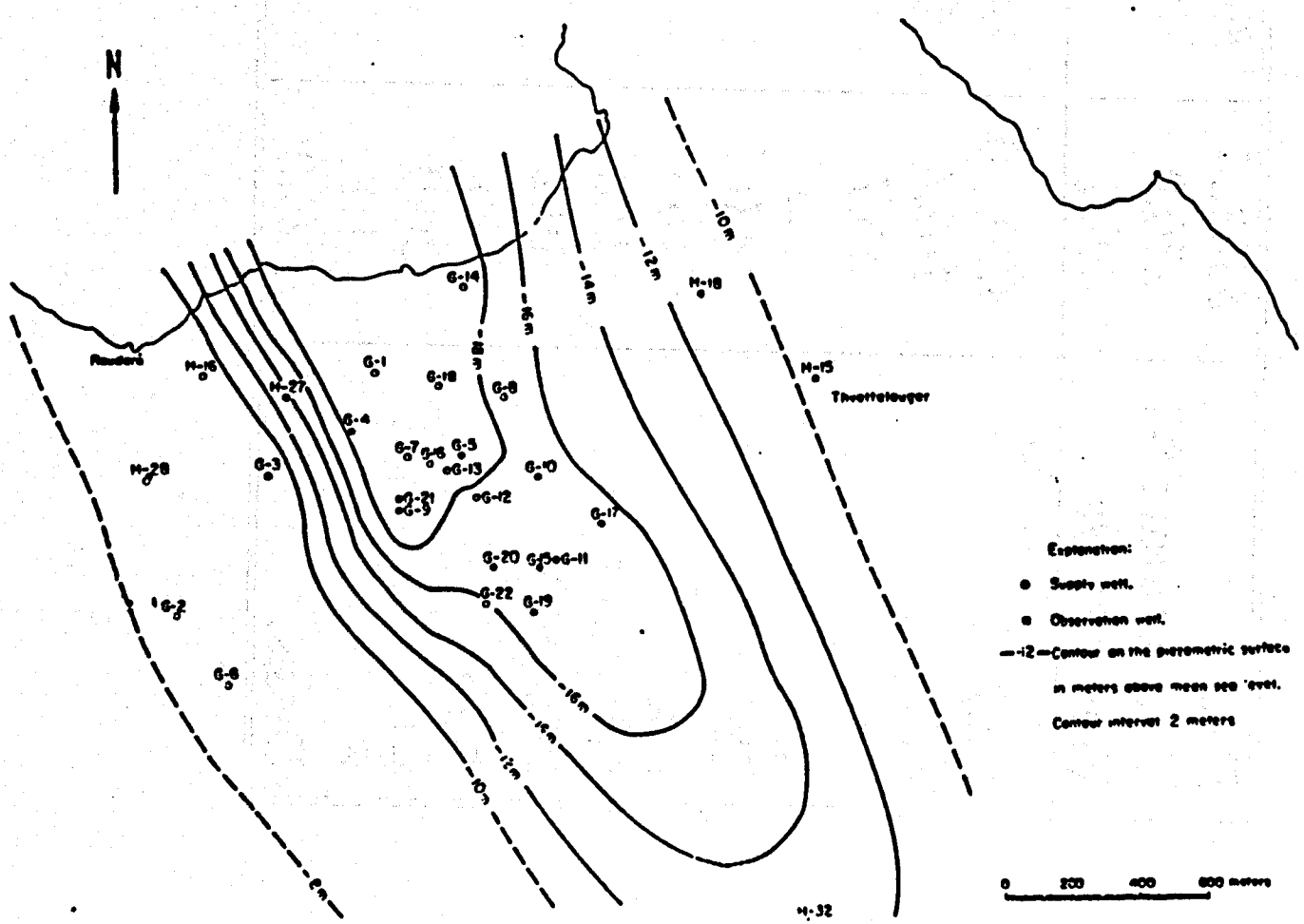

LAUGARNES FIELD.

Elevation of the pizometric surface on November 15, 1967.

LAUGARNES FIELD WELL RV-5
Chemical analysis of production fluid, 1963 and 1989.

Date	630306	890110
Temperature °C	130.0	129.9
Flowrate l/s	29.0	52.0
pH/°C	8.70/20	9.47/21
SiO_2	162.4	143.6
Na	56.7	75.8
K	2.5	3.0
Ca	4.0	3.8
Mg	<0.1	0.01
CO_2(tot)	22.0	15.3
SO_4(tot)	19.2	31.8
H_2S	0.5	0.21
Cl	30.0	61.6
F	1.1	1.0
Diss.s.	324.0	

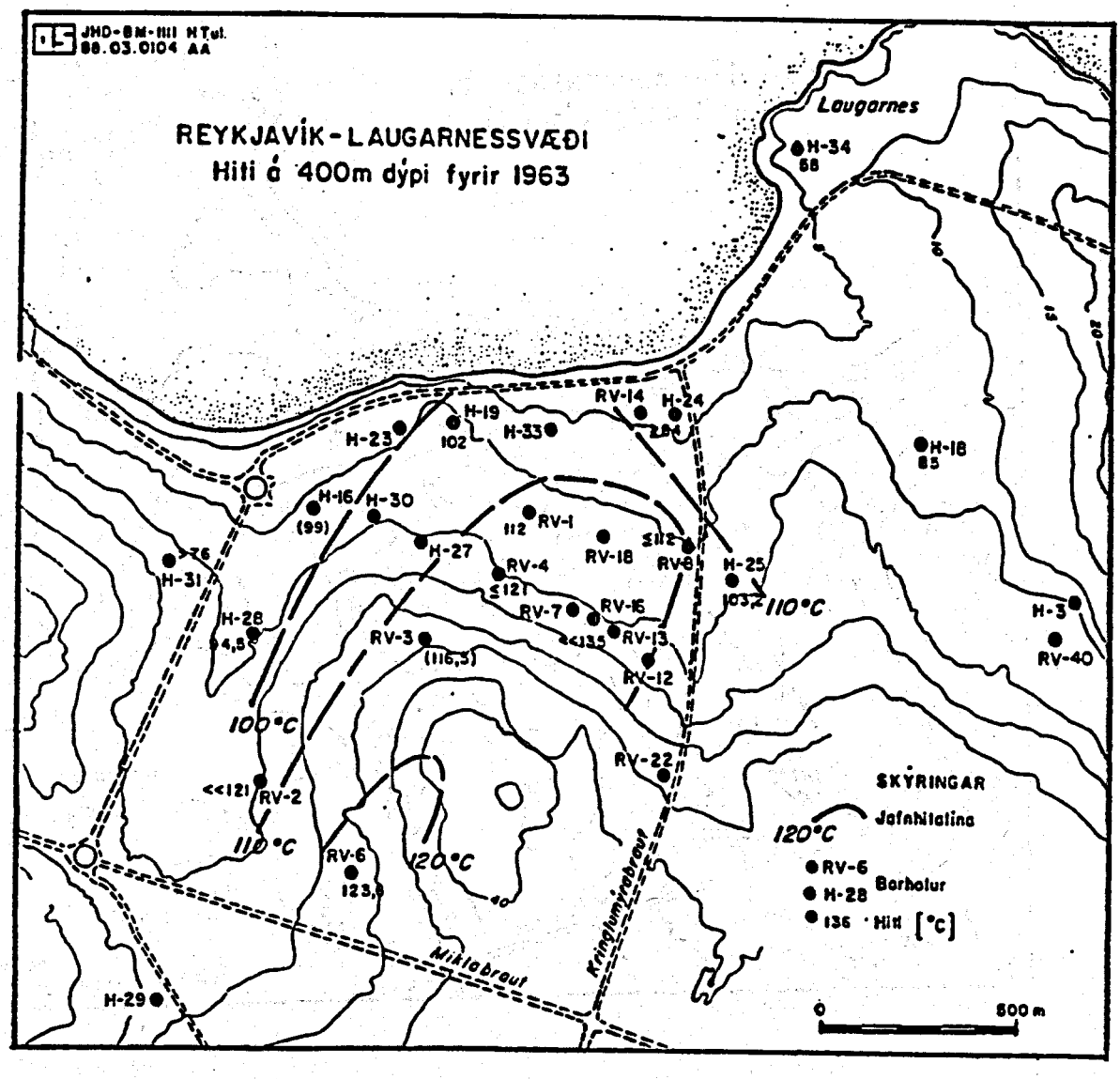

LAUGARNES FIELD.

Temperature distribution at 400 m depth. 1963

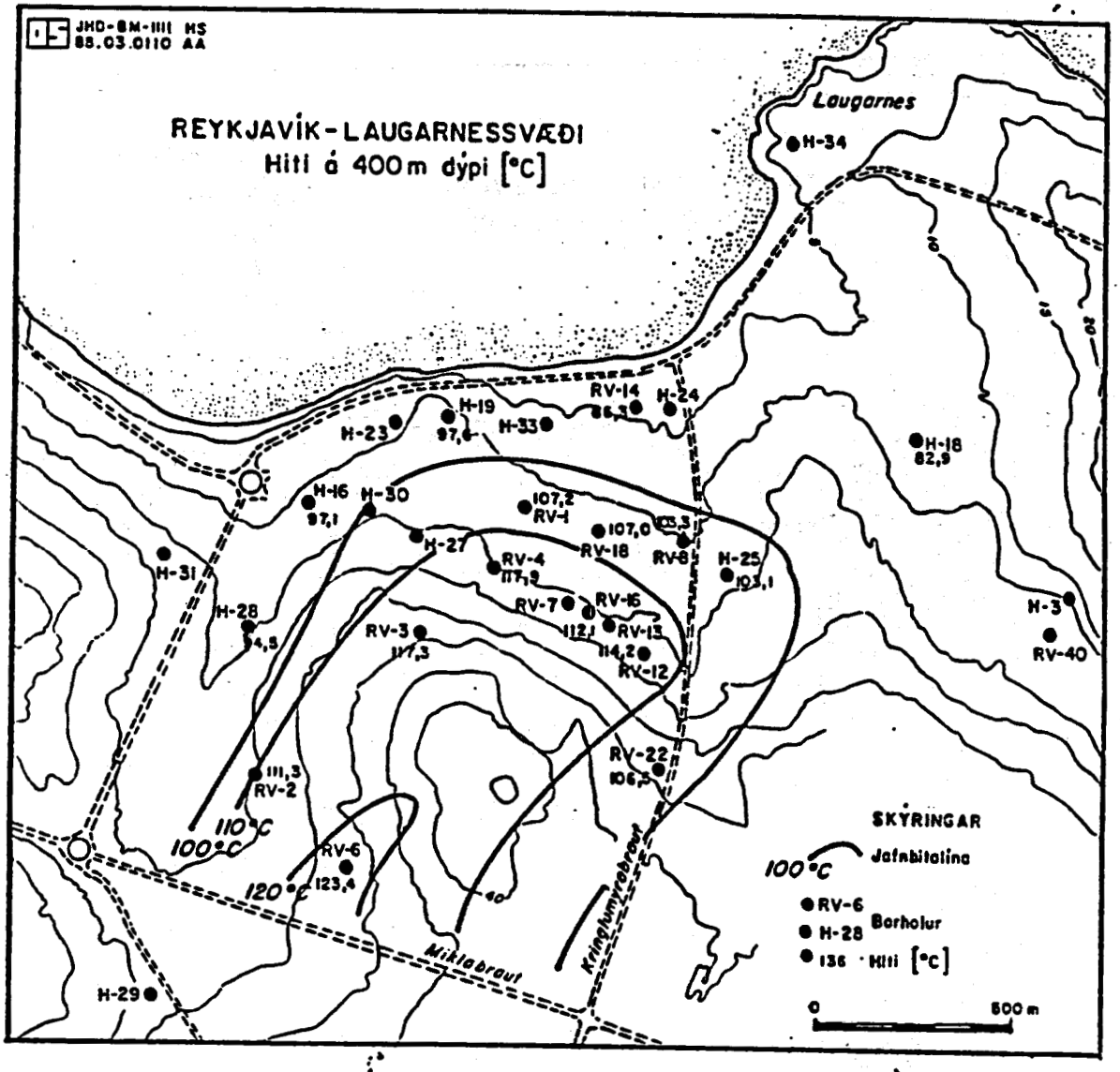

LAUGARNES FIELD.

Temperature distribution at 400 m depth. 1987

Reykjavík hola RV-5

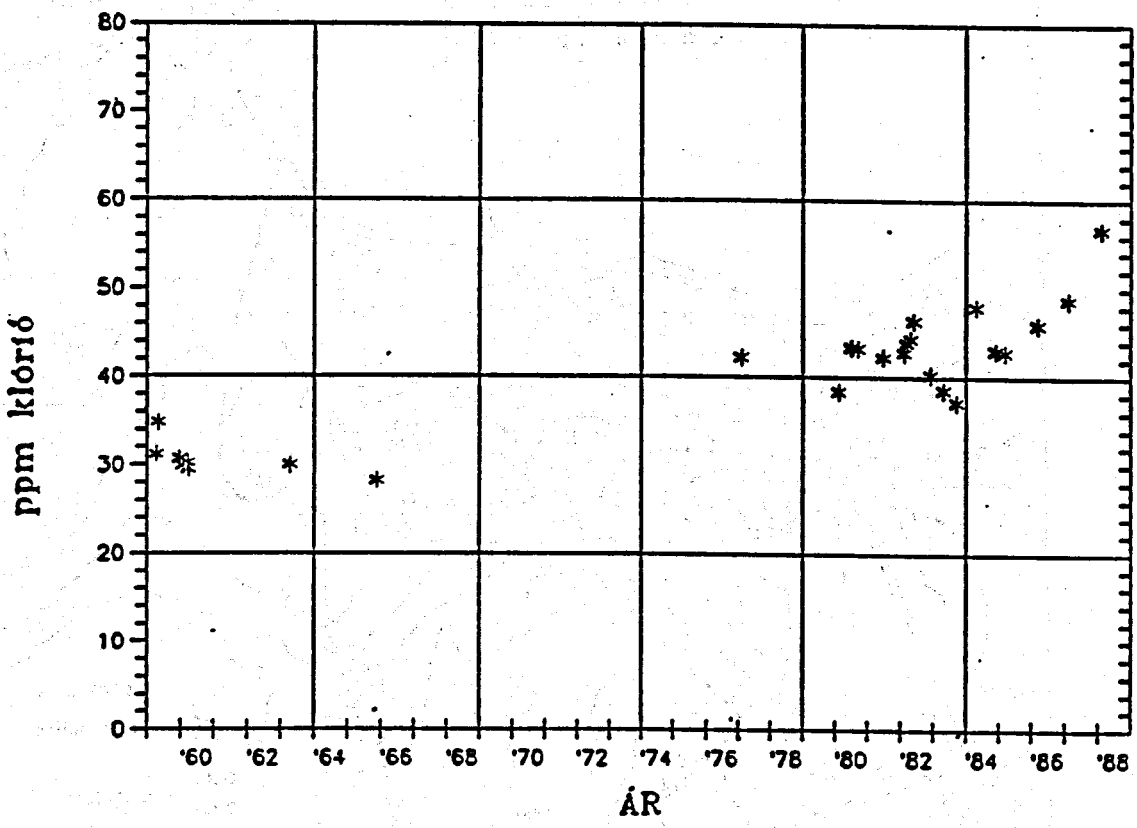

LAUGARNES FIELD. WELL RV-5.

Variations in cloride concentration 1958-1988.

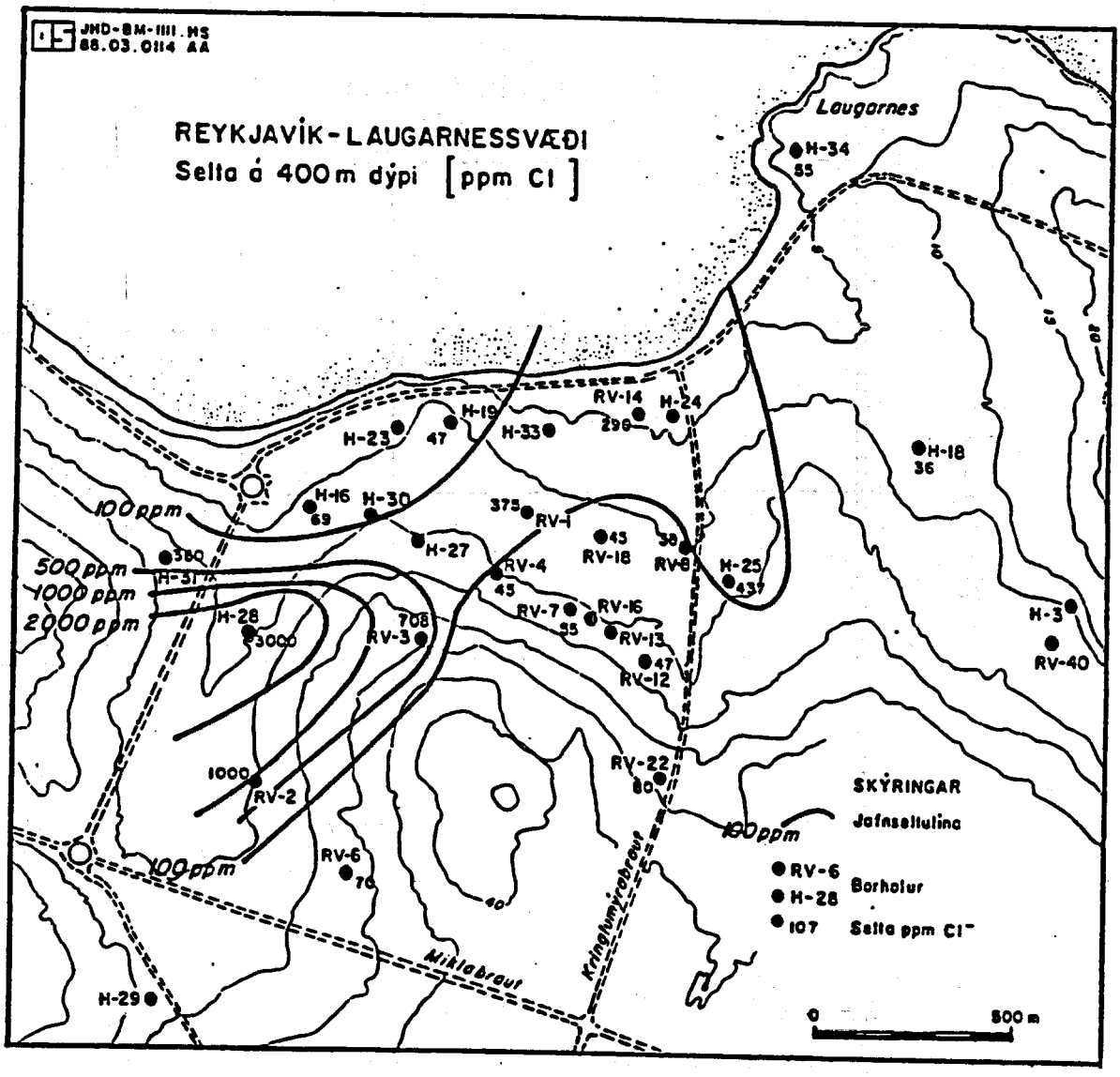

LAUGARNES FIELD.

Salinity at 400 m depth. 1987

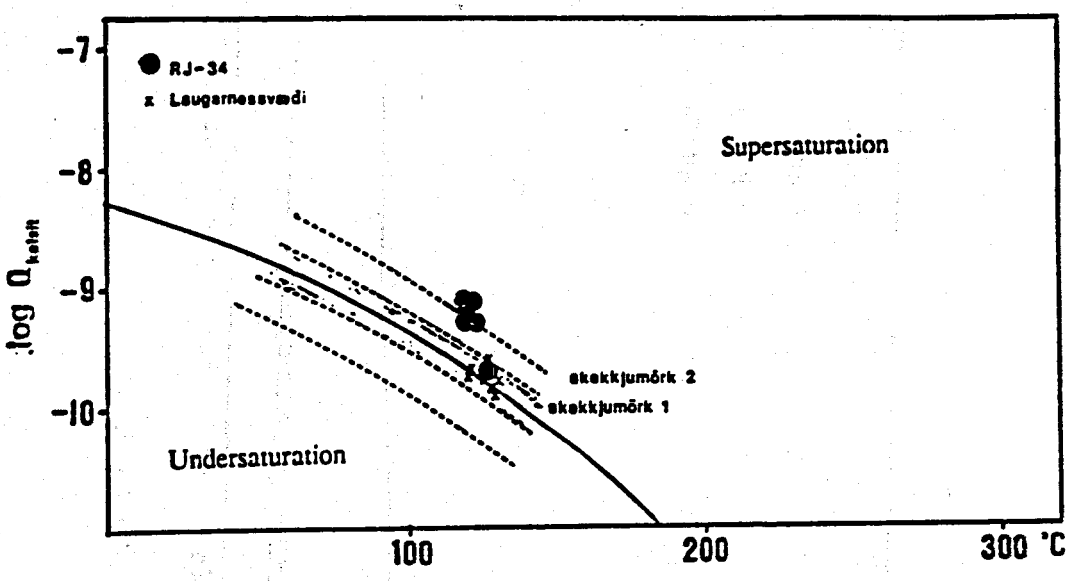

LAUGARNES FIELD.

Solubility of calsite as a function of temperature.

The solid circles are for water from well RJ-34.

The crosses are for wells with low cloride concentrations.

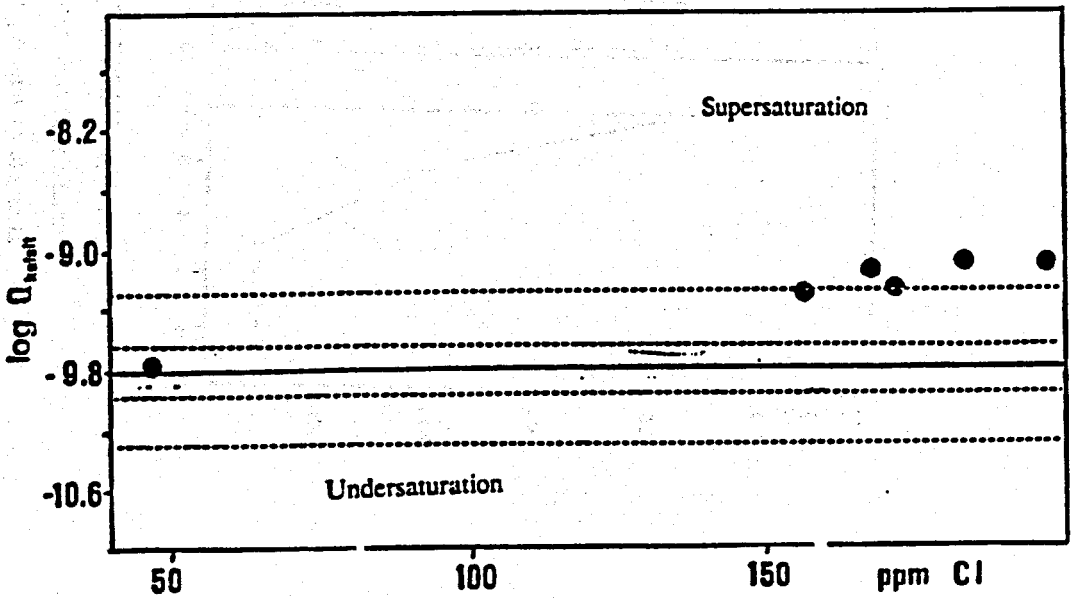

LAUGARNES FIELD. WELL RJ-34.

Solubility of calsite as a function of salinity.

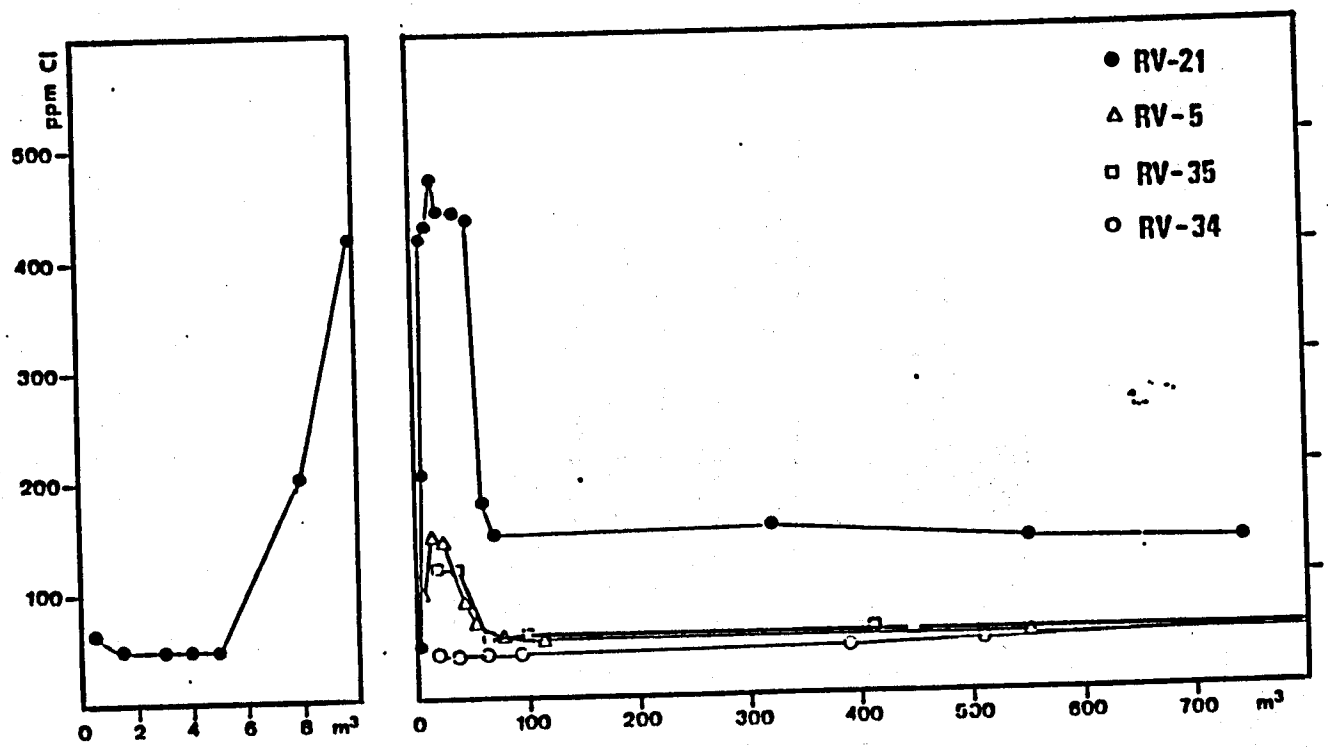

LAUGARNES FIELD. WELLS RV-5, 21, 34 AND 35.

Initial cloride concentration when pumping starts

after a few mounths production stop.

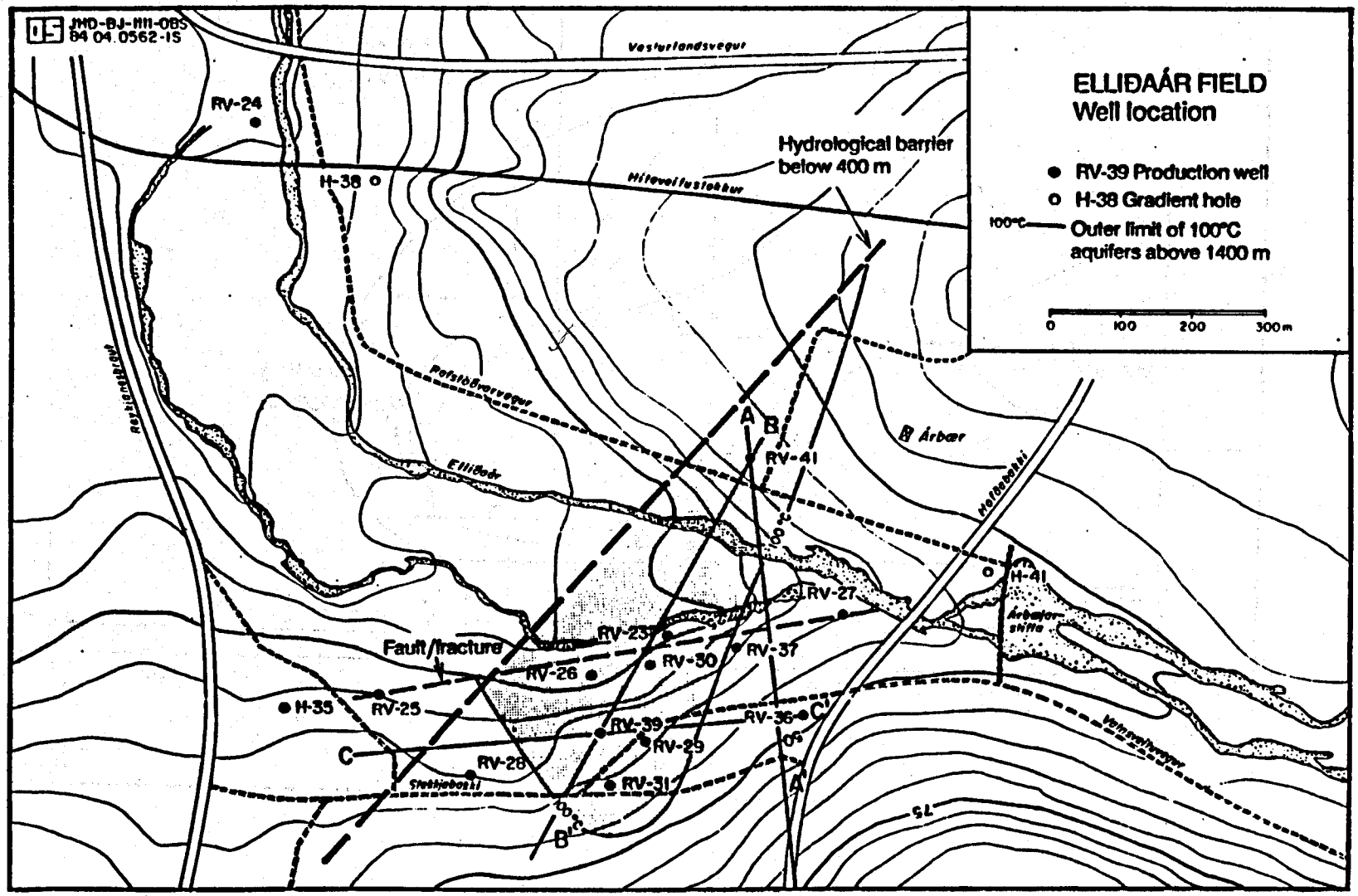
ELLIÐAÁR FIELD
Well location
RV-39 Production well
H-38 Gradient hole
100°C Outer limit of 100°C aquifers above 1400 m
0 100 200 300 m
Hydrological barrier below 400 m
Vesturlandsvegur
Hitaveitustokkur
RV-24
H-38
RV-41
RV-27
RV-23
RV-26
RV-30
RV-37
H-41
Fault/fracture
H-35
RV-25
RV-39
RV-36
RV-29
RV-28
RV-31
A
B
C
A'
B'
C'

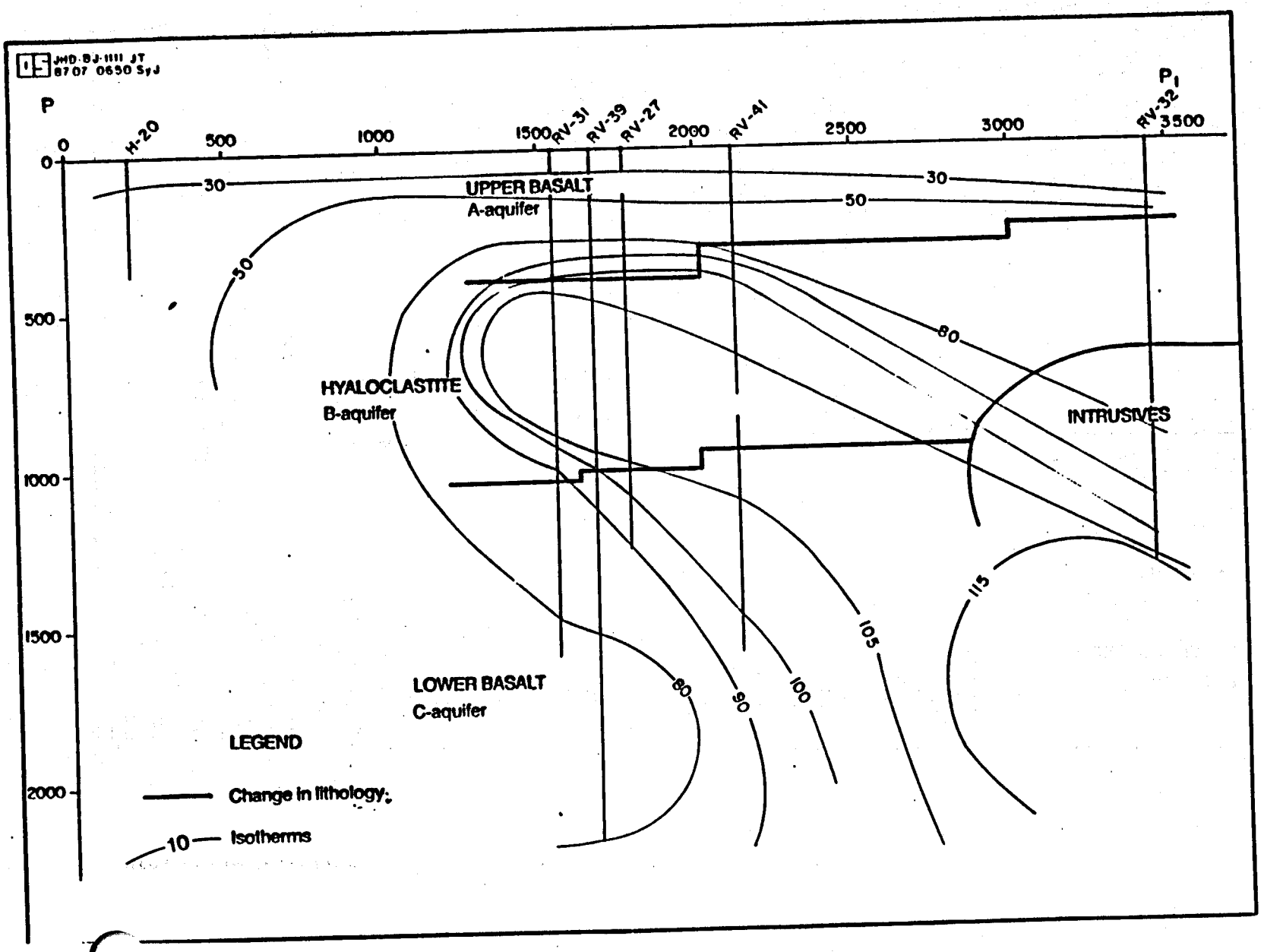
P
P1
0
500
1000
1500
2000
2500
3000
3500
H-20
RV-31
RV-39
RV-27
RV-41
RV-32
30
50
80
105
115
90
100
UPPER BASALT
A-aquifer
HYALOCLASTITE
B-aquifer
INTRUSIVES
LOWER BASALT
C-aquifer
LEGEND
Change in lithology
Isotherms

ELLIDAÁR FIELD.

Annual mass extraction 1968-1988.

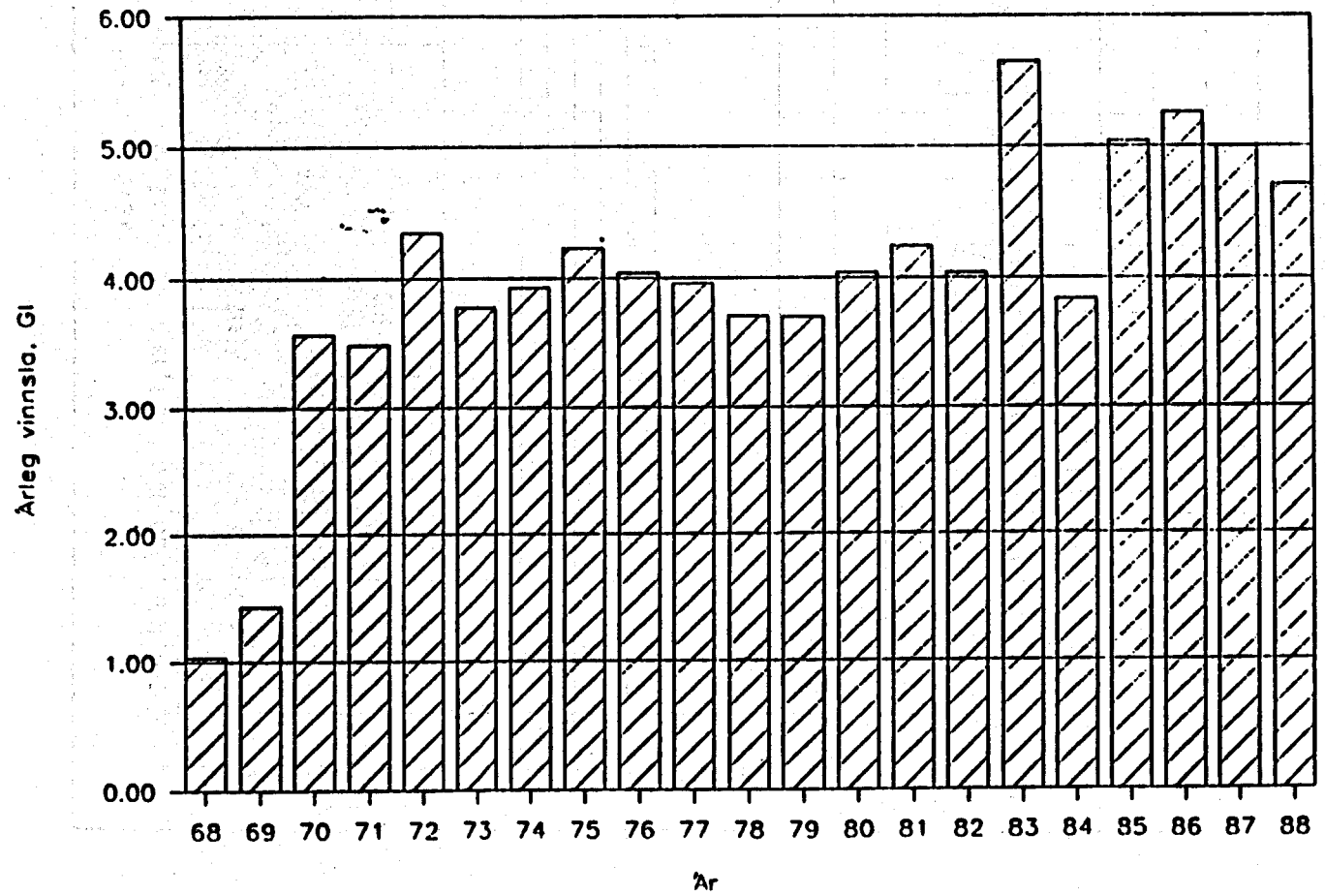

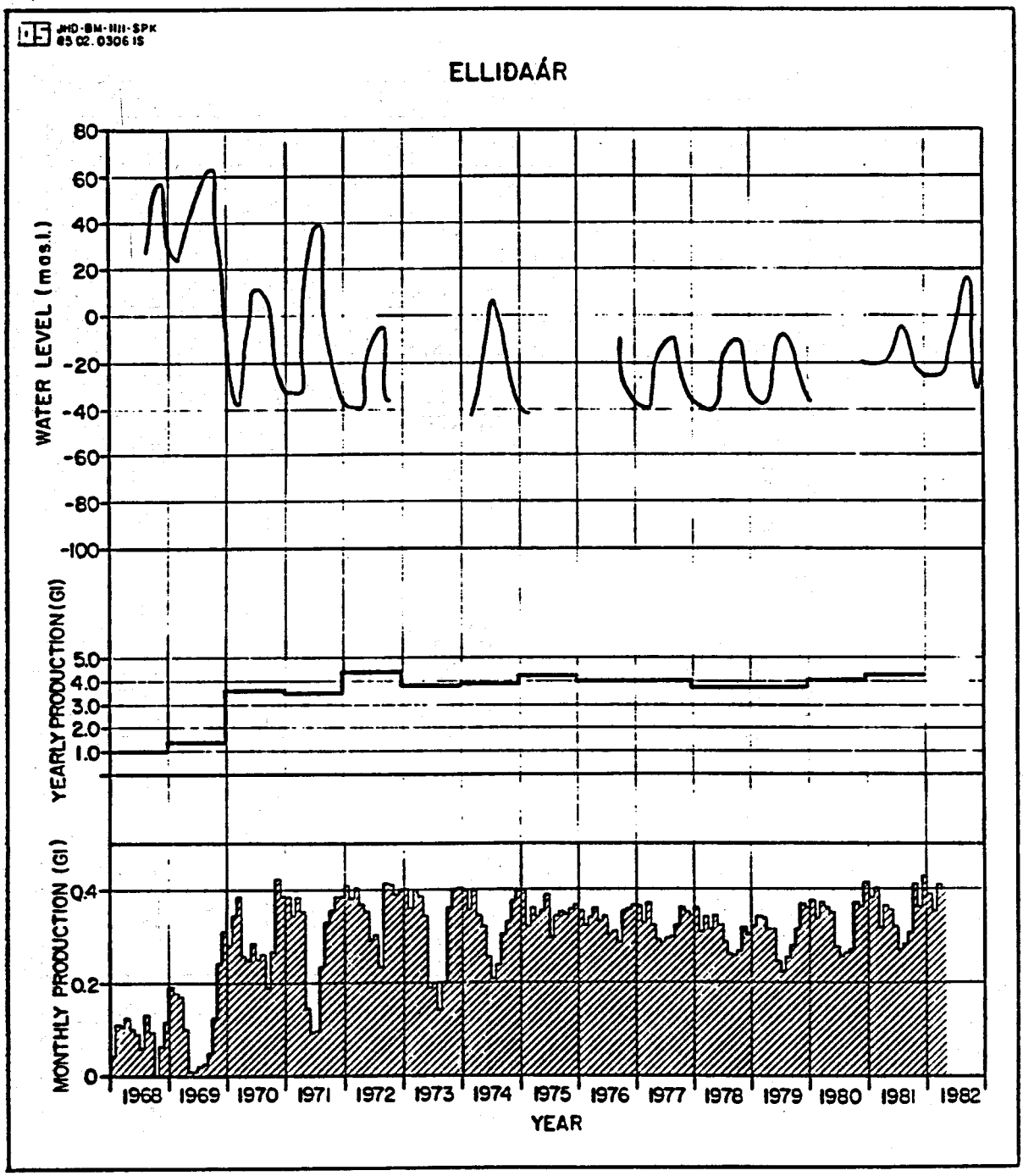
JHD-BM-IIII-SPK
85 02. 0306 IS
ELLIDAÁR
WATER LEVEL (m.s.l.)
80
60
40
20
0
-20
-40
-60
-80
-100
YEARLY PRODUCTION (Gl)
5.0
4.0
3.0
2.0
1.0
MONTHLY PRODUCTION (Gl)
0.4
0.2
0
1968
1969
1970
1971
1972
1973
1974
1975
1976
1977
1978
1979
1980
1981
1982
YEAR

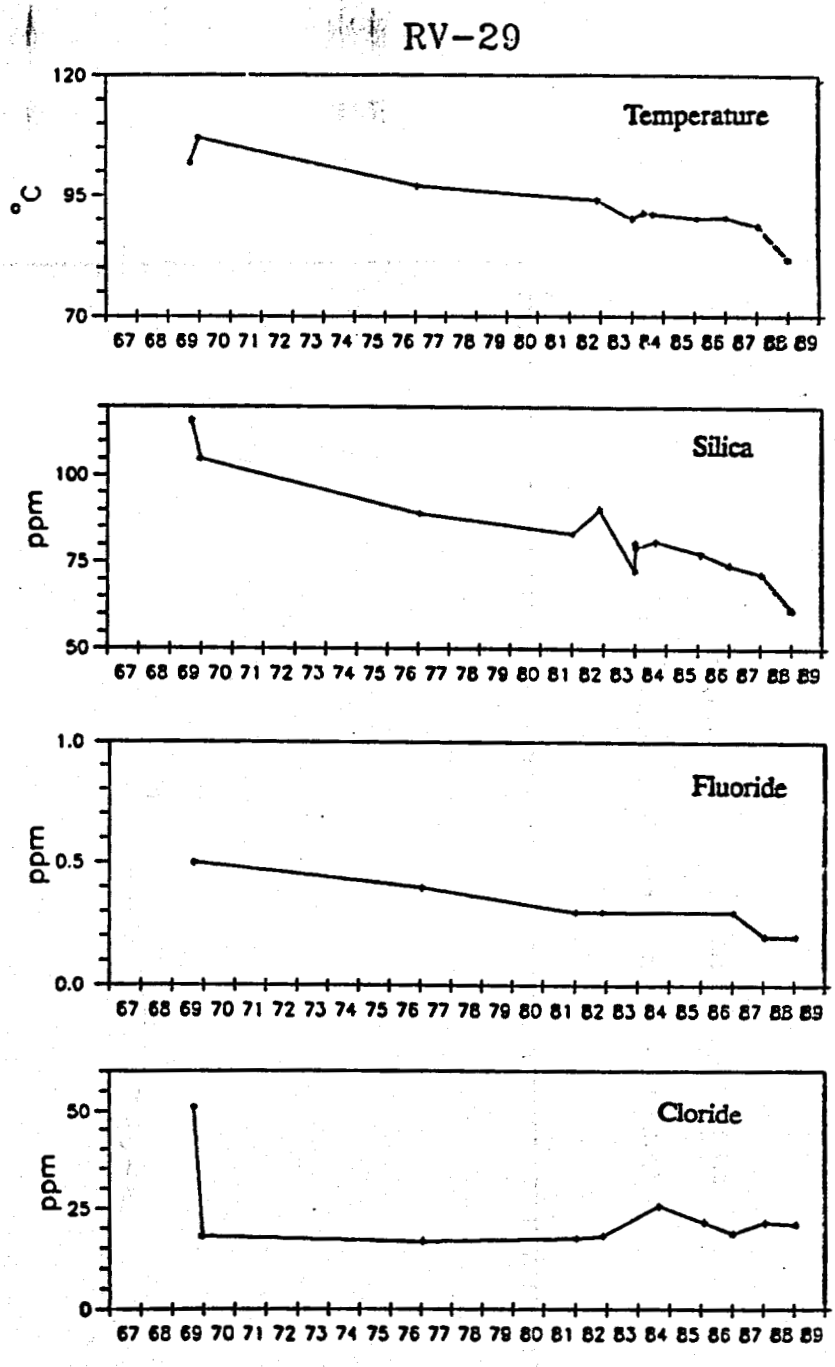

ELLIÐAÁR FIELD. WELL RV-29

Variations in fluid temperature and chemistry 1968-1989.

ELLIÐAÁR FIELD. WELL RV-29

Production temperatures after 3 months stop.

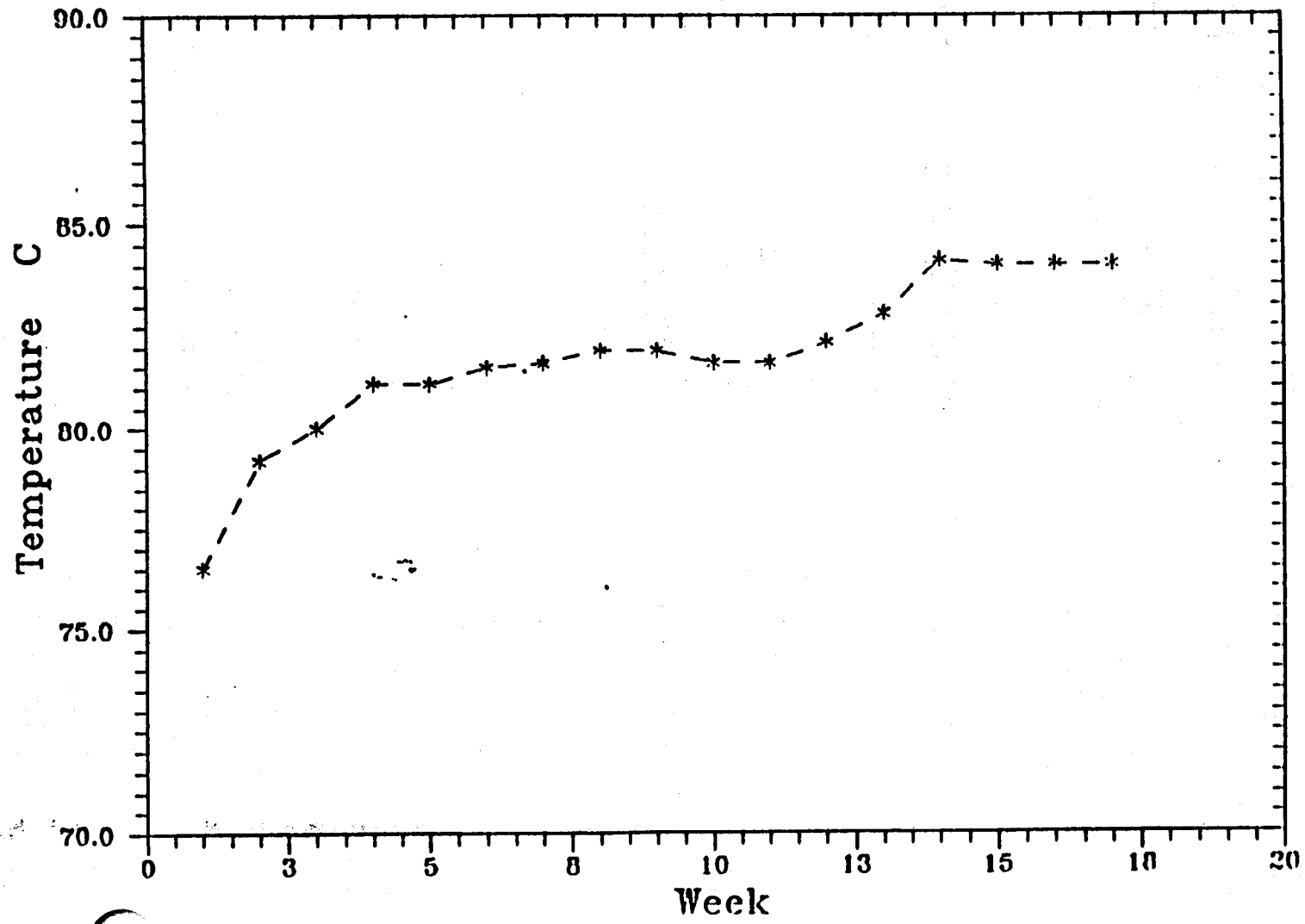

ELLIDAÁR FIELD.

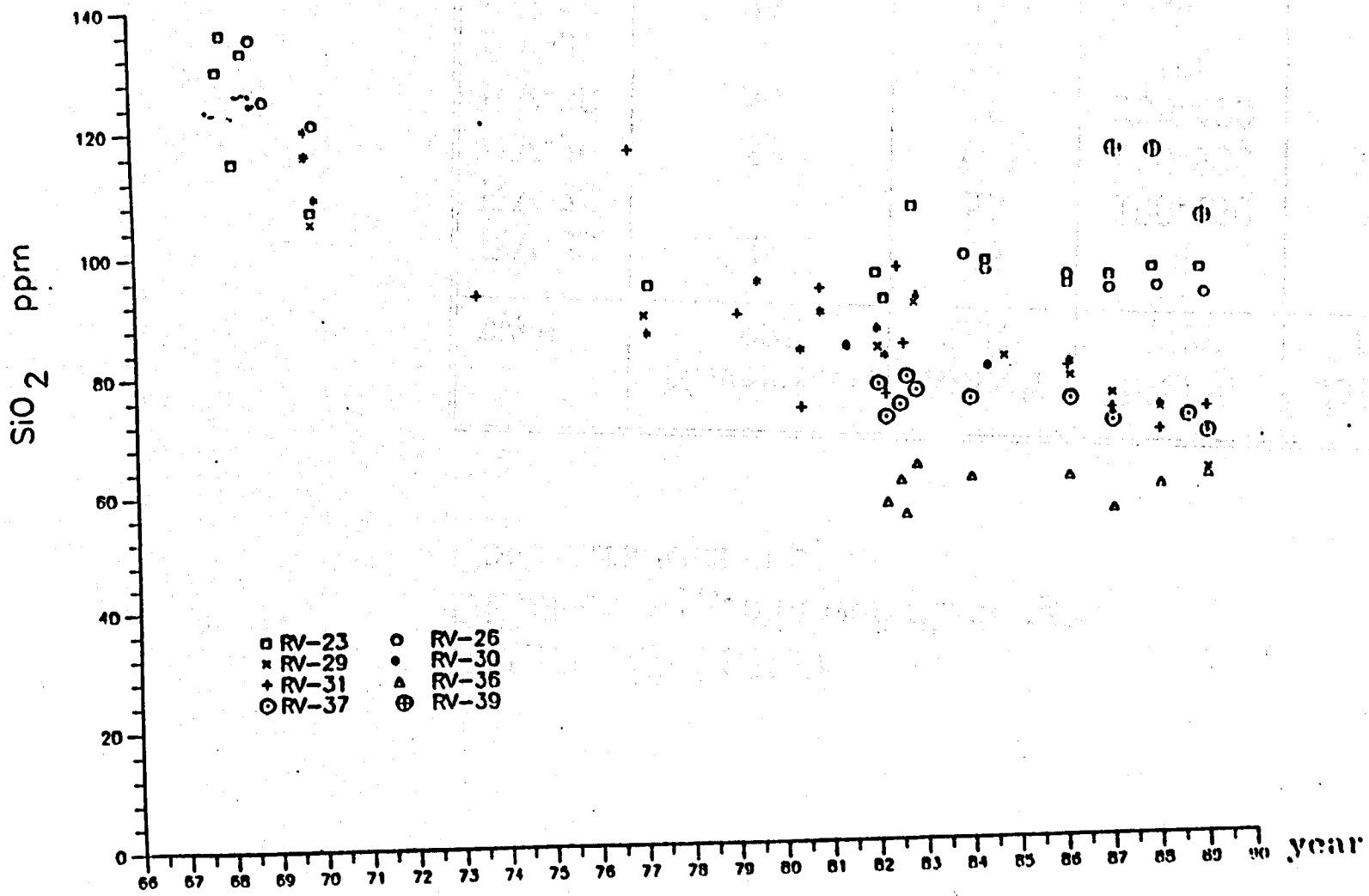

Changes in concentration of SiO_2 in drillholes.

ELLIÐAÁR FIELD
Dissolved oxygen in well discharges.
Concentrations in ppb.

Well	November 1982	March 1983	March 1988	January 1989
RV-23	0	25	0	0
RV-26		50	100-150	150
RV-29	50	120	400-500	800
RV-30	50	35	300-400	800
RV-31		25	150	300
RV-36	25	15	60	150
RV-37	30	35	150	250
RV-39			2-3	5-10

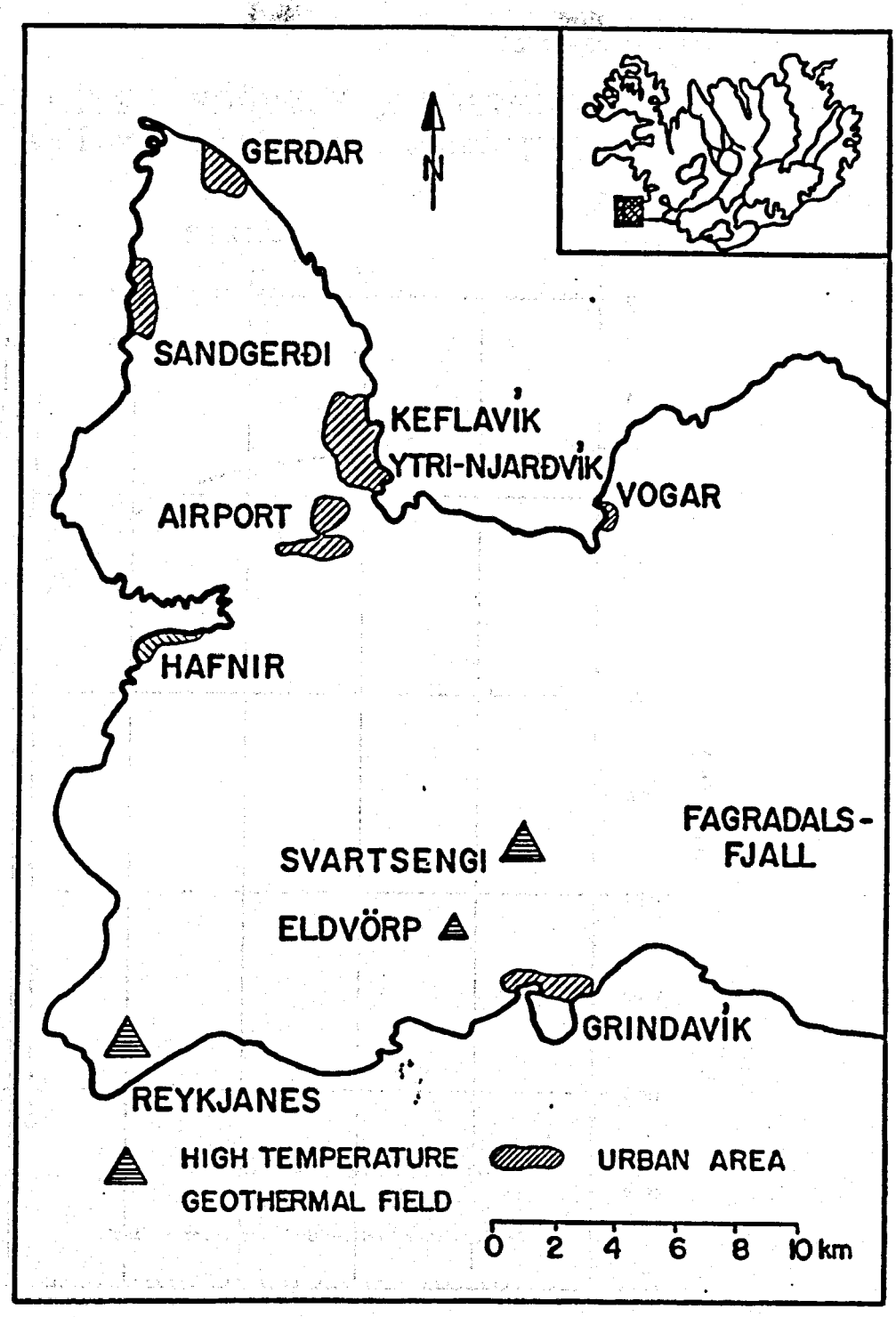
GERDAR
N
SANDGERÐI
KEFLAVÍK
YTRI-NJARÐVÍK
VOGAR
AIRPORT
HAFNIR
FAGRADALS-
FJALL
SVARTSENGI
ELDVÖRP
GRINDAVÍK
REYKJANES
HIGH TEMPERATURE
GEOTHERMAL FIELD
URBAN AREA
0 2 4 6 8 10 km

OS-JHD
89-06-07 BS

SVARTSENGI, ELDVÖRP, REYKJANES
Typical temperature profiles

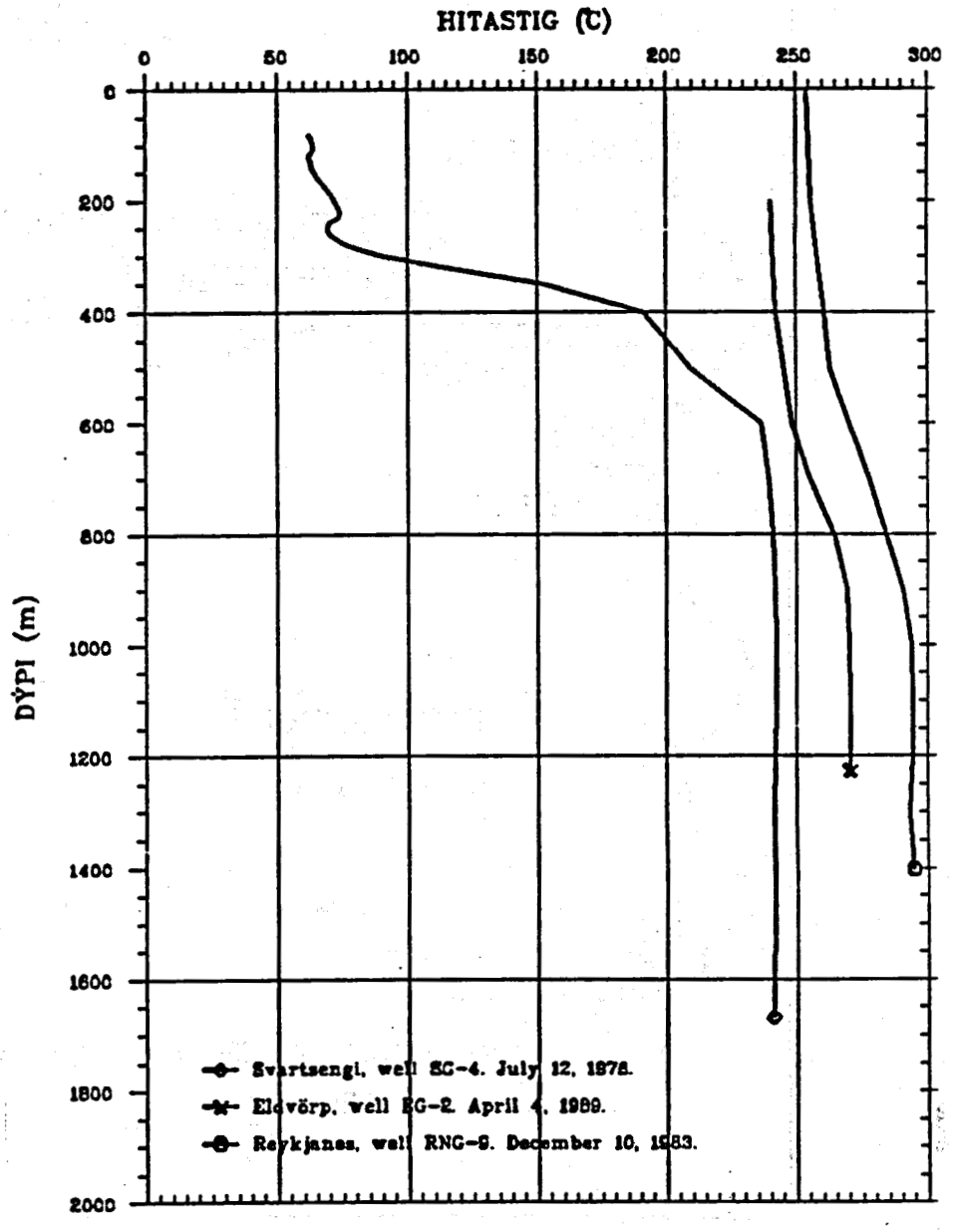

VERKFRÆÐISTOFAN 8702
VATNASKIL 89-06-06 SPK

ORKUSTOFNUN

SVARTSENGI

Estimated temperature distribution at 600 m depth

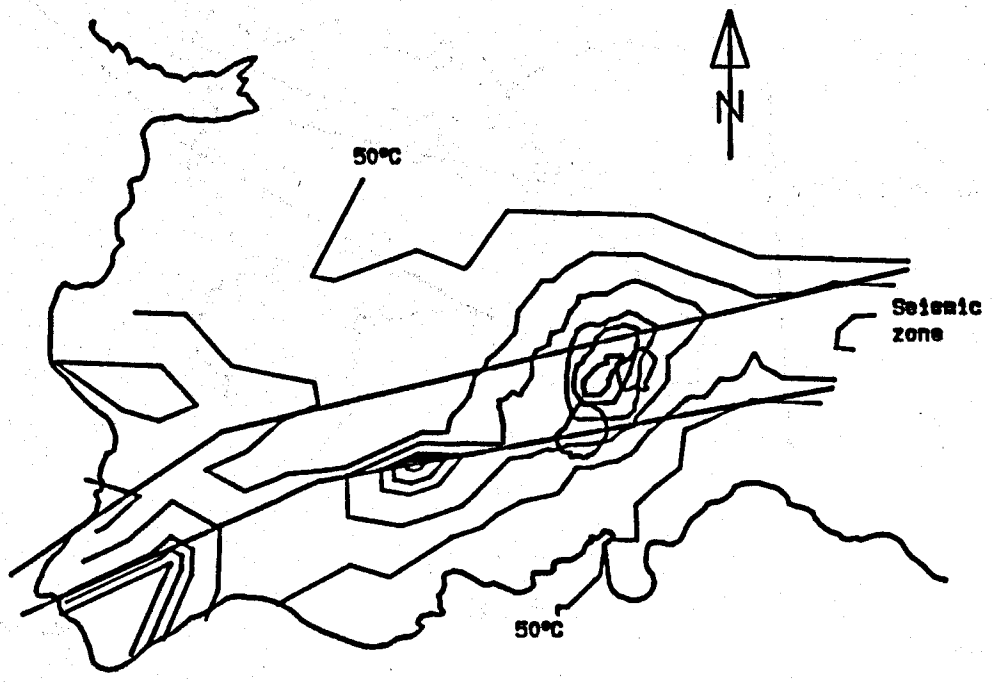

Contour interval:
Green: 50 °C
Red: 220 and 240 °C

Scale : 1:200000

VERKFRÆÐISTOFAN 8702
VATNASKIL 89-06-06 SPK

ORKUSTOFNUN

SVARTSENGI
Model area

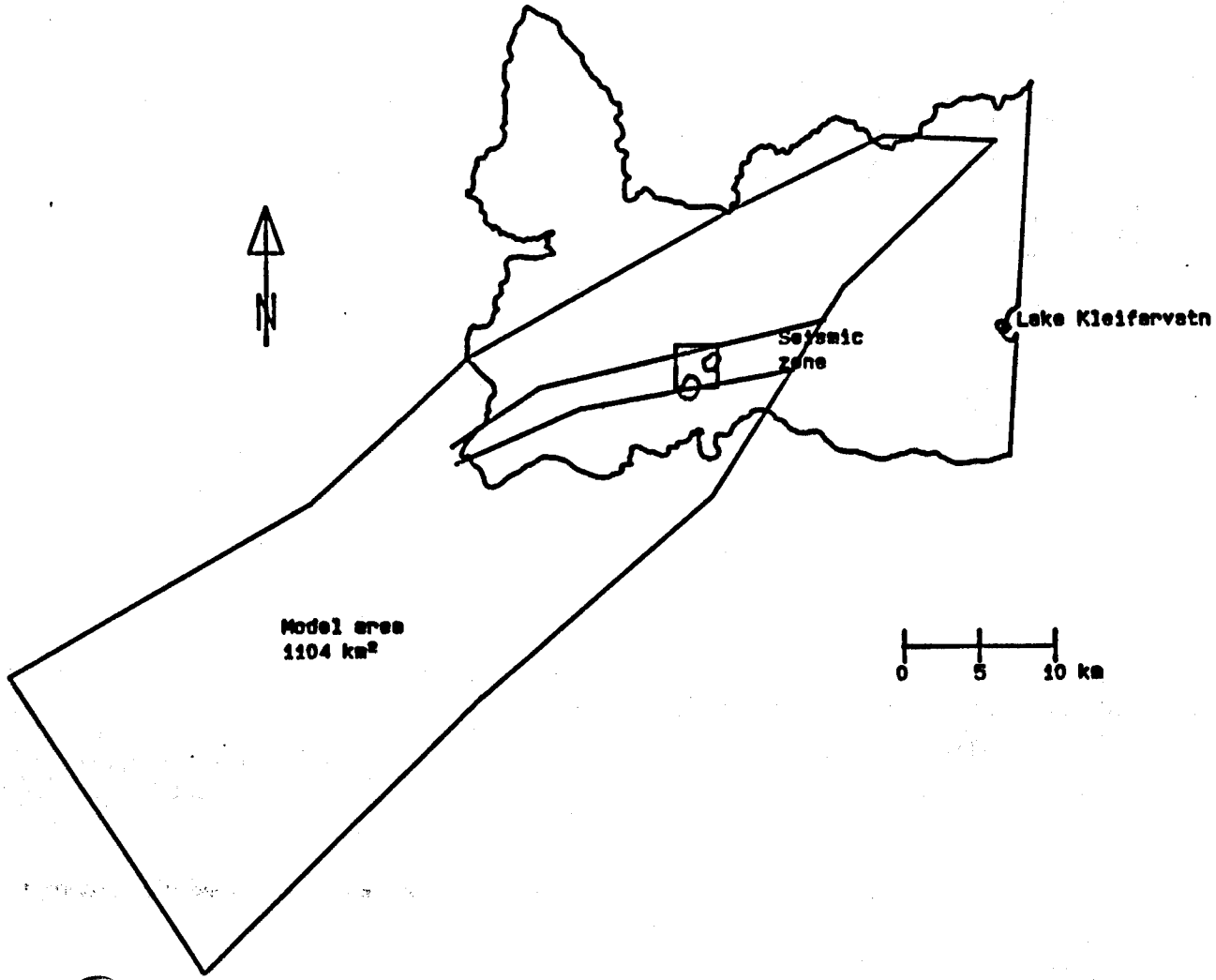

VERKFRÆÐISTOFAN 8702
VATNASKIL 89-06-06 SPK

ORKUSTOFNUN

SVARTSENGI

Two phase area above 600 m depth

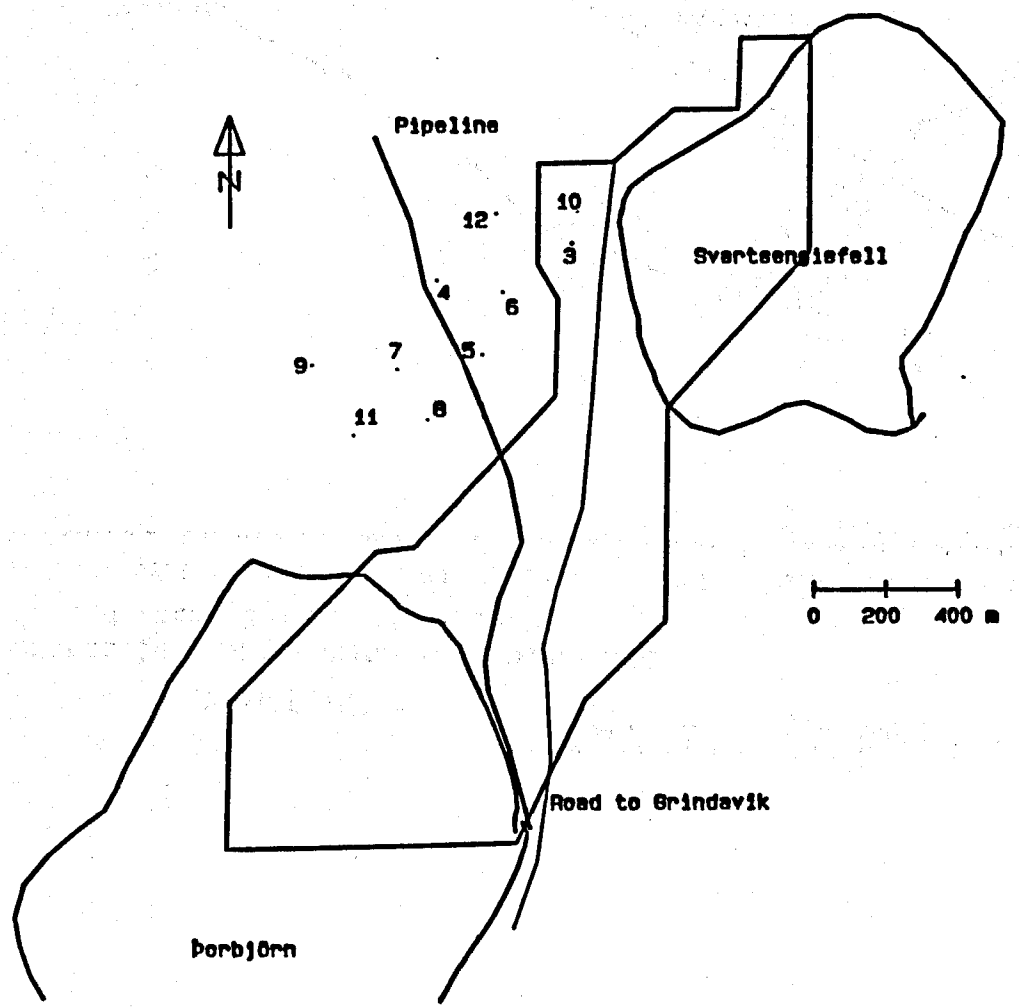

VERKFRÆÐISTOFAN 85.11
VATNASKIL 89-06-06 SPK

HITAVEITA SUÐURNESJA

SVARTSENGI

Net extraction (production - reinjection)
and water level 1976 - 1988

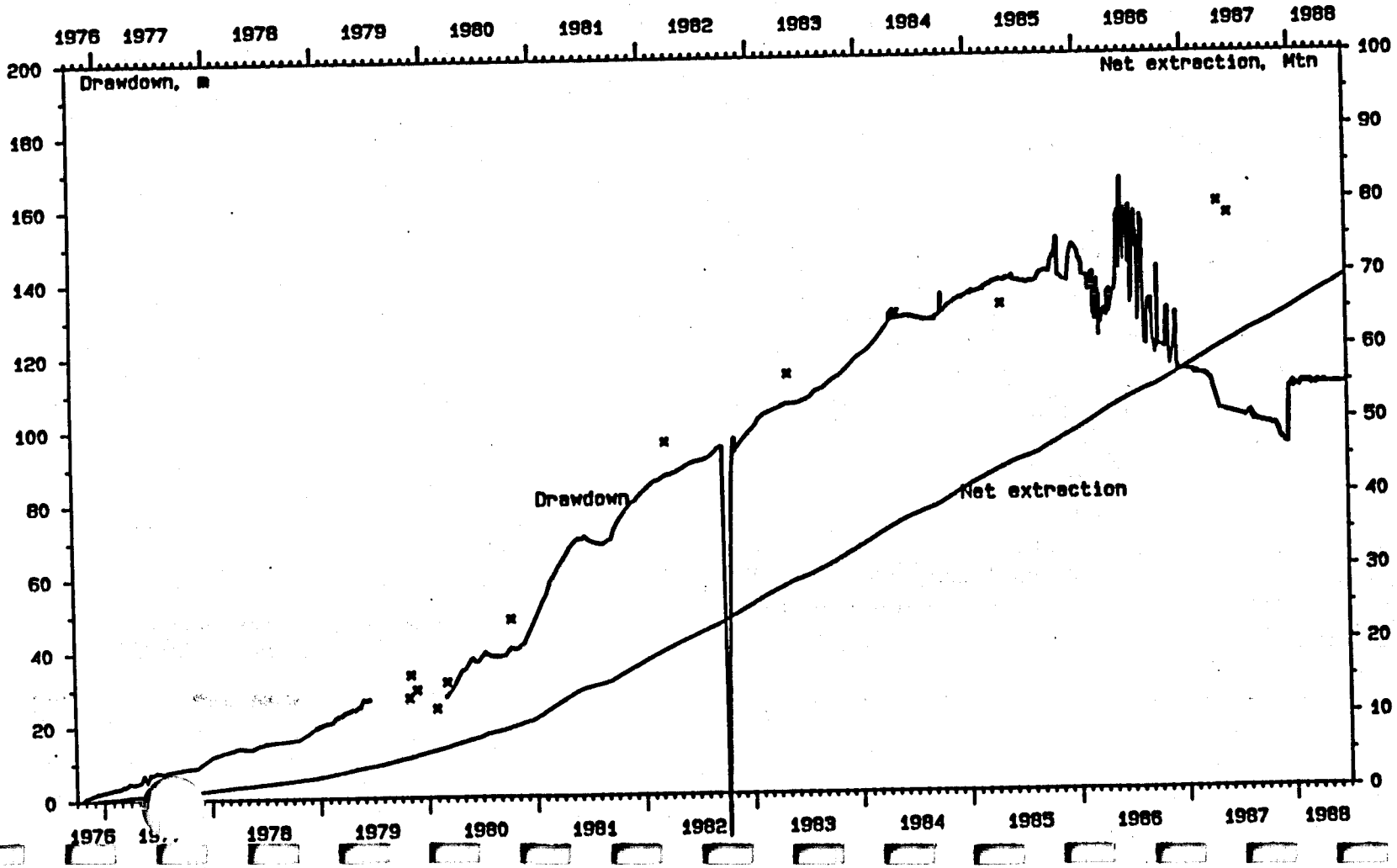

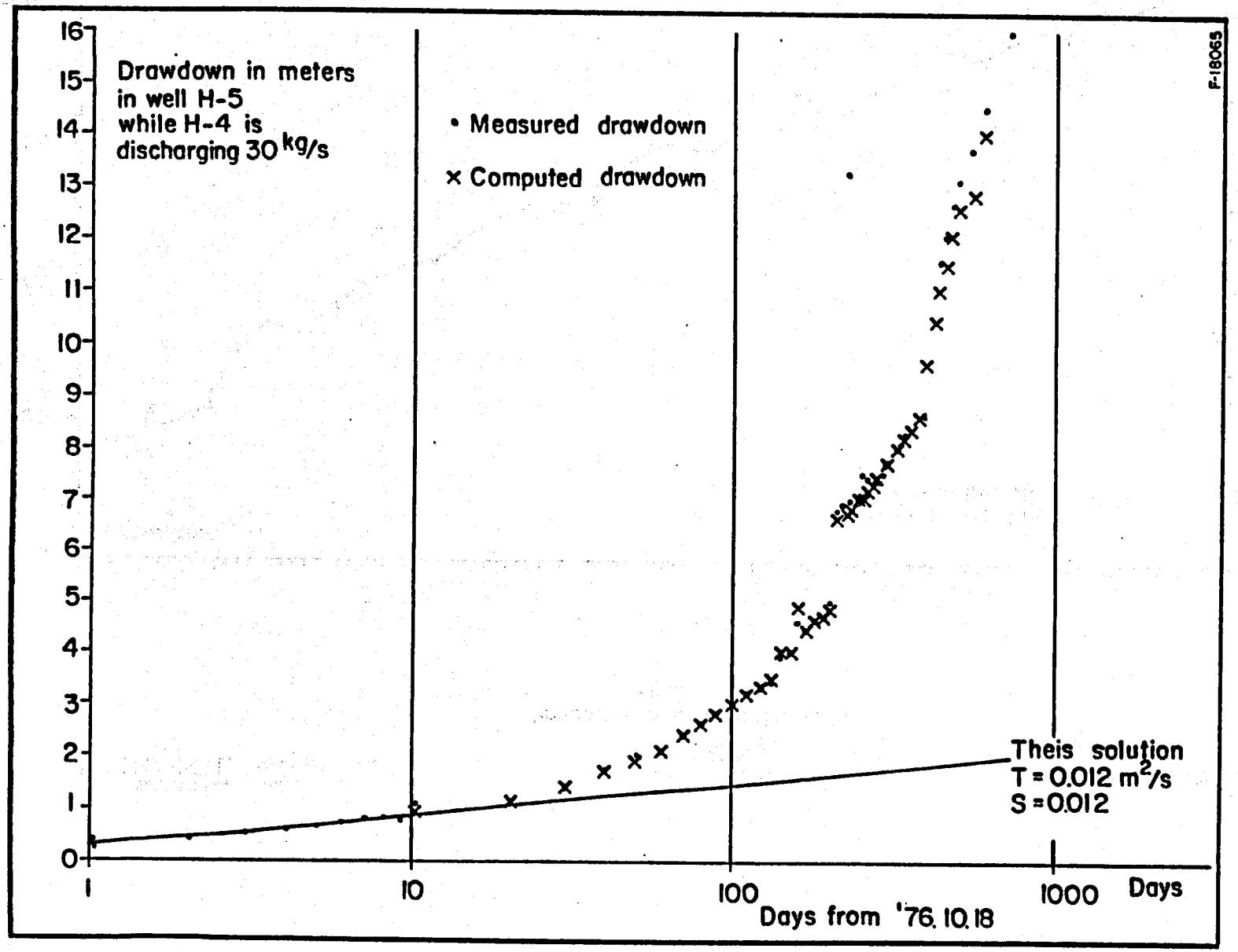
Drawdown in meters
in well H-5
while H-4 is
discharging 30 kg/s
• Measured drawdown
× Computed drawdown
Theis solution
T = 0.012 m²/s
S = 0.012
Days from '76. 10. 18
Days
F-18065
0
1
2
3
4
5
6
7
8
9
10
11
12
13
14
15
16
1
10
100
1000

VERKFRÆÐISTOFAN 8702
VATNASKIL 89-06-06 SPK

ORKUSTOFNUN

SVARTSENGI

Pressure drawdown in well 8
1980 - 1988

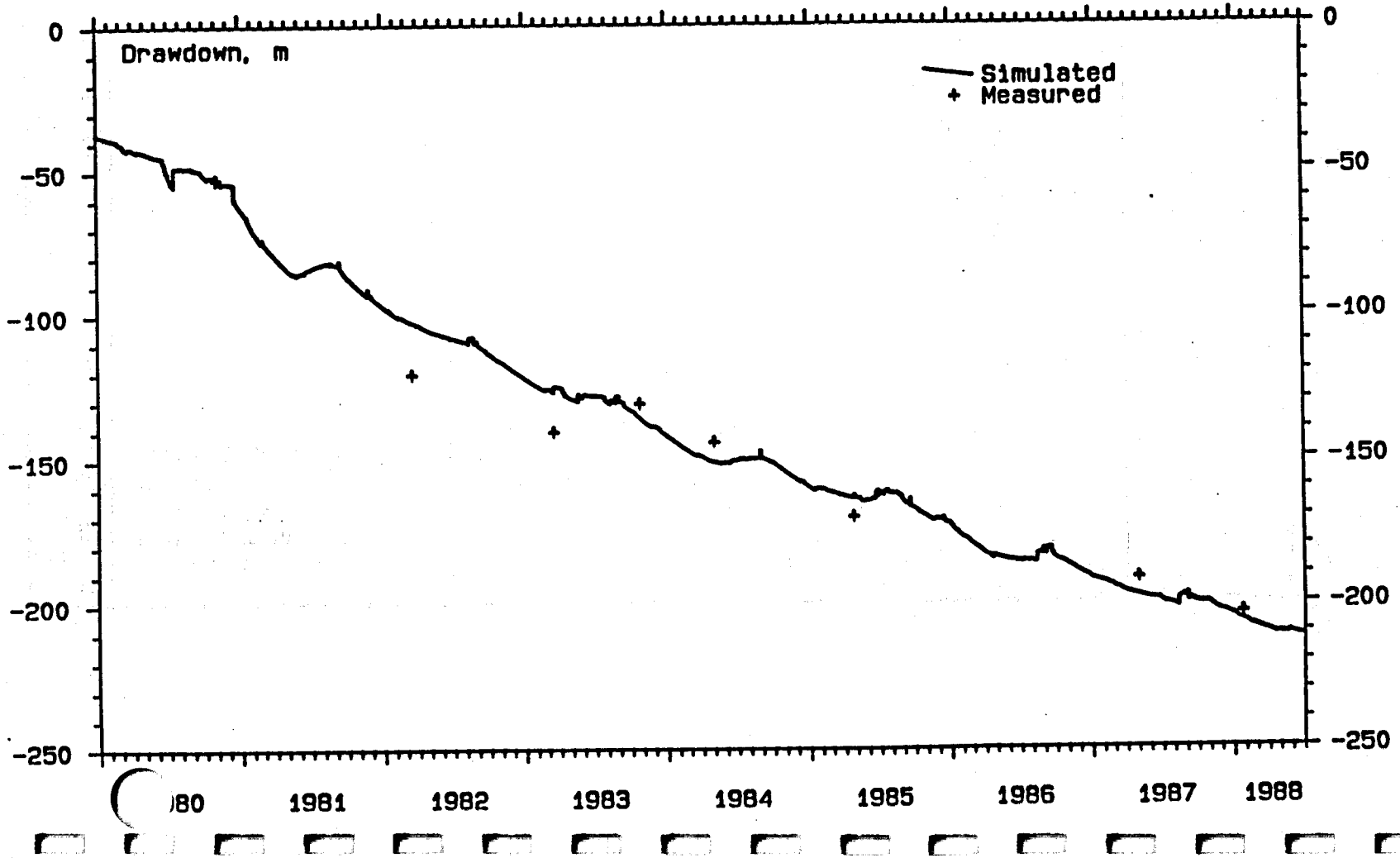

VERKFRÆÐISTOFAN 8702
VATNASKIL 89-06-06 SPK

ORKUSTOFNUN

SVARTSENGI

Simulated drawdown distribution
Spring 1988

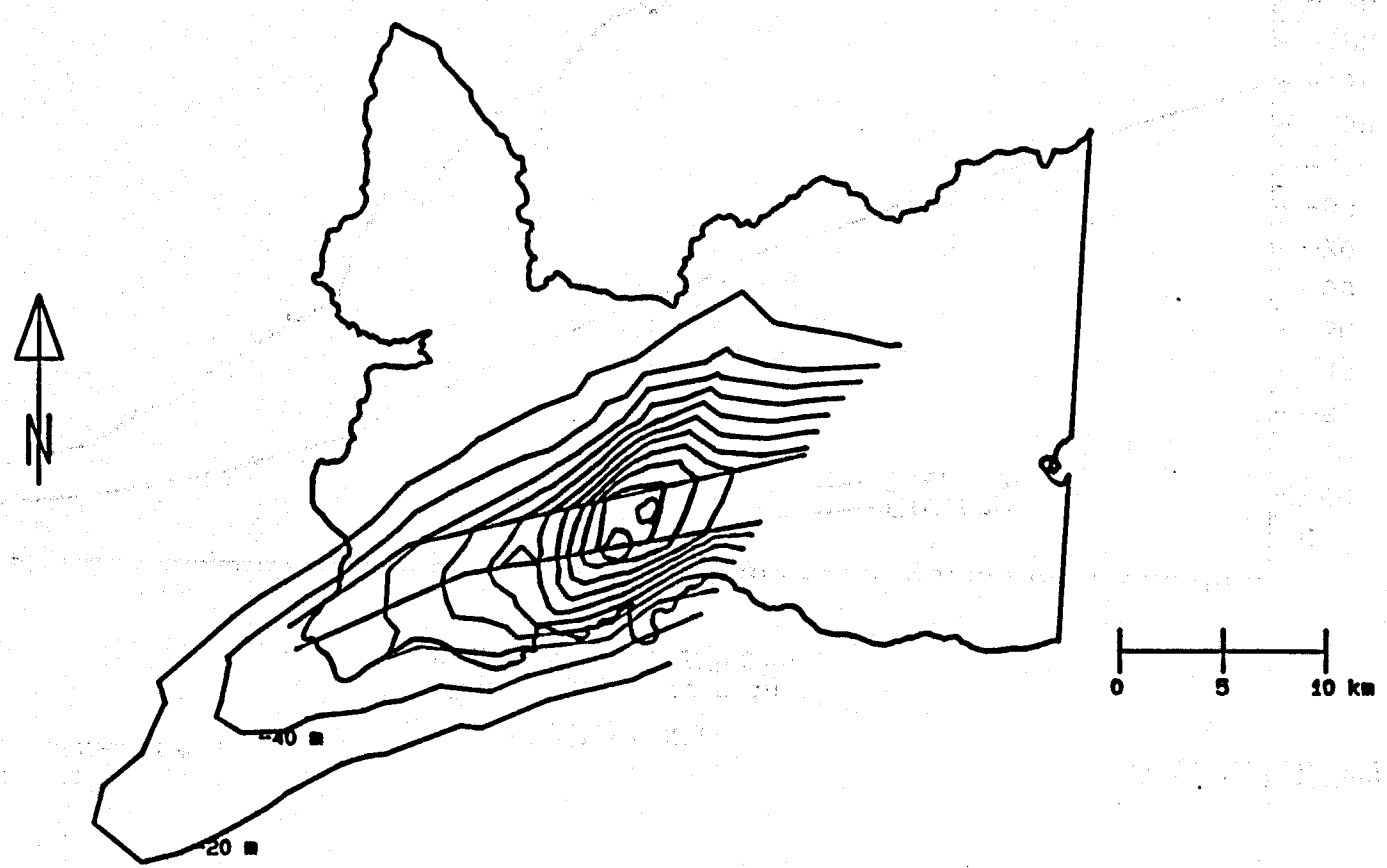

VERKFRÆÐISTOFAN 8702
VATNASKIL 89-06-06 SPK

ORKUSTOFNUN

SVARTSENGI

Simulated drawdown in
Svartsengi and Eldvörp

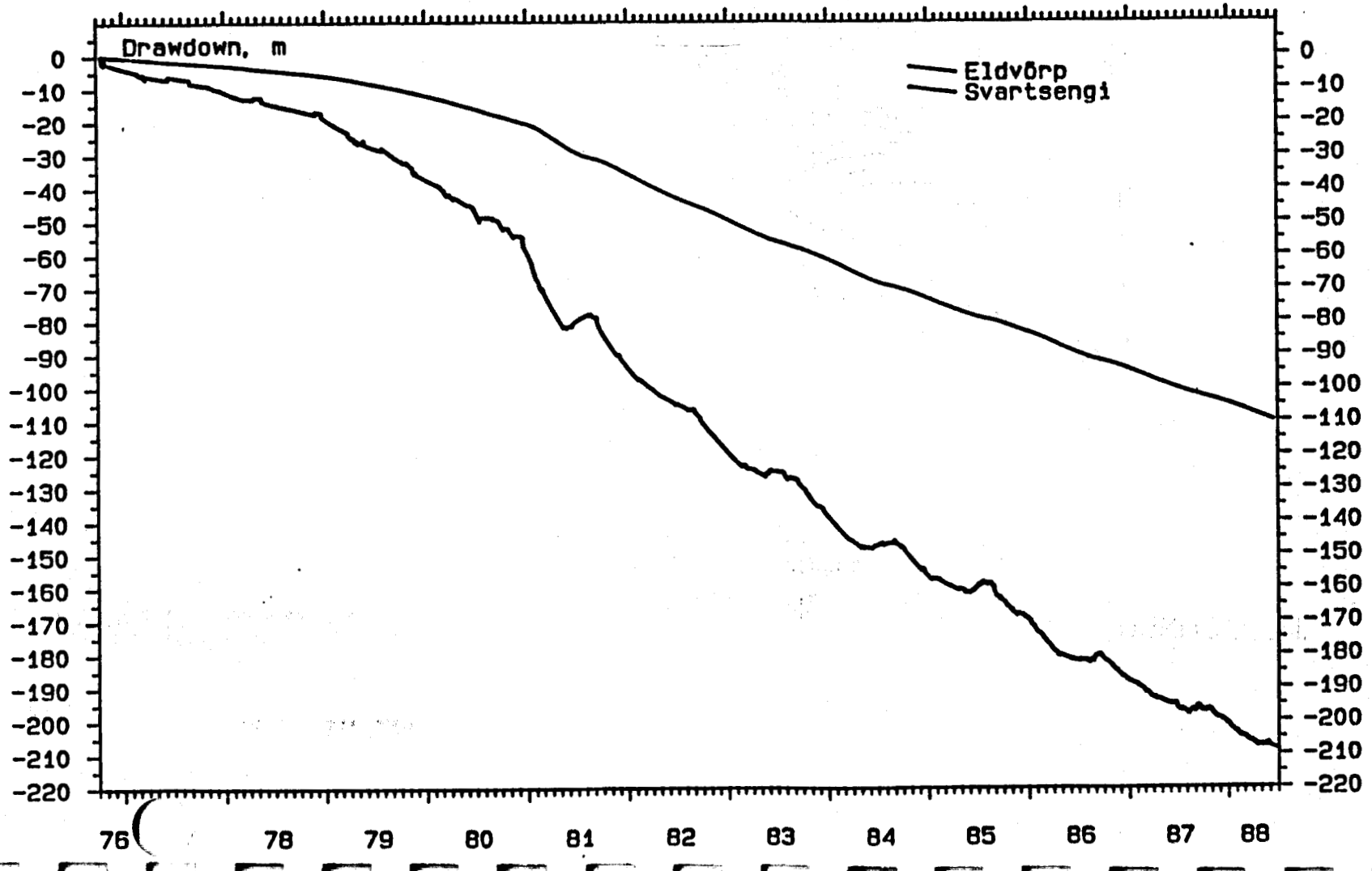

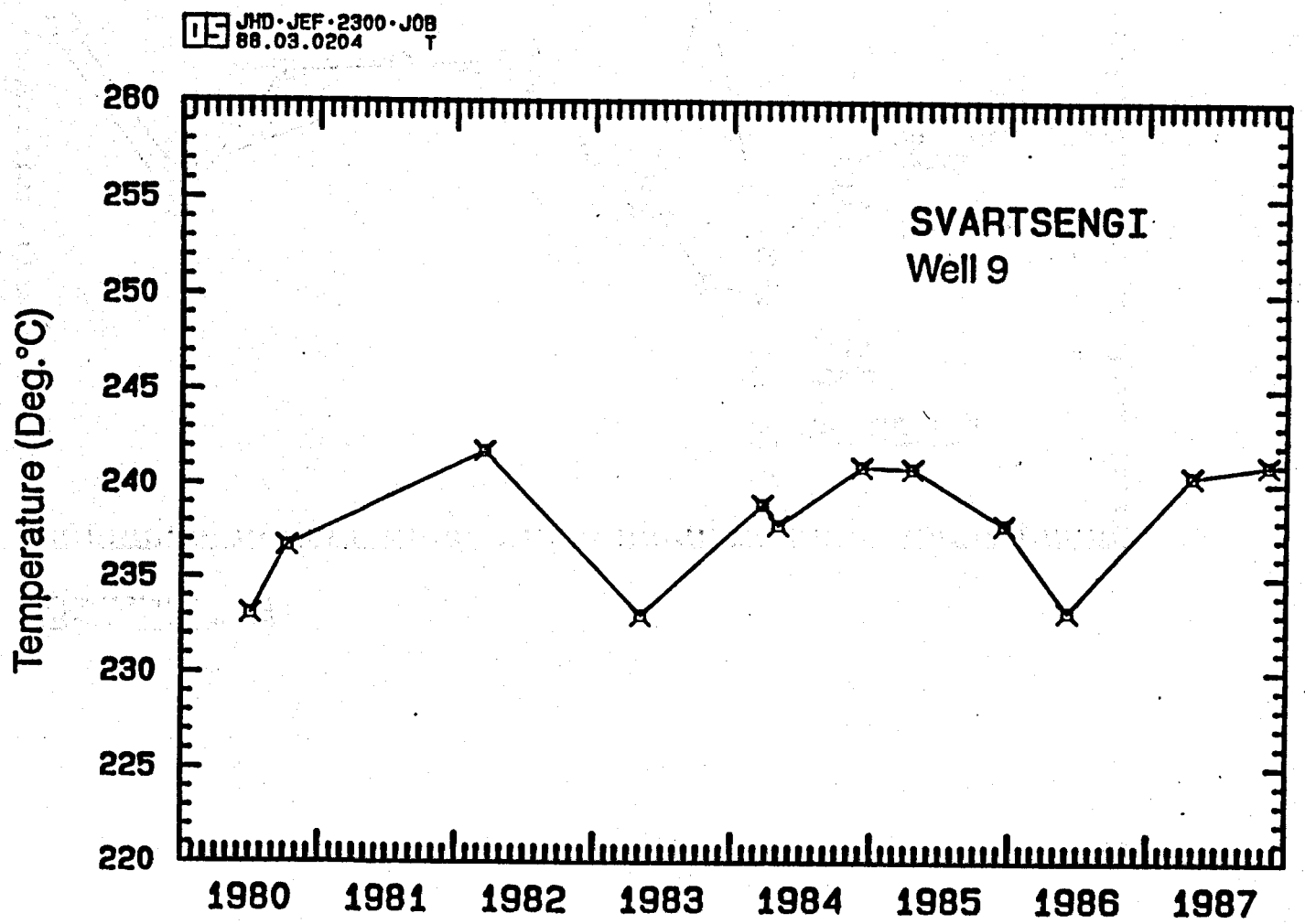
OS JHD·JEF·2300·JOB
88.03.0204 T
SVARTSENGI
Well 9
Temperature (Deg.°C)
260
255
250
245
240
235
230
225
220
1980
1981
1982
1983
1984
1985
1986
1987

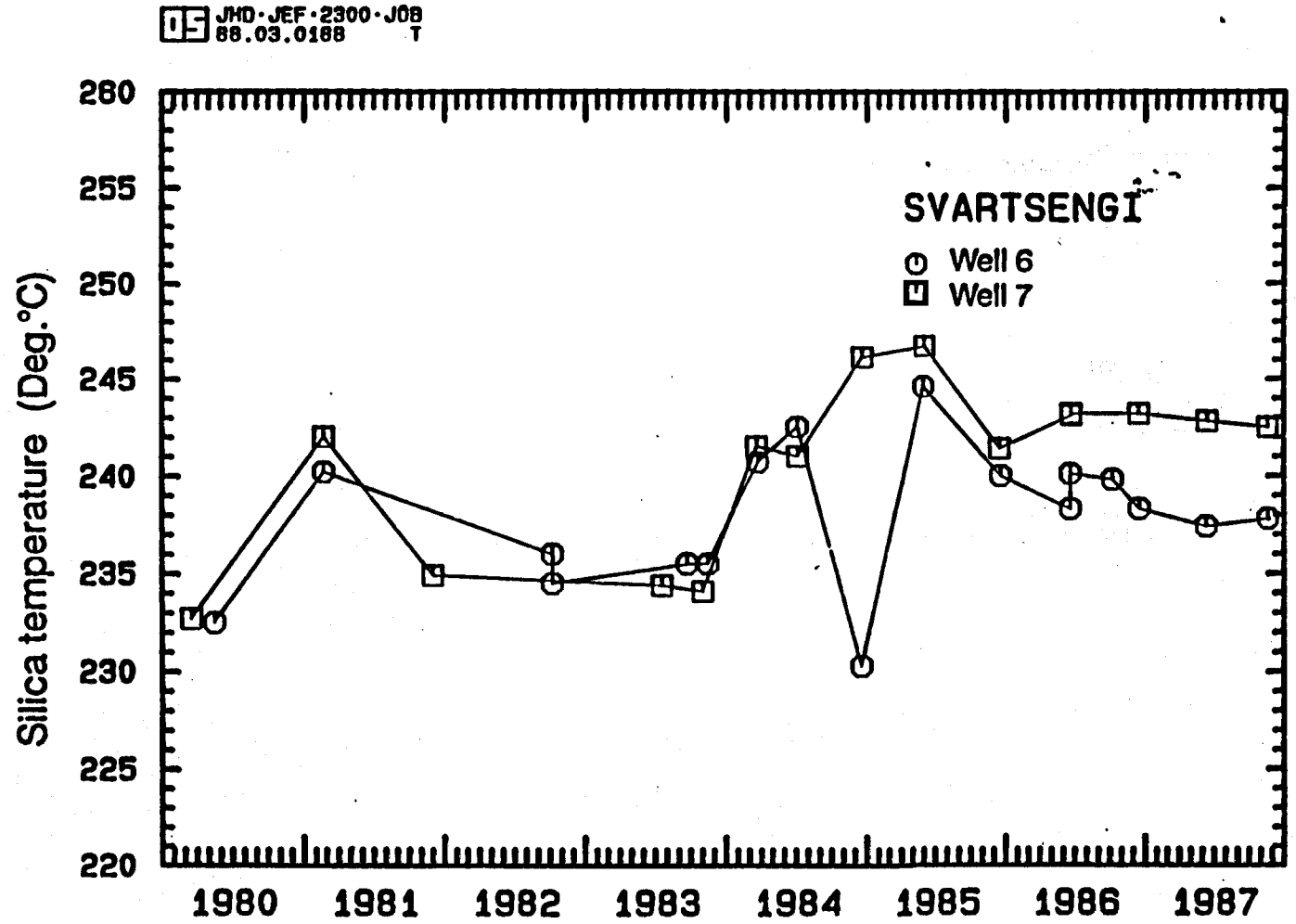
JHD·JEF·2300·J08
88.03.0188 T
SVARTSENGI
Well 6
Well 7
Silica temperature (Deg.°C)
260
255
250
245
240
235
230
225
220
1980
1981
1982
1983
1984
1985
1986
1987

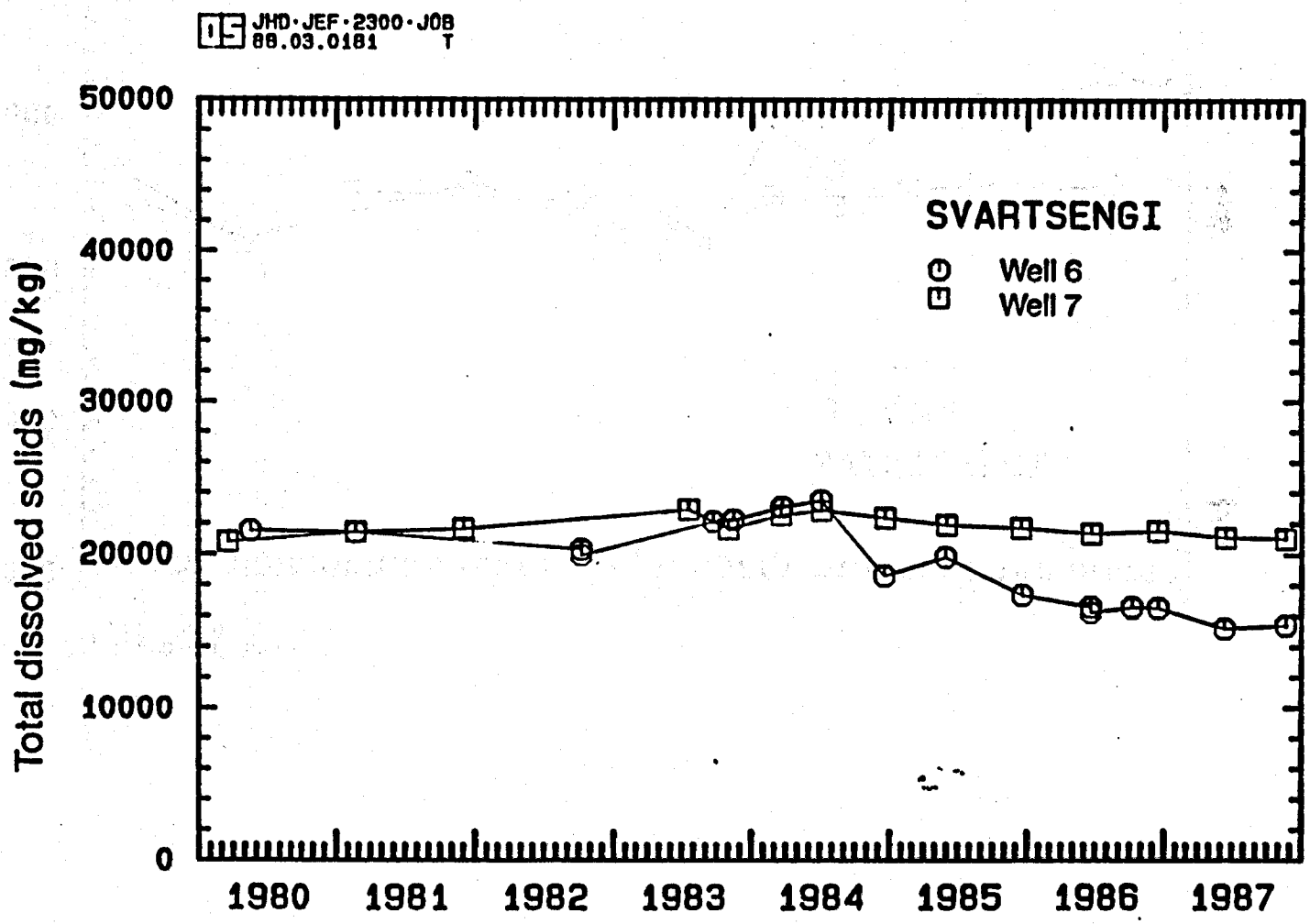
JHD·JEF·2300·JOB
88.03.0181 T
SVARTSENGI
Well 6
Well 7
Total dissolved solids (mg/kg)
50000
40000
30000
20000
10000
0
1980
1981
1982
1983
1984
1985
1986
1987

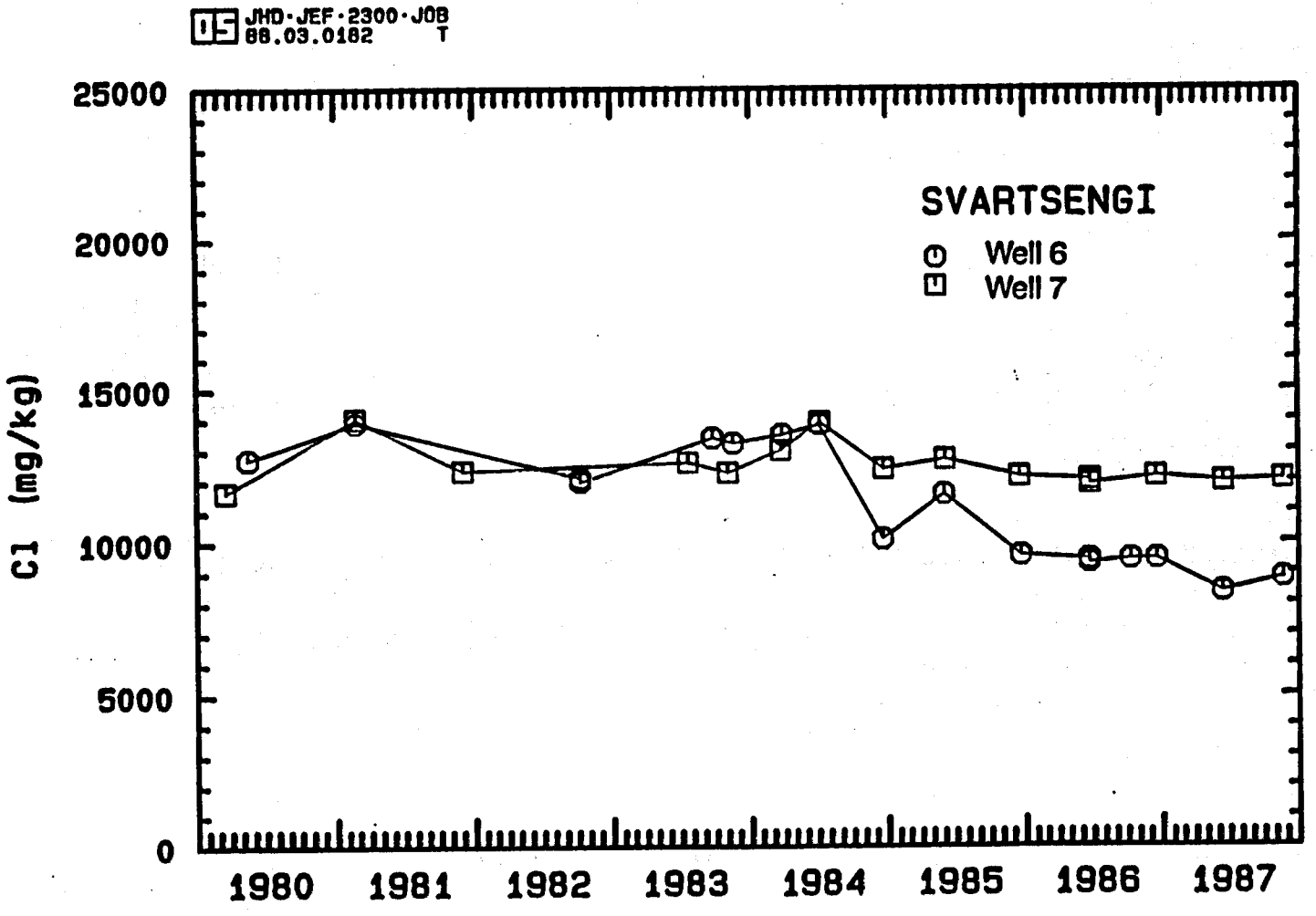
JHD·JEF·2300·JOB
88.03.0182 T
SVARTSENGI
Well 6
Well 7
Cl (mg/kg)
25000
20000
15000
10000
5000
0
1980
1981
1982
1983
1984
1985
1986
1987

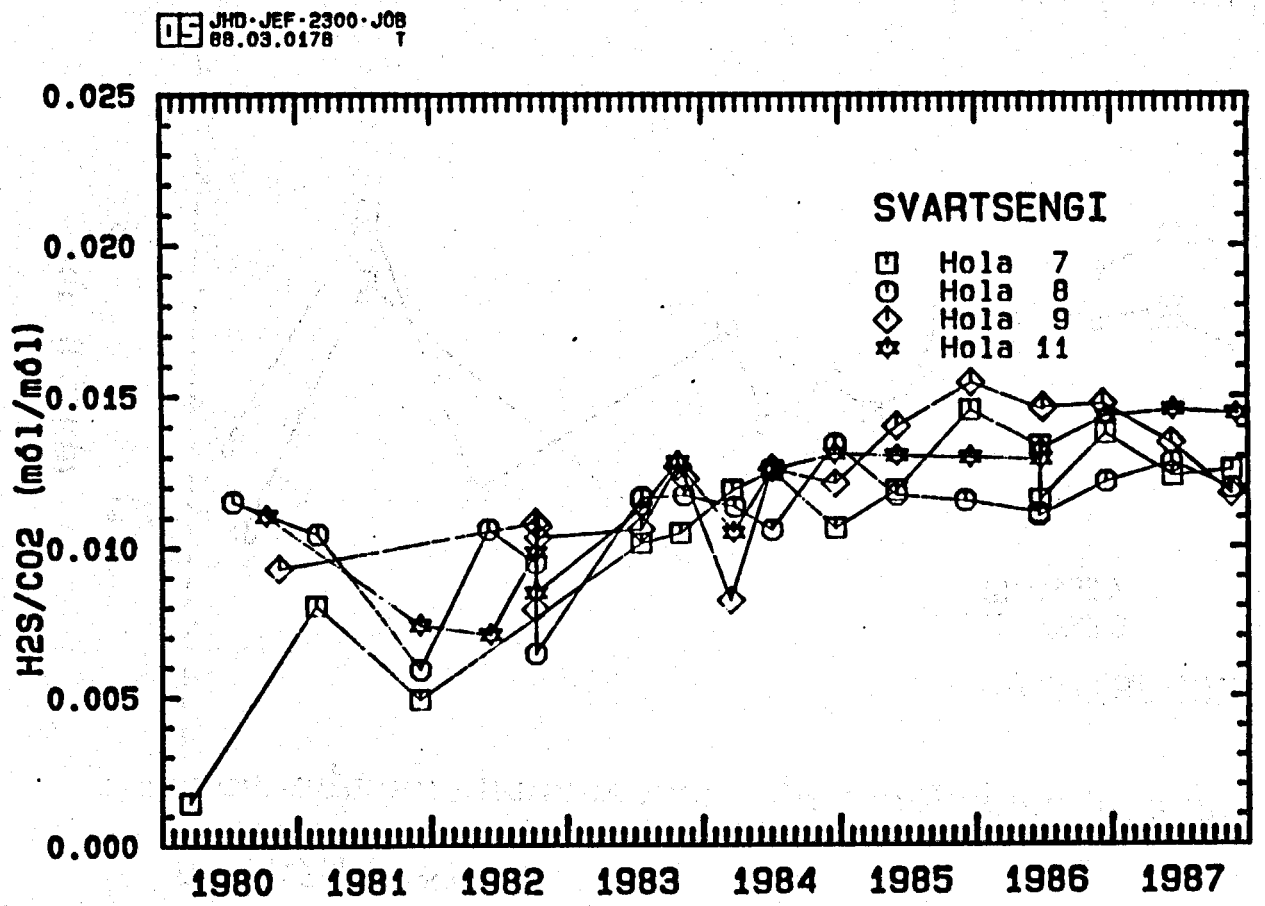

SVARTSENGI WELLS 7,8,9 AND 11.

Hydrogen sulfide and carbon dioxide ratios of resevoir fluids, 1980-1987.

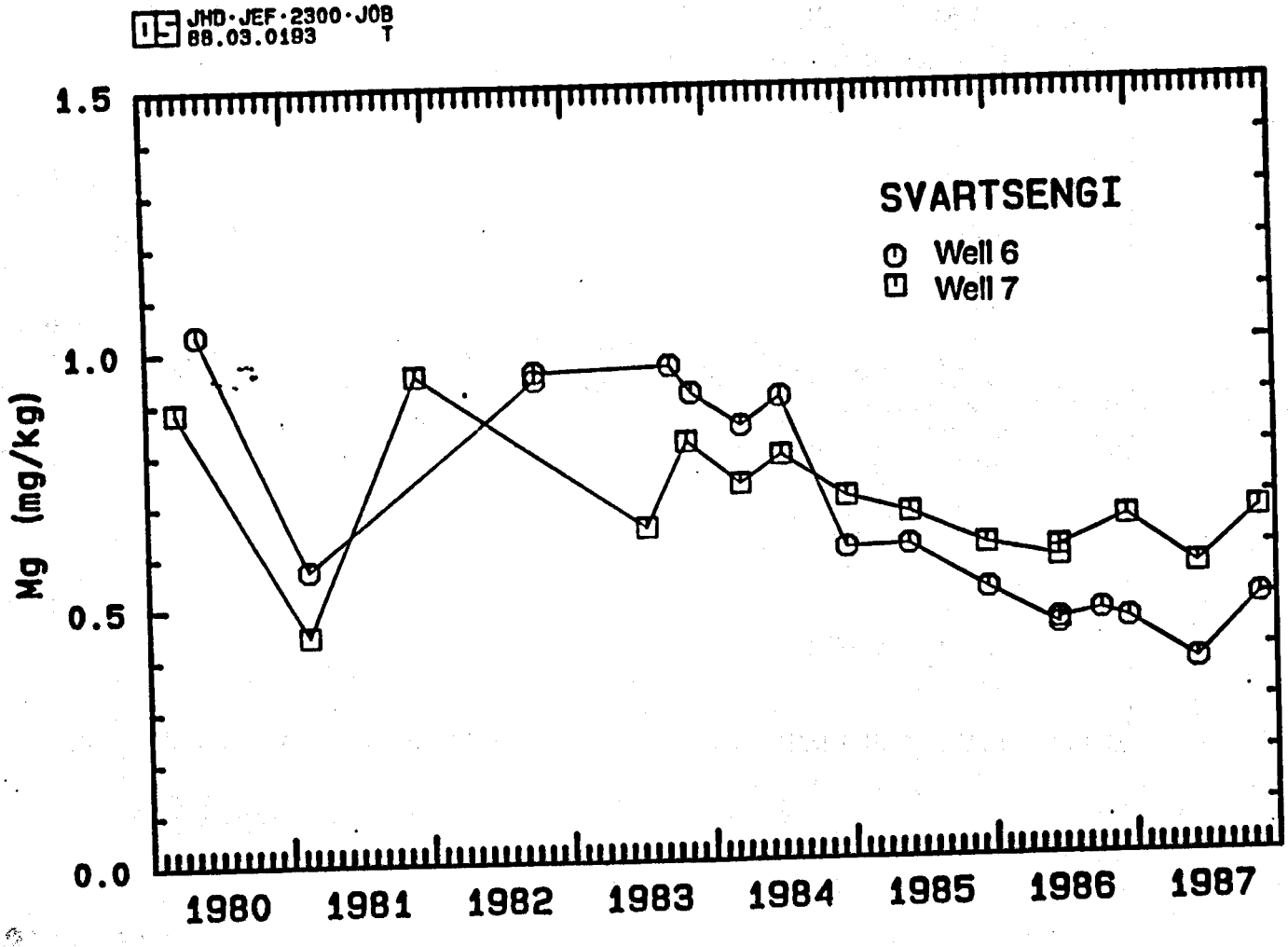
JHD·JEF·2300·JOB
88.03.0183 T
SVARTSENGI
Well 6
Well 7
Mg (mg/kg)
1.5
1.0
0.5
0.0
1980
1981
1982
1983
1984
1985
1986
1987

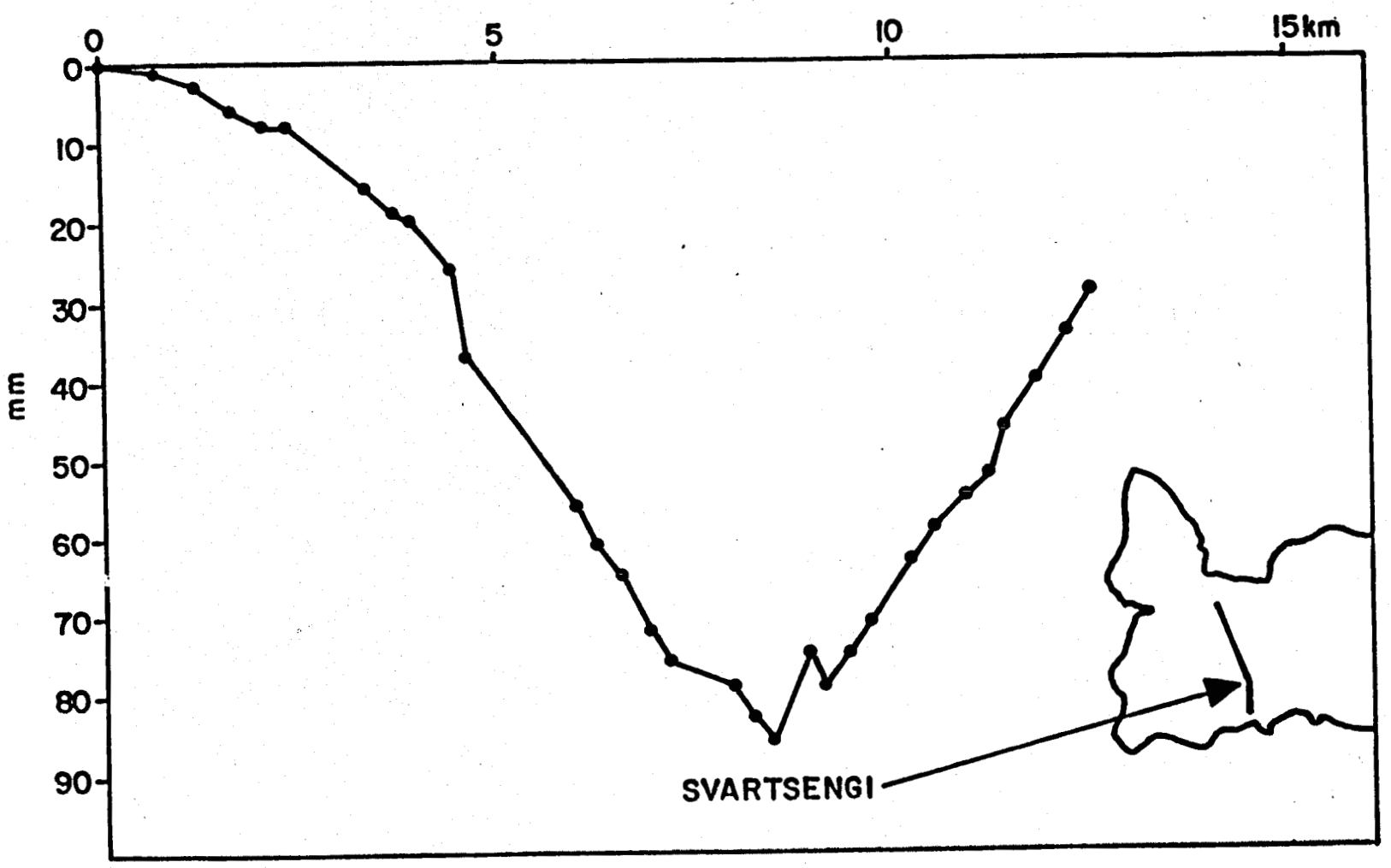

SVARTSENGI.

Subsidence during 1975 to 1982.

GEOTHERMAL RESOURCES COUNCIL

Workshop On

Responses of a Geothermal Field During Exploitation

A Reservoir Management Plan

Presentation by
Alfred H. Truesdell

15-16 June 1989
The Shattuck Hotel
Berkeley Conference Center
Berkeley, California

CHEMICAL PROCESSES AND CHANGES DURING EXPLOITATION -- BOILING, MIXING AND PRECIPITATION

- Natural State

  Heat excess systems
  - Vapor dominated (The Geysers, Larderello)
  - Some 2-phase (Cerro Prieto β, Los Azufres)

  Liquid excess systems
  - Other 2-phase (Cerro Prieto α, Wairakei)
  - Low temperature

- Exploited State

  Mass removed → Pressure decline

  Response with heat excess

  Boiling
  - Superheating of steam
  - Excess steam production
  - Mineral deposition
  - HCl appearance

  Response with liquid excess

  Recharge with cooler water
  - Decrease of temperature
  - Cold sweep

- Solutions

  Injection for heat excess
  Well location for liquid excess

Geochemically Important Distinctions Between Reservoir Types in Their Natural State

- Vapor-Dominated Reservoir
  - Formed by boil down of hot-water system from increased heat or decreased recharge
  - Liquid is immobile; vapor is highly mobile
  - Produces only steam -- only gas and isotope analyses
  - Liquids include condensate (sampled) and deep brine (never sampled)
  - Naturally cools by release of steam
  - Example: The Geysers

- Two-Phase Reservoir
  - Liquid and vapor mobile
  - At boiling point to depth
  - Chemistry of liquid and vapor well known
  - Usually meteoric water with solutes from rock reaction
  - Cools by boiling with ascent of steam and water and/or by mixing with cooler water
  - Example: Cerro Prieto deep reservoir
  - Reservoir may have fracture or matrix porosity and permeability

- Hot-Water Reservoir
  - Contains only compressed liquid otherwise similar to two-phase
  - Liquid may boil during ascent to the surface
  - Cools mostly by mixing with cooler water (and conduction?)
  - Example: Wairakei(?), Klamath Falls

- Exploitation Effects -- Boiling

When pressures decline from mass removal well sealed reservoirs boil (Broadlands(?), Cerro Prieto β)

Boiling has these effects:
- Pressure is related to rock temperature and stabilized
- Lowers temperature -- affects all temperature-sensitive equilibria
- Produces a vapor phase -- gases partition into vapor
- Concentrates solutes } Minerals precipitate
- Increases pH
- Heat transfers from rock to fluid } Excess steam produced
- Steam may segregate and enter wells
- Mineral precipitation reduces permeability (Okay if distributed; a problem if localized)
- Boiling process differs in fracture and matrix reservoirs

Extreme boiling has these effects:
- Liquid may become immobile and only steam is produced (two-phase)
- Liquid may disappear and only superheated steam is produced (vapor-dominated)
- Pressure no longer linked to rock temperature may drop rapidly
- Steam no longer from liquid may become gas rich
- HCl may be produced and tranported to wells

- Exploitation Effects -- Cool-Water Entry

With lowered pressures, poorly sealed reservoirs suck in surrounding cooler water (Cerro Prieto α, Old Travale)

Entry of cooler water has these effects:
- Rock heat is transferred to cool water -- heat sweep
- Reservoir fluid and rock cools
- Vapor (if present) dissolves in liquid, lowering pH
- These changes cause quartz to precipitate, calcite and anhydrite to dissolve
- Cold and hot waters mix also causing quartz precipitation
- Fluid enthalpy and steam production decrease

Extreme effects are more of the above

- Reservoir Management Actions

Prevention of boiling requires pressure maintenance, therefore inject liquid to equal that removed

Liquid injection will:

- Maintain pressure and prevent boiling
- Prevent reservoir plugging (provided chemistry is okay)
- Prevent HCl production and transport
- In vapor systems, provide additional steam and prevent rapid pressure decline
- If sited correctly, injected liquid can sweep heat to wells

Prevention of cool-water entry is more difficult

Two responses are possible:

Site wells so that natural water inflow sweeps heat toward them. This exploits natural pressure maintenance and can mine heat efficiently. No injection wells are needed.

Inject sufficient liquid to maintain pressure and keep cooler water out. Location of injectors relative to producers and natural inflow is important.

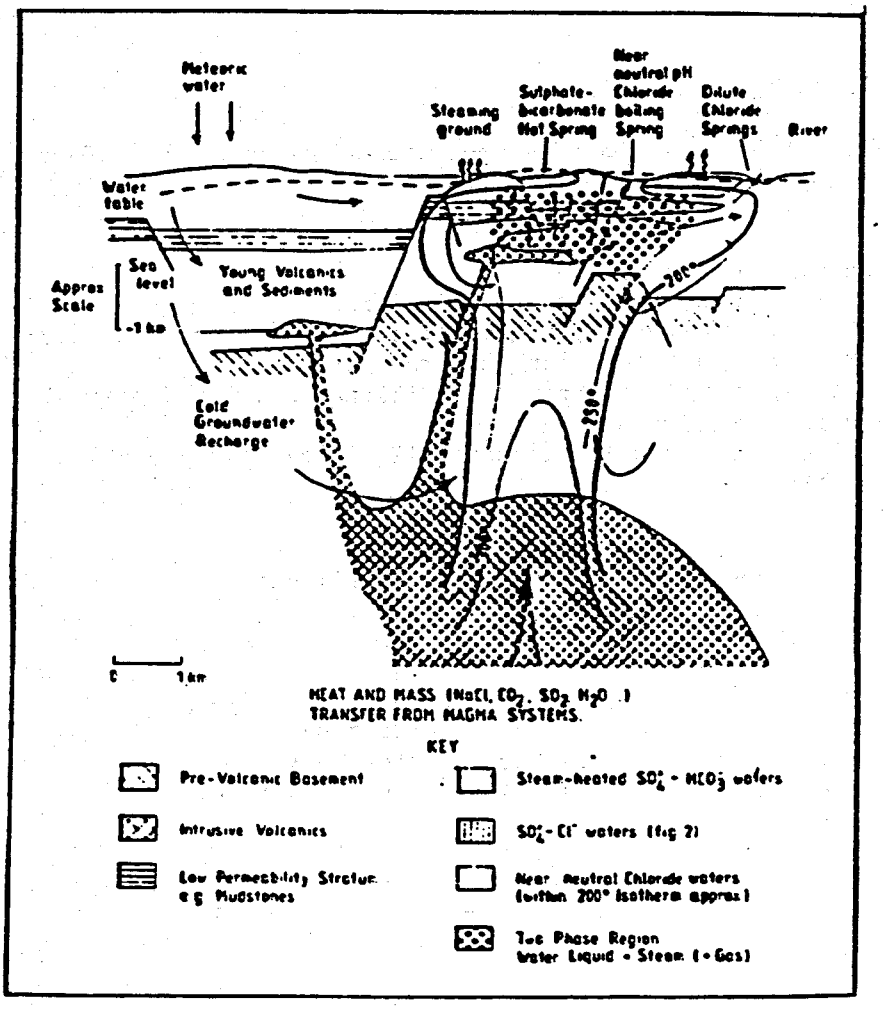
Meteoric water
Steaming ground
Sulphate-bicarbonate Hot Spring
Near neutral pH Chloride boiling Spring
Dilute Chloride Springs
River
Water table
Sea level
Approx Scale
-1 km
Young Volcanics and Sediments
Cold Groundwater Recharge
250°
300°
200°
0
1 km
HEAT AND MASS (NaCl, CO_2, SO_2 H_2O) TRANSFER FROM MAGMA SYSTEMS.
KEY
Pre-Volcanic Basement
Intrusive Volcanics
Low Permeability Stratum e.g. Mudstones
Steam-heated SO_4^- - HCO_3^- waters
SO_4^- - Cl^- waters (Fig 2)
Near Neutral Chloride waters (within 200° isotherm approx.)
Two Phase Region Water Liquid + Steam (+ Gas)

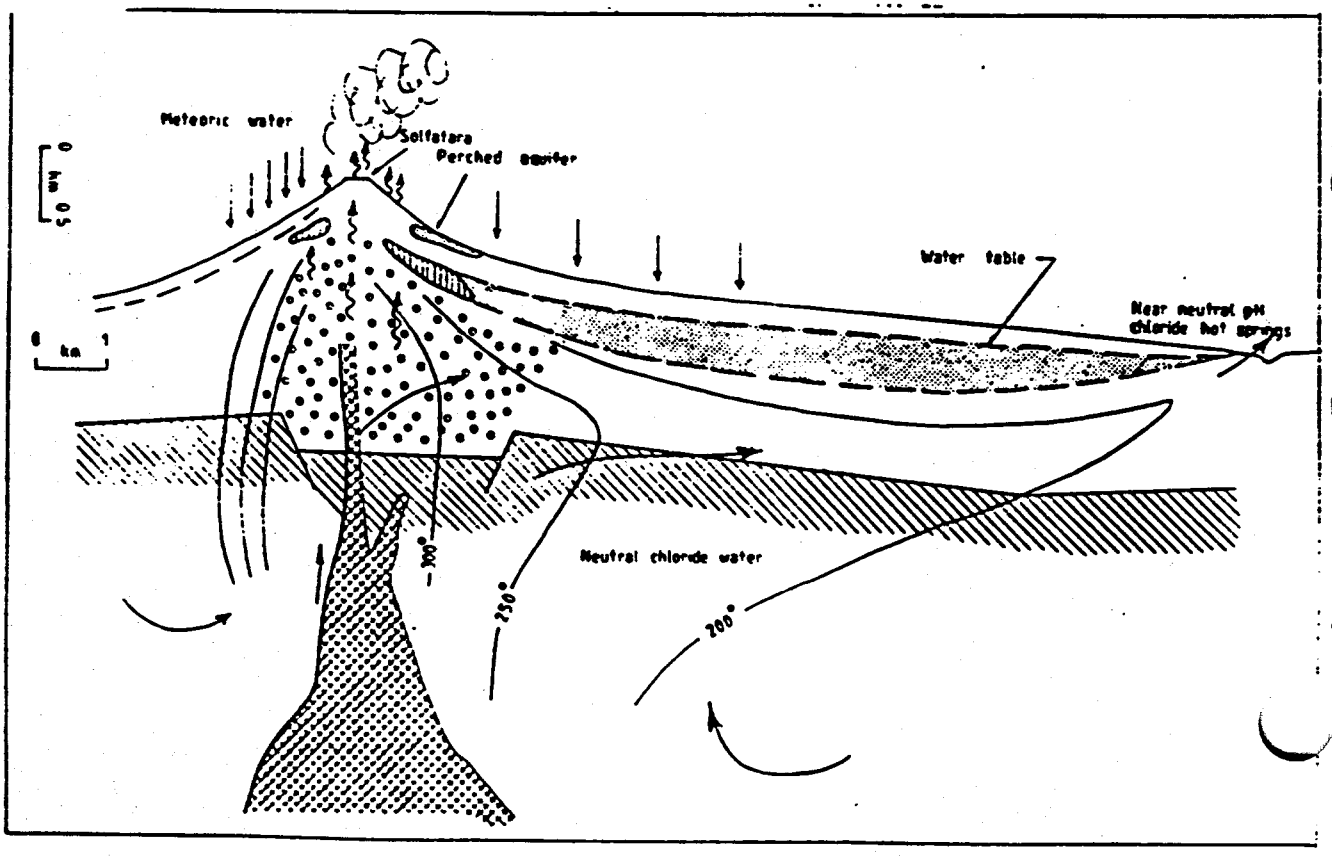
Meteoric water
Solfatara
Perched aquifer
0
0.5 km
0
1 km
Water table
Near neutral pH chloride hot springs
Neutral chloride water
300°
250°
200°

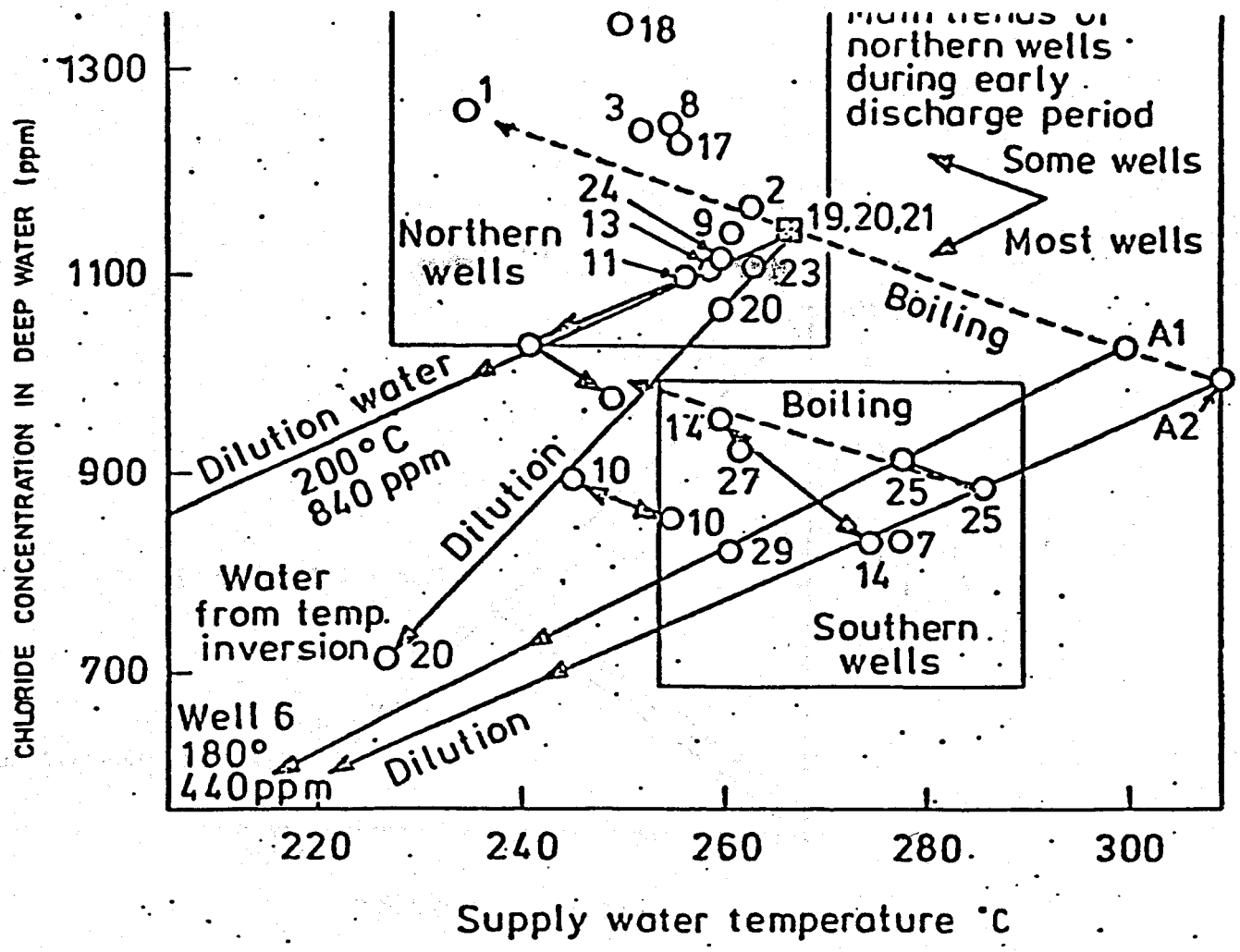
CHLORIDE CONCENTRATION IN DEEP WATER (ppm)
1300
1100
900
700
220
240
260
280
300
Supply water temperature °C
O18
Northern wells
Some wells
Most wells
Boiling
A1
A2
Dilution water
200°C
840 ppm
Dilution
Boiling
Water from temp. inversion
Southern wells
Well 6
180°
440ppm
Dilution

Figure 16

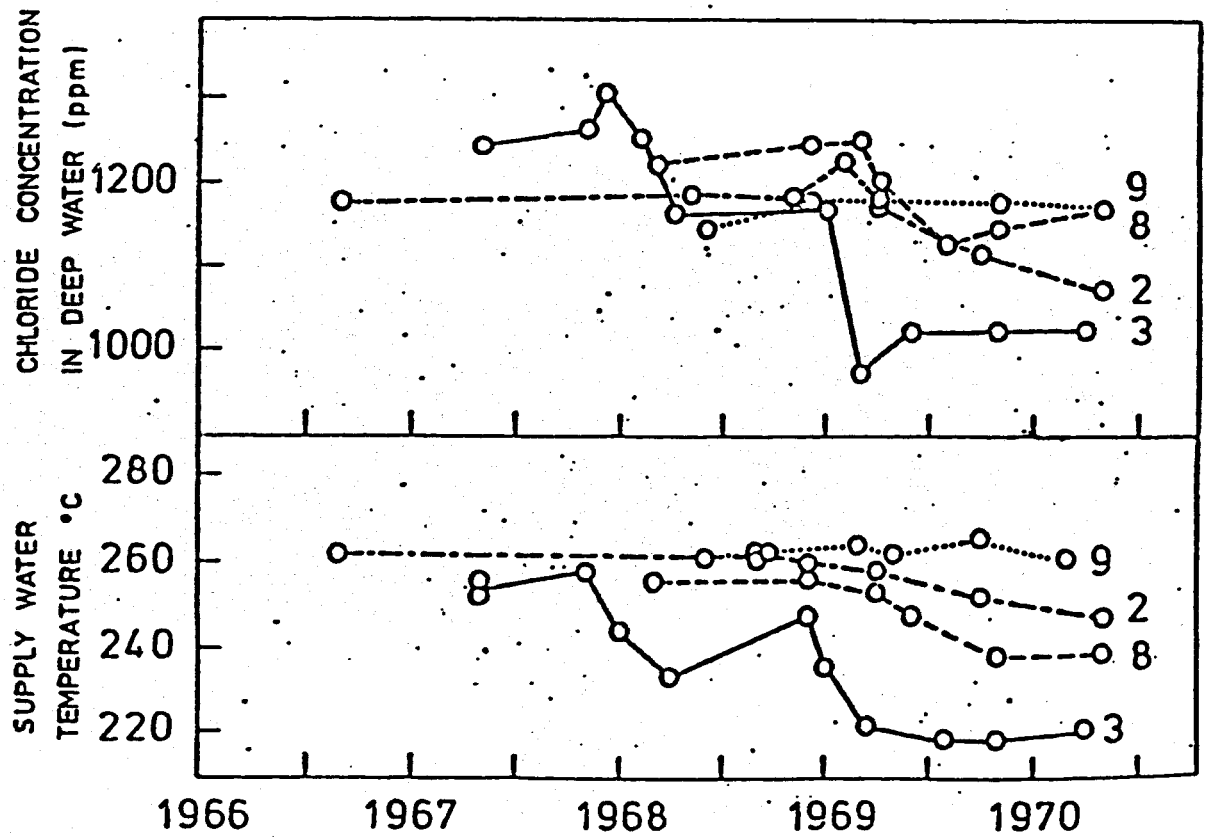
CHLORIDE CONCENTRATION IN DEEP WATER (ppm)
1200
1000
SUPPLY WATER TEMPERATURE °C
280
260
240
220
1966
1967
1968
1969
1970

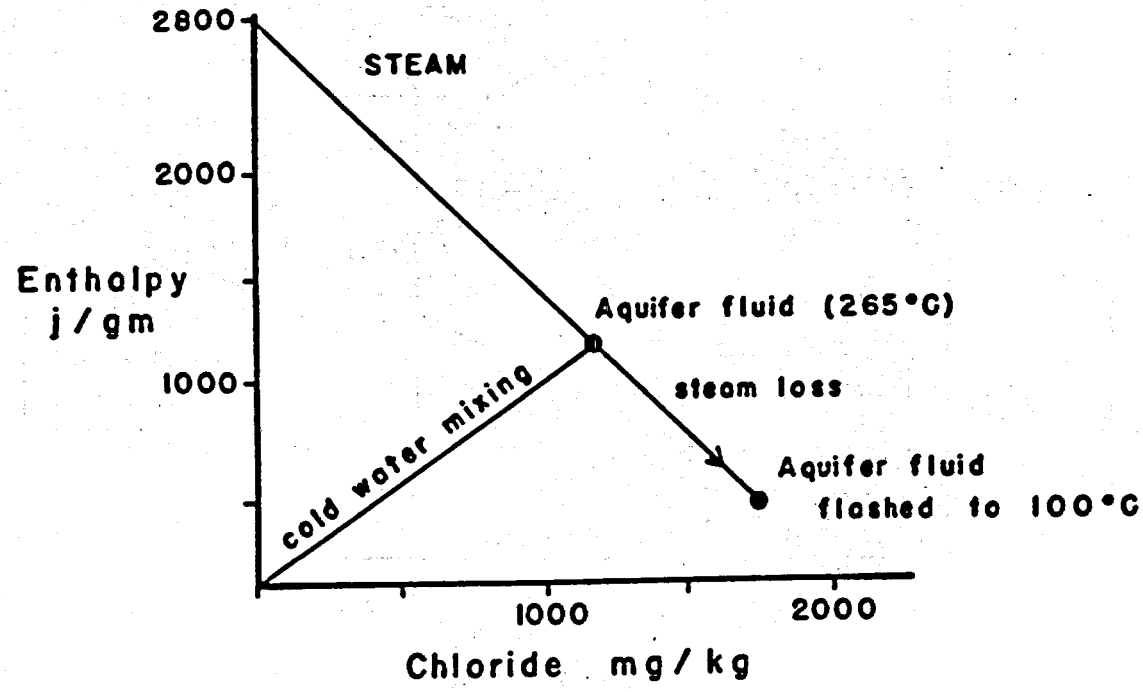

Figure 2.7. A typical enthalpy-chloride mixing diagram showing the effects of boiling and dilution on the 265°C aquifer fluid discussed in the text.

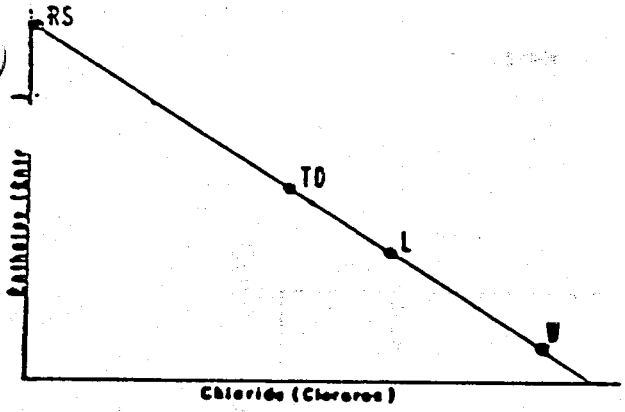

Figure 1a. Concentration-enthalpy plot for a model system with widely distributed boiling. (W:weirbox composition, L: reservoir liquid, TD: total discharge composition, RS: reservoir steam).

Figura 1a. Gráfico de concentración-entalpía de un sistema modelo con ebullición distribuida ampliamente. (W: composición del vertedor, L: líquido del yacimiento, TD: composición del fluido total, RS: vapor del yacimiento.

←

Figure 1b. Gas-enthalpy plot for a model system like that of figure 1a.

Figura 1b. Gráfico de gas-entalpía de un sistema modelo como el de la figura 1a.

→

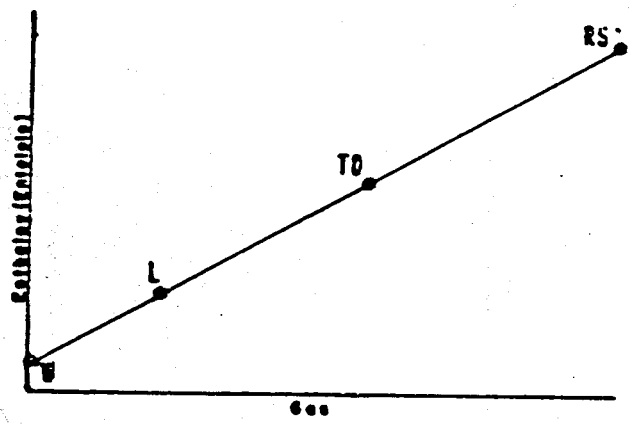

Figure 2a. Concentration-enthalpy plot for a model system with heat transfer from rock to fluid. (TDH: total discharge composition with heat transfer from rock, TDHS: mixture of reservoir steam and steam produced by heat transfer).

Figura 2a. Gráfico de concentración-entalpía de un sistema modelo con transferencia de calor de la roca al fluido. (TDH: composición del fluido total con transferencia de calor de la roca, TDHS: mezcla de vapor del yacimiento y vapor producido por transferencia de calor).

←

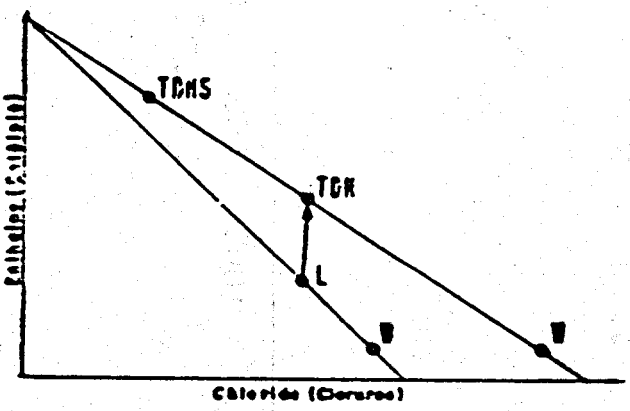

Figure 2b. Gas-enthalpy plot for a model system like that of figure 2a. (SS: separated steam, SSH: separated steam with heat transfer from rock, SSNG: mixture of separated steam and gas free steam.

Figura 2b. Gráfico de gas-entalpía de un sistema modelo como el de la figura 2a. (SS: vapor separado, SSH: vapor separado con transferencia de calor de la roca, SSNG: mezcla de vapor separado y sin gas).

→

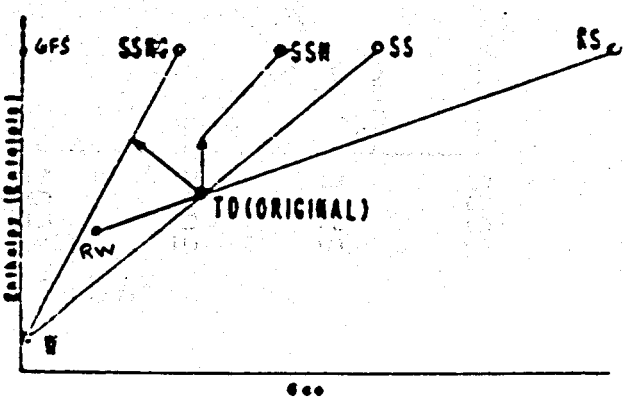

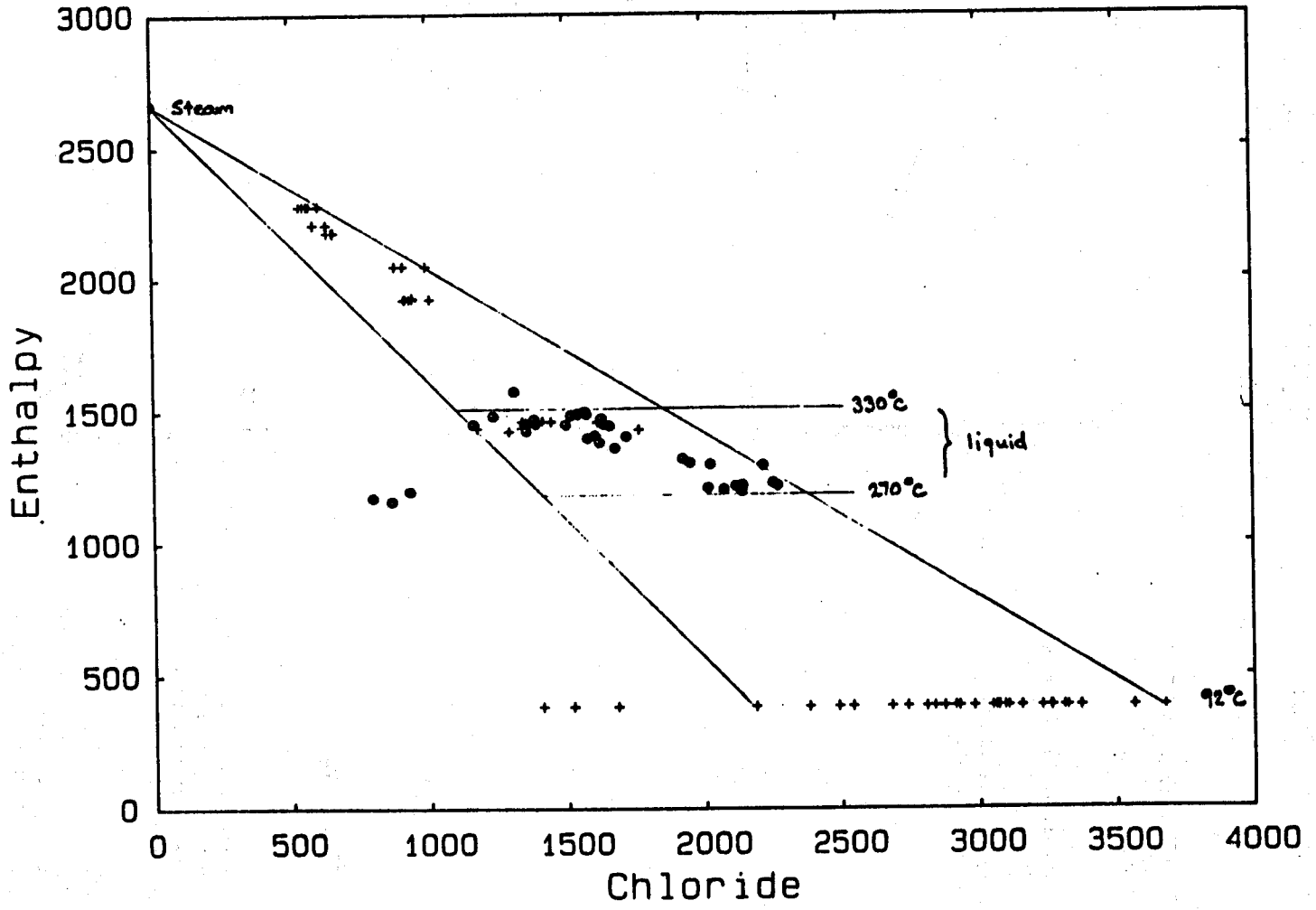
3000
2500
2000
1500
1000
500
0
Enthalpy
Steam
330°C
liquid
270°C
92°C
0
500
1000
1500
2000
2500
3000
3500
4000
Chloride

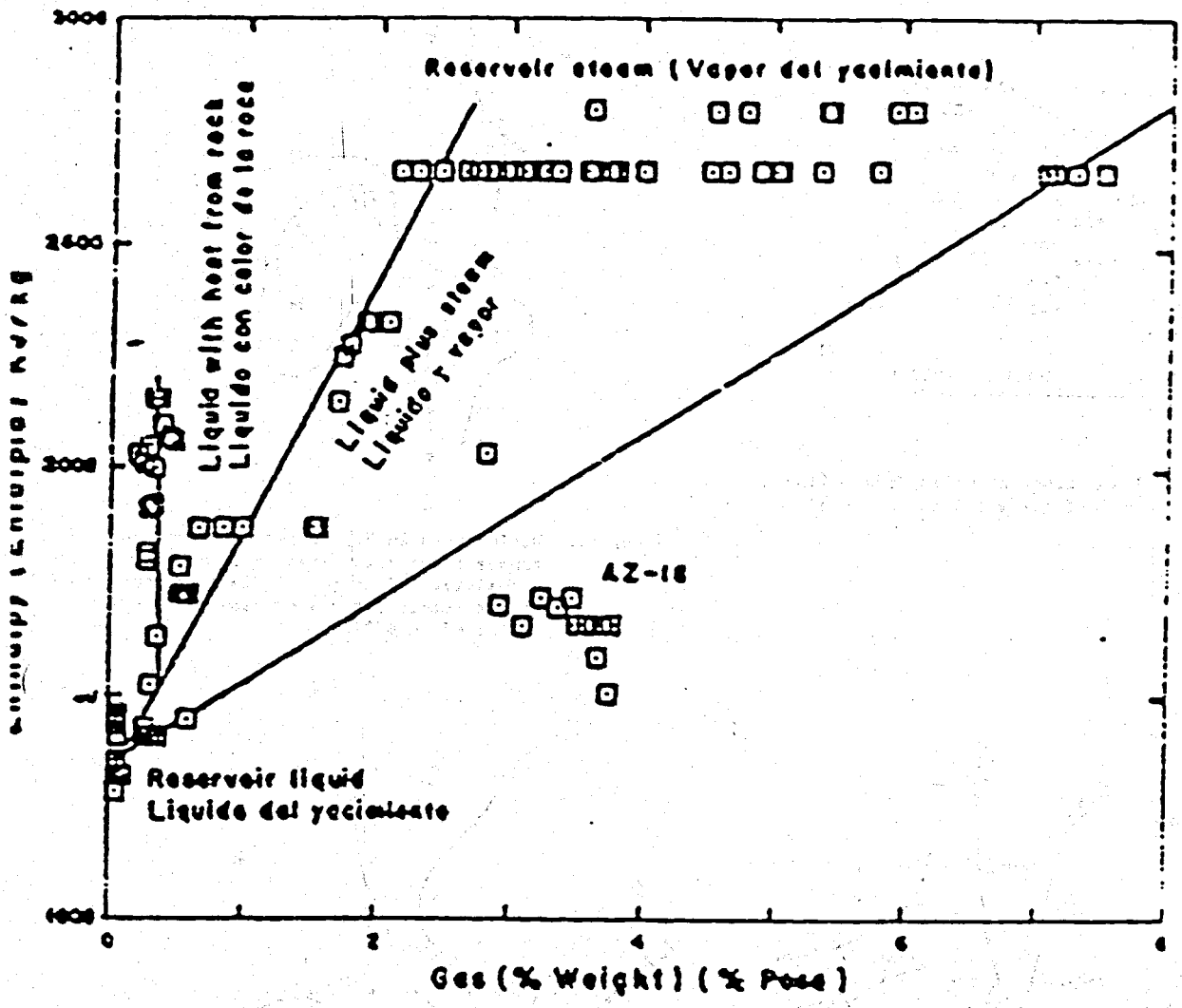
Reservoir steam (Vapor del yacimiento)
Liquid with heat from rock
Líquido con calor de la roca
Liquid plus steam
Líquido y vapor
AZ-18
Reservoir liquid
Líquido del yacimiento
2000
2400
2800
0
2
4
6
8
Gas (% Weight) (% Peso)

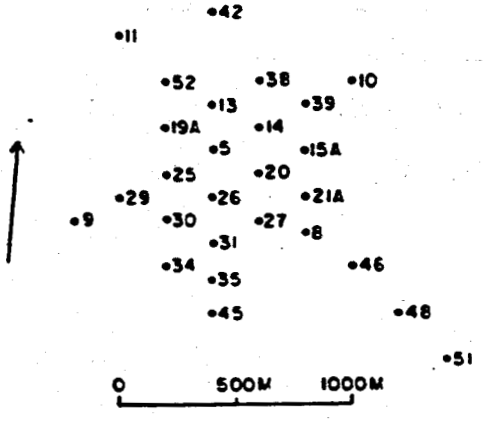

Figure 1. Well locations at Cerro Prieto (the area shown in figures 1-4 is the same).

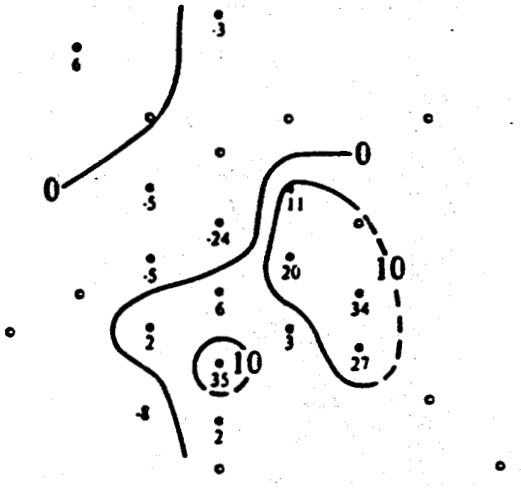

Figure 4. Differences in °C between aquifer temperatures calculated from measured enthalpies and those calculated from silica concentrations of fluids collected in 6/77.

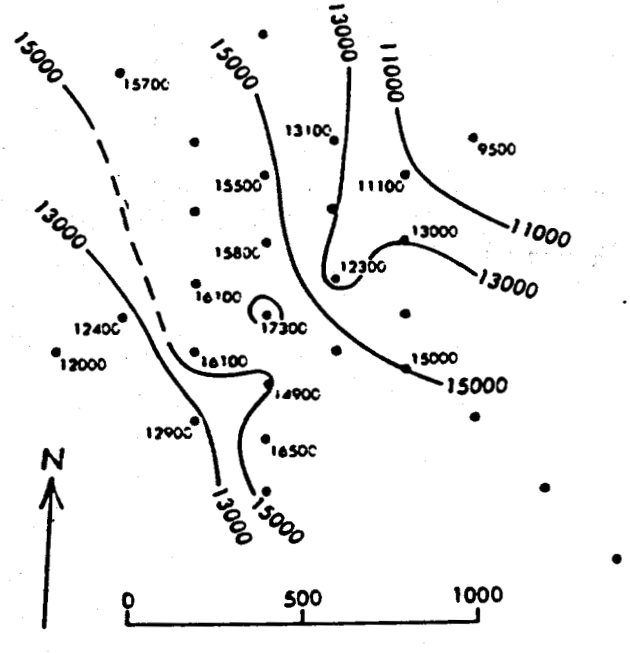

Figure 2. 1973-74 average brine chloride concentrations in mg/kg after flashing to one atmosphere. Data from Manon et al.[1] and Reed[2]

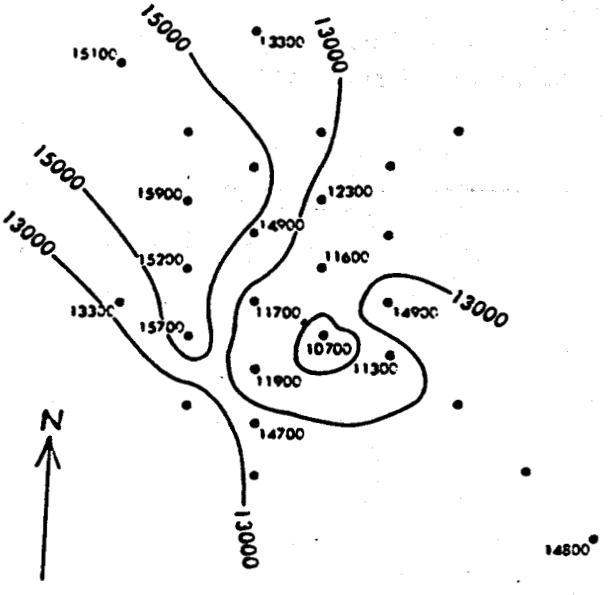

Figure 3. 1977-78 average brine chloride concentrations in mg/kg after flashing. Data from Manon et al.[1] and unpublished data[3]

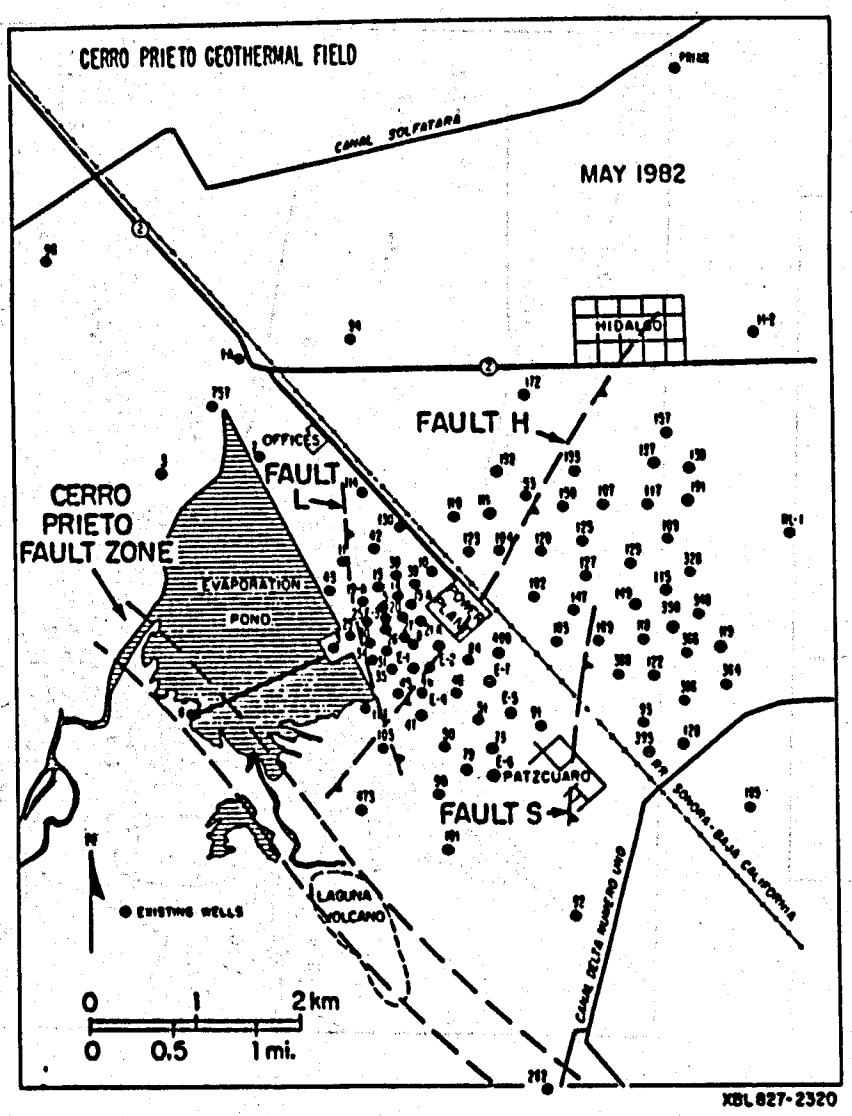
CERRO PRIETO GEOTHERMAL FIELD
MAY 1982
CANAL SOLFATARA
HIDALGO
FAULT H
OFFICES
FAULT L
CERRO PRIETO FAULT ZONE
EVAPORATION POND
PLANT
PATZCUARO
FAULT S
LAGUNA VOLCANO
EXISTING WELLS
CANAL DELTA RIO HONDO
SONORA - BAJA CALIFORNIA
0 1 2km
0 0.5 1 mi.
XBL 827-2320

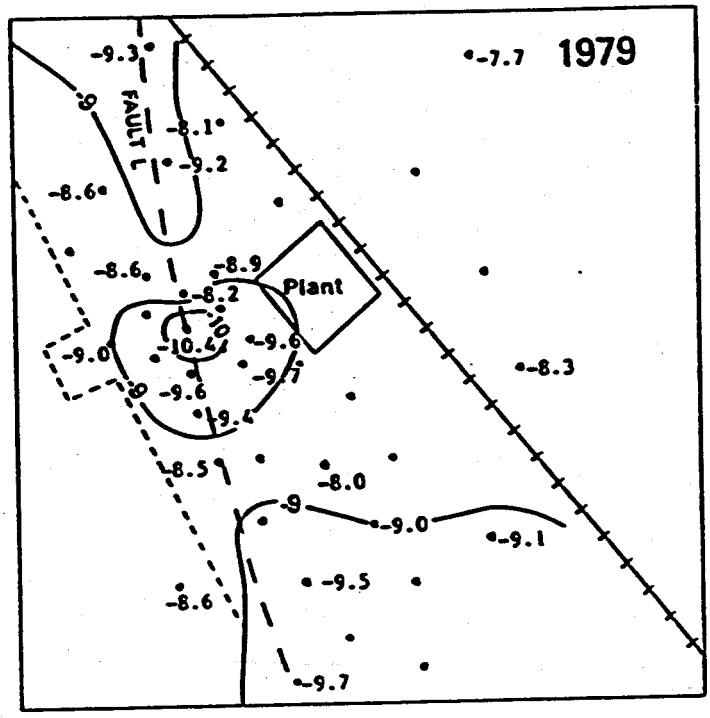
1979
FAULT L
Plant
-9.3
-8.1
-9.2
-8.6
-8.9
-8.2
-10.4
-9.6
-9.7
-9.0
-9.6
-9.4
-8.5
-8.0
-9
-9.0
-9.1
-8.6
-9.5
-9.7
-7.7
-8.3

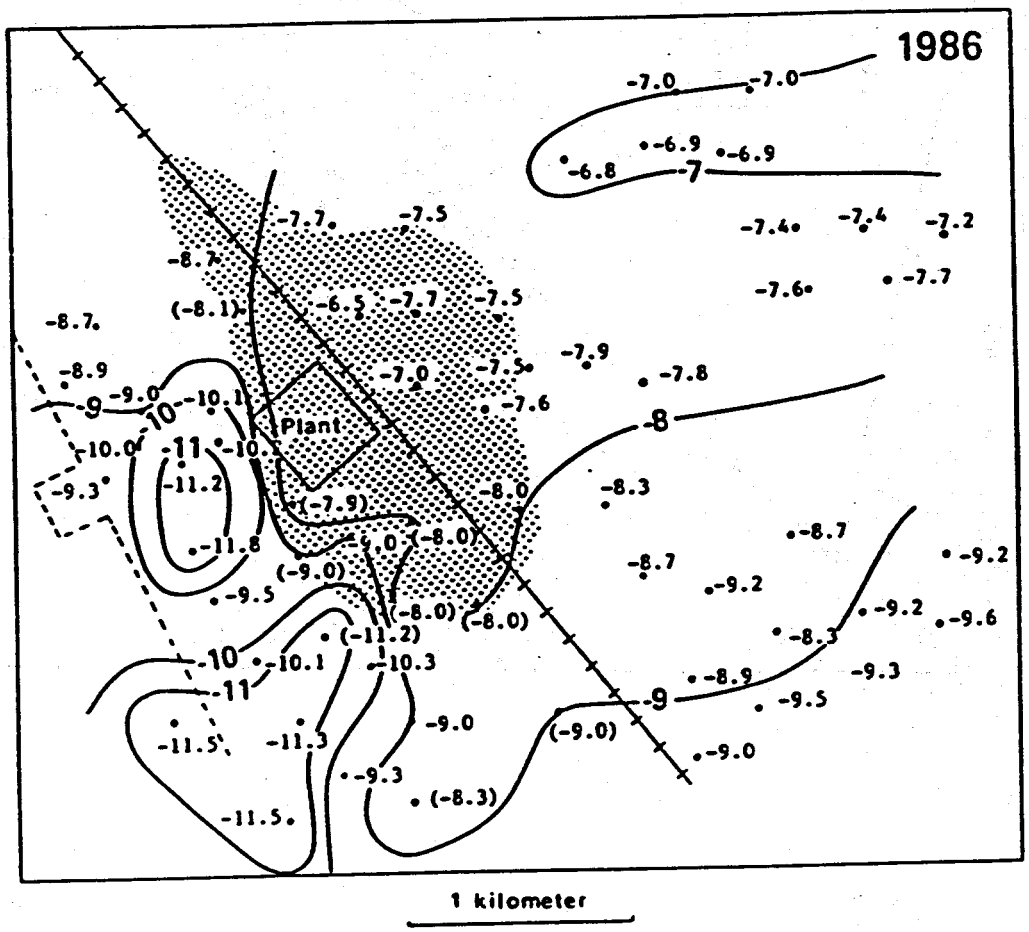
1986
Plant
-7.0
-7.0
-6.9
-6.9
-6.8
-7
-7.4
-7.4
-7.2
-7.6
-7.7
-7.7
-7.5
-8.7
(-8.1)
-6.5
-7.7
-7.5
-8.7
-8.9
-9.0
-9
-10
-10.1
-7.0
-7.5
-7.9
-7.8
-7.6
-8
-10.0
-11
-10.2
-9.3
-11.2
(-7.9)
-8.0
-8.3
-11.8
-9.0
(-8.0)
-8.7
-9.2
(-9.0)
-9.5
-8.7
-9.2
(-8.0)
(-8.0)
-9.2
-9.6
-8.3
(-11.2)
-10
-10.1
-10.3
-11
-8.9
-9.3
-9
-9.5
-11.5
-11.3
-9.0
(-9.0)
-9.0
-9.3
(-8.3)
-11.5

1 kilometer

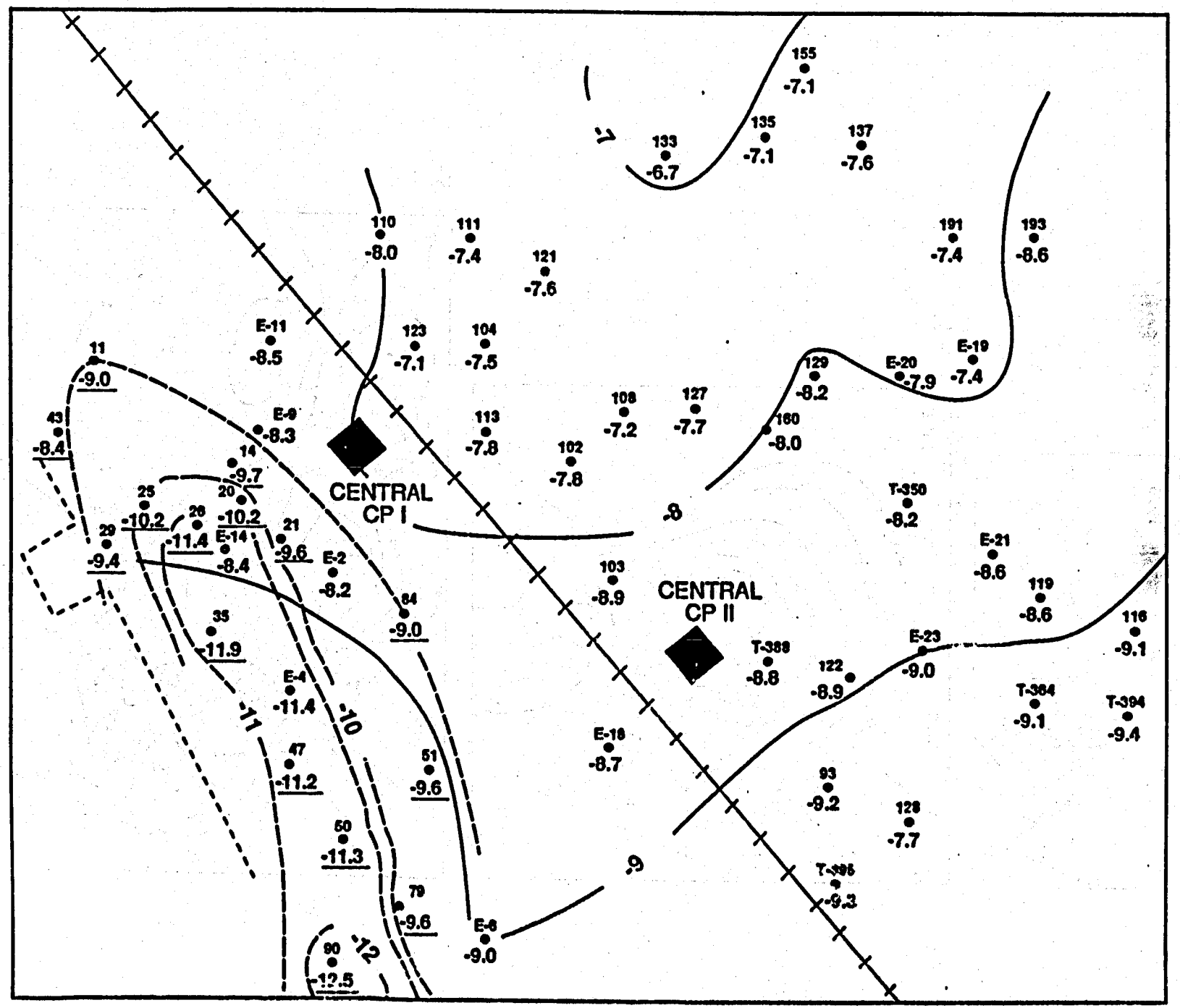
CENTRAL
CP I
CENTRAL
CP II
-7
-8
-9
-10
-11
-12
155
-7.1
133
-6.7
135
-7.1
137
-7.6
110
-8.0
111
-7.4
121
-7.6
191
-7.4
193
-8.6
E-11
-8.5
123
-7.1
104
-7.5
11
-9.0
E-19
-7.4
129
-8.2
E-20
-7.9
108
-7.2
127
-7.7
43
-8.4
E-9
-8.3
113
-7.8
160
-8.0
14
-9.7
102
-7.8
T-350
-8.2
25
-10.2
20
-10.2
26
-11.4
21
-9.6
E-14
-8.4
E-21
-8.6
29
-9.4
E-2
-8.2
103
-8.9
119
-8.6
84
-9.0
116
-9.1
35
-11.9
T-388
-8.8
E-23
-9.0
122
-8.9
E-4
-11.4
T-364
-9.1
T-394
-9.4
E-18
-8.7
47
-11.2
51
-9.6
93
-9.2
128
-7.7
50
-11.3
T-395
-9.3
79
-9.6
E-6
-9.0
90
-12.5

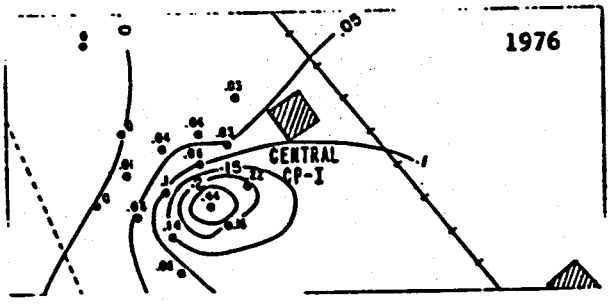

Figure 5a

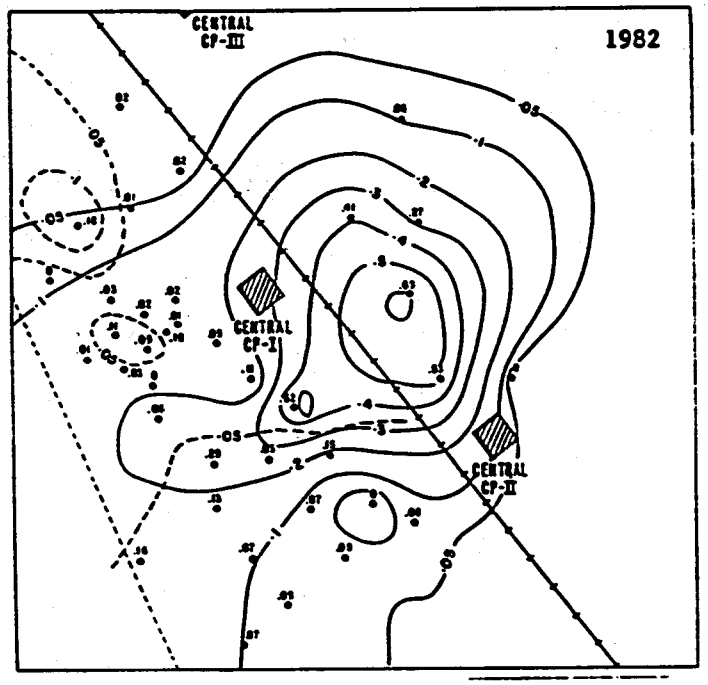

5b.

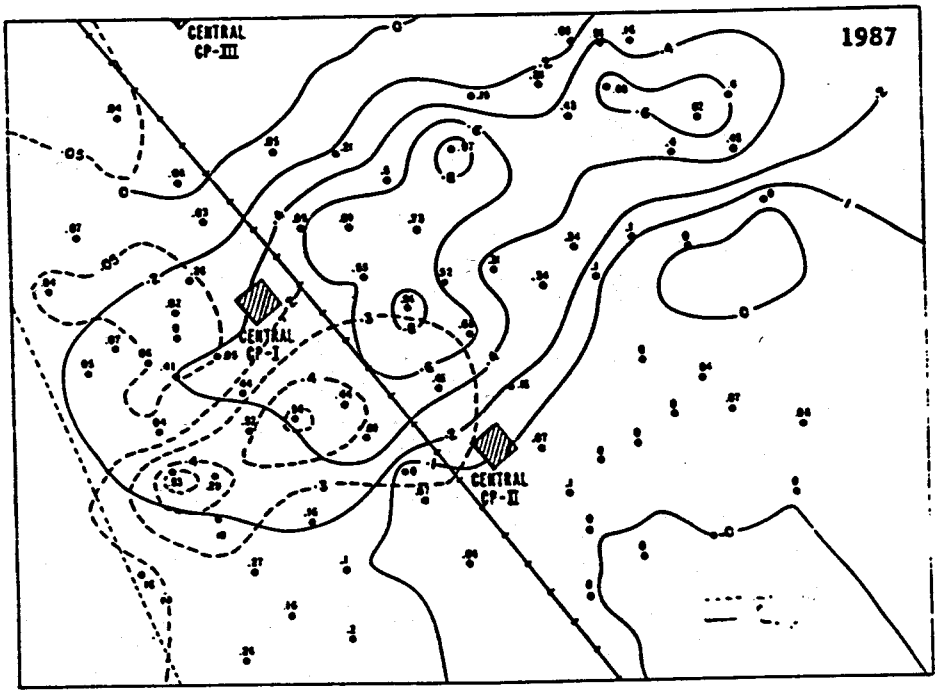

5c.

Figure 4a.

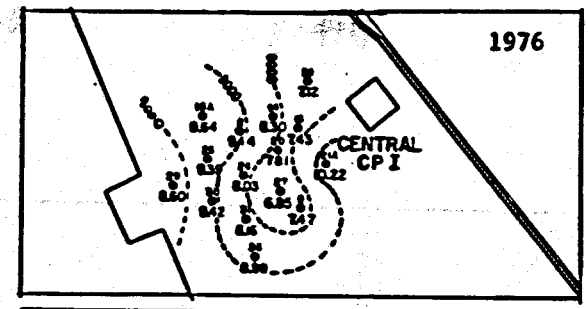

4b.

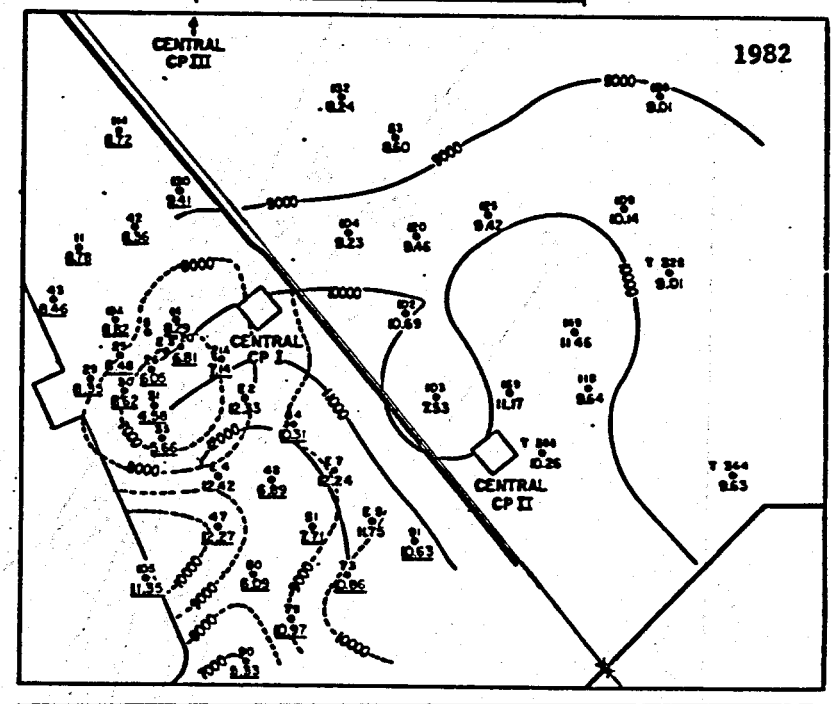

4c.

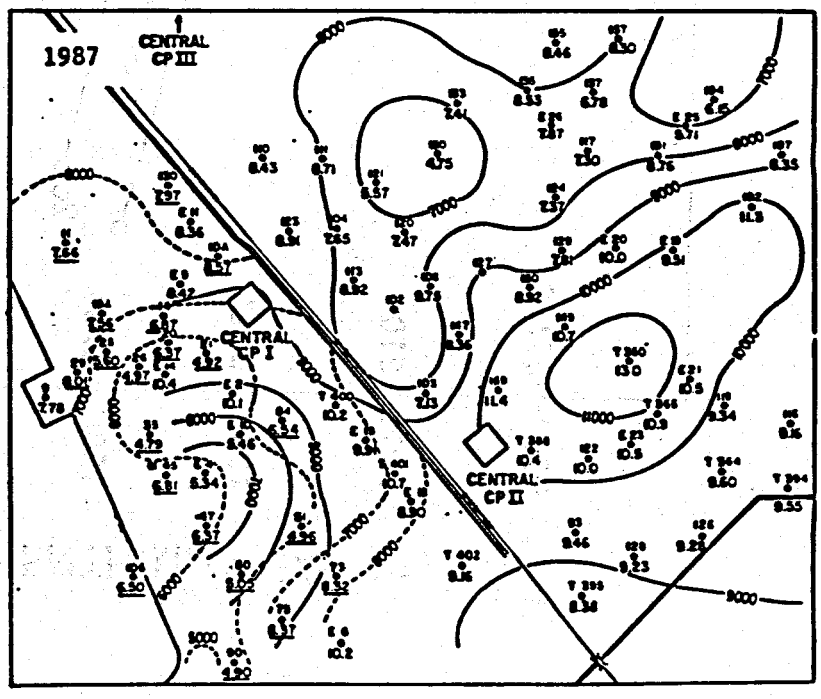

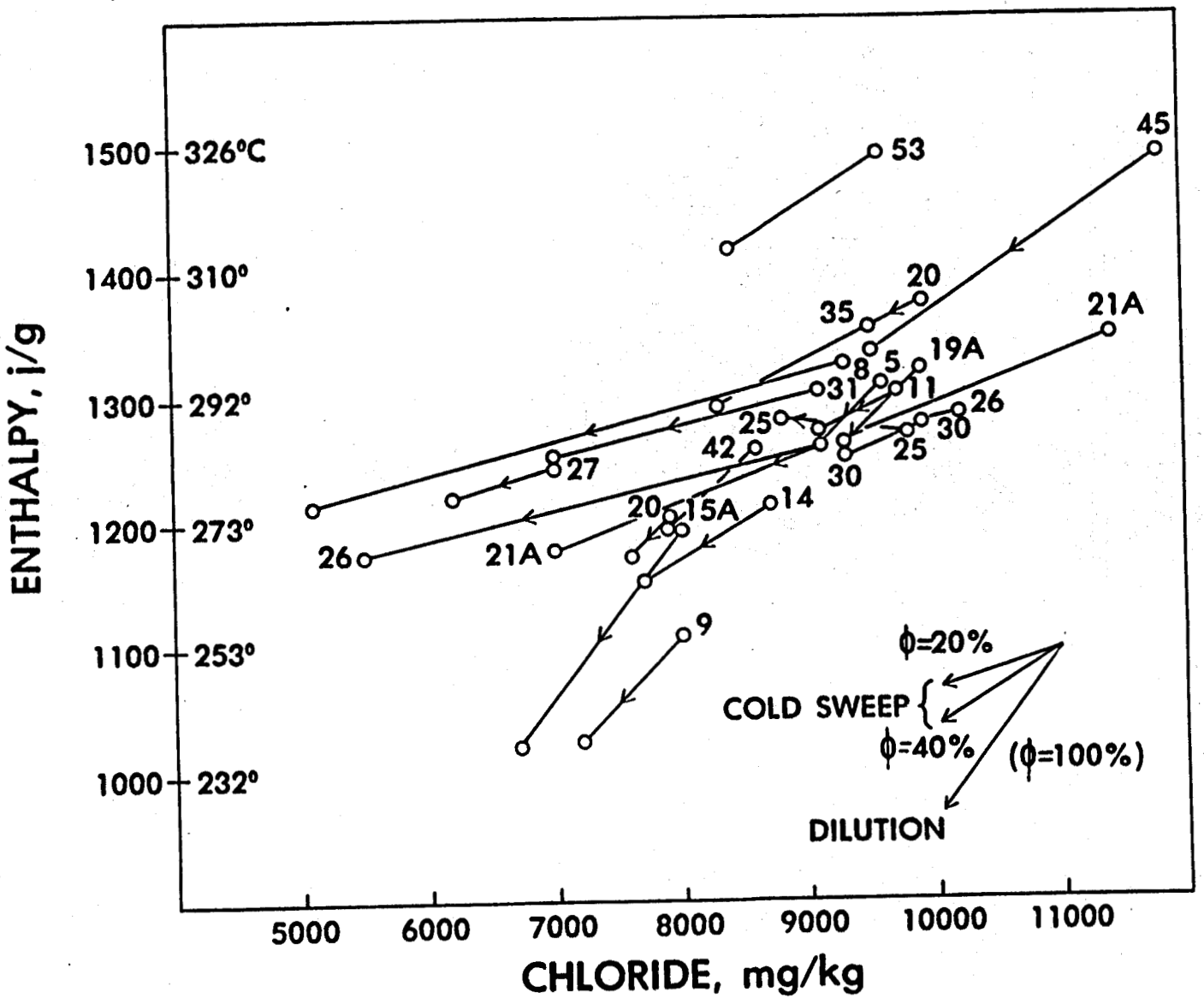
ENTHALPY, j/g
1500
326°C
1400
310°
1300
292°
1200
273°
1100
253°
1000
232°
5000
6000
7000
8000
9000
10000
11000
CHLORIDE, mg/kg
53
45
20
35
21A
19A
8
5
31
11
26
25
30
42
27
25
30
20
15A
14
26
21A
9
ϕ=20%
COLD SWEEP
ϕ=40%
(ϕ=100%)
DILUTION

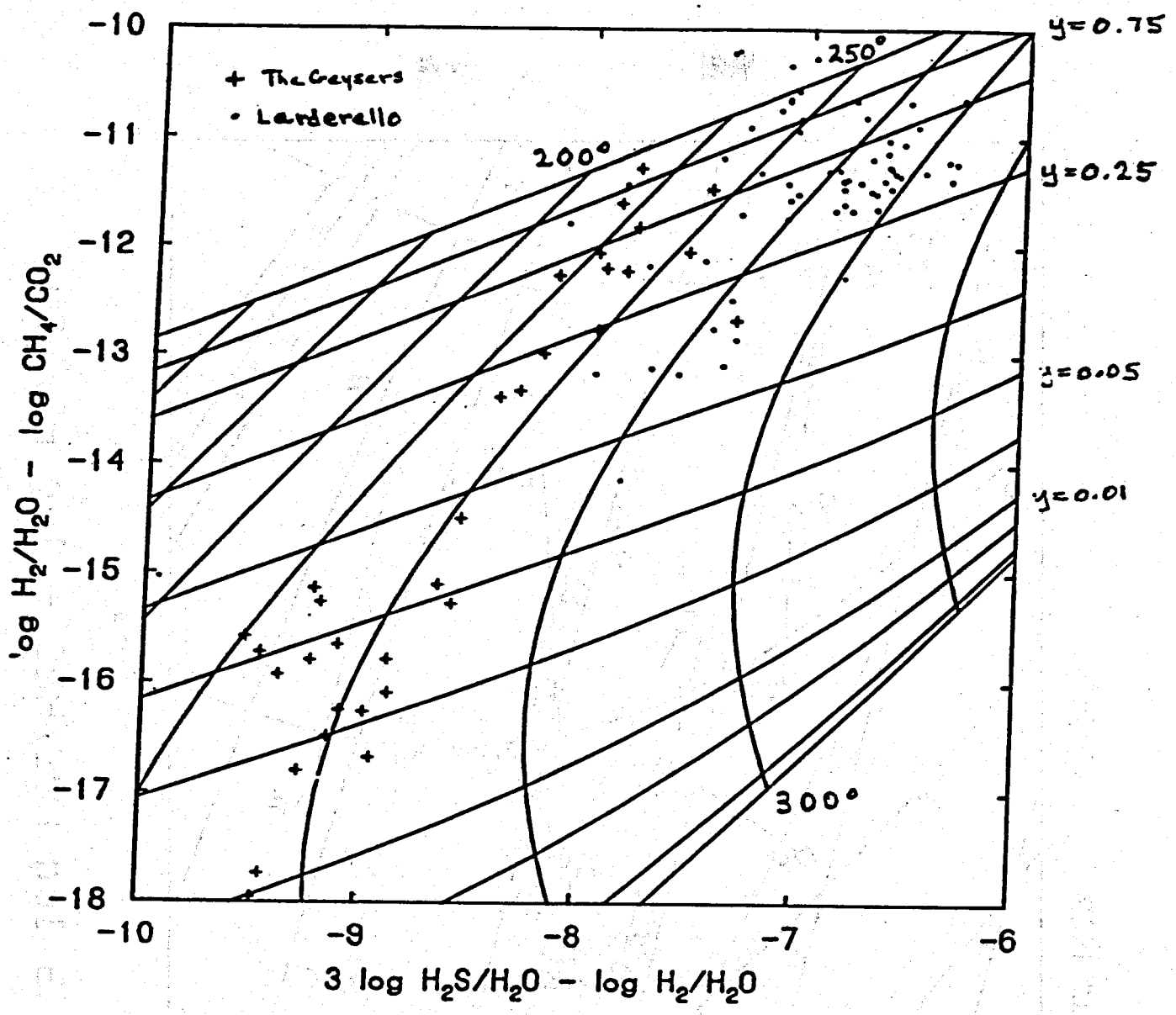
+ The Geysers
• Larderello
250°
200°
300°
y=0.75
y=0.25
y=0.05
y=0.01
-10
-11
-12
-13
-14
-15
-16
-17
-18
-10
-9
-8
-7
-6
log H2/H2O - log CH4/CO2
3 log H2S/H2O - log H2/H2O

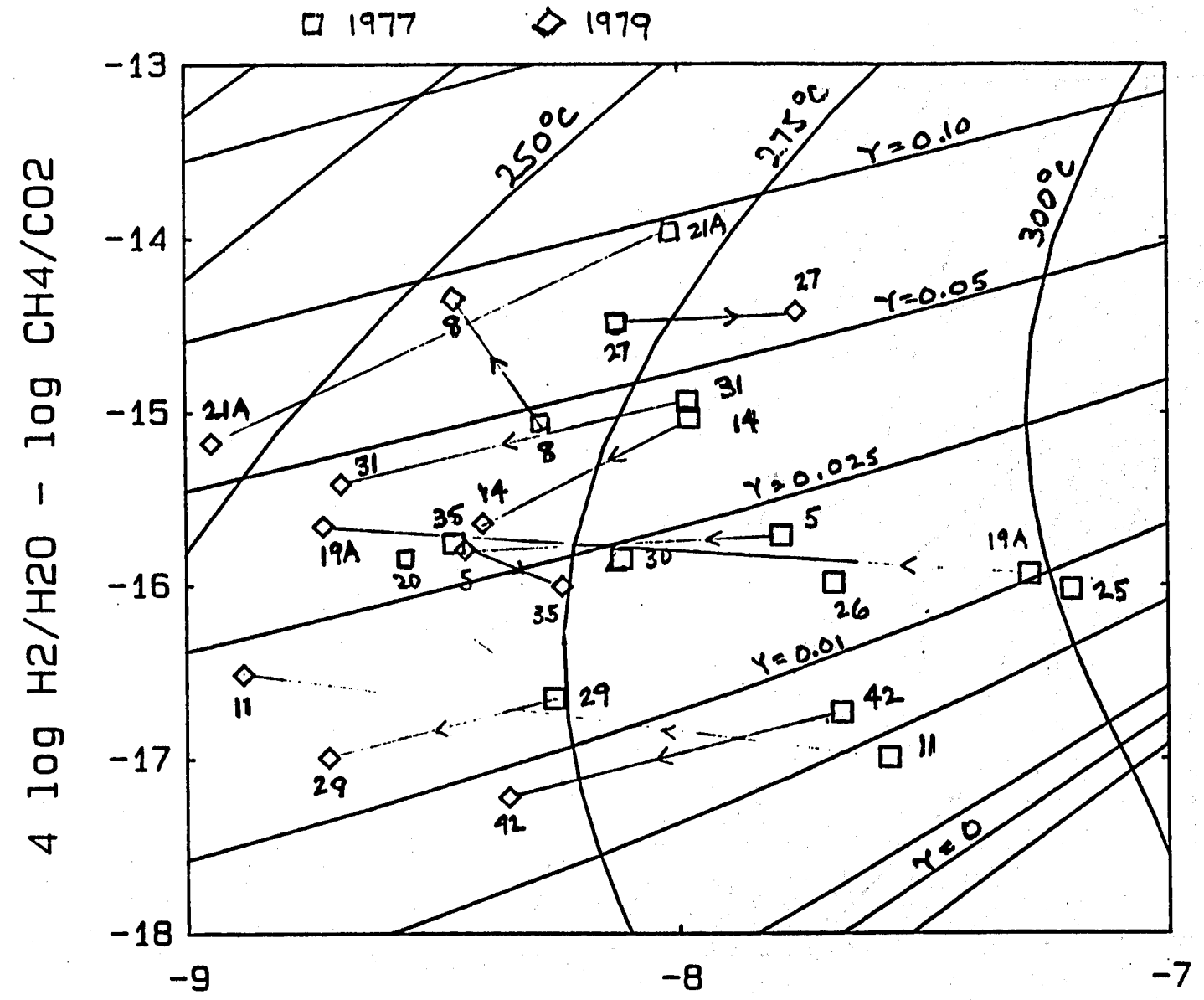
1977
1979
250°C
275°C
300°C
Y=0.10
Y=0.05
Y=0.025
Y=0.01
Y=0
21A
27
8
31
14
35
5
19A
20
30
26
25
11
29
42
92
-13
-14
-15
-16
-17
-18
-9
-8
-7
4 log H2/H20 - log CH4/CO2
3 log H2S/H20 - log H2/H20

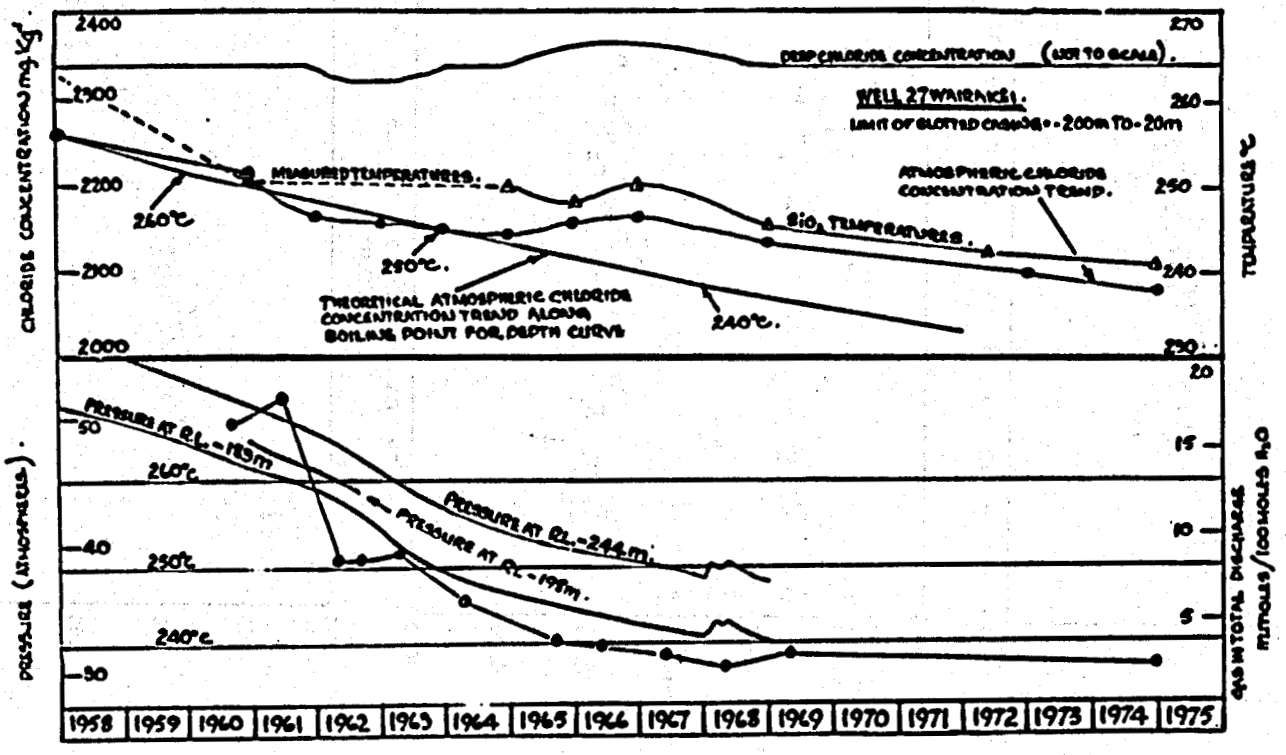

Figure 2. Well 27, Wairakei, New Zealand. Trends in gas and chloride concentrations with exploitation.

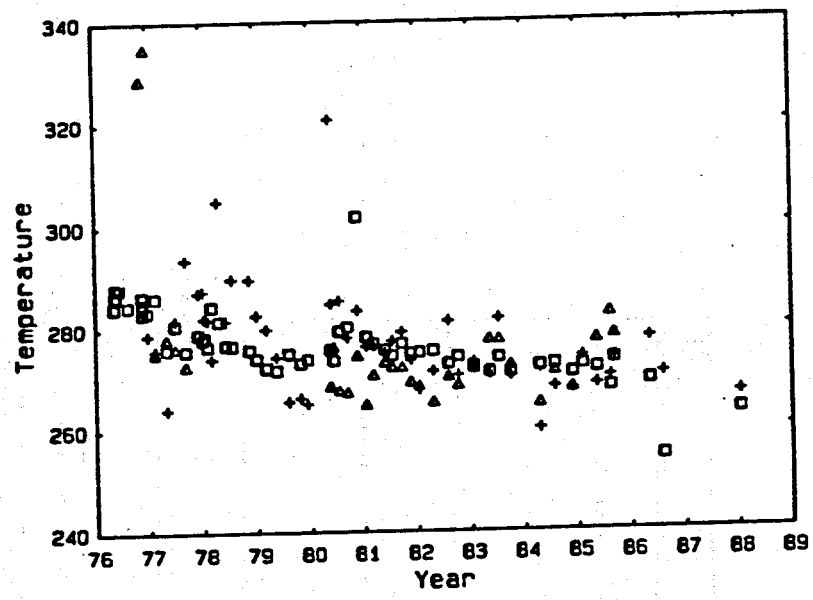
Temperature
340
320
300
280
260
240
76 77 78 79 80 81 82 83 84 85 86 87 88 89
Year

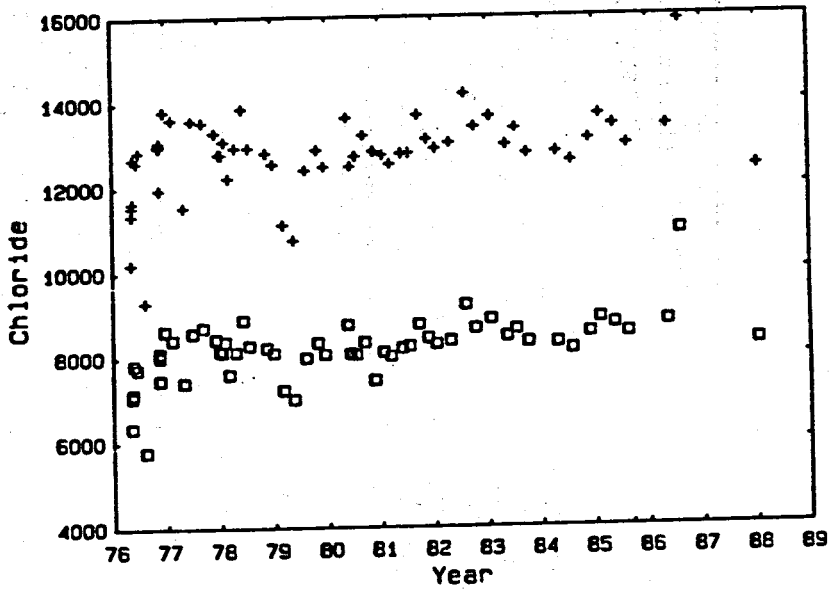
Chloride
16000
14000
12000
10000
8000
6000
4000
76 77 78 79 80 81 82 83 84 85 86 87 88 89
Year

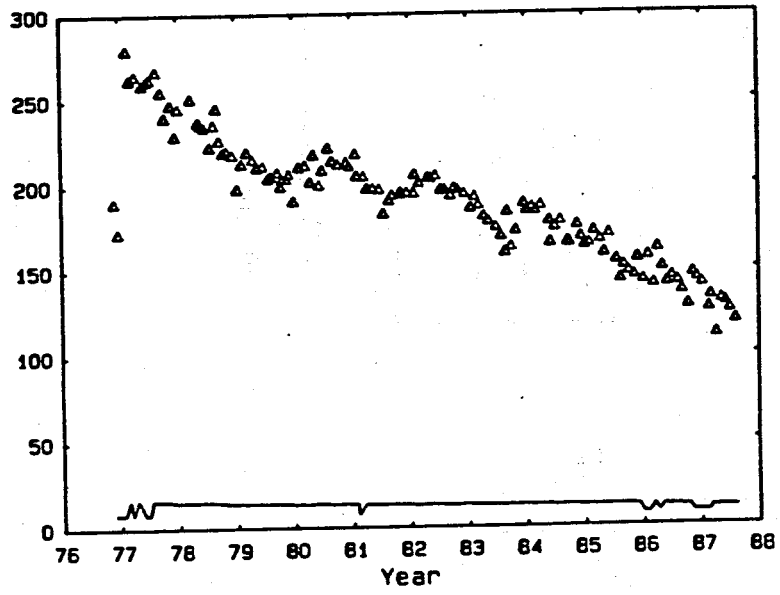
300
250
200
150
100
50
0
76 77 78 79 80 81 82 83 84 85 86 87 88
Year

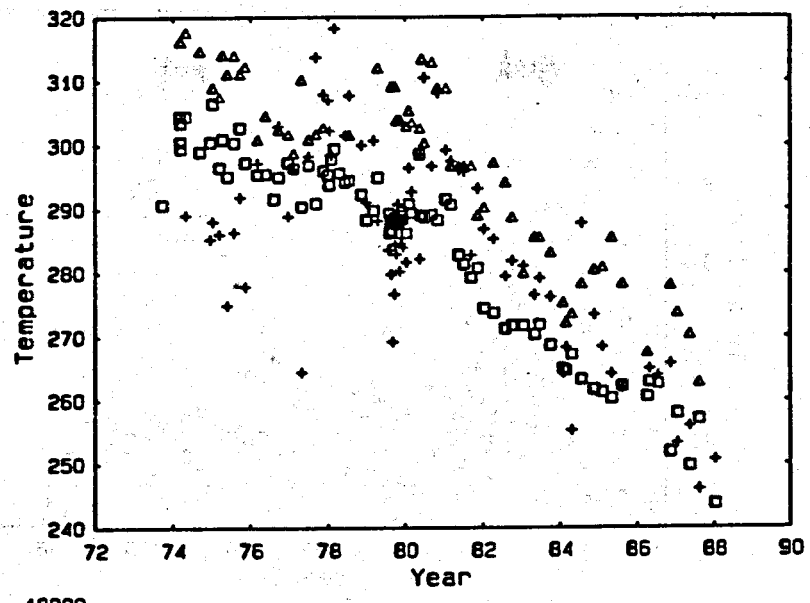
Temperature
320
310
300
290
280
270
260
250
240
72
74
76
78
80
82
84
86
88
90
Year

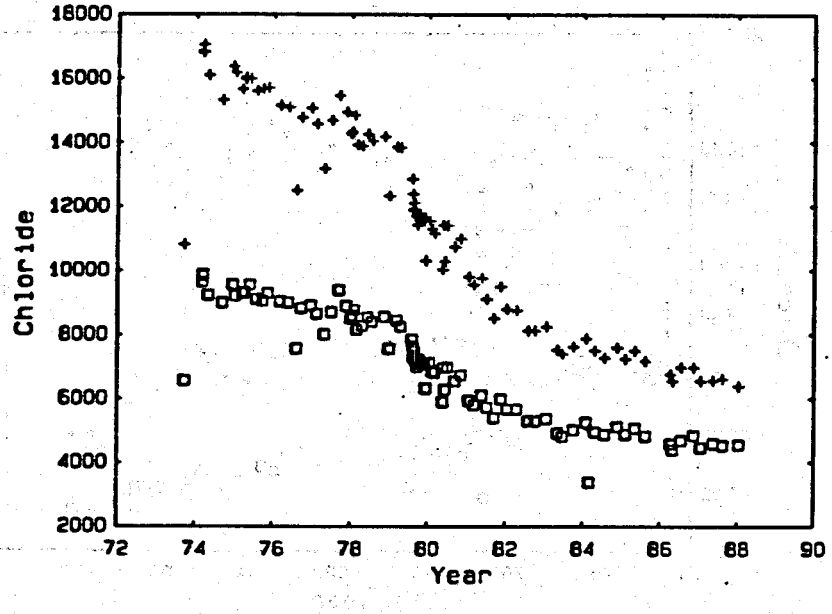
Chloride
18000
16000
14000
12000
10000
8000
6000
4000
2000
72
74
76
78
80
82
84
86
88
90
Year

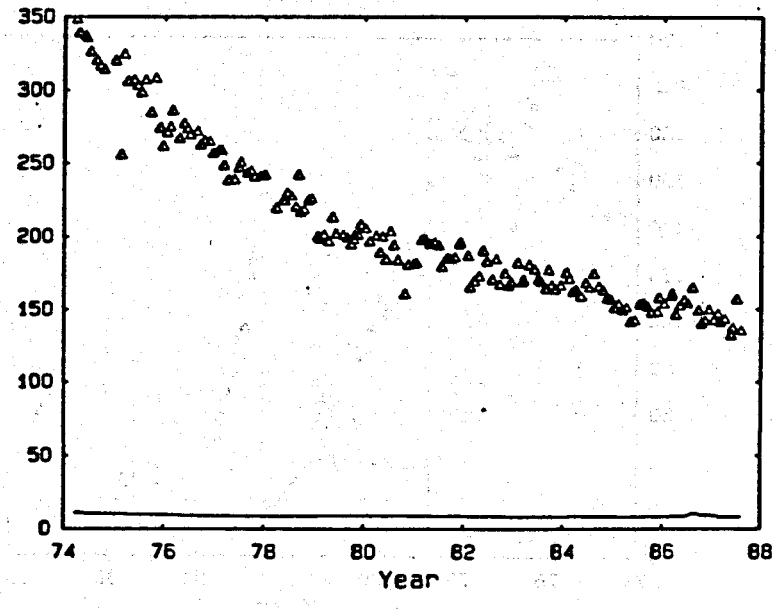
350
300
250
200
150
100
50
0
74
76
78
80
82
84
86
88
Year

M-21A

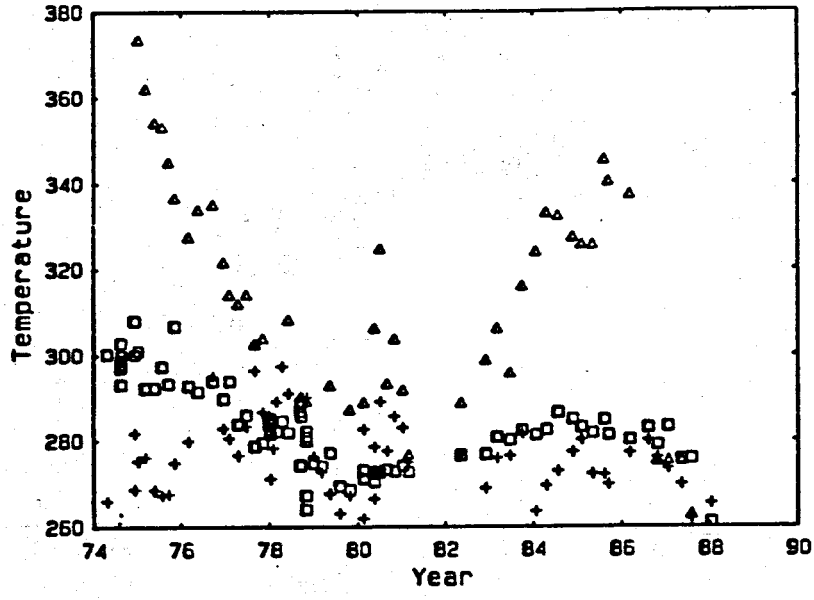
Temperature
380
360
340
320
300
280
260
74
76
78
80
82
84
86
88
90
Year

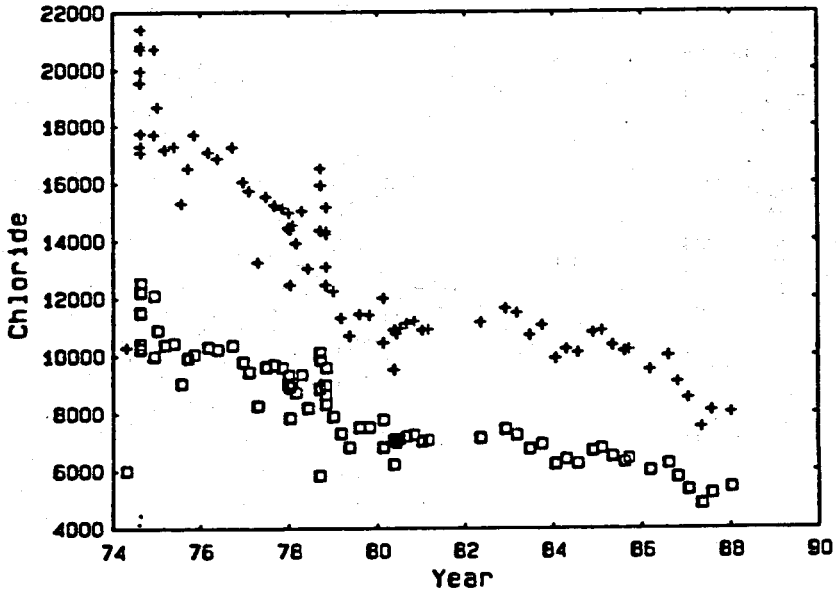
Chloride
22000
20000
18000
16000
14000
12000
10000
8000
6000
4000
74
76
78
80
82
84
86
88
90
Year

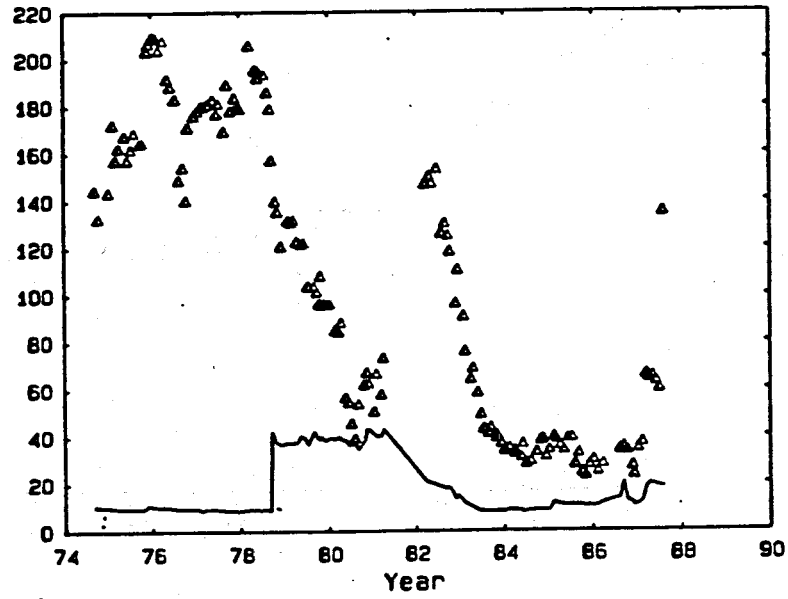
220
200
180
160
140
120
100
80
60
40
20
0
74
76
78
80
82
84
86
88
90
Year

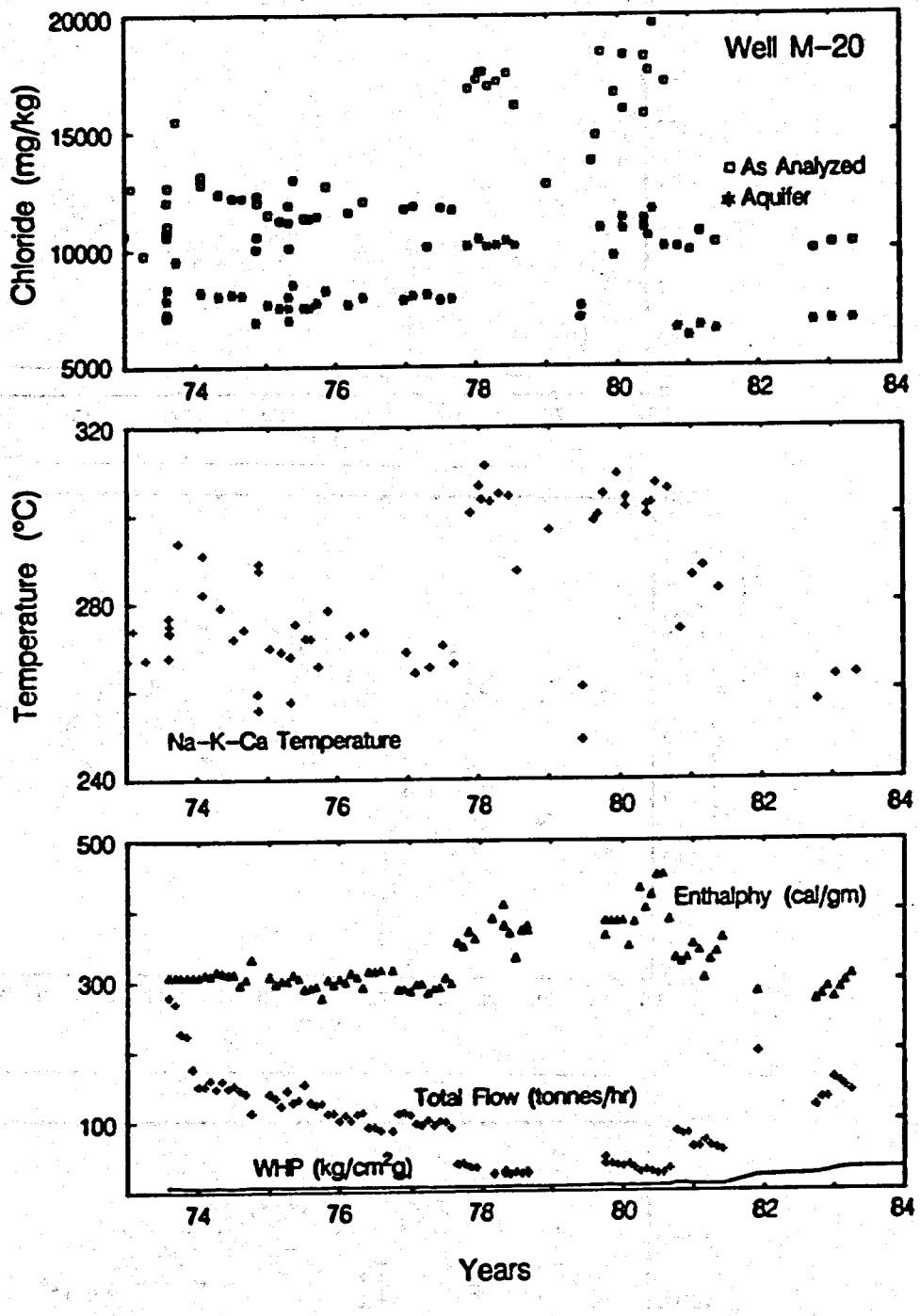

XBL 865-10815

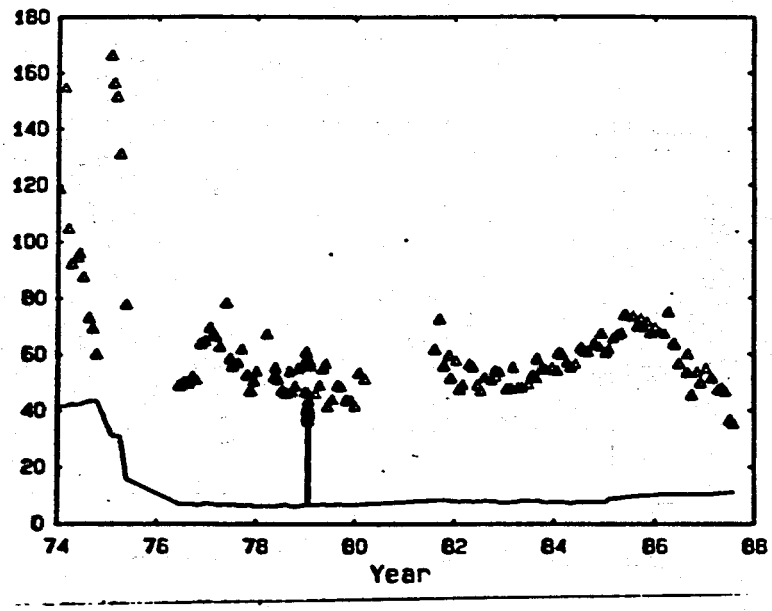
180
160
140
120
100
80
60
40
20
0
74
76
78
80
82
84
86
88
Year

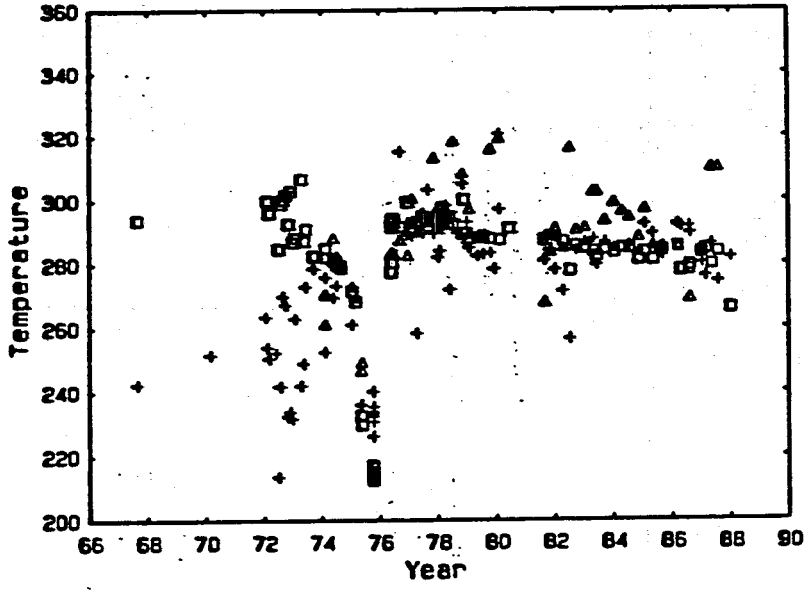
Temperature
360
340
320
300
280
260
240
220
200
66
68
70
72
74
76
78
80
82
84
86
88
90
Year

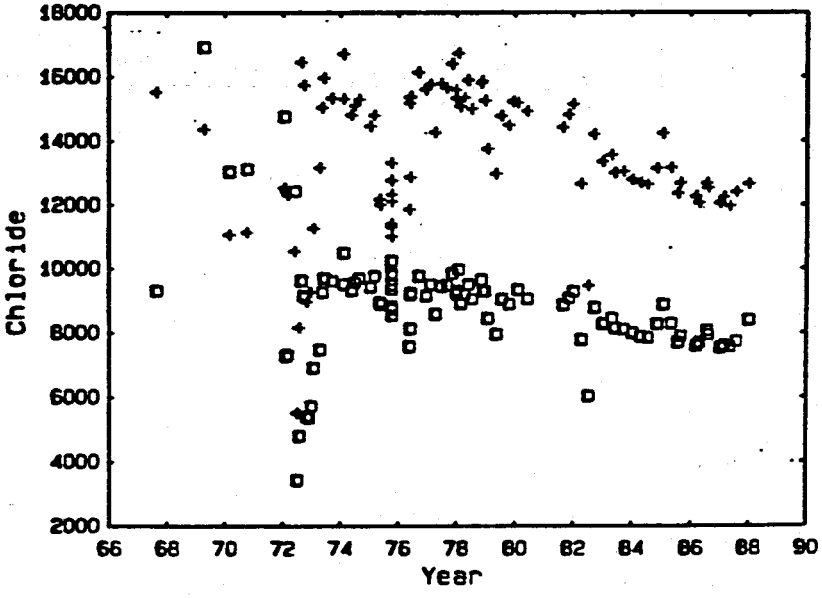
Chloride
18000
16000
14000
12000
10000
8000
6000
4000
2000
66
68
70
72
74
76
78
80
82
84
86
88
90
Year

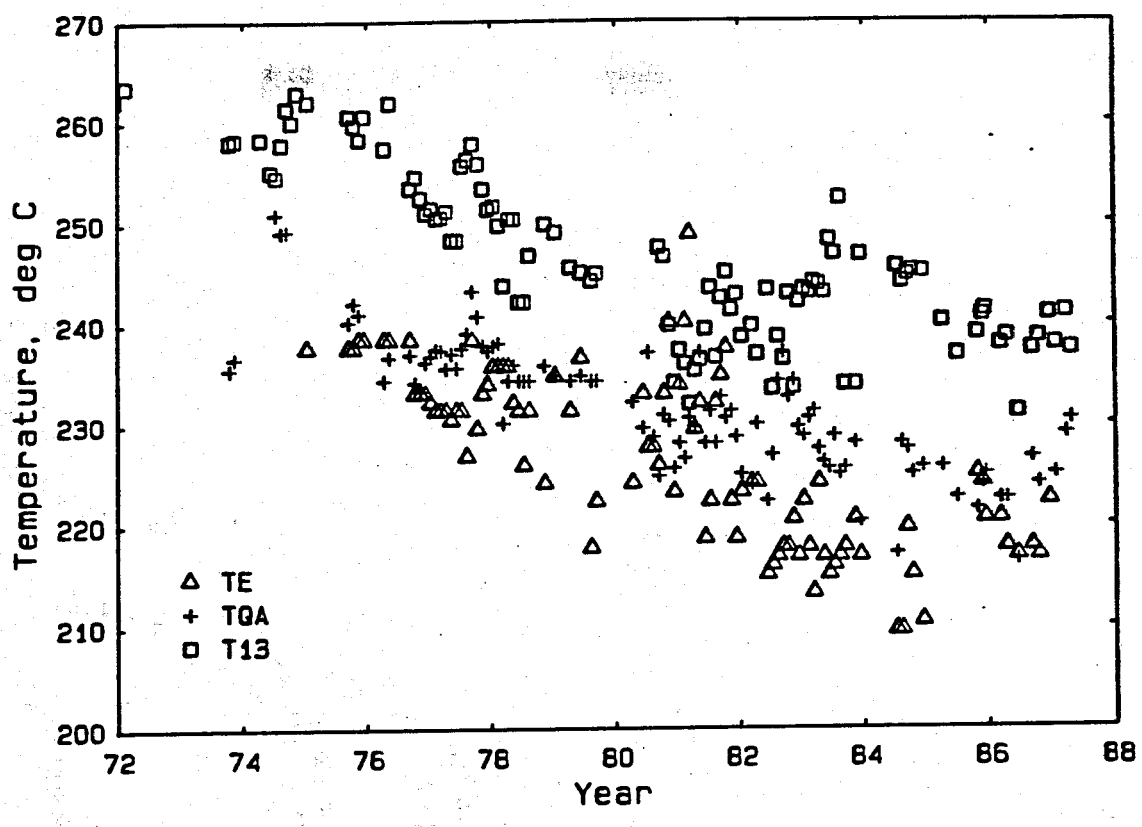
Temperature, deg C
270
260
250
240
230
220
210
200
72
74
76
78
80
82
84
86
88
Year
TE
TQA
T13

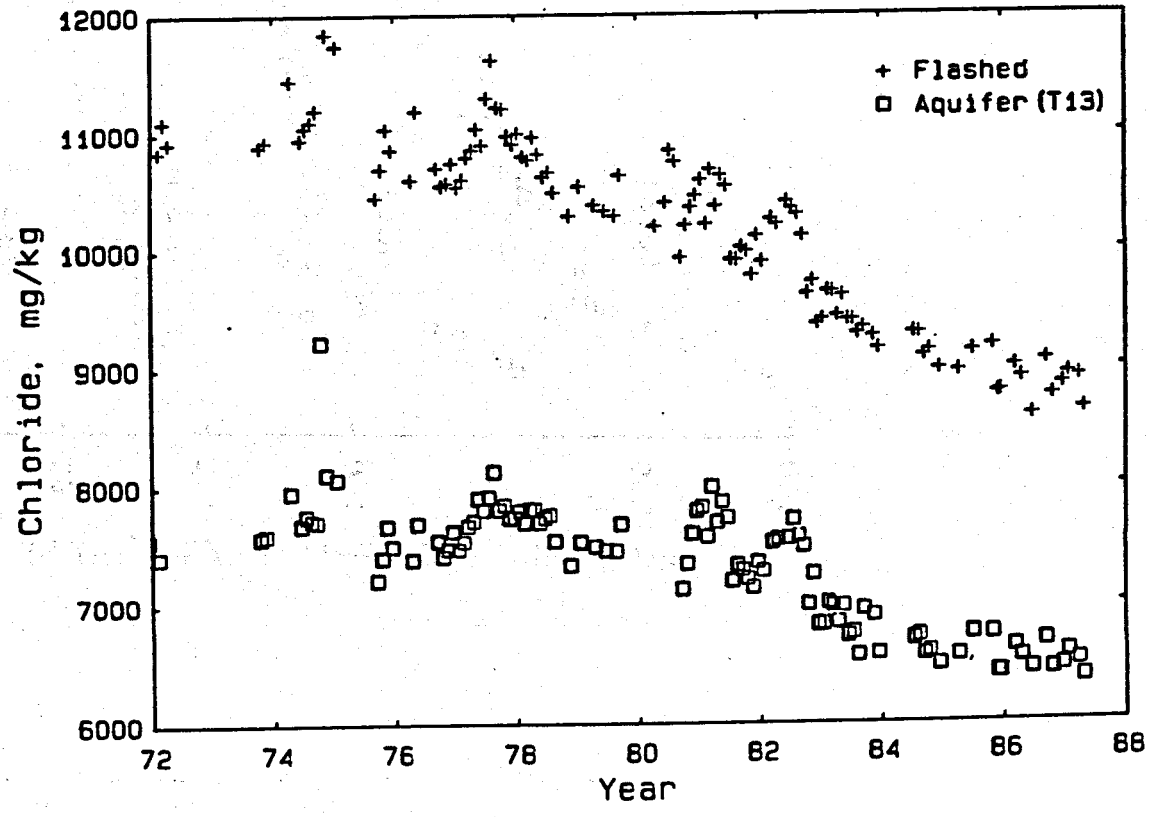
Chloride, mg/kg
12000
11000
10000
9000
8000
7000
6000
72
74
76
78
80
82
84
86
88
Year
Flashed
Aquifer (T13)

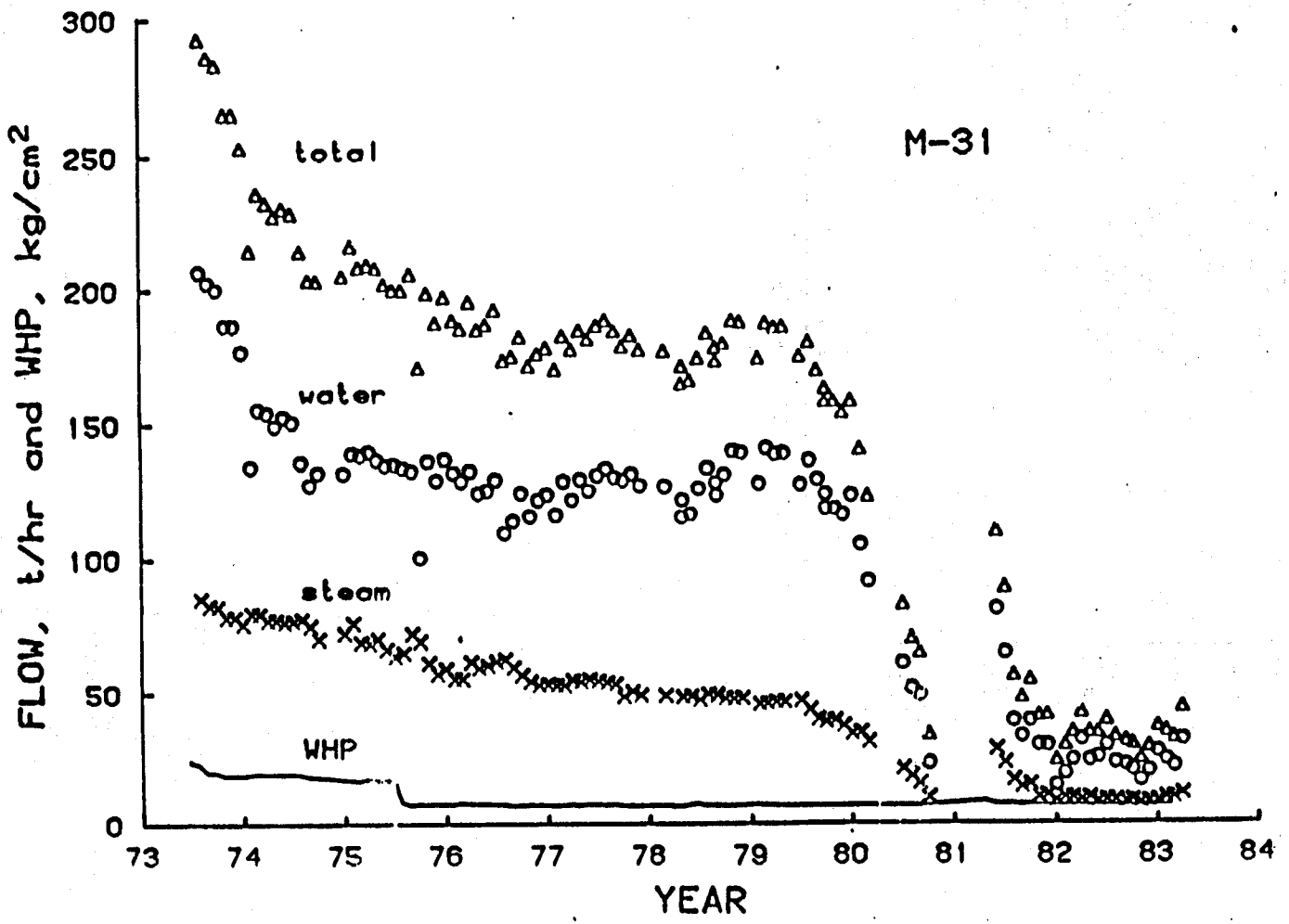
M-31
total
water
steam
WHP
FLOW, t/hr and WHP, kg/cm²
YEAR
300
250
200
150
100
50
0
73
74
75
76
77
78
79
80
81
82
83
84

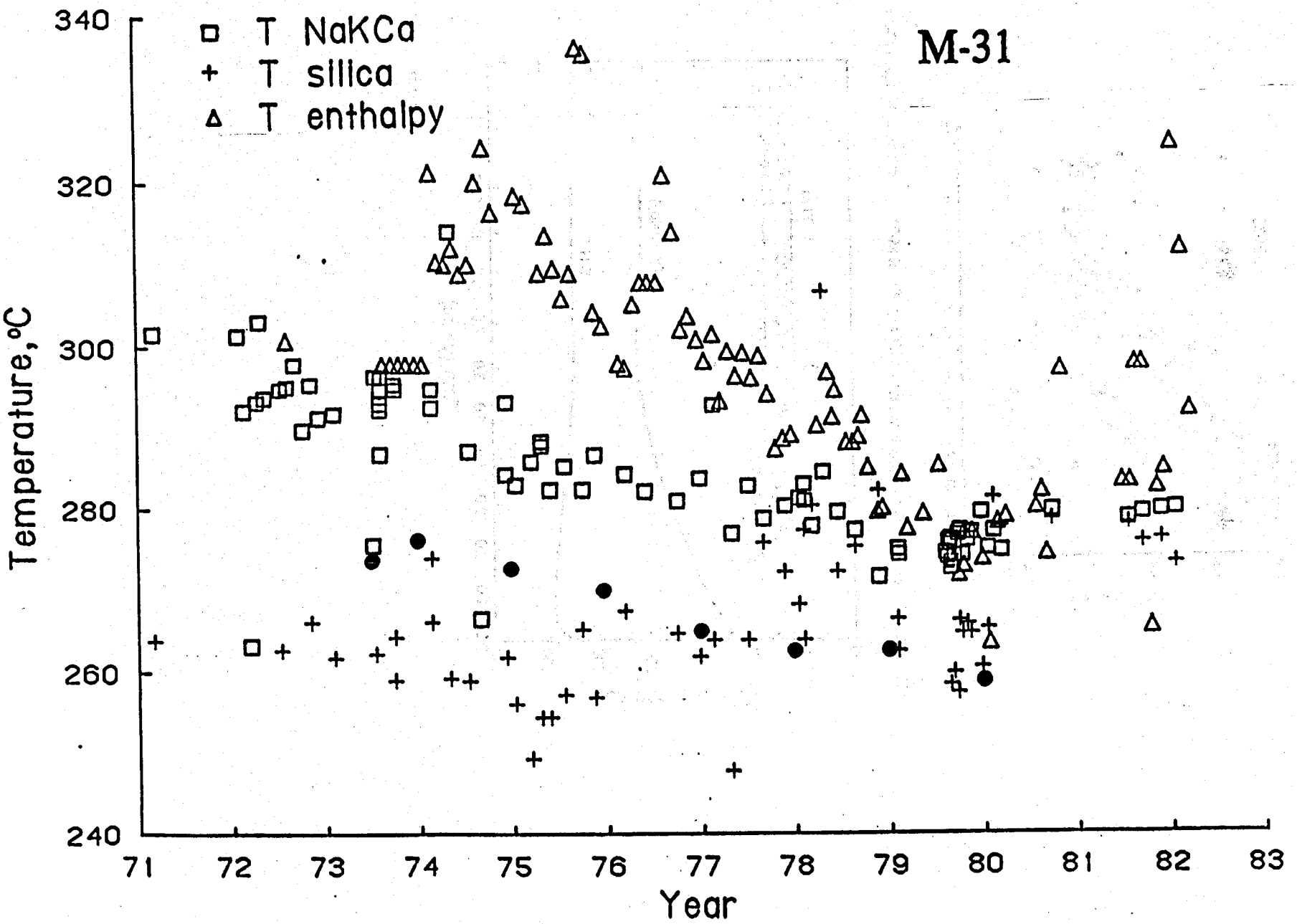
M-31
T NaKCa
T silica
T enthalpy
Temperature, °C
340
320
300
280
260
240
71
72
73
74
75
76
77
78
79
80
81
82
83
Year

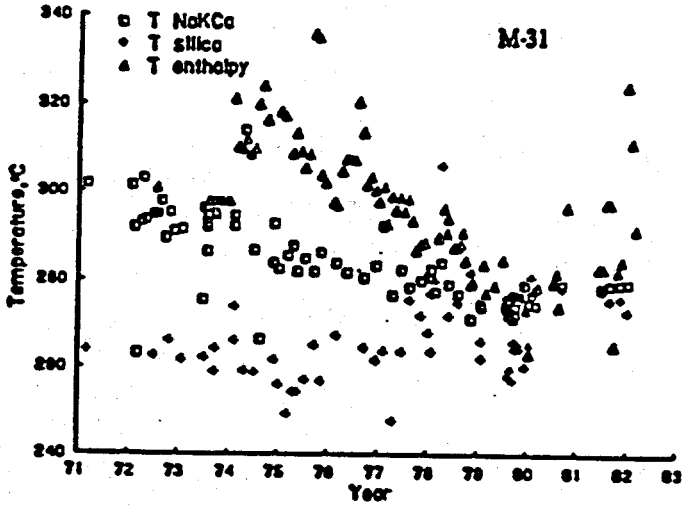

Figure 7. Chemical and enthalpy temperature history of well M-31. (from Truesdell et al, 1984a)

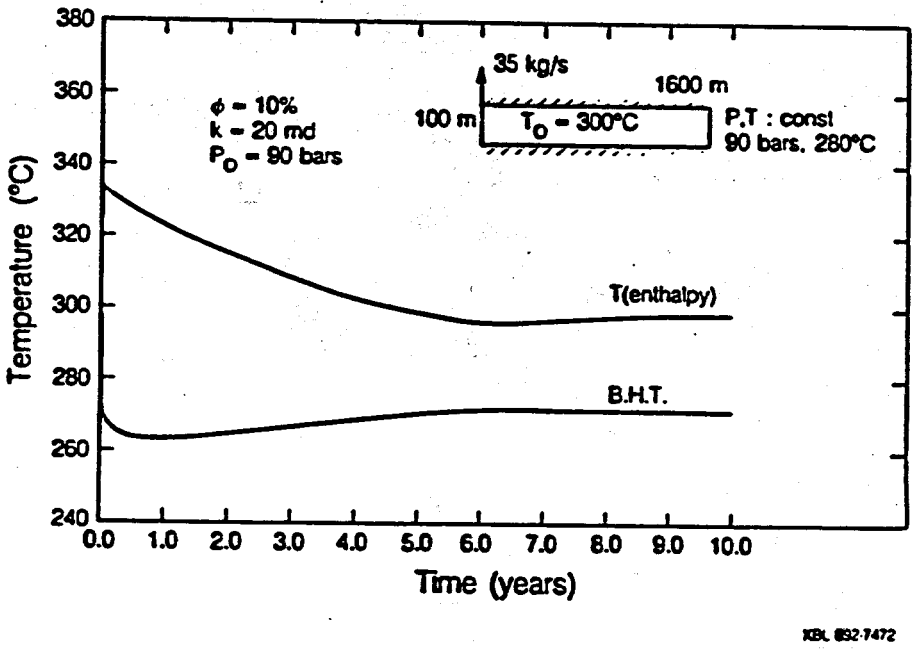

XBL 892-7472

FLUID PROPERTIES AFFECTED BY AQUIFER BOILING

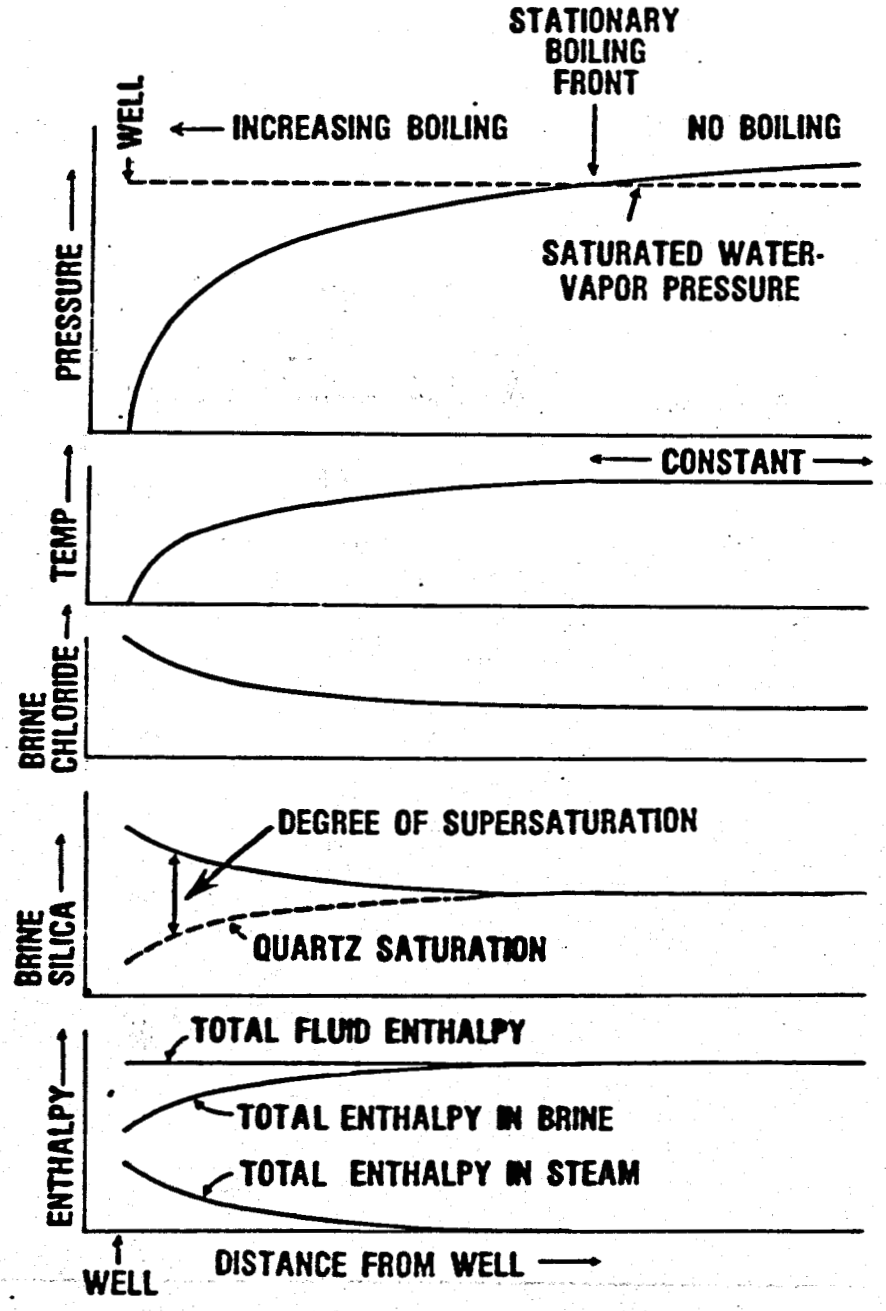

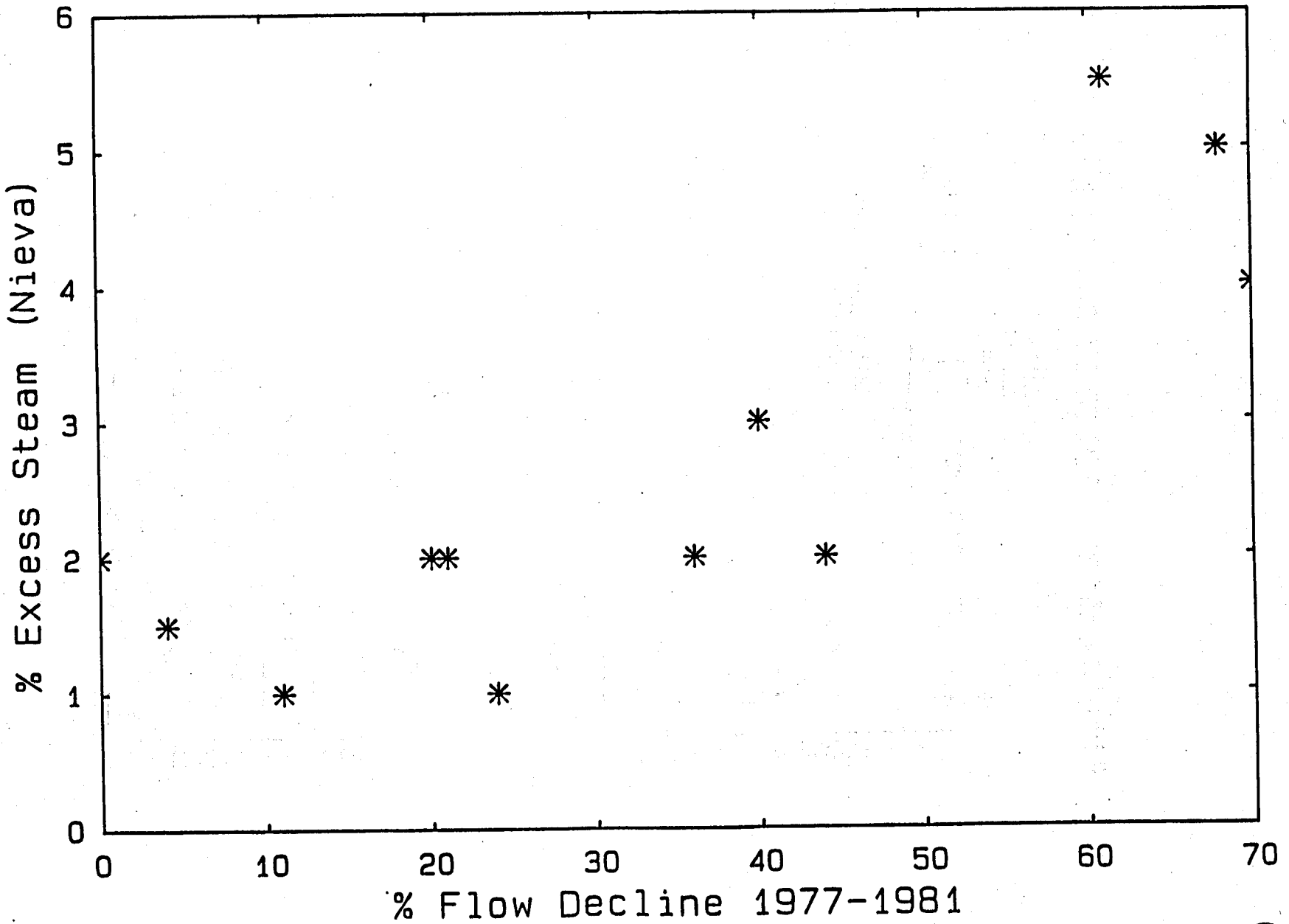
% Excess Steam (Nieva)
% Flow Decline 1977-1981
0
1
2
3
4
5
6
0
10
20
30
40
50
60
70

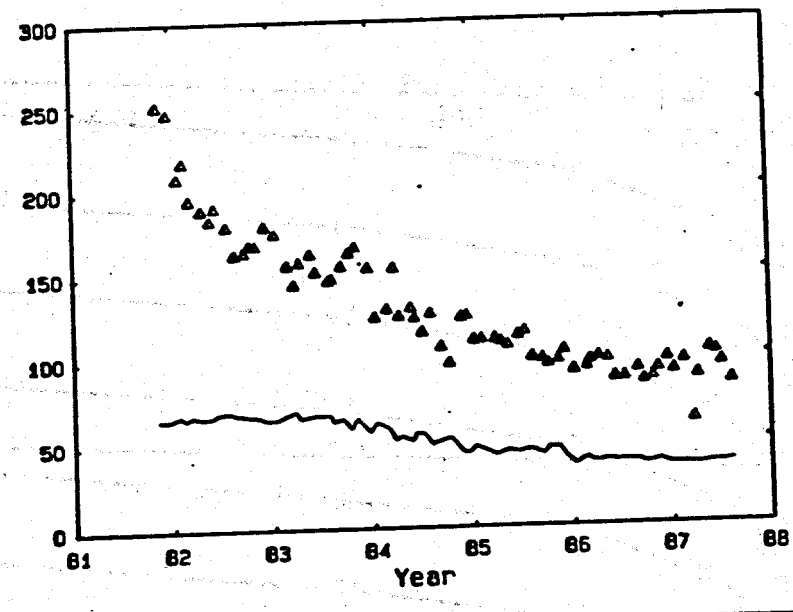
300
250
200
150
100
50
0
81
82
83
84
85
86
87
88
Year

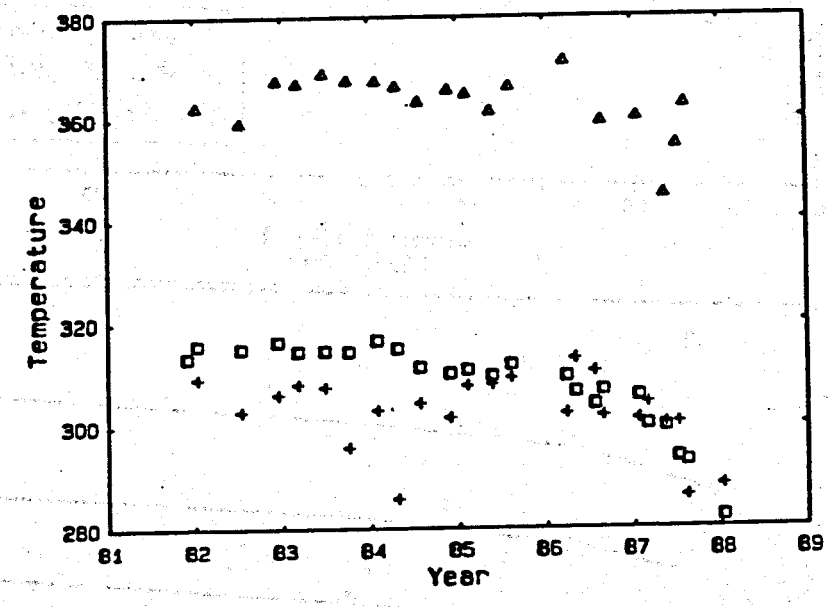
380
360
340
320
300
280
Temperature
81
82
83
84
85
86
87
88
89
Year

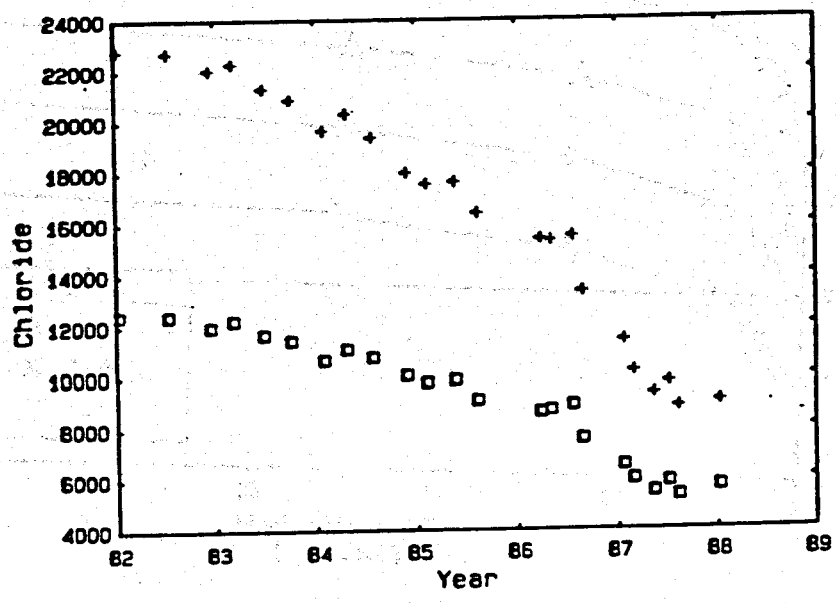
24000
22000
20000
18000
16000
14000
12000
10000
8000
6000
4000
Chloride
82
83
84
85
86
87
88
89
Year

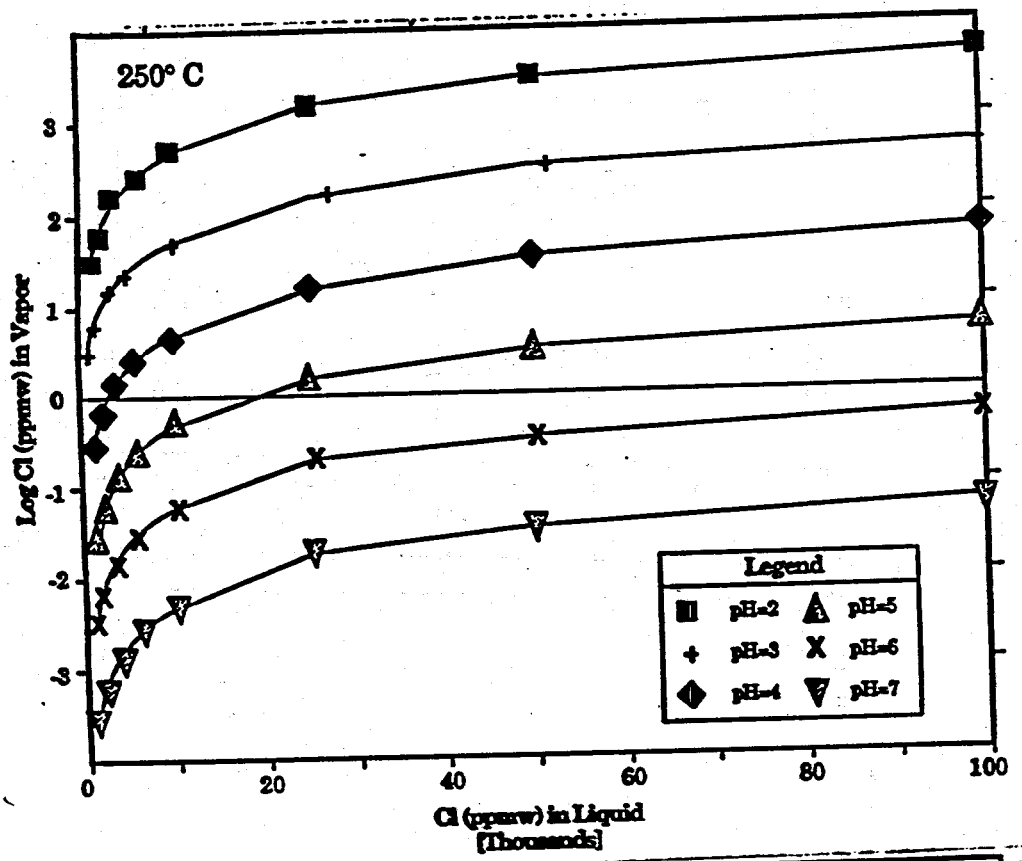
250° C
Log Cl (ppmw) in Vapor
3
2
1
0
-1
-2
-3
0
20
40
60
80
100
Cl (ppmw) in Liquid
[Thousands]
Legend
pH=2
pH=3
pH=4
pH=5
pH=6
pH=7

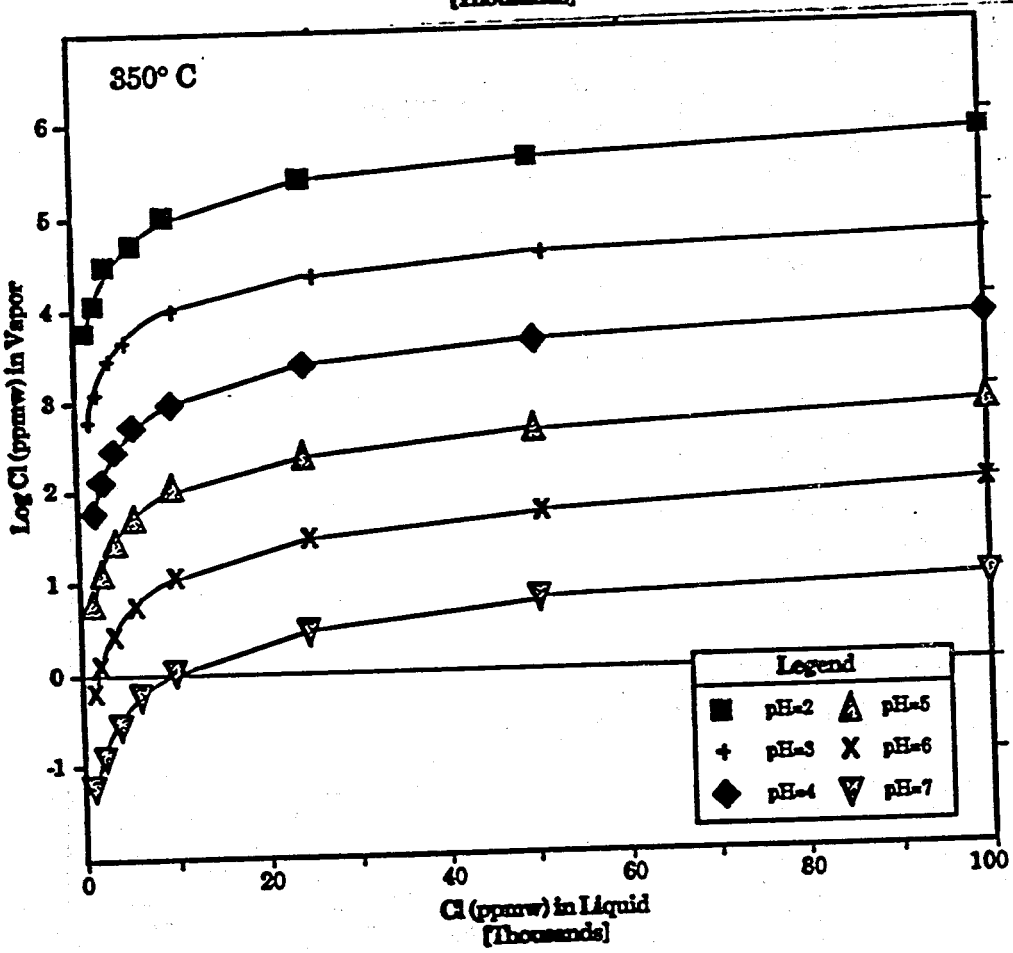
350° C
Log Cl (ppmw) in Vapor
6
5
4
3
2
1
0
-1
0
20
40
60
80
100
Cl (ppmw) in Liquid
[Thousands]
Legend
pH=2
pH=3
pH=4
pH=5
pH=6
pH=7

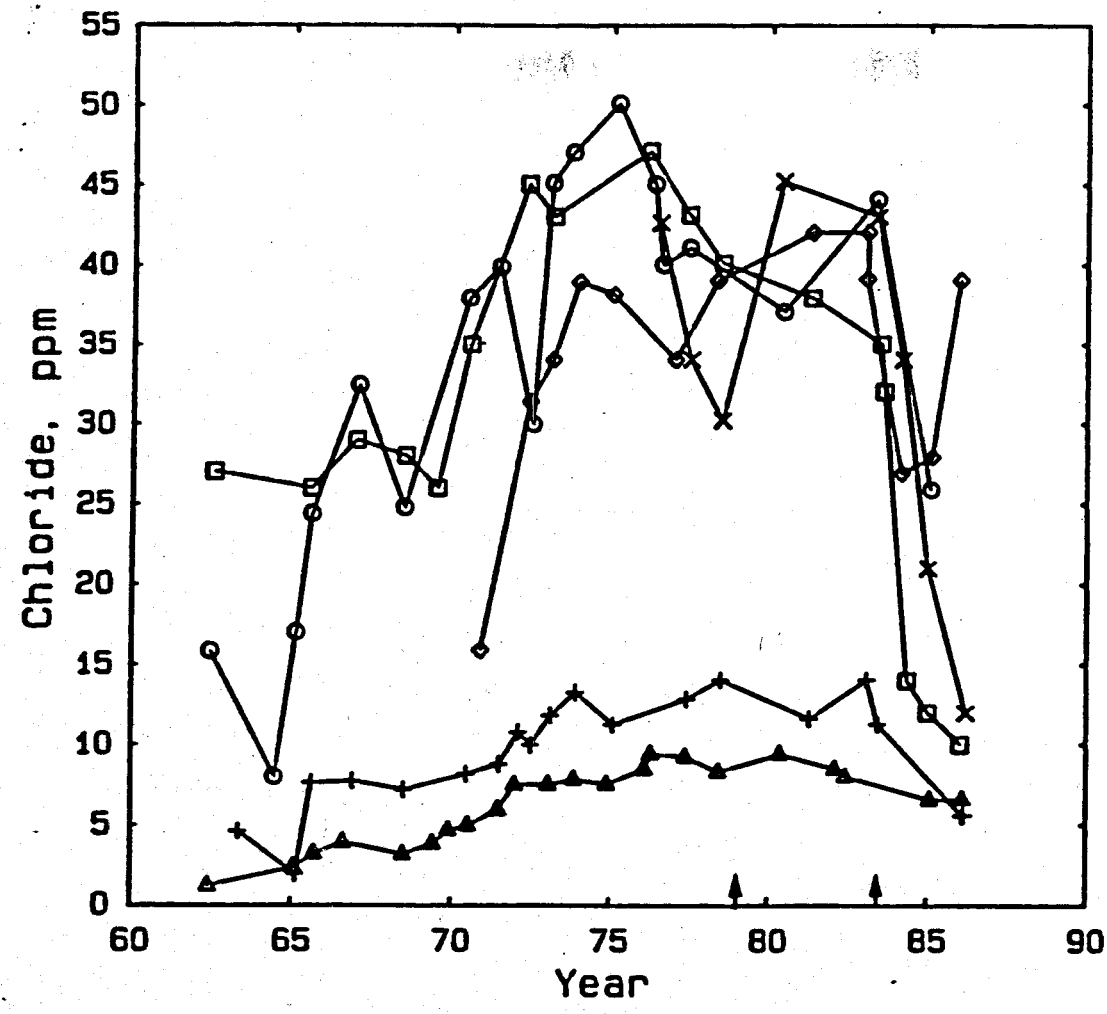
Chloride, ppm
55
50
45
40
35
30
25
20
15
10
5
0
60
65
70
75
80
85
90
Year

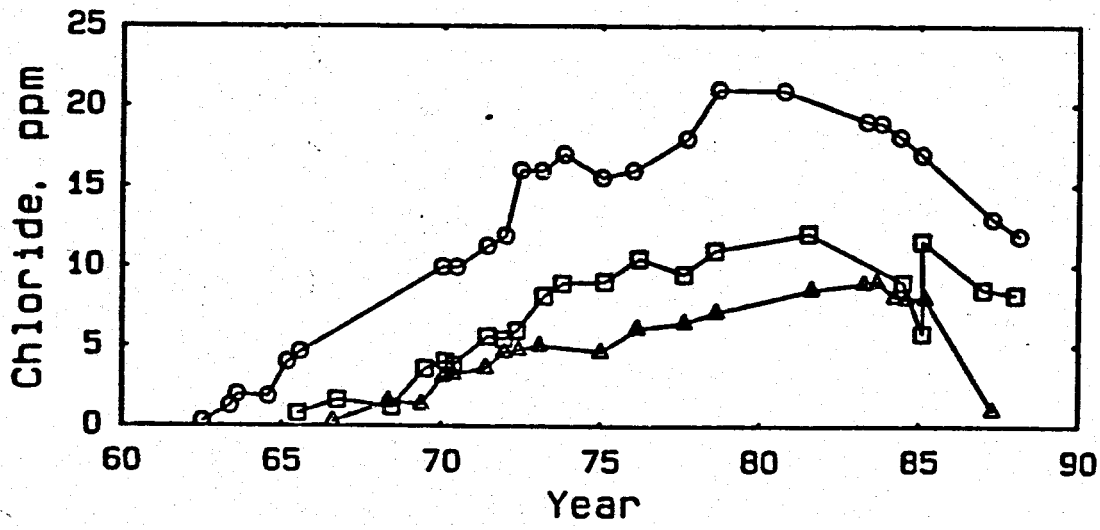
Chloride, ppm
25
20
15
10
5
0
60
65
70
75
80
85
90
Year